



THE UNIVERSITY OF QUEENSLAND
AUSTRALIA

Synthesis of Cyclic Macromolecular Architectures

Md. Daloar Hossain

BSc (Hons), ME

A thesis submitted for the degree of Doctor of Philosophy at

The University of Queensland in 2014

Australian Institute for Bioengineering and Nanotechnology

Abstract

Design and synthesis of complex polymer architectures is a promising field in polymer chemistry to produce new materials with unprecedented macroscopic properties. Recent advances in 'living' radical polymerization and polymer coupling chemistries has facilitated the fabrication of new polymer topologies. The main goal of this thesis is to develop novel methods to fabricate cyclic polymers with pendent functional groups, and use them as building blocks in the synthesis of complex polymer topologies. The 'click' reaction used to couple the cyclic polymers was by copper-catalyzed azide/alkyne cycloaddition reaction (CuAAC). The thermal properties of the resultant complex structures were investigated by Differential Scanning Calorimetry to determine the effect of topology on the glass transition temperature (T_g).

First, the combination of RAFT polymerization and CuAAC reaction were used for the synthesis of cyclic polymer with pendent hydroxyl group. An alkyne functional RAFT agent was used for the synthesis of linear polystyrene (PSTY), in which the RAFT moiety was then converted to an azide moiety and a free OH group via a two step synthetic reaction. This linear polymer was cyclized in high yield and considered as a highly efficient method, and has the potential to be applied to a wide range of polymers made by RAFT. Although the monocyclic polymer was synthesized in high yield, we observed ester cleavage during the synthesis of more complex topologies from the monocyclic precursor building blocks. A detail degradation study was conducted using different catalyst/ligand complexes, and finally the methodology for the synthesis of different topologies of cyclics was amended to reduce this degradative side reaction. However, for the fabrication of more complex topologies, the synthetic methodology was redirected towards a more stable synthetic approach.

A modular approach was followed for the synthesis of multifunctional linear polymer precursors through modulating the Cu(I) activity towards the click reaction over radical formation. The post-modification approach allowed for the synthesis of α , ω -heterotelechelic linear polymer precursors which was cyclised by using a modified CuAAC cyclization reaction in which the hydroxyl functional groups were equally spaced. The hydroxyl groups were converted to azides or alkynes and then further coupled together through the CuAAC reaction to produce complex structures, including a spiro tricyclic and 1st generation dendritic structures. All these structures were produced in high yields with good 'click' efficiencies. The purity and 'click' efficiencies were calculated by fitting the experimental SEC traces with a log-normal distribution (LND) model based on fitting

multiple Gaussian functions for each polymer species. The crude polymer was purified by preparative SEC that essentially removes all the unreacted species and by-products.

In the follow up work, a range of different topologies of cyclic homo and copolymers were synthesized by combining of ATRP, SET-LRP and CuAAC coupling reactions. The homopolystyrene architectures ranged from di-block to 3-armed star polymers, consisting of both linear and cyclic polymer building blocks. Additionally, the di-block, AB, miktoarm AB₂ and A₂B type of amphiphilic copolymers consisting of PSTY and polyacrylic acid (PAA) and their cyclic analogues were successfully synthesized. All these topologically diverse polymers were purified by preparative SEC to remove any impurities formed during 'click' reaction. To investigate the topology effect on thermal property such as T_g, the polymers were characterized by differential scanning calorimetry (DSC). The results revealed that the topologies which possessed higher number of cyclic units (i.e., lower number of chain ends) showed higher T_g values. The thin film self-assemblies of block copolymers of both linear and cyclic analogues were also characterized by AFM to investigate the effect of cyclic topology on the morphology. The thin film domain spacing of cyclic block copolymer decreased by ~50% compared to the linear analogue due to the structural compactness.

Finally, a range of complex polymer architectures such as linear, cyclic, spiro di and tricyclic, star tricyclic, G1 star tetracyclic and dendrimer pentacyclic were used to investigate the effect of placing knots in different locations in a cyclic polymer on the glass transition temperature. The molecular weight of all these polymers was kept essentially the same to avoid the influence of molecular weight effect on T_g. To form a knot, we used covalent linkages that produce irreversible knots. The experimental results revealed that the T_g for this series of polymers was not only affected by the number of knots but also the type and location of the knots.

Declaration by author

This thesis is composed of my original work, and contains no material previously published or written by another person except where due reference has been made in the text. I have clearly stated the contribution by others to jointly-authored works that I have included in my thesis.

I have clearly stated the contribution of others to my thesis as a whole, including statistical assistance, survey design, data analysis, significant technical procedures, professional editorial advice, and any other original research work used or reported in my thesis. The content of my thesis is the result of work I have carried out since the commencement of my research higher degree candidature and does not include a substantial part of work that has been submitted to qualify for the award of any other degree or diploma in any university or other tertiary institution. I have clearly stated which parts of my thesis, if any, have been submitted to qualify for another award.

I acknowledge that an electronic copy of my thesis must be lodged with the University Library and, subject to the General Award Rules of The University of Queensland, immediately made available for research and study in accordance with the *Copyright Act 1968*.

I acknowledge that copyright of all material contained in my thesis resides with the copyright holder(s) of that material. Where appropriate I have obtained copyright permission from the copyright holder to reproduce material in this thesis.

Publications during candidature

1) Hossain, M. D.; Valade, D.; Jia, Z.; Monteiro, M. J., Cyclic polystyrene topologies via RAFT and CuAAC. *Polymer Chemistry* **2012**, 3 (10), 2986-2995.

Publications included in this thesis

1) Hossain, M. D.; Valade, D.; Jia, Z.; Monteiro, M. J., Cyclic polystyrene topologies via RAFT and CuAAC. *Polymer Chemistry* **2012**, 3 (10), 2986-2995. – Incorporated as Chapter 2.

Hossain, M. D. was responsible for 45% of analysis and interpretation of data, 40% of drafting and writing and 50% of conception and design. Valade, D. was responsible for 5 % of analysis and interpretation of data and 10% of drafting and writing. Jia, Z. was responsible for 10% of analysis and interpretation of data and 10% of drafting and writing. Monteiro, M. J. was responsible for 40% of analysis and interpretation of data, 40% of drafting and writing and 50% of conception and design.

Contributions by others to the thesis

The author acknowledges the following individuals who have contributed to this thesis:

Prof. Michael J. Monteiro for contributing to the conception, design, analysis and interpretation of the research detailed in this thesis.

Dr. Zhongfan Jia for contributing to the later parts of the conception, design, analysis and interpretation of the research detailed in this thesis.

Statement of parts of the thesis submitted to qualify for the award of another degree

None.

Acknowledgements

First and foremost, I would like to express my gratitude and special thanks to my supervisor, Prof. Michael J. Monteiro for his support, guidance and encouragement in pursuing my PhD thesis. He has been a steady influence throughout my program and patiently guided me step by step to achieve a high standard thesis. He has oriented and mentored me with promptness and care, and has always been positive in times of new ideas and in solving any research problem. I admire his high scientific standards, and hard work which can be set an example in scientific community. I would also like to express my sincere appreciation to my co-supervisor, Dr. Zhongfan Jia for picking me up at the critical stage of my Ph.D. His intuitive thoughts and creative suggestions made my lab work so easy and prolific. I would like to thank my ex co-supervisor Dr. Davide Valade for guiding me at the early stage of my program and for maintaining a good working relationship with flexibility in scheduling, gentle encouragement and relaxed demeanor.

I am deeply indebted to all my past and present group members for support, sharing their knowledge and precious friendships that made my life abroad so enjoyable. I wish to acknowledge receipt of the scholarship from UQ international, UQ graduate school and the Australian Institute for Bioengineering and Nanotechnology (AIBN) to pursue my PhD research smoothly. I would like to express my gratitude to AIBN for their state-of-the-art facilities and support from the staff members.

I am forever indebted to my parents and my siblings for their support in achieving my university degree. Without their help and generosity, I would never be where I am today. Finally and most importantly, I would like to convey my special thanks to my wife Fatema Johra (Liza) for her endless love and patience to realise this dream and my little baby, Yashfee Shayan Hossain, who missed out on a lot of Daddy time while I sought intellectual enlightenment.

Keywords

Living radical polymerization, complex polymer topologies, CuAAC, cyclic polymer, glass transition temperature.

Australian and New Zealand Standard Research Classifications (ANZSRC)

030301, Chemical Characterisation of Materials, 20 %

030305, Polymerization Mechanisms, 5 %

030306, Synthesis of Materials, 75 %

Fields of Research (FoR) Classification

0303, Macromolecular and Materials Chemistry, 90%

0305, Organic Chemistry, 10 %

TABLE OF CONTENTS

Abstract.....	ii
Declaration by author.....	iv
Publications during candidature.....	v
Publications included in this thesis.....	v
Contributions by others to the thesis.....	v
Statement of parts of the thesis submitted to qualify for the award of another degree.....	v
Acknowledgements.....	vi
Keywords.....	vii
Australian and New Zealand standard research classifications (ANZSRC).....	vii
Fields of Research (FoR) Classification.....	vii
Table of Contents.....	viii
List of Figures.....	xiii
List of Schemes.....	xvii
List of Tables.....	xviii
List of Abbreviations.....	xix

Chapter 1

Introduction

1.1 Reversible Addition Fragmentation Chain transfer (RAFT) polymerization.....	1
1.2 Atom Transfer Radical Polymerization (ATRP)	3
1.3 Single-Electron Transfer (SET) LRP.....	4
1.4 Cu Catalyzed Azide/Alkyne Click (CuAAC) Reaction.....	5
1.5 Cyclic polymers	6
1.6 Synthetic strategies towards the macro-cyclization.....	7
1.6.1 Ring-closure techniques.....	8
1.6.2 Ring-expansion techniques.....	10
1.7 Synthetic route towards the macro-cyclization.....	11
1.8 Complex Topologies from Monocyclic Polymers.....	14
1.9 Cyclic Polymer Topologies and Their Properties.....	15
1.10 Objectives and Outlines of this thesis.....	16
1.11 References.....	17

Chapter 2

Cyclic polystyrene topologies via RAFT and CuAAC.

2.1 Introduction.....	26
2.1.1 Aim of the Chapter.....	26
2.2 Experimental.....	27
2.2.1 Materials.....	27
2.2.2 Instruments and measurements.....	28
2.2.3 Synthetic Procedures.....	30
2.2.3.1 Synthesis of 4-benzyl-1-(1-phenylethyl)-1H-1,2,3-triazole ligand.....	30
2.2.3.2 Synthesis of prop-2-ynyl-2-(butylthiocarbonothioylthio)-2-methylpropanoate alkyne	
RAFT.....	30
2.2.3.3 Synthesis of RAFT-PSTY-Alk by RAFT polymerization.....	31
2.2.3.4 Synthesis of Epo-PSTY-Alk.....	31
2.2.3.5 Synthesis of N ₃ -PSTY-Alk.....	32
2.2.3.6 Synthesis of c-PSTY-OH by CuAAC.....	32
2.2.3.7 Synthesis of c-PSTY-Br.....	32
2.2.3.8 Synthesis of c-PSTY-N ₃	33
2.2.3.9 Kinetic studies in the synthesis of dicyclic PSTY by one pot.....	33
2.2.3.10 Kinetic studies in the synthesis tricyclic PSTY by one pot.....	33
2.2.2.11. Synthesis of di-cyclic and tri-cyclic PSTY by one pot.....	33
2.3 Results and discussion.....	34
2.4 Conclusion.....	42
2.5 References.....	43

Chapter 3

Complex Polymer Topologies Built from Tailored Multifunctional Cyclic Polymers

3.1 Introduction.....	46
3.1.1 Aim of the Chapter.....	48
3.2 Experimental.....	49
3.2.1 Materials.....	49
3.2.2 Analytical Methods.....	49
3.2.3. Synthetic Procedures.....	51
3.2.3.1 Synthesis of Protected Alkyne (hydroxyl) Functional Initiator (6).....	51
3.2.3.2 Synthesis of 3-(1, 1, 1-Triisopropylsilyl)-2-propyn-1-ol (2).....	51

3.2.3.3 Synthesis of 3-Bromo-prop-1-ynyl 3-(1, 1, 1-triisopropyl)-silane 3.....	52
3.2.3.4 Synthesis of Compound 4.....	52
3.2.3.5 Synthesis of Compound 5.....	53
3.2.3.6 Synthesis of Protected Alkyne Functional Initiator, Comp. 6.....	53
3.2.3.7 Synthesis of Linear PSTY by Atom Transfer Radical Polymerization (ATRP).....	54
3.2.3.8 Cyclization Reaction by CuAAC Using Argon Flow Technique.....	55
3.2.3.9 Chain-end Modification of Hydroxyl Functional Cyclic Polymer.....	55
3.2.3.10 Synthesis of Protected Alkyne Functional Linear PSTY by ATRP.....	56
3.2.3.11 Cyclization Reaction of $\equiv(\text{OH-PSTY}_{25})_2\text{-N}_3$ by CuAAC Using Argon Flow Technique.....	58
3.2.3.12 Chain-end Modification of Di-hydroxy Functional Cyclic.....	58
3.2.3.13 Synthesis of tri-functional linear PSTY.....	60
3.2.3.14 Cyclization reaction of $\equiv(\text{OH-PSTY}_{25})_3\text{-N}_3$ by CuAAC Using Argon Flow Technique.....	61
3.2.3.15 Chain-end Modification of Tri-hydroxy Functional Cyclic.....	61
3.2.3.16 Synthesis of Complex Topologies.....	62
3.3 Results and discussion.....	64
3.4 Conclusion.....	76
3.5 References.....	76

Chapter 4

Complex Polymer Topologies and Their Glass Transition Studies

4.1 Introduction.....	79
4.1.1 Aim of the Chapter.....	81
4.2 Experimental.....	81
4.2.1 Materials.....	81
4.2.2 Synthetic Procedures.....	82
4.2.2.1 Synthesis of the initiator 3-hydroxy-2-methyl-2-((prop-2-yn-1-yloxy) methyl)propyl 2- bromo-2-methylpropanoate (1).....	82
4.2.2.2 Synthesis of PSTY ₄₄ -Br, 2a by ATRP.....	83
4.2.2.3 Synthesis of PSTY ₄₄ -N ₃ , 3a by azidation with NaN ₃	83
4.2.2.4 Synthesis of PSTY ₄₄ - \equiv , 4a	83
4.2.2.5 Synthesis of PSTY ₄₄ -(\equiv) ₂ , 5a.....	84
4.2.2.6 Synthesis of PtBA ₄₄ -Br, 2b by ATRP.....	84

4.2.2.7 Synthesis of PtBA ₄₄ -N ₃ 3b by azidation with NaN ₃	85
4.2.2.8 Synthesis of PtBA-(≡) ₂ , 5b.....	85
4.2.2.9 Synthesis of ≡(OH)-PSTY ₄₇ -Br, 6a.....	85
4.2.2.10 Synthesis of ≡(OH)-PSTY ₄₇ -N ₃ , 7a.....	86
4.2.2.11 Cyclization reaction of ≡(OH)-PSTY ₄₇ -N ₃ , 7a by CuAAC chemistry.....	86
4.2.2.12 Chain-end modification of functional cyclic polymers.....	86
4.2.2.13 Synthesis of ≡(OH)-P ^t BA ₄₄ -Br, 6b.....	88
4.2.2.14 Synthesis of ≡(OH)-P ^t BA ₄₄ -N ₃ , 7b.....	89
4.2.2.15 Cyclization reaction of ≡(OH)-P ^t BA ₄₄ -N ₃ , 7b by CuAAC chemistry.....	89
4.2.2.16 Chain-end modification of functional cyclic polymers.....	89
4.2.2.17 Synthesis of complex architectures via CuAAC chemistry.....	91
4.2.2.18 Deprotection of ^t BA from 23-28– General Procedure.....	97
4.2.2.19 Thin Film Studies.....	97
4.2.3 Analytical Methodologies.....	98
4.3 Results and discussion.....	100
4.4 Conclusion.....	111
4.5 References.....	112

Chapter 5

Polymeric Knots on Glass Transition Temperature: A Model Study

5.1 Introduction.....	115
5.1.1 Aim of the Chapter.....	117
5.2 Experimental.....	117
5.2.1 Materials.....	117
5.2.2 Analytical Methods.....	118
5.2.3 Synthetic Procedures.....	119
5.2.3.1 Synthesis of Alkyne (hydroxyl) Functional Initiator (1).....	119
5.2.3.2 Synthesis of Protected Alkyne (hydroxyl) Functional Initiator (6).....	119
5.2.3.3 Synthesis of ≡(HO)-PSTY ₂₅ -Br 7a by ATRP.....	120
5.2.3.4 Synthesis of ≡(HO)-PSTY ₂₅ -N ₃ 8a by Azidation with NaN ₃	120
5.2.3.5 Synthesis of c-PSTY ₂₅ -OH, 9a.....	121
5.2.3.6 Synthesis of c-PSTY ₂₅ -Br 10a.....	121
5.2.3.7 Synthesis of c-PSTY ₂₅ -N ₃ 11a.....	121
5.2.3.8 Synthesis of c-PSTY ₂₅ -≡ 14a.....	122

5.2.3.9 Synthesis of $\equiv(\text{HO})\text{-PSTY}_{58}\text{-Br}$ 7b by ATRP.....	122
5.2.3.10 Synthesis of $\equiv(\text{HO})\text{-PSTY}_{58}\text{-N}_3$ 8b by Azidation with NaN_3	123
5.2.3.11 Synthesis of $\text{c-PSTY}_{58}\text{-OH}$, 9b.....	123
5.2.3.12 Synthesis of $\text{c-PSTY}_{58}\text{-Br}$, 10b.....	123
5.2.3.13 Synthesis of $\text{c-PSTY}_{58}\text{-N}_3$ 11b.....	124
5.2.3.14 Synthesis of $\text{c-PSTY}_{58}\text{-}\equiv$, 14b.....	124
5.2.3.15 Synthesis of $\text{c-PSTY}_{58}\text{-}(\equiv)_2$, 15b.....	124
5.2.3.16 Synthesis of $\equiv(\text{HO})\text{-PSTY}_{84}\text{-Br}$ 7c by ATRP.....	125
5.2.3.17 Synthesis of $\equiv(\text{HO})\text{-PSTY}_{84}\text{-N}_3$ 8c by Azidation with NaN_3	125
5.2.3.18 Synthesis of $\text{c-PSTY}_{84}\text{-OH}$, 9c.....	125
5.2.3.19 Synthesis of $\text{c-PSTY}_{84}\text{-Br}$, 10c.....	126
5.2.3.20 Synthesis of $\text{c-PSTY}_{84}\text{-N}_3$ 11c.....	126
5.2.3.21 Synthesis of $\text{c-PSTY}_{84}\text{-}\equiv$, 14c.....	126
5.2.3.22 Synthesis of $\equiv(\text{HO})\text{-PSTY}_{163}\text{-Br}$ 7d by ATRP.....	127
5.2.3.23 Synthesis of $\equiv(\text{HO})\text{-PSTY}_{163}\text{-N}_3$ 8d by Azidation with NaN_3	127
5.2.3.24 Synthesis of $\text{c-PSTY}_{163}\text{-OH}$, 9d.....	128
5.2.3.25 Synthesis of Complex Topologies.....	128
5.3 Results and discussion.....	131
5.4 Conclusion.....	136
5.5 References.....	137

Chapter 6

Summary.....	139
6.1 Cyclic polystyrene topologies via RAFT and CuAAC.....	139
6.2 Multifunctional Cyclic Polymers and Their Complex Topologies.....	140
6.3 Complex Polymer Topologies and Their Glass transition Studies.....	140
6.4 Future Perspective of the Thesis.....	141
Appendix A	142
Appendix B	150
Appendix C	183
Appendix D	217

LIST OF FIGURES

Fig. 2.1 (A) SEC chromatograms for cyclization of (a) RAFT-PSTY-Alk (b) Epo-PSTY-Alk, and (c) N₃-PSTY-Alk, SEC analysis based on polystyrene calibration curve. (B) UV-vis spectra at 311 nm of (a) RAFT-PSTY-Alk, 2 and (b) the aminolyzed Epo-PSTY-Alk, elution solvent THF 35

Figure 2.2. ¹H-NMR spectra of (A) RAFT-PSTY-Alk (B) Epo-PSTY-Alk (C) N₃-PSTY-Alk and (D) c-PSTY-OH in CDCl₃ (* methanol). 36

Figure 2.3: SEC chromatograms of (a) N₃-PSTY-Alk, (b) c-PSTY-OH, crude, (c) c-PSTY-OH after purification by preparatory SEC and (d) LND simulation of with hydrodynamic volume change of 0.76. SEC analysis based on polystyrene calibration curve..... 37

Figure 2.4. MALDI-ToF mass spectrometry of cPSTY-Br, **6** with Ag salt as cationization agent and DCTB matrix in reflectron mode: (A) full molecular weight distribution, (B) expanded spectrum; calculated [M+Ag⁺] = 4335.22, DP_n = 36..... 38

Figure 2.5: SEC chromatograms for the kinetics of (A) dicyclic cleavage using CuBr/PMDETA in toluene; (a) Alk-PSTY- N₃ **4** (b) cPSTY-N₃ **7**; degradation after (c) 10 min (d) 30 min (e) 1 h (f) 3 h (g) 7 h and (h) 24 h; (B) tricyclic cleavage using CuBr/PMDETA in toluene; (a) Alk-PSTY-N₃ **4** (b) c-PSTY-N₃ **7**; degradation after (c) 10 min (d) 30 min (e) 1h (f) 2 h (g) 5 h and (h) 24 h. SEC analysis based on polystyrene calibration curve. 39

Figure 2.6: (A) The percent of di-cyclic formed *versus* time using (a) CuBr-PMDETA in toluene, (b) CuBr in DMF and (c) CuBr-triazole in toluene; (B) The percent of tricyclic formed *versus* time using (a) CuBr-PMDETA in toluene, (b) CuBr in DMF and (c) CuBr-triazole in toluene. 39

Figure 2.7: SEC chromatograms of CuAAC coupling reactions by one pot using cPSTY-N₃ **7** with (A) propargyl ether in CuBr/DMF to produce (cPSTY)₂ **8**; (a) cPSTY-N₃ **7**; (b) (cPSTY)₂-crude and (c) LND simulation of **8**. (d) (cPSTY)₂ **8** after preparatory SEC purification. (B) tripropargylamine in CuBr/triazole to produce (cPSTY)₃ **9**; (a) cPSTY-N₃ **7**; (b) (cPSTY)₃-crude and (c) LND simulation of **9** with hydrodynamic volume change of 0.91. (d) (c-PSTY)₃ **9** after preparatory SEC purification. All chromatograms are based on PSTY calibration. 40

Figure 2.8. 500 MHz ^1H 1D DOSY NMR spectra of (A) c-PSTY- N_3 **7** (B) (c-PSTY) $_2$ **8** and (C) (c-PSTY) $_3$ **9**.....41

Figure 3.1. Protected and unprotected alkyne ATRP initiators.....51

Figure 3.2. Molecular weight distributions (MWDs) for starting polymer and products obtained from SEC with RI detection. Synthesis of (A) TIPS- $\equiv(\text{OH-PSTY}_{25})_2\text{-Br}$ **16** (curve c - crude product) from **7** (curve a) and **15** (curve b); and (B) TIPS- $\equiv(\text{OH-PSTY}_{25})_3\text{-Br}$ **24** (curve c - crude product) from **7** (curve a) and **17** (curve b). Curve d represents the LND fit to the product MWD..... 65

Figure 3.3. 500 MHz ^1H 1D DOSY NMR spectra in CDCl_3 of (A) TIPS- $\equiv(\text{OH-PSTY}_{25})_2\text{-N}_3$ **17**, (B) $\equiv(\text{OH-PSTY}_{25})_2\text{-N}_3$ **18**, (C) TIPS- $\equiv(\text{OH-PSTY}_{25})_3\text{-N}_3$ **25**, and (D) $\equiv(\text{OH-PSTY}_{25})_3\text{-N}_3$, **26**....68

Figure 3.4: Molecular weight distributions (MWDs) for starting linear and cyclic polymers. (A) (a) **8**, (b) crude **9**, (c) **9** purified by prep SEC; (B) (a) **18**, (b) crude **19**, (c) **19** purified by prep SEC; and (C) **26**, (b) crude **27**, (c) **27** purified by prep SEC. Curve d represents the LND fit to the product MWD using a hydrodynamic volume change between 0.75 and 0.76. 70

Figure 3.5. 500 MHz ^1H 1D DOSY NMR spectra in CDCl_3 of (A) $\equiv(\text{OH})\text{-PSTY}_{25}\text{-N}_3$ **8**, (B) c-PSTY $_{25}\text{-OH}$ **9**, (C) $\equiv(\text{OH-PSTY}_{25})_2\text{-N}_3$ **18**, (D) c-PSTY $_{50}\text{-(OH)}_2$ **19**, (E) $\equiv(\text{OH-PSTY}_{25})_3\text{-N}_3$ **26**, and (F) cPSTY $_{75}\text{-(OH)}_3$ **27**. (*small molecules impurities)..... 71

Figure 3.6. MALDI-TOF mass spectrum using Ag salt as cationizing agent and DCTB matrix. (A) c-PSTY $_{25}\text{-OH}$, **9** acquired in reflectron mode, (B) c-PSTY $_{50}\text{-(OH)}_2$, **19** and (C) cPSTY $_{75}\text{-(OH)}_3$, **27** acquired in linear mode. (i) Full spectra, and (ii) expanded spectra.....72

Figure 3.7. Molecular weight distribution (MWDs) for starting polymers and products. (A) SEC RI distribution of (a) c-PSTY $_{25}\text{-}\equiv$ **13** and (b) c-PSTY $_{50}\text{-(N}_3)_2$ **21** to produce (c) spiro (c-PSTY) $_3$ **31**, (d) purified by preparative SEC. (B) SEC RI distribution of (a) c-PSTY $_{25}\text{-N}_3$ **11** and (b) c-PSTY $_{50}\text{-(}\equiv)_4$ **23** to produce (c) G1 (c-PSTY) $_5$ **32**, (d) purified by preparative SEC. (C) SEC RI distribution of (a) c-PSTY $_{25}\text{-}\equiv$ **13** and (b) c-PSTY $_{75}\text{-(N}_3)_3$ **29** to produce (c) G1- (c-PSTY) $_4$ **33**, (d) purified by preparative SEC. (D) SEC RI distribution of (a) c-PSTY $_{25}\text{-N}_3$ **11** and (b) c-PSTY $_{75}\text{-(}\equiv)_6$ **30** to produce (c) G1 (c-PSTY) $_7$ **34**, (d) purified by preparative SEC. SEC analysis based on polystyrene calibration curve..... 74

Figure 4.1. SEC chromatograms for cyclization of (A) (a) $\equiv(\text{OH})\text{-PSTY}_{47}\text{-N}_3$ **7a** (b) c-PSTY $_{47}\text{-OH}$ crude, **8a** (c) c-PSTY $_{47}\text{-OH}$ purified by prep and (d) LND simulation of **8a** crude with hydrodynamic volume change of 0.75; (B) (a) $\equiv(\text{OH})\text{-P}^t\text{BA}_{44}\text{-N}_3$ **7b** (b) c-P t BA $_{44}\text{-OH}$ crude, **8b** (c)

c-P^tBA₄₄-OH purified by prep and (d) LND simulation of 8b crude with hydrodynamic volume change of 0.78 SEC analysis based on polystyrene calibration curve.....101

Figure 4.2: SEC of molecular weight distributions (MWDs) for the synthesis of (A) (PSTY₄₄)₂ 15 by CuAAC of (a) PSTY₄₄-≡, 4a, and (b) PSTY₄₄-N₃, 3a; (c) (PSTY₄₄)₂ 15, crude, (d) (PSTY₄₄)₂ prepped and (e) LND simulation of crude, (B) c-PSTY₄₇-b-PSTY₄₄, 16 by CuAAC of (a) PSTY₄₄-≡, 4a and (b) c-PSTY₄₇-N₃, 10a; (c) c-PSTY₄₇-b-PSTY₄₄, 16, crude, (d) c-PSTY₄₇-b-PSTY₄₄, prep and (e) LND simulation of crude and (C) (c-PSTY₄₇)₂, 17 by CuAAC of (a) c-PSTY₄₇-≡, 11a and (b) c-PSTY₄₇-N₃, 10a; (c) (c-PSTY₄₇)₂, 17 crude, (d) (c-PSTY₄₇)₂, prep and (e) LND simulation of crude. SEC analysis based on polystyrene calibration curve. Simulation was achieved by adding M_ps of reactants (RI SEC) to fit with the crude products (RI SEC).....103

Figure 4.3: SEC of molecular weight distributions (MWDs) for the synthesis of (A) (PSTY₄₄)₃ 18 by CuAAC of (a) PSTY₄₄-(≡)₂, 5a, and (b) PSTY₄₄-N₃, 3a; (c) (PSTY₄₄)₃ 18, crude, (d) (PSTY₄₄)₃ prepped and (e) LND simulation of crude, (B) c-PSTY₄₇-b-(PSTY₄₄)₂, 19 by CuAAC of (a) PSTY₄₄-(≡)₂, 4a and (b) c-PSTY₄₇-N₃, 10a; (c) c-PSTY₄₇-b-PSTY₄₄, 16, crude, (d) c-PSTY₄₇-b-PSTY₄₄, prep and (e) LND simulation of crude and (C) (c-PSTY₄₇)₂, 17 by CuAAC of (a) c-PSTY₄₇-≡, 11a and (b) c-PSTY₄₇-N₃, 10a; (c) (c-PSTY₄₇)₂, 17 crude, (d) (c-PSTY₄₇)₂, prep and (e) LND simulation of crude. SEC analysis based on polystyrene calibration curve. Simulation was achieved by adding M_ps of reactants (RI SEC) to fit with the crude products (RI SEC). 104

Figure 4.4: SEC of molecular weight distributions (MWDs) for the synthesis of (A) PSTY₄₄-b-P^tBA₄₄ 23 by CuAAC of (a) PSTY₄₄-≡, 4a, and (b) P^tBA₄₄-N₃, 3b; (c) PSTY₄₄-b-P^tBA₄₄ 23, crude, (d) PSTY₄₄-b-P^tBA₄₄ prepped and (e) LND simulation of crude, (B) c-PSTY₄₇-b-c-P^tBA₄₄, 24 by CuAAC of (a) c-PSTY₄₇-≡, 11a and (b) c-P^tBA₄₄-N₃, 10b; (c) c-PSTY₄₇-b-c-P^tBA₄₄, 24, crude, (d) c-PSTY₄₇-b-c-P^tBA₄₄, prep and (e) LND simulation of crude, (C) PSTY₄₄-b-(P^tBA₄₄)₂, 25 by CuAAC of (a) PSTY₄₄-(≡)₂, 5a and (b) P^tBA₄₄-N₃, 3b; (c) PSTY₄₄-b-(P^tBA₄₄)₂, 25 crude, (d) PSTY₄₄-b-(P^tBA₄₄)₂, prep and (e) LND simulation of crude, (D) c-PSTY₄₇-b-(c-P^tBA₄₄)₂, 26 by CuAAC of (a) c-PSTY₄₇-≡, 12a and (b) c-P^tBA₄₄-N₃, 10b; (c) c-PSTY₄₇-b-(c-P^tBA₄₄)₂, 26 crude, (d) c-PSTY₄₇-b-(P^tBA₄₄)₂, prep and (e) LND simulation of crude. (E) (PSTY₄₄)₂-b-P^tBA₄₄, 27 by CuAAC of (a) PSTY₄₄-N₃, 3a and (b) P^tBA₄₄-(≡)₂, 5b; (c) (PSTY₄₄)₂-b-P^tBA₄₄, 27 crude, (d) (PSTY₄₄)₂-b-P^tBA₄₄, prep and (e) LND simulation of crude. (F) (c-PSTY₄₇)₂-b-c-P^tBA₄₄, 28 by CuAAC of (a) c-PSTY₄₇-N₃, 10a and (b) c-P^tBA₄₄-(≡)₂, 12b; (c) (c-PSTY₄₇)₂-b-c-P^tBA₄₄, 28 crude, (d) (c-PSTY₄₇)₂-b-c-P^tBA₄₄, prep and (e) LND simulation of crude. SEC analysis based on

polystyrene calibration curve. Simulation was achieved by adding M_{ps} of reactants (RI SEC) to fit with the crude products (RI SEC)..... 106

Figure 4.5. The change of glass transition temperature with the increase of no of cyclic unit, Series 1 polymers: 15, 16, 17 and series 2 polymers: 18, 19, 20 and 22)..... 108

Figure 4.6. Schematic representation of AB di-block copolymers, showing areas (the dotted circles) of aggregation of the higher T_g blocks (red), joined by the lower T_g block (black).. 110

Figure 4.7. Atomic force microscopy height images for (a) PSTY₄₄-b-PAA₄₄, **23** and (b) c-PSTY₄₇-b-c-PAA₄₄, **24**..... 111

Figure 5.1. SEC chromatograms for cyclization of (A) (a) $\equiv(\text{OH})\text{-PSTY}_{25}\text{-N}_3$ 8a (b) c-PSTY₂₅-OH crude, 9a (c) c-PSTY₂₅-OH purified by prep and (d) LND simulation of 9a crude with hydrodynamic volume change of 0.75; (B) (a) $\equiv(\text{OH})\text{-PSTY}_{58}\text{-N}_3$ 8b (b) c-PSTY₅₈-OH crude, 9b (c) c-PSTY₅₈-OH purified by prep and (d) LND simulation of 9b crude with hydrodynamic volume change of 0.75; (C) (a) $\equiv(\text{OH})\text{-PSTY}_{84}\text{-N}_3$ 8c (b) c-PSTY₈₄-OH crude, 9c (c) c-PSTY₈₄-OH purified by prep and (d) LND simulation of 9c crude with hydrodynamic volume change of 0.76; (D) (a) $\equiv(\text{OH})\text{-PSTY}_{163}\text{-N}_3$ 8d (b) c-PSTY₁₆₃-OH crude, 9d (c) c-PSTY₁₆₃-OH purified by prep and (d) LND simulation of 9d crude with hydrodynamic volume change of 0.765; SEC analysis based on polystyrene calibration curve..... 132

Figure 5.2: SEC of molecular weight distributions (MWDs) for the synthesis of (A) (c-PSTY)₂ **31** by CuAAC of (a) c-PSTY₈₄- \equiv , **14c**, and (b) c-PSTY₈₄-N₃, **11c**; (c) (c-PSTY)₂ **31**, crude, (d) (c-PSTY)₂ prepped and (e) LND simulation of crude, (B) (c-PSTY)₃, **32** by CuAAC of (a) c-PSTY₅₈- \equiv , **15b** and (b) c-PSTY₅₈-N₃, **11b**; (c) star (c-PSTY)₃, **32**, crude, (d) (c-PSTY)₃, prep and (e) LND simulation of crude, (C) spiro (c-PSTY)₃, **33** by CuAAC of (a) c-PSTY₅₈- \equiv , **14b** and (b) c-PSTY₅₀-(N₃)₂, **23**; (c) spiro (c-PSTY)₃, **33** crude, (d) spiro (c-PSTY)₃, prep and (e) LND simulation of crude, (D) den (c-PSTY)₅, **34** by CuAAC of (a) c-PSTY₅₀- \equiv , **24** and (b) c-PSTY₂₅-N₃, **11a**; (c) den (c-PSTY)₅, **34** crude, (d) den (c-PSTY)₅, prep and (e) LND simulation of crude and (D) G1 star (c-PSTY)₄, **35** by CuAAC of (a) c-PSTY₇₅-(N₃)₃, **30** and (b) c-PSTY₂₅- \equiv , **14a**; (c) G1 star (c-PSTY)₄, **35** crude, (d) G1-star (c-PSTY)₄, prep and (e) LND simulation of crude. SEC analysis based on polystyrene calibration curve. Simulation was achieved by adding M_{ps} of reactants (RI SEC) to fit with the crude products (RI SEC)..... 134

LIST OF SCHEMES

Scheme 1.1 Mechanism for RAFT polymerisation.....	2
Scheme 1.2 Mechanism for ATRP polymerisation. Mt^m = transition metal species in oxidation state m, L = ligand.....	3
Scheme 1.3 Mechanism of SET-LRP.....	4
Scheme 1.4 Generalized scheme for copper catalysed alkyne-azide click (CuAAC) reaction.....	6
Scheme 1.5 Encounter pair model for a chemical reaction.....	10
Scheme 1.6 Schematic representation of the ring-expansion technique for the synthesis of cyclic polymers.....	10
Scheme 1.7 Synthetic route for the preparation of cyclic polystyrene from linear precursors made by living anionic polymerization.....	11
Scheme 1.8 Synthesis of cyclic polymers via a combination of ATRP and ATRC and subsequent ring expansion by NMP.....	12
Scheme 1.9 Synthesis of cyclic PNIPAM via a combination of RAFT and CuAAC.....	13
Scheme 1.10 Synthesis of cyclic polystyrene via a combination of ATRP and CuAAC.....	14
Scheme 2.1 Synthetic route for the preparation of cyclic polystyrene by combining RAFT and CuAAC reactions to form dicyclic (8) and tricyclic PSTY (9). Reaction conditions: (i) AIBN, bulk polymerization at 65 °C for 15.5 h, (ii) glycidyl methacrylate, hexylamine, TEA and TCEP in DMF at 25 °C (iii) NaN_3-NH_4Cl in DMF at 50 °C (iv) CuBr, PMDETA in toluene at 25 °C, feed rate = 0.1 mL min ⁻¹ over 4.17 h and then kept for 3 h (v) 2-bromopropionyl bromide, TEA in THF at 0 °C-RT for 48 h (vi) NaN_3 in DMF at 25 °C for 16 h (vii) CuBr in DMF, at 25 °C for 1.0 h and (viii) CuBr-triazole in toluene at 25 °C for 12.0 h.....	27
Scheme 3.1. Synthetic methodology to build complex topologies from multifunctional cyclic polymers.....	48
Scheme 4.1. Graphical representation of different architectures homo and amphiphilic block copolymers where black and red lines represent the PSTY and PAA segments respectively.....	81
Scheme 5.1. General Synthetic Strategy for the Construction of Spiro Tricyclic, G1 Star Tetracyclic, G1 Dendrimer Pentacyclic and G1 Star Heptacyclic Topologies.....	116
Scheme 5.2. Synthetic scheme for protected alkyne (hydroxyl) functional initiator.....	120

LIST OF TABLES

Table 2.1 RI and triple detection molecular weight distributions data for PSTY starting, chain end modified and click coupled polymers	35
Table 2.2 Click efficiency and molecular weight data for synthesis of dicyclic and tricyclic PSTY.....	42
Table 3.1: Purity, coupling efficiency, molecular weight data (RI and triple detection) and change in hydrodynamic volume for all starting building blocks and products.	66
Table 3.2. LND simulation data for the synthesis of TIPS-≡(OH-PSTY ₂₅) ₂ -Br (16) and TIPS-≡(OH-PSTY ₂₅) ₃ -Br (24) polymers by LND based on weight distribution (w(M)).....	67
Table 4.1. Click efficiency and molecular weight data for the synthesis of complex topologies (15-28).. ..	107
Table 4.2. DSC results of linear, cyclic and their complex topologies and amphiphilic block and mikto-arm star copolymers.	109
Table 5.1: Molecular weight data and Tg results for the products (8d , 9d and 31-35).....	136

LIST OF ABBREVIATIONS

AFM-Atomic Force Microscopy

AIBN- Azobisisobutyronitrile

ATNRC- Atom Transfer Nitroxide Radical Coupling

ATRC – Atom Transfer Radical Coupling

ATR-FTIR – Attenuated Total Reflectance Fourier Transform Infra-Red

ATRP – Atom Transfer Radical Polymerization

ATRA- atom transfer radical addition

BiB – 2-Bromoisobutyryl Bromide

BPB – 2-Bromopropionyl Bromide

CHCl₃ – Chloroform

CSIRO- Commonwealth Scientific and Industrial Research Organization

CTA-Chain Transfer Agent

CuAAC – Copper-Catalyzed Azide-Alkyne Cycloaddition

CuBr – Copper(I) Bromide

CuBr₂ – Copper(II) Bromide

CuSO₄-Copper Sulfate

c-PMA – Cyclic Polymethyl Acrylate

c-PSTY – Cyclic Polystyrene

c-P^tBA – Cyclic Poly(*Tert* Butyl Acrylate)

DCC – *N,N*-dicyclohexylcarbodiimide

DCM – Dichloromethane

DCTB- Trans-2-[3-(4-*tert*-butylphenyl)-2- methyl-propenylidene]malononitrile

DMAP- Dimethyl(amino)pyridine

DMAc- *N,N*-dimethylacetamide

DMF – *N,N*-Dimethylformamide

DMSO – Dimethylsulfoxide

DSC-Differential Scanning Colorimetry

DOSY-Diffusion Ordered Spectroscopy

DP-Degree of polymerization

EBiB – Ethyl-2-bromo Isobutyrate

EtOAc – Ethyl Acetate

EtOH- Ethanol

ESA-CF- Electrostatic self-assembly and covalent fixation

GC-MS- Gas chromatography/mass spectrometry
GPC-Gel permeation chromatography
HDV- Hydrodynamic change
KBr- Potassium Bromide
K₂CO₃- Potassium carbonate
K₃PO₄- Potassium phosphate tri-basic
LND – Log Normal Distribution
LRP – Living Radical Polymerization
MALDI-ToF – Matrix-Assisted Laser Desorption Ionization – Time-of-Flight
Me₆tren – Tris[2-dimethylamino]ethyl]amine
MBP – Methyl-2-Bromopropionate
MeOH – Methanol
MWD – Molecular Weight Distribution
NaN₃ – Sodium Azide
NH₄Cl-Ammonium Chloride
NMP – Nitroxide-Mediated Polymerization
NMR – Nuclear Magnetic Resonance
NRC – Nitroxide Radical Coupling
PAA – Poly(acrylic acid)
PDI – Polydispersity Index
PDMS- poly(dimethyl siloxane)
PMA – Poly(methyl acrylate)
PMDETA – N,N,N',N'',N'''-Pentamethyldiethylenetriamine
PNIPAM-Poly(*N*-isopropylacrylamide)
PREP-SEC – Preparative Size Exclusion Chromatography
PSTY – Polystyrene
RAFT – Reversible Addition-Fragmentation Chain Transfer
RI – Refractive Index
RT – Room Temperature
SEC – Size Exclusion Chromatography
SET – Single-Electron Transfer
STY – Styrene
^tBA – *tert*-Butyl Acrylate
TCEP- Tris(2-carboxyethyl)phosphine Hydrochloride

TEA – Triethylamine

TEMPO-(2,2,6,6-Tetramethylpiperidin-1-yl)oxy

THF – Tetrahydrofuran

TIPS-Cl-1,1,1-triisopropylsilyl chloride

UV-Vis – Ultraviolet-Visible

Chapter 1 - Introduction

The opportunity to build complex polymer architectures from linear polymer building blocks has driven the potential to design new materials with unprecedented macroscopic properties. Polymers with controlled topology and chemical functionality are an essential component in the design of materials in biomedical applications, including drug and vaccine delivery, tissue engineering and medical imaging.¹⁻⁴ New polymerization methods coupled with highly efficient coupling reactions are providing Polymer Scientists the tools to create polymers with precise molecular engineering that in the near future could mimic the function of proteins.

There are many types of polymeric architectures that can now be made by coupling linear polymers to produce, for example, rings, grafts, branched, star-shaped, cross-linked network, and dendrimers. Cyclic (or ring) polymers are the most intriguing due to the absence of chain ends,⁵⁻¹¹ in which the conventional reptation theory for linear systems is no longer applicable.

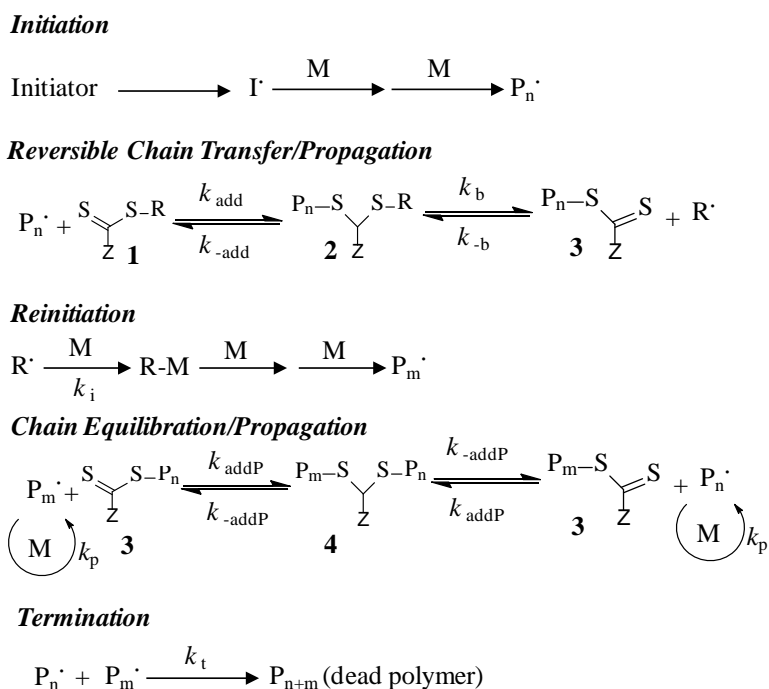
The most recent methods to create well-defined complex architectures with a range of macromolecular characteristic features include combining 'living' radical polymerization (LRP) with 'click' quantitative reactions. 'Living' radical polymerization produces macromolecules with predetermined molecular weights, narrow molecular weight distributions, and high chain-end functionality (essential for the fabrication of complex polymer architectures). The most used LRP techniques are reversible addition-fragmentation chain transfer (RAFT)¹²⁻¹⁶ polymerization, atom transfer radical polymerization (ATRP)¹⁷⁻²², nitroxide-mediated polymerization (NMP)²³⁻²⁵ and single electron transfer living radical polymerization (SET-LRP).^{26,27}

1.1 Reversible Addition-Fragmentation Chain-Transfer Polymerisation (RAFT)

Reversible Addition-Fragmentation chain Transfer (RAFT) polymerisation was developed simultaneously by the Commonwealth Scientific and Industrial Research Organization (CSIRO) in 1998¹² and French company (Rhodia)²⁸ in 1997. RAFT polymerisation is the most versatile 'living radical polymerisation' technique due to the large range of monomers that can be polymerised while still maintaining control

over molecular weight, polydispersity and end-group control.²⁹ The RAFT polymerisation technique has been widely accepted due to its broad synthetic scope such as polymerization in bulk, in both aqueous and organic solvents over a wide range of temperature.³⁰⁻³²

A typical RAFT polymerisation mixture contains monomer, radical initiator and a RAFT chain transfer agent. Initiation, propagation and termination events occur similarly to conventional free-radical polymerisation. After propagating, macro-radical add to the carbon sulfur-double bond of the RAFT agent (with a rate constant of addition k_{add} , see Scheme 1.1), the radical adduct that is formed undergoes β -scission and either yields back the reactants ($k_{-\text{add}}$) or releases another initiating (macro) radical (with a rate constant of fragmentation, k_{β}). In this way, equilibrium between dormant and active species is established. The structural diversity of RAFT agents is considerably larger, which ultimately allows for greater control over a wider range of monomers.³³ Both the R and Z groups of a RAFT agent should be carefully selected to provide appropriate control.³⁴ In order to efficiently fragment and initiate polymerization, $R\cdot$ should be more stable than $P_n\cdot$. The stability of dormant species and rate of addition of $R\cdot$ to a given monomer depends on the proper selection of the R group and this is important for a successful RAFT polymerization.



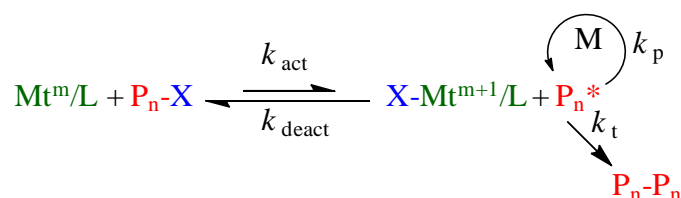
Scheme 1.1 Mechanism for RAFT polymerisation.³⁵

Although RAFT is a versatile tool in polymer synthesis, it also has some disadvantages. The synthesis of RAFT agent typically requires a multistep procedure and laborious purification; additionally RAFT agents decompose gradually, yielding sulphur compounds that are undesirable for many applications.

1.2 Atom Transfer Radical Polymerisation (ATRP)

Atom transfer radical polymerization (ATRP) was developed in 1995 independently by Matyjaszewski and Wang^{36,37} and Kato *et al*³⁸ as an expansion of transition metal catalysed atom transfer radical addition (ATRA). This technique has become the most widely applied LRP technique. ATRP produces well-defined polymers with low polydispersity and allows post-polymerisation synthetic diversity due to the resulting halogen end-group.

The polymerization mechanism is based on the reversible abstraction of the halogen atom from the polymer chain-end by a transition metal complex. The mechanism is illustrated in the Scheme 1.2. Homolytic cleavage of the halide occurs to form a carbon-centred radical on the polymer chain-end ($P\cdot$).³⁷ For a successful ATRP reaction, a low concentration of propagating radical intermediates ($P_n\cdot$) must be maintained and their fast but reversible transformation into the dormant species (P_n-X , where X is a halide group) via deactivation. In order to create a low concentration of propagating radicals, the deactivation rate must be significantly higher than the activation rate, and the concentration dormant species must be significantly greater than the dormant species. If the deactivation rate slows or becomes non-existent, bimolecular radical termination will dominant, resulting in poor control of molecular weight and high polydispersity.³⁹



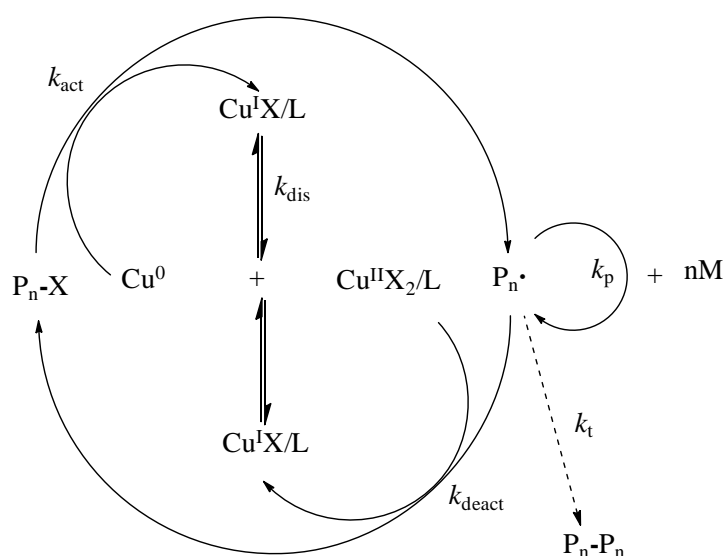
Scheme 1.2 Mechanism for ATRP polymerisation. Mt^m = transition metal species in oxidation state m, L = ligand.¹⁷

ATRP is strongly influenced by the values of the rate constants, k_{act} ,⁴⁰ and k_{deact} ,⁴¹ and their ratio, K_{ATRP} .^{40,42} Rates of ATRP increase with catalysts activity (K_{ATRP}) but

under some conditions may decrease due to radical termination and a resulting low $[M^{m+1}]/[X-M^{m+1}/L]$ ratio, and build-up in the concentration of deactivator via the persistent radical effect.⁴³ The low concentration of radicals, along with a build-up of M^{m+1} deactivator suppresses the radical termination side reactions, maintaining control over the molecular weight distribution. These key rate parameters produce polymers with halide end groups in high quantitative yields. ATRP is thus the most convenient way to introduce an chemical functional groups on the polymer chain-end, which can be used as macro-initiator for further polymerization or post functional modification.

1.3 Single-Electron Transfer (SET) LRP

Compared to other metal catalysed LRP techniques, SET-LRP mediates an ultrafast polymerization of acrylates, methacrylates and vinyl chloride under mild reaction conditions (e.g. at room temperature or below).^{26,27} Favourable solvent and ligand selection is required to mediate the disproportionation of Cu(I) to Cu(0) activator and Cu(II) deactivator. SET LRP allows the preparation of unprecedented high molecular weight polymer rapidly with excellent control over the molecular weight distribution and near perfect retention of halide chain-end functionality.^{44,45} The heterogenous Cu(0) activator and homogenous Cu(II) deactivator are formed simultaneously by disproportionation of Cu(I)/L produced *in-situ* during the generation of radicals from alkyl halides (Scheme 1.3).²⁶



Scheme 1.3 Mechanism of SET-LRP²⁶

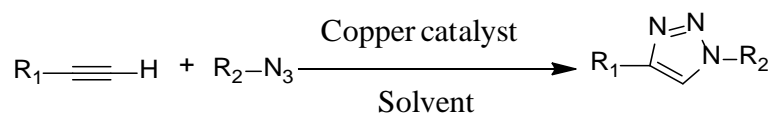
The main mechanistic difference between SET and ATRP is the formation of deactivator Cu(II)/L. The deactivator Cu(II) forms in SET through the disproportionation of Cu(I) via a self-regulated mechanism, whereas in ATRP, deactivator forms from the abstraction of halide from the polymer chain-end. The build-up of Cu(II)/L deactivator proceeds without the usual need for bimolecular termination in SET. On the other hand, the formation of Cu(II)/L undergoes bimolecular termination to generate persistent radical effect in ATRP.⁴⁶ This mechanistic feature enables the synthesis of polymers with essentially near perfect retention of chain-end functionality, and no detectable structural defects even at very high monomer conversions. The ultrafast activation of alkyl halides occurs due to the extreme reactivity of nascent Cu(0), generated by disproportionation of Cu(I) in appropriate solvent and ligand conditions. This facilitates faster polymerization compared to other techniques.

The main advantages in SET are the use of copper wire as the catalyst, which allows for a simpler experimental setup and ease of purification of copper catalyst from the reaction mixtures. Although there are number of advantages in the synthetic utility and final polymer products from SET-LRP, the mechanistic features are complex and are still being investigated.

1.4 Cu-Catalysed Azide/Alkyne Click (CuACC) Reaction

Building new macromolecular architectures by connecting readily accessible building blocks in the presence of other functional groups under a wide range of conditions is a challenge in synthetic polymer chemistry. In recent years, a number of reactions have been developed, exemplified as ‘click’ chemistry, which enables the efficient formation of a specific covalent linkage by addition reaction, even within a highly complex chemical environment.⁴⁷⁻⁵³ Among these reactions, the Huisgen 1,3-dipolar cycloaddition reaction of organic azides and alkynes^{54,55} has gained considerable attention due to the near quantitative yields, highly regio-selectivity, robustness, insensitivity, and most importantly, the lack of by-product formation. The triazole ring formed in the reaction is essentially chemically inert to reactive conditions, e.g. oxidation, reduction, and hydrolysis.⁵⁶ The ‘click’ reaction most often utilised with polymers typically proceeds through a Cu(I) catalysed 1,3-dipolar cycloaddition

between an azide and an alkyne (Scheme 1.4). The Cu(I) catalyst used in ‘click’ reaction lowers the activation barrier by 11 kcal/mol, which is sufficient to rapidly drive the reaction forward with high selectivity.^{57,58} The reaction is quite insensitive to reaction conditions as long as Cu(I) is present and can be performed in an aqueous⁵⁹⁻⁶² or organic⁶³ environment.



Scheme 1.4. Generalised scheme for copper catalysed alkyne-azide click (CuAAC) reaction.

In the field of polymer chemistry, combination of LRP and ‘click’ reactions provide powerful tools in tailoring macromolecular architectures through the coupling of different functional polymer chains.⁶⁴ The highly efficient CuAAC reaction has become a powerful tool in macromolecular engineering because azide and alkyne moieties can easily be introduced at different locations in the polymer chains.⁶⁵⁻⁶⁹

Despite the excellent reaction kinetics, high specificity, and bio-orthogonality, CuAAC reaction has some limitations. The reaction has been used to a far lesser extent in the cellular context because of toxicity caused by the metal catalyst. Recently, strain-promoted copper free cyclooctane-azide addition reaction was introduced for more sensitive biologic systems.⁷⁰⁻⁷³ Due to the presence of inherent halide functional polymer chain ends after ATRP or SET-LRP polymerizations, the conversion of halide to azide in the presence of NaN₃ in DMF is usually quantitative under mild condition. Therefore, the combination of ATRP or SET-LRP and CuAAC is the most used and successful method for synthesis of complex polymer architectures.

1.5 Cyclic Polymers

One of the most interesting fields of polymer chemistry is tailoring architecture from conventional linear structures to nonlinear and complex topologies to understand their properties. Remarkable progress has been achieved in the synthesis of different complex topologies, intriguing researchers as they exhibit different physical and mechanical properties in dilute solution or bulk conditions. Among the various types of topologies, cyclic polymers show very different distinct properties compared to

their linear counterparts. In bulk conditions, linear polymers diffuse through a polymer matrix via reptation (i.e., they move in a snake-like manner) due to their chain-ends; as chain-ends explore a much greater volume than the interior of the chain.^{74,75} On the other hand, cyclic polymers that have no chain ends and cannot reptate like their linear analogues, rather they move with an amoeba-like motion.¹¹ The different conformation and internal chain dynamics of cyclic polymers to their linear analogues result in different properties, such as a higher density,⁷⁶ lower intrinsic viscosity,⁷⁷ higher glass transition temperatures,⁷⁷ lower translational friction coefficients,⁷⁸ higher critical solution temperature,⁷⁹ increased rate of crystallization,⁸⁰ and higher refractive index.⁸¹ In dilute solution, cyclic polymers show a more compact nature than their linear analogues. Theory⁸² predicts that the ratio of the radius of gyration for a cyclic to linear polymer of the same MW (i.e., $\langle R_g^2 \rangle_c / \langle R_g^2 \rangle_L$) equals to 0.5 in a theta solvent and 0.526 in a good solvent, and have found to agree with experimental values.⁸³ The more compact nature of cyclic polymers compared to their linear analogues was also found from their smaller hydrodynamic diameters. This characteristic feature is typically used to identify the presence of cyclic polymers by size exclusion chromatography (SEC).⁸⁴ Significant progress has been made in producing a wide variety of single cyclic polymers using different methods in order to assess how these changes affect their properties. However, the first and foremost difficulty was to synthesise absolutely pure cyclic polymer as even trace amount of linear contaminants in the cyclic polymer influences the properties significantly.⁸⁵ This impurity may be present when carrying out cyclization reactions in a good solvent under dilute conditions. In addition, one cannot ignore the dependence of polymer concentration during cyclization, especially when it exceeds the critical overlap concentration (c^* or c^{**}). This could lead to catenane or Olympic ring-type structures. Therefore, the synthetic strategy plays a vital role in determining the purity and types of cyclic topologies. For the application of cyclic polymers, one must have the capability to make cyclic structure in large scale and high purity.

1.6 Synthetic Strategies towards the Macro-cyclization

Macrocyclic polymers were suggested to be theoretically possible in 1950,⁸⁶ and the first observation for the synthesis of macrocyclic has been tested for poly(dimethyl

siloxane) (PDMS) in 1965.⁸⁷ A series of publications^{78,88,89} on the preparation and characterisation of cyclic PDMS was followed by the reporting of cyclic polystyrene by Gieser and Hocker in 1980.^{90,91} However, the above methods encounter difficulties in purifying pure cyclic product from crude sample due to the polydispersity of product and inability to isolate corresponding linear precursors and high molecular weight by-products. To date several procedures have been developed for the synthesis of cyclic polymers based on end-to-end coupling, i.e., ring closure techniques⁹²⁻⁹⁹ as well as on an alternative ring-expansion polymerization.¹⁰⁰⁻¹⁰⁷ The ring closure techniques involve the coupling of a linear polymer's two chain ends to yield a cyclic polymer. The key step of this method is to select highly efficient coupling reactions to afford the well-defined monocyclic polymer under ultra-dilute conditions to prevent intermolecular coupling reaction. On the other hand, the ring-expansion technique involves the insertion of cyclic monomer units into an activated cyclic chain through a cycle-chain equilibrium process.

1.6.1 Ring Closure Techniques

Ring-closure technique was the first successful approach for the preparation of relatively pure cyclic polymers. Cyclization via ring closure technique depends on the end-to-end distance between the two chain ends in random coil conformation of polymer.⁷⁷ To occur a chemical reaction, the chain ends have to diffuse within a capture volume with a rate constant K_{c1} , a covalent bond can form through a chemical reaction at k_2 , or the chain ends can diffuse apart at k_{-1} (Scheme 1.5). This kinetic scheme is equivalent to that of an “encounter-pair” model. Two important cases for the model are diffusion controlled and activation controlled reaction. If $k_2 \gg k_{-1}$, i.e., the activation energy of the reaction is very small or if the diffusion of chain ends apart is difficult, the kinetics will be dominated by k_{c1} which is termed as diffusion controlled reaction. In the reverse case ($k_2 \ll k_{-1}$), the activation energy of the reaction dominates the kinetics, and the reaction is controlled by its equilibrium kinetics. This concept allows us to use the well-known Jacobson–Stockmayer⁸⁶ equation to determine the probability of cyclization at a given polymer molecular weight. As the rate of chemical reaction, k_2 , to form a monocyclic species via an intra-molecular process is equal to that for the formation of multi-block by intermolecular process, the percentage of monocyclic species only depends on the probability of a chain end

being within the capture volume, v_s with its other chain end (P_C) over that of another chain end (P_L). According to Jacobson and Stockmayer theory for Case II type condensation, the relative probabilities are as follows:

$$P_c = \left(\frac{3}{2\pi} \right)^{3/2} \frac{v_s}{\langle r^2 \rangle^{3/2}} \dots\dots\dots (1)$$

$$P_L = 2N \frac{v_s}{V} = \frac{2N_A c}{M} v_s \dots\dots\dots (2)$$

Where v_s is the capture volume, P_c is the probability when the two ends of the same chain are within the capture volume, P_L is the probability when chain ends from other chains are within the capture volume, $\langle r^2 \rangle$ is the mean-square end-to-end distance of the chain, N is the total number of polymer molecules in total volume V , N_A is Avogadro's number, M is the molecular weight of the polymer, and c is the concentration of polymer in g mL^{-1} . The ratio between monocyclic and other condensed species is given by¹⁰⁸

$$\frac{P_c}{P_L} = \left(\frac{3}{2\pi \langle r^2 \rangle} \right)^{3/2} \frac{2000}{N_A [P]} = \frac{k_c}{k_l [P]} \dots\dots\dots (3)$$

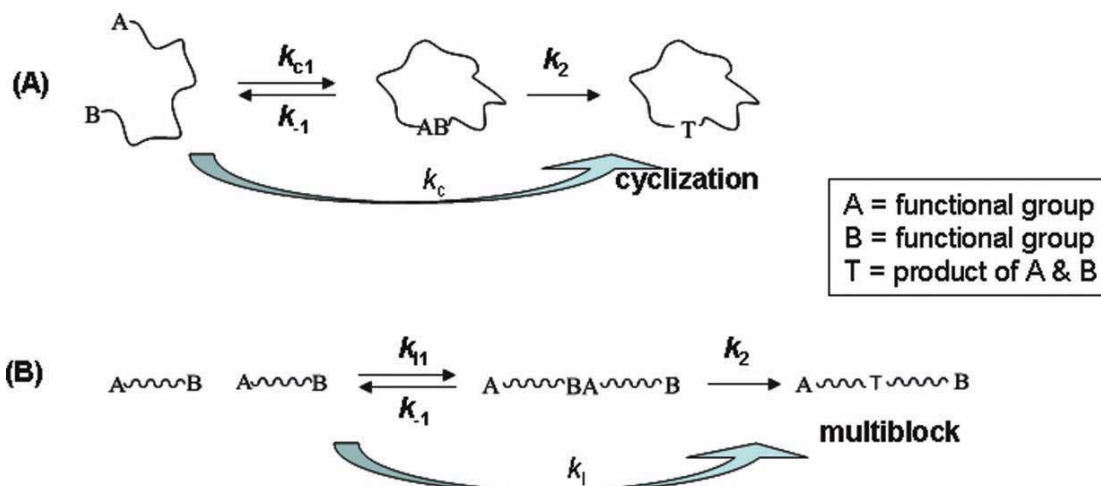
So that

$$\frac{k_c}{k_l} = \left(\frac{3}{2\pi \langle r^2 \rangle} \right)^{3/2} \frac{2000}{N_A} \dots\dots\dots (4)$$

and therefore the theoretical % monocyclic is derived by

$$\% \text{ cyclic} = \frac{P_c}{P_c + P_L} \times 100 \dots\dots\dots (5)$$

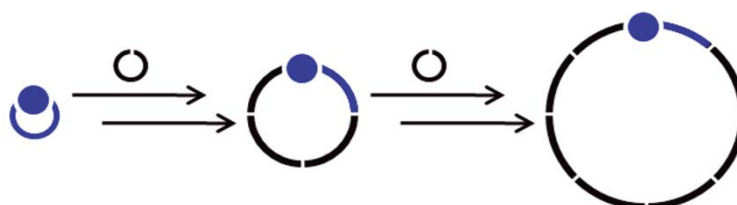
Where $[P]$ is the concentration (mol L^{-1}) of starting linear polymer in solution. From equation 3, if the polymer concentration decreases in batch condition, percent of monocyclic formation will increase. Another way to reach high percentages of monocyclic would be through a feed of linear polymer into a solution already containing the catalyst (semi-batch condition). In any ring closure type cyclization reaction, the polymer concentration should be maintained in such a way that the rate of cyclization will be closer to or greater than the feed rate to maintain the corresponding instantaneous concentration to meet the minimum requirement of desired percent of monocyclic.



Scheme 1.5. Encounter pair model for a chemical reaction.¹⁰⁹

1.6.2 Ring Expansion Techniques

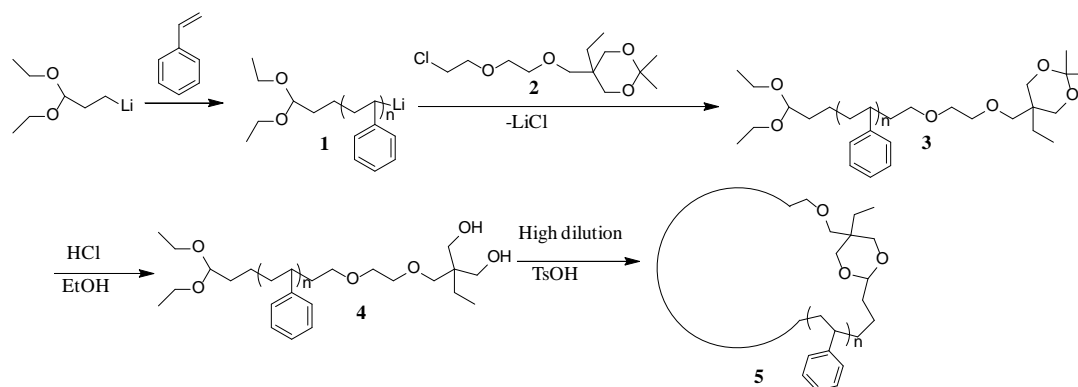
Cyclization by ring-expansion techniques are based on the insertion of monomer units into an activated cyclic chain, typically involve a catalyst or initiator that yields a growing cyclic polymer chain. The critical advantage of ring expansion technique is that it does not require high dilute condition to yield cyclic polymers. As a result, the synthetic condition can easily be optimised on the large scale synthesis. Unlike ring closure technique, ring expansion techniques do not require linear precursors to form cyclic that greatly reduce linear by-products formation. Another advantage of this technique is that the high molecular weight cyclic polymers can easily be prepared without the entropic penalty associated with the “ring-closure” approach, as the cyclic structure is maintained throughout the propagation process. Although the method has few advantages over ring-closure technique, the main challenges include severe polymerization condition, limited types of suitable monomers, and time-consuming process for synthesizing cyclic initiator along with their sensitivity to functional groups.



Scheme 1.6 Schematic representation of the ring-expansion technique for the synthesis of cyclic polymers.⁷

1.7 Synthetic routes towards the macrocyclic structures

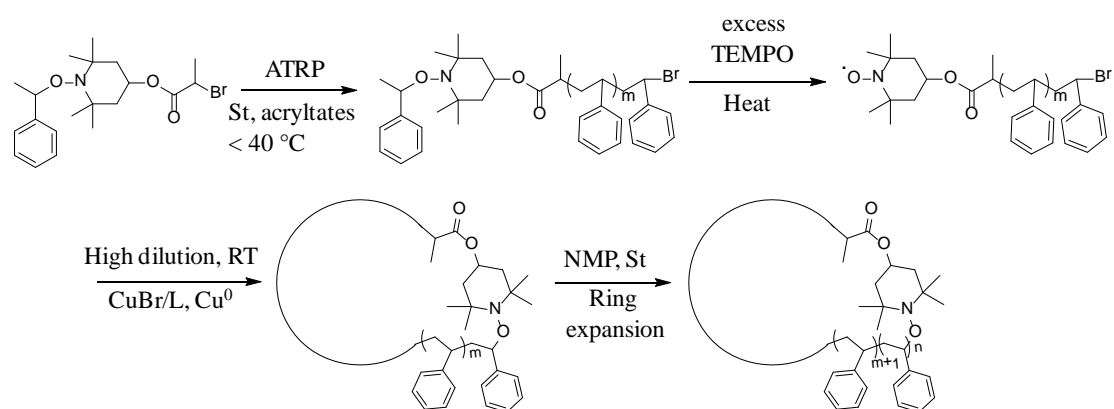
The main challenge in preparing macrocyclic polymers using a CuAAC cyclization is to find a suitable polymer that has structurally well-defined architecture, narrow molecular weight distribution and amenable to efficient end-group modification. In this regards, living ionic polymerization methods such as anionic and cationic polymerization are very efficient.¹¹⁰⁻¹¹² One of the first cyclization techniques used historically was the quenching of α, ω -homo-difunctional anionic polymers with a difunctional electrophilic agent. Roovers *et al.* pioneered this field; they synthesised cyclic polystyrenes through anionic polymerization from a difunctional initiator and quenching with a dimethyl dichlorosilane under extreme dilute conditions.¹¹³ Deffieux and Schappacher have used this technique extensively for the synthesis of a number of cyclic architectures including monocyclic polymers, bi-cycle figure 8's, and even tri-cyclic compounds from the polymer precursors by anionic polymerization.¹¹⁴⁻¹¹⁶ The main drawback for this technique is that to synthesise polymer precursors, it requires rigorously controlled conditions, involving stringent drying and very low reaction temperatures ($< -70^{\circ}\text{C}$).⁴⁶



Scheme 1.7. Synthetic route for the preparation of cyclic polystyrene from linear precursors made by living anionic polymerization.¹¹⁴

Recently, nitroxide-mediated radical polymerization (NMP) was combined with Huisgen 1, 3-dipolar cycloaddition reaction to prepare a range of cyclic polymers. First, linear precursor polymer was synthesised by NMP method followed by post-modification to achieve α, ω heterotelechelic functional groups. Then, cyclization was achieved via a CuAAC under high dilution.⁹⁷ In another approach, α, ω -heterotelechelic functional linear polymer with alkoxyamine functional group was prepared by ATRP. After cyclization by CuAAC, the polymer was further chain extended by NMP method to afford cyclic polymer with extended degree of

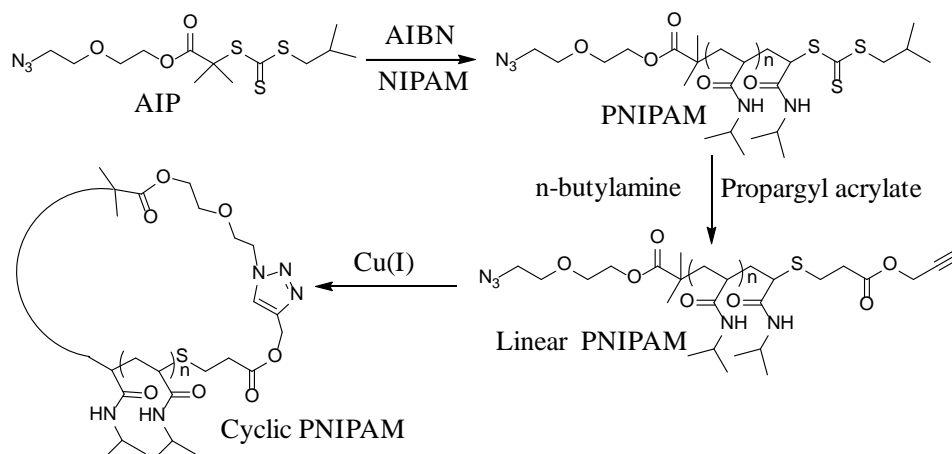
polymerization.^{117,118} Lepoittevin *et al.* also utilised NMP to form a linear polystyrene precursor which contained an alcohol functionality from the stable nitroxide radical (4-hydroxy-TEMPO) and an carboxylic acid from the initiator 4,4'-azobis(4-cyanovaleric acid).¹¹⁹ Esterification reaction between carboxylic acid and hydroxyl chain ends followed the procedure of Kubo *et al.*,¹²⁰ enabled the ring-closure to yield the macromolecular lactone. However, this procedure was only efficient for the production of low molecular weight cyclic polystyrene (<4 kDa) and yielded increasing amounts of oligomeric contaminants in larger polymers. This was attributed to the thermal instability of the nitroxide group present in the backbone of the cyclic polymer.



Scheme 1.8. Synthesis of cyclic polymers via a combination of ATRP and ATRC and subsequent ring expansion by NMP.¹¹⁷

Nowadays, a significant effort has been directed toward the reversible addition-fragmentation chain transfer (RAFT) polymerization to prepare cyclic polymer.^{79,121,122} Winnik *et al.* were pioneer in this area who utilised RAFT technique to prepare linear precursor and subsequently synthesised cyclic PNIPAM in aqueous solution.¹²³ An azide functional RAFT agent was used to prepare linear polymer precursor. The propargyl group was introduced by a one-pot aminolysis/Michael addition sequence. The polymer was then cyclised in the presence of CuSO₄ and sodium ascorbate in aqueous media at dilute condition. Monteiro and co-workers used a difunctional RAFT agent in the polymerization of styrene with subsequent conversion of the dithioester groups to thiols, in which monocyclic polymers were produced under dilute conditions in high yields through the oxidation reaction to form disulfide linkages.⁹² Shi *et al.*¹²² reported the synthesis of amphiphilic ‘‘tad-pole’’ shaped block copolymers having polystyrene and PNIPAM blocks via a post-

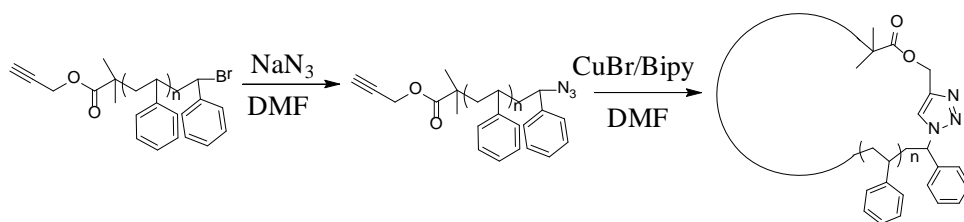
polymerization CuAAC approach. Alkyne functional RAFT macro CTA was treated with maleic anhydride resulting in the introduction of a single maleic anhydride unit. Chain extension with NIPAM yielded the target amphiphilic block copolymer in which the two blocks were “linked” by a single maleic anhydride unit in the interface. Finally, intramolecular cyclization was achieved via CuAAC coupling reaction generating the target tadpole shaped copolymer with the polystyrene block formed the head and PNIPAM the tail.



Scheme 1.9. Synthesis of cyclic PNIPAM via a combination of RAFT and CuAAC.¹³⁰

The present thesis was aimed to synthesise a range of complex polymer architectures using LRP and click reaction to investigate their properties. In the first attempt, we successfully synthesised monocyclic polymer by combining RAFT and CuAAC reaction.¹²⁴ An alkyne functional RAFT agent was used for the synthesis of polystyrene, in which the RAFT moiety was then modified to an epoxide group in one-pot through aminolysis followed by the Michael-addition of glycidyl methacrylates. The epoxide end group of the polymer chain was then directly converted to an azide and an alcohol groups using NaN_3 and NH_4Cl in DMF at $50\text{ }^\circ\text{C}$. This linear polymer was cyclised by efficient CuAAC in high yield following our previous method.⁸⁴ The above synthetic methodology was thought to be highly potential as the cyclic possess free alcohol group that can be further modified to prepare a range of cyclic polymers with different topologies. However, we observed an unforeseen degradation profile while building up complex topologies and required to circumvent the strategy by following a more suitable and reliable technique. In the past few years, significant efforts were paid for the synthesis of macrocyclic polymers by combining ATRP and CuAAC reaction using intramolecular ring closure

approach. While the bromide end group of an ATRP polymer presents an ideal substrate for a nucleophilic displacement with an azide, incorporation of an alkyne within the ATRP initiator provides the requisite functional groups at opposite (i.e., α , ω) ends of the polymer chain for subsequent cyclization via CuAAC reactions. A strategy to prepare macrocyclic polymer via the combination of ATRP and CuAAC chemistry was reported by Grayson et. al.⁹⁵ Linear polymer precursors were prepared by ATRP of styrene, using propargyl 2-bromoisobutyrate as an initiator, followed by nucleophilic substitution of the terminal bromide group by an azido group. The cyclization reaction was conducted under high dilute conditions, with Cu(I)/L complexes as catalyst. The functionalization and the cyclization were essentially quantitative, eliminating the need for purification. This approach was subsequently extended to the synthesis of cyclic poly (N-isopropylacrylamide)¹²⁵ (PNIPAM) and cyclic poly(methyl acrylate)-b-polystyrene (PMA-b-PSTY) block copolymers.⁹⁹ However, in the latter case, the alkyne moiety of the ATRP initiator had to be protected with a trimethylsilyl group, which added an additional deprotection step to the synthesis. Recently, a rapid and effective synthetic methodology was developed by our group to prepare a high purity monocyclic polymer in less than 9 min in non-dilute condition.⁸⁴ The higher solubility of Cu(I)Br/PMDETA complex in toluene facilitated the catalytic activity which is the key for making such a high purity monocyclic polymer. The technique allowed introducing a pendant functional group on the cyclic chain which is a promising candidate to build up complex architectures by the post-modification approach.



Scheme 1.10. Synthesis of cyclic polystyrene via a combination of ATRP and CuAAC.⁹⁵

1.8. Complex Topologies from Monocyclic Polymers

The advances for the synthesis of well-defined monocyclic polymers has now made great opportunities to synthesise more complex polymer topologies based on monocyclic building blocks. Tezuka et. al., is pioneer to synthesise a variety of single

cyclic polymers of different segment components that have specific functional groups at designated position. At very low concentration, a variety of spiro and bridged-type multicyclic polymer, and fused polymer topologies have been constructed mainly electrostatic self-assembly and covalent fixation process, in some cases with the combination of CuAAC 'click' reaction.¹²⁶⁻¹²⁹ Nevertheless, cyclization under very dilute condition and limited chemical variations are the major drawback of the method for the practical application. Mostly, monocyclic polymers bearing a pendant functional group provide opportunities for building different complex polymer topologies through post cyclization modification.^{93,124,130-133} Therefore, elaboration of synthetic methodologies to generate multiple chemical functionalities in the cyclic polymer is appealing for the synthesis of a wide range of complex cyclic topologies. In the present thesis, we have synthesised a range of different polymer topologies and studied their glass transition temperature and also we employed a novel strategy for the synthesis cyclic polymers having mono, di and trihydroxy functional groups in the predetermined position. The post-modification of these multifunctional cyclic and subsequent click reaction allowed preparing different unusual cyclic topologies.

1.9 Cyclic Polymer Topologies and Their Properties

The fundamental goal in polymer science is to achieve precise control over the structure and properties of macromolecules and investigate their special properties and function. A significant success in introducing the function in the complex polymer system specially arises from the unique cyclic topology effect has been reported recently.¹³⁴⁻¹³⁷ The amphiphillic mikto-arm stars, AB₂ (where A is hydrophobic cyclic polystyrene and B is hydrophilic linear poly(acrylic acid)) showed 4-fold increase in the aggregation number, resulting in a highly compact hydrophobic core and a densely packed hydrophilic corona compared with linear analogue.¹³¹ Due to the smaller hydrodynamic volume and higher packing parameter of cyclic than linear counterpart can significantly enhance the aggregation number. The outstanding topology effect substantially enhances the properties of polymeric materials which is impossible through the conventional process. Recently, Tezuka et. al., investigated the self-assembly behaviour of amphiphillic block copolymers of both linear and cyclic analogues and they found that cyclic exhibited a dramatic elevation (40 °C) of cloud point temperature (T_c) than the linear analogue.¹³⁵ Furthermore, they found a

significant salt and thermal stability of self-assembled micelles which led the control of the performance of polymeric materials for designing highly functional materials.¹³⁴

A significant amount of research has been carried out to understand and control the complex polymer system in solution but the basic structural properties play a major role in determining bulk physical properties of the polymer which is almost ignored in material science. Bulk properties describe how the chains interact through various physical forces in nano-scale, how the bulk polymer interacts with other chemicals and solvents in macro-scale. In the present thesis, we have demonstrated the synthesis of unusually different cyclic topologies and investigate their glass transition temperature in bulk state.

1.10. Objectives and Outlines of this thesis

The main objective of this thesis is to develop a facile strategy to synthesise different polymer topologies based on cyclic polymers by combining 'living' radical polymerization such as RAFT, ATRP and high efficient CuAAC reaction. The thermal properties (i.e. the glass transition temperature by DSC) for a range of cyclic topologies were determined. The objective is subdivided into the following chapters: Chapter 2 describes the facile synthesis of cyclic polymer topologies by CuAAC from the linear polymers made by RAFT polymerization. Unexpected degradation behaviour was observed and the degradation profile has been investigated extensively in three different CuAAC 'click' reaction conditions.

A novel synthetic protocol was employed to synthesise different complex polymer topologies in Chapter 3. The multi-functional cyclic polymers were synthesised first by combining modular approach and CuAAC reaction. The post-modification and further click reaction allowed synthesizing different complex polymer topologies.

Topology effect on the glass transition temperature has been studied thoroughly in the Chapter 4. Different topologies of both homo and block polymers (total 18 polymers) were synthesised and studied their glass transition temperature by DSC.

In Chapter 5, a series of polymeric architectures were used to investigate the knots effect on the glass transition temperature in cyclic system. The hydrodynamic volume and chain segment stiffness of these polymeric knots (which have the same molecular

weight) on their thermal property (i.e. glass transition temperature- T_g) have been studied.

1.11. References

- (1) Duncan, R. *Nat Rev Drug Discov* **2003**, 2, 347-360.
- (2) Putnam, D. *Nat Mater* **2006**, 5, 439-451.
- (3) Langer, R.; Vacanti, J. *Science* **1993**, 260, 920-926.
- (4) Langer, R.; Tirrell, D. A. *Nature* **2004**, 428, 487-492.
- (5) Hadjichristidis, N.; Pitsikalis, M.; Pispas, S.; Iatrou, H. *Chemical Reviews* **2001**, 101, 3747-3792.
- (6) Kobayashi, S.; Editor. *New Frontiers in Polymer Synthesis. [In: Adv. Polym. Sci., 2008; 217]*; Springer GmbH, 2008, p 187 pp.
- (7) Laurent, B. A.; Grayson, S. M. *Chemical Society Reviews* **2009**, 38, 2202-2213.
- (8) Kricheldorf, H. R. *Journal of Polymer Science Part A: Polymer Chemistry* **2010**, 48, 251-284.
- (9) Jia, Z.; Monteiro, M. J. *Journal of Polymer Science Part A: Polymer Chemistry* **2012**, 50, 2085-2097.
- (10) McLeish, T. *Science* **2002**, 297, 2005-2006.
- (11) Obukhov, S. P.; Rubinstein, M.; Duke, T. *Physical Review Letters* **1994**, 73, 1263-1266.
- (12) Chiefari, J.; Chong, Y. K.; Ercole, F.; Krstina, J.; Jeffery, J.; Le, T. P. T.; Mayadunne, R. T. A.; Meijs, G. F.; Moad, C. L.; Moad, G.; Rizzardo, E.; Thang, S. H. *Macromolecules* **1998**, 31, 5559-5562.
- (13) Stenzel, M. H.; Davis, T. P. *Journal of Polymer Science Part A: Polymer Chemistry* **2002**, 40, 4498-4512.
- (14) Barner, L.; Barner-Kowollik, C.; Davis, T. P.; Stenzel, M. H. *Australian Journal of Chemistry* **2004**, 57, 19-24.
- (15) Goh, Y.-K.; Whittaker, A. K.; Monteiro, M. J. *Journal of Polymer Science Part A: Polymer Chemistry* **2007**, 45, 4150-4153.
- (16) Stenzel-Rosenbaum, M. H.; Davis, T. P.; Fane, A. G.; Chen, V. *Angewandte Chemie International Edition* **2001**, 40, 3428-3432.
- (17) Matyjaszewski, K. *Macromolecules* **2012**, 45, 4015-4039.

- (18) Moad, G. *The Chemistry of Radical Polymerization*, 2nd edition ed.; Elsevier: Oxford, 2006.
- (19) Tsarevsky, N. V.; Bencherif, S. A.; Matyjaszewski, K. *Macromolecules* **2007**, *40*, 4439-4445.
- (20) An, S. G.; Li, G. H.; Cho, C. G. *Polymer* **2006**, *47*, 4154-4162.
- (21) Matyjaszewski, K.; Tsarevsky, N. V. *Nat Chem* **2009**, *1*, 276-288.
- (22) Liu, C.; Pan, M.; Zhang, Y.; Huang, J. *Journal of Polymer Science Part A: Polymer Chemistry* **2008**, *46*, 6754-6761.
- (23) Nicolas, J.; Guillaneuf, Y.; Lefay, C.; Bertin, D.; Gigmes, D.; Charleux, B. *Progress in Polymer Science* **2013**, *38*, 63-235.
- (24) Hawker, C. J.; Bosman, A. W.; Harth, E. *Chemical Reviews* **2001**, *101*, 3661-3688.
- (25) Karaky, K.; Clisson, G.; Reiter, G.; Billon, L. *Macromolecular Chemistry and Physics* **2008**, *209*, 715-722.
- (26) Percec, V.; Guliashvili, T.; Ladislaw, J. S.; Wistrand, A.; Stjerndahl, A.; Sienkowska, M. J.; Monteiro, M. J.; Sahoo, S. *Journal of the American Chemical Society* **2006**, *128*, 14156-14165.
- (27) Percec, V.; Popov, A. V.; Ramirez-Castillo, E.; Monteiro, M.; Barboiu, B.; Weichold, O.; Asandei, A. D.; Mitchell, C. M. *Journal of the American Chemical Society* **2002**, *124*, 4940-4941.
- (28) Charmot, D.; Corpart, P.; Adam, H.; Zard, S. Z.; Biadatti, T.; Bouhadir, G. *Macromolecular Symposia* **2000**, *150*, 23-32.
- (29) Shipp, D. A. *Journal of Macromolecular Science, Part C* **2005**, *45*, 171-194.
- (30) Lowe, A. B.; McCormick, C. L. *Progress in Polymer Science* **2007**, *32*, 283-351.
- (31) McCormick, C. L.; Lowe, A. B. *Accounts of Chemical Research* **2004**, *37*, 312-325.
- (32) Smith, A. E.; Xu, X.; McCormick, C. L. *Progress in Polymer Science* **2010**, *35*, 45-93.
- (33) Perrier, S.; Takolpuckdee, P. *Journal of Polymer Science Part A: Polymer Chemistry* **2005**, *43*, 5347-5393.
- (34) Favier, A.; Charreyre, M.-T. *Macromolecular Rapid Communications* **2006**, *27*, 653-692.
- (35) Moad, G.; Rizzardo, E.; Thang, S. H. *Australian Journal of Chemistry* **2005**, *58*, 379-410.

- (36) Wang, J.-S.; Matyjaszewski, K. *Journal of the American Chemical Society* **1995**, *117*, 5614-5615.
- (37) Wang, J.-S.; Matyjaszewski, K. *Macromolecules* **1995**, *28*, 7901-7910.
- (38) Kato, M.; Kamigaito, M.; Sawamoto, M.; Higashimura, T. *Macromolecules* **1995**, *28*, 1721-1723.
- (39) Matyjaszewski, K. *Journal of Macromolecular Science, Part A* **1997**, *34*, 1785-1801.
- (40) Tang, W.; Matyjaszewski, K. *Macromolecules* **2006**, *39*, 4953-4959.
- (41) Tang, W.; Kwak, Y.; Braunecker, W.; Tsarevsky, N. V.; Coote, M. L.; Matyjaszewski, K. *Journal of the American Chemical Society* **2008**, *130*, 10702-10713.
- (42) Matyjaszewski, K.; Paik, H.-j.; Zhou, P.; Diamanti, S. J. *Macromolecules* **2001**, *34*, 5125-5131.
- (43) Fischer, H. *Chemical Reviews* **2001**, *101*, 3581-3610.
- (44) Lligadas, G.; Percec, V. *Journal of Polymer Science Part A: Polymer Chemistry* **2008**, *46*, 6880-6895.
- (45) Lligadas, G.; Percec, V. *Journal of Polymer Science Part A: Polymer Chemistry* **2007**, *45*, 4684-4695.
- (46) Matyjaszewski, K. *Chemistry – A European Journal* **1999**, *5*, 3095-3102.
- (47) Inglis, A. J.; Sinnwell, S.; Davis, T. P.; Barner-Kowollik, C.; Stenzel, M. H. *Macromolecules* **2008**, *41*, 4120-4126.
- (48) Becer, C. R.; Hoogenboom, R.; Schubert, U. S. *Angewandte Chemie International Edition* **2009**, *48*, 4900-4908.
- (49) Killops, K. L.; Campos, L. M.; Hawker, C. J. *Journal of the American Chemical Society* **2008**, *130*, 5062-5064.
- (50) Fairbanks, B. D.; Scott, T. F.; Kloxin, C. J.; Anseth, K. S.; Bowman, C. N. *Macromolecules* **2008**, *42*, 211-217.
- (51) Li, H.; Yu, B.; Matsushima, H.; Hoyle, C. E.; Lowe, A. B. *Macromolecules* **2009**, *42*, 6537-6542.
- (52) Becer, C. R.; Babiuch, K.; Pilz, D.; Hornig, S.; Heinze, T.; Gottschaldt, M.; Schubert, U. S. *Macromolecules* **2009**, *42*, 2387-2394.
- (53) Rosen, B. M.; Lligadas, G.; Hahn, C.; Percec, V. *Journal of Polymer Science Part A: Polymer Chemistry* **2009**, *47*, 3940-3948.
- (54) Huisgen, R. *Pure and Applied Chemistry* **1989**, *61*, 613-628.

- (55) Huisgen, R.; Szeimies, G.; Möbius, L. *Chemische Berichte* **1967**, *100*, 2494-2507.
- (56) Wu P, F. V., V. *Aldrich Chimica Acta*; Aldrich Chemistry, 2007; Vol. 40, p 7.
- (57) Bock, V. D.; Hiemstra, H.; van Maarseveen, J. H. *European Journal of Organic Chemistry* **2006**, *2006*, 51-68.
- (58) Hein, C.; Liu, X.-M.; Wang, D. *Pharm Res* **2008**, *25*, 2216-2230.
- (59) Rostovtsev, V. V.; Green, L. G.; Fokin, V. V.; Sharpless, K. B. *Angewandte Chemie International Edition* **2002**, *41*, 2596-2599.
- (60) Cho, S. H.; Chang, S. *Angewandte Chemie International Edition* **2007**, *46*, 1897-1900.
- (61) Asano, K.; Matsubara, S. *Organic Letters* **2010**, *12*, 4988-4991.
- (62) Gaulier, C.; Hospital, A.; Legeret, B.; Delmas, A. F.; Aucagne, V.; Cisnetti, F.; Gautier, A. *Chemical Communications* **2012**, *48*, 4005-4007.
- (63) Gonda, Z.; Novak, Z. *Dalton Transactions* **2010**, *39*, 726-729.
- (64) Matyjaszewski, K. *Progress in Polymer Science* **2005**, *30*, 858-875.
- (65) Lutz, J.-F. *Angewandte Chemie International Edition* **2007**, *46*, 1018-1025.
- (66) Binder, W. H.; Sachsenhofer, R. *Macromolecular Rapid Communications* **2007**, *28*, 15-54.
- (67) Golas, P. L.; Matyjaszewski, K. *QSAR & Combinatorial Science* **2007**, *26*, 1116-1134.
- (68) Fournier, D.; Hoogenboom, R.; Schubert, U. S. *Chemical Society Reviews* **2007**, *36*, 1369-1380.
- (69) Nandivada, H.; Jiang, X.; Lahann, J. *Advanced Materials* **2007**, *19*, 2197-2208.
- (70) Johnson, J. A.; Baskin, J. M.; Bertozzi, C. R.; Koberstein, J. T.; Turro, N. J. *Chemical Communications* **2008**, 3064-3066.
- (71) Agard, N. J.; Prescher, J. A.; Bertozzi, C. R. *Journal of the American Chemical Society* **2004**, *126*, 15046-15047.
- (72) Agard, N. J.; Baskin, J. M.; Prescher, J. A.; Lo, A.; Bertozzi, C. R. *ACS Chemical Biology* **2006**, *1*, 644-648.
- (73) Baskin, J. M.; Prescher, J. A.; Laughlin, S. T.; Agard, N. J.; Chang, P. V.; Miller, I. A.; Lo, A.; Codelli, J. A.; Bertozzi, C. R. *Proceedings of the National Academy of Sciences* **2007**, *104*, 16793-16797.
- (74) de Gennes, P. G. *The Journal of Chemical Physics* **1971**, *55*, 572-579.

- (75) Doi, M.; Edwards, S. F. *Journal of the Chemical Society, Faraday Transactions 2: Molecular and Chemical Physics* **1978**, *74*, 1789-1801.
- (76) Orrah, D. J.; Semlyen, J. A.; Ross-Murphy, S. B. *Polymer* **1988**, *29*, 1455-1458.
- (77) Clarson, S. J.; Semlyen, J. A. *Polymer* **1986**, *27*, 1633-1636.
- (78) Edwards, C. J. C.; Stepto, R. F. T.; Semlyen, J. A. *Polymer* **1980**, *21*, 781-786.
- (79) Qiu, X.-P.; Tanaka, F.; Winnik, F. M. *Macromolecules* **2007**, *40*, 7069-7071.
- (80) Shin, E. J.; Jeong, W.; Brown, H. A.; Koo, B. J.; Hedrick, J. L.; Waymouth, R. M. *Macromolecules* **2011**, *44*, 2773-2779.
- (81) Bannister, D. J.; Semlyen, J. A. *Polymer* **1981**, *22*, 377-381.
- (82) Casassa, E. F. *Journal of Polymer Science Part A: General Papers* **1965**, *3*, 605-614.
- (83) Roovers, J. *Journal of Polymer Science: Polymer Physics Edition* **1985**, *23*, 1117-1126.
- (84) Lonsdale, D. E.; Bell, C. A.; Monteiro, M. J. *Macromolecules* **2010**, *43*, 3331-3339.
- (85) McKenna, G. B.; Hadziioannou, G.; Lutz, P.; Hild, G.; Strazielle, C.; Straupe, C.; Rempp, P.; Kovacs, A. J. *Macromolecules* **1987**, *20*, 498-512.
- (86) Jacobson, H.; Stockmayer, W. H. *The Journal of Chemical Physics* **1950**, *18*, 1600-1606.
- (87) Brown, J. F.; Slusarczuk, G. M. J. *Journal of the American Chemical Society* **1965**, *87*, 931-932.
- (88) Carmichael, J. B.; Winger, R. *Journal of Polymer Science Part A: General Papers* **1965**, *3*, 971-984.
- (89) Carmichael, J. B.; Gordon, D. J.; Isackson, F. J. *The Journal of Physical Chemistry* **1967**, *71*, 2011-2015.
- (90) Geiser, D.; Höcker, H. *Polymer Bulletin* **1980**, *2*, 591-597.
- (91) Geiser, D.; Höcker, H. *Macromolecules* **1980**, *13*, 653-656.
- (92) Whittaker, M. R.; Goh, Y.-K.; Gemici, H.; Legge, T. M.; Perrier, S.; Monteiro, M. J. *Macromolecules* **2006**, *39*, 9028-9034.
- (93) Peng, Y.; Liu, H.; Zhang, X.; Liu, S.; Li, Y. *Macromolecules* **2009**, *42*, 6457-6462.
- (94) Misaka, H.; Kakuchi, R.; Zhang, C.; Sakai, R.; Satoh, T.; Kakuchi, T. *Macromolecules* **2009**, *42*, 5091-5096.

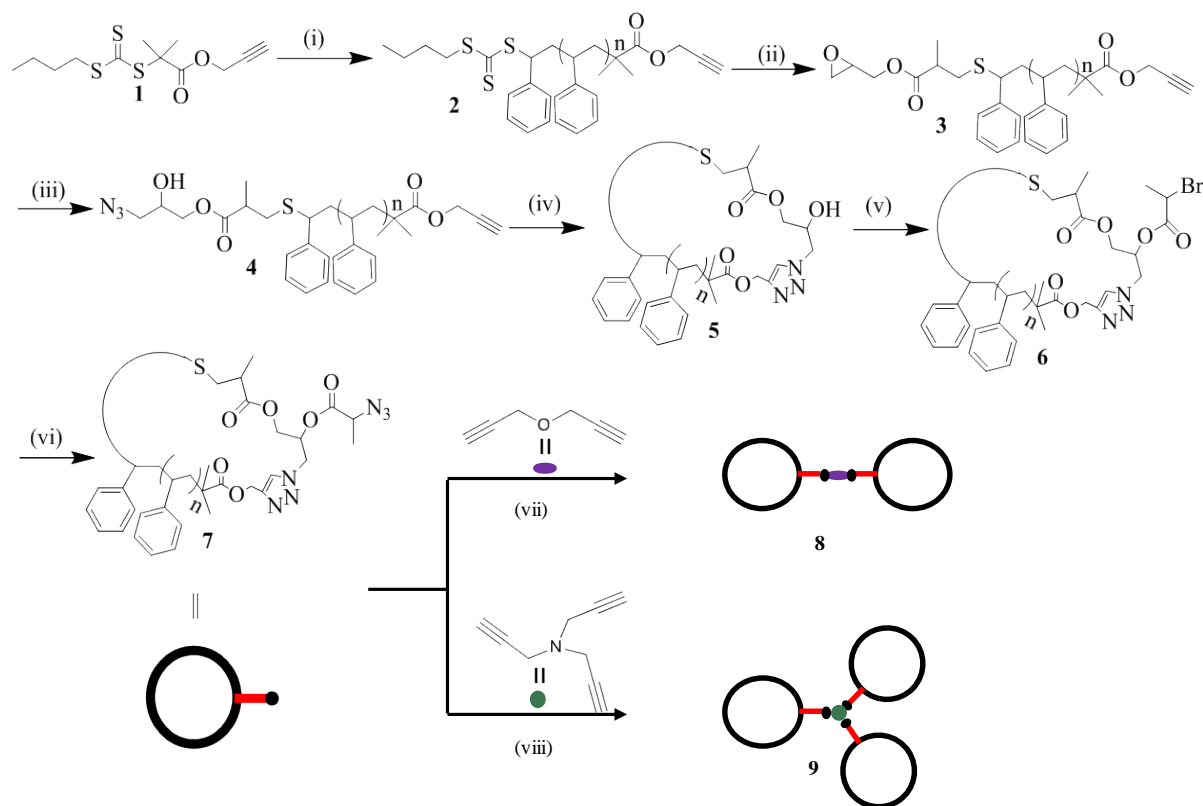
- (95) Laurent, B. A.; Grayson, S. M. *Journal of the American Chemical Society* **2006**, *128*, 4238-4239.
- (96) Ge, Z.; Zhou, Y.; Xu, J.; Liu, H.; Chen, D.; Liu, S. *Journal of the American Chemical Society* **2009**, *131*, 1628-1629.
- (97) O'Bryan, G.; Ningnuek, N.; Braslau, R. *Polymer* **2008**, *49*, 5241-5248.
- (98) Hoskins, J. N.; Grayson, S. M. *Macromolecules* **2009**, *42*, 6406-6413.
- (99) Eugene, D. M.; Grayson, S. M. *Macromolecules* **2008**, *41*, 5082-5084.
- (100) Bielawski, C. W.; Benitez, D.; Grubbs, R. H. *Science* **2002**, *297*, 2041-2044.
- (101) Boydston, A. J.; Xia, Y.; Kornfield, J. A.; Gorodetskaya, I. A.; Grubbs, R. H. *Journal of the American Chemical Society* **2008**, *130*, 12775-12782.
- (102) Kudo, H.; Sato, M.; Wakai, R.; Iwamoto, T.; Nishikubo, T. *Macromolecules* **2008**, *41*, 521-523.
- (103) Culkin, D. A.; Jeong, W.; Csihony, S.; Gomez, E. D.; Balsara, N. P.; Hedrick, J. L.; Waymouth, R. M. *Angewandte Chemie International Edition* **2007**, *46*, 2627-2630.
- (104) Jeong, W.; Hedrick, J. L.; Waymouth, R. M. *Journal of the American Chemical Society* **2007**, *129*, 8414-8415.
- (105) Herbert, D. E.; Gilroy, J. B.; Chan, W. Y.; Chabanne, L.; Staubitz, A.; Lough, A. J.; Manners, I. *Journal of the American Chemical Society* **2009**, *131*, 14958-14968.
- (106) Zhang, F.; Götz, G.; Winkler, H. D. F.; Schalley, C. A.; Bäuerle, P. *Angewandte Chemie International Edition* **2009**, *48*, 6632-6635.
- (107) Zhang, K.; Lackey, M. A.; Wu, Y.; Tew, G. N. *Journal of the American Chemical Society* **2011**, *133*, 6906-6909.
- (108) Rique-Lurbet, L.; Schappacher, M.; Deffieux, A. *Macromolecules* **1994**, *27*, 6318-6324.
- (109) Lonsdale, D. E.; Monteiro, M. J. *Journal of Polymer Science Part A: Polymer Chemistry* **2010**, *48*, 4496-4503.
- (110) Hsieh, H. L., Quirk, R. P., *Anionic Polymerization, Principles and Practical Applications*: New York, 1996.
- (111) Jenkins, A. D. *Polymer International* **1993**, *30*, 281-281.
- (112) Matyjaszewski, K. *Cationic Polymerization: Mechanisms, Synthesis and Applications*: New York, 1996.
- (113) Roovers, J.; Toporowski, P. M. *Macromolecules* **1983**, *16*, 843-849.
- (114) Schappacher, M.; Deffieux, A. *Macromolecules* **2001**, *34*, 5827-5832.

- (115) Beinat, S.; Schappacher, M.; Deffieux, A. *Macromolecules* **1996**, *29*, 6737-6743.
- (116) Schappacher, M.; Deffieux, A. *Macromolecules* **1995**, *28*, 2629-2636.
- (117) Nicolaÿ, R.; Matyjaszewski, K. *Macromolecules* **2010**, *44*, 240-247.
- (118) Narumi, A.; Zeidler, S.; Barqawi, H.; Enders, C.; Binder, W. H. *Journal of Polymer Science Part A: Polymer Chemistry* **2010**, *48*, 3402-3416.
- (119) Lepoittevin, B.; Perrot, X.; Masure, M.; Hemery, P. *Macromolecules* **2001**, *34*, 425-429.
- (120) Kubo, M.; Hayashi, T.; Kobayashi, H.; Tsuboi, K.; Itoh, T. *Macromolecules* **1997**, *30*, 2805-2807.
- (121) Goldmann, A. S.; Quémener, D.; Millard, P.-E.; Davis, T. P.; Stenzel, M. H.; Barner-Kowollik, C.; Müller, A. H. E. *Polymer* **2008**, *49*, 2274-2281.
- (122) Shi, G.-Y.; Tang, X.-Z.; Pan, C.-Y. *Journal of Polymer Science Part A: Polymer Chemistry* **2008**, *46*, 2390-2401.
- (123) Qiu, X.-P.; Winnik, F. M. *Macromolecular Symposia* **2009**, *278*, 10-13.
- (124) Hossain, M. D.; Valade, D.; Jia, Z.; Monteiro, M. J. *Polymer Chemistry* **2012**, *3*, 2986-2995.
- (125) Xu, J.; Ye, J.; Liu, S. *Macromolecules* **2007**, *40*, 9103-9110.
- (126) Tezuka, Y.; Fujiyama, K. *Journal of the American Chemical Society* **2005**, *127*, 6266-6270.
- (127) Tezuka, Y.; Takahashi, N.; Satoh, T.; Adachi, K. *Macromolecules* **2007**, *40*, 7910-7918.
- (128) Sugai, N.; Heguri, H.; Ohta, K.; Meng, Q.; Yamamoto, T.; Tezuka, Y. *Journal of the American Chemical Society* **2010**, *132*, 14790-14802.
- (129) Igari, M.; Heguri, H.; Yamamoto, T.; Tezuka, Y. *Macromolecules* **2013**, *46*, 7303-7315.
- (130) Lonsdale, D. E.; Monteiro, M. J. *Chemical Communications* **2010**, *46*, 7945-7947.
- (131) Lonsdale, D. E.; Monteiro, M. J. *Journal of Polymer Science Part A: Polymer Chemistry* **2011**, *49*, 4603-4612.
- (132) Jia, Z.; Lonsdale, D. E.; Kulis, J.; Monteiro, M. J. *ACS Macro Letters* **2012**, *1*, 780-783.
- (133) Kulis, J.; Jia, Z.; Monteiro, M. J. *Macromolecules* **2012**, *45*, 5956-5966.
- (134) Honda, S.; Yamamoto, T.; Tezuka, Y. *Nat Commun* **2013**, *4*, 1574.

- (135) Honda, S.; Yamamoto, T.; Tezuka, Y. *Journal of the American Chemical Society* **2010**, *132*, 10251-10253.
- (136) Isono, T.; Satoh, Y.; Miyachi, K.; Chen, Y.; Sato, S.-i.; Tajima, K.; Satoh, T.; Kakuchi, T. *Macromolecules* **2014**, *47*, 2853-2863.
- (137) Zhang, B.; Zhang, H.; Li, Y.; Hoskins, J. N.; Grayson, S. M. *ACS Macro Letters* **2013**, *2*, 845-848.

Chapter 2

Cyclic polystyrene topologies via RAFT and CuAAC



Cyclic polymers have attracted interest due to their different self-assembly behaviour and physical properties compared to their linear counterparts with the same molecular weight. This chapter describes a facile and efficient synthesis of cyclic polymers by combining RAFT and CuAAC reaction followed by post-modification for the fabrication of complex topologies. There are only a few examples of using polymers made by RAFT to create cyclic polymers, and no reports of coupling these cyclic polymers together to form stars. In this work, we have demonstrated a novel approach to produce cyclic polymers by RAFT with the required functionality for further coupling to form 2- and 3- arm stars. Cyclization of a chemically modified linear RAFT polystyrene (PSTY) using the copper catalyzed azide–alkyne cycloaddition (CuAAC) gave cyclic polystyrene (c-PSTY) with a purity of 95% as determined by simulating the experimental molecular weight distribution using the log-normal distribution (LND) method. The –OH group on c-PSTY was converted to an azide via a two-step procedure, allowing the cyclic polymers to be coupled together using propargyl ether or tripropargylamine via the CuAAC reaction to form 2- and 3-arm stars, respectively. When the conventional ligand complex and solvent was used (i.e. CuBr–PMDETA in toluene), the linkage between the cyclic arms degraded fully after 24 h due to base cleavage. We overcame this by changing the ligand to a triazole or carrying out the reaction in ligand-free conditions (i.e. CuBr in

DMF). These latter experimental conditions gave ‘click’ efficiencies of greater than 82% without degradation of the final structures. Our methodology for producing cyclic polymers by RAFT will not only extend to other monomers but allow one to utilise these cyclic polymers as building blocks in the formation of more complex polymer architectures.

2.1 Introduction

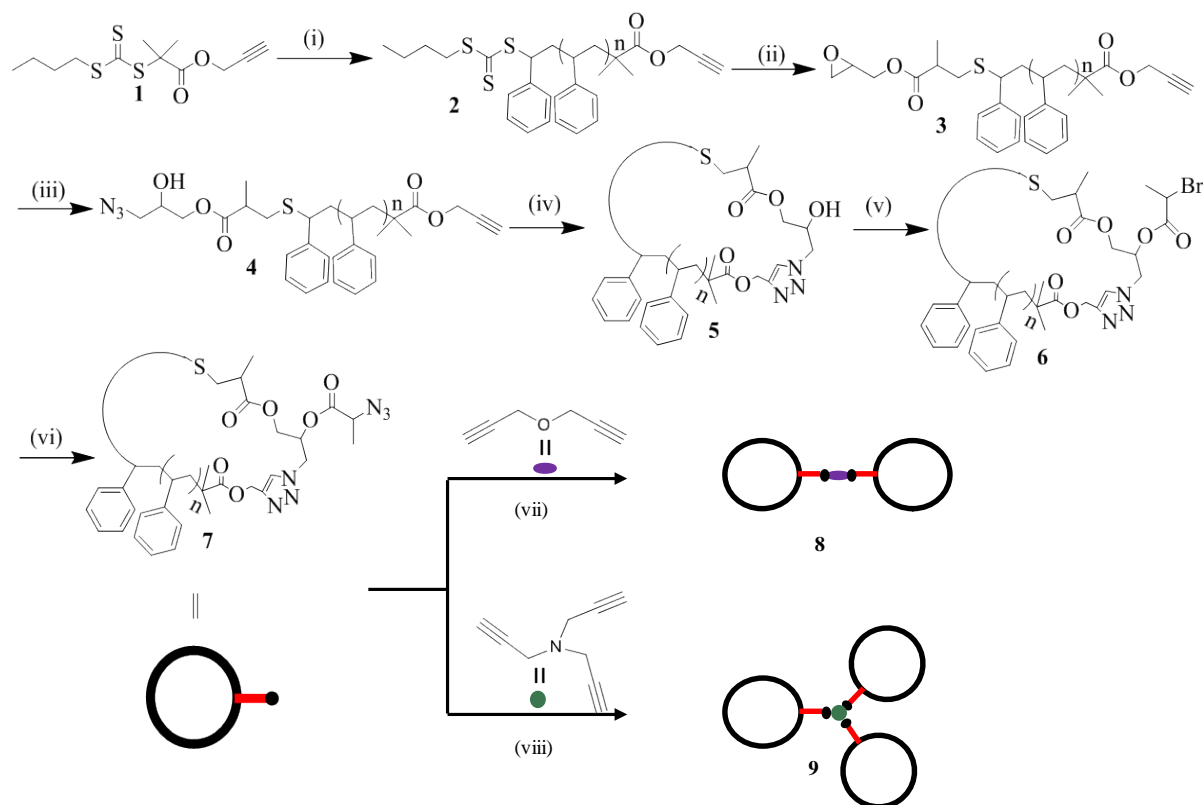
Considerable interest has been paid to the synthesis of cyclic polymers.¹⁻⁵ The different diffusion process of cyclic polymers in a concentrated matrix compared to their linear counterparts was postulated to result in very different physical properties.⁶ Cyclic polymers are more compact and thought to move with an amoebae-like motion.⁷ This results in a higher density,⁸ lower intrinsic viscosity,⁹ lower translational friction coefficients, higher glass transition temperatures,⁹ higher critical solution temperature,¹⁰ increased rate of crystallization,¹¹ higher refractive index¹² and enhancement of fluorescence.¹³ Cyclic polymers have been self-assembled in water to display similar and unique properties to cyclic lipids used by microorganisms to stabilise their cell membranes in hot springs.¹⁴ The self-assembly of tadpole structures in which the hydrophobic block was cyclic produced a dense micelle core with a 4-fold increase in the aggregation number compare to their linear counterparts.¹⁵

There have been many reports for the synthesis of cyclic polymers through ring closure using the combination of ATRP (atom transfer radical polymerization) and CuAAC (copper catalyzed azide–alkyne cycloaddition).^{3-5,16,17} This has eventuated in the production of 2- and 3-arm stars in which at least one arm consisted of a cyclic polymer.^{15,18} We recently showed that ABC 3-miktoarm stars¹⁹ consisting of all cyclic building blocks could be made using ATRP²⁰ or SET-LRP²¹ in combination with CuAAC and NRC²² (nitroxide radical coupling) through modulating the copper activity.^{23,24} However, there have been only a few reports using reversible addition–fragmentation chain transfer (RAFT) polymerization to construct cyclic polymers.^{10,25-27} This is surprising as the range of polymers, especially the water soluble polymers, can be extended when using RAFT. There are no reports to our knowledge that use cyclic polymers made by RAFT and CuAAC and subsequently construct more complex architectures such as 2- and 3- arm stars.

2.1.1 Aim of the Chapter

The aim of the work was to develop a novel strategy to synthesise of different topologies cyclic polymer by combining RAFT and CuAAC reactions. An alkyne functional RAFT agent (**1**) was used for the synthesis of polystyrene (**2**), in which the RAFT moiety was then modified to an epoxide group in one-pot through aminolysis followed by the Michael-addition of glycidyl

methacrylate to form polymer **3** (Scheme 2.1). The epoxide endgroup of the polymer chain was directly converted to an azide and an alcohol group using sodium azide (**4**).²⁸ This linear polymer was cyclised in high yield following our previous method,¹⁷ and the alcohol (**5**) then converted to an azide (**7**). This cyclic polymer was finally coupled with either propargyl ether or tri-propargyl amine to form 2- and 3-arm stars under appropriate ligand and solvent conditions for the ‘click’ reaction. This method has the potential to be applied to a wide range of polymers made by RAFT.



Scheme 2.1 Synthetic route for the preparation of cyclic polystyrene by combining RAFT and CuAAC reactions to form dicyclic (**8**) and tricyclic PSTY (**9**). Reaction conditions: (i) AIBN, bulk polymerization at 65 °C for 15.5 h, (ii) glycidyl methacrylate, hexylamine, TEA and TCEP in DMF at 25 °C (iii) NaN₃–NH₄Cl in DMF at 50 °C (iv) CuBr, PMDETA in toluene at 25 °C, feed rate = 0.1 mL min⁻¹ over 4.17 h and then kept for 3 h (v) 2-bromopropionyl bromide, TEA in THF at 0 °C–RT for 48 h (vi) NaN₃ in DMF at 25 °C for 16 h (vii) CuBr in DMF, at 25 °C for 1.0 h and (viii) CuBr–triazole in toluene at 25 °C for 12.0 h.

2.2 Experimental

2.2.1 Materials

The following chemicals were analytical grade and used as received unless otherwise stated: activated basic alumina (Aldrich: Brockmann I, standard grade, ~150 mesh, 58 Å),

dimethyl(amino)pyridine (DMAP, Aldrich, 99%), Dowex ion-exchange resin (Sigma-Aldrich, 50WX8-200), magnesium sulphate, anhydrous (MgSO_4 : Scharlau, extra pure), potassium carbonate (K_2CO_3 : AnalaR, 99.9%), silica gel 60 (230–400 mesh ATM (SDS)), potassium phosphate tri-basic (K_3PO_4 : Sigma-Aldrich $\geq 98\%$), triethylamine (TEA: Fluka, 98%), 2-bromopropionyl bromide (BPB: Aldrich 98%), propargyl bromide solution (80 wt% in toluene, Aldrich), propargyl ether (Aldrich, 99%), tripropargylamine (TPA: Aldrich, 98%), sodium azide (NaN_3 : Aldrich, 99.5%), *N,N,N',N'',N''*-pentamethyldiethylenetriamine (PMDETA: Aldrich, 99%), copper(I) bromide (Cu(I)Br : Aldrich, 99.999%), copper(II) bromide (Cu(II)Br_2 : Aldrich, 99%); tris(2-carboxyethyl) phosphine hydrochloride (TCEP, 98%, Aldrich); styrene (Sty, Aldrich, >99%) was purified from inhibitor prior to use by passing through a basic alumina column. Azobisisobutyronitrile (AIBN, Riedel-de Haen) was recrystallised from methanol twice prior to use. All other chemicals used were of at least analytical grade and used as received.

The following solvents were used as received: acetone (Chem Supply, AR), chloroform (CHCl_3 : Univar, AR grade), dichloromethane (DCM: Labscan, AR grade), diethyl ether (Univar, AR grade), ethanol (EtOH: ChemSupply, AR), ethyl acetate (EtOAc: Univar, AR grade), hexane (Wacol, technical grade, distilled), hydrochloric acid (HCl, Univar, 32%), anhydrous methanol (MeOH: Mallinckrodt, 99.9%, HPLC grade), Milli-Q water (Biolab, 18.2 $\text{M}\Omega$ cm), *N,N*-dimethylformamide (DMF: Labscan, AR grade), tetrahydrofuran (THF: Labscan, HPLC grade), toluene (HPLC, LABSCAN, 99.8%).

2.2.2 Instruments and measurements

Size Exclusion Chromatography (SEC).

For SEC analysis, polymer solution was prepared by dissolving in tetrahydrofuran (THF) to a concentration of 1 mg mL^{-1} and then filtered through a 0.45 mm PTFE syringe filter. A waters 2695 separations module, fitted with a waters 410 refractive index detector maintained at 35°C , a waters 996 photodiode array detector, and two Ultra-styragel linear columns ($7.8 \times 300 \text{ mm}$) arranged in series were used to analyze the molecular weight distribution of the polymers. For all analysis, these columns were maintained at 40°C and are capable of separating polymers in the molecular weight range of 500 to 4 million g mol^{-1} with high resolution. All samples were eluted at a flow rate of 1.0 mL min^{-1} . Calibration was performed using narrow molecular weight PSTY standards ($\text{PDI} \leq 1.1$) ranging from 500 to 2 million g mol^{-1} . Data acquisition was performed using Empower software, and molecular weights were calculated relative to polystyrene standards.

Absolute molecular weight determination by triple detection-SEC.

Absolute molecular weights of polymers were determined using a Polymer Labs GPC50 Plus equipped with dual angle laser light scattering detector, viscometer and differential refractive index detector. HPLC grade tetrahydrofuran was used as eluent at flow rate 1 mL min⁻¹. Separations were achieved using two PLGel Mixed C (7.8 × 300 mm) SEC columns connected in series and held at a constant temperature of 40 °C. The triple detection system was calibrated using a 4 mg mL⁻¹ PSTY standard (Polymer Laboratories: Mw = 110 K, dn/dc = 0.185 and IV = 0.4872 mL g⁻¹). Polymer samples of known concentration were freshly prepared in THF and passed through a 0.45 mm PTFE syringe filter just prior to injection.

Preparative Size Exclusion Chromatography (Prep-SEC).

Linear polystyrene was purified using a Varian Pro-Star preparative SEC system equipped with a manual injector, differential refractive index detector, and single wave-length ultra-violet visible detector. Flow rate was maintained 10 mL min⁻¹ and HPLC grade tetrahydrofuran was used as the eluent. Separations were achieved using a PLgel 10 mm 10 × 10³ Å, 300 mm × 25 mm preparative SEC column held at 25 °C. The dried crude polymer was dissolved in THF at 100 mg mL⁻¹ concentration and filtered through a 0.45 mm PTFE syringe filter prior to inject. Different fractions were collected manually, and the composition of each was determined using the Polymer Laboratories GPC50 Plus equipped with triple detection as described above.

¹H Nuclear Magnetic Resonance (NMR).

All NMR spectra were recorded on a Bruker DRX 300 MHz and 500 MHz spectrometer using an external lock (CDCl₃) and referenced to the residual non-deuterated solvent (CHCl₃). Then a DOSY experiment was run to acquire spectra presented herein by increasing the pulse gradient from 2 to 85% of the maximum gradient strength and increasing d (p30) from 1 ms to 2 ms, using 64 scans.

Attenuated Total Reflectance Fourier Transform Spectroscopy (ATR-FTIR).

ATR-FTIR spectra were obtained using a horizontal, single bounce, diamond ATR accessory on a Nicolet Nexus 870 FT-IR. Spectra were recorded between 4000 and 500 cm⁻¹ for 64 scans at 4 cm⁻¹ resolutions with an OPD velocity of 0.6289 cm s⁻¹. Solids were pressed directly onto the diamond internal reflection element of the ATR without further sample preparation.

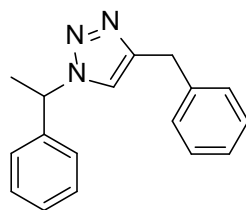
Matrix-Assisted Laser Desorption Ionization-Time-of-Flight (MALDI-ToF) mass spectrometry.

MALDI-ToF MS spectra were obtained using a Bruker MALDI-ToF autoflex III smart beam equipped with a nitrogen laser (337 nm, 200 Hz maximum firing rate) with a mass range of 600–400 000 Da. Spectra were recorded in both reflectron mode (2000–5000 Da) and linear mode (5000–20 000 Da). Trans-2-[3-(4-tert-butylphenyl)-2- methyl-propenyldiene]malononitrile (DCTB;

20 mg mL⁻¹ in THF) was used as the matrix and Ag-(CF₃COO) (1 mg mL⁻¹ in THF) as the cation source. Samples were prepared by co-spotting the matrix (20 mL), Ag (CF₃COO) (1 mL), and polymer (20 mL, 1 mg mL⁻¹ in THF) solutions on the target plate.

2.2.3 Synthetic Procedures

2.2.3.1 Synthesis of 4-benzyl-1-(1-phenylethyl)-1H-1,2,3-triazole ligand.



This ligand was synthesised according to our previous method.²⁹

2.2.3.2 Synthesis of prop-2-ynyl-2-(butylthiocarbonothioylthio)-2-methylpropanoate alkyne RAFT (1)

First, 2-(butylthiocarbonothioylthio)-2-methylpropanoic acid was prepared as follows. Butyl mercaptan (1.00 g, 7.35×10⁻³ mol) was added to a stirred suspension of K₃PO₄ (1.72 g, 8.09 mmol) in acetone (20 mL) and stirring for 1 h. CS₂ (1.68 g, 22.06×10⁻³ mol) was added, and the solution turned bright yellow. After stirring for a further 2 h, 2-bromoisobutyric acid (1.26 g, 7.35×10⁻³ mol) was added and KBr instantaneously precipitated. After stirring overnight, the suspension was filtered and the cake washed with acetone (2 × 20 mL). After removing the solvent from the filtrate under reduced pressure, the resulting yellow residue was purified by column chromatography on silica using a petroleum ether (37– 55 °C)–ethyl acetate gradient to yield a bright yellow oil (96%) that crystallised on refrigeration. Alkyne RAFT agent (1) was synthesised as follows: 2-(butylthiocarbonothioylthio)-2- methylpropanoic acid (2.0 g 7.92×10⁻³ mol), DCC (1.96 g, 9.5×10⁻³ mol) and DMAP (0.049 g, 0.79×10⁻³ mol) were introduced in a round bottom flask and 35 mL DCM was added to dissolve all the components. The solution was cooled to 0 °C in an ice bath and stirred under argon for 30 min. Propargyl alcohol (0.49 g, 8.77×10⁻³ mol) was added drop-wise and the solution was stirred under argon atmosphere. After 48 h, DCM was removed in vacuum. The residue was dissolved in ether and filtered, and the solvent removed by rotary evaporator. The organic yellow oil was then further purified by column chromatography (eluent: ethyl acetate (10%)

+ petroleum spirit (90%)) using silica as stationary phase. The first fraction was collected and solvent was removed by rotary evaporator. The yield was calculated to be 85.5%. $^1\text{H NMR}$ (δ , ppm, CDCl_3): 0.95 (t, 3H, $\text{CH}_3\text{CH}_2\text{CH}_2$), 1.45 (m, 2H, $\text{CH}_3\text{CH}_2\text{CH}_2$), 1.65 (2H, p, $\text{CH}_3\text{CH}_2\text{CH}_2$), 1.69 (3H, s, SCH_3COO) 2.45 (m, H, $\text{OCH}_2\text{C}\equiv\text{CH}$), 3.28 (t, 2H $\text{CH}_2\text{CH}_2\text{CH}_2\text{S}$), 4.69 (m, 2H, $\text{OCH}_2\text{C}\equiv\text{CH}$).

2.2.3.3 Synthesis of RAFT-PSTY₃₆-≡ (2) by RAFT polymerization.

Bulk polymerization of styrene was conducted to synthesise alkyne functional polystyrene with a targeted molecular weight of 4000. For a typical polymerization, alkyne RAFT (**1**, 0.5 g, 1.72×10^{-3} mol) and AIBN (0.028 g, 0.17×10^{-3} mol) were dissolved in 20 mL of styrene (18.12 g, 173.98×10^{-3} mol). The solution was purged with argon for 30 min, and then placed into a temperature controlled oil bath at 65 °C. After 15 h, the conversion was found to be 38% by $^1\text{H NMR}$. The polymerization was stopped after 15 h 30 min by quenching reaction in ice bath. The viscous solution was dissolved in DCM, precipitated in MeOH and filtered – this was repeated three times to remove monomer. The polymer was dried overnight and characterised by SEC, $^1\text{H NMR}$ and MALDI-ToF. ($M_n = 4110$, PDI = 1.08 (SEC-RI calibrated using narrow monodisperse polystyrene standards in tetrahydrofuran) and triple detection SEC ($M_n = 4270$, PDI = 1.05).

2.2.3.4 Synthesis of Epo-PSTY₃₆-≡ (3).

A typical Michael addition reaction was run as follows: RAFT-PSTY₃₆-≡, **2** (6.0 g, 1.5×10^{-3} mol), glycidyl methacrylates (4.0 mL, 30.0×10^{-3} mol) and TCEP (43 mg, 0.3×10^{-3} mol) were dissolved in 40 mL of dry DMF in a 100 mL Schlenk flask. In another flask, TEA (1.0 mL, 4.5×10^{-3} mol) and hexylamine (1.0 mL, 4.5×10^{-3} mol) were mixed in 5 mL of dry DMF. Both the flasks were purged with argon for 30 min and the amine solution was transferred to the polymer solution using a double tip needle by applying argon pressure. The reaction was run under argon atmosphere for 24 h. The polymer solution was then precipitated in MeOH and filtered, and repeated to remove impurities. The polymer was dried overnight and characterised by SEC, $^1\text{H NMR}$, ATR-FTIR and MALDI-ToF. ($M_n = 4150$, PDI = 1.08 (SEC-RI calibrated using narrow monodisperse polystyrene standards in THF) and triple detection SEC ($M_n = 4060$, PDI = 1.05).

2.2.3.5 Synthesis of N₃-PSTY₃₆-≡ (4).

Epo-PSTY₃₆-≡ **3** (5.0 g, 1.25×10^{-3} mol), NaN_3 (0.81 g 12.5×10^{-3} mol) and NH_4Cl (0.67 g, 12.5×10^{-3} mol) were added in 40 mL of DMF. The reaction was carried out under argon atmosphere at 50 °C for 24 h. The turbid solution was then added in 300 mL of DCM and filtered to remove salts. The volume of DCM was decreased by rotary evaporator and polymer precipitated in MeOH and

filtered. The polymer was dried overnight and characterised by SEC, ^1H NMR, ATR-FTIR and MALDI-ToF. ($M_n = 4270$, PDI = 1.08 (SEC-RI calibrated using narrow monodisperse polystyrene standards in THF) and triple detection SEC ($M_n = 4090$, PDI = 1.05).

2.2.3.6 Synthesis of *c*-PSTY₃₆-OH (**5**).

A solution of N₃-PSTY₃₆-≡ **4** (0.5 g, 0.125×10^{-3} mol) in 25 mL of dry toluene was purged with argon for 30 min to remove oxygen. This polymer solution was added via syringe pump at a flow rate of 0.1 mL min^{-1} to a deoxygenated solution of Cu(I)Br (0.896 g, 6.25×10^{-3} mol) and PMDETA (1.31 mL, 6.25×10^{-3} mol) in 25 mL toluene at 25 °C. After the addition of polymer solutions, which was 4.17 h, the reaction mixture was further stirred for 3 h. At the end of this period (i.e., feed time plus an additional 3 h), toluene was evaporated and the copper salts were removed through CHCl₃-water extraction. The residual copper salts were removed by passage through activated basic alumina column. The polymer was recovered by precipitation into MeOH (20 fold excess to polymer solution) and then by filtration. The polymer was dried in vacuo for 24 h at 25 °C. The purity of cyclic polymer was 95%, which was determined from the simulation of the MWD by the LND method using the experimental M_n and PDI values of the linear polymer **4** and the hydrodynamic change (ΔHDV) of 0.76. The procedure was then repeated. The crude products were purified by preparative SEC ($M_n = 2910$, PDI = 1.06) and triple detection SEC ($M_n = 4040$, PDI = 1.04).

2.2.3.7 Synthesis of *c*-PSTY₃₆-Br (**6**).

c-PSTY₃₆-OH, **5** (1.0 g, 0.25×10^{-3} mol), TEA (1.74 mL, 12.5×10^{-3} mol) and 15 mL of dry THF were added under an argon blanket to a dry Schlenk flask that has been flushed with argon. The reaction was then cooled on ice. To this stirred mixture, a solution of 2-bromopropionyl bromide (1.31 mL, 12.5×10^{-3} mol) in 5 mL of dry THF was added drop wise under argon via an air-tight syringe over 5 min. After stirring the reaction mixture for 48 h at room temperature, the polymer was precipitated into MeOH, filtered and washed three times with MeOH. The polymer was dried for 24 h in high vacuum oven at 25 °C. The polymer was characterised using SEC (both PSTY standards and triple detection), ^1H NMR, ATR-FTIR and MALDI-ToF.

2.2.3.8 Synthesis of *c*-PSTY₃₆-N₃ (**7**).

c-PSTY₃₆-Br, **6** (1.0 g, 0.25×10^{-3} mol) was dissolved in 15 mL of DMF in a reaction vessel equipped with magnetic stirrer. To this solution, NaN₃ (0.163 g, 2.5×10^{-3} mol) was added and the mixture stirred for 17 h at room temperature. The polymer was precipitated into MeOH, recovered by vacuum filtration and washed exhaustively with water and MeOH, then dried in vacuo for 24 h

at 25 °C. The polymer was characterised using SEC (both PSTY standards and triple detection), ¹H NMR, ATR-FTIR and MALDI-ToF.

2.2.3.9 Kinetic studies in the synthesis of dicyclic PSTY by one pot.

c-PSTY₃₆-N₃, **7** (0.02 g, 0.005×10⁻³ mol), propargyl ether (0.26 μL, 0.0025×10⁻³ mol; from a stock solution prepared by adding 5.2×10⁻³ mL propargyl ether in 10 mL toluene) and PMDETA (5.22×10⁻³ mL 0.025×10⁻³ mol) were dissolved in 0.5 mL of dry toluene to a vial. CuBr (0.0036 g, 0.025×10⁻³ mol) was added in a 10 mL Schlenk flask equipped with magnetic stirrer. Both of the vessels were purged with argon for 12 min and the polymer solution was transferred to CuBr flask using double tipped needle by applying argon pressure. The reaction mixture was purged with argon for further 2 min and the flask was placed in a temperature controlled oil bath at 25 °C. After a certain time interval, aliquots were taken and analyzed by SEC. Kinetic studies using CuBr in DMF and CuBr–triazole in toluene followed the same procedure.

2.2.3.10 Kinetic studies in the synthesis tricyclic PSTY by one pot.

c-PSTY₃₆-N₃, **7** (0.02 g, 0.005×10⁻³ mol), tripropargylamine (0.25×10⁻³ mL, 0.0017×10⁻³ mol; from a stock solution prepared by adding 5.0×10⁻³ mL tripropargylamine in 10 mL toluene) and PMDETA (5.22×10⁻³ mL, 0.025×10⁻³ mol) were dissolved in 0.5 mL of dry toluene to a vial. CuBr (0.0036 g, 0.025×10⁻³ mol) was added in a 10 mL Schlenk flask equipped with magnetic stirrer. Both of the vessels were purged with argon for 12 min, and the polymer solution was transferred to CuBr flask using double tipped needle by applying argon pressure. The reaction mixture was purged with argon for a further 2 min and the flask was placed in a temperature controlled oil bath at 25 °C. After a certain time interval, aliquots were analyzed by SEC. Kinetic studies using CuBr in DMF and CuBr–triazole in toluene followed the same procedure.

2.2.3.11 Synthesis of dicyclic and tricyclic PSTY by one pot

Synthesis of (c-PSTY)₂ (**8**). c-PSTY₃₆-N₃, **7** (0.04 g, 0.01×10⁻³ mol) and propargyl ether (0.62×10⁻³ mL, 0.006×10⁻³ mol; from a stock solution prepared by adding 6.2×10⁻³ mL propargyl ether in 5 mL DMF) were dissolved in 0.5 mL of dry DMF to a vial. CuBr (0.007 g, 0.05×10⁻³ mol) was added in a 10 mL Schlenk flask equipped with magnetic stirrer. Both of the vessels were purged with argon for 12 min, and the polymer solution was transferred to CuBr flask using double tipped needle by applying argon pressure. The reaction mixture was purged with argon for further 2 min and the flask was placed in a temperature controlled oil bath at 25 °C. After 30 min, an aliquot was analysed by SEC. The reaction was stopped after 1 h, and the mixture diluted in 2.0 mL of THF. The solution was then passed through activated basic alumina column to remove copper. Solvent

was removed by rotary evaporator, precipitated in MeOH, filtered and dried overnight. The crude product was then purified by preparative SEC.

Synthesis of (c-PSTY)₃ (9). c-PSTY₃₆-N₃, **7** (0.06 g, 0.015×10⁻³ mol), tripropargylamine (0.74×10⁻³ mL, 0.005×10⁻³ mol; from a stock solution prepared by adding 7.4×10⁻³ mL tripropargylamine in 5 mL toluene) and triazole (0.019 g, 0.075×10⁻³ mol) were dissolved in 0.5 mL of dry toluene to a vial. CuBr (0.011 g, 0.075×10⁻³ mol) was added in a 10 mL Schlenk flask equipped with magnetic stirrer. Both of the vessels were purged with argon for 12 min and the polymer solution was transferred to CuBr flask using double tipped needle by applying argon pressure. The reaction mixture was purged with argon for further 2 min and the flask was placed in a temperature controlled oil bath at 25 °C. After 10 h, an aliquot was analyzed by SEC. The reaction was stopped after 12 h, and the mixture diluted with 2.0 mL of THF. The solution was then passed through activated basic alumina column to remove copper. Solvent was removed by rotary evaporator, precipitated in MeOH, filtered and dried overnight. The crude product was then purified by preparative SEC.

2.3 Results and discussion

Synthesis of the precursor linear polystyrene

A linear polystyrene (PSTY, **2**) with an alkyne and trithioester on either end of the polymer chain was synthesised using the RAFT technique (Scheme 2.1). The polymerization was carried out in bulk at 65 °C and stopped after 15.5 h with a conversion of 38%, number-average molecular weight (M_n) of 4110, and polydispersity of 1.08 (Table 2.1). There was no requirement to protect the alkyne group during the polymerization as the M_n was close to theory and with a low polydispersity. The SEC trace showed no trace of higher molecular weight polymer from alkyne–alkyne coupling (see curve a in Fig. 2.1(A)). The next step was to convert the trithioester moiety on the polymer to an epoxide in a one-pot reaction to produce **3**. A solution of hexylamine in dry DMF was added slowly to a mixture of polymer **2**, glycidyl methacrylate, and TCEP (to eliminate disulfide formation) in dry DMF. After 24 h, the molecular weight distribution (MWD) remained essentially unchanged (curve b in Fig. 2.1(A)), and there was no detection of the RAFT end-group at 311 nm as shown in Fig. 2.1(B).

The direct azidation of the epoxide ring is a key feature to make cyclic polymers with an alcohol functionality required for further coupling reactions. The ring-opening of the epoxide on **3** (Epo-PSTY-≡) in the presence of the nucleophile, NaN₃, gave near quantitative ring-opening and formation of an azide and alcohol after 24 h at 50 °C to give **4** (N₃-PSTY-≡). This was supported by

^1H NMR analysis (Fig. 2.2), in which the signals at 3.23, 2.84, and 2.64 ppm attributed to the methine and methylene protons of the epoxide disappeared with the formation of new peaks at 3.73–4.07 ppm, representing the methylene protons next to the ester groups and the methine proton adjacent to the hydroxyl groups (CO_2CH_2 and CH-OH), and at 3.30 and 3.32 ppm representing methylene protons adjacent to azide groups (CH_2N_3).

Table 2.1 RI and triple detection molecular weight distributions data for PSTY starting, chain end modified and click coupled polymers

Polymer code	RI Detection ^a			Triple Detection ^b		
	M_n	M_p	PDI	M_n	M_p	PDI
RAFT-PSTY-≡ (2)	4110	4317	1.08	4270	4490	1.05
Epo-PSTY-≡ (3)	4150	4353	1.08	4060	4190	1.05
N ₃ -PSTY-≡ (4)	4270	4425	1.08	4090	4210	1.05
c-PSTY-OH (5)	2910	2930	1.06	4040	4130	1.04
c-PSTY-Br (6)	3180	3210	1.06	4280	4470	1.03
c-PSTY-N ₃ (7)	3230	3350	1.07	4680	4720	1.02
(c-PSTY) ₂ (8)	6490	6850	1.05	7830	8300	1.02
(c-PSTY) ₃ (9)	8770	9180	1.05	11000	13370	1.05

^a The data was acquired using SEC (RI detector) and is based on PSTY calibration curve. ^b The data was acquired using triple detection SEC.

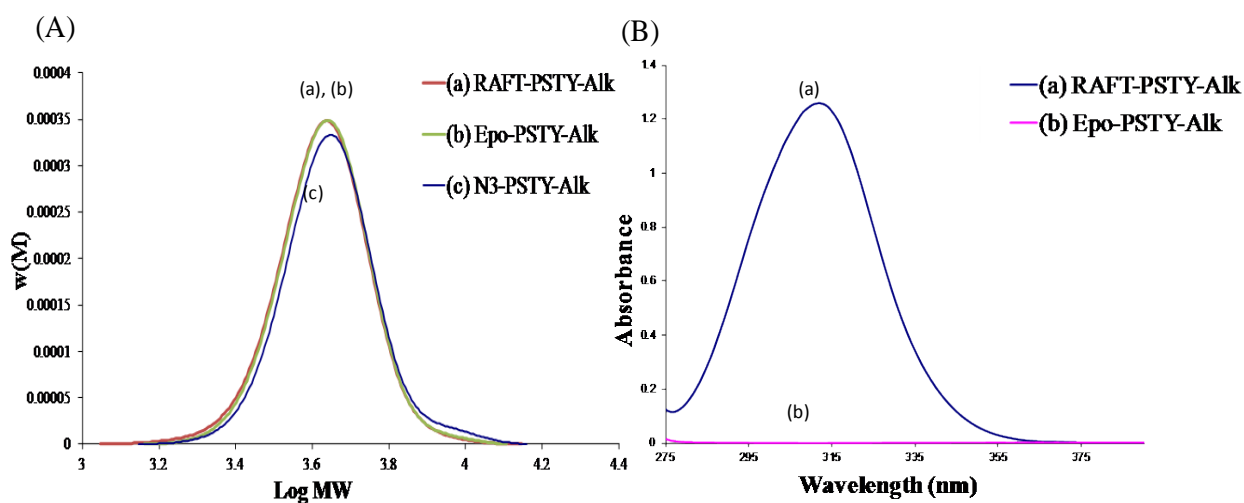


Fig. 2.1 (A) SEC chromatograms for cyclization of (a) RAFT-PSTY-Alk **2** (b) Epo-PSTY-Alk, **3** and (c) N₃-PSTY-Alk, **4**, SEC analysis based on polystyrene calibration curve. (B) UV-vis spectra

at 311 nm of (a) RAFT-PSTY-Alk, **2** and (b) the aminolyzed Epo-PSTY-Alk, **3**, elution solvent THF.

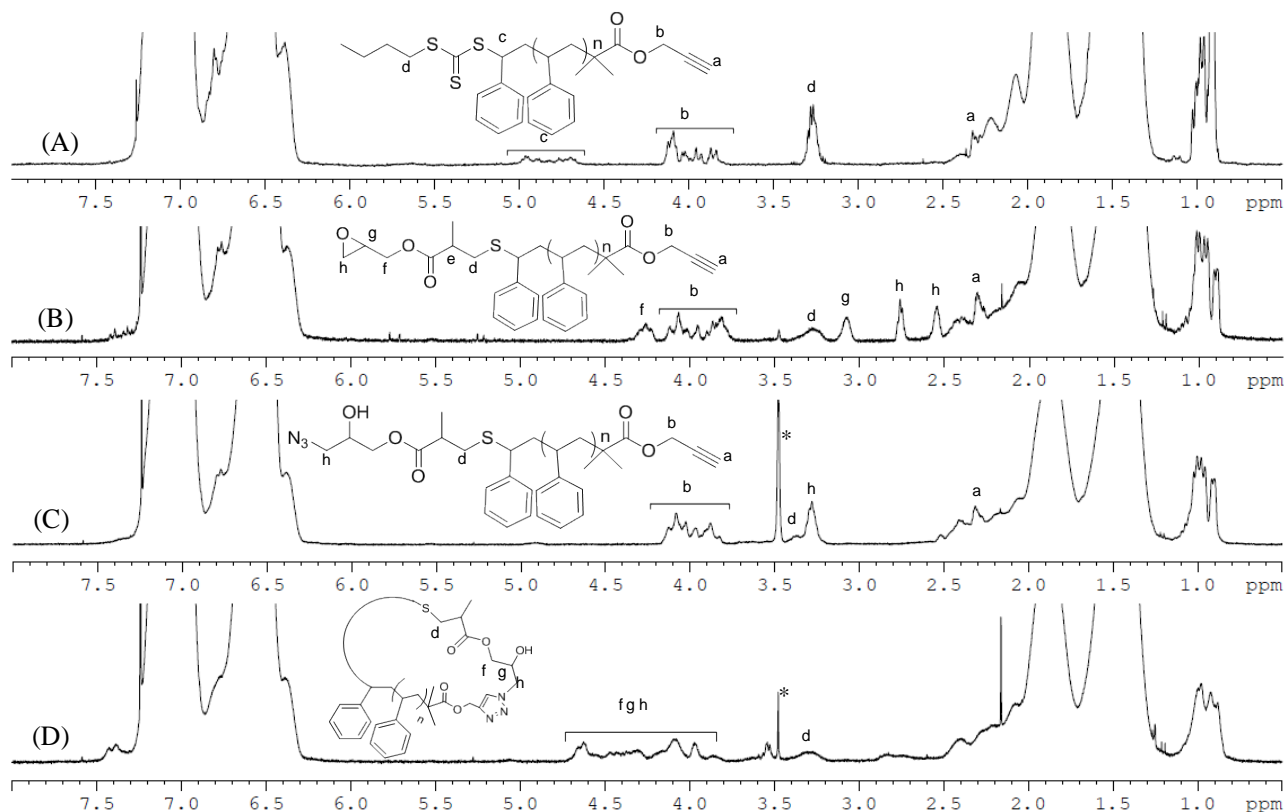


Figure 2.2. $^1\text{H-NMR}$ spectra of (A) RAFT-PSTY-Alk **2** (B) Epo-PSTY-Alk **3** (C) N_3 -PSTY-Alk **4** and (D) c-PSTY-OH **5** in CDCl_3 (* methanol).

Cyclization of linear polystyrene and chain-end modification

Cyclization of **4** to give **5** (c-PSTY-OH) was carried out by feeding a solution of **4** (0.5 g in 25 mL) dissolved in toluene at a feed rate of 0.1 mL min^{-1} into the reaction mixture containing Cu(I)Br-PMDETA (as the catalyst for the CuAAC reaction) and 25 mL of toluene at $25 \text{ }^\circ\text{C}$. After the feed, the reaction was stirred for a further 30 min to ensure complete conversion of starting polymer **4**. The formation of **5** was evident from a shift to a lower MWD to that of the starting linear species. Such a reduction in hydrodynamic volume is typical for cyclic PSTY chains due to their more compact topology.^{17,30} The cyclic purity of **5** was calculated from the ratio of the cyclic product to that of all polymer species determined from the normalised weight distribution using the Gaussian simulation (Fig. 2.3). The experimental MWD ($w(M)$) after cyclization was simulated using the LND method^{19,24} using the experimental M_n and PDI values of the linear polymer **4** (N_3 -PSTY-Alk) and the hydrodynamic change (ΔHDV) of 0.76 (curve d in Fig. 2.3). The LND simulation provides

a sensitive method to analyze the amount of monocyclic formed after the cyclization reaction. It can be seen that the simulated MWD overlaps near perfectly with the MWD after cyclization, allowing us to calculate a 95% purity for the monocyclic polymer. Purification of **5** by preparative SEC gave essentially pure c-PSTY-OH ($M_n = 2950$, PDI = 1.06; see Table 2.1) in which all higher molecular weight polymers were removed.

When the purified polymer was subsequently injected into the triple detection SEC (to obtain an absolute MWD independent of topology), it gave an essentially identical MWD to that of the starting linear species **4**, further confirming the production of cyclic polymer. The ^1H NMR (Fig. 2.2(D)) and ATR-FTIR (see appendix A) of purified **5** showed near quantitative loss of azide groups. Compared to the linear PSTY precursor **4**, new resonance peaks between 4.2 and 4.7 ppm were observed with the disappearance of protons adjacent to azide group at 3.3 ppm, suggesting the near quantitative loss of starting linear polystyrene due to the formation of a triazole ring.

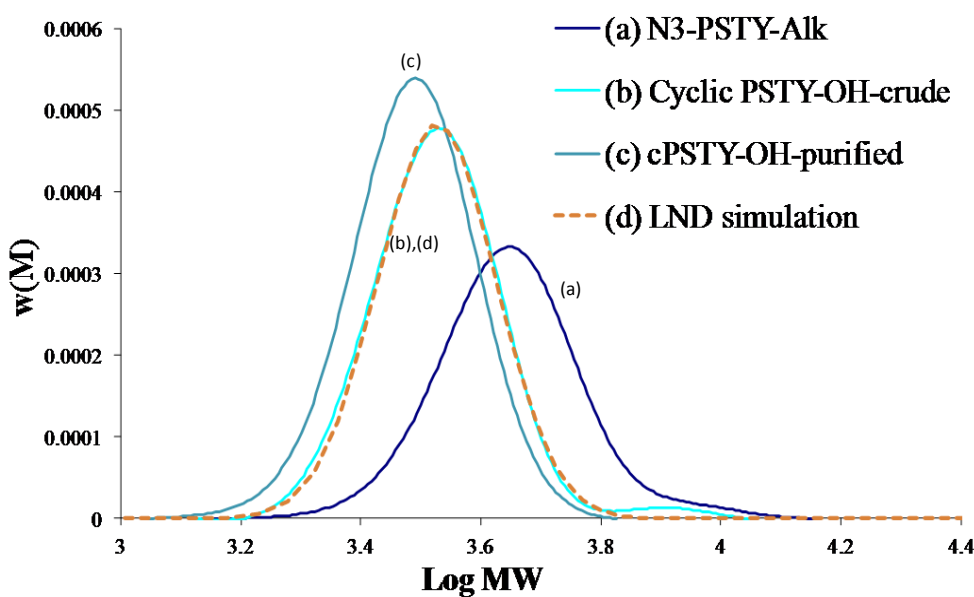


Figure 2.3: SEC chromatograms of (a) N₃-PSTY-Alk **4**, (b) c-PSTY-OH, **5** crude, (c) c-PSTY-OH **5** after purification by preparatory SEC and (d) LND simulation of **5** with hydrodynamic volume change of 0.76. SEC analysis based on polystyrene calibration curve.

The -OH functionality on **5** was then converted to cyclic PSTY azide via a two-step reaction (Scheme 2.1): first, bromination using excess of 2-bromopropionyl bromide, and second, azidation to form **6**. The bromo functional cyclic product was confirmed by MALDI-ToF spectroscopy acquired in reflectron mode. The molecular weight distribution and expanded spectra between 4100 and 4500 were given in Fig. 2.4, exhibiting a theoretical value $[M + \text{Ag}^+]$ of 4335.22 that was nearly identical with experimental value $[M + \text{Ag}^+]$ 4335.02, indicating quantitative conversion of

hydroxyl of cyclic PSTY to bromo functional cyclic PSTY **6** (c-PSTY-Br). In addition, there was no distinctive change in the SEC traces after functionalization to the bromine and azide groups (see Fig. A7 in appendix A), suggesting high end-group functionality.

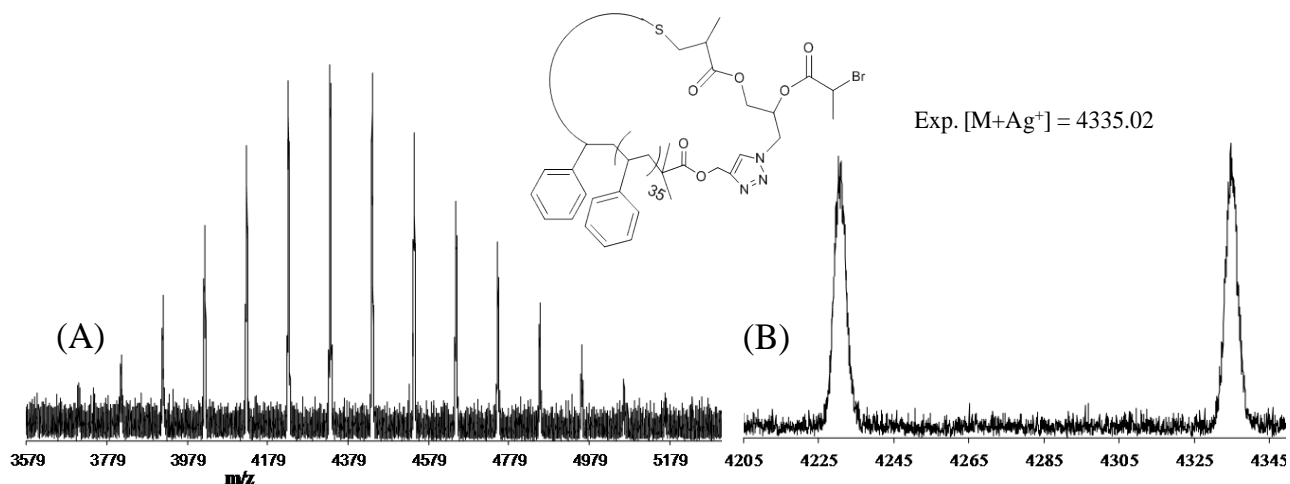


Figure 2.4. MALDI-ToF mass spectrometry of cPSTY-Br, **6** with Ag salt as cationization agent and DCTB matrix in reflectron mode: (A) full molecular weight distribution, (B) expanded spectrum; calculated $[M+Ag^+] = 4335.22$, $DP_n = 36$.

Synthesis of 2- and 3-arm topologies in one-pot built from cyclic polymer

The 2- and 3-arm stars were coupled in a one pot using c-PSTY- N_3 (**7**, 20 mg in 0.5 mL, 1 eq.) and either propargyl ether (0.5 eq.) or tripropargylamine (0.33 eq.) at 25 °C (Scheme 2.1). Conventional experimental CuAAC conditions of Cu(I)Br and PMDETA in toluene were first used in the ‘click’ reaction. After 10 min, the SEC trace (curve c in Fig. 2.5(A)) showed the formation of a distribution at twice the molecular weight of **7**, corresponding to the 2-arm species. However, with time this peak decreased and the distribution corresponding to the **7** increased (Fig. 2.5(A)), suggesting the susceptibility of the 2-arm species to cleavage. This result was further supported from the coupling efficiency which decreased from approximately 80% after 10 min to near full cleavage of the 2-arm species after 24 h (curve a in Fig. 2.6(A)). The cleavage of the 2-arm star occurred at the linker between the cyclic arms since no linear PSTY was observed in the SEC traces, leaving the c-PSTY intact. The presence of base (i.e. PMDETA ligand) most likely cleaves the ester group after ‘clicking’ with propargyl ether, and has been the cause of degradation in other systems.^{31,32} A similar result was found when **7** was coupled via the CuAAC with tripropargylamine (Fig. 2.5(B) and 2.6(B)).

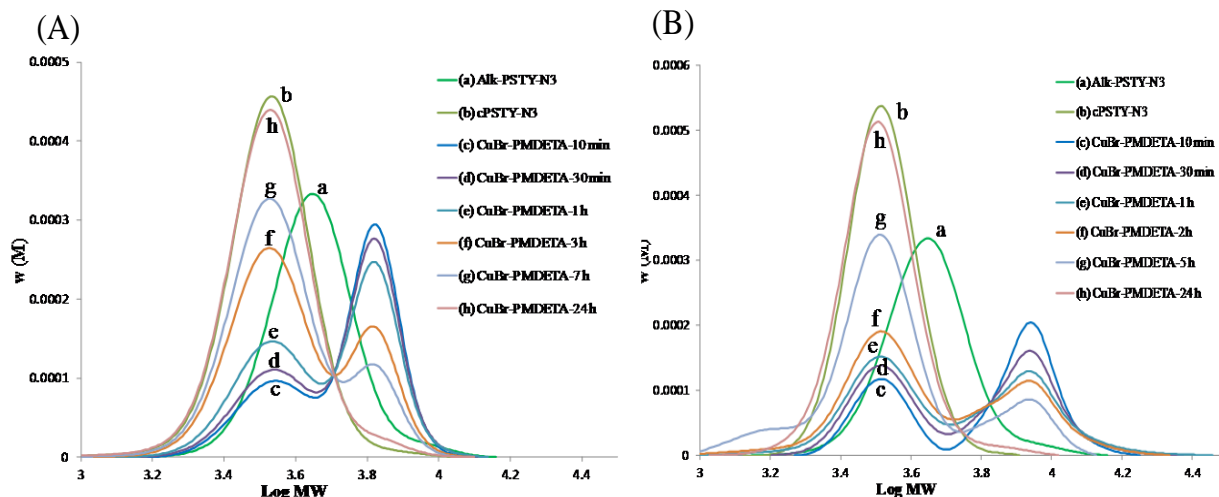


Figure 2.5: SEC chromatograms for the kinetics of (A) dicyclic cleavage using CuBr/PMDETA in toluene; (a) Alk-PSTY-N₃ **4** (b) cPSTY-N₃ **7**; degradation after (c) 10 min (d) 30 min (e) 1 h (f) 3 h (g) 7 h and (h) 24 h; (B) tricyclic cleavage using CuBr/PMDETA in toluene; (a) Alk-PSTY-N₃ **4** (b) c-PSTY-N₃ **7**; degradation after (c) 10 min (d) 30 min (e) 1 h (f) 2 h (g) 5 h and (h) 24 h. SEC analysis based on polystyrene calibration curve.

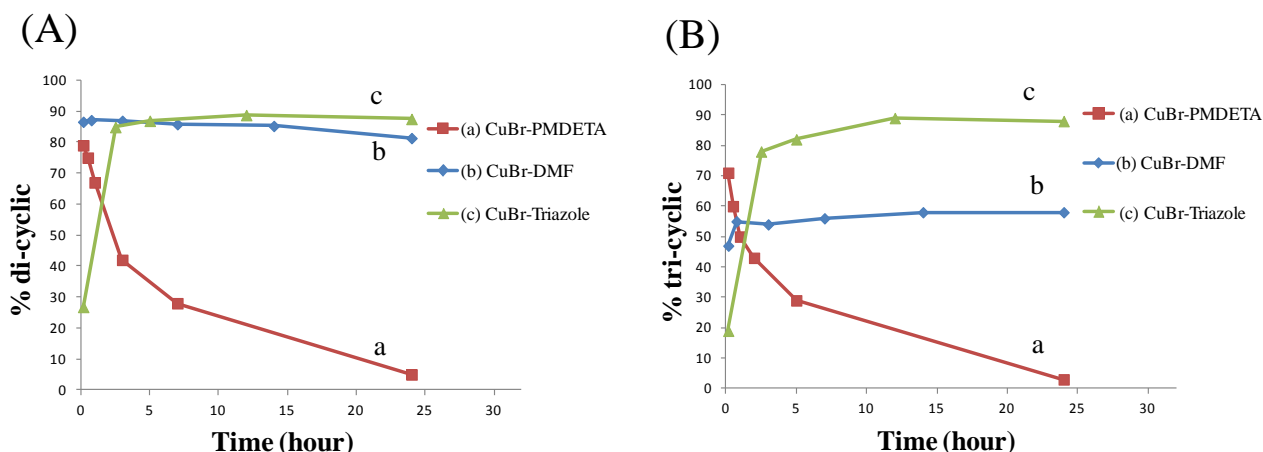


Figure 2.6: (A) The percent of di-cyclic formed *versus* time using (a) CuBr-PMDETA in toluene, (b) CuBr in DMF and (c) CuBr-triazole in toluene; (B) The percent of tri-cyclic formed *versus* time using (a) CuBr-PMDETA in toluene, (b) CuBr in DMF and (c) CuBr-triazole in toluene.

In the next experiment, we exchanged the PMDETA for the neutral triazole ligand (4-benzyl-1-(1-phenylethyl)-1H-1,2,3-triazole)²⁹ and carried out the CuAAC reaction in toluene. The results showed that the ‘click’ reaction was slower than with PMDETA and reached a coupling efficiency of close to 90% (curve b in Fig. 2.6(A) and (B)). The data also showed no degradation of either the 2- or 3-arm species over time. In another experiment, in which the reaction was carried out in DMF without any ligand (i.e. ligand-free), the 2-arm species formed in less than 1 h with approximately 90% coupling efficiency (curve c in Fig. 2.6(A)). It has been established previously that the click

reaction can be quite efficient in the absence of ligand if the solvent (e.g. DMF) can facilitate sufficient solubility of copper catalyst.²⁹ In the case of the 3-arm species (curve c in Fig. 2.6(B)), the coupling efficiency was close to 50% after 1 h, and increased to 60% after 24 h. This reaction was repeated, giving a similar result. The reason for such a low coupling efficiency under these conditions is not clear, but could be due to DMF reducing the enhanced CuAAC rates from adjacent triazole rings in the linker due to DMF's preferential binding to CuBr.²⁹

Based on the kinetic analysis above, we chose the ligand-free conditions of CuBr in dry DMF to catalyze the CuAAC coupling reaction between c-PSTY-N₃ (**7**, 0.04 g in 0.5 mL, 1 eq.) and propargyl ether to form the 2-arm species **8** (c-PSTY)₂. The formation of **8** at 25 °C after 1 h showed a molecular weight distribution at twice that of the starting polymer as shown in Fig. 2.7(A) (curve b). Fitting a LND (curve c) to the MWD of the crude SEC trace of **8** allowed us to calculate the purity and coupling efficiency to be 84% (Table 2.2). This crude polymer was purified using preparative SEC (curve d), removing all low molecular weight starting polymer. The formation of 2-arm polymer structure in a one-pot reaction was further confirmed by ¹H NMR (Fig. 2.8) and MALDI ToF (see appendix A13). The ¹H NMR spectra in Fig. 2.8 showed a near quantitative loss of azide group as determined from the loss of the peak for the proton adjacent to the azide moiety (denoted as i at 3.82, COCH(CH₃)N₃) and the appearance of peaks at 4.65 denoted as k for CH₂-O of propargyl ether.

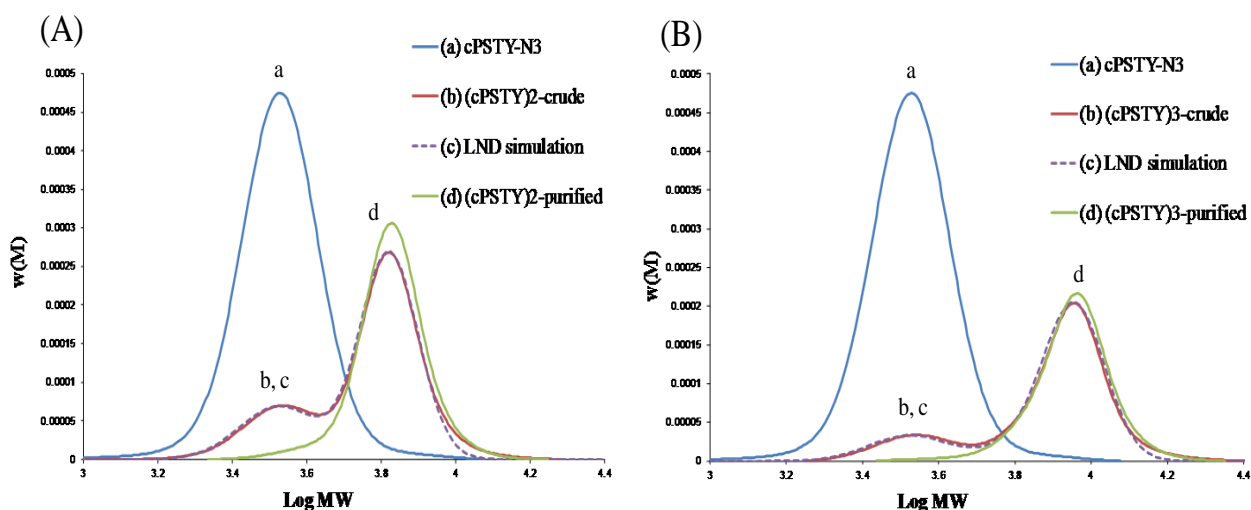


Figure 2.7: SEC chromatograms of CuAAC coupling reactions by one pot using cPSTY-N₃ **7** with (A) propargyl ether in CuBr/DMF to produce (c-PSTY)₂ **8**; (a) c-PSTY-N₃ **7**; (b) (c-PSTY)₂-crude and (c) LND simulation of **8**. (d) (c-PSTY)₂ **8** after preparatory SEC purification. (B) tripropargylamine in CuBr/triazole to produce (c-PSTY)₃ **9**; (a) c-PSTY-N₃ **7**; (b) (c-PSTY)₃-crude and (c) LND simulation of **9** with hydrodynamic volume change of 0.91. (d) (c-PSTY)₃ **9** after preparatory SEC purification. All chromatograms are based on PSTY calibration.

Based on the poor coupling efficiency for the 3-arm star (i.e. 0.06 g of **7** in 0.5 mL of DMF and tripropargylamine) using CuBr in DMF from the kinetic analysis above, we carried out the CuAAC reaction using CuBr–triazole. The kinetic data from Fig. 2.6(B) suggested that the CuAAC reaction to form **9** was complete in approximately 10 h. The SEC trace after 10 h showed a molecular weight distribution at triple that of the starting polymer as shown in Fig. 2.7(B) (curve b). The full experimental MWD of crude **9** was fit using the LND method (curve c), giving a 3-arm star purity of 82% (Table 2.2) and a small amount of 2-arm (dicyclic, 11%) resulting in a coupling efficiency of close to 90%. Purification of the crude **9** by preparative SEC gave near pure 3-arm star as shown in curve d (Fig. 2.7(B)). The ^1H NMR spectra in Fig. 2.8 showed a nearly quantitative loss of azide group as determined from the loss of peak for the proton adjacent to the azide moiety (denoted as i at 3.82, $\text{COCH}(\text{CH}_3)\text{N}_3$).

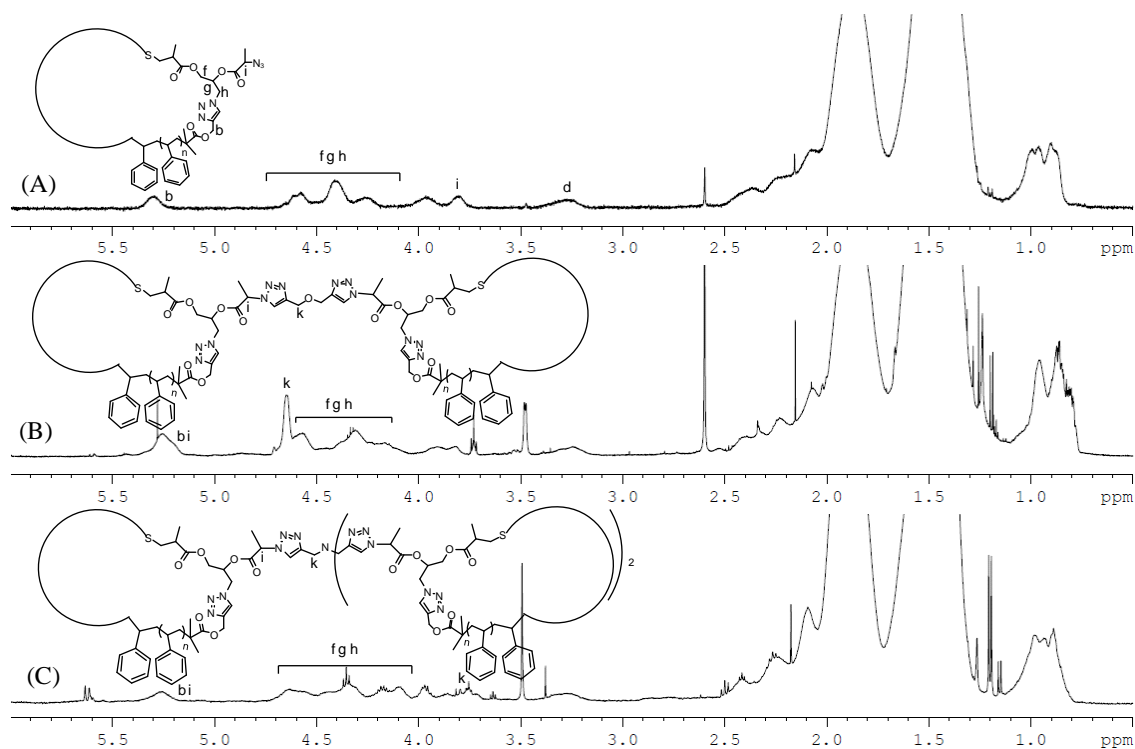


Figure 2.8. 500 MHz ^1H 1D DOSY NMR spectra of (A) c-PSTY- N_3 **7** (B) (c-PSTY) $_2$ **8** and (C) (c-PSTY) $_3$ **9**.

Table 2.2 Click efficiency and molecular weight data for synthesis of dicyclic and tricyclic PSTY

Product	Before purification by prep SEC			After purification by prep SEC						Δ HDV ^f
	Max. Purity ^a %	Purity by SEC ^b	Coupling efficiency ^c	RI (PSTY calibration) ^d			Absolute MW (triple detection) ^e			
				Mn	Mp	PDI	Mn	Mp	PDI	
(c-PSTY) ₂ (8)	100	84.0	84.0	6490	6850	1.05	7830	8300	1.02	0.83
(c-PSTY) ₃ (9)	100	82.0	82.0	8770	9180	1.05	11000	13370	1.05	0.69

^a Maximum purity by theory. ^b Purity determined using LND by Gaussian simulation. ^c Coupling efficiency calculated as follows: $\text{purity (SEC)}^b / \text{max. purity}^a \times 100$. ^d The data acquired using SEC (RI detector) based on PSTY calibration curve. ^e Data acquired using triple detection SEC. ^f Δ HDV = $M_p(\text{RI})/M_p(\text{triple detection})$.

2.4 Conclusions

In conclusion, we have demonstrated a novel approach to produce cyclic polymers by RAFT with functionality required for further coupling to form 2- and 3-arm cyclic stars. Cyclization of the linear RAFT polymer gave cyclic with a purity of 95% as determined by simulating the experimental MWD using the LND method. This method has been found to be accurate for determining the purity of the product and relative amounts of side products and reactants. The alcohol moiety on the cyclic polymer (c-PSTY-OH) was then converted to an azide and ‘clicked’ together using the CuAAC reaction to form either 2- or 3-arm stars. The cyclic arms of the 2- and 3-arm stars degraded to the starting monocyclic polymers when CuAAC coupling was attempted using CuBr–PMDETA in toluene. The best condition to form the stars without degradation was to carry out the CuAAC reaction in either CuBr in DMF solvent or CuBr–triazole in toluene. Our approach to build stars from cyclic RAFT polymers will allow many chemically different polymers to be cyclised, and may provide a new tool to design polymer architecture with greater function.

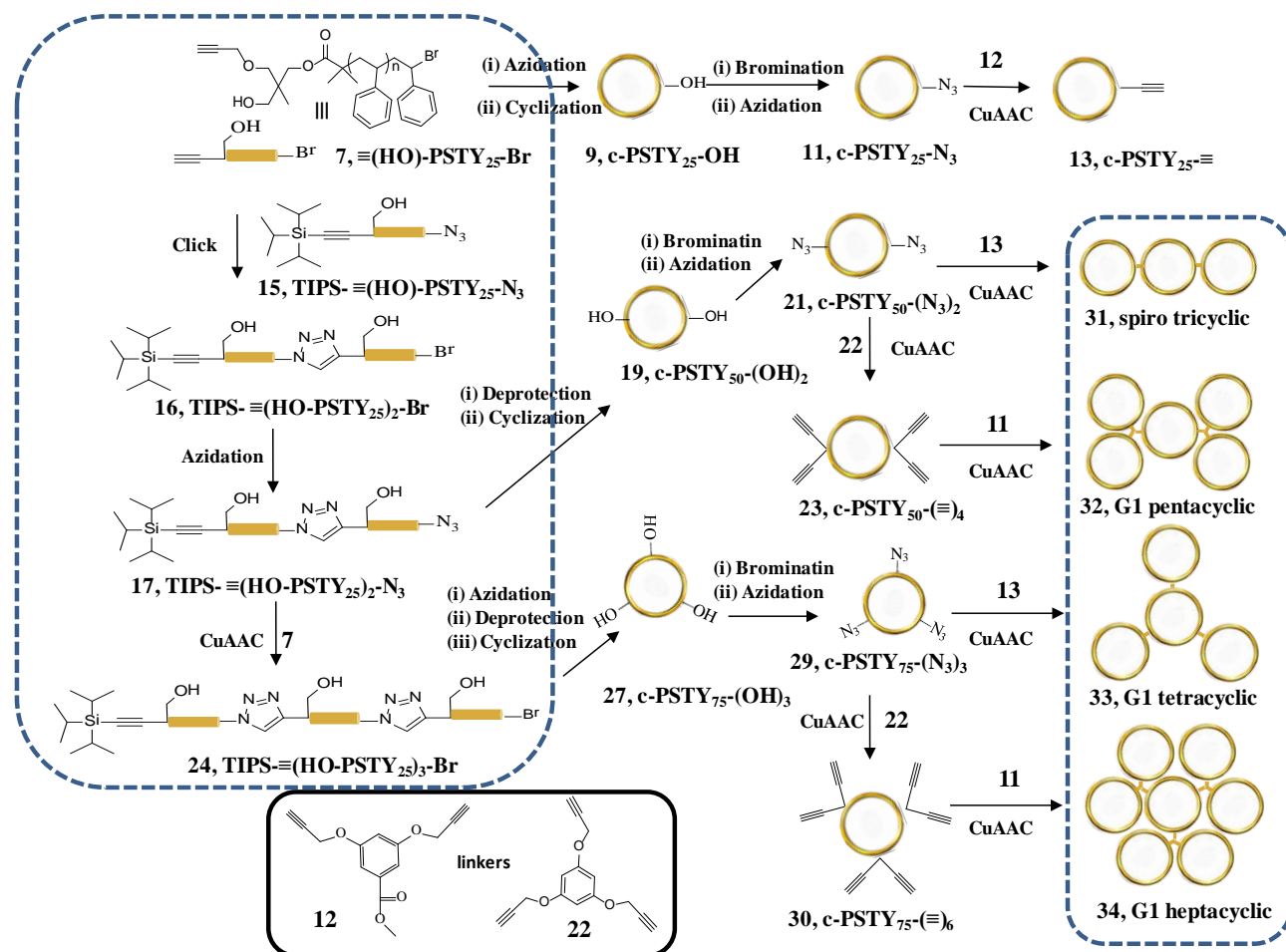
2.5 References

- (1) Hadjichristidis, N.; Pitsikalis, M.; Pispas, S.; Iatrou, H. *Chemical Reviews* **2001**, *101*, 3747-3792.
- (2) Endo, K. In *New Frontiers in Polymer Synthesis*, Kobayashi, S., Ed.; Springer Berlin Heidelberg, 2008, pp 121-183.
- (3) Laurent, B. A.; Grayson, S. M. *Chemical Society Reviews* **2009**, *38*, 2202-2213.
- (4) Kricheldorf, H. R. *Journal of Polymer Science Part A: Polymer Chemistry* **2010**, *48*, 251-284.
- (5) Jia, Z.; Monteiro, M. J. *Journal of Polymer Science Part A: Polymer Chemistry* **2012**, *50*, 2085-2097.
- (6) McLeish, T. *Science* **2002**, *297*, 2005-2006.
- (7) Obukhov, S. P.; Rubinstein, M.; Duke, T. *Physical Review Letters* **1994**, *73*, 1263-1266.
- (8) Orrah, D. J.; Semlyen, J. A.; Ross-Murphy, S. B. *Polymer* **1988**, *29*, 1455-1458.
- (9) Clarson, S. J.; Semlyen, J. A. *Polymer* **1986**, *27*, 1633-1636.
- (10) Qiu, X.-P.; Tanaka, F.; Winnik, F. M. *Macromolecules* **2007**, *40*, 7069-7071.
- (11) Shin, E. J.; Jeong, W.; Brown, H. A.; Koo, B. J.; Hedrick, J. L.; Waymouth, R. M. *Macromolecules* **2011**, *44*, 2773-2779.
- (12) Bannister, D. J.; Semlyen, J. A. *Polymer* **1981**, *22*, 377-381.
- (13) Gan, Y.; Dong, D.; Carlotti, S.; Hogen-Esch, T. E. *Journal of the American Chemical Society* **2000**, *122*, 2130-2131.
- (14) Honda, S.; Yamamoto, T.; Tezuka, Y. *Journal of the American Chemical Society* **2010**, *132*, 10251-10253.
- (15) Lonsdale, D. E.; Monteiro, M. J. *Journal of Polymer Science Part A: Polymer Chemistry* **2011**, *49*, 4603-4612.
- (16) Laurent, B. A.; Grayson, S. M. *Journal of the American Chemical Society* **2006**, *128*, 4238-4239.
- (17) Lonsdale, D. E.; Bell, C. A.; Monteiro, M. J. *Macromolecules* **2010**, *43*, 3331-3339.
- (18) Lonsdale, D. E.; Monteiro, M. J. *Chemical Communications* **2010**, *46*, 7945-7947.
- (19) Jia, Z.; Lonsdale, D. E.; Kulis, J.; Monteiro, M. J. *ACS Macro Letters* **2012**, *1*, 780-783.
- (20) Matyjaszewski, K.; Xia, J. *Chemical Reviews* **2001**, *101*, 2921-2990.
- (21) Percec, V.; Guliashvili, T.; Ladislav, J. S.; Wistrand, A.; Stjern Dahl, A.; Sienkowska, M. J.; Monteiro, M. J.; Sahoo, S. *Journal of the American Chemical Society* **2006**, *128*, 14156-14165.
- (22) Kulis, J.; Bell, C. A.; Micallef, A. S.; Jia, Z.; Monteiro, M. J. *Macromolecules* **2009**, *42*, 8218-8227.
- (23) Jia, Z.; Bell, C. A.; Monteiro, M. J. *Chemical Communications* **2011**, *47*, 4165-4167.

- (24) Bell, C. A.; Jia, Z.; Kulis, J.; Monteiro, M. J. *Macromolecules* **2011**, *44*, 4814-4827.
- (25) Whittaker, M. R.; Goh, Y.-K.; Gemici, H.; Legge, T. M.; Perrier, S.; Monteiro, M. J. *Macromolecules* **2006**, *39*, 9028-9034.
- (26) Shi, G.-Y.; Tang, X.-Z.; Pan, C.-Y. *Journal of Polymer Science Part A: Polymer Chemistry* **2008**, *46*, 2390-2401.
- (27) Goldmann, A. S.; Quémener, D.; Millard, P.-E.; Davis, T. P.; Stenzel, M. H.; Barner-Kowollik, C.; Müller, A. H. E. *Polymer* **2008**, *49*, 2274-2281.
- (28) Tsarevsky, N. V.; Bencherif, S. A.; Matyjaszewski, K. *Macromolecules* **2007**, *40*, 4439-4445.
- (29) Bell, C. A.; Jia, Z.; Perrier, S.; Monteiro, M. J. *Journal of Polymer Science Part A: Polymer Chemistry* **2011**, *49*, 4539-4548.
- (30) Roovers, J.; Toporowski, P. M. *Macromolecules* **1983**, *16*, 843-849.
- (31) Whittaker, M. R.; Urbani, C. N.; Monteiro, M. J. *Journal of the American Chemical Society* **2006**, *128*, 11360-11361.
- (32) Urbani, C. N.; Bell, C. A.; Whittaker, M. R.; Monteiro, M. J. *Macromolecules* **2008**, *41*, 1057-1060.

Chapter 3

Complex Polymer Topologies Built from Tailored Multifunctional Cyclic Polymers



Chapter 3 describes the synthesis of complex polymer structures using multifunctional cyclic polymer combining ATRP and CuAAC reaction. Complex polymer structures, including a spiro tricyclic and 1st generation dendritic structures, were constructed from cyclic polymer building blocks. We described a new method to produce mono-cyclic polymers with hydroxyl groups equally spaced along the polymer backbone. A key synthetic feature was carrying out the CuAAC reaction of telechelic polymer chains in the presence of a bromine group through modulating the Cu(I) activity towards the 'click' reaction over radical formation. This allowed the precise control over the location of the OH-groups. Azidation of the bromine groups and cyclization using a modified feed approach resulted in multifunctional cyclics in high amounts and high purity of greater than 99% of multifunctional mono-cyclic after fractionation. Conversion of the OH-groups to either azide or alkyne functionality produced the central core macromolecule from which the

more complex topologies were built. All four complex topologies, including a spiro tricyclic, and dendritic structures consisting of a G1 pentacyclic, G1 tertacyclic, and a G1 heptacyclic were produced in high amounts with good 'click' efficiencies.

3.1 Introduction

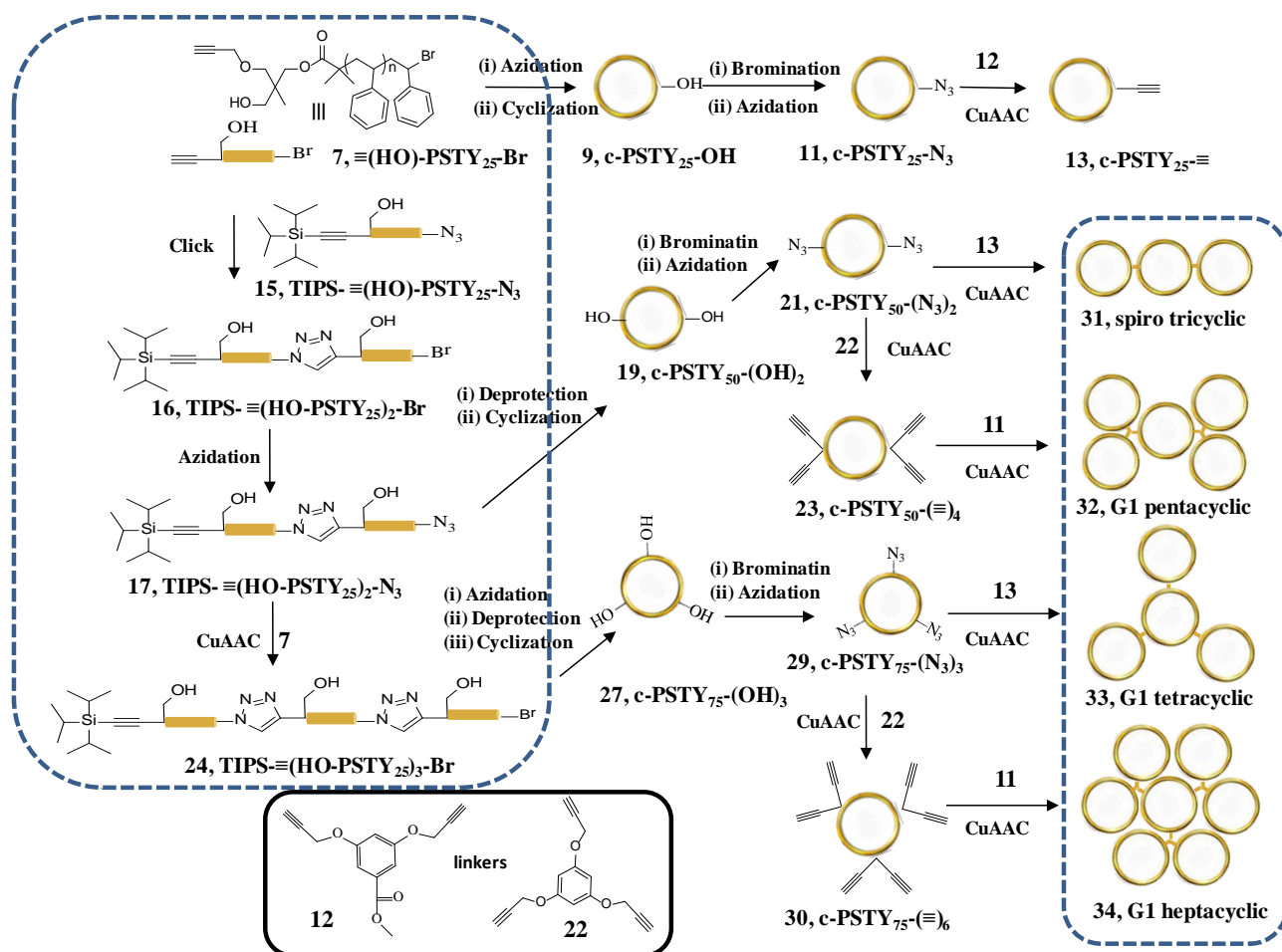
Building complex polymer topologies from polymer building blocks is now possible through the combination of 'living' radical polymerization (LRP)¹ and 'click'²⁻⁴ reactions. This advance in synthetic polymer chemistry has led to the precise control over the architecture to form stars,⁵ dendrimers,⁶⁻⁸ hyperbranched polymers,⁹ multiblock copolymers,¹⁰ and bioconjugates.^{11, 12} Such synthetic protocols enabled the synthesis of the more intriguing cyclic and multicyclic polymers,¹³⁻¹⁷ which through their different diffusion mechanisms and greater compact topology have very different properties to linear polymers.¹⁸ Linear polymers diffuse through a matrix via reptation, in which its path is determined by the chain-ends. In the case of a cyclic polymer with the absence of chain-ends, diffusion is faster with an amoeba-like motion;¹⁹ although the true mechanism of diffusion is yet to be elucidated. Cyclic polymers also have a more compact topology, resulting in a lower hydrodynamic volume (by a factor of ~0.71 for polystyrene) compared to a linear polymer of the same molecular weight.^{20, 21} This shift in hydrodynamic volume is a characteristic feature used to identify the formation of cyclic polymers by size exclusion chromatography (SEC), and can also be used to quantify and separate cyclic polymer species from linear polymer precursors made by the ring-closure method.²²

The ring-closure method represents a straightforward synthetic protocol to link functional chain-ends together on the same polymer chain, forming cyclic or ring polymers.²³⁻²⁷ The advantages of this method include the preparation of monodisperse cyclics, a wide variety of cyclic compositions, and predetermined location of functional groups on the cyclic. It should be noted that other efficient methods for making cyclic polymers have been described.²⁸⁻³² 'Living' radical polymerization has been widely used to form chemically functional telechelic polymers that can then be coupled through 'click' chemistry to form the cyclics. It was recently reported that cyclic polymers with a single chemical functionality could be coupled together to form mikto-arm stars.²² The more complex bridged and fused cyclic topologies could be prepared using a different technique; the elegant electrostatic self-assembly and covalent fixation (ESA-CF) process as first exemplified by Tezuka and coworkers.³³⁻³⁶ The self-assembly of the chain-ends through the electrostatic process, however, requires dilute conditions, followed by a heat treatment to form a covalent bond between the chain-ends.

Our laboratory has described the optimal conditions for the general 'click' ring-closure method.^{14, 37} Utilizing the Jacobson-Stockmayer equation,³⁸ we produced significantly higher concentrations of high purity cyclic polymer within less than 9 min under feed conditions, and the cyclic polymer could be easily separated and isolated from the linear precursor by preparative SEC. The aim of this current work was to develop a new synthetic strategy to produce multifunctional cyclic polymers through the LRP/'click' ring-closure method at high concentrations. The functional groups on the cyclics were then coupled to other polymer building blocks to produce complex structures. The advantage of producing polymers by LRP are the wide range of polymer types and compositions, allowing for greater design and control over polymer topology, chemical composition and functionality.

Here, we elaborate a new synthetic approach to form cyclic polymers with two and three functional hydroxyl groups equidistant from each other (see polymers **19** and **27** in Scheme 3.1) via the LRP/'click' procedure. The hydroxyl groups were converted to azides or alkynes and then coupled through the copper catalyzed azide-alkyne cycloaddition (CuAAC) reaction with monofunctional cyclic to produce complex structures, including a spiro tricyclic and 1st generation dendritic structures (see Scheme 3.1). To produce the precursor linear polymers with equally spaced hydroxyl groups, we coupled **7** directly to **15** or **17** without loss of the Br end-group in products **16** or **24**. This was accomplished through modulating the copper(I) catalytic activity (i.e. by using the combination of PMDETA ligand and toluene as solvent) to facilitate a significantly faster CuAAC reaction over abstraction of Br end-group by either atom transfer or single electron transfer reactions to form the incipient polymeric radicals.³⁹ Our group has demonstrated that the catalytic activity of Cu(I) can be modulated by changing ligand and solvent to facilitate or inhibit the CuAAC reaction compared to either atom transfer nitroxide radical coupling (ATNRC) or single electron transfer-nitroxide radical coupling (SET-NRC).⁴⁰⁻⁴³

Scheme 3.1. Synthetic methodology to build complex topologies from multifunctional cyclic polymers.



Conditions: (a) azidation: NaN₃ in DMF at 25 °C, (b) cyclization: CuBr, PMDETA in toluene by feed at 25 °C, (c) bromination: 2-BPB, TEA in THF; 0 °C- RT, (d) deprotection: TBAF in THF at 25 °C. (e) CuAAC ‘click’ reaction: CuBr, PMDETA in toluene at 25 °C

3.1.1 Aim of the Chapter

The initial aim of the work described in this chapter was to synthesise multifunctional cyclic polymers in which the functional groups located in the equally spaced position. Linear polymer precursors were synthesised by CuAAC reaction in the presence of a bromine group through modulating the Cu(I) activity towards the click reaction over radical formation. The azidation and subsequent deprotection of linear polymers reveals α, ω hetero-telechelic linear polymer precursors which were cyclised by using modified CuAAC cyclization providing hydroxyl functional groups equally spaced from each other. The multifunctional cyclic polymers were then utilised to synthesise different complex topologies such as spiro tricyclic and 1st generation dendritic structures by CuAAC reaction.

3.2 Experimental

3.2.1 Materials

The following chemicals were analytical grade and used as received unless otherwise stated: alumina, activated basic (Aldrich: Brockmann I, standard grade, ~150 mesh, 58 Å), Dowex ion-exchange resin (sigma-aldrich, 50WX8-200), magnesium sulphate, anhydrous (MgSO₄: Scharlau, extra pure) potassium carbonate (K₂CO₃: analaR, 99.9%), silica gel 60 (230-400 mesh ATM (SDS)), pyridine (99%, Univar reagent), 1,1,1-triisopropylsilyl chloride (TIPS-Cl: Aldrich, 99%), phosphorus tribromide (Aldrich, 99%), tetrabutylammonium fluoride (TBAF: Aldrich, 1.0 M in THF), ethylmagnesium bromide solution (Aldrich, 3.0 M in diethyl ether), triethylamine (TEA: Fluka, 98%), 2-bromopropionyl bromide (BPB: Aldrich 98%), 2-bromoisobutyryl bromide (BIB: Aldrich, 98%), propargyl bromide solution (80% wt% in xylene, Aldrich), 1,1,1-(trihydroxymethyl) ethane (Aldrich, 96%), sodium hydride (60% dispersion in mineral oil), sodium azide (NaN₃: Aldrich, 99.5%), TLC plates (silica gel 60 F254), *N,N,N',N'',N''*-pentamethyldiethylenetriamine (PMDETA: Aldrich, 99%), copper (II) bromide (Cu(II)Br₂: Aldrich, 99%). Copper(I)bromide and Cu(II)Br₂/PMDETA complex were synthesised in our group. Styrene (STY: Aldrich, >99 %) was de-inhibited before use by passing through a basic alumina column. Methyl 3,5-bis (propargyloxy) benzoate⁴⁴ (**12**) and 1,3,5-tris(prop-2-ynyloxy)benzene⁴⁵ (**22**) linkers were prepared according to the literature procedure. All other chemicals used were of at least analytical grade and used as received.

The following solvents were used as received: acetone (ChemSupply, AR), chloroform (CHCl₃: Univar, AR grade), dichloromethane (DCM: Labscan, AR grade), diethyl ether (Univar, AR grade), dimethyl sulfoxide (DMSO: Labscan, AR grade), ethanol (EtOH: ChemSupply, AR), ethyl acetate (EtOAc: Univar, AR grade), hexane (Wacol, technical grade, distilled), hydrochloric acid (HCl, Univar, 32 %), anhydrous methanol (MeOH: Mallinckrodt, 99.9 %, HPLC grade), Milli-Q water (Biolab, 18.2 MΩ cm), *N,N*-dimethylformamide (DMF: Labscan, AR grade), tetrahydrofuran (THF: Labscan, HPLC grade), toluene (HPLC, LABSCAN, 99.8%).

3.2.2 Analytical Methods

Size Exclusion Chromatography (SEC)

The molecular weight distributions of the polymers was determined using a Waters 2695 separations module, fitted with a Waters 410 refractive index detector maintained at 35 °C, a Waters 996 photodiode array detector, and two Ultrastyrigel linear columns (7.8 x 300 mm) arranged in series. These columns were maintained at 40 °C for all analyses and are capable of separating polymers in the

molecular weight range of 500 to 4 million g/mol with high resolution. All samples were eluted at a flow rate of 1.0 mL/min. Calibration was performed using narrow molecular weight PSTY standards ($PDI_{SEC} \leq 1.1$) ranging from 500 to 2 million g/mol. Data acquisition was performed using Empower software, and molecular weights were calculated relative to polystyrene standards.

Absolute Molecular Weight Determination by Triple Detection SEC

Absolute molecular weights of polymers were determined using a Polymer Laboratories GPC50 Plus equipped with dual angle laser light scattering detector, viscometer, and differential refractive index detector. HPLC grade *N,N*-dimethylacetamide (DMAc, containing 0.03 wt % LiCl) was used as the eluent at a flow rate of 1.0 mL·min⁻¹. Separations were achieved using two PLGel Mixed B (7.8 x 300 mm) SEC columns connected in series and held at a constant temperature of 50 °C. The triple detection system was calibrated using a 2 mg·mL⁻¹ PSTY standard (Polymer Laboratories: $M_{wt} = 110$ K, $dn/dc = 0.16$ mL·g⁻¹ and $IV = 0.5809$). Samples of known concentration were freshly prepared in DMAc + 0.03 wt % LiCl and passed through a 0.45 μm PTFE syringe filter prior to injection. The absolute molecular weights and dn/dc values were determined using Polymer Laboratories Multi Cirrus software based on the quantitative mass recovery technique.

Preparative Size Exclusion Chromatography (Prep SEC).

Crude polymers were purified using a Varian Pro-Star preparative SEC system equipped with a manual injector, differential refractive index detector, and single wave-length ultraviolet visible detector. The flow rate was maintained at 10 mL min⁻¹ and HPLC grade tetrahydrofuran was used as the eluent. Separations were achieved using a PL Gel 10 μm 10 × 10³ Å, 300 × 25 mm preparative SEC column at 25 °C. The dried crude polymer was dissolved in THF at 100 mg mL⁻¹ and filtered through a 0.45 μm PTFE syringe filter prior to injection. Fractions were collected manually, and the composition of each was determined using the Polymer Laboratories GPC50 Plus equipped with triple detection as described above.

¹H Nuclear Magnetic Resonance (¹H NMR). All NMR spectra were recorded on a Bruker DRX 500 MHz spectrometer using an external lock (CDCl₃) and referenced to the residual non-deuterated solvent (CHCl₃). A DOSY experiment was run to acquire spectra presented herein by increasing the pulse gradient from 2 to 85 % of the maximum gradient strength and increasing d (**p30**) from 1 ms to 2 ms, using 64-128 scans.

Matrix-Assisted Laser Desorption Ionization-Time-of-Flight (MALDI-ToF) Mass Spectrometry. MALDI-ToF MS spectra were obtained using a Bruker MALDI-ToF autoflex III smart beam equipped

with a nitrogen laser (337 nm, 200 Hz maximum firing rate) with a mass range of 600-400 000 Da. Spectra were recorded in both reflectron mode (500-5000 Da) and linear mode (5000-20000 Da). Trans- 2-[3-(4-tert-butylphenyl)-2-methyl-propenylidene] malononitrile (DCTB; 20 mg/mL in THF) was used as the matrix and Ag-(CF₃COO) (1 mg/mL in THF) as the cation source of all the polystyrene samples. 20 μ L polymer solution (1 mg/mL in THF), 20 μ L DCTB solutions and 2 μ L Ag-(CF₃COO) solution were mixed in an ependorf tube, vortexed and centrifuged. 1 μ L of solution was placed on the target plate spot, evaporated the solvent at ambient condition and run the measurement.

Gas chromatography/mass spectrometry analysis (GC-MS)

Small organic compounds were analyzed by gas chromatography/mass spectrometry (Thermo Fisher Trace GC Ultra and DSQ II Quadrupole Mass Spectrometer) in electron ionization mode. The analysis was carried out by introducing methanol solution headspace into the GC/MS system by means of direct injection (3×10^{-3} mL by volume) using a gastight syringe.

3.2.3 Synthetic Procedures

The alkyne (hydroxyl) functional initiator **1** (Figure 3.1) was synthesised according to the literature procedure previously reported by our group.²² The scheme for the synthesis of **1** was given in Scheme B1 in appendix B.

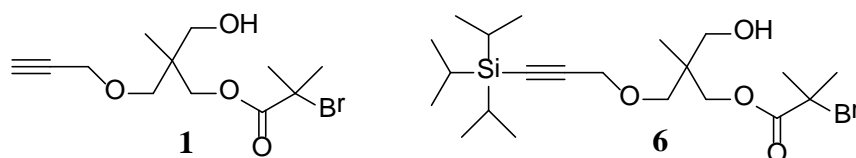


Figure 3.1. Protected and unprotected alkyne ATRP initiators.

3.2.3.1 Synthesis of Protected Alkyne (hydroxyl) Functional Initiator (6)

The synthetic strategy to produce **6** (Figure 3.1) was given in Scheme B2 in appendix B.

3.2.3.2 Synthesis of 3-(1, 1, 1-Triisopropylsilyl)-2-propyn-1-ol (2)

A solution of propargyl alcohol (2.847 g, 5.08×10^{-2} mol) in THF (50 mL) was added drop wise at room temperature to a 3.0 M solution of ethylmagnesium bromide (50.78 mL, 15.23×10^{-2} mol) in 100 mL THF. The reaction mixture was refluxed for 24 h and allowed to cool to room temperature. 7.24 mL of 1,1,1-triisopropylsilyl chloride (TIPS-Cl) (6.53 g, 16.92×10^{-3} mol) in THF (25 mL) was added drop wise, and subsequently refluxed for a further 5 h. Formation of the product was observed by TLC (petroleum spirit/ethyl acetate = 9:1). The reaction mixture was cooled to room temperature and poured into a 10% (m/m) HCl solution (20.27 mL). The aqueous layer was separated and the product

was extracted with ether 2 times. The combined organic layers were washed with brine, dried with anhydrous magnesium sulphate and the solvent was removed *in vacuo*. The crude product was isolated as yellow oil and used without further purification (yield=57.02 %).

$^1\text{H NMR}^{46}$ (CDCl_3 , 298K, 500 MHz); δ (ppm) 4.28 (s, 2H Si-C \equiv C-CH $_2$ -OH), 1.06 (s, 3H, ((CH $_3$) $_2$ -CH) $_3$ -Si-C \equiv C), 1.05 (s, 18H, ((CH $_3$) $_2$ -CH) $_3$ -Si-C \equiv C); $^{13}\text{C NMR}$ (CDCl_3 , 298K, 500 MHz); δ 105.75 (Si-C \equiv C-CH $_2$ -OH), 86.95 (Si-C \equiv C-CH $_2$ -OH), 51.88 (Si-C \equiv C-CH $_2$ -OH), 18.65 ((CH $_3$) $_2$ -CH) $_3$ -Si-C \equiv C), 11.23 ((CH $_3$) $_2$ -CH) $_3$ -Si-C \equiv C). GC-MS (EI): m/z 212.2 (calcd m/z 212.14 for M+H $^+$), 169.07 (calcd m/z 170.32 for M $_1$ +H $^+$)).

3.2.3.3 Synthesis of 3-Bromo-prop-1-ynyl 3-(1,1,1-triisopropyl)-silane 3

A solution of 3-(1,1,1-triisopropylsilyl)-2-propyn-1-ol **2** (6.0 g, 28.25×10^{-3} mol) and pyridine (13.7×10^{-3} mL, 1.69×10^{-3} mol) in anhydrous diethyl ether (100 mL) was cooled to 0 °C in an ice-bath. Phosphorus tri-bromide (3.186 mL, 33.9×10^{-3} mol) was added slowly and the mixture was stirred for two hours at 0 °C and then warmed to room temperature. After stirring overnight, ice water was added slowly to quench the reaction. The organic layer was separated and the aqueous layer was extracted with diethyl ether three times. The combined organic extracts were washed with saturated sodium bicarbonate solution, saturated sodium chloride solution and dried over anhydrous magnesium sulphate. Solvent was removed *in vacuo* and the residue was purified by silica gel column chromatography to give the product as colorless oil (yield=50.66 %). TLC: R $_f$ (hexane/ethyl acetate, 4/1) = 0.85. $^1\text{H NMR}^{47}$ (CDCl_3 , 298K, 500 MHz); δ (ppm) 3.93 (s, 2H, Si-C \equiv C-CH $_2$ -Br), 1.05 (s, 21H, ((CH $_3$) $_2$ -CH) $_3$ -Si-C \equiv C). $^{13}\text{C NMR}$ (CDCl_3 , 298K, 500 MHz); δ 101.93 (Si-C \equiv C-CH $_2$ -Br), 89.2 (Si-C \equiv C-CH $_2$ -Br), 18.62 ((CH $_3$) $_2$ -CH) $_3$ -Si-C \equiv C), 15.1 (Si-C \equiv C-CH $_2$ -Br), 11.26 ((CH $_3$) $_2$ -CH) $_3$ -Si-C \equiv C-), GC-MS (EI): m/z 276.5 (calcd m/z 275.3 for M+H $^+$), 231.97 (calcd m/z 233.22 for M $_1$ +H $^+$)).

3.2.3.4 Synthesis of Compound 4

3.85 g (24.0×10^{-3} mol) of 2,2,5-trimethyl-1,3-dioxan-5-yl methanol was dissolved in 60 mL dry THF in a 250 mL two-neck round bottom flask connected to the argon line, and the solution cooled to 0 °C in an ice-bath. 1.0 g (24.0×10^{-3} mol) NaH (60 % in mineral oil) was added proportionally to the above solution over 10 min. The reaction was stirred for 2 h and the reaction vessel cooled to -78 °C in a dry ice/acetone mixture. 5.5 g (20.0×10^{-3} mol) of **3** was added to the solution drop-wise over 30 min. The reaction was then allowed to warm to RT and stirred overnight. The reaction mixture was filtered to remove the salt and concentrated to remove all the solvent and low b.p impurities at room temperature. The crude brown liquid product was purified by silica gel column chromatography to give the product as colorless oil (yield = 97%). TLC: R $_f$ (petroleum spirit/ethyl acetate 9:1, v/v) = 0.62. $^1\text{H NMR}^3$

(CDCl₃, 298K, 500 MHz); δ (ppm) 4.16 (s, 2H, Si-C \equiv C-CH₂-O), 3.68-3.7 (d, 2H, J = 11.81 Hz, -CH₂-O-C(CH₃)₂-), 3.50-3.52 (d, 2H, J = 11.81 Hz, -CH₂-O-C(CH₃)₂-), 3.5 (s, 2H, Si-C \equiv C-CH₂-O-CH₂-), 1.36-1.4 (d, 6H, J = 15.82 Hz, (O-C(CH₃)₂), 1.05 (s, 21H, ((CH₃)₂-CH)₃-Si-C \equiv C), 0.87 (s, 3H, C \equiv C-CH₂-O-CH₂-C(CH₃)). ¹³C NMR (CDCl₃, 298K, 500 MHz); δ (ppm) 103.77 (Si-C \equiv C-CH₂-O), 97.94 (O-C(CH₃)₂), 87.3 (Si-C \equiv C-CH₂-O), 72.66 (C \equiv C-CH₂-O-CH₂), 66.7 (-CH₂-O-C(CH₃)₂-), 59.47 (C \equiv C-CH₂-O-CH₂-), 34.27 (C \equiv C-CH₂-O-CH₂-C(CH₃)), 25.9 (-CH₂-O-C(CH₃)₂-), 21.79 (O-C(CH₃)₂), 18.67 ((CH₃)₂-CH)₃-Si-C \equiv C), 18.48 (O-C(CH₃)₂), 11.25 ((CH₃)₂-CH)₃-Si-C \equiv C), GC-MS (EI): m/z 339.19 (calcd m/z 340.62 for M₁+H⁺) 311.16 (calcd m/z 312.52 for M₂+H⁺).

3.2.3.5 Synthesis of Compound 5

4.8 g (13.5 \times 10⁻³ mol) of compound **4** was dissolved in 25 mL dry methanol, DOWEX 2 g was added to the solution and stirred at 40 °C overnight. The DOWEX resin was filtered out and the solution was concentrated and further applied on high vacuum to remove any trace of methanol. 4.1 g of colorless viscous liquid product **5** was obtained with 96.5% yield. The product was directly used for the characterization and the next reaction without any further purification. TLC: R_f (petroleum spirit/ethyl acetate 3:2, v/v) = 0.7. ¹H NMR³ (CDCl₃, 298K, 500 MHz); δ (ppm) 4.16 (s, 2H, Si-C \equiv C-CH₂O-), 3.56-3.58 (m, 4H, -C(CH₃)-CH₂-OH), 3.55 (s, 2H, C \equiv C-CH₂O-CH₂-) 1.05 (s, 21H, ((CH₃)₂-CH)₃-Si-C \equiv C), 0.82 (s, 3H, -C(CH₃)-CH₂-OH). ¹³C NMR (CDCl₃, 298K, 500 MHz); δ (ppm) 103.15 (Si-C \equiv C-CH₂-O), 88.3 (Si-C \equiv C-CH₂O-), 74.7 (C \equiv C-CH₂OCH₂-), 68.16 (-C(CH₃)-CH₂-OH), 59.56 (Si-C \equiv C-CH₂-O), 40.84 (-C(CH₃)-CH₂-OH), 18.64 ((CH₃)₂-CH)₃-Si-C \equiv C), 17.3 ((-C(CH₃)-CH₂-OH), 11.23 ((CH₃)₂-CH)₃-Si-C \equiv C), GC-MS (EI): m/z 271.12 (calcd m/z 272.46 for M₁+H⁺).

3.2.3.6 Synthesis of Protected Alkyne Functional Initiator, Comp. 6

3.13 g (9.95 \times 10⁻³ mol) of **5** and 1.73 g (12.44 \times 10⁻³ mol) of TEA were dissolved in 30.0 mL of dry THF and cooled to 0 °C in an ice-bath. To the above solution, 1.48 g (11.94 \times 10⁻³ mol) bromo isobutryl bromide was added drop-wise over 10 min. The reaction was warmed up to room temperature and stirred for 24 h. The reaction mixture was filtered to remove the solid, concentrated under high vacuum at RT. The brown crude product was purified by column chromatography. Eluent ethyl acetate: petroleum spirit = 2:1 (v/v). The fraction with R_f as 0.27 was collected and concentrated. 6.5 g colorless viscous liquid product **6** was obtained with the yield as 48.5 %.

¹H NMR³ (CDCl₃, 298K, 500 MHz); δ (ppm) 4.1-4.2 (dt, J = 6.4, 20.55 Hz, 4H, -C \equiv C-CH₂-O-CH₂C(CH₃)-CH₂OCO-), 3.53 (s, 2H, -C \equiv C-CH₂-O-CH₂C(CH₃)), 3.48-3.53 (d, 2H, -C(CH₃)-CH₂OH, J = 5.85 Hz), 1.05 (s, 21H, ((CH₃)₂-CH)₃-Si-C \equiv C), 0.94 (s, 3H, -C(CH₃)-CH₂OH). ¹³C NMR (CDCl₃, 298K, 500 MHz); δ (ppm) 171.89 (O-CH₂C(CH₃)-CH₂OCO-), 102.98 (Si-C \equiv C-CH₂-

O), 88.29 (Si-C≡C-CH₂-O), 73.9 (C≡C-CH₂-O-CH₂-), 68.18 (CH₂OCO-C(CH₃)₂-), 67.03 (-C(CH₃)-CH₂-OH), 59.62 (Si-C≡C-CH₂-O), 55.92 (CH₂OCO-C(CH₃)₂-), 40.67 (-C(CH₃)-CH₂-OH), 30.89 (CH₂OCO-C(CH₃)₂-), 18.66 ((CH₃)₂-CH)₃-Si-C≡C), 17.2 (-C(CH₃)-CH₂-OH), 11.23 ((CH₃)₂-CH)₃-Si-C≡C), GC-MS (EI): *m/z* 421.10 (calcd *m/z* 421.44 for M₁+H⁺).

3.2.3.7 Synthesis of Linear PSTY by Atom Transfer Radical Polymerization (ATRP)

Synthesis of ≡(HO)-PSTY₂₅-Br **7** by ATRP

Styrene (8.11 g, 77.86×10⁻³ mol), PMDETA (0.17 mL, 8.1×10⁻⁴ mol), CuBr₂/PMDETA (6.4×10⁻² g, 4.05×10⁻⁴ mol) and initiator (0.5 g, 1.6277×10⁻³ mol) were added to a 100 mL schlenk flask equipped with a magnetic stirrer and purged with argon for 40 min to remove oxygen. Cu(I)Br (0.12 g, 8.1×10⁻⁴ mol) was then carefully added to the solution under an argon blanket. The reaction mixture was further degassed for 5 min and then placed into a temperature controlled oil bath at 80 °C. After 4 h, an aliquot was taken to check the conversion. The reaction was quenched by cooling to 0 °C in ice bath, exposed to air, and diluted with THF (*ca.* 3 fold to the reaction mixture volume). The copper salts were removed by passage through an activated basic alumina column. The solution was concentrated by rotary evaporation and the polymer was recovered by precipitation into large volume of MeOH (20 fold excess to polymer solution) and vacuum filtration two times. The polymer was dried in high *vacuo* overnight at 25 °C, SEC (*M_n* = 2890, PDI = 1.11). Final conversion was calculated by gravimetry (53.3%). The polymer was further characterised by ¹H NMR and MALDI-ToF. Another batch of ≡(HO)-PSTY₂₅-Br, **7'** was also synthesised by following similar procedure.

Synthesis of ≡(HO)-PSTY₂₅-N₃ **8** by Azidation with NaN₃

Polymer **7** (2.9 g, 1.0×10⁻³ mol) was dissolved in 20 mL of DMF in a reaction vessel equipped with a magnetic stirrer. To this solution, NaN₃ (0.65 g, 10.0×10⁻³ mol) was added and the mixture stirred for 24 h at 25 °C. The polymer solution was directly precipitated into MeOH/H₂O (95/5, v/v) (20 fold excess to polymer solution) from DMF, recovered by vacuum filtration and washed exhaustively with MeOH. The polymer was dried in *vacuo* for 24 h at 25 °C, SEC (*M_n* = 2880, PDI = 1.11). The polymer was further characterised by ¹H NMR and MALDI-ToF.

3.2.3.8 Cyclization Reaction by CuAAC Using Argon Flow Technique (see Scheme B4 in appendix B)

Synthesis of c-PSTY₂₅-OH 9

A solution of polymer **8** (2.0 g, 6.667×10^{-4} mol) in 80.0 ml of dry toluene and 6.97 mL of PMDETA (33.35×10^{-3} mol) in 80 mL of dry toluene in another flask were purged with argon for 45 min to remove oxygen. 4.78 g of CuBr (33.35×10^{-3} mol) was taken in a 250 mL of dry schlenk flask and maintained under an argon flow in the flask at the same time. A PMDETA solution was transferred to CuBr flask by applying argon pressure using a double tip needle to prepare CuBr/PMDETA complex. After complex formation, the polymer solution was added via syringe pump using a syringe that is pre-filled with argon. The feed rate of argon was set at 1.24 mL/min. After the addition of the polymer solution (after 65 min), the reaction mixture was further stirred for 3 h. At the end of this period (i.e., feed time plus an additional 3 h), toluene was evaporated by air-flow and the copper salts were removed by passage through activated basic alumina column by adding few drops of glacial acetic acid. The polymer was recovered by precipitation into MeOH (20 fold excess to polymer solution) and then by filtration. The polymer was dried *in vacuo* for 24 h at 25 °C. (Purity by SEC=88.9%). A small fraction of crude product was purified by preparative SEC for characterization. SEC ($M_n=2140$, PDI=1.04), Triple Detection SEC ($M_n=2780$, PDI=1.02). The polymer was further characterised by ¹H NMR and MALDI-ToF.

*3.2.3.9 Chain-end Modification of Hydroxyl Functional Cyclic Polymer**Synthesis of c-PSTY₂₅-Br 10*

c-PSTY₂₅-OH **9** (1.6 g, 5.867×10^{-4} mol), TEA (1.63 mL, 11.73×10^{-3} mol) and 30.0 mL of dry THF were added under an argon blanket to a dry schlenk flask that has been flushed with argon. The reaction was then cooled on ice bath. To this stirred mixture, a solution of 2-bromopropionyl bromide (1.23 mL, 11.73×10^{-3} mol) in 10 mL of dry THF was added drop wise under argon via an air-tight syringe over 10 min. After stirring the reaction mixture for 48 h at room temperature, the crude polymer solution was added in 300 mL of acetone and filtered to remove salt precipitate. Solvent was removed by rotavap and precipitated into MeOH, filtered and washed three times with MeOH. A fraction of crude product was purified by preparative SEC for characterization. The polymer was dried for 24 h in high vacuum oven at 25 °C. SEC ($M_n=2350$, PDI=1.04). The polymer was further characterised by ¹H NMR and MALDI-ToF.

Synthesis of c-PSTY₂₅-N₃ 11

Polymer c-PSTY₂₅-Br **10** (1.5 g, 0.5×10^{-3} mol) was dissolved in 10 mL of DMF in a reaction vessel equipped with magnetic stirrer. To this solution, NaN₃ (0.65 g, 1.0×10^{-3} mol) was added and the mixture stirred for 24 h at room temperature. The polymer solution was directly precipitated into MeOH/H₂O (95/5, v/v) (20 fold excess to polymer solution) from DMF, recovered by vacuum filtration and washed exhaustively with MeOH. A fraction of the polymer was purified by preparative SEC and precipitated and filtered. The polymer was dried *in vacuo* for 24 h at 25 °C, SEC ($M_n = 2250$, PDI = 1.04) and Triple Detection SEC ($M_n = 2930$, PDI=1.02). The polymer was further characterised by ¹H NMR and MALDI-ToF.

*Synthesis of c-PSTY₂₅-≡ **13***

Polymer c-PSTY₂₅-N₃ **11** (0.4 g, 0.133×10^{-3} mol), PMDETA (27.87×10^{-3} mL, 0.133×10^{-3} mol) and methyl 3,5-bis (propargyloxy) benzoate **12** (0.49 g, 1.99×10^{-3} mol) were dissolved in 3.0 mL toluene. CuBr (19.0×10^{-3} g, 1.33×10^{-4} mol) was added to a 10 mL schlenk flask equipped with magnetic stirrer and both of the reaction vessels were purged with argon for 20 min. The polymer solution was then transferred to CuBr flask by applying argon pressure using double tip needle. The reaction mixture was purged with argon for a further 2 min and the flask was placed in a temperature controlled oil bath at 25 °C for 1.5 h. The reaction was then diluted with THF (*ca.* 3 fold to the reaction mixture volume), and passed through activated basic alumina to remove the copper salts. The solution was concentrated by rotary evaporator and the polymer was recovered by precipitation into a large amount of MeOH (20 fold excess to polymer solution) and filtration. The polymer was purified by preparative SEC to remove excess linker as well as high MW impurities. After precipitation and filtration, the polymer was dried *in vacuo* for 24 h at 25 °C. SEC ($M_n = 2440$, PDI=1.04) and Triple Detection SEC ($M_n = 3170$, PDI=1.02). The polymer was further characterised by ¹H NMR and MALDI-ToF.

3.2.3.10 Synthesis of Protected Alkyne Functional Linear PSTY by Atom Transfer Radical Polymerization (ATRP)

*Synthesis of TIPS-≡(HO)-PSTY₂₅-Br **14***

Styrene (5.47 g, 5.3×10^{-2} mol), PMDETA (1.13×10^{-1} mL, 5.4×10^{-4} mol), CuBr₂/PMDETA (4.3×10^{-2} g, 1.08×10^{-4} mol) and initiator (0.5 g, 1.08×10^{-3} mol) were added to a 100 mL schlenk flask equipped with a magnetic stirrer and sparged with argon for 30 min to remove oxygen. Cu(I)Br (7.7×10^{-2} g, 5.4×10^{-4} mol) was then carefully added to the solution under an argon blanket. The reaction mixture was further degassed for 5 min and then placed into a temperature controlled oil bath at 80 °C. After 4 h an aliquot was taken to check the conversion. The reaction was quenched by cooling the reaction mixture to 0 °C, exposure to air, and dilution with THF (*ca.* 3 fold to the reaction mixture volume). The copper salts were removed by passage through an activated basic

alumina column. The solution was concentrated by rotary evaporator and the polymer was recovered by precipitation into large volume of MeOH (20 fold excess to polymer solution) and vacuum filtration two times. The polymer was dried *in high vacuo* overnight at 25 °C. SEC ($M_n = 2870$, PDI = 1.08). Final conversion was calculated by gravimetry (46%). The polymer was further characterised by ^1H NMR and MALDI-ToF.

Synthesis of TIPS- \equiv (OH)-PSTY₂₅-N₃ 15 by Azidation with NaN₃

Polymer TIPS- \equiv (OH)-PSTY₂₅-Br **14** (1.3 g, 4.5×10^{-4} mol) was dissolved in 10 mL of DMF in a 20 mL reaction vessel equipped with magnetic stirrer. To this solution NaN₃ (2.8×10^{-1} g, 4.5×10^{-3} mol) was added and the mixture stirred for 24 h at 25 °C. The polymer solution was directly precipitated into MeOH/H₂O (95/5, v/v) (20 fold excess to polymer solution) from DMF, recovered by vacuum filtration and washed exhaustively with MeOH. The polymer was dried *in vacuo* for 24 h at 25 °C. SEC ($M_n = 2890$, PDI = 1.06). The polymer was further characterised by ^1H NMR and MALDI-ToF.

Synthesis of TIPS- \equiv (OH-PSTY₂₅)₂-Br 16 by CuAAC

Polymer TIPS- \equiv (OH)-PSTY₂₅-N₃ **15** (1.2 g, 4.2×10^{-4} mol) and \equiv (OH)-PSTY₂₅-Br **7a** (1.07 g, 4.2×10^{-4} mol) and PMDETA (8.75×10^{-2} mL, 4.2×10^{-4} mol) were dissolved in 20.0 mL of dry toluene in a 50 mL reaction vessel equipped with magnetic stirrer. To this solution CuBr (6.0×10^{-2} g, 4.2×10^{-4} mol) was added under argon blanket and the mixture was stirred at 25 °C under argon atmosphere. An aliquot was taken to check SEC. The reaction was stopped after 1.5 h and added 3 fold excess of THF, passed through alumina column to remove copper salts. Solvent was removed by rotary evaporator and precipitated in 20 fold excess of MeOH and filtered. The polymer was dried *in vacuo* for 24 h at 25 °C. SEC for **16** ($M_n = 5510$, PDI = 1.05). The polymer was further characterised by ^1H NMR and MALDI-ToF.

Synthesis of TIPS- \equiv (OH-PSTY₂₅)₂-N₃ 17 by Azidation with NaN₃

Polymer TIPS- \equiv (OH-PSTY₂₅)₂-Br (2.2 g, 4.02×10^{-4} mol) was dissolved in 10 mL of DMF in a 20 mL reaction vessel equipped with magnetic stirrer. To this solution NaN₃ (2.6×10^{-1} g, 4.02×10^{-3} mol) was added and the mixture stirred for 24 h at 25 °C. The polymer solution was directly precipitated into MeOH/H₂O (95/5, v/v) (20 fold excess to polymer solution) from DMF, recovered by vacuum filtration and washed exhaustively with MeOH. The polymer was dried *in vacuo* for 24 h at 25 °C. SEC ($M_n = 5510$, PDI = 1.06). The polymer was further characterised by ^1H NMR and MALDI-ToF.

Synthesis of $\equiv(\text{OH-PSTY}_{25})_2\text{-N}_3$ 18 by Deprotection with TBAF

Polymer TIPS- $\equiv(\text{OH-PSTY}_{25})_2\text{-N}_3$ **17** (1.7 g, 3.08×10^{-4} mol) was dissolved in 15 mL of dry THF in a 50 mL schlenk flask equipped with magnetic stirrer. To this solution, 3.07 mL of TBAF (1.0 M in THF solution, 3.08×10^{-3} mol) solution was added and the mixture stirred for 24 h at 25 °C under argon atmosphere. The polymer solution was directly precipitated into MeOH (20 fold excess to polymer solution), recovered by vacuum filtration and washed exhaustively with MeOH. The polymer was dried and purified by preparative SEC to remove undesired high and low molecular weight impurities. SEC ($M_n=5350$, PDI=1.06). The polymer was further characterised by ^1H NMR and MALDI-ToF.

*3.2.3.11 Cyclization Reaction of $\equiv(\text{OH-PSTY}_{25})_2\text{-N}_3$ by CuAAC Using Argon Flow Technique**Synthesis of $c\text{-PSTY}_{50}\text{-(OH)}_2$ 19*

A solution of $\equiv(\text{OH-PSTY}_{25})_2\text{-N}_3$ **18** (0.5 g, 9.5×10^{-5} mol) in 20.0 mL of dry toluene and 1.0 mL of PMDETA (4.76×10^{-3} mol) in 20.0 mL of dry toluene in another flask were purged with argon for 45 min to remove oxygen. 0.68 g of CuBr (4.76×10^{-3} mol) was taken in a 250 mL of dry schlenk flask and maintained argon flow at the same time. PMDETA solution was transferred to CuBr flask by applying argon pressure using a double tip needle to prepare CuBr/PMDETA complex. After complex formation, polymer solution was added via syringe pump using a syringe that is pre-filled with argon. The feed rate of argon was set at 1.24 mL/min. After the addition of polymer solutions (16 min), the reaction mixture was further stirred for 3 h. At the end of this period (i.e., feed time plus an additional 3 h), toluene was evaporated by air-flow and the copper salts were removed by passage through activated basic alumina column by adding few drops of glacial acetic acid. The polymer was recovered by precipitation into MeOH (20 fold excess to polymer solution) and then by filtration. The polymer was dried *in vacuo* for 24 h at 25 °C. (Purity by SEC=82.1%). A small fraction of crude product was purified by preparative SEC for characterization. SEC ($M_n = 4110$, PDI = 1.03). Triple Detection SEC ($M_n=5350$, PDI=1.02). The polymer was further characterised by ^1H NMR and MALDI-ToF.

*3.2.3.12 Chain-end Modification of Di-hydroxy Functional Cyclic**Synthesis of $c\text{-PSTY}_{50}\text{-Br}_2$ 20*

$c\text{-PSTY}_{50}\text{-(OH)}_2$ **19** (1.4×10^{-1} g, 2.57×10^{-5} mol), TEA (0.18 mL, 1.285×10^{-3} mol) and 3.5 mL of dry THF were added under an argon blanket to a dry schlenk flask that has been flushed with argon. The reaction was then cooled on ice. To this stirred mixture, a solution of 2-bromopropionyl bromide (0.13

mL, 1.285×10^{-3} mol) in 0.5 mL of dry THF was added drop wise under argon via an air-tight syringe over 3 min. After stirring the reaction mixture for 48 h at room temperature, the polymer was precipitated into MeOH, filtered and washed three times with MeOH. The polymer was dried for 24 h in high vacuum oven at 25 °C. SEC ($M_n = 4350$, PDI = 1.03). The polymer was further characterised by ^1H NMR and MALDI-ToF.

Synthesis of c-PSTY₅₀-(N₃)₂ 21

Polymer c-PSTY₅₀-Br₂ **20** (1.2×10^{-1} g, 2.2×10^{-5} mol) was dissolved in 2.0 mL of DMF in a reaction vessel equipped with magnetic stirrer. To this solution, NaN₃ (2.8×10^{-2} g, 4.4×10^{-4} mol) was added and the mixture stirred for 17 h at room temperature. The polymer solution was directly precipitated into MeOH/H₂O (95/5, v/v) (20 fold excess to polymer solution) from DMF, recovered by vacuum filtration and washed exhaustively with MeOH. A fraction of crude polymer was further purified by preparative SEC and recovered by precipitation. The polymer was dried *in vacuo* for 24 h at 25 °C. SEC ($M_n = 4470$, PDI=1.03), Triple Detection SEC ($M_n = 5850$, PDI=1.005). The polymer was further characterised by ^1H NMR and MALDI-ToF.

Synthesis of c-PSTY₅₀-(≡)₄ 23

Polymer cPSTY₅₀-(N₃)₂ **21** (0.15 g, 2.4×10^{-5} mol), PMDETA (10.12×10^{-3} mL, 4.8×10^{-5} mol) and 1,3,5-tris(prop-2-ynyloxy)benzene **22** (8.7×10^{-2} g, 3.6×10^{-4} mol) were dissolved in 1.0 mL of toluene/DMSO (0.8/0.2 mL) mixed solvent. CuBr (7.0×10^{-3} g, 4.8×10^{-5} mol) was added to a 10 mL schlenk flask equipped with magnetic stirrer and both of the reaction vessels were purged with argon for 12 min. The polymer solution was then transferred to CuBr flask by applying argon pressure using double tip needle. The reaction mixture was purged with argon for a further 2 min and the flask was placed in a temperature controlled oil bath at 25 °C for 1.5 h. The reaction was then diluted with THF (*ca.* 3 fold to the reaction mixture volume), and passed through activated basic alumina to remove the copper salts. The solution was concentrated by rotary evaporator and the polymer was recovered by precipitation into a large amount of MeOH (20 fold excess to polymer solution) and filtration. The polymer was then further purified by preparative SEC to remove undesired high molecular weight polymers and residual linker. The polymer was dried *in vacuo* for 24 h at 25 °C. SEC ($M_n = 4470$, PDI=1.04), Triple Detection SEC ($M_n = 6420$, PDI=1.001). The polymer was further characterised by ^1H NMR and MALDI-ToF.

3.2.3.13 Synthesis of tri-functional linear PSTY

Synthesis of TIPS- \equiv (OH-PSTY₂₅)₃-Br **24** by CuAAC

Polymer TIPS- \equiv (OH-PSTY₂₅)₂-N₃ **17** (2.7×10^{-4} g, 4.53×10^{-5} mol) and \equiv (OH)-PSTY₂₅-Br **7** (1.3×10^{-1} g, 4.53×10^{-5} mol) and PMDETA (9.5×10^{-3} mL, 4.53×10^{-5} mol) were dissolved in 3.5 mL of dry toluene in a vial. CuBr (6.5×10^{-3} g, 4.53×10^{-5} mol) was added to a 10 mL schlenk flask equipped with magnetic stirrer and both of the reaction vessels were purged with argon for 12 min. The polymer solution was then transferred to CuBr flask by applying argon pressure using double tip needle. The reaction mixture was purged with argon for a further 2 min and the flask was placed in a temperature controlled oil bath at 25 °C. After 1.0 h an aliquot was taken to check SEC. The reaction was stopped after 1.5 h and added 3 fold excess of THF, passed through alumina column to remove CuBr. Solvent was removed by rotary evaporator and precipitated in excess of MeOH and filtered. The polymer was dried *in vacuo* for 24 h at 25 °C. SEC ($M_n=8830$, PDI=1.06). The polymer was further characterised by ¹H NMR and MALDI-ToF.

Synthesis of TIPS- \equiv (OH-PSTY₂₅)₃-N₃ **25** by Azidation with NaN₃

Polymer TIPS- \equiv (OH-PSTY₂₅)₃-Br **24** (0.35 g, 3.9×10^{-5} mol) was dissolved in 3.5 mL of DMF in a 20 mL reaction vessel equipped with magnetic stirrer. To this solution NaN₃ (3.9×10^{-2} g, 5.9×10^{-4} mol) was added and the mixture stirred for 24 h at 25 °C. The polymer solution was directly precipitated into MeOH/H₂O (95/5, v/v) (20 fold excess to polymer solution) from DMF, recovered by vacuum filtration and washed exhaustively with water and MeOH. The polymer was dried *in vacuo* for 24 h at 25 °C. SEC ($M_n=8750$, PDI=1.06). The polymer was further characterised by ¹H NMR and MALDI-ToF.

Synthesis of \equiv (OH-PSTY₂₅)₃-N₃ **26** by Deprotection with TBAF

Polymer TIPS- \equiv (OH-PSTY₂₅)₃-N₃ **25** (0.33 g, 3.96×10^{-5} mol) was dissolved in 15 mL of dry THF in a schlenk flask equipped with magnetic stirrer. To this solution, 0.8 mL of TBAF (1.0 M in THF solution, 7.9×10^{-4} mol) solution was added and the mixture stirred for 24 h at 25 °C under argon atmosphere. The polymer solution was directly precipitated into MeOH (20 fold excess to polymer solution), recovered by vacuum filtration and washed exhaustively with MeOH. The polymer was dried *in vacuo* for 24 h at 25 °C and the polymer was purified by preparative SEC to remove undesired impurities. SEC ($M_n=8720$, PDI=1.05). The polymer was further characterised by ¹H NMR and MALDI-ToF.

3.2.3.14 Cyclization reaction of $\equiv(\text{OH-PSTY}_{25})_3\text{-N}_3$ by CuAAC Using Argon Flow Technique

Synthesis of *c*-PSTY₇₅-(OH)₃ **27**

A solution of $\equiv(\text{OH-PSTY}_{25})_3\text{-N}_3$ **26** (0.17 g, 1.87×10^{-5} mol) in 10 mL of dry toluene and 0.19 mL of PMDETA (9.4×10^{-4} mol) in 10 mL of dry toluene in another flask were purged with argon for 45 min to remove oxygen. CuBr (0.13 g, 9.4×10^{-4} mol) was taken in a 100 mL of dry schlenk flask and maintained argon flow at the same time. PMDETA solution was transferred to CuBr flask by argon pressure using a double tip needle to prepare CuBr/PMDETA complex. After complex formation, polymer solution was added via syringe pump with the help of a syringe that is pre-filled with argon. The feed rate was set at 0.25 mL/min. After the addition of polymer solutions, which was 43 min, the reaction mixture was further stirred for 3 h. At the end of this period (i.e., feed time plus an additional 3 h), toluene was evaporated by air-flow and the copper salts were removed by passage through activated basic alumina column by adding few drops of glacial acetic acid. The polymer was recovered by precipitation into MeOH (20 fold excess to polymer solution) and then by filtration. The polymer was dried *in vacuo* for 24 h at 25 °C. The purity of cyclic polymer was 76.5 % by SEC. A small fraction of crude product was purified by preparative SEC for characterization. SEC ($M_n = 6600$, PDI = 1.03). Triple Detection SEC, ($M_n = 8830$, PDI = 1.007). The polymer was further characterised by ¹H NMR and MALDI-ToF.

3.2.3.15 Chain-end Modification of Tri-hydroxy Functional Cyclic

Synthesis of *c*-PSTY₇₅-Br₃ **28**

c-PSTY₇₅-(OH)₃ **19** (9.0×10^{-2} g, 1.0×10^{-5} mol), TEA (85.5×10^{-3} mL, 6.0×10^{-4} mol) and 1.5 mL of dry THF were added under an argon blanket to a dry schlenk flask that has been flushed with argon. The reaction was then cooled on ice bath. To this stirred mixture, a solution of 2-bromopropionyl bromide (64.3×10^{-3} mL, 6.0×10^{-4} mol) in 0.5 mL of dry THF was added drop wise under argon via an air-tight syringe over 3 min. After stirring the reaction mixture for 48 h at room temperature, the polymer was precipitated into MeOH, filtered and washed three times with MeOH. The polymer was dried for 24 h in high vacuum oven at 25 °C. SEC ($M_n = 7210$, PDI = 1.03). The polymer was further characterised by ¹H NMR and MALDI ToF.

Synthesis of *c*-PSTY₇₅-(N₃)₃ **29**

Polymer *c*-PSTY₇₅-Br₃ **28** (8.0×10^{-2} g, 9.2×10^{-6} mol) was dissolved in 1.0 mL of DMF in a reaction vessel equipped with magnetic stirrer. To this solution, NaN₃ (1.8×10^{-2} g, 2.76×10^{-4} mol) was added

and the mixture stirred for 24 h at room temperature. The polymer solution was directly precipitated into MeOH/H₂O (95/5, v/v) (20 fold excess to polymer solution) from DMF, recovered by vacuum filtration and washed exhaustively with MeOH. The polymer was dried *in vacuo* for 24 h at 25 °C and the polymer was purified by preparative SEC to remove undesired impurities. SEC ($M_n=7070$, PDI=1.03), Triple Detection SEC ($M_n=9250$, PDI=1.004). The polymer was further characterised by ¹H NMR and MALDI ToF.

Synthesis of c-PSTY₇₅-(≡)₆ 30

Polymer cPSTY₇₅-(N₃)₃ **29** (1.2×10^{-1} g, 1.26×10^{-5} mol), PMDETA (7.92×10^{-3} mL, 3.8×10^{-5} mol) and 1,3,5-tris(prop-2-ynoxy)benzene **22** (9.1×10^{-2} g, 3.6×10^{-4} mol) were dissolved in 1.0 mL of toluene/DMSO (0.8/0.2 mL) mixed solvent. CuBr (5.0×10^{-3} g, 3.8×10^{-5} mol) was added to a 10 mL schlenk flask equipped with magnetic stirrer and both of the reaction vessels were purged with argon for 20 min. The polymer solution was then transferred to CuBr flask by applying argon pressure using double tip needle. The reaction mixture was purged with argon for a further 2 min and the flask was placed in a temperature controlled oil bath at 25 °C for 1.5 h. The reaction was then diluted with THF (*ca.* 3 fold to the reaction mixture volume), and passed through activated basic alumina to remove the copper salts. The solution was concentrated by rotary evaporator and the polymer was recovered by precipitation into a large amount of MeOH (20 fold excess to polymer solution) and filtration. The polymer was then further purified by preparative SEC to remove undesired high molecular weight polymers and residual linker. The polymer was dried *in vacuo* for 24 h at 25 °C. SEC ($M_n=7640$, PDI=1.03), Triple Detection SEC ($M_n=9980$, PDI=1.004). The polymer was further characterised by ¹H NMR and MALDI ToF.

3.2.3.16 Synthesis of Complex Topologies

Synthesis of Spiro Tricyclic 31

Polymer c-PSTY₅₀-(N₃)₂ **21** (3.0×10^{-2} g, 5.0×10^{-6} mol), polymer c-PSTY₂₅-≡ **13** (3.4×10^{-2} g, 1.0×10^{-5} mol) and PMDETA (2.13×10^{-3} mL, 1.0×10^{-5} mol) were dissolved in 0.5 mL of toluene. CuBr (1.5×10^{-3} g, 1.0×10^{-5} mol) was added to a 10 mL schlenk flask equipped with magnetic stirrer and both of the reaction vessels were purged with argon for 15 min. The polymer solution was then transferred to CuBr flask using double tip needle by applying argon pressure. The reaction mixture was purged with argon for a further 2 min and the flask was placed in a temperature controlled oil bath at 25 °C for 1.5 h. The reaction was then diluted with THF (*ca.* 3 fold to the reaction mixture volume), and passed through activated basic alumina to remove the copper salts. The solution was concentrated by rotary evaporator and the polymer was recovered by precipitation into a large amount of MeOH (20 fold excess to polymer solution) and filtration. The polymer was then purified

by preparatory SEC to remove undesired high molecular weight polymers and residual reactant polymers. The polymer was dried *in vacuo* for 24 h at 25 °C and characterised. SEC ($M_n=9820$, PDI=1.05), Triple Detection SEC ($M_n=12420$, PDI=1.004). The polymer was further characterised by ^1H NMR and MALDI-ToF.

Synthesis of G1 Dendrimer Pentacyclic 32

Polymer c-PSTY₅₀-(≡)₄ **23** (2.5×10^{-2} g, 3.8×10^{-6} mol), polymer c-PSTY₂₅-N₃ (4.8×10^{-5} g, 1.6×10^{-5} mol) and PMDETA (3.16×10^{-3} mL, 1.5×10^{-5} mol) were dissolved in 0.5 mL of toluene. CuBr (2.2×10^{-3} g, 0.015×10^{-3} mol) was added to a 10 mL schlenk flask equipped with magnetic stirrer and both of the reaction vessels were purged with argon for 15 min. The polymer solution was then transferred to CuBr flask using double tip needle by applying argon pressure. The reaction mixture was purged with argon for a further 2 min and the flask was placed in a temperature controlled oil bath at 25 °C for 1.5 h. The reaction was then diluted with THF (*ca.* 3 fold to the reaction mixture volume), and passed through activated basic alumina to remove the copper salts. The solution was concentrated by rotary evaporator and the polymer was recovered by precipitation into a large amount of MeOH (20 fold excess to polymer solution) and filtration. The polymer was then further purified by preparatory SEC to remove undesired high molecular weight polymers and residual reactant polymers. The polymer was dried *in vacuo* for 24 h at 25 °C and characterised. SEC ($M_n=12890$, PDI=1.04), Triple Detection SEC ($M_n=18900$, PDI=1.005). The polymer was further characterised by ^1H NMR and MALDI-ToF.

Synthesis of G1 Star Tetracyclic 33

Polymer c-PSTY₇₅-(N₃)₃ **29** (3.0×10^{-2} g, 3.2×10^{-6} mol), polymer c-PSTY₂₅-≡ **13** (3.2×10^{-2} g, 1.0×10^{-5} mol) and PMDETA (2.0×10^{-3} mL, 9.5×10^{-6} mol) were dissolved in 0.6 mL of toluene. CuBr (1.4×10^{-3} g, 9.5×10^{-6} mol) was added to a 10 mL schlenk flask equipped with magnetic stirrer and both of the reaction vessels were purged with argon for 15 min. The polymer solution was then transferred to CuBr flask using double tipped needle by applying argon pressure. The reaction mixture was purged with argon for a further 2 min and the flask was placed in a temperature controlled oil bath at 25 °C for 1.5 h. The reaction was then diluted with THF (*ca.* 3 fold to the reaction mixture volume), and passed through activated basic alumina to remove the copper salts. The solution was concentrated by rotary evaporator and the polymer was recovered by precipitation into a large amount of MeOH (20 fold excess to polymer solution) and filtration. The polymer was then further purified by preparatory SEC to remove undesired high molecular weight polymers and residual reactant polymers. The polymer was dried *in vacuo* for 24 h at 25 °C and characterised.

SEC ($M_n=13920$, PDI=1.05), Triple Detection SEC ($M_n=19680$, PDI=1.002). The polymer was further characterised by ^1H NMR and MALDI-ToF.

Synthesis of G1 Star Heptacyclic 34

Polymer c-PSTY₇₅-(≡)₆ **30** (1.9×10^{-2} g, 2.0×10^{-6} mol), polymer c-PSTY₂₅-N₃ **11** (3.8×10^{-3} g, 1.3×10^{-5} mol) and PMDETA (2.54×10^{-3} mL, 1.2×10^{-5} mol) were dissolved in 0.6 mL of toluene. CuBr (1.7×10^{-3} g, 1.2×10^{-5} mol) was added to a 10 mL schlenk flask equipped with magnetic stirrer and both of the reaction vessels were purged with argon for 15 min. The polymer solution was then transferred to CuBr flask using double tipped needle by applying argon pressure. The reaction mixture was purged with argon for a further 2 min and the flask was placed in a temperature controlled oil bath at 25 °C for 1.5 h. The reaction was then diluted with THF (*ca.* 3 fold to the reaction mixture volume), and passed through activated basic alumina to remove the copper salts. The solution was concentrated by rotary evaporator and the polymer was recovered by precipitation into a large amount of MeOH (20 fold excess to polymer solution) and filtration. The polymer was then further purified by preparatory SEC to remove undesired high molecular weight polymers and residual reactant polymers. The polymer was dried *in vacuo* for 24 h at 25 °C and characterised. SEC ($M_n=18930$, PDI=1.05), Triple Detection SEC ($M_n=29800$, PDI=1.007). The polymer was further characterised by ^1H NMR and MALDI-ToF.

3.3 Results and Discussion

Synthesis of Functional Precursor Linear Polymers.

The functional alcohol groups can be incorporated directly into the polymer chain by using two functional ATRP initiators **1** and **6** (Figure 3.1). Initiator **1** has three different functionalities: an alkyne group for the CuAAC coupling, a bromine group that can readily transformed to an azide, and an alcohol group for post modification. Initiator **6** was similar but with the alkyne group protected with TIPS (1,1,1-triisopropylsilyl moiety); full characterization of **6** was given in appendix B. The polymerization in bulk at 80 °C using initiator **1** for styrene in the presence of Cu(I)Br and Cu(II)Br₂/PMDETA resulted in the production of polystyrene ((≡(HO)-PSTY₂₅-Br, **7**) with a number-average molecular weight, M_n , of 2890 (M_n , theory = 2651) and polydispersity index (PDI) of 1.11 (see Table 3.1). The presence of Cu(II)Br₂ in the reaction mixture and stopping the polymerization close to 50% conversion should minimise radical termination products. However, the molecular weight distribution (MWD) determined by SEC (curve b in Figure 3.2(A)) showed a bimodal distribution, in which the peak maximum of the second distribution was approximately twice that of the first distribution. This second distribution most probably occurred through alkyne-

alkyne (i.e. Glaser) coupling rather than radical termination (*vide infra*). The polymerization using initiator **6** with the protected alkyne also gave a polymer (**14**) with a narrow MWD and an M_n close to theory (Table 3.1). In this case, there was no observable bimodal distribution (Figure B25 in appendix B), supporting the postulate that Glaser coupling in **7** was dominated over radical termination for initiator **1**.

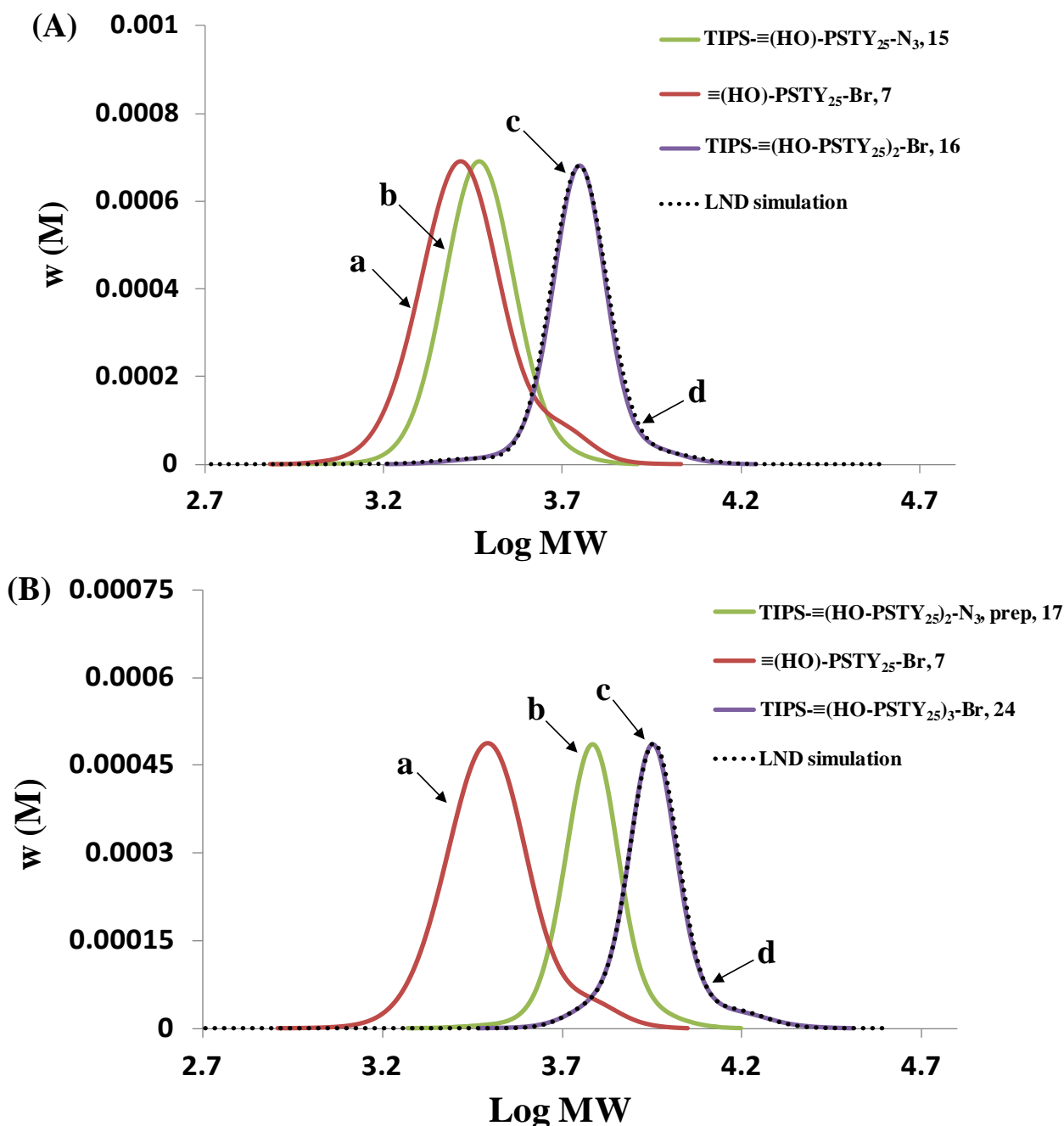


Figure 3.2. Molecular weight distributions (MWDs) for starting polymer and products obtained from SEC with RI detection. Synthesis of (A) TIPS-≡(OH-PSTY₂₅)₂-Br **16** (curve c - crude product) from **7** (curve a) and **15** (curve b); and (B) TIPS-≡(OH-PSTY₂₅)₃-Br **24** (curve c - crude product) from **7** (curve a) and **17** (curve b). Curve d represents the LND fit to the product MWD.

Table 3.1: Purity, coupling efficiency, molecular weight data (RI, triple detection and NMR) and change in hydrodynamic volume for all starting building blocks and products.

Polymer	Purity by LND (%)		Coupling efficiency (%) ^a by LND	RI detection ^b			Triple detection ^c			M _n by NMR	Δ HDV ^d
	Crude	Prep		M _n	M _p	PDI	M _n	M _p	PDI		
7	84.0			2890	2900	1.11				3120	
8	84.0			2880	2900	1.11				2980	
9	40.3	>99		2140	2180	1.04	2780	2860	1.016	2980	0.76
10				2350	2400	1.04				3110	
11				2250	2300	1.04	2930	3090	1.018	3180	0.75
13				2440	2470	1.04	3170	3320	1.021	3520	0.74
14				2870	3040	1.08				2960	
15	98.5			2890	2910	1.06				3030	
16	90.8		90.8	5510	5600	1.05				6350	
17	88.3	94.5		5510	5550	1.06				6210	
18	87.0	91.0		5350	5400	1.06				6420	
19	52.7	>99		4110	4170	1.03	5350	5500	1.020	6470	0.76
20				4350	4370	1.03				6220	
21				4470	4590	1.03	5850	5990	1.005	6250	0.77
23				4720	4830	1.04	6420	6500	1.001	6840	0.74
24	82.0		82.0	8830	8990	1.06				9230	
25	82.5			8750	8860	1.06				9400	
26	82.0	86.0		8720	8890	1.05				9660	
27	38.5	>99		6600	6780	1.03	8830	8980	1.007	8930	0.76
28				7210	7320	1.03				9230	
29				7070	7220	1.03	9250	9390	1.004	8910	0.77
30				7640	7790	1.03	9980	10120	1.004	9740	0.77
31	68.5	77.6	70.8	9820	9750	1.05	12420	12720	1.004	12990	0.77
32	77.8	97.0	80.9	12890	13130	1.04	18900	19400	1.005	18410	0.68
33	70.5	84.2	73.2	13920	13980	1.05	19680	19800	1.002	18450	0.71
34	71.2	84.9	74.25	18930	18870	1.06	29800	30310	1.007	29950	0.62

^aCuAAC coupling efficiency was determined from the RI traces of SEC. Coupling efficiency calculated as follows: purity (LND)/max. purity by theory×100. ^bThe data was acquired using SEC (RI detector) and is based on PSTY calibration curve. ^cThe data was acquired using DMAc Triple Detection SEC with 0.03 wt% of LiCl as eluent. ^dΔHDV was calculated by dividing M_p of RI with M_p of triple detection.

A key synthetic challenge is to place functional groups in desired locations on the cyclic polymer chain. It requires that the precursor linear polymer (i.e. before ring formation) should have the functional groups in the desired locations. Producing such linear polymer required the coupling of two or more functional polymers by using a new strategy as illustrated in Scheme 3.1. This strategy involved the coupling of two polymer chains 'clicked' together via the CuAAC reaction, in which one of the chains contained a bromine group (which is normally susceptible to form a radical in the presence of Cu(I)). Coupling polymers **7** and **15** resulted in the loss of nearly all reactants and formation of high purity diblock **16** (TIPS-≡-(HO-PSTY₂₅)₂-Br) as shown by the SEC chromatograms in Figure 3.2(A). The purity was determined by fitting the experimental SEC trace (denoted as crude - i.e. prior to fractionation) with a log-normal distribution (LND) model⁴⁸ based on fitting multiple Gaussian functions for each polymer species.^{22, 49} The purity of **16** using the LND method was 90.8 % (Table 3.2). In addition to the main product **16**, there was 0.04 and 0.80% of the starting polymers **7** and **15**, and 8.0% of higher molecular weight polymer. Coupling **7** and **17** resulted in high purity (82.0%) of **24** (TIPS-≡-(HO-PSTY₂₅)₃-Br) and approximately 4.75% of remaining starting polymer **17**. The reason for the higher amount of unreacted **17** could be a consequence of the difficulty in determining the stoichiometry of reactants since neither **16** nor **17** were fractionated by preparative SEC. It can be clearly seen from Scheme 3.1 that the OH-groups are equally spaced and in the desired location for **17** and **24**.

Table 3.2. LND simulation data for the synthesis of TIPS-≡(OH-PSTY₂₅)₂-Br (**16**) and TIPS-≡(OH-PSTY₂₅)₃-Br (**24**) polymers by LND based on weight distribution (w(M)).

Polymer		Purity w(M) (%)	Unreacted reactants and by-products (%)									
			15	15*2	7	7*2	15+7*2	16*2	17	7*2+17	7+17*2	(7+17)*2
7	Crude	90.3	--	--	90.3	9.7	--	--	--	--	--	--
15	Crude	98.5	98.5	1.5	--	--	--	--	--	--	--	--
16	Crude	90.8	0.8	--	0.4	--	4	4	--	--	--	--
17	Crude	88.3	0.8	--	0.4	--	6	4.5	--	--	--	--
	Prep	94.5	0.5	--	--	--	--	1	--	4	--	--
24	Crude	82.0	--	--	--	--	--	--	4.75	4.75	4.5	4

The deprotection of the TIPS of the alkyne group from **17** using TBAF gave **18** (\equiv -(HO-PSTY₂₅)₂-N₃) with near complete loss of TIPS as shown from the ¹H NMR (i.e. loss of proton a' at 1.1 ppm in Figure 3.3(B)). In addition, after deprotection the SEC chromatogram showed little or no change in the MWD, suggesting minimal Glaser coupling (see Figure B32 in appendix B). Azidation and deprotection of **24** to form **26** also showed little or no change in the SEC traces (Figures B44 in appendix B) and complete loss of the TIPS (Figure 3.3(D)). The next step involves the ring-closure of **18** and **26** via the CuAAC under feed conditions.

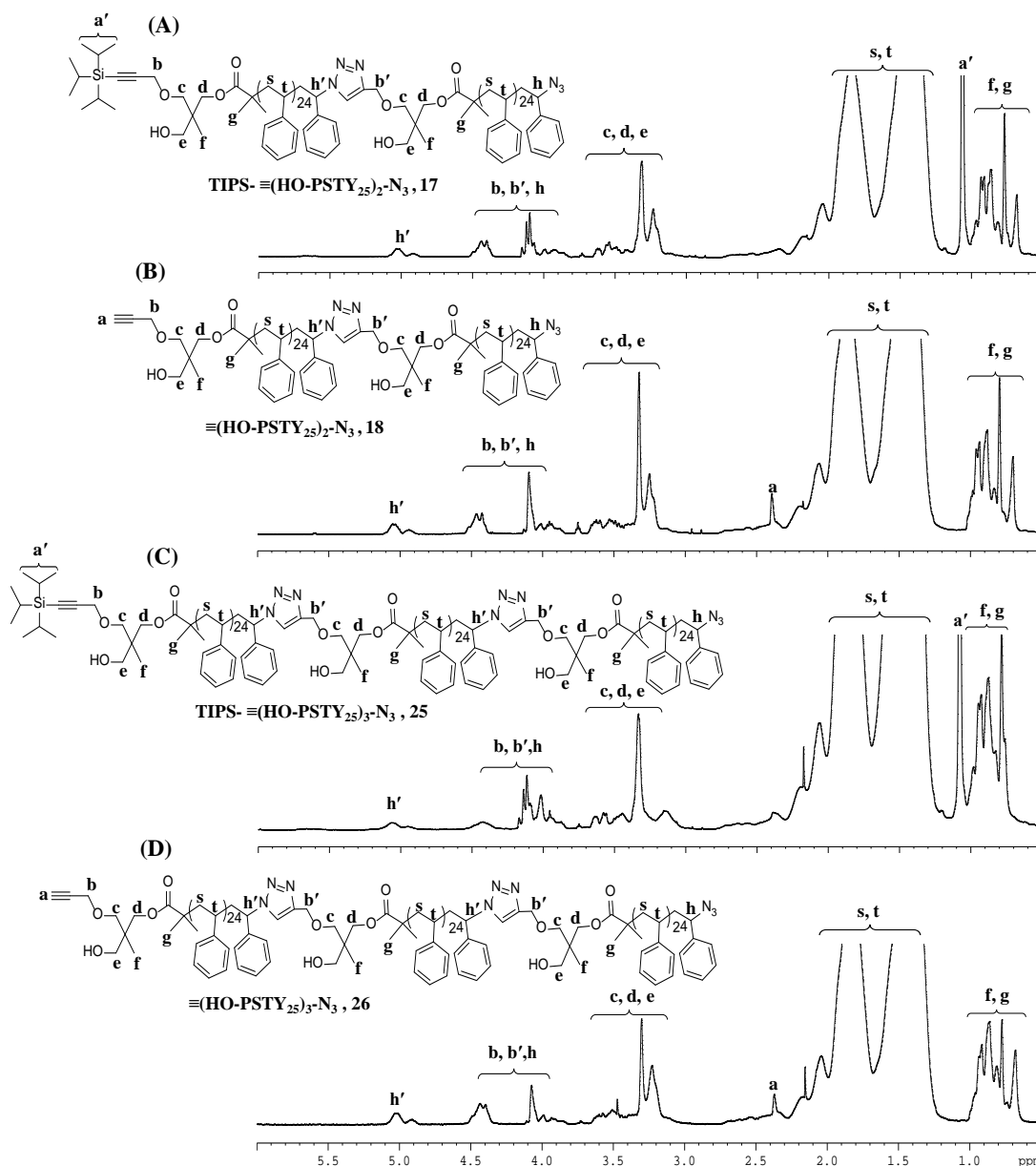


Figure 3.3. 500 MHz ¹H 1D DOSY NMR spectra in CDCl₃ of (A) TIPS-≡(OH-PSTY₂₅)₂-N₃ **17**, (B) ≡(OH-PSTY₂₅)₂-N₃ **18**, (C) TIPS-≡(OH-PSTY₂₅)₃-N₃ **25**, and (D) ≡(OH-PSTY₂₅)₃-N₃ **26**.

Cyclization of Multifunctional Precursor Linear Polymers.

The most used method for cyclization of polymers using the CuAAC reaction involved, for example, feeding a polymer solution (0.02 g of polymer in 1 mL of toluene) at a feed rate of 0.124 mL/min into a Cu(I)Br/PMDETA solution (in 1 mL of toluene). Such small scales provide high purity cyclic polymers in 9 min, and as long as oxygen is excluded the reaction proceeded in accord with theory.^{14, 37} Scaling up to produce significantly more amounts of cyclic polymer required a new method to always keep the polymer and Cu(I) solutions under an inert atmosphere (see Scheme B4 in appendix B). Diffusion of even a small amount of oxygen into the polymer or Cu(I) solutions during the feed process will slow the CuAAC reaction and thus the rate of cyclization with the production of greater amounts of multiblock instead of cyclic polymer. This becomes a major problem when the gas tight syringe loses its seal after multiple uses, resulting in poor reproducibility when the polymer solution is directly fed from the syringe into the Cu(I) solution (results not shown). Our new method avoids this problem by injecting a syringe filled with argon into a flask filled with polymer solution under argon, in which the pressure drives the polymer solution into the next flask (with Cu(I)Br/PMDETA) under argon (Scheme B4 in appendix B). This method provided an easy method to scale up to 2 g of polymer (i.e. an increase of two orders of magnitude) while maintaining the same feed rate (0.124 mL/min) and high purity of cyclic polymer.

Cyclization of **8** ($\equiv(\text{OH})\text{-PSTY}_{25}\text{-N}_3$) to form **9** (c-PSTY₂₅-OH) using our synthetic strategy resulted in nearly complete loss of starting polymer **8** (see curve a in Figure 3.4(A)) and formation of large peak at lower molecular weight, indicative of a change of hydrodynamic volume upon cyclization (curve b). In addition, a broad high molecular weight peak in curve b suggested multiblock formation. The low molecular weight peak (corresponding to the cyclic) could be accurately fit via the LND method by implementing a hydrodynamic volume shift of 0.75 to that of the linear precursor polymer **8** (curve d). The purity of **9** was determined to be 82.1% (Table 3.1); the lower than expected purity was most probably due to the high molecular weight polymer by-product in **8** (as seen from the high molecular weight shoulder in curve b). Fractionation of the crude **9** by preparative SEC gave pure cyclic (>99%, curve c) further supported by the excellent fit of the LND SEC trace (curve d). Cyclization of **18** ($\equiv(\text{OH-PSTY}_{25})_2\text{-N}_3$) to produce **19** (c-PSTY₅₀-(OH)₂) gave a purity of 85.9% (Table 3.1 and curve b in Figure 3.4(B)). The LND fit showed that the apparent low molecular weight peak consisted entirely of cyclic polymer (curve d). Fractionation similar to that for **9** gave > 99% purity of **19** cyclic with two OH group located equidistant from each other. In the final cyclization, **26** ($\equiv(\text{OH-PSTY}_{25})_3\text{-N}_3$) gave a purity of 76.8% (curve b in Figure 3.4(C)), and after fractionation a purity of > 99% as supported from the LND fit (curve d).

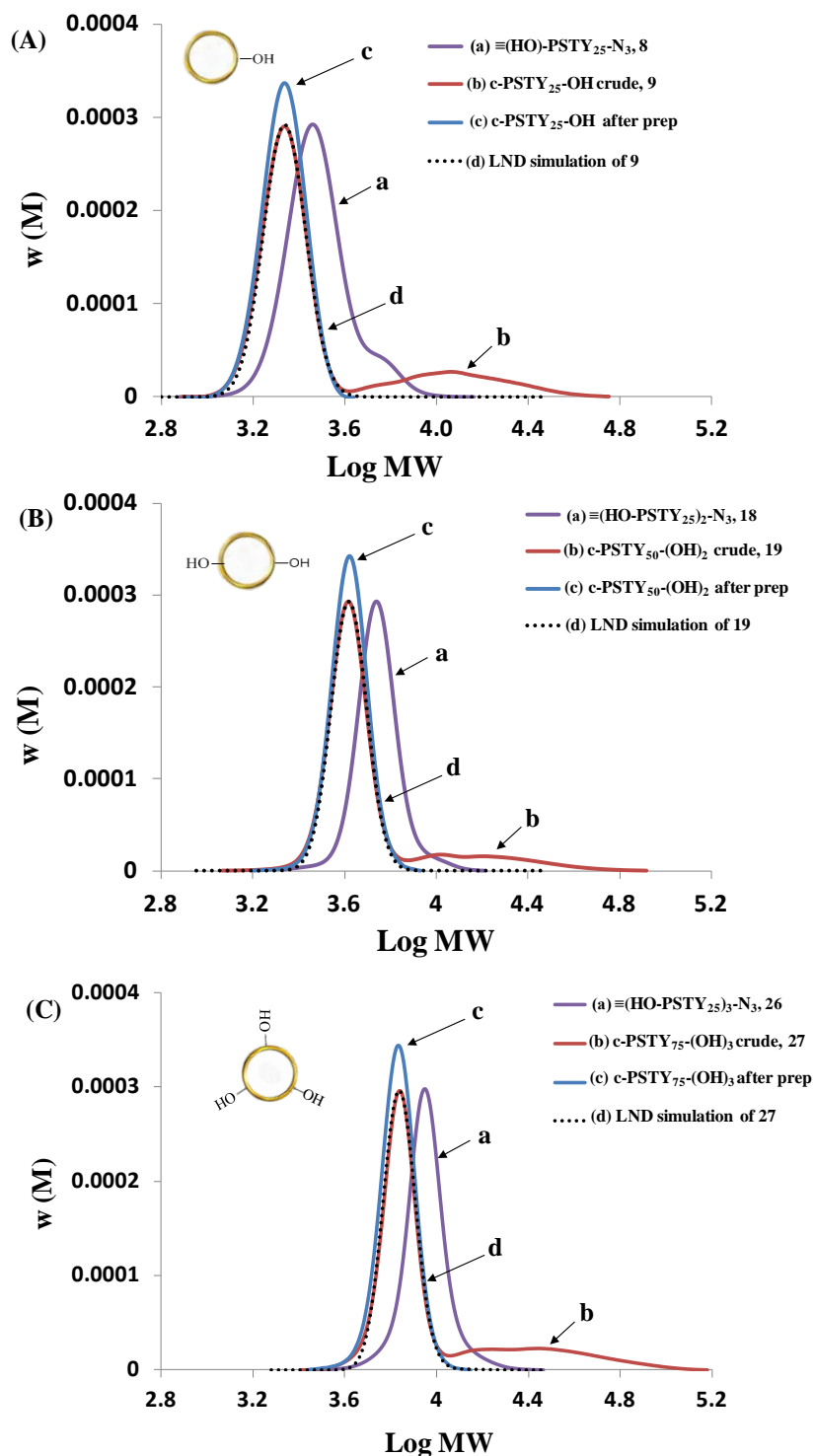


Figure 3.4: Molecular weight distributions (MWDs) for starting linear and cyclic polymers. (A) (a) **8**, (b) crude **9**, (c) **9** purified by prep SEC; (B) (a) **18**, (b) crude **19**, (c) **19** purified by prep SEC; and (C) **26**, (b) crude **27**, (c) **27** purified by prep SEC. Curve d represents the LND fit to the product MWD using a hydrodynamic volume change between 0.75 and 0.76.

The ^1H NMR before and after cyclization showed the complete loss of the protons adjacent to the alkyne and azide groups (peaks b and h in Figure 3.5) and loss of the alkyne proton a. The MALDI

(Figure 3.6) acquired in linear mode showed that the distributions (i.e. the full spectrum) were similar to that found by SEC, with the main peak corresponding to the expected molecular weight of the cyclic polymer product. For example, the experimental peak at $m/z = 3086.87$ (adduct with Ag^+) matched closely with the theoretical $m/z = 3085.09$ for cyclic **9**, suggesting complete cyclic formation. The other two cyclic products, **19** and **27**, also gave similar results. Take together, the SEC, NMR and MALDI data support that the cyclic polymer with one, two and three OH groups can be prepared with high purity.

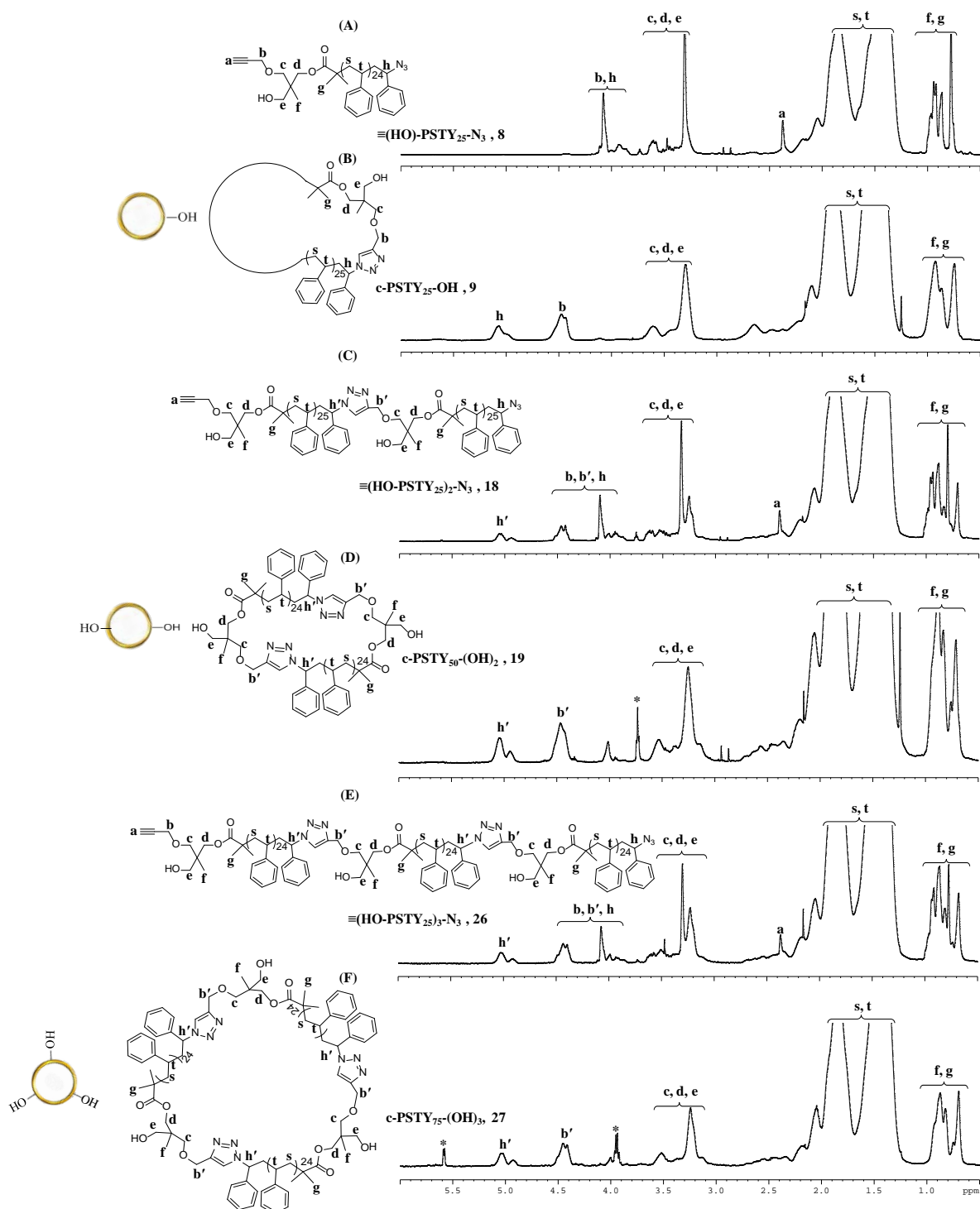


Figure 3.5. 500 MHz ^1H 1D DOSY NMR spectra in CDCl_3 of (A) $\equiv(\text{OH})\text{-PSTY}_{25}\text{-N}_3$ **8**, (B) $c\text{-PSTY}_{25}\text{-OH}$ **9**, (C) $\equiv(\text{OH-PSTY}_{25})_2\text{-N}_3$ **18**, (D) $c\text{-PSTY}_{50}\text{-}(\text{OH})_2$ **19**, (E) $\equiv(\text{OH-PSTY}_{25})_3\text{-N}_3$ **26**, and (F) $c\text{PSTY}_{75}\text{-}(\text{OH})_3$ **27**. (*small molecules impurities)

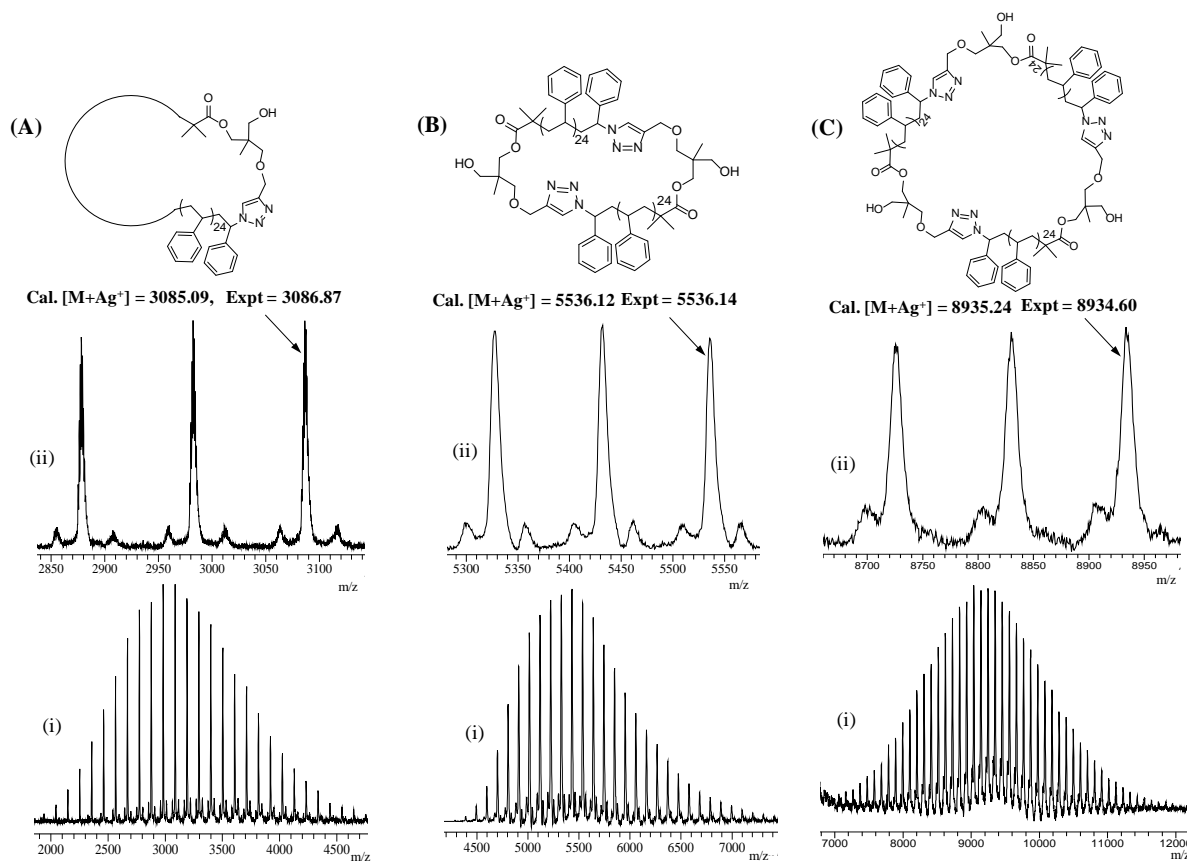


Figure 3.6. MALDI-TOF mass spectrum using Ag salt as cationizing agent and DCTB matrix. (A) $c\text{-PSTY}_{25}\text{-OH}$, **9** acquired in reflectron mode, (B) $c\text{-PSTY}_{50}\text{-}(\text{OH})_2$, **19** and (C) $c\text{PSTY}_{75}\text{-}(\text{OH})_3$, **27** acquired in linear mode. (i) Full spectra, and (ii) expanded spectra.

Construction of Multicyclic Topologies.

The hydroxyl groups attached to the cyclic polystyrene (**9**, **19** and **27**) can be converted to azide groups as shown in Scheme 3.1 through a reaction with 2-bromopropionyl bromide (BPB) followed by azidation of the bromide group with NaN_3 . The conversion of the OH groups to bromine (via reaction with BPB) produced $c\text{-PSTY}_{25}\text{-Br}$ (**10**), $c\text{-PSTY}_{50}\text{-Br}_2$ (**20**) and $c\text{-PSTY}_{75}\text{-Br}_3$ (**28**) in near quantitative yields supported by both ^1H NMR and MALDI ToF (see appendix B). Further conversion of the bromine to azide groups using excess NaN_3 in DMF at 25°C was also near quantitative as found by ^1H NMR from the complete loss of the methine proton (CH-Br) at 4.2 ppm for polymer **10** (see in Figure B17 in appendix B) and the emergence of the CH-N_3 peak at 3.9 ppm

in **11** (Figure B20 in appendix B). Near complete CuAAC coupling of the azide group on **11** with an alkyne PSTY (results not shown) further supported high azide functionality. Similar results were found for the formation of **21** and **29**.

Polymers **11**, **21** and **29** were then converted to alkyne groups through a CuAAC reaction with excess multi-alkyne linker (see Scheme 3.1). Linkers **12** and **22** are less sterically hindered, offering greater coupling efficiency, and in addition the benzyl core provides greater thermal stability compared to other linkers (e.g. tripropagyl amine). The product from the CuAAC reactions between the polymers and the linkers showed high coupling efficiencies. There was no observable alkyne-alkyne coupling product from the MALDI for **13**, **23** and **30** (see Figures B24, B41 and B53 in appendix B) and there was the expected change in M_n values with the addition of the linker molecules (see Table 3.1). These three polymers formed the core cyclic structures to prepare four complex topologies, **31** to **34**.

The first structure, a spiro type tricyclic polymer **31**, was synthesised by coupling two *c*-PSTY₂₅-≡ (**13**, 2.1 equiv.) and one *c*-PSTY₅₀-(N₃)₂ (**21**, 1.0 equiv.) catalysed by CuBr (2.0 equiv.) in toluene for 1.5 h. The SEC trace (curve c, Figure 3.7(A)) of the polymer after the CuAAC 'click' reaction showed MWDs corresponding to the starting polymer **13** (3.8%), little or no observed peak of the *c*-PSTY₅₀-(N₃)₂ (0.4%), and a dominant high MWD corresponding to the **31** (69%, and 'click' efficiency was calculated to be 70.8% as shown in Table 3.1). The amount (i.e. %) of each species was determined by fitting curve c using the LND method. In addition, there was approximately 12.5% of a product corresponding to the 'click' between one *c*-PSTY₂₅-≡, **13** and one *c*-PSTY₅₀-(N₃)₂, **21**, 1.7% of a glazer coupling product of two **13** polymers, and a high percentage (16.4%) of high molecular weight polymer. The mechanism for the formation of this latter high molecular weight polymer is unknown but observed in all the complex topologies. Preparative SEC allowed the removal of this high molecular weight polymer as observed from curve d in Figure 3.7(A). The MALDI of **31** gave a MWD similar to that found by SEC, and the molecular weight was in agreement with the theoretical value including Ag⁺ (see Figure B55 in appendix B). Triple detection SEC also showed that the M_n was similar to the theoretically calculated molecular weight value (Table 3.1).

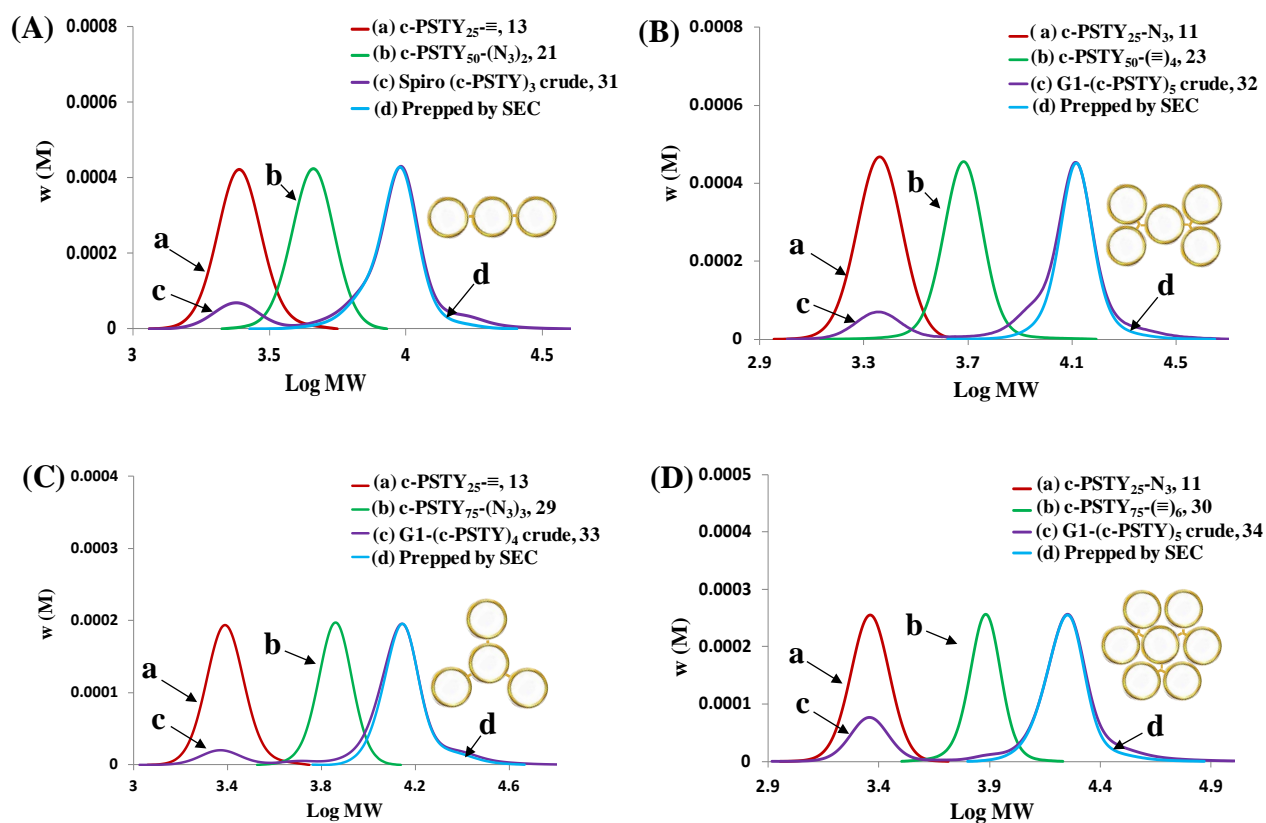


Figure 3.7. Molecular weight distribution (MWDs) for starting polymers and products. (A) SEC RI distribution of (a) c-PSTY₂₅-≡ **13** and (b) c-PSTY₅₀-(N₃)₂ **21** to produce (c) spiro (c-PSTY)₃ **31**, (d) purified by preparative SEC. (B) SEC RI distribution of (a) c-PSTY₂₅-N₃ **11** and (b) c-PSTY₅₀-(≡)₄ **23** to produce (c) G1-(c-PSTY)₅ **32**, (d) purified by preparative SEC. (C) SEC RI distribution of (a) c-PSTY₂₅-≡ **13** and (b) c-PSTY₇₅-(N₃)₃ **29** to produce (c) G1-(c-PSTY)₄ **33**, (d) purified by preparative SEC. (D) SEC RI distribution of (a) c-PSTY₂₅-N₃ **11** and (b) c-PSTY₇₅-(≡)₆ **30** to produce (c) G1-(c-PSTY)₇ **34**, (d) purified by preparative SEC. SEC analysis based on polystyrene calibration curve.

The 1st generation pentacyclic dendrimer **32** was formed by coupling four c-PSTY₂₅-N₃ (**11**, 4.2 equiv.) onto a c-PSTY₅₀-(≡)₄ (**23**, 1.0 equiv.). The SEC trace (curve c, Figure 3.7(B)) after the 'click' reaction showed MWDs corresponding to the product **32** (78%, and 'click' efficiency of 81%), 3.8% of the starting polymer **11**, little or no of the other starting polymer **23** (< 0.4%), 1% of one **11** coupled with **23**, 8% of two **11** polymers coupled with **23**, and 10% of high molecular weight polymers probably formed through glazer coupling of **23**. After preparative SEC, **32** was found to be 97% pure, which was further confirmed from MALDI (see Figure B57 in appendix B). The G1 tetracyclic dendrimer **33** was formed by coupling three c-PSTY₂₅-≡ (**13**, 3.15 equiv.) and c-PSTY₇₅-(N₃)₃ (**29**, 1.0 equiv.). The SEC trace (curve c, Figure 3.7(C)) after the 'click' reaction showed MWDs corresponding to the product **33** (71%, and 'click' efficiency of 73%), 1.5% of the

starting polymer **13**, little or no of the other starting polymer **29** (<0.4%), 4% of one **13** coupled with **29**, 0.8% of two **13** polymers coupled with **29**, 4% of the glazer coupling product between two **13** polymers, and 19% of high molecular weight polymers. After preparative SEC, **33** was found to be 84% pure. A similar result was also found for the formation of G1 tetracyclic dendrimer **34** by coupling six c-PSTY₂₅-N₃ (**11**, 6.3 equiv.) with one c-PSTY₇₅-(≡)₆ (**23**, 1.0 equiv.). The SEC trace (curve c, Figure 3.7(D)) after the 'click' reaction showed MWDs corresponding to the product **34** (71%, and 'click' efficiency of 74%), 3 and 1% of the starting polymer **11** and **30**, 3.7% of two **11** polymers coupled with **30**, 2.4% of three **11** polymers coupled with **30**, and 19% of high molecular weight polymers. After preparative SEC, **34** was found to be 85% pure. The MALDI and triple detection SEC data for **33** and **34** showed that the molecular weights corresponded to the theoretical values, confirming the formation of these structures in high percentages. The change in hydrodynamic volume in Table 3.1 (determined from the ratio of the M_p from RI detection to the M_p from triple detection) showed that the value of 0.77 for **31** was similar to the change observed after cyclization of a linear polymer (e.g. **9**). However, the star-like structures showed a more compact conformation, in which the hydrodynamic volume decreased with complexity of the dendrimer from 0.68 to 0.62.

3.4 Conclusion

In conclusion, we have described a new method to produce mono-cyclic polymers with hydroxyl groups equally spaced along the polymer backbone. Carrying out the CuAAC reaction of telechelic polymer chains in the presence of a bromine group through modulating the Cu(I) activity towards the 'click' reaction over radical formation produced linear polymers with the OH-groups located at each 'click' site. Azidation of the bromine groups and cyclization using a modified feed approach resulted in multifunctional cyclics in high amounts and high purity. Fractionation of the low hydrodynamic mono-cyclic from the high molecular weight multiblock polymers gave greater than 99% of multifunctional mono-cyclic. Conversion of the OH-groups on the cyclic polymer to either alkyne or azide moieties produced cyclics that would be the core to form complex topologies, in which all the building blocks consisted of cyclic polymers. The complex topologies included a spiro tricyclic, and dendritic structures consisting of a G1 pentacyclic, G1 tertacyclic, and a G1 heptacyclic. All these structures were produced in high amounts with good 'click' efficiencies. This work demonstrated the utility for the formation of complex polymer topologies from cyclic building blocks. The synthetic strategy used here provides a useful methodology for the production of more complex topologies with varying copolymer compositions.

3.5 References

1. Matyjaszewski, K.; Davis, T. P., *Handbook of Radical Polymerization*. John Wiley and Sons: USA, 2002.
2. Kolb, H. C.; Finn, M. G.; Sharpless, K. B. *Angew. Chem., Int. Ed.* **2001**, 40, (11), 2004-2021.
3. Lutz, J. F. *Angew Chem Int Edit* **2007**, 46, (7), 1018-1025.
4. Lutz, J. F.; Borner, H. G.; Weichenhan, K. *Macromolecules* **2007**, 40, (19), 7060-7060.
5. Lammens, M.; Fournier, D.; Fijten, M. W. M.; Hoogenboom, R.; Du Prez, F. *Macromol Rapid Comm* **2009**, 30, (23), 2049-2055.
6. Whittaker, M. R.; Urbani, C. N.; Monteiro, M. J. *J. Am. Chem. Soc.* **2006**, 128, (35), 11360-11361.
7. Urbani, C. N.; Bell, C. A.; Whittaker, M. R.; Monteiro, M. J. *Macromolecules* **2008**, 41, (4), 1057-1060.
8. Urbani, C. N.; Lonsdale, D. E.; Bell, C. A.; Whittaker, M. R.; Monteiro, M. J. *J. Polym. Sci., Part A Polym. Chem.* **2008**, 46, (5), 1533-1547.
9. Konkolewicz, D.; Monteiro, M. J.; Petrie, S. *Macromolecules* **2011**, 44, (18), 7067-7087.
10. Hu, D.; Zheng, S. X. *Eur Polym J* **2009**, 45, (12), 3326-3338.

11. Pan, P. J.; Fujita, M.; Ooi, W. Y.; Sudesh, K.; Takarada, T.; Goto, A.; Maeda, M. *Polymer* **2011**, 52, (4), 895-900.
12. Lutz, J. F.; Borner, H. G.; Weichenhan, K. *Macromolecules* **2006**, 39, (19), 6376-6383.
13. Laurent, B. A.; Grayson, S. M. *J. Am. Chem. Soc.* **2006**, 128, (13), 4238-4239.
14. Lonsdale, D. E.; Bell, C. A.; Monteiro, M. J. *Macromolecules* **2010**, 43, (7), 3331-3339.
15. Lonsdale, D. E.; Monteiro, M. J. *Chem. Commun.* **2010**, 46, (42), 7945-7947.
16. Dong, Y.-Q.; Tong, Y.-Y.; Dong, B.-T.; Du, F.-S.; Li, Z.-C. *Macromolecules* **2009**, 42, (8), 2940-2948.
17. Eugene, D. M.; Grayson, S. M. *Macromolecules* **2008**, 41, (14), 5082-5084.
18. McLeish, T. *Science* **2002**, 297, (5589), 2005-2006.
19. Obhukov, S. P.; Rubinstein, M.; Duke, T. *Phys. Rev. Lett.* **1994**, 73, 1263-1266.
20. Geiser, D.; Hoecker, H. *Macromolecules* **1980**, 13, (3), 653-6.
21. Roovers, J.; Toporowski, P. M. *Macromolecules* **1983**, 16, (6), 843-849.
22. Jia, Z. F.; Lonsdale, D. E.; Kulis, J.; Monteiro, M. J. *Acs Macro Letters* **2012**, 1, (6), 780-783.
23. Jia, Z. F.; Monteiro, M. J. *J. Polym. Sci., Part A Polym. Chem.* **2012**, 50, (11), 2085-2097.
24. Endo, K. *Adv. Polym. Sci.* **2008**, 217, (New Frontiers in Polymer Synthesis), 121-183.
25. Laurent, B. A.; Grayson, S. M. *Chem. Soc. Rev.* **2009**, 38, (8), 2202-2213.
26. Kricheldorf, H. R. *J. Polym. Sci., Part A Polym. Chem.* **2010**, 48, (2), 251-284.
27. Yamamoto, T.; Tezuka, Y. *Polym. Chem.* **2011**, 2, (9), 1930-1941.
28. Bielawski, C. W.; Benitez, D.; Grubbs, R. H. *Science* **2002**, 297, (5589), 2041-2044.
29. Shin, E. J.; Brown, H. A.; Gonzalez, S.; Jeong, W.; Hedrick, J. L.; Waymouth, R. M. *Angew Chem Int Edit* **2011**, 50, (28), 6388-6391.
30. Shin, E. J.; Jeong, W.; Brown, H. A.; Koo, B. J.; Hedrick, J. L.; Waymouth, R. M. *Macromolecules* **2011**, 44, (8), 2773-2779.
31. Zhang, K.; Lackey, M. A.; Cui, J.; Tew, G. N. *J. Am. Chem. Soc.* **2011**, 133, (11), 4140-4148.
32. Zhang, K.; Lackey, M. A.; Wu, Y.; Tew, G. N. *J. Am. Chem. Soc.* **2011**, 133, (18), 6906-6909.
33. Tezuka, Y.; Komiya, R.; Washizuka, M. *Macromolecules* **2003**, 36, (1), 12-17.
34. Tezuka, Y.; Oike, H. *J. Am. Chem. Soc.* **2001**, 123, (47), 11570-11576.
35. Tezuka, Y.; Oike, H. *Macromol. Rapid Commun.* **2001**, 22, (13), 1017-1029.
36. Sugai, N.; Heguri, H.; Ohta, K.; Meng, Q.; Yamamoto, T.; Tezuka, Y. *J. Am. Chem. Soc.* **2010**, 132, (42), 14790-14802.
37. Lonsdale, D. E.; Monteiro, M. J. *J. Polym. Sci., Part A Polym. Chem.* **2010**, 48, (20), 4496-4503.
38. Jacobson, H.; Stockmayer, W. H. *J. Chem. Phys.* **1950**, 18, 1600-1606.

-
39. Bell, C. A.; Jia, Z. F.; Kulis, J.; Monteiro, M. J. *Macromolecules* **2011**, 44, (12), 4814-4827.
40. Kulis, J.; Bell, C. A.; Micallef, A. S.; Jia, Z. F.; Monteiro, M. J. *Macromolecules* **2009**, 42, (21), 8218-8227.
41. Jia, Z. F.; Bell, C. A.; Monteiro, M. J. *Chem Commun* **2011**, 47, (14), 4165-4167.
42. Kulis, J.; Bell, C. A.; Micallef, A. S.; Monteiro, M. J. *Aust J Chem* **2010**, 63, (8), 1227-1236.
43. Kulis, J.; Bell, C. A.; Micallef, A. S.; Monteiro, M. J. *J. Polym. Sci., Part A Polym. Chem.* **2010**, 48, (10), 2214-2223.
44. Cai, H. H.; Jiang, G. L.; Shen, Z. H.; Fan, X. H. *Macromolecules* **2012**, 45, (15), 6176-6184.
45. Li, Y. T.; Mullen, K. M.; Claridge, T. D. W.; Costa, P. J.; Felix, V.; Beer, P. D. *Chem Commun* **2009**, (46), 7134-7136.
46. Vaz, B.; Otero, L.; Alvarez, R.; de Lera, A. R. *Chem-Eur J* **2013**, 19, (39), 13065-13074.
47. Schaefer, M.; Hanik, N.; Kilbinger, A. F. M. *Macromolecules* **2012**, 45, (17), 6807-6818.
48. Cabaniss, S. E.; Zhou, Q. H.; Maurice, P. A.; Chin, Y. P.; Aiken, G. R. *Environmental Science & Technology* **2000**, 34, (6), 1103-1109.
49. Hossain, M. D.; Valade, D.; Jia, Z. F.; Monteiro, M. J. *Polymer Chemistry* **2012**, 3, (10), 2986-2995.

Chapter 4

Complex Cyclic Polymer Topologies and Their Glass Transition Studies

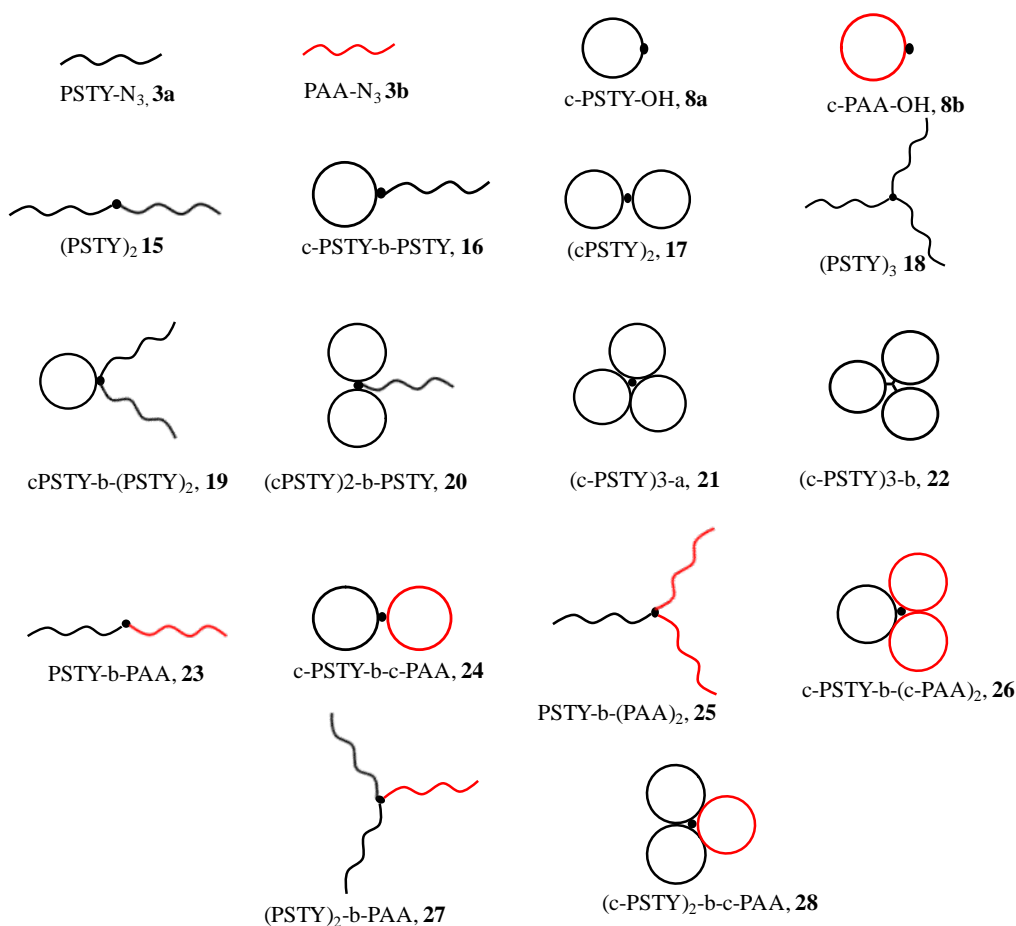
In this chapter, different architectures of polystyrene homopolymers and polystyrene (PSTY)/polyacrylic acid (PAA) copolymers were synthesised by combining of ATRP, SET-LRP and CuAAC coupling reactions. The architectures of polystyrene homopolymers ranged from diblock copolymer to 3-arms star polymers, consisting of both linear and cyclic polymer building blocks. The diblock, AB, miktoarm AB₂ and A₂B type of amphiphilic copolymers of both linear and cyclic counterparts were also successfully synthesised. These polymers were characterised by ¹H NMR, SEC, MALDI ToF mass spectroscopy and differential scanning calorimetry (DSC). The DSC was used to investigate the effect of topology of amorphous PSTY and PSTY/PAA copolymers by determining the glass transition temperature (T_g). The results revealed that the topologies that possessed higher number of cyclic units (i.e., lower number of chain ends) showed higher T_g values. The thin film self-assemblies of block copolymers were also characterised by AFM to investigate the morphology of linear block copolymer and its cyclic analogue. The thin film domain spacing of cyclic block copolymer decreased by ~50% compared to the linear analogue due to the structural compactness.

4.1 Introduction

Great attention has been paid for the synthesis of polymers with tailored architectures from conventional linear structures to form nonlinear and complex topologies. Combination of 'living' radical polymerization and highly efficient 'click' reactions led to a significant breakthrough in the synthesis of different complex polymer topologies, including stars, brush, graft, dendrimers, hyper-branched polymers, multiblock copolymers, gel and networks, polymers conjugated to nanomaterials and even more intriguing cyclic and multicyclic polymers. Among the various types of topologies, cyclic polymers are unique class of topologies that do not have any chain-ends, and show very distinct properties compared to their linear counterparts.¹⁻⁷ A great deal of effort has been paid to understand the macromolecular motion of linear polymers but to a lesser extent to cyclic.⁷⁻¹¹ The conventional theory for diffusion of linear polymers occurs via reptation through the matrix while cyclic polymers diffuse via amoeba-like motion.^{7,8} However, the above theories for cyclic polymers do not include the formation of duplex conformations that interpenetrate each other by opening up the folded structures. A quantitative theory for interpenetrated duplex structures of cyclic has been proposed recently,⁹ though the true mechanism is yet to found.

Before understanding the diffusion processes and deriving a unifying theory, one must first synthesise precisely defined cyclic polymers in high purity. Even trace amount of linear contaminants in the cyclic polymer can influence the properties.⁸ Significant progress has now been made to produce a wide variety of single cyclic polymers based on end-to-end coupling processes,¹²⁻²⁰ as well as on an alternative ring-expansion polymerization.²¹⁻²⁷ Recently, a rapid and effective synthetic methodology was developed by our group to prepare a high purity monocyclic polymer in less than 9 min in non-dilute condition.²⁸ The higher solubility of Cu(I)Br/PMDETA complex in toluene facilitated the catalytic activity. However, cyclic polymer having a pendant functional group is fascinating as the post modification approach allows in building different complex polymer topologies.^{13,29-33} Tezuka *et al.* pioneered the synthetic strategies to produce a variety of single cyclic polymers of different segment components that have specific functional groups at designated position.³⁴⁻³⁶ A variety of spiro and bridged-type multicyclic polymer, different polymeric graphs and fused polymer topologies have been constructed through the CuAAC addition in conjunction with electrostatic self-assembly and covalent fixation process.³⁷⁻⁴⁰ Nevertheless, cyclization was carried under very dilute condition, limiting this technique for practical applications. Therefore, the elaboration of synthetic methodologies to generate precise chemical functionality in the cyclic polymer is appealing for the synthesis of a wide range of complex cyclic topologies.

In this work, a facile and efficient strategy was used to synthesise single cyclic polymer with hydroxyl functional group by combining 'living' radical polymerization and effective CuAAC reaction. The subsequent functionalization of the hydroxyl group allows the fabrication of a range of complex structures through topological and compositional control. Linear polymer precursors for the cyclic polymers were herein synthesised by 'living' radical polymerization that essentially produce a wide range of polymer with near uniform chain length (i.e. with low polydispersity indexes) and high chain-end functionality. After post-modification and subsequent 'click' reaction allows preparation of cyclic, linear di-block, tadpole, spiro di-cyclic, linear tri-block star, twin-tailed tadpole, twin-headed tadpole and cyclic tri-block star and amphiphilic linear di-block, spiro di-block, mikto-arm linear and analogous cyclic architectures that are illustrated in the Scheme 4.1. The molecular weights of linear and cyclic analogues in all the topologies were almost the same to avoid the any effect from the chain length. All the structures were purified using preparatory SEC, which allowed most if not all linear and intermediate species to be removed. The present work is designed to study the effect of topologies on glass transition temperature, and the results may be useful for the fabrication of new materials.



Scheme 4.1. Graphical representation of different architectures homo and amphiphilic block copolymers where black and red lines represent the PSTY and PAA segments respectively.

4.1.1 Aim of the Chapter

The aim of the work described in this chapter was to synthesise a range of different topologies of polymers having both linear and cyclic analogues and investigate their glass transition temperature. The chain-ends play a vital role in determining the polymer's bulk properties. The present work demonstrates a systematic synthetic protocol that used simple linear polymers to form star tricyclic polymers, and showed the influence of topology effects on the T_g . A range of copolymers of PSTY and PAA were also synthesised, and the effects of topology of two distinct blocks on the glass transition temperature were assessed.

4.2 Experimental

4.2.1 Materials

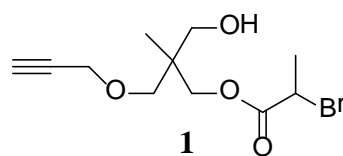
The following chemicals were analytical grade and used as received unless otherwise stated: alumina, activated basic (Aldrich: Brockmann I, standard grade, ~150 mesh, 58 Å), dimethyl(amino)pyridine (DMAP, Aldrich, 99%), Dowex ion-exchange resin (sigma-aldrich, 50WX8-200), magnesium

sulphate, anhydrous (MgSO_4 : Scharlau, extra pure) potassium carbonate (K_2CO_3 : analaR, 99.9%), silica gel 60 (230-400 mesh ATM (SDS)), triethylamine (TEA: Fluka, 98%), 2-bromopropionyl bromide (BPB: Aldrich 98%), propargyl bromide solution (80% wt% in xylene, Aldrich), propargyl ether (Aldrich, 99%), tripropargylamine (TPA: Aldrich, 98%), sodium azide (NaN_3 : Aldrich, 99.5%), *N,N,N',N'',N'''*-pentamethyldiethylenetriamine (PMDETA: Aldrich, 99%), copper(I) bromide (Cu(I)Br : Aldrich, 99.999%), copper (II) bromide (Cu(II)Br_2 : Aldrich, 99%). The following monomers were de-inhibited before use by passing through a basic alumina column: styrene (STY: Aldrich, >99%), *tert*-butyl acrylate (*t*BA: Aldrich, >99%). 1,3,5-tris(prop-2-ynoxy)benzene⁴¹ (**13**) linkers were prepared according to the literature procedure. All other chemicals used were of at least analytical grade and used as received.

The following solvents were used as received: acetone (ChemSupply, AR), chloroform (CHCl_3 : Univar, AR grade), dichloromethane (DCM: Labscan, AR grade), diethyl ether (Univar, AR grade), ethanol (EtOH: ChemSupply, AR), ethyl acetate (EtOAc: Univar, AR grade), hexane (Wacol, technical grade, distilled), hydrochloric acid (HCl, Univar, 32%), anhydrous methanol (MeOH: Mallinckrodt, 99.9%, HPLC grade), Milli-Q water (Biolab, 18.2 M Ω cm), *N,N*-dimethylformamide (DMF: Labscan, AR grade), tetrahydrofuran (THF: Labscan, HPLC grade), toluene (HPLC, LABSCAN, 99.8%).

4.2.2 Synthetic Procedures

The alkyne (hydroxyl) functional initiator **1** was synthesised according to the literature procedure previously reported by our group with a slight modification.³²



4.2.2.1 Synthesis of the initiator 3-hydroxy-2-methyl-2-((prop-2-yn-1-yloxy)methyl)propyl 2-bromo-2-methylpropanoate (**1**)

5.0 g (3.16×10^{-2} mol) of 2-methyl-2-((prop-2-yn-1-yloxy)methyl)propane-1,3-diol and 6.6 mL (4.74×10^{-2} mol) TEA were dissolved in 60 mL of dry THF and cooled to 0 °C in an ice-bath. To the above solution, 4.14 mL (3.95×10^{-2} mol) of 2-bromopropionyl bromide was added drop-wise in 10 min. The reaction was stirring overnight at room temperature. The reaction mixture was filtered to remove the solid, concentrated and applied under vacuum at room temperature. The brown color crude product was purified by column chromatography with EtOAc/petroleum spirit (3/2, v/v) as

eluent. The fraction with R_f as 0.30 was collected and concentrated. 3.9 g colorless viscous liquid product **1** was obtained with the yield as 42.0 %. $^1\text{H NMR}$ (CDCl_3 , 298K, 500 MHz); δ 4.17 (s, 2H; $-\text{CH}_2\text{-OC(=O)-}$), 4.14 (d, 2H, $J=4.04$, 2.39 Hz; $\text{HC}\equiv\text{C-CH}_2\text{O-}$), 3.54 (d, 2H, $J=3.41$ Hz; $\text{HOCH}_2\text{-}$), 3.49 (s, 2H; $\text{HC}\equiv\text{C-CH}_2\text{OCH}_2\text{-}$), 2.43 (t, 1H, $J=2.33$ Hz; $\text{HC}\equiv\text{C-CH}_2\text{O-}$), 1.82 (d, 3H; methyl protons), 0.95 (s, 3H; methyl protons).

4.2.2.2 Synthesis of $\text{PSTY}_{44}\text{-Br}$, **2a** by ATRP

Styrene (4.54 g, 4.4×10^{-2} mol), PMDETA (0.05 mL, 2.4×10^{-4} mol), $\text{CuBr}_2/\text{PMDETA}$ (19.23×10^{-3} g, 4.8×10^{-5} mol) and initiator (94.5×10^{-3} g, 4.8×10^{-4} mol) were added to a 100 mL schlenk flask equipped with a magnetic stirrer and purged with argon for 30 min to remove oxygen. Cu(I)Br (35.0 g, 2.4×10^{-4} mol) was then carefully added to the solution under an argon blanket. The reaction mixture was further degassed for 5 min and then placed into a temperature controlled oil bath at 80 °C. After 4 h an aliquot was taken to check the conversion. The reaction was then quenched by cooling the reaction mixture to 0 °C, exposure to air, and dilution with THF (*ca.* 3 fold to the reaction mixture volume). The copper salts were removed by passage through an activated basic alumina column. The solution was concentrated by rotary evaporator and the polymer was recovered by precipitation into large volume of MeOH (20 fold excess to polymer solution) and vacuum filtration. The polymer was dried *in vacuo* for 24 h at 25 °C, SEC ($M_n=4670$, PDI = 1.07). The polymer was further characterised by $^1\text{H NMR}$ and MALDI-ToF.

4.2.2.3 Synthesis of $\text{PSTY}_{44}\text{-N}_3$, **3a** by azidation with NaN_3

Polymer PSTY-Br , **2a** (1.0 g, 0.20×10^{-3} mol) was dissolved in 7 mL of DMF in a reaction vessel equipped with magnetic stirrer. To this solution NaN_3 (0.13 g, 0.20×10^{-3} mol) was added and the mixture stirred for 24 h at 25 °C. The polymer solution was directly precipitated into MeOH (20 fold excess to polymer solution) from DMF, recovered by vacuum filtration and washed exhaustively with water and MeOH. The polymer was dried *in vacuo* for 24 h at 25 °C, SEC ($M_n=4650$, PDI = 1.07). The polymer was further characterised by $^1\text{H NMR}$ and MALDI-ToF.

4.2.2.4 Synthesis of $\text{PSTY}_{44}\text{-}\equiv$, **4a**

Polymer $\text{PSTY}_{44}\text{-N}_3$, **3a** (0.2 g, 4.0×10^{-5} mol), PMDETA (8.36×10^{-3} mL, 4.0×10^{-5} mol) and propargyl ether (123.5×10^{-3} mL, 1.2×10^{-3} mol) were dissolved in toluene (1.5 mL). CuBr (0.006 g, 4.0×10^{-5} mol) was added to a 10 mL schlenk flask equipped with magnetic stirrer and both of the reaction vessels were purged with argon for 12 min. The polymer solution was then transferred to a CuBr flask using double tipped needle by applying argon pressure. The reaction mixture was purged with argon for a further 2 min and the flask was placed in a temperature controlled oil bath

at 25 °C for 1.5 h. The reaction was then diluted with THF (*ca.* 3 fold to the reaction mixture volume), and passed through activated basic alumina to remove the copper salts. The solution was concentrated by rotary evaporator and the polymer was recovered by precipitation into a large amount of MeOH (20 fold excess to polymer solution) and filtration. The polymer was re-precipitated twice to ensure complete purity of the final product from propargyl ether. The polymer was dried *in vacuo* for 24 h at 25 °C, SEC ($M_n = 4800$, PDI = 1.07). The polymer was further characterised by ^1H NMR and MALDI-ToF.

4.2.2.5 Synthesis of $\text{PSTY}_{44-(\equiv)}_2$, **5a**

Polymer $\text{PSTY}_{44-\text{N}_3}$, **3a** (0.2 g, 4.0×10^{-5} mol), PMDETA (8.36×10^{-3} mL, 4.0×10^{-5} mol) and tripropargyl amine (169.8×10^{-3} mL, 1.2×10^{-3} mol) were dissolved in toluene (1.5 mL). CuBr (0.006 g, 4.0×10^{-5} mol) was added to a 10 mL schlenk flask equipped with magnetic stirrer and both of the reaction vessels were purged with argon for 12 min. The polymer solution was then transferred to CuBr flask using double tipped needle by applying argon pressure. The reaction mixture was purged with argon for a further 2 min and the flask was placed in a temperature controlled oil bath at 25 °C for 1.5 h. The reaction was then diluted with THF (*ca.* 3 fold to the reaction mixture volume), and passed through activated basic alumina to remove the copper salts. The solution was concentrated by rotary evaporator and the polymer was recovered by precipitation into a large amount of MeOH (20 fold excess to polymer solution) and filtration. The polymer was re-precipitated twice to ensure complete purity of the final product from tripropargyl amine. The polymer was dried *in vacuo* for 24 h at 25 °C, SEC ($M_n = 4850$, PDI = 1.07). The polymer was further characterised by ^1H NMR and MALDI-ToF.

4.2.2.6 Synthesis of $\text{PtBA}_{44-\text{Br}}$, **2b** by ATRP

^tBA (4.375 g, 3.4×10^{-5} mol), PMDETA (0.04 mL, 1.89×10^{-4} mol), $\text{CuBr}_2/\text{PMDETA}$ (15.04×10^{-3} g, 3.7×10^{-5} mol), initiator (74.2×10^{-3} g, 3.7×10^{-4} mol) and 2.0 mL of acetone were added to a 100 mL schlenk flask equipped with a magnetic stirrer and purged with argon for 30 min to remove oxygen. Cu(I)Br (27.2×10^{-3} g, 1.89×10^{-3} mol) was then carefully added to the solution under an argon blanket. The reaction mixture was further degassed for 5 min and then placed into a temperature controlled oil bath at 50 °C. After 4 h an aliquot was taken to check the conversion. The reaction was quenched by cooling the reaction mixture to 0 °C, exposure to air, and dilution with THF (*ca.* 3 fold to the reaction mixture volume). The copper salts were removed by passage through an activated basic alumina column. The solution was concentrated by rotary evaporator and the polymer was recovered by precipitation into large volume of MeOH/water (50/50) and vacuum

filtration. The polymer was dried *in vacuo* for 24 h at 25 °C, SEC ($M_n=5660$, PDI = 1.10). The polymer was further characterised by ^1H NMR and MALDI-ToF.

4.2.2.7 Synthesis of $\text{PtBA}_{44}\text{-N}_3$ **3b** by azidation with NaN_3

The $\text{P}^t\text{BA}_{44}\text{-Br}$, **2b** polymers were azidated in a similar way to PSTY polymer (in DMF, with x 10 NaN_3 mole excess to polymer chain-end, 24 h, at 25 °C) with the exception of the precipitation/polymer collection procedure. The azidated polymers were precipitated into cold water (20 fold excess to polymer solution) from DMF. Polymers $\text{P}^t\text{BA}_{44}\text{-N}_3$, **2b** were collected via vacuum filtration and washed with H_2O . The viscous polymer $\text{P}^t\text{BA}_{44}\text{-N}_3$ was collected via decanting of the solution, re-dissolving in DCM, drying with MgSO_4 , filtration and rotary evaporation of DCM. All polymers were dried *in vacuo* for 24 h at 25 °C, SEC ($M_n=5540$, PDI = 1.10). The polymer was further characterised by ^1H NMR and MALDI-ToF.

4.2.2.8 Synthesis of $\text{PtBA}_{44}\text{-}(=)$, **5b**

Polymer $\text{PtBA}_{44}\text{-N}_3$ **2b** (0.2 g, 3.3×10^{-5} mol), PMDETA (6.89×10^{-3} mL, 3.3×10^{-3} mol) and tripropargyl amine (140.1×10^{-3} mL, 9.9×10^{-4} mol) were dissolved in toluene (1.5 mL). CuBr (0.0047 g, 3.3×10^{-5} mol) was added to a 10 mL schlenk flask equipped with magnetic stirrer and both of the reaction vessels were purged with argon for 12 min. The polymer solution was then transferred to CuBr flask using double tipped needle by applying argon pressure. The reaction mixture was purged with argon for a further 2 min and the flask was placed in a temperature controlled oil bath at 25 °C for 1.5 h. The reaction was then diluted with THF (*ca.* 3 fold to the reaction mixture volume), and passed through activated basic alumina to remove the copper salts. The solution was concentrated by rotary evaporator and the polymer was recovered by precipitation into a large amount of MeOH/water (50/50) and filtration. The polymer was re-precipitated twice to ensure complete purity of the final product from tripropargyl amine. The polymer was dried *in vacuo* for 24 h at 25 °C, SEC ($M_n=5770$, PDI = 1.09). The polymer was further characterised by ^1H NMR and MALDI-ToF.

4.2.2.9 Synthesis of $\equiv(\text{OH})\text{-PSTY}_{47}\text{-Br}$, **6a**

Styrene (18.18 g, 1.75×10^{-1} mol), PMDETA (0.2 mL, 87.5×10^{-3} mol), $\text{CuBr}_2/\text{PMDETA}$ (0.077 g, 1.94×10^{-4} mol) and initiator (0.57 g, 1.94×10^{-3} mol) were added to a 100 mL schlenk flask equipped with a magnetic stirrer and purged with argon for 30 min to remove oxygen. Cu(I)Br (0.139 g, 87.5×10^{-3} mol) was then carefully added to the solution under an argon blanket. The reaction mixture was further degassed for 5 min and then placed into a temperature controlled oil bath at 80 °C. After 3.5 h an aliquot was taken to check the conversion. The reaction was quenched by cooling

the reaction mixture to 0 °C, exposure to air, and dilution with THF (*ca.* 3 fold to the reaction mixture volume). The copper salts were removed by passage through an activated basic alumina column. The solution was concentrated by rotary evaporator and the polymer was recovered by precipitation into large volume of MeOH (20 fold excess to polymer solution) and vacuum filtration. The polymer was dried *in vacuo* for 24 h at 25 °C, SEC ($M_n = 5220$, PDI = 1.10) and Triple Detection SEC ($M_n = 4890$, PDI = 1.05). The polymer was further characterised by ^1H NMR and MALDI-ToF.

4.2.2.10 Synthesis of $\equiv(\text{OH})\text{-PSTY}_{47}\text{-N}_3$, **7a**

Polymer $\equiv(\text{OH})\text{-PSTY}_{47}\text{-Br}$, **6a** (3.0 g, 6.0×10^{-4} mol) was dissolved in 20 mL of DMF in a reaction vessel equipped with magnetic stirrer. To this solution, NaN_3 (0.390 g, 6.0×10^{-3} mol) was added and the mixture stirred for 17 h at room temperature. The polymer was precipitated into MeOH, recovered by vacuum filtration and washed exhaustively with water and MeOH, then dried *in vacuo* for 24 h at 25 °C, SEC ($M_n = 5070$, PDI = 1.10) and Triple Detection SEC ($M_n = 4920$, PDI = 1.05). The polymer was further characterised by ^1H NMR and MALDI-ToF.

4.2.2.11 Cyclization reaction of $\equiv(\text{OH})\text{-PSTY}_{47}\text{-N}_3$, **7a** by CuAAC reaction

Synthesis of *c*-PSTY₄₇-OH **8a**

A solution of $\equiv(\text{OH})\text{-PSTY}_{47}\text{-N}_3$, **7a** (0.5 g, 1.0×10^{-4} mol) in 25 ml of dry toluene was purged with argon for 30 min to remove oxygen. This polymer solution was added via syringe pump, at a flow rate of 1.24 mL/min, to a deoxygenated solution of Cu (I) Br (0.703 g, 5.0×10^{-3} mol) and PMDETA (1.02 mL, 5.0×10^{-3} mol) in 25 ml toluene at 25 °C. After the addition of polymer solutions, which was 20.16 min for feed rate 1.24 ml/min, the reaction mixture was further stirred for 3 h. At the end of this period (i.e., feed time plus an additional 3 h), toluene was evaporated by air-flow and the copper salts were removed through CHCl_3 /water extraction. The residual copper salts were removed by passage through activated basic alumina column. The polymer was recovered by precipitation into MeOH (20 fold excess to polymer solution) and then by filtration. The polymer was dried *in vacuo* for 24 h at 25 °C (Purity by number distribution LND $f(\text{N}) = 81.46\%$). The crude products were fractionated by preparative SEC. SEC ($M_n = 3780$, PDI=1.06), Triple Detection SEC ($M_n = 5450$, PDI=1.04). The polymer was further characterised by ^1H NMR and MALDI-ToF.

4.2.2.12 Chain-end modification of functional cyclic polymers

Synthesis of *c*-PSTY₄₇-Br, **9a**

Polymer *c*-PSTY₄₇-OH, **8a** (0.5 g, 1.0×10^{-4} mol), TEA (0.273 mL, 2.0×10^{-3} mol) and 8.0 ml of dry THF were added under an argon blanket to a dry schlenk flask that has been flushed with argon. The reaction was then cooled on ice. To this stirred mixture, a solution of 2-bromopropionyl bromide (0.21 mL, 2.0×10^{-3} mol) in 2 mL of dry THF was added drop wise under argon via an air-tight syringe over 3 min. After stirring the reaction mixture for 48 h at room temperature, the polymer was precipitated into MeOH, filtered and washed three times with MeOH. The polymer was dried for 24 h in high vacuum oven at 25 °C, SEC ($M_n=3870$, PDI=1.05). The polymer was further characterised by ¹H NMR and MALDI-ToF.

Synthesis of c-PSTY₄₇-N₃, 10a

Polymer *c*-PSTY₄₇-Br, **9a** (0.4 g, 8.0×10^{-5} mol) was dissolved in 5 mL of DMF in a reaction vessel equipped with magnetic stirrer. To this solution, NaN₃ (0.052 g, 8.0×10^{-4} mol) was added and the mixture stirred for 17 h at room temperature. The polymer was precipitated into MeOH, recovered by vacuum filtration and washed exhaustively with water and MeOH, then dried *in vacuo* for 24 h at 25 °C, SEC ($M_n=3920$, PDI=1.05). The polymer was further characterised by ¹H NMR and MALDI-ToF.

Synthesis of c-PSTY₄₇-≡, 11a

Polymer *c*-PSTY₄₇-N₃, **10a** (0.1 g, 2.0×10^{-5} mol), PMDETA (4.18×10^{-3} mL, 2.0×10^{-5} mol) and propargyl ether (61.8×10^{-3} mL, 6.0×10^{-3} mol) were dissolved in toluene (0.8 mL). CuBr (0.003 g, 2.0×10^{-5} mol) was added to a 10 mL schlenk flask equipped with magnetic stirrer and both of the reaction vessels were purged with argon for 12 min. The polymer solution was then transferred to CuBr flask using double tipped needle by applying argon pressure. The reaction mixture was purged with argon for a further 2 min and the flask was placed in a temperature controlled oil bath at 25 °C for 1.5 h. The reaction was then diluted with THF (*ca.* 3 fold to the reaction mixture volume), and passed through activated basic alumina to remove the copper salts. The solution was concentrated by rotary evaporator and the polymer was recovered by precipitation into a large amount of MeOH (20 fold excess to polymer solution) and filtration. The polymer was re-precipitated twice to ensure complete purity of the final product from propargyl ether. The polymer was dried *in vacuo* for 24 h at 25 °C, SEC ($M_n=3920$, PDI=1.05). The polymer was further characterised by ¹H NMR and MALDI-ToF.

Synthesis of c-PSTY₄₇-(≡)₂-A, 12a

Polymer *c*-PSTY₄₇-N₃, **10a** (0.1 g, 2.0×10^{-5} mol), PMDETA (4.18×10^{-3} mL, 2.0×10^{-5} mol) and tripropargyl amine (84.89×10^{-3} mL, 6.0×10^{-4} mol) were dissolved in toluene (0.8 mL). CuBr (0.003 g, 2.0×10^{-5} mol) was added to a 10 mL schlenk flask equipped with magnetic stirrer and both of the reaction vessels were purged with argon for 12 min. The polymer solution was then transferred to

CuBr flask using double tipped needle by applying argon pressure. The reaction mixture was purged with argon for a further 2 min and the flask was placed in a temperature controlled oil bath at 25 °C for 1.5 h. The reaction was then diluted with THF (*ca.* 3 fold to the reaction mixture volume), and passed through activated basic alumina to remove the copper salts. The solution was concentrated by rotary evaporator and the polymer was recovered by precipitation into a large amount of MeOH (20 fold excess to polymer solution) and filtration. The polymer was re-precipitated twice to ensure complete purity of the final product from propargyl ether. The polymer was dried *in vacuo* for 24 h at 25 °C, SEC ($M_n=3820$, PDI=1.06). The polymer was further characterised by ^1H NMR and MALDI-ToF.

Synthesis of c-PSTY-(≡)₂-B, 14

Polymer c-PSTY₄₇-N₃, **10a** (0.1 g, 2.0×10^{-5} mol), PMDETA (4.18×10^{-3} mL, 2.0×10^{-5} mol) and 1,3,5-tris(prop-2-ynyloxy)benzene, **13** (0.144 g, 6.0×10^{-4} mol) were dissolved in toluene (1.5 mL). CuBr (0.0035 g, 2.0×10^{-5} mol) was added to a 10 mL schlenk flask equipped with magnetic stirrer and both of the reaction vessels were purged with argon for 10 min. The polymer solution was then transferred to CuBr flask using double tipped needle by applying argon pressure. The reaction mixture was purged with argon for a further 2 min and the flask was placed in a temperature controlled oil bath at 25 °C for 1.5 h. The reaction was then diluted with THF (*ca.* 3 fold to the reaction mixture volume), and passed through activated basic alumina to remove the copper salts. The solution was concentrated by rotary evaporator and the polymer was recovered by precipitation into a large amount of MeOH (20 fold excess to polymer solution) and filtration. The polymer was re-precipitated twice to ensure complete purity of the final product from **13**. The polymer was dried *in vacuo* for 24 h at 25 °C, SEC ($M_n=4420$, PDI=1.05). The polymer was further characterised by ^1H NMR and MALDI-ToF.

4.2.2.13 Synthesis of ≡(OH)-P^tBA₄₄-Br, 6b

tert-Butyl Acrylate (^tBA) (12.36 g, 9.6×10^{-2} mol), Me₆TREN (0.67 mL, 2.4×10^{-3} mol), CuBr₂/Me₆TREN (0.49 g, 10.82×10^{-4} mol), initiator (0.70 g, 2.39×10^{-3} mol), DMSO (1.2 mL) and acetone (8.4 mL) were added to a 50 mL Schlenk flask equipped with a magnetic stirrer. The reaction mixture was cooled down to 0 °C and purged with argon for 30 min to remove oxygen. Cu (0) (0.15 g, 2.39×10^{-3} mol) was then carefully added to the solution under an argon blanket. The reaction mixture was further degassed for 5 min at 0 °C and then placed into a temperature controlled water bath at 23 °C. After 30 min, an aliquot was taken to check the conversion. The reaction was quenched by cooling in liquid nitrogen, exposure to air, and dilution with THF (*ca.* 3 fold to the reaction mixture volume). The copper salts were removed by passage through an

activated basic alumina column. The solution was concentrated by rotary evaporator and the polymer was precipitated into cold MeOH/water mixture (40:60 v/v, 20 fold excess to polymer solution) twice. The polymer (viscous glassy solid) was dried *in vacuo* for 24 h at 25 °C, SEC ($M_n=5890$, PDI=1.13). The polymer was further characterised by ^1H NMR and MALDI-ToF.

4.2.2.14 Synthesis of $\equiv(\text{OH})\text{-P}^t\text{BA}_{44}\text{-N}_3$, **7b**

Polymer $\equiv(\text{OH})\text{-PtBA}_{44}\text{-Br}$, **6b** (10.00 g, 1.667×10^{-3} mol) was dissolved in 50 mL of DMF in a 100 mL reaction vessel equipped with magnetic stirrer. To this solution NaN_3 (1.08 g, 16.67×10^{-3} mol) was added and the mixture stirred overnight at room temperature. The polymer solution was then directly precipitated into cold MeOH/water mixture (20:80 v/v, ~15 fold excess to polymer solution) from DMF. All liquid was decanted and the polymer (viscous solid) was then dried *in vacuo* for 24 h at 25 °C, SEC ($M_n=6080$, PDI=1.13), and Triple Detection SEC ($M_n=6040$, PDI = 1.09). The polymer was further characterised by ^1H NMR and MALDI-ToF.

4.2.2.15 Cyclization reaction of $\equiv(\text{OH})\text{-P}^t\text{BA}_{44}\text{-N}_3$, **7b** by CuAAC reaction

A solution of $\equiv(\text{OH})\text{-P}^t\text{BA}_{44}\text{-N}_3$, **7b** (0.50 g, 8.30×10^{-5} mol) in toluene (25 mL) was purged with argon for 40 min to remove oxygen. This polymer solution was added via syringe pump, at a flow rate of 1.240 mL/min, to a deoxygenated solution of Cu(I)Br (0.6 g, 4.15×10^{-3} mol) and PMDETA (0.87 mL, 4.15×10^{-3} mol) in toluene (25 mL) at 25 °C. After the addition of the polymer solution the reaction mixture was stirred for further 3 h. At the end of this period, toluene was evaporated and the copper salts were removed through $\text{CHCl}_3/\text{H}_2\text{O}$ extraction. The residual copper salts were removed by passage through activated basic alumina column with THF and the solvent was then removed by rotary evaporator. (Purity by number distribution LND $f(\text{N})=71.6\%$). The crude products were fractionated by preparative SEC and fractions combined. SEC ($M_n=4890$, PDI = 1.05) and Triple Detection SEC ($M_n=6260$, PDI = 1.04). The polymer was further characterised by ^1H NMR and MALDI-ToF.

4.2.2.16 Chain-end modification of functional cyclic polymers

Synthesis of $c\text{-P}^t\text{BA}_{44}\text{-Br}$, **9b**

Polymer $c\text{-P}^t\text{BA}_{44}\text{-OH}$, **8b** (0.5 g, 8.30×10^{-5} mol), TEA (0.232 mL, 16.6×10^{-4} mol) and 20.0 ml of dry THF were added under an argon blanket to a dry schlenk flask that has been flushed with argon. The reaction was then cooled on ice. To this stirred mixture, a solution of 2-bromopropionyl bromide (0.173 mL, 16.6×10^{-4} mol) in 5 mL of dry THF was added drop wise under argon via an air-tight syringe over 5 min. After stirring the reaction mixture for 48 h at room temperature, the

polymer solution was directly precipitated into cold MeOH/water mixture (20:80v/v, ~15 fold excess to polymer solution) from DMF. The polymer was dried for 24 h in high vacuum oven at 25 °C, SEC ($M_n = 4930$, PDI = 1.05). The polymer was further characterised by ^1H NMR and MALDI-ToF.

Synthesis of c-P^tBA₄₄-N₃, 10b

Polymer c-P^tBA₄₄-Br, **9b** (0.35 g, 5.83×10^{-5} mol) was dissolved in 3.0 mL of DMF in a reaction vessel equipped with magnetic stirrer. To this solution, NaN₃ (0.038 g, 5.83×10^{-4} mol) was added and the mixture stirred for 17 h at room temperature. After stirring the reaction mixture for 48 h at room temperature, the polymer solution was directly precipitated into cold MeOH/water mixture (20:80 v/v, ~15 fold excess to polymer solution) from DMF, recovered by vacuum filtration, then dried in vacuo for 24 h at 25 °C, SEC ($M_n = 4940$, PDI = 1.05). The polymer was further characterised by ^1H NMR and MALDI-ToF.

Synthesis of c-P^tBA₄₄-(≡)₂, 12b

Polymer c-P^tBA₄₄-N₃ **10b** (0.12 g, 2.14×10^{-5} mol), tripropargylamine (0.09 mL, 6.4×10^{-4} mol) and PMDETA (4.47×10^{-3} mL, 2.14×10^{-5} mol) were dissolved in toluene (1.0 mL). CuBr (0.003 g, 2.14×10^{-5} mol) was added to a 10 mL schlenk flask equipped with magnetic stirrer and both of the reaction vessels were purged with argon for 12 min. The polymer solution was then transferred to CuBr flask using double tipped needle by applying argon pressure. The reaction mixture was purged with argon for a further 2 min and then flask was placed in a temperature controlled oil bath at 25 °C for 1.0 h. The reaction was then diluted with THF (*ca.* 3 fold to the reaction mixture volume), and passed through activated basic alumina to remove the copper salts. The solution was concentrated by rotary evaporation to near-dryness and the polymer was re-dissolved in MeOH (2.0 mL). The polymer solution was then transferred to dialysis bag (presoaked in water, Pierce Snakeskin, MWCO 3.5 K) and dialyzed against a large volume of MeOH for 3 days (replacing the large volume of MeOH twice a day). The final purification was performed by Preparative SEC to ensure complete purity of the final product from tripropargyl amine. The polymer was finally dried in *vacuo* for 24 h at 25 °C, SEC ($M_n = 4940$, PDI = 1.07). The polymer was further characterised by ^1H NMR and MALDI-ToF.

4.2.2.17 Synthesis of complex architectures via CuAAC Reaction

Synthesis of (PSTY₄₄)₂ **15** by CuAAC

PSTY₄₄-≡, **4a** (0.03 g, 6.0×10⁻⁶ mol), PSTY₄₄-N₃, **3a** (0.03 g, 6.0×10⁻⁶ mol) and PMDETA (1.25×10⁻³ mL, 6.0×10⁻⁶ mol) were dissolved in 0.5 ml of dry toluene in a vial. CuBr (0.86×10⁻³ g, 6.0×10⁻⁶ mol) was added in a 10 mL Schlenk flask equipped with magnetic stirrer. Both of the vessels were purged with argon for 5 minutes and the polymer solution was transferred to CuBr flask using double tipped needle by applying argon pressure. The reaction mixture was purged with argon for further 2 min and the flask was placed in a temperature controlled oil bath at 25 °C. After 30 min, an aliquot was taken to check SEC. The reaction was stopped after 1 hr and the mixture was diluted with 3.0 mL of THF. The solution was then passed through activated basic alumina column to remove copper. The solution was concentrated by rotary evaporator and the crude product was further purified by preparative SEC. The polymer was recovered by precipitation into a large amount of MeOH (20 fold excess to polymer solution) and then recovered by vacuum filtration. The polymer was dried *in vacuo* for 48 h at 25 °C, SEC ($M_n = 9710$, PDI = 1.03) and Triple Detection SEC ($M_n = 9820$, PDI = 1.02). The polymer was further characterised by ¹H NMR and MALDI-ToF.

Synthesis of *c*-PSTY₄₇-*b*-PSTY₄₄, **16** by CuAAC

PSTY₄₄-≡, **4a** (0.03 g, 6.0×10⁻⁶ mol), *c*-PSTY₄₇-N₃, **10a** (0.03 g, 6.0×10⁻⁶ mol) and PMDETA (1.25×10⁻³ mL, 6.0×10⁻⁶ mol) were dissolved in 0.5 ml of dry toluene in a vial. CuBr (0.86×10⁻³ g, 6.0×10⁻⁶ mol) was added in a 10 mL Schlenk flask equipped with magnetic stirrer. Both of the vessels were purged with argon for 5 minutes and the polymer solution was transferred to CuBr flask using double tipped needle by applying argon pressure. The reaction mixture was purged with argon for further 2 min and the flask was placed in a temperature controlled oil bath at 25 °C. After 30 min, an aliquot was taken to check SEC. The reaction was stopped after 1 hr and the mixture was diluted with 3.0 mL of THF. The solution was then passed through activated basic alumina column to remove copper. The solution was concentrated by rotary evaporator and the crude product was further purified by preparative SEC. The polymer was recovered by precipitation into a large amount of MeOH (20 fold excess to polymer solution) and then recovered by vacuum filtration. The polymer was dried *in vacuo* for 48 h at 25 °C, SEC ($M_n = 8400$, PDI = 1.03) and Triple Detection SEC ($M_n = 10180$, PDI = 1.03). The polymer was further characterised by ¹H NMR and MALDI-ToF.

Synthesis of (*c*-PSTY₄₇)₂ **17** by CuAAC

Polymer *c*-PSTY₄₇-≡, **11a** (0.03 g, 6.0×10⁻⁶ mol), *c*-PSTY₄₇-N₃ **10a** (0.03 g, 6.0×10⁻⁶ mol) and PMDETA (1.25×10⁻³ mL, 6.0×10⁻⁶ mol) were dissolved in 0.5 ml of dry toluene in a vial. CuBr

(0.86×10^{-3} g, 6.0×10^{-6} mol) was added in a 10 mL Schlenk flask equipped with magnetic stirrer. Both of the vessels were purged with argon for 5 minutes and the polymer solution was transferred to CuBr flask using double tipped needle by applying argon pressure. The reaction mixture was purged with argon for further 2 min and the flask was placed in a temperature controlled oil bath at 25 °C. After 30 min, an aliquot was taken to check SEC. The reaction was stopped after 1 hr and the mixture was diluted with 3.0 mL of THF. The solution was then passed through activated basic alumina column to remove copper. The solution was concentrated by rotary evaporator and the crude product was further purified by preparative SEC. The polymer was recovered by precipitation into a large amount of MeOH (20 fold excess to polymer solution) and then recovered by vacuum filtration. The polymer was dried *in vacuo* for 48 h at 25 °C, SEC ($M_n = 7630$, PDI = 1.02) and Triple Detection SEC ($M_n = 10230$, PDI = 1.03). The polymer was further characterised by ^1H NMR and MALDI-ToF.

Synthesis of (PSTY₄₄)₃ 18 by CuAAC

PSTY₄₄-(\equiv)₂, **5a** (0.02 g, 4.0×10^{-6} mol), PSTY₄₄-N₃, **3a** (0.04 g, 8.0×10^{-6} mol) and PMDETA (1.67×10^{-3} mL, 8.0×10^{-6} mol) were dissolved in 0.5 ml of dry toluene in a vial. CuBr (1.15×10^{-3} g, 8.0×10^{-6} mol) was added in a 10 mL Schlenk flask equipped with magnetic stirrer. Both of the vessels were purged with argon for 5 minutes and the polymer solution was transferred to CuBr flask using double tipped needle by applying argon pressure. The reaction mixture was purged with argon for further 2 min and the flask was placed in a temperature controlled oil bath at 25 °C. After 30 min, an aliquot was taken to check SEC. The reaction was stopped after 1 hr and the mixture was diluted with 3.0 mL of THF. The solution was then passed through activated basic alumina column to remove copper. The solution was concentrated by rotary evaporator and the crude product was further purified by preparative SEC. The polymer was recovered by precipitation into a large amount of MeOH (20 fold excess to polymer solution) and then recovered by vacuum filtration. The polymer was dried *in vacuo* for 48 h at 25 °C, SEC ($M_n = 13170$, PDI = 1.03) and Triple Detection SEC ($M_n = 15110$, PDI = 1.04). The polymer was further characterised by ^1H NMR and MALDI-ToF.

Synthesis of c-PSTY_{47-b}-(PSTY₄₄)₂ 19 by CuAAC

c-PSTY_{47-b}-(\equiv)₂ **12a** (0.02 g, 4.0×10^{-6} mol), PSTY₄₄-N₃ **3a** (0.04 g, 8.0×10^{-6} mol) and PMDETA (1.67×10^{-3} mL, 8.0×10^{-6} mol) were dissolved in 0.5 ml of dry toluene in a vial. CuBr (1.15×10^{-3} g, 8.0×10^{-6} mol) was added in a 10 mL Schlenk flask equipped with magnetic stirrer. Both of the vessels were purged with argon for 5 minutes and the polymer solution was transferred to CuBr

flask using double tipped needle by applying argon pressure. The reaction mixture was purged with argon for further 2 min and the flask was placed in a temperature controlled oil bath at 25 °C. After 30 min, an aliquot was taken to check SEC. The reaction was stopped after 1 hr and the mixture was diluted with 3.0 mL of THF. The solution was then passed through activated basic alumina column to remove copper. The solution was concentrated by rotary evaporator and the crude product was further purified by preparative SEC. The polymer was recovered by precipitation into a large amount of MeOH (20 fold excess to polymer solution) and then recovered by vacuum filtration. The polymer was dried *in vacuo* for 48 h at 25 °C, SEC ($M_n = 12410$, PDI = 1.03) and Triple Detection SEC ($M_n = 15550$, PDI = 1.04). The polymer was further characterised by ^1H NMR and MALDI-ToF.

Synthesis of (c-PSTY₄₇)₂-b-PSTY₄₄ 20 by CuAAC

PSTY₄₄-(\equiv)₂, **5a** (0.02 g, 4.0×10^{-6} mol), c-PSTY₄₇-N₃, **10a** (0.04 g, 8.0×10^{-6} mol) and PMDETA (1.67×10^{-3} mL, 8.0×10^{-6} mol) were dissolved in 0.5 ml of dry toluene in a vial. CuBr (1.15×10^{-3} g, 8.0×10^{-6} mol) was added in a 10 mL Schlenk flask equipped with magnetic stirrer. Both of the vessels were purged with argon for 5 minutes and the polymer solution was transferred to CuBr flask using double tipped needle by applying argon pressure. The reaction mixture was purged with argon for further 2 min and the flask was placed in a temperature controlled oil bath at 25 °C. After 30 min, an aliquot was taken to check SEC. The reaction was stopped after 1 hr and the mixture was diluted with 3.0 mL of THF. The solution was then passed through activated basic alumina column to remove copper. The solution was concentrated by rotary evaporator and the crude product was further purified by preparative SEC. The polymer was recovered by precipitation into a large amount of MeOH (20 fold excess to polymer solution) and then recovered by vacuum filtration. The polymer was dried *in vacuo* for 48 h at 25 °C, SEC ($M_n = 10750$, PDI = 1.04) and Triple Detection SEC ($M_n = 15580$, PDI = 1.03). The polymer was further characterised by ^1H NMR and MALDI-ToF.

Synthesis of (c-PSTY₄₇)₃-A 21 by CuAAC

c-PSTY₄₇-(\equiv)₂, **12a** (0.02 g, 4.0×10^{-6} mol), c-PSTY₄₇-N₃, **10a** (0.04 g, 8.0×10^{-6} mol) and PMDETA (1.67×10^{-3} mL, 8.0×10^{-6} mol) were dissolved in 0.5 ml of dry toluene in a vial. CuBr (1.15×10^{-3} g, 8.0×10^{-6} mol) was added in a 10 mL Schlenk flask equipped with magnetic stirrer. Both of the vessels were purged with argon for 5 minutes and the polymer solution was transferred to CuBr flask using double tipped needle by applying argon pressure. The reaction mixture was purged with argon for further 2 min and the flask was placed in a temperature controlled oil bath at 25 °C. After 30 min, an aliquot was taken to check SEC. The reaction was stopped after 1 hr and the mixture was

diluted with 3.0 mL of THF. The solution was then passed through activated basic alumina column to remove copper. The solution was concentrated by rotary evaporator and the crude product was further purified by preparative SEC. The polymer was recovered by precipitation into a large amount of MeOH (20 fold excess to polymer solution) and then recovered by vacuum filtration. The polymer was dried *in vacuo* for 48 h at 25 °C, SEC ($M_n = 9910$, PDI = 1.03) and Triple Detection SEC ($M_n = 15800$, PDI = 1.03). The polymer was further characterised by ^1H NMR and MALDI-ToF.

Synthesis of (c-PSTY₄₇)₃-B 22 by CuAAC

c-PSTY₄₇-≡₂-B, **14** (0.025 g, 4.8×10^{-6} mol), c-PSTY₄₇-N₃, **10a** (0.05 g, 9.6×10^{-6} mol) and PMDETA (2.0×10^{-3} mL, 9.6×10^{-6} mol) were dissolved in 0.5 ml of dry toluene in a vial. CuBr (1.37×10^{-3} g, 9.6×10^{-6} mol) was added in a 10 mL Schlenk flask equipped with magnetic stirrer. Both of the vessels were purged with argon for 5 minutes and the polymer solution was transferred to CuBr flask using double tipped needle by applying argon pressure. The reaction mixture was purged with argon for further 2 min and the flask was placed in a temperature controlled oil bath at 25 °C. After 30 min, an aliquot was taken to check SEC. The reaction was stopped after 1.5 hr and the mixture was diluted with 3.0 mL of THF. The solution was then passed through activated basic alumina column to remove copper. The solution was concentrated by rotary evaporator and the crude product was further purified by preparative SEC. The polymer was recovered by precipitation into a large amount of MeOH (20 fold excess to polymer solution) and then recovered by vacuum filtration. The polymer was dried *in vacuo* for 48 h at 25 °C, SEC ($M_n = 10490$, PDI = 1.03) and Triple Detection SEC ($M_n = 16100$, PDI = 1.03). The polymer was further characterised by ^1H NMR and MALDI-ToF.

Synthesis of PSTY₄₄-b-P^tBA₄₄ 23

PSTY₄₄-≡, **4a** (0.05 g, 10.0×10^{-6} mol), P^tBA₄₄-N₃, **3b** (0.06 g, 10.0×10^{-6} mol) and PMDETA (4.18×10^{-3} mL, 20.0×10^{-6} mol) were dissolved in 1.0 ml of dry toluene in a vial. CuBr (0.0029 g, 20.0×10^{-6} mol) was added in a 10 mL Schlenk flask equipped with magnetic stirrer. Both of the vessels were purged with argon for 15 minutes and the polymer solution was transferred to CuBr flask using double tipped needle by applying argon pressure. The reaction mixture was purged with argon for further 2 min and the flask was placed in a temperature controlled oil bath at 25 °C. After 30 min, an aliquot was taken to check SEC. The reaction was stopped after 1 hr and the mixture was diluted with 3.0 mL of THF. The solution was then passed through activated basic alumina column to remove copper. The solution was concentrated by rotary evaporator and the crude product was

further purified by preparative SEC. The polymer was recovered by precipitation into a cold solution of MeOH/H₂O (20/80 v/v, 15 fold excess to polymer solution) and then recovered by vacuum filtration. The polymer was dried *in vacuo* for 48 h at 25 °C, SEC ($M_n = 10630$, PDI = 1.04) and Triple Detection SEC ($M_n = 10450$, PDI = 1.03). The polymer was further characterised by ¹H NMR and MALDI-ToF.

Synthesis of c-PSTY₄₇-b-c-P^tBA₄₄, 24

Polymer c-PSTY₄₇-≡, **11a** (0.03 g, 6.0×10^{-6} mol), c-P^tBA₄₄-N₃, **10b** (0.034 g, 6.0×10^{-6} mol) and PMDETA (2.5×10^{-3} mL, 1.2×10^{-5} mol) were dissolved in 1.0 ml of dry toluene in a vial. CuBr (0.0017 g, 1.2×10^{-5} mol) was added in a 10 mL Schlenk flask equipped with magnetic stirrer. Both of the vessels were purged with argon for 15 minutes and the polymer solution was transferred to CuBr flask using double tipped needle by applying argon pressure. The reaction mixture was purged with argon for further 2 min and the flask was placed in a temperature controlled oil bath at 25 °C. After 30 min, an aliquot was taken to check SEC. The reaction was stopped after 1 hr and the mixture was diluted with 3.0 mL of THF. The solution was then passed through activated basic alumina column to remove copper. The solution was concentrated by rotary evaporator and the crude product was further purified by preparative SEC. The polymer was recovered by precipitation into a cold solution of MeOH/H₂O (20/80 v/v, 15 fold excess to polymer solution) and then recovered by vacuum filtration. The polymer was dried *in vacuo* for 48 h at 25 °C, SEC ($M_n = 8790$, PDI = 1.06) and Triple Detection SEC ($M_n = 12050$, PDI = 1.06). The polymer was further characterised by ¹H NMR and MALDI-ToF.

Synthesis of PSTY₄₄-b-(P^tBA₄₄)₂, 25

PSTY₄₄-(≡)₂ **5a** (0.04 g, 8.0×10^{-6} mol), P^tBA₄₄-N₃ **3b** (0.12 g, 16.0×10^{-6} mol) and PMDETA (6.689×10^{-3} mL, 32.0×10^{-6} mol) were dissolved in 1.0 ml of dry toluene in a vial. CuBr (0.0046 g, 32.0×10^{-6} mol) was added in a 10 mL Schlenk flask equipped with magnetic stirrer. Both of the vessels were purged with argon for 15 minutes and the polymer solution was transferred to CuBr flask using double tipped needle by applying argon pressure. The reaction mixture was purged with argon for further 2 min and the flask was placed in a temperature controlled oil bath at 25 °C. After 30 min, an aliquot was taken to check SEC. The reaction was stopped after 1.0 hr and the mixture was diluted with 3.0 mL of THF. The solution was then passed through activated basic alumina column to remove copper. The solution was concentrated by rotary evaporator and the crude product was further purified by preparative SEC. The polymer was recovered by precipitation into a cold solution of MeOH/H₂O (20/80 v/v, 15 fold excess to polymer solution) and then recovered by vacuum filtration. The polymer was dried *in vacuo* for 48 h at 25 °C, SEC ($M_n = 14730$, PDI = 1.07)

and Triple Detection SEC ($M_n=17510$, PDI=1.06). The polymer was further characterised by ^1H NMR and MALDI-ToF.

Synthesis of c-PSTY₄₇-b-(c-P^tBA₄₄)₂, 26

c-PSTY₄₇-(\equiv)₂, **12a** (0.02 g, 4.0×10^{-6} mol), c-P^tBA₄₄-N₃, **10b** (0.045 g, 8.0×10^{-6} mol) and PMDETA (3.34×10^{-3} mL, 1.6×10^{-5} mol) were dissolved in 1.0 ml of dry toluene in a vial. CuBr (0.0023 g, 1.6×10^{-5} mol) was added in a 10 mL Schlenk flask equipped with magnetic stirrer. Both of the vessels were purged with argon for 15 minutes and the polymer solution was transferred to CuBr flask using double tipped needle by applying argon pressure. The reaction mixture was purged with argon for further 2 min and the flask was placed in a temperature controlled oil bath at 25 °C. After 30 min, an aliquot was taken to check SEC. The reaction was stopped after 1.0 hr and the mixture was diluted with 3.0 mL of THF. The solution was then passed through activated basic alumina column to remove copper. The solution was concentrated by rotary evaporator and the crude product was further purified by preparative SEC. The polymer was recovered by precipitation into a cold solution of MeOH/H₂O (20/80 v/v, 15 fold excess to polymer solution) and then recovered by vacuum filtration. The polymer was dried *in vacuo* for 48 h at 25 °C, SEC ($M_n = 12210$, PDI = 1.07) and Triple Detection SEC ($M_n=17070$, PDI=1.05). The polymer was further characterised by ^1H NMR and MALDI-ToF.

Synthesis of (PSTY₄₄)₂-b-P^tBA₄₄ 27

PSTY₄₄-N₃ **3a** (0.05 g, 10.0×10^{-6} mol), P^tBA₄₄-(\equiv)₂, **5b** (0.03 g, 5.0×10^{-6} mol) and PMDETA (4.18×10^{-3} mL, 20.0×10^{-6} mol) were dissolved in 1.0 ml of dry toluene in a vial. CuBr (0.0029 g, 20.0×10^{-6} mol) was added in a 10 mL Schlenk flask equipped with magnetic stirrer. Both of the vessels were purged with argon for 15 minutes and the polymer solution was transferred to CuBr flask using double tipped needle by applying argon pressure. The reaction mixture was purged with argon for further 2 min and the flask was placed in a temperature controlled oil bath at 25 °C. After 30 min, an aliquot was taken to check SEC. The reaction was stopped after 1.0 hr and the mixture was diluted with 3.0 mL of THF. The solution was then passed through activated basic alumina column to remove copper. The solution was concentrated by rotary evaporator and the crude product was further purified by preparative SEC. The polymer was recovered by precipitation into a cold solution of MeOH/H₂O (20/80 v/v, 15 fold excess to polymer solution) and then recovered by vacuum filtration. The polymer was dried *in vacuo* for 48 h at 25 °C, SEC ($M_n = 13460$, PDI = 1.06) and Triple Detection SEC ($M_n=16530$, PDI=1.06). The polymer was further characterised by ^1H NMR and MALDI-ToF.

Synthesis of (c-PSTY₄₇)₂-b-c-P^tBA₄₄, 28

Polymer, c-PSTY₄₇-N₃, **10a** (0.058 g, 4.0×10⁻⁶ mol), c-P^tBA₄₄-(≡)₂, **12b** (0.045 g, 8.0×10⁻⁶ mol) and PMDETA (3.34×10⁻³ mL, 1.6×10⁻⁵ mol) were dissolved in 1.0 ml of dry toluene in a vial. CuBr (0.0023 g, 1.6 x 10⁻⁵ mol) was added in a 10 mL Schlenk flask equipped with magnetic stirrer. Both of the vessels were purged with argon for 15 minutes and the polymer solution was transferred to CuBr flask using double tipped needle by applying argon pressure. The reaction mixture was purged with argon for further 2 min and the flask was placed in a temperature controlled oil bath at 25 °C. After 30 min, an aliquot was taken to check SEC. The reaction was stopped after 1.0 hr and the mixture was diluted with 3.0 mL of THF. The solution was then passed through activated basic alumina column to remove copper. The solution was concentrated by rotary evaporator and the crude product was further purified by preparative SEC. The polymer was recovered by precipitation into a cold solution of MeOH/H₂O (20/80 v/v, 15 fold excess to polymer solution) and then recovered by vacuum filtration. The polymer was dried *in vacuo* for 48 h at 25 °C, SEC (M_n = 11120, PDI = 1.06) and Triple Detection SEC (M_n =15900, PDI=1.06). The polymer was further characterised by ¹H NMR and MALDI-ToF.

4.2.2.18 Deprotection of ^tBA from 23-28– General Procedure

The hydrolysis of ^tBA side groups on the polymer architectures to acrylic acid (AA) was carried out following a literature procedure.³ TFA (5 times excess to the *tert*-butyl groups) was added dropwise to a solution of polymer in DCM. The reaction mixture was stirred at room temperature for 24 hours. The organics were removed using N₂ flow and the residue re-dissolved in a minimum amount of THF. The polymer was recovered by precipitation in hexane to afford a white solid. The polymers were dried *in vacuo* for 24 h at 25 °C.

4.2.2.19 Thin Film Studies

Thin films of the amphiphillic cyclic block copolymers and their linear analogues were prepared by spin coating 2 wt% of polymer (**23** and **24**) solutions in THF onto silicon wafer substrates. The concentration of the polymer solutions and spin speed were kept constant for direct comparison of thin films with all films having essentially the same thickness, and all were thermally annealed at 130 °C overnight. The resulting nanophase-separated thin films were characterised by atomic force

microscopy (AFM) in order to determine the effect of macromolecular architecture on nanophase-separated polymer thin films.

4.2.3 Analytical Methodologies

Size Exclusion Chromatography (SEC)

For SEC analysis, polymer solution was prepared by dissolving in tetrahydrofuran (THF) to a concentration of 1 mg mL^{-1} and then filtered through a $0.45 \text{ }\mu\text{m}$ PTFE syringe filter. A water 2695 separations module, fitted with a water 410 refractive index detector maintained at $35 \text{ }^\circ\text{C}$, a water 996 photodiode array detector, and two Ultrastyrigel linear columns ($7.8 \times 300 \text{ mm}$) arranged in series were used to analyse the molecular weight distribution of the polymers. For all analysis, these columns were maintained at $40 \text{ }^\circ\text{C}$ and are capable of separating polymers in the molecular weight range of 500 to 4 million g mol^{-1} with high resolution. All samples were eluted at a flow rate of 1.0 mL min^{-1} . Calibration was performed using narrow molecular weight PSTY standards ($\text{PDI} \leq 1.1$) ranging from 500 to 2 million g mol^{-1} . Data acquisition was performed using Empower software, and molecular weights were calculated relative to polystyrene standards.

Absolute Molecular Weight Determination by Triple Detection SEC

Absolute molecular weights of polymers were determined using a Polymer Labs GPC50 Plus equipped with dual angle laser light scattering detector, viscometer and differential refractive index detector. HPLC grade tetrahydrofuran was used as eluent at flow rate 1 mL min^{-1} . Separations were achieved using two PLGel Mixed C ($7.8 \times 300 \text{ mm}$) SEC columns connected in series and held at a constant temperature of $40 \text{ }^\circ\text{C}$. The triple detection system was calibrated using a 4 mg/mL PSTY Standard (Polymer Laboratories: $M_{\text{wt}} = 110 \text{ K}$, $dn/dc = 0.185$ and $IV = 0.4872 \text{ mL g}^{-1}$). Polymer samples of known concentration were freshly prepared in THF and passed through a $0.45 \text{ }\mu\text{m}$ PTFE syringe filter just prior to injection.

Preparative Size Exclusion Chromatography (Prep SEC).

Linear polystyrene was purified using a Varian Pro-Star preparative SEC system equipped with a manual injector, differential refractive index detector, and single wave-length ultraviolet visible detector. Flow rate was maintained 10 mL min^{-1} and HPLC grade tetrahydrofuran was used as the eluent. Separations were achieved using a PL Gel $10 \text{ }\mu\text{m}$ $10 \times 10^3 \text{ A}^\circ$, $300 \times 25 \text{ mm}$ preparative SEC column held at $25 \text{ }^\circ\text{C}$. The dried crude polymer was dissolved in THF at 100 mg mL^{-1} concentration

and filtered through a 0.45 μm PTFE syringe filter prior to use. Different fractions were collected manually, and the composition of each was determined using the Polymer Laboratories GPC50 Plus equipped with triple detection as described above.

¹H Nuclear Magnetic Resonance (NMR).

All NMR spectra were recorded on a 300 MHz and Bruker DRX 500 MHz spectrometer using an external lock (CDCl_3) and referenced to the residual non-deuterated solvent (CHCl_3). Then a DOSY experiment was run to acquire spectra presented herein by increasing the pulse gradient from 2 to 85 % of the maximum gradient strength and increasing d (**p30**) from 1 ms to 2 ms, using 64 to 128 scans.

Attenuated Total Reflectance Fourier Transform Spectroscopy (ATR-FTIR)

ATR-FTIR spectra were obtained using a horizontal, single bounce, diamond ATR accessory on a Nicolet Nexus 870 FT-IR. Spectra were recorded between 4000 and 500 cm^{-1} for 64 scans at 4 cm^{-1} resolution with an OPD velocity of 0.6289 cm/s . Solids were pressed directly onto the diamond internal reflection element of the ATR without further sample preparation.

Matrix-Assisted Laser Desorption Ionization-Time-of-Flight (MALDI-ToF) Mass Spectrometry.

MALDI-ToF MS spectra were obtained using a Bruker MALDI-ToF autoflex III smart beam equipped with a nitrogen laser (337 nm, 200 Hz maximum firing rate) with a mass range of 600-400 000 Da. Spectra were recorded in both reflectron mode (2000-5000 Da) and linear mode (5000-20000 Da). Trans- 2-[3-(4-tert-butylphenyl)-2-methyl-propenylidene] malononitrile (DCTB; 20 mg/mL in THF) was used as the matrix and Ag-(CF_3COO) (1 mg/mL in THF) as the cation source of all the polystyrene samples. For poly (t-butylacrylate) Na-(CF_3COO) (1 mg/mL in THF) was used as the cation source in the same matrix. Samples were prepared by co-spotting the matrix (20 μL), Ag (CF_3COO) or Na-(CF_3COO) (2×10^{-3} mL) and polymer (20×10^{-3} mL, 1 mg/mL in THF) solutions on the target plate.

Differential Scanning Calorimetry

Differential scanning calorimetry (DSC) was carried out on a Mettler Toledo DSC1 STARe System calorimeter. For the DSC measurements, samples of 3–5 mg were first heated from 20 to 150 $^\circ\text{C}$ at a heating rate of 5 $^\circ\text{C}/\text{min}$ under nitrogen atmosphere, followed by cooling to 20 $^\circ\text{C}$ at a rate of 5 $^\circ\text{C}/\text{min}$ after stopping at 150 $^\circ\text{C}$ for 3 min, and finally heating to 150 $^\circ\text{C}$ at the rate of 5 $^\circ\text{C}/\text{min}$. The mid-point of inflection of the obtained DSC curves in final heating process was used to determine the glass-transition temperature.

Determination of glass transition temperature (T_g)

T_g of amphiphilic copolymers were evaluated using differential scanning calorimetry (DSC). Each sample (3–5 mg) was loaded onto a DSC aluminium crucible cell (40 μ L, Mettler Toledo International Inc.), heated under nitrogen at a constant heating rate of 5 $^{\circ}$ C /min from 20 $^{\circ}$ C up to 150 $^{\circ}$ C, cooled back down to 20 $^{\circ}$ C, and heated back up again to 150 $^{\circ}$ C. T_g values of all samples for both PSTY and PAA blocks were chosen from the second heating cycle.

Atomic Force Microscopy

A Cypher atomic force microscope (Asylum Research) was used for all the measurements. The cantilevers used were HA_NC (Etalon) from NT-MDT, Russia having a nominal resonant frequency of 145 kHz. The images were obtained by employing the Tapping Mode of the AFM in air.

4.3 Results and Discussion

Synthesis of c-PSTY₄₇-OH and c-P^tBA₄₄-OH by CuAAC

Cyclic polystyrene (c-PSTY) and polybutyl acrylate (c-P^tBA) were prepared with a single OH group on each chain. c-PSTY₄₇-OH, **8a** and c-P^tBA₄₄-OH, **8b** were synthesised according to our previously described literature procedure.³² Highly functional linear polymer precursors \equiv (OH)-PSTY₄₇-Br, **6a** and \equiv (OH)-P^tBA₄₄-Br, **6b** were synthesised by ATRP and SET-LRP using an alkyne-functional initiator, **1**, producing a polymers with number-average molecular weights (M_n) of 5220 and 5890, and PDI values of 1.10 and 1.13, respectively (see Table C1 in appendix C). The Br chain-end functionalities of **6a** and **6b** were calculated by ¹H NMR integration as 96 and 97%, respectively. However, the LND simulation⁴² based on weight distribution (w(M)) of **6a** and **6b** gave ~12 % of double molecular weight products. The formation of double molecular weight products can occur by radical termination or alkyne-alkyne coupling reaction during or after polymerization. The Br chain-ends of two polymers were converted to azide groups quantitatively, and the linear polymers then cyclised using CuAAC reaction.⁴³ The general synthetic route to produce different functional linear and cyclic polymers and their complex architectures is shown in Scheme C1 in Appendix C.

An effective and rapid cyclization procedure was followed to prepare monocyclic polymer with high yield and purity. The linear polymer solution in toluene, was fed into a toluene solution of an excess of Cu(I)Br and PMDETA at a feed rate of 1.24 mL min⁻¹ at 25 $^{\circ}$ C over 20.16 min and then stirred for 3 h, following a procedure shown to be highly effective in producing monocyclic

polymer. The reason for using the [Cu(PMDETA)Br] complex to activate the CuAAC reaction in toluene is that the complex forms a neutral, distorted square planar structure and is more soluble and thus more reactive in toluene than other ionised and partially soluble copper complexes.⁴⁴ The monocyclic polymers **8a** and **8b** under these feed conditions gave conversions of 85.0 and 78%, respectively, as determined from SEC distributions. SEC traces for cyclization of PSTY and P^tBA are shown in Figure 4.1.

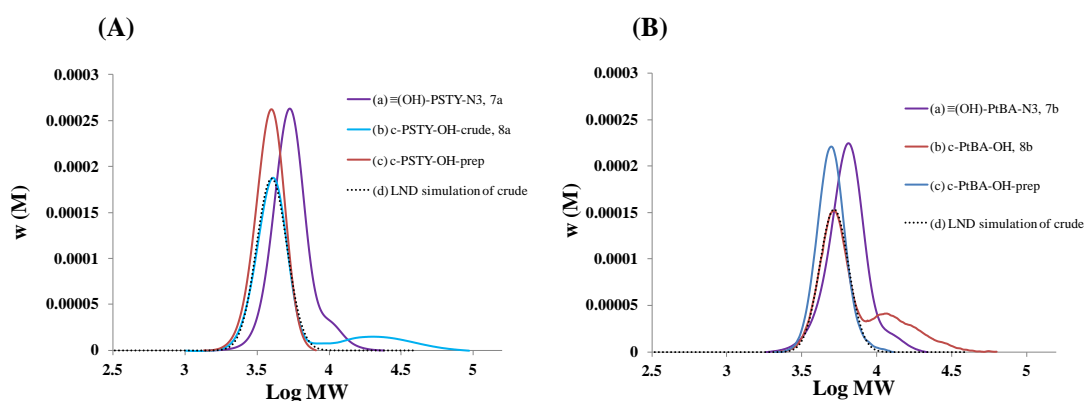


Figure 4.1. SEC chromatograms for cyclization of (A) (a) $\equiv(\text{OH})\text{-PSTY}_{47}\text{-N}_3$ **7a** (b) $\text{c-PSTY}_{47}\text{-OH}$ crude, **8a** (c) $\text{c-PSTY}_{47}\text{-OH}$ purified by prep and (d) LND simulation of **8a** crude with hydrodynamic volume change of 0.75; (B) (a) $\equiv(\text{OH})\text{-P}^t\text{BA}_{44}\text{-N}_3$ **7b** (b) $\text{c-P}^t\text{BA}_{44}\text{-OH}$ crude, **8b** (c) $\text{c-P}^t\text{BA}_{44}\text{-OH}$ purified by prep and (d) LND simulation of **8b** crude with hydrodynamic volume change of 0.78 SEC analysis based on polystyrene calibration curve.

The resultant crude cyclic polymer was purified by prep SEC to remove any unreacted starting polymers and high-molecular-weight by-products formed through either alkyne-alkyne coupling or multi-block formation from CuAAC reactions. The M_n of **8a** after prep was 3780 (PDI = 1.06) and **8b** was 4890 (PDI = 1.05) as determined by RI detection alone and was in accord with a reduced hydrodynamic volume of more compact cyclic topology 0.75 and 0.78 respectively. Analysis of the purified cyclic polymers by triple-detection SEC (to obtain an absolute MWD independent of topology) gave $M_n = 5450$ (PDI = 1.04) for **8a** and $M_n = 6260$ (PDI=1.04) for **8b** are almost identical to the starting linear polymers. For detailed characterization of **8a** and **8b** using ^1H NMR and MALDI-ToF, see appendix C.

Functionalization of **8a** and **8b**

The free OH group on the cyclic polymers, was then further functionalised using 2-bromopropionyl bromide to obtain $\text{c-PSTY}_{47}\text{-Br}$, **9a** and $\text{c-P}^t\text{BA}_{44}\text{-Br}$, **9b** and subsequent azidation using NaN_3 gave $\text{c-PSTY}_{47}\text{-N}_3$ **10a** and $\text{c-P}^t\text{BA}_{44}\text{-N}_3$ **10b** in near quantitative yields, as confirmed by ^1H NMR and MALDI analysis shown in appendix C. These polymers were further

functionalised to mono-alkyne moiety (**11a**) using excess propargyl ether and di-alkyne moieties (**12a**, **12b** and **14**) using excess tripropargyl amine and 1, 3, 5-tris(prop-2-ynyloxy)benzene, **13** as small linkers. The mono and di-alkyne functionalised polymers were characterised by SEC, NMR and MALDI, see appendix C.

Coupling reaction for complex topologies

The mono-alkyne, di-alkyne and azide functional linear and cyclic polymers were utilised to form a variety of complex architectures using the CuAAC 'click' coupling reaction (see Scheme C1 in Appendix C). First, topologies **15-17** (MW~10K) were prepared by a simple CuAAC reaction between two blocks, one having an alkyne and another with azide functional group. For example, c-PSTY₄₇-N₃, **10a** was coupled with PSTY₄₄-≡, **4a**, to produce a tadpole like di-block **16** by CuAAC reaction in 1.0 h at 25 °C with 89.7% product purity as determined from the LND simulation based on weight distribution (Figure 4.2 (B)). The 'click' efficiency for the formation of the coupled products was 89.7 % from the ratio of purity determined by LND to that of the maximum theoretical purity expected from the stoichiometric ratios of the reactants. The MW data and 'click' efficiency are summarised in the Table 4.1. Preparative SEC gave essentially pure **16** in which most of the higher molecular weight polymers was removed. When the purified polymer was subsequently injected through the triple detection SEC (to obtain an absolute MWD independent of topology), it gave a near identical MWD to that of the sum of M_p of starting reactants **10a** and **4a** and with a polydispersity index 1.03 (see Table 4.1 and Figure C26 in appendix C). These results demonstrate the isolation of a well-defined and essentially pure structure. The ¹H NMR of purified **16** (Figure C27 in Appendix C) showed a near quantitative loss of CH₂ protons adjacent to alkyne moiety (denoted as f, $\delta=4.12$ ppm) from **3a** and appearance of a CH proton near triazole moiety (denoted as i, $\delta=4.12$ ppm) as determined by integration suggested quantitative click reaction without any unreacted reactants left. The purified product was further characterised by MALDI ToF mass spectroscopy that produced a MWD that could only result from the coupling of **10a** and **4a** (see Figure C28 in Appendix C). The calculated $[M+Ag^+]$ value (9765.8) in expanded spectra was nearly identical to the experimental value (9764.34), suggesting that after purification there was little or no reactant species left. Similarly, the CuAAC of **3a** with **4a** produced **15** with 92.9 % product purity and coupling efficiency and the coupling of **11a** with **10a** produced **17** with 89.5 % product purity and coupling efficiency. **15** and **17** were also further characterised by NMR and MALDI as shown in Appendix C.

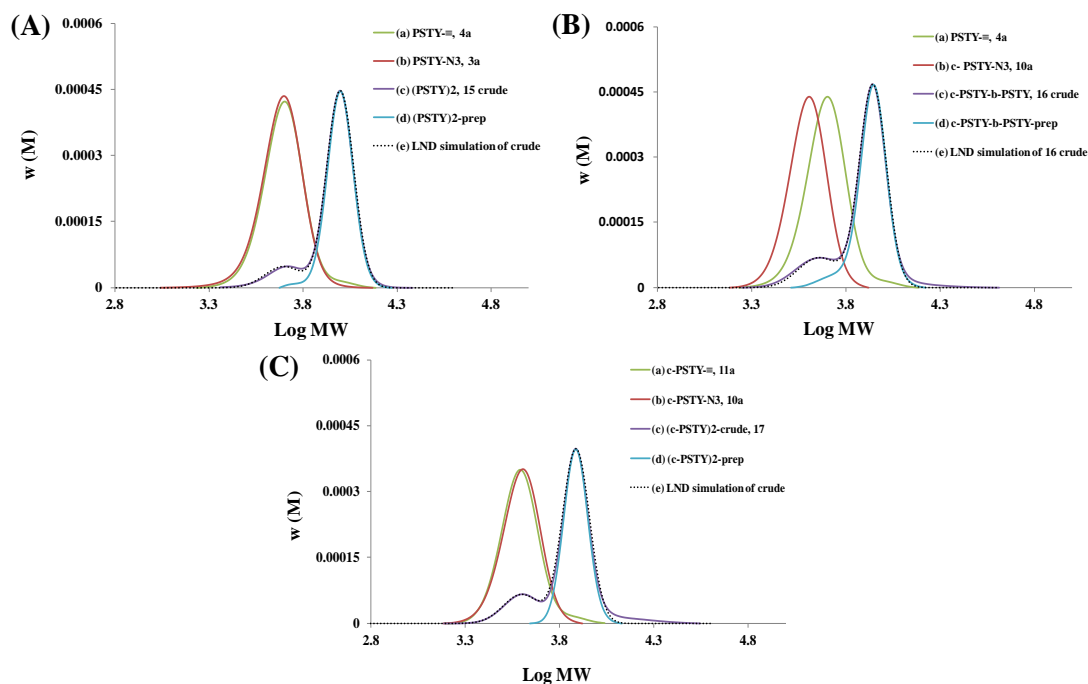


Figure 4.2: SEC of molecular weight distributions (MWDs) for the synthesis of (A) $(\text{PSTY}_{44})_2$ **15** by CuAAC of (a) $\text{PSTY}_{44}\text{-}\equiv$, **4a**, and (b) $\text{PSTY}_{44}\text{-N}_3$, **3a**; (c) $(\text{PSTY}_{44})_2$ **15**, crude, (d) $(\text{PSTY}_{44})_2$ prepped and (e) LND simulation of crude, (B) $\text{c-PSTY}_{47}\text{-b-PSTY}_{44}$, **16** by CuAAC of (a) $\text{PSTY}_{44}\text{-}\equiv$, **4a** and (b) $\text{c-PSTY}_{47}\text{-N}_3$, **10a**; (c) $\text{c-PSTY}_{47}\text{-b-PSTY}_{44}$, **16**, crude, (d) $\text{c-PSTY}_{47}\text{-b-PSTY}_{44}$, prep and (e) LND simulation of crude and (C) $(\text{c-PSTY}_{47})_2$, **17** by CuAAC of (a) $\text{c-PSTY}_{47}\text{-}\equiv$, **11a** and (b) $\text{c-PSTY}_{47}\text{-N}_3$, **10a**; (c) $(\text{c-PSTY}_{47})_2$, **17** crude, (d) $(\text{c-PSTY}_{47})_2$, prep and (e) LND simulation of crude. SEC analysis based on polystyrene calibration curve. Simulation was achieved by adding M_p s of reactants (RI SEC) to fit with the crude products (RI SEC).

Likewise, the topologies (MW~ 15.0 K) **18**, **19**, **20** and **22** were produced by CuAAC from alkyne and azide precursors with the yield of 94.5, 85.8, 83.5, and 92% product purity and the crude products were further purified by preparative SEC essentially gave 98.0, 99.0, 95.3 and 99.5% product purity respectively. The SEC traces for the synthesis of **18**, **19**, **20** and **22** were shown in Figure 4.3. The purified polymers were further characterised by ^1H NMR and MALDI as shown in Appendix C.

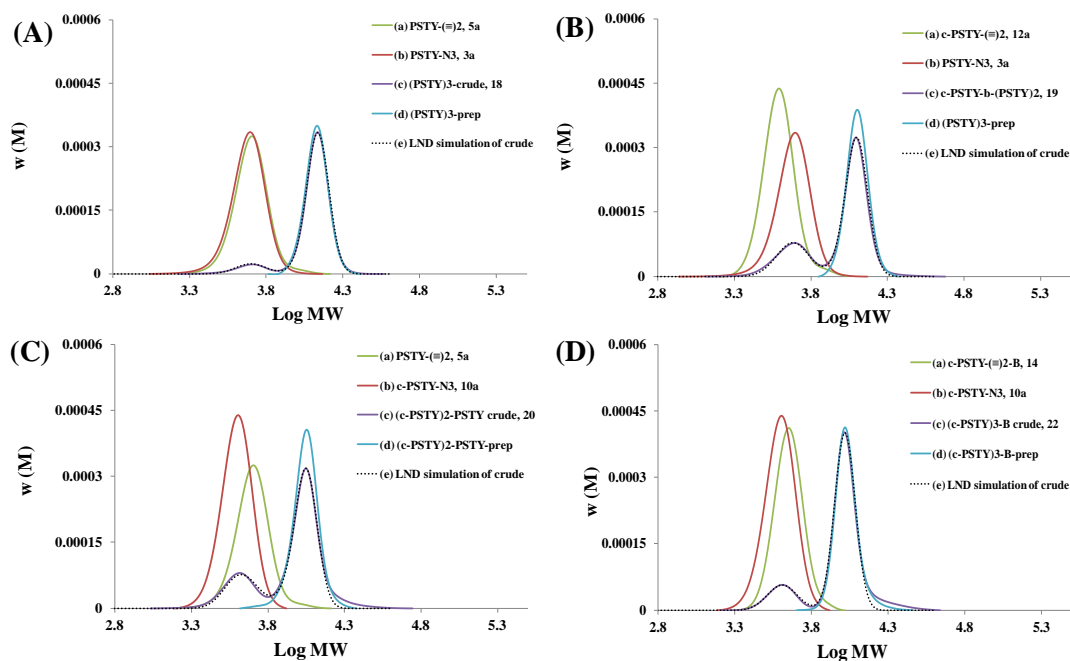


Figure 4.3: SEC of molecular weight distributions (MWDs) for the synthesis of (A) (PSTY₄₄)₃ **18** by CuAAC of (a) PSTY₄₄-≡₂, **5a**, and (b) PSTY₄₄-N₃, **3a**; (c) (PSTY₄₄)₃ **18**, crude, (d) (PSTY₄₄)₃ prepped and (e) LND simulation of crude, (B) c-PSTY₄₇-b-(PSTY₄₄)₂, **19** by CuAAC of (a) PSTY₄₄-≡₂, **4a** and (b) c-PSTY₄₇-N₃, **10a**; (c) c-PSTY₄₇-b-PSTY₄₄, **16**, crude, (d) c-PSTY₄₇-b-PSTY₄₄, prep and (e) LND simulation of crude and (C) (c-PSTY₄₇)₂, **17** by CuAAC of (a) c-PSTY₄₇-≡₂, **11a** and (b) c-PSTY₄₇-N₃, **10a**; (c) (c-PSTY₄₇)₂, **17** crude, (d) (c-PSTY₄₇)₂, prep and (e) LND simulation of crude. SEC analysis based on polystyrene calibration curve. Simulation was achieved by adding M_ps of reactants (RI SEC) to fit with the crude products (RI SEC).

The di-block (**23**, **24**) and mikto-arm star (**25-28**) copolymers were also synthesised by the CuAAC reaction from the azide, mono and di-alkyne functional polymer precursors. First, mono-alkyne functional polymer precursors, PSTY₄₄-≡, **4a** and c-PSTY₄₇-≡, **11a**, were coupled to an equimolar ratio of P^tBA₄₄-N₃, **4b**, and c-P^tBA₄₄-N₃, **10b**, to produced PSTY₄₄-b-P^tBA₄₄, **23**, and c-PSTY₄₇-b-c-P^tBA₄₄, **24**, respectively. The 'click' efficiency for the formation **23** was 92.3%, which was much higher than that of formation of **24** (83%). The reason can be attributed to the higher functionality of **4b** compared to **10b**, as the later one undergoes multiple reaction steps that may decrease the chain-end functionality. The crude products **23** and **24** were purified by preparative SEC to remove all starting polymers and undesired coupling products. When the purified polymers were injected in triple detection SEC, the M_p of **24** increased to 12270, while it was 8490 on RI detection (Table 4.1). On the other hand, there was no apparent change of M_p in product **23** observed. The significant difference in hydrodynamic volume of **24** is a consequence of the change in

hydrodynamic volume from the combination of individual cyclic polymers and the formation of a di-cyclic block copolymer, resulting in a hydrodynamic shift of 0.73. The LND model was used to fit RI traces for **23** and **24** with M_{ps} of 10890 and 12270 from triple detection and multiplied by the factor of hydrodynamic volume changes of 1 and 0.73 respectively. The fits were excellent, suggesting that **23** and **24** were pure with no remaining starting polymers left. The peak maximum (M_p) of the polymers after purification by prep SEC were also similar to theoretical M_{ps} , which were calculated from the addition of the M_{ps} of the starting compounds. The di-alkyne functional polymers PSTY₄₄-(≡)₂, **5a**, and c-PSTY₄₇-(≡)₂ **12a** were coupled with two equivalents of P^tBA₄₄-N₃, **4b**, and c-P^tBA₄₄-N₃, **10b**, to produce mikto-arm stars PSTY₄₄-b-(P^tBA₄₄)₂, **25**, and c-PSTY₄₇-b-(c-P^tBA₄₄)₂, **26**, respectively. Topologies **27** and **28** were also synthesised by coupling di-alkyne functional polymers, PtBA-(≡)₂, **5b**, and c-P^tBA-(≡)₂, **12b**, with two equivalents of PSTY₄₄-N₃, **3a**, and c-PSTY₄₇-N₃, **10a**, respectively. The higher coupling efficiency and product purity were observed in the formation of all the topologies except **28**. The lower product purity of **28** might be due to the lower chain end functionality of **12b** from the multiple reaction steps and subsequent purification. The crude products **25-28** were purified by preparative SEC to remove all starting polymers as well as undesired coupling products. The purified polymers were injected in triple detection SEC to measure the absolute MW, and it was observed that the M_{ps} of products **25-28** were almost identical to the theoretical M_{ps} calculated by adding corresponding reactants M_{ps} . These results supported that the products **25-28** were essentially pure with no remaining starting polymers left. The significant change in hydrodynamic volume for **25**, **26**, **27** and **28** of 0.82, 0.62, 0.79 and 0.59, respectively, suggested that the products were topologically constrained. All the SEC results for the synthesis of **23-28** are shown in Figure 4.4. The products were further characterised by ¹H NMR as shown in Appendix C.

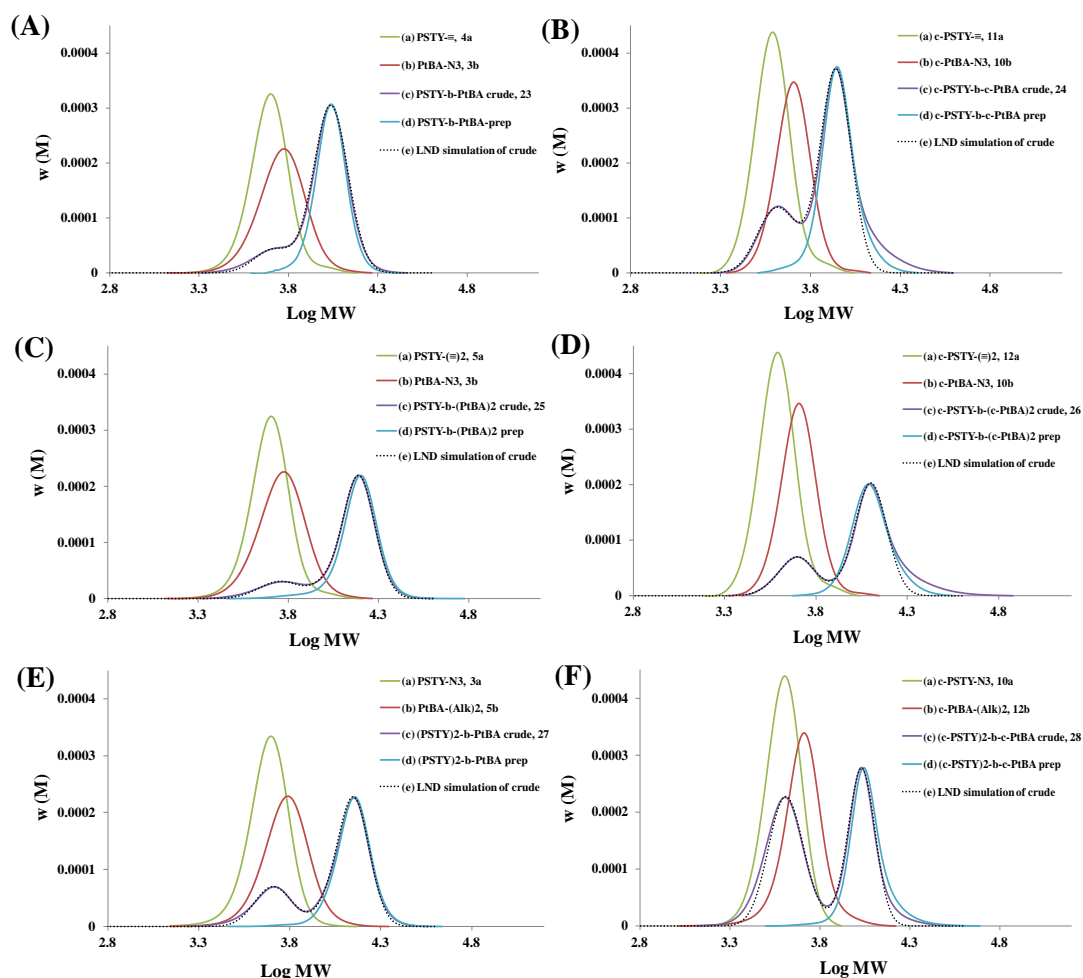


Figure 4.4: SEC of molecular weight distributions (MWDs) for the synthesis of (A) $\text{PSTY}_{44}\text{-b-P}^t\text{BA}_{44}$ **23** by CuAAC of (a) $\text{PSTY}_{44}\text{-}\equiv$, **4a**, and (b) $\text{P}^t\text{BA}_{44}\text{-N}_3$, **3b**; (c) $\text{PSTY}_{44}\text{-b-P}^t\text{BA}_{44}$ **23**, crude, (d) $\text{PSTY}_{44}\text{-b-P}^t\text{BA}_{44}$ prepped and (e) LND simulation of crude, (B) $\text{c-PSTY}_{47}\text{-b-c-P}^t\text{BA}_{44}$, **24** by CuAAC of (a) $\text{c-PSTY}_{47}\text{-}\equiv$, **11a** and (b) $\text{c-P}^t\text{BA}_{44}\text{-N}_3$, **10b**; (c) $\text{c-PSTY}_{47}\text{-b-c-P}^t\text{BA}_{44}$, **24**, crude, (d) $\text{c-PSTY}_{47}\text{-b-c-P}^t\text{BA}_{44}$, prep and (e) LND simulation of crude, (C) $\text{PSTY}_{44}\text{-b-(P}^t\text{BA}_{44})_2$, **25** by CuAAC of (a) $\text{PSTY}_{44}\text{-}(\equiv)_2$, **5a** and (b) $\text{P}^t\text{BA}_{44}\text{-N}_3$, **3b**; (c) $\text{PSTY}_{44}\text{-b-(P}^t\text{BA}_{44})_2$, **25** crude, (d) $\text{PSTY}_{44}\text{-b-(P}^t\text{BA}_{44})_2$, prep and (e) LND simulation of crude, (D) $\text{c-PSTY}_{47}\text{-b-(c-P}^t\text{BA}_{44})_2$, **26** by CuAAC of (a) $\text{c-PSTY}_{47}\text{-}(\equiv)_2$, **12a** and (b) $\text{c-P}^t\text{BA}_{44}\text{-N}_3$, **10b**; (c) $\text{c-PSTY}_{47}\text{-b-(c-P}^t\text{BA}_{44})_2$, **26** crude, (d) $\text{c-PSTY}_{47}\text{-b-(P}^t\text{BA}_{44})_2$, prep and (e) LND simulation of crude. (E) $(\text{PSTY}_{44})_2\text{-b-P}^t\text{BA}_{44}$, **27** by CuAAC of (a) $\text{PSTY}_{44}\text{-N}_3$, **3a** and (b) $\text{P}^t\text{BA}_{44}\text{-}(\equiv)_2$, **5b**; (c) $(\text{PSTY}_{44})_2\text{-b-P}^t\text{BA}_{44}$, **27** crude, (d) $(\text{PSTY}_{44})_2\text{-b-P}^t\text{BA}_{44}$, prep and (e) LND simulation of crude. (F) $(\text{c-PSTY}_{47})_2\text{-b-c-P}^t\text{BA}_{44}$, **28** by CuAAC of (a) $\text{c-PSTY}_{47}\text{-N}_3$, **10a** and (b) $\text{c-P}^t\text{BA}_{44}\text{-}(\equiv)_2$, **12b**; (c) $(\text{c-PSTY}_{47})_2\text{-b-c-P}^t\text{BA}_{44}$, **28** crude, (d) $(\text{c-PSTY}_{47})_2\text{-b-c-P}^t\text{BA}_{44}$, prep and (e) LND simulation of crude. SEC analysis based on polystyrene calibration curve. Simulation was achieved by adding M_{ps} of reactants (RI SEC) to fit with the crude products (RI SEC).

Deprotection of tertiary butyl acrylate (^tBA) groups in the polymers (**23-28**) to acrylic acid (AA) using TFA gave amphiphillic architectures in which the chain length of the PSTY (n=44 for linear and n=47 for cyclic) and PAA (n=44 for both linear and cyclic) were nearly identical in all the equivalent architectures.

Table 4.1. Click efficiency and molecular weight data for the synthesis of complex topologies (**15-28**).

Polymer	Purity by LND (%)		Coupling efficiency (%) ^a	RI detection ^b			Triple detection ^c			M _n by NMR	Δ HDV ^d
	Crude	Prep		M _n	M _p	PDI	M _n	M _p	PDI		
15	92.9	99.5	92.9	9710	9950	1.03	9820	10030	1.02	9890	0.99
16	89.7	96.0	89.7	8400	8880	1.03	10180	10480	1.03	10290	0.85
17	89.5	> 99.0	89.5	7630	7660	1.02	10230	10530	1.03	11000	0.73
18	94.5	98.0	94.5	13170	13500	1.03	15110	15720	1.04	14560	0.86
19	85.8	99.0	85.8	12410	12710	1.03	15550	16170	1.04	15380	0.79
20	83.5	95.3	83.5	10750	11290	1.04	15580	16200	1.03	15890	0.70
21	90.7	97.5	90.7	9910	10060	1.03	15800	16270	1.03	15930	0.62
22	92.0	99.5	92.0	10490	10410	1.03	16100	16580	1.03	17020	0.63
23	92.3	98.5	92.3	10630	10900	1.04	10450	10890	1.03	10600	1.00
24	83.0	98.5	83.0	8790	8920	1.06	12050	12270	1.06	11950	0.73
25	90.0	97.0	90.0	14730	15930	1.07	17510	19400	1.06	16540	0.82
26	85.5	98.5	85.5	12210	12300	1.07	17070	19710	1.05	17830	0.62
27	83.8	95.5	83.8	13460	14380	1.06	16530	18220	1.06	14970	0.79
28	68.8	97.7	68.8	11120	11000	1.06	15900	18770	1.06	16700	0.59

^aCuAAC coupling efficiency was determined by dividing the purity calculated by LND over the maximum theoretical purity expected from the stoichiometric ratios of the reactants. ^bThe data was acquired using SEC (RI detector) and is based on PSTY calibration curve. ^cThe data was acquired using Triple Detection SEC. ^dΔHDV was calculated by dividing M_p of RI with M_p of triple detection.

Topology effect on glass transition temperature

The homopolystyrene of different architectures were divided by two series based on molecular weight or no. of block. Series 1 polymers included architectures, **15-17**, with di-blocks (MW~10K), and Series 2 polymers included architectures, **18-22**, with tri-blocks (MW~15K) polymers. DSC thermograms of Series 1 polymer **15**, **16** and **17** are shown in Figure **C45** in Appendix C. An increase (11.0 °C) of T_g was observed from linear di-block, **15**, to tadpole, **16**, of the similar molecular weight (see Table 4.2). A simple linear polymer consists of two free chain-ends that play

a role on the free volume. Chain-ends require more free volume to move than the segment in its interior chain. When, thermal energy is applied, the chain ends rotate or translate more readily than the rest of the chain and the more chain-ends a sample has the greater the contribution to the free volume. Therefore, polymers having higher number of chain ends contribute greater degree of configurational freedom that resulted lowering the T_g of **15** than **16**. However, the topology effect on T_g is more significant than molecular weight effect as it is observed that the cyclic **8a** (MW~5.0 K) shows higher T_g than both **15** and **16** (MW~10.0 K). An increasing trend of T_g vs no. of cyclic unit (or no. of chain-ends) in different topologies of polymer are shown in Figure 4.5.

The DSC thermo-grams of 3 arms star **18**, twin-tailed tadpole **19**, twin-headed tadpole **20**, tri-cyclic star with amine core, **21** and benzene core, **22** are shown in the Figure C46 in Appendix C. As can be seen in topologies **15-17**, decreasing the number of chain end leads to the increase of glass transition temperature at same molecular weight. Cleavage (see Figure C51 in Appendix C) was observed for the amine core based **21** during the running of the DSC and did not show any specific glass transition. The reason can be attributed by the ester cleavage for the restricted segmental mobility in highly compact core. Therefore, we synthesised topology **22** using a benzene based tri-alkyne core, and the topology showed a higher value of glass transition than the other topologies of similar molecular weight. Thus, the polymer having multiple cyclic units tethering in a single point restrict their mobility due to the compactness of polymer chains to the tethering point.

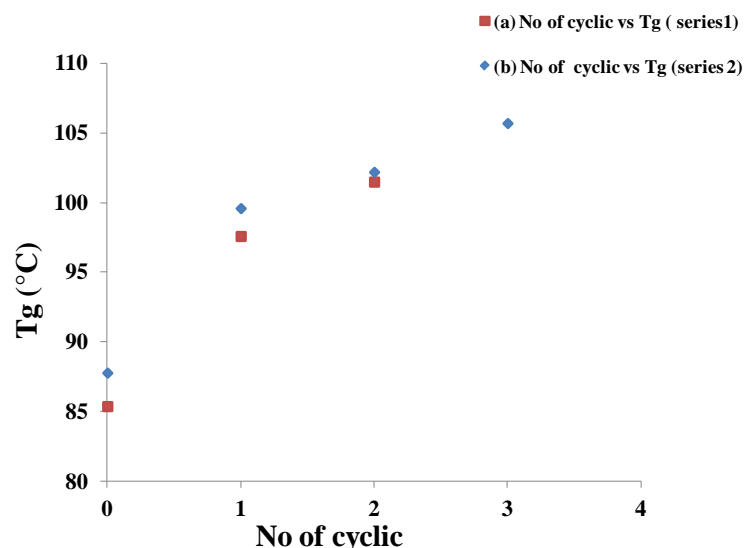


Figure 4.5. The change of glass transition temperature with the increase of no of cyclic unit, Series 1 polymers: **15**, **16**, **17** and series 2 polymers: **18**, **19**, **20** and **22**).

A number of amphiphillic cyclic block copolymers and their linear counterparts were also investigated to study the effect of polymer topology of block copolymers on the glass transition temperature. Generally, most polymer blends, as well as their graft and block copolymer and interpenetrating polymer networks, phase-separate, in which each phase exhibits their own characteristic chain mobility.⁴⁵ From the thermo-grams in Figure C48 in Appendix C, two clear and separated glass transitions were observed for both blocks in **23** and **24**, which corresponded to the T_g s of the PSTY and PAA phases, respectively. The PSTY block in **23** shows a 10 °C higher T_g than **3a** homopolystyrene, which suggested that the segmental mobility of the PSTY blocks was influenced by the increasing restrictions of the PAA blocks at the block changing point⁴⁶ and the PAA block segment also shifted to a slight higher T_g presumably due to more effective hydrogen bonding when PAA blocks are phase separated by PS block.⁴⁷

Table 4.2. DSC results of linear, cyclic and their complex topologies and amphiphillic block and mikto-arm star copolymers.

Polymer	Polymer code	Type of topology	Glass transition temp. (°C)	
			PSTY segment	PAA segment
3a	PSTY₄₄-N₃	Linear	85.4	--
8a	c-PSTY₄₇-OH	Mono-cyclic	99.8	--
15	(PSTY₄₄)₂	Linear di-block	86.6	--
16	c-PSTY₄₇-b-PSTY₄₄	Tadpole	97.6	--
17	(c-PSTY₄₇)₂	Spiro di-cyclic	101.5	--
18	(PSTY₄₄)₃	3-arms linear star	87.8	--
19	c-PSTY₄₇-b-(PSTY₄₄)₂	Twin-tailed tadpole	99.6	--
20	(c-PSTY₄₇)₂-b-PSTY₄₄	Twin-headed tadpole	102.2	--
21	(c-PSTY₄₇)₃-A	Tri-cyclic star-A	--	--
22	(c-PSTY₄₇)₃-B	Tri-cyclic star-B	105.7	--
2b	PAA₄₄-N₃	Linear	--	113.3
8b	c-PAA₄₄-OH	Mono-cyclic	--	115.1
23	PSTY₄₄-b-PAA₄₄	Linear di-block-AB	95.5	118.7
24	c-PSTY₄₇-b-c-PAA₄₄	Cyclic di-block-AB	108.5	120.9
25	PSTY₄₄-b-(PAA₄₄)₂	Mikto-arm linear-AB ₂	93.8	126.5
26	c-PSTY₄₇-b-(c-PAA₄₄)₂	Mikto-arm cyclic-AB ₂	109.0	128.4
27	(PSTY₄₄)₂-b-PAA₄₄	Mikto-arm linear-A ₂ B	96.5	118.9
28	(c-PSTY₄₇)₂-b-c-PAA₄₄	Mikto-arm cyclic-A ₂ B	109.5	123.2

The property enhancement of these block copolymers can also be explained in terms of domain concept illustrated schematically in Figure 4.6. The block with higher T_g tends to aggregates in domains that act as both cross-linking points and filler particles. These aggregated regions serve to anchor the lower T_g block and act as effective cross-linking points, thereby increasing T_g to the

second block. The T_g of polystyrene segments in cyclic block copolymer, **24** shows 13 °C higher than that of linear counterparts, **23**. So the increase of T_g can be attributed to the topological constraints conferred by cyclic moieties anchoring to aggregated domains.

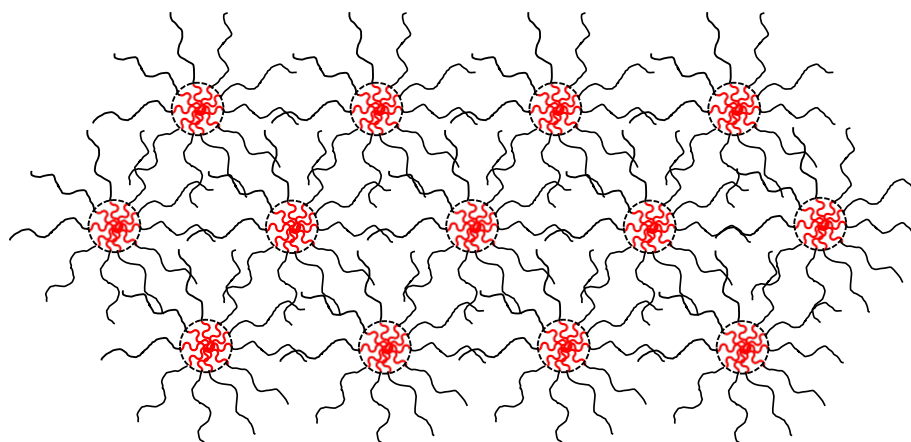


Figure 4.6. Schematic representation of AB di-block copolymers, showing areas (the dotted circles) of aggregation of the higher T_g blocks (red), joined by the lower T_g block (black).

The block copolymer phase separation was further confirmed by the formation of self-assembled thin films by thermally annealed above 130 °C. The resulting nanophase-separated thin films were characterised by atomic force microscopy (AFM) in order to determine the effect of macromolecular architectures on the thin films. AFM height images of the linear **23** and cyclic analogue, **24** are shown in Figure 4.7. The cyclic block copolymer, **24** displays a considerable (~50%) decrease in domain spacing than linear analogue. Hawker and co-workers,⁴⁸ have also demonstrated a decrease in domain spacing by ~30% for cyclic polystyrene-*b*-polyethylene oxide (c-(PSTY-*b*-PEO)) over the corresponding linear polymers (PSTY-*b*-PEO). Compared with their work, our result was consistent with the more compact structure (c-PSTY₄₇-*b*-c-PAA₄₄, **24**) than the linear analogue (PSTY₄₄-*b*-PAA₄₄, **23**) and additional constraints resulting from the folding of two opposite chain ends to a common junction point that forms spiro bi-cyclic type topology.

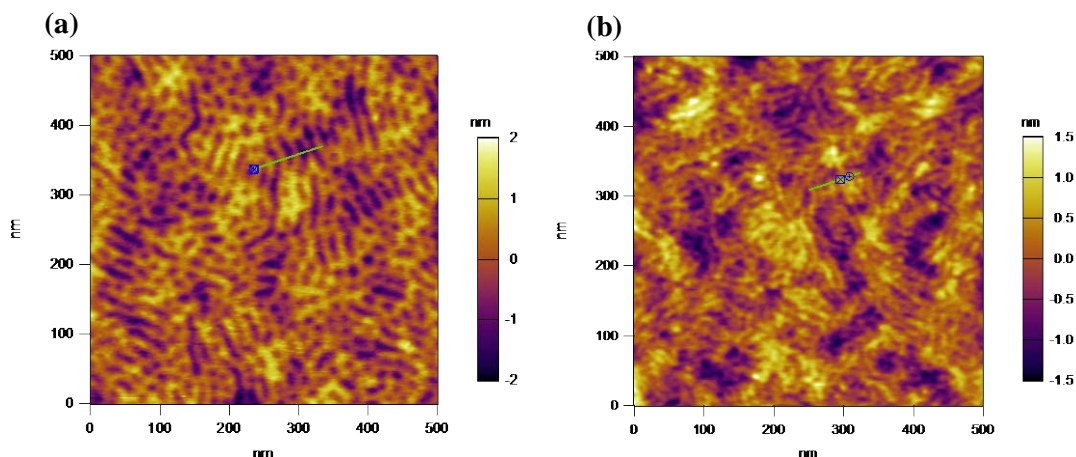


Figure 4.7. Atomic force microscopy height images for (a) PSTY₄₄-b-PAA₄₄, **23** and (b) c-PSTY₄₇-b-c-PAA₄₄, **24**.

Compared to the T_g ($T_{g(\text{PAA})}=118.7$ °C) of di-block (AB) **23**, mikto-arm star (AB₂) **25** shows higher T_g ($T_{g(\text{PAA})}=126.5$ °C). This result is contradictory to the free volume theory as the higher number of chain end possess more free volume which results low T_g value. The reason of higher T_g of PAA in **25** can be explained by the fact that the hydrogen bond between the two PAA chains of **25** help to squeeze them together that restrict the segmental mobility and may lead to higher glass transition temperature.⁴⁹ Furthermore, a little change in T_g value of the topologies **23** and **27** was observed although the number of PS chains were higher in **27**. In addition, PS segment in topology **26** and **28** has pronounce effect on T_g compared with their linear analogues, but this effect is less in case of PAA segments.

4.4 Conclusion

In summary, we have demonstrated the synthesis of different homopolystyrene and amphiphilic architectures, including di-block and miktoarm star copolymer of both linear and cyclic counterparts by combining ATRP, SET-LRP and CuAAC coupling reactions. The products were then further purified using preparative SEC to remove any starting polymers and other polymeric species from side reactions. All the P^tBA arms on the structures were deprotected to the hydrophilic PAA using TFA, producing amphiphilic macrocyclic structures. The effect of topology of homo and copolymers was investigated by measuring the glass transition temperature using DSC. The topology having higher no. of cyclic units (or lower no. of chain end), provides higher glass transition temperature, than the topology with the lower no. of cyclic units of same molecular weight. The tricyclic star homopolymer, thus having no chain end showed relatively higher T_g than the other topologies. Phase-separated block copolymers also showed the enhance glass transition

temperature due the influence of segmental mobility of one block to another. Hydrogen bonding in PAA segments also play important role in the glass transition temperature.

4.5 References

- (1) Hadjichristidis, N.; Pitsikalis, M.; Pispas, S.; Iatrou, H. *Chemical Reviews* **2001**, *101*, 3747-3792.
- (2) Kobayashi, S.; *New frontiers in polymer synthesis*; Springer: Berlin :, 2008.
- (3) Laurent, B. A.; Grayson, S. M. *Chemical Society Reviews* **2009**, *38*, 2202-2213.
- (4) Kricheldorf, H. R. *Journal of Polymer Science Part A: Polymer Chemistry* **2010**, *48*, 251-284.
- (5) Jia, Z.; Monteiro, M. J. *Journal of Polymer Science Part A: Polymer Chemistry* **2012**, *50*, 2085-2097.
- (6) McLeish, T. *Science* **2002**, *297*, 2005-2006.
- (7) Obukhov, S. P.; Rubinstein, M.; Duke, T. *Physical Review Letters* **1994**, *73*, 1263-1266.
- (8) Kapnistos, M.; Lang, M.; Vlassopoulos, D.; Pyckhout-Hintzen, W.; Richter, D.; Cho, D.; Chang, T.; Rubinstein, M. *Nat Mater* **2008**, *7*, 997-1002.
- (9) Lo, W.-C.; Turner, M. S. *EPL (Europhysics Letters)* **2013**, *102*, 58005.
- (10) Klein, J. *Macromolecules* **1986**, *19*, 105-118.
- (11) McLeish, T. *Nat Mater* **2008**, *7*, 933-935.
- (12) Whittaker, M. R.; Goh, Y.-K.; Gemici, H.; Legge, T. M.; Perrier, S.; Monteiro, M. J. *Macromolecules* **2006**, *39*, 9028-9034.
- (13) Peng, Y.; Liu, H.; Zhang, X.; Liu, S.; Li, Y. *Macromolecules* **2009**, *42*, 6457-6462.
- (14) Misaka, H.; Kakuchi, R.; Zhang, C.; Sakai, R.; Satoh, T.; Kakuchi, T. *Macromolecules* **2009**, *42*, 5091-5096.
- (15) Laurent, B. A.; Grayson, S. M. *Journal of the American Chemical Society* **2006**, *128*, 4238-4239.
- (16) Ge, Z.; Zhou, Y.; Xu, J.; Liu, H.; Chen, D.; Liu, S. *J. Am. Chem. Soc.* **2009**, *131*, 1628-1629.
- (17) O'Bryan, G.; Ningnuek, N.; Braslau, R. *Polymer* **2008**, *49*, 5241-5248.
- (18) Hoskins, J. N.; Grayson, S. M. *Macromolecules* **2009**, *42*, 6406-6413.
- (19) Qiu, X.-P.; Tanaka, F.; Winnik, F. M. *Macromolecules* **2007**, *40*, 7069-7071.
- (20) Eugene, D. M.; Grayson, S. M. *Macromolecules* **2008**, *41*, 5082-5084.
- (21) Bielawski, C. W.; Benitez, D.; Grubbs, R. H. *Science* **2002**, *297*, 2041-2044.
- (22) Boydston, A. J.; Xia, Y.; Kornfield, J. A.; Gorodetskaya, I. A.; Grubbs, R. H. *J. Am. Chem. Soc.* **2008**, *130*, 12775-12782.

- (23) Kudo, H.; Sato, M.; Wakai, R.; Iwamoto, T.; Nishikubo, T. *Macromolecules* **2008**, *41*, 521-523.
- (24) Culkin, D. A.; Jeong, W.; Csihony, S.; Gomez, E. D.; Balsara, N. P.; Hedrick, J. L.; Waymouth, R. M. *Angew. Chem., Int. Ed.* **2007**, *46*, 2627-2630.
- (25) Jeong, W.; Hedrick, J. L.; Waymouth, R. M. *J. Am. Chem. Soc.* **2007**, *129*, 8414-8415.
- (26) Herbert, D. E.; Gilroy, J. B.; Chan, W. Y.; Chabanne, L.; Staubitz, A.; Lough, A. J.; Manners, I. *J. Am. Chem. Soc.* **2009**, *131*, 14958-14968.
- (27) Zhang, F.; Götz, G.; Winkler, H. D. F.; Schalley, C. A.; Bäuerle, P. *Angew. Chem., Int. Ed.* **2009**, *48*, 6632-6635.
- (28) Lonsdale, D. E.; Bell, C. A.; Monteiro, M. J. *Macromolecules* **2010**, *43*, 3331-3339.
- (29) Lonsdale, D. E.; Monteiro, M. J. *Chemical Communications* **2010**, *46*, 7945-7947.
- (30) Lonsdale, D. E.; Monteiro, M. J. *Journal of Polymer Science Part A: Polymer Chemistry* **2011**, *49*, 4603-4612.
- (31) Hossain, M. D.; Valade, D.; Jia, Z.; Monteiro, M. J. *Polym Chem-Uk* **2012**, *3*, 2986-2995.
- (32) Jia, Z.; Lonsdale, D. E.; Kulis, J.; Monteiro, M. J. *ACS Macro Letters* **2012**, *1*, 780-783.
- (33) Kulis, J.; Jia, Z.; Monteiro, M. J. *Macromolecules* **2012**, *45*, 5956-5966.
- (34) Oike, H.; Imaizumi, H.; Mouri, T.; Yoshioka, Y.; Uchibori, A.; Tezuka, Y. *J. Am. Chem. Soc.* **2000**, *122*, 9592-9599.
- (35) Oike, H.; Hamada, M.; Eguchi, S.; Danda, Y.; Tezuka, Y. *Macromolecules* **2001**, *34*, 2776-2782.
- (36) Tezuka, Y.; Mori, K.; Oike, H. *Macromolecules* **2002**, *35*, 5707-5711.
- (37) Tezuka, Y.; Fujiyama, K. *J. Am. Chem. Soc.* **2005**, *127*, 6266-6270.
- (38) Tezuka, Y.; Takahashi, N.; Satoh, T.; Adachi, K. *Macromolecules* **2007**, *40*, 7910-7918.
- (39) Sugai, N.; Heguri, H.; Ohta, K.; Meng, Q.; Yamamoto, T.; Tezuka, Y. *J. Am. Chem. Soc.* **2010**, *132*, 14790-14802.
- (40) Igari, M.; Heguri, H.; Yamamoto, T.; Tezuka, Y. *Macromolecules* **2013**, *46*, 7303-7315.
- (41) Li, Y.; Mullen, K. M.; Claridge, T. D. W.; Costa, P. J.; Felix, V.; Beer, P. D. *Chemical Communications* **2009**, 7134-7136.
- (42) Cabaniss, S. E.; Zhou, Q.; Maurice, P. A.; Chin, Y.-P.; Aiken, G. R. *Environmental Science & Technology* **2000**, *34*, 1103-1109.
- (43) Kolb, H. C.; Finn, M. G.; Sharpless, K. B. *Angewandte Chemie International Edition* **2001**, *40*, 2004-2021.
- (44) Bell, C. A.; Jia, Z.; Kulis, J.; Monteiro, M. J. *Macromolecules* **2011**, *44*, 4814-4827.
- (45) Sperling, L. H. *Polymeric Multicomponent Materials: An Introduction*; Wiley, 1997, p 397 pp.
- (46) Magnusson, H.; Malmström, E.; Hult, A.; Johansson, M. *Polymer* **2002**, *43*, 301-306.

- (47) Wong, C. L. H.; Kim, J.; Torkelson, J. M. *Journal of Polymer Science Part B: Polymer Physics* **2007**, *45*, 2842-2849.
- (48) Poelma, J. E.; Ono, K.; Miyajima, D.; Aida, T.; Satoh, K.; Hawker, C. J. *ACS Nano* **2012**, *6*, 10845-10854.
- (49) Mori, H.; Müller, A. H. E. *Progress in Polymer Science* **2003**, *28*, 1403-1439.

Chapter 5

Polymeric Knots on Glass Transition Temperature: A Model Study

In this chapter, different topological conformations using polystyrene cyclic building blocks were constructed all with the same molecular weight. The cyclic building blocks were coupled together by combining ATRP and the high efficient CuAAC 'click' reaction. A series of topologies such as linear, monocyclic, spiro dicyclic, star tricyclic, spiro tricyclic, G1 pentacyclic, and a G1 tetracyclic were built from the multifunctional polymeric cyclic blocks (see Scheme 5.1). A modular approach was used for the synthesis of linear polymer precursors to make cyclic polymers with a different number of chemical functionalities. The configurations could represent the many types of knots found when preparing cyclic polymers via the ring closure method, and the change in the glass transition temperature (T_g) could provide some insight into the affect of chain restriction on chain dynamics.

5.1 Introduction

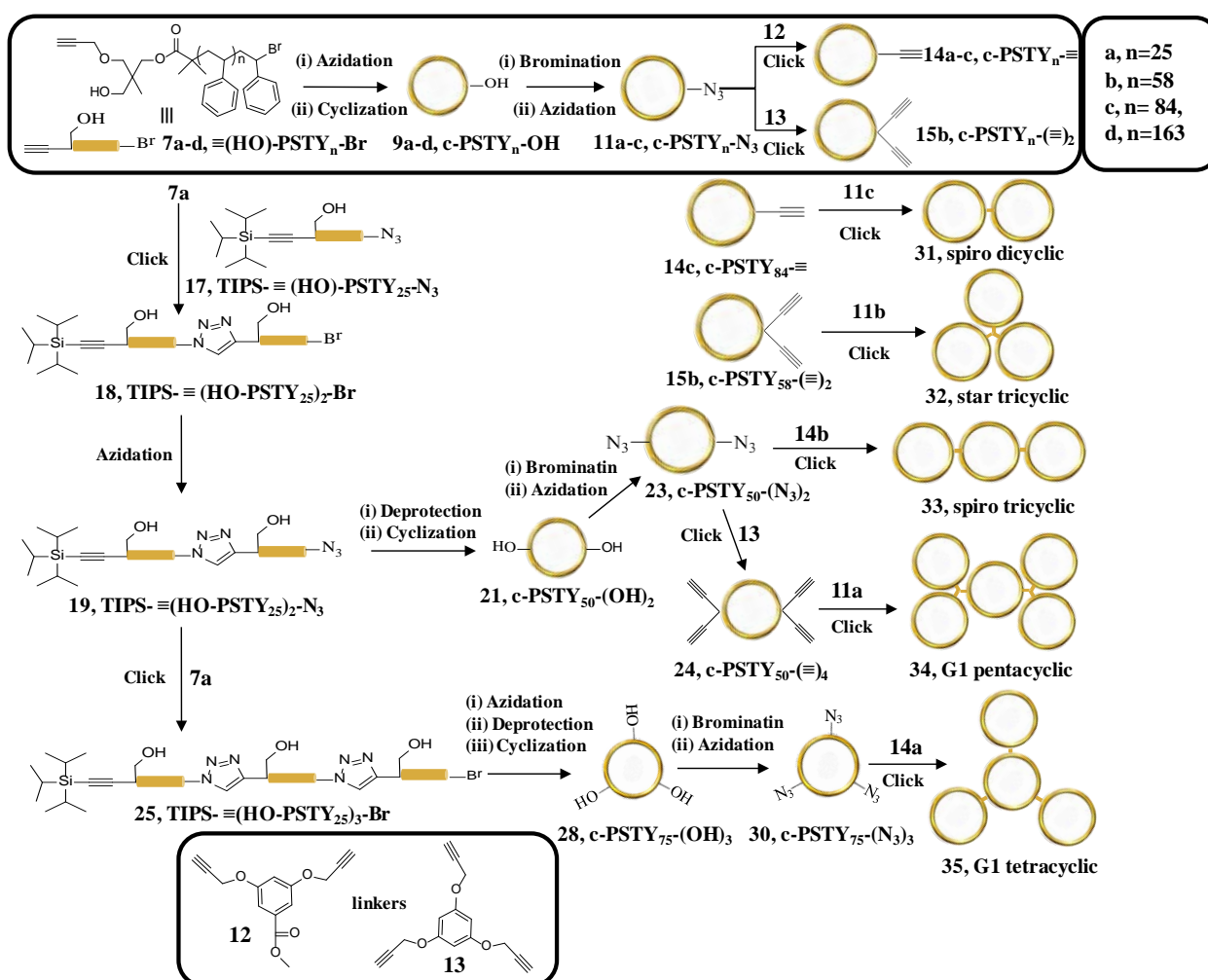
Among the various type of topologies, cyclic polymers have very different properties compared to their linear analogues due to the absence of chain end.¹ Significant progress has now been achieved to produce a wide variety of single cyclic polymers based on the end-to-end coupling processes²⁻¹⁰ as well as on an alternative ring-expansion polymerization.¹¹⁻¹⁷ Tezuka *et al.*¹⁸⁻²⁰ have pioneered the synthesis of multifunctional cyclic polymers, including spiro and bridged-type multicyclic polymer, and a variety of polymeric grafts and fused polymer topologies constructed through CuAAC addition in conjunction with electrostatic self-assembly and covalent fixation process.²¹⁻²⁴ This work inspired us to build similar topologies to investigate the effect of predesigned knots on T_g .

Knots and links play a prominent role in biological systems and polymer processing.²⁵ Knotting is involved in chromosomes during cell replication.²⁶ Knots are also observed in bacterial DNA²⁷, or in the native states of proteins²⁸. Long (or high molecular weight) polymer almost certainly form a wide range of knots that correlate to that found from theory.²⁹

In this work, a facile and efficient strategy was followed to produce a range of polymer architectures starting from a simple linear to dendrimer-like complex topologies in which each link corresponded to an irreversible knot. A facile modular approach in conjunction with post modification and effective CuAAC reaction was used for the synthesis of multi-hydroxy functional cyclic polymers in which the locations of hydroxyl groups were precisely designated. The subsequent functionalization of these hydroxyl groups allows the fabrication of new structures through topological and compositional control. Our strategy as shown in Scheme 5.1 allows the

fabrication of multi-functional cyclic polymers that upon post-modification are coupled with other cyclic polymers to produce the desired topologies. The molecular weight of all these polymers was kept essentially the same to avoid the contribution from the effect of molecular weight on any the glass transition temperature. All the topologies except linear polymer can be exemplified by knotted from monocyclic polymer. For example, formation of spiro di-cyclic via click between two functional cyclic is equivalent to a single knot in a monocyclic. In this chapter, we have investigated the effect of knot on the glass transition temperature and observed that placing knots in different locations within a cyclic polymer has a direct correlation with the glass transition temperature.

Scheme 5.1. General Synthetic Strategy for the Construction of Spiro Tricyclic, G1 Star Tetracyclic, G1 Dendrimer Pentacyclic and G1 Star Heptacyclic Topologies.



Conditions: (a) **Azidation:** NaN_3 in DMF at 25 °C, (b) **Cyclization:** CuBr, PMDETA in toluene by feed at 25 °C, (c) **Bromination:** 2-BPB, TEA in THF; 0-25 °C, (d) **Deprotection:** TBAF in THF at 25 °C. (e) **'Click':** CuBr, PMDETA in toluene at 25 °C.

5.1.1 Aim of the Chapter

The aim of the work described in this chapter was to synthesise a range polymeric architectures having irreversible knots placed in different places of a cyclic polymer, and investigate their effect on the glass transition temperature. Spiro, di and tricyclic polymers, star tricyclic, G1 tetracyclic polymers and G1 dendrimeric architectures were successfully synthesised by combing ATRP and CuAAC reaction.

5.2. Experimental

5.2.1 Materials

The following chemicals were analytical grade and used as received unless otherwise stated: alumina, activated basic (Aldrich: Brockmann I, standard grade, ~150 mesh, 58 Å), Dowex ion-exchange resin (sigma-aldrich, 50WX8-200), magnesium sulphate, anhydrous (MgSO₄: Scharlau, extra pure) potassium carbonate (K₂CO₃: analaR, 99.9%), silica gel 60 (230-400 mesh ATM (SDS)), pyridine (99%, Univar reagent), 1,1,1-triisopropylsilyl chloride (TIPS-Cl: Aldrich, 99%), phosphorus tribromide (Aldrich, 99%), tetrabutylammonium fluoride (TBAF: Aldrich, 1.0 M in THF), ethylmagnesium bromide solution (Aldrich, 3.0 M in diethyl ether), triethylamine (TEA: Fluka, 98%), 2-bromopropionyl bromide (BPB: Aldrich 98%), 2-bromoisobutyryl bromide (BIB: Aldrich, 98%), propargyl bromide solution (80% wt% in xylene, Aldrich), 1,1,1-(trihydroxymethyl) ethane (Aldrich, 96%), sodium hydride (60% dispersion in mineral oil), sodium azide (NaN₃: Aldrich, 99.5%), TLC plates (silica gel 60 F254), *N,N,N',N'',N''*-pentamethyldiethylenetriamine (PMDETA: Aldrich, 99%), copper (II) bromide (Cu(II)Br₂: Aldrich, 99%). Copper(I)bromide and Cu(II)Br₂/PMDETA complex were synthesised in our group. Styrene (STY: Aldrich, >99 %) was de-inhibited before use by passing through a basic alumina column. Methyl 3,5-bis (propargyloxy) benzoate³⁰ (**12**) and 1,3,5-tris(prop-2-ynyloxy)benzene³¹ (**13**) linkers were prepared according to the literature procedure. All other chemicals used were of at least analytical grade and used as received.

The following solvents were used as received: acetone (ChemSupply, AR), chloroform (CHCl₃: Univar, AR grade), dichloromethane (DCM: Labscan, AR grade), diethyl ether (Univar, AR grade), dimethyl sulfoxide (DMSO: Labscan, AR grade), ethanol (EtOH: ChemSupply, AR), ethyl acetate (EtOAc: Univar, AR grade), hexane (Wacol, technical grade, distilled), hydrochloric acid (HCl, Univar, 32 %), anhydrous methanol (MeOH: Mallinckrodt, 99.9 %, HPLC grade), Milli-Q water (Biolab, 18.2 MΩ cm), *N,N*-dimethylformamide (DMF: Labscan, AR grade), tetrahydrofuran (THF: Labscan, HPLC grade), toluene (HPLC, LABSCAN, 99.8%).

5.2.2 Analytical Methods

Size Exclusion Chromatography (SEC)

All polymers were dried under vacuum for at least 24 hr before analysis. Water 2695 separations module, fitted with a Water 410 refractive index detector maintained at 35 °C, a Waters 996 photodiode array detector, and two Ultrastyrigel linear columns (7.8 x 300 mm) arranged in series were used to determine the molecular weight distribution. These columns were maintained at 40 °C for all analyses and are capable of separating polymers in the molecular weight range of 500 to 4 million g/mol with high resolution. All samples were eluted at a flow rate of 1.0 mL/min. Calibration was performed using narrow molecular weight PSTY standards ($PDI_{SEC} \leq 1.1$) ranging from 500 to 2 million g/mol. Data acquisition was performed using Empower software, and molecular weights were calculated relative to polystyrene standards. All SEC chromatograms were weight normalised and then replotted as $w(M)$ versus Log (MW).

Absolute Molecular Weight Determination by Triple Detection SEC

Absolute molecular weights of polymers were determined using a Polymer Laboratories GPC50 Plus equipped with dual angle laser light scattering detector, viscometer, and differential refractive index detector. HPLC grade *N,N*-dimethylacetamide (DMAc, containing 0.03 wt % LiCl) was used as the eluent at a flow rate of 1.0 mL.min⁻¹. Separations were achieved using two PLGel Mixed B (7.8 x 300 mm) SEC columns connected in series and held at a constant temperature of 50 °C. The triple detection system was calibrated using a 2 mg.mL⁻¹ PSTY standard (Polymer Laboratories: $M_{wt} = 110$ K, $dn/dc = 0.16$ mL.g⁻¹ and $IV = 0.5809$). Samples of known concentration were freshly prepared in DMAc + 0.03 wt % LiCl and passed through a 0.45 µm PTFE syringe filter prior to injection. The absolute molecular weights and dn/dc values were determined using Polymer Laboratories Multi Cirrus software based on the quantitative mass recovery technique.

Preparative Size Exclusion Chromatography (Prep SEC).

Crude polymers were purified using a Varian Pro-Star preparative SEC system equipped with a manual injector, differential refractive index detector, and single wave-length ultraviolet visible detector. The flow rate was maintained at 10 mL min⁻¹ and HPLC grade tetrahydrofuran was used as the eluent. Separations were achieved using a PL Gel 10 µm 10×10^3 Å, 300 × 25 mm preparative SEC column at 25 °C. The dried crude polymer was dissolved in THF at 100 mg mL⁻¹ and filtered through a 0.45 µm PTFE syringe filter prior to injection. Fractions were collected manually, and the composition of each was determined using the Polymer Laboratories GPC50 Plus equipped with triple detection as described above.

¹H Nuclear Magnetic Resonance (NMR).

All NMR spectra were recorded on a Bruker DRX 500 MHz spectrometer using an external lock (CDCl₃) and referenced to the residual non-deuterated solvent (CHCl₃). A DOSY experiment was run to acquire spectra presented herein by increasing the pulse gradient from 2 to 85 % of the maximum gradient strength and increasing d (**p30**) from 1 ms to 2 ms, using 64-128 scans.

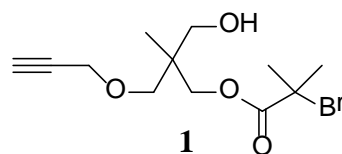
Matrix-Assisted Laser Desorption Ionization-Time-of-Flight (MALDI-ToF) Mass Spectrometry.

MALDI-ToF MS spectra were obtained using a Bruker MALDI-ToF autoflex III smart beam equipped with a nitrogen laser (337 nm, 200 Hz maximum firing rate) with a mass range of 600-400 000 Da. Spectra were recorded in both reflectron mode (500-5000 Da) and linear mode (5000-20000 Da). Trans- 2-[3-(4-tert-butylphenyl)-2-methyl-propenylidene] malononitrile (DCTB; 20 mg/mL in THF) was used as the matrix and Ag-(CF₃COO) (1 mg/mL in THF) as the cation source of all the polystyrene samples. 20 μL polymer solution (1 mg/mL in THF), 20 μL DCTB solutions and 2 μL Ag-(CF₃COO) solution were mixed in an ependorf tube, vortexed and centrifuged. 1 μL of solution was placed on the target plate spot, evaporated the solvent at ambient condition and run the measurement.

5.2.3 Synthetic Procedures

5.2.3.1 Synthesis of Alkyne (hydroxyl) Functional Initiator (**1**)

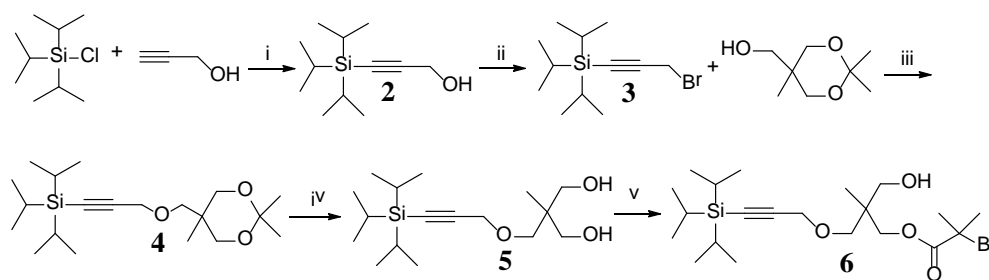
The alkyne (hydroxyl) functional initiator **1** was synthesised according to the literature procedure previously reported by our group.³²



5.2.3.2 Synthesis of Protected Alkyne (hydroxyl) Functional Initiator (**6**)

The detailed synthesis of protected alkyne (hydroxyl) functional initiator **6** was explained in the chapter 3.

Scheme 5.2. Synthetic scheme for protected alkyne (hydroxyl) functional initiator.



Reactants and conditions: (i) EtMgBr, THF, reflux at 76 °C, (ii) PBr₃, pyridine, diethyl ether 0~ 25 °C (iii) NaH/ THF, -78 °C - 25 °C (iv) DOWEX resin in MeOH at 40 °C (v) 2-bromoisobutyryl bromide, TEA in THF at 0 °C-25 °C for 24 h.

5.2.3.3 Synthesis of $\equiv(\text{HO})\text{-PSTY}_{25}\text{-Br}$ **7a** by ATRP

Styrene (8.11 g, 77.86×10^{-3} mol), PMDETA (0.17 mL, 8.1×10^{-4} mol), CuBr₂/PMDETA (6.4×10^{-2} g, 4.05×10^{-4} mol) and initiator (0.5 g, 1.6277×10^{-3} mol) were added to a 100 mL schlenk flask equipped with a magnetic stirrer and purged with argon for 40 min to remove oxygen. Cu(I)Br (0.12 g, 8.1×10^{-4} mol) was then carefully added to the solution under an argon blanket. The reaction mixture was further degassed for 5 min and then placed into a temperature controlled oil bath at 80 °C. After 4 h an aliquot was taken to check the conversion. The reaction was quenched by cooling to 0 °C in ice bath, exposed to air, and diluted with THF (*ca.* 3 fold to the reaction mixture volume). The copper salts were removed by passage through an activated basic alumina column. The solution was concentrated by rotary evaporation and the polymer was recovered by precipitation into large volume of MeOH (20 fold excess to polymer solution) and vacuum filtration two times. The polymer was dried *in high vacuo* overnight at 25 °C, SEC ($M_n = 2890$, PDI = 1.11). Final conversion was calculated by gravimetry 53.3%. The polymer was further characterised by ¹H NMR and MALDI-ToF.

5.2.3.4 Synthesis of $\equiv(\text{HO})\text{-PSTY}_{25}\text{-N}_3$ **8a** by Azidation with NaN₃

Polymer **7a** (2.9 g, 1.0×10^{-3} mol) was dissolved in 20 mL of DMF in a reaction vessel equipped with a magnetic stirrer. To this solution NaN₃ (0.65 g, 10.0×10^{-3} mol) was added and the mixture stirred for 24 h at 25 °C. The polymer solution was directly precipitated into MeOH/H₂O (95/5, v/v) (20 fold excess to polymer solution) from DMF, recovered by vacuum filtration and washed exhaustively with MeOH. The polymer was dried *in vacuo* for 24 h at 25 °C, SEC ($M_n = 2880$, PDI = 1.11). The polymer was further characterised by ¹H NMR and MALDI-ToF.

5.2.3.5 Synthesis of *c*-PSTY₂₅-OH, **9a**

A solution of polymer **8a** (2.0 g, 6.667×10^{-4} mol) in 80.0 ml of dry toluene and 6.97 mL of PMDETA (33.35×10^{-3} mol) in 80 mL of dry toluene in another flask were purged with argon for 45 min to remove oxygen. 4.78 g of CuBr (33.35×10^{-3} mol) was taken in a 250 mL of dry schlenk flask and maintained argon flow in the flask at the same time. PMDETA solution was transferred to CuBr flask by applying argon pressure using a double tip needle to prepare CuBr/PMDETA complex. After complex formation, polymer solution was added via syringe pump using a syringe that is pre-filled with argon. The feed rate of argon was set at 1.24 mL/min. After the addition of polymer solutions (65 min), the reaction mixture was further stirred for 3 h. At the end of this period (i.e., feed time plus an additional 3 h), toluene was evaporated by air-flow and the copper salts were removed by passage through activated basic alumina column by adding few drops of glacial acetic acid. The polymer was recovered by precipitation into MeOH (20 fold excess to polymer solution) and then by filtration. The polymer was dried *in vacuo* for 24 h at 25 °C. (Purity by SEC=88.9%). A small fraction of crude product was purified by preparative SEC for characterization. SEC ($M_n=2140$, PDI=1.04), Triple Detection SEC ($M_n=2780$, PDI=1.02). The polymer was further characterised by ¹H NMR and MALDI-ToF.

5.2.3.6 Synthesis of *c*-PSTY₂₅-Br **10a**

c-PSTY₂₅-OH, **9a** (1.6 g, 5.867×10^{-4} mol), TEA (1.63 mL, 11.73×10^{-3} mol) and 30.0 ml of dry THF were added under an argon blanket to a dry schlenk flask that has been flushed with argon. The reaction was then cooled on ice bath. To this stirred mixture, a solution of 2-bromopropionyl bromide (1.23 mL, 11.73×10^{-3} mol) in 10 mL of dry THF was added drop wise under argon via an air-tight syringe over 10 min. After stirring the reaction mixture for 48 h at room temperature, the crude polymer solution was added in 300 mL of acetone and filtered to remove salt precipitate. Solvent was removed by rotavap and precipitated into MeOH, filtered and washed three times with MeOH. A fraction of crude product was purified by preparative SEC for characterization. The polymer was dried for 24 h in high vacuum oven at 25 °C. SEC ($M_n=2350$, PDI=1.04). The polymer was further characterised by ¹H NMR and MALDI-ToF.

5.2.3.7 Synthesis of *c*-PSTY₂₅-N₃ **11a**

Polymer *c*-PSTY₂₅-Br **10a** (1.5 g, 0.5×10^{-3} mol) was dissolved in 10 mL of DMF in a reaction vessel equipped with magnetic stirrer. To this solution, NaN₃ (0.65 g, 1.0×10^{-3} mol) was added and the mixture stirred for 24 h at room temperature. The polymer solution was directly precipitated into MeOH/H₂O (95/5, v/v) (20 fold excess to polymer solution) from DMF, recovered by vacuum

filtration and washed exhaustively with MeOH. A fraction of the polymer was purified by preparative SEC and precipitated and filtered. The polymer was dried *in vacuo* for 24 h at 25 °C, SEC ($M_n = 2250$, PDI = 1.04) and Triple Detection SEC ($M_n = 2930$, PDI=1.02). The polymer was further characterised by ^1H NMR and MALDI-ToF.

5.2.3.8 Synthesis of *c*-PSTY₂₅-≡ **14a**

Polymer *c*-PSTY₂₅-N₃ **11a** (0.4 g, 0.133×10^{-3} mol), PMDETA (27.87×10^{-3} mL, 0.133×10^{-3} mol) and methyl 3,5-bis (propargyloxy) benzoate **12** (0.49 g, 1.99×10^{-3} mol) were dissolved in 3.0 mL toluene. CuBr (19.0×10^{-3} g, 1.33×10^{-4} mol) was added to a 10 mL schlenk flask equipped with magnetic stirrer and both of the reaction vessels were purged with argon for 20 min. The polymer solution was then transferred to CuBr flask by applying argon pressure using double tip needle. The reaction mixture was purged with argon for a further 2 min and the flask was placed in a temperature controlled oil bath at 25 °C for 1.5 h. The reaction was then diluted with THF (*ca.* 3 fold to the reaction mixture volume), and passed through activated basic alumina to remove the copper salts. The solution was concentrated by rotary evaporator and the polymer was recovered by precipitation into a large amount of MeOH (20 fold excess to polymer solution) and filtration. The polymer was purified by preparative SEC to remove excess linker as well as high MW impurities. After precipitation and filtration, the polymer was dried *in vacuo* for 24 h at 25 °C. SEC ($M_n = 2440$, PDI=1.04) and Triple Detection SEC ($M_n = 3170$, PDI=1.02). The polymer was further characterised by ^1H NMR and MALDI-ToF.

5.2.3.9 Synthesis of ≡(HO)-PSTY₅₈-Br **7b** by ATRP

Styrene (3.7 g, 35.53×10^{-3} mol), PMDETA (0.034 mL, 1.63×10^{-4} mol), CuBr₂/PMDETA (1.3×10^{-2} g, 0.32×10^{-4} mol) and initiator (0.1 g, 3.2×10^{-4} mol) were added to a 50 mL schlenk flask equipped with a magnetic stirrer and purged with argon for 40 min to remove oxygen. Cu(I)Br (0.023 g, 1.63×10^{-4} mol) was then carefully added to the solution under an argon blanket. The reaction mixture was further degassed for 5 min and then placed into a temperature controlled oil bath at 80 °C. After 4 h an aliquot was taken to check the conversion. The reaction was quenched by cooling to 0 °C in ice bath, exposed to air, and diluted with THF (*ca.* 3 fold to the reaction mixture volume). The copper salts were removed by passage through an activated basic alumina column. The solution was concentrated by rotary evaporation and the polymer was recovered by precipitation into large volume of MeOH (20 fold excess to polymer solution) and vacuum filtration two times. The polymer was dried *in high vacuo* overnight at 25 °C, SEC ($M_n = 6470$, PDI = 1.08). Final

conversion was calculated by gravimetry 53.1%. The polymer was further characterised by ^1H NMR and MALDI-ToF.

5.2.3.10 Synthesis of $\equiv(\text{HO})\text{-PSTY}_{58}\text{-N}_3$ **8b** by Azidation with NaN_3

Polymer **7b** (1.0 g, 1.6×10^{-4} mol) was dissolved in 10 mL of DMF in a reaction vessel equipped with a magnetic stirrer. To this solution NaN_3 (0.16 g, 2.4×10^{-3} mol) was added and the mixture stirred for 24 h at 25 °C. The polymer solution was directly precipitated into MeOH/ H_2O (95/5, v/v) (20 fold excess to polymer solution) from DMF, recovered by vacuum filtration and washed exhaustively with MeOH. The polymer was dried *in vacuo* for 24 h at 25 °C, SEC ($M_n = 6390$, PDI = 1.08). The polymer was further characterised by ^1H NMR and MALDI-ToF.

5.2.3.11 Synthesis of *c*- $\text{PSTY}_{58}\text{-OH}$, **9b**

A solution of polymer **8b** (0.75 g, 1.19×10^{-4} mol) in 37.5 ml of dry toluene and 1.24 mL of PMDETA (5.95×10^{-3} mol) in 37.5 mL of dry toluene in another flask were purged with argon for 45 min to remove oxygen. 0.854 g of CuBr (5.95×10^{-3} mol) was taken in a 100 mL of dry schlenk flask and maintained argon flow in the flask at the same time. PMDETA solution was transferred to CuBr flask by applying argon pressure using a double tip needle to prepare CuBr/PMDETA complex. After complex formation, polymer solution was added via syringe pump using a syringe that is pre-filled with argon. The feed rate of argon was set at 0.5 mL/min. After the addition of polymer solutions (75 min), the reaction mixture was further stirred for 3 h. At the end of this period (i.e., feed time plus an additional 3 h), toluene was evaporated by air-flow and the copper salts were removed by passage through activated basic alumina column by adding few drops of glacial acetic acid. The polymer was recovered by precipitation into MeOH (20 fold excess to polymer solution) and then by filtration. The polymer was dried *in vacuo* for 24 h at 25 °C. (Purity by LND (based on number distribution) =80.0%). A small fraction of crude product was purified by preparative SEC for characterization. SEC ($M_n=4690$, PDI=1.04), Triple Detection SEC ($M_n= 6220$, PDI=1.005). The polymer was further characterised by ^1H NMR and MALDI-ToF.

5.2.3.12 Synthesis of *c*- $\text{PSTY}_{58}\text{-Br}$, **10b**

c- $\text{PSTY}_{58}\text{-OH}$, **9b** (0.15 g, 2.4×10^{-5} mol), TEA (0.066 mL, 4.8×10^{-4} mol) and 2.0 ml of dry THF were added under an argon blanket to a dry schlenk flask that has been flushed with argon. The reaction was then cooled on ice bath. To this stirred mixture, a solution of 2-bromopropionyl bromide (0.05 mL, 4.8×10^{-4} mol) in 1 mL of dry THF was added drop wise under argon via an air-tight syringe over 2 min. After stirring the reaction mixture for 48 h at room temperature, the crude polymer solution was precipitated into MeOH, filtered and washed three times with MeOH. The polymer was dried for 24 h

in high vacuum oven at 25 °C. SEC ($M_n=4580$, PDI=1.04). The polymer was further characterised by ^1H NMR and MALDI-ToF.

5.2.3.13 Synthesis of *c*-PSTY₅₈-N₃ **11b**

Polymer *c*-PSTY₅₈-Br **10b** (0.134 g, 2.12×10^{-5} mol) was dissolved in 1.5 mL of DMF in a reaction vessel equipped with magnetic stirrer. To this solution, NaN₃ (0.028 g, 4.25×10^{-4} mol) was added and the mixture stirred for 24 h at room temperature. The polymer solution was directly precipitated into MeOH/H₂O (95/5, v/v) (20 fold excess to polymer solution) from DMF, recovered by vacuum filtration and washed exhaustively with MeOH. The polymer was dried *in vacuo* for 24 h at 25 °C, SEC ($M_n = 4750$, PDI = 1.04) and Triple Detection SEC ($M_n = 6420$, PDI=1.01). The polymer was further characterised by ^1H NMR and MALDI-ToF.

5.2.3.14 Synthesis of *c*-PSTY₅₈-≡, **14b**

Polymer *c*-PSTY₅₈-N₃ **11b** (0.1 g, 1.59×10^{-5} mol), PMDETA (3.32×10^{-3} mL, 1.59×10^{-5} mol) and methyl 3,5-bis(propargyloxy) benzoate **12** (0.039 g, 1.59×10^{-4} mol) were dissolved in toluene/DMSO (0.75 mL/0.05 mL) mixed solvent. CuBr (2.28×10^{-3} g, 1.59×10^{-5} mol) was added to a 10 mL schlenk tube equipped with magnetic stirrer and both of the reaction vessels were purged with argon for 25 min. The polymer solution was then transferred to CuBr flask by applying argon pressure using double tip needle. The reaction mixture was purged with argon for a further 2 min and the flask was placed in a temperature controlled oil bath at 25 °C for 1.5 h. The reaction was then diluted with THF (*ca.* 3 fold to the reaction mixture volume), and passed through activated basic alumina to remove the copper salts. The solution was concentrated by rotary evaporator and the polymer was recovered by precipitation into a large amount of MeOH (20 fold excess to polymer solution) and filtration. The polymer was purified by preparative SEC to remove excess linker as well as high MW impurities. After precipitation and filtration, the polymer was dried *in vacuo* for 24 h at 25 °C. SEC ($M_n=4930$, PDI=1.04) and Triple Detection SEC ($M_n=6520$, PDI=1.004). The polymer was further characterised by ^1H NMR and MALDI-ToF.

5.2.3.15 Synthesis of *c*-PSTY₅₈-(≡)₂, **15b**

Polymer *c*-PSTY₅₈-N₃, **11b** (0.09 g, 1.42×10^{-5} mol), PMDETA (2.98×10^{-3} mL, 1.42×10^{-5} mol) and 1,3,5-tris(prop-2-ynyloxy)benzene, **13** (0.034 g, 1.42×10^{-4} mol) were dissolved in 0.5 mL toluene. CuBr (2.0×10^{-3} g, 1.42×10^{-5} mol) was added to a 10 mL schlenk flask equipped with magnetic stirrer and both of the reaction vessels were purged with argon for 15 min. The polymer solution was then transferred to CuBr flask using double tipped needle by applying argon pressure. The

reaction mixture was purged with argon for a further 2 min and the flask was placed in a temperature controlled oil bath at 25 °C for 1.5 h. The reaction was then diluted with THF (*ca.* 3 fold to the reaction mixture volume), and passed through activated basic alumina to remove the copper salts. The solution was concentrated by rotary evaporator and the polymer was recovered by precipitation into a large amount of MeOH (20 fold excess to polymer solution) and filtration. The polymer was further purified by preparative SEC to remove residual linker as well as high MW impurities. After precipitation and filtration, the polymer was dried *in vacuo* for 24 h at 25 °C, SEC ($M_n=5020$, PDI=1.03) and Triple Detection SEC ($M_n=6500$, PDI=1.004). The polymer was further characterised by ^1H NMR and MALDI-ToF.

5.2.3.16 Synthesis of $\equiv(\text{HO})\text{-PSTY}_{84}\text{-Br}$ **7c** by ATRP

Styrene (4.23 g, 40.7×10^{-3} mol), PMDETA (0.026 mL, 1.2×10^{-4} mol), $\text{CuBr}_2/\text{PMDETA}$ (9.68×10^{-3} g, 2.4×10^{-5} mol) and initiator (0.075 g, 2.4×10^{-4} mol) were added to a 50 mL schlenk flask equipped with a magnetic stirrer and purged with argon for 40 min to remove oxygen. Cu(I)Br (0.018 g, 1.2×10^{-4} mol) was then carefully added to the solution under an argon blanket. The reaction mixture was further degassed for 5 min and then placed into a temperature controlled oil bath at 80 °C. After 4 h an aliquot was taken to check the conversion. The reaction was quenched by cooling to 0 °C in ice bath, exposed to air, and diluted with THF (*ca.* 3 fold to the reaction mixture volume). The copper salts were removed by passage through an activated basic alumina column. The solution was concentrated by rotary evaporation and the polymer was recovered by precipitation into large volume of MeOH (20 fold excess to polymer solution) and vacuum filtration two times. The polymer was dried *in high vacuo* overnight at 25 °C, SEC ($M_n = 9130$, PDI = 1.08). Final conversion was calculated by gravimetry 46.0%. The polymer was further characterised by ^1H NMR and MALDI-ToF.

5.2.3.17 Synthesis of $\equiv(\text{HO})\text{-PSTY}_{84}\text{-N}_3$ **8c** by Azidation with NaN_3

Polymer **7c** (1.0 g, 1.1×10^{-4} mol) was dissolved in 10 mL of DMF in a reaction vessel equipped with a magnetic stirrer. To this solution NaN_3 (0.14 g, 2.2×10^{-3} mol) was added and the mixture stirred for 24 h at 25 °C. The polymer solution was directly precipitated into MeOH/ H_2O (95/5, v/v) (20 fold excess to polymer solution) from DMF, recovered by vacuum filtration and washed exhaustively with MeOH. The polymer was dried *in vacuo* for 24 h at 25 °C, SEC ($M_n = 9020$, PDI = 1.08). The polymer was further characterised by ^1H NMR and MALDI-ToF.

5.2.3.18 Synthesis of *c*-PSTY₈₄-OH, **9c**

A solution of polymer **8c** (0.5 g, 5.5×10^{-5} mol) in 25 ml of dry toluene and 0.575 mL of PMDETA (2.75×10^{-3} mol) in 25 mL of dry toluene in another flask were purged with argon for 45 min to remove oxygen. 0.394 g of CuBr (2.75×10^{-3} mol) was taken in a 100 mL of dry schlenk flask and maintained argon flow in the flask at the same time. PMDETA solution was transferred to CuBr flask by applying argon pressure using a double tip needle to prepare CuBr/PMDETA complex. After complex formation, polymer solution was added via syringe pump using a syringe that is pre-filled with argon. The feed rate of argon was set at 0.5 mL/min. After the addition of polymer solutions (50 min), the reaction mixture was further stirred for 3 h. At the end of this period (i.e., feed time plus an additional 3 h), toluene was evaporated by air-flow and the copper salts were removed by passage through activated basic alumina column by adding few drops of glacial acetic acid. The polymer was recovered by precipitation into MeOH (20 fold excess to polymer solution) and then by filtration. The polymer was dried *in vacuo* for 24 h at 25 °C. (Purity by LND (based on number distribution) =74.5%). A small fraction of crude product was purified by preparative SEC for characterization. SEC ($M_n=6890$, PDI=1.04), Triple Detection SEC ($M_n=9190$, PDI=1.005). The polymer was further characterised by ¹H NMR and MALDI-ToF.

5.2.3.19 Synthesis of *c*-PSTY₈₄-Br, **10c**

c-PSTY₈₄-OH, **9c** (0.2 g, 2.2×10^{-5} mol), TEA (0.092 mL, 1.1×10^{-3} mol) and 3.0 ml of dry THF were added under an argon blanket to a dry schlenk flask that has been flushed with argon. The reaction was then cooled on ice bath. To this stirred mixture, a solution of 2-bromopropionyl bromide (0.069 mL, 1.1×10^{-3} mol) in 1 mL of dry THF was added drop wise under argon via an air-tight syringe over 2 min. After stirring the reaction mixture for 48 h at room temperature, the crude polymer solution was precipitated into MeOH, filtered and washed three times with MeOH. The polymer was dried for 24 h in high vacuum oven at 25 °C. SEC ($M_n=6670$, PDI=1.04). The polymer was further characterised by ¹H NMR and MALDI-ToF.

5.2.3.20 Synthesis of *c*-PSTY₈₄-N₃ **11c**

Polymer *c*-PSTY₈₄-Br **10c** (0.195 g, 2.12×10^{-5} mol) was dissolved in 2.0 mL of DMF in a reaction vessel equipped with magnetic stirrer. To this solution, NaN₃ (0.041 g, 6.4×10^{-4} mol) was added and the mixture stirred for 24 h at room temperature. The polymer solution was directly precipitated into MeOH/H₂O (95/5, v/v) (20 fold excess to polymer solution) from DMF, recovered by vacuum filtration and washed exhaustively with MeOH. The polymer was dried *in vacuo* for 24 h at 25 °C,

SEC ($M_n = 6880$, PDI = 1.04) and Triple Detection SEC ($M_n = 8900$, PDI=1.006). The polymer was further characterised by ^1H NMR and MALDI-ToF.

5.2.3.21 Synthesis of *c*-PSTY₈₄-≡, **14c**

Polymer *c*-PSTY₈₄-N₃ **11c** (0.12 g, 1.3×10^{-5} mol), PMDETA (2.72×10^{-3} mL, 1.3×10^{-5} mol) and methyl 3,5-bis (propargyloxy) benzoate **12** (0.031 g, 1.3×10^{-4} mol) were dissolved in toluene/DMSO (0.75 mL/0.05 mL) mixed solvent. CuBr (1.86×10^{-3} g, 1.3×10^{-5} mol) was added to a 10 mL schlenk tube equipped with magnetic stirrer and both of the reaction vessels were purged with argon for 25 min. The polymer solution was then transferred to CuBr flask by applying argon pressure using double tip needle. The reaction mixture was purged with argon for a further 2 min and the flask was placed in a temperature controlled oil bath at 25 °C for 1.5 h. The reaction was then diluted with THF (*ca.* 3 fold to the reaction mixture volume), and passed through activated basic alumina to remove the copper salts. The solution was concentrated by rotary evaporator and the polymer was recovered by precipitation into a large amount of MeOH (20 fold excess to polymer solution) and filtration. The polymer was purified by preparative SEC to remove excess linker as well as high MW impurities. After precipitation and filtration, the polymer was dried *in vacuo* for 24 h at 25 °C. SEC ($M_n = 7050$, PDI=1.04) and Triple Detection SEC ($M_n = 9040$, PDI=1.007). The polymer was further characterised by ^1H NMR and MALDI-ToF.

5.2.3.22 Synthesis of ≡(HO)-PSTY₁₆₃-Br **7d** by ATRP

Styrene (5.76 g, 55.3×10^{-3} mol), PMDETA (0.018 mL, 8.5×10^{-5} mol), CuBr₂/PMDETA (6.78×10^{-3} g, 2.4×10^{-5} mol) and initiator (0.075 g, 2.4×10^{-4} mol) were added to a 50 mL schlenk flask equipped with a magnetic stirrer and purged with argon for 40 min to remove oxygen. Cu(I)Br (0.018 g, 1.7×10^{-5} mol) was then carefully added to the solution under an argon blanket. The reaction mixture was further degassed for 5 min and then placed into a temperature controlled oil bath at 80 °C. After 4 h an aliquot was taken to check the conversion. The reaction was quenched by cooling to 0 °C in ice bath, exposed to air, and diluted with THF (*ca.* 3 fold to the reaction mixture volume). The copper salts were removed by passage through an activated basic alumina column. The solution was concentrated by rotary evaporation and the polymer was recovered by precipitation into large volume of MeOH (20 fold excess to polymer solution) and vacuum filtration two times. The polymer was dried *in high vacuo* overnight at 25 °C, SEC ($M_n = 17110$, PDI = 1.09). Final conversion was calculated by gravimetry 33.3%. The polymer was further characterised by ^1H NMR and MALDI-ToF.

5.2.3.23 Synthesis of $\equiv(\text{HO})\text{-PSTY}_{163}\text{-N}_3$ **8d** by Azidation with NaN_3

Polymer **7d** (1.0 g, 5.6×10^{-5} mol) was dissolved in 10 mL of DMF in a reaction vessel equipped with a magnetic stirrer. To this solution NaN_3 (0.11 g, 16.8×10^{-4} mol) was added and the mixture stirred for 24 h at 25 °C. The polymer solution was directly precipitated into MeOH/H₂O (95/5, v/v) (20 fold excess to polymer solution) from DMF, recovered by vacuum filtration and washed exhaustively with MeOH. The polymer was dried *in vacuo* for 24 h at 25 °C, SEC ($M_n = 17300$, PDI = 1.06). The polymer was further characterised by ¹H NMR and MALDI-ToF.

5.2.3.24 Synthesis of *c*-PSTY₁₆₃-OH, **9d**

A solution of polymer **8d** (0.1 g, 5.5×10^{-6} mol) in 10 ml of dry toluene and 0.116 mL of PMDETA (5.5×10^{-4} mol) in 25 mL of dry toluene in another flask were purged with argon for 45 min to remove oxygen. 0.08 g of CuBr (2.75×10^{-3} mol) was taken in a 50 mL of dry schlenk flask and maintained argon flow in the flask at the same time. PMDETA solution was transferred to CuBr flask by applying argon pressure using a double tip needle to prepare CuBr/PMDETA complex. After complex formation, polymer solution was added via syringe pump using a syringe that is pre-filled with argon. The feed rate of argon was set at 0.2 mL/min. After the addition of polymer solutions (50 min), the reaction mixture was further stirred for 3 h. At the end of this period (i.e., feed time plus an additional 3 h), toluene was evaporated by air-flow and the copper salts were removed by passage through activated basic alumina column by adding few drops of glacial acetic acid. The polymer was recovered by precipitation into MeOH (20 fold excess to polymer solution) and then by filtration. The polymer was dried *in vacuo* for 24 h at 25 °C. (Purity by LND (based on number distribution) = 73.4%). A small fraction of crude product was purified by preparative SEC for characterization. SEC ($M_n = 13430$, PDI = 1.04), Triple Detection SEC ($M_n = 18330$, PDI = 1.003). The polymer was further characterised by ¹H NMR and MALDI-ToF.

The detail synthesis and characterization of multi-functional cyclic polymers such as *c*-PSTY-(N₃)₂, **23**, *c*-PSTY-(\equiv)₄, **24** and *c*-PSTY-(N₃)₃, **30** were explained in chapter 3.

5.2.3.25 Synthesis of Complex Topologies

Synthesis of spiro dicyclic, (*c*-PSTY₈₄)₂ **31**

Polymer *c*-PSTY₈₄-N₃ **11c** (2.97×10^{-2} g, 3.2×10^{-6} mol), polymer *c*-PSTY₈₄- \equiv **14c** (3.0×10^{-2} g, 3.2×10^{-6} mol) and PMDETA (6.7×10^{-4} mL, 3.2×10^{-6} mol) were dissolved in 0.5 mL of toluene. CuBr (4.6×10^{-4} g, 3.2×10^{-6} mol) was added to a 10 mL schlenk flask equipped with magnetic stirrer and both of the reaction vessels were purged with argon for 20 min. The polymer solution was then transferred to CuBr flask using double tip needle by applying argon pressure. The reaction mixture

was purged with argon for a further 2 min and the flask was placed in a temperature controlled oil bath at 25 °C for 1.5 h. The reaction was then diluted with THF (*ca.* 3 fold to the reaction mixture volume), and passed through activated basic alumina to remove the copper salts. The solution was concentrated by rotary evaporator and the polymer was recovered by precipitation into a large amount of MeOH (20 fold excess to polymer solution) and filtration. The polymer was then purified by preparatory SEC to remove undesired high molecular weight polymers and residual reactant polymers. The polymer was dried *in vacuo* for 24 h at 25 °C and characterised. SEC ($M_n=13320$, PDI=1.04), Triple Detection SEC ($M_n=19140$, PDI=1.003). The polymer was further characterised by ^1H NMR and MALDI-ToF.

Synthesis of star tricyclic, (c-PSTY₅₈)₃, 32

Polymer c-PSTY₅₈-N₃ **11b** (4.9×10^{-2} g, 7.68×10^{-6} mol), polymer c-PSTY₅₈-(≡)₂, **15b** (2.5×10^{-2} g, 3.8×10^{-6} mol) and PMDETA (1.6×10^{-3} mL, 7.68×10^{-6} mol) were dissolved in 0.5 mL of toluene. CuBr (1.12×10^{-3} g, 7.68×10^{-6} mol) was added to a 10 mL schlenk flask equipped with magnetic stirrer and both of the reaction vessels were purged with argon for 20 min. The polymer solution was then transferred to CuBr flask using double tip needle by applying argon pressure. The reaction mixture was purged with argon for a further 2 min and the flask was placed in a temperature controlled oil bath at 25 °C for 1.5 h. The reaction was then diluted with THF (*ca.* 3 fold to the reaction mixture volume), and passed through activated basic alumina to remove the copper salts. The solution was concentrated by rotary evaporator and the polymer was recovered by precipitation into a large amount of MeOH (20 fold excess to polymer solution) and filtration. The polymer was then purified by preparatory SEC to remove undesired high molecular weight polymers and residual reactant polymers. The polymer was dried *in vacuo* for 24 h at 25 °C and characterised. SEC ($M_n=12850$, PDI=1.04), Triple Detection SEC ($M_n=19700$, PDI=1.017). The polymer was further characterised by ^1H NMR and MALDI-ToF.

Synthesis of spiro tricyclic, (c-PSTY)₃, 33

Polymer c-PSTY₅₀-(N₃)₂ **23** (2.0×10^{-2} g, 3.2×10^{-6} mol), polymer c-PSTY₅₈-≡ **14b** (4.4×10^{-2} g, 6.77×10^{-6} mol) and PMDETA (1.35×10^{-3} mL, 3.2×10^{-6} mol) were dissolved in 0.5 mL of toluene. CuBr (9.25×10^{-4} g, 3.2×10^{-6} mol) was added to a 10 mL schlenk flask equipped with magnetic stirrer and both of the reaction vessels were purged with argon for 25 min. The polymer solution was then transferred to CuBr flask using double tip needle by applying argon pressure. The reaction mixture was purged with argon for a further 2 min and the flask was placed in a temperature controlled oil bath at 25 °C for 1.5 h. The reaction was then diluted with THF (*ca.* 3 fold to the reaction mixture volume), and passed through activated basic alumina to remove the copper salts.

The solution was concentrated by rotary evaporator and the polymer was recovered by precipitation into a large amount of MeOH (20 fold excess to polymer solution) and filtration. The polymer was then purified by preparatory SEC to remove undesired high molecular weight polymers and residual reactant polymers. The polymer was dried *in vacuo* for 24 h at 25 °C and characterised. SEC ($M_n=14050$, PDI=1.06), Triple Detection SEC ($M_n=19080$, PDI=1.001). The polymer was further characterised by ^1H NMR and MALDI-ToF.

Synthesis of G1 Dendrimer Pentacyclic (c-PSTY)₅, 34

Polymer c-PSTY₅₀-(≡)₄ **24** (2.5×10^{-2} g, 3.8×10^{-6} mol), polymer c-PSTY₂₅-N₃, **11a** (4.8×10^{-2} mg, 1.6×10^{-5} mol) and PMDETA (3.16×10^{-3} mL, 1.5×10^{-5} mol) were dissolved in 0.5 mL of toluene. CuBr (2.2 mg, 0.015 mmol) was added to a 10 mL schlenk flask equipped with magnetic stirrer and both of the reaction vessels were purged with argon for 15 min. The polymer solution was then transferred to CuBr flask using double tip needle by applying argon pressure. The reaction mixture was purged with argon for a further 2 min and the flask was placed in a temperature controlled oil bath at 25 °C for 1.5 h. The reaction was then diluted with THF (*ca.* 3 fold to the reaction mixture volume), and passed through activated basic alumina to remove the copper salts. The solution was concentrated by rotary evaporator and the polymer was recovered by precipitation into a large amount of MeOH (20 fold excess to polymer solution) and filtration. The polymer was then further purified by preparatory SEC to remove undesired high molecular weight polymers and residual reactant polymers. The polymer was dried *in vacuo* for 24 h at 25 °C and characterised. SEC ($M_n=12890$, PDI=1.04), Triple Detection SEC ($M_n=18900$, PDI=1.005). The polymer was further characterised by ^1H NMR and MALDI-ToF.

Synthesis of G1 Star Tetracyclic (c-PSTY)₄, 35

Polymer c-PSTY₇₅-(N₃)₃ **30** (3.0×10^{-2} g, 3.2×10^{-6} mol), polymer c-PSTY₂₅-≡ **14a** (3.2×10^{-2} g, 1.0×10^{-5} mol) and PMDETA (2.0×10^{-3} mL, 9.5×10^{-6} mol) were dissolved in 0.6 mL of toluene. CuBr (1.4×10^{-3} g, 9.5×10^{-6} mol) was added to a 10 mL schlenk flask equipped with magnetic stirrer and both of the reaction vessels were purged with argon for 15 min. The polymer solution was then transferred to CuBr flask using double tipped needle by applying argon pressure. The reaction mixture was purged with argon for a further 2 min and the flask was placed in a temperature controlled oil bath at 25 °C for 1.5 h. The reaction was then diluted with THF (*ca.* 3 fold to the reaction mixture volume), and passed through activated basic alumina to remove the copper salts. The solution was concentrated by rotary evaporator and the polymer was recovered by precipitation into a large amount of MeOH (20 fold excess to polymer solution) and filtration. The polymer was

then further purified by preparatory SEC to remove undesired high molecular weight polymers and residual reactant polymers. The polymer was dried *in vacuo* for 24 h at 25 °C and characterised. SEC ($M_n=13920$, PDI=1.05), Triple Detection SEC ($M_n=19680$, PDI=1.002). The polymer was further characterised by ^1H NMR and MALDI-ToF.

5.3 Results and Discussion

Synthesis of c-PSTY_n-OH by CuAAC

c-PSTY_n-OH, **9a-d**, were synthesised according to our previously described literature procedure.³² Highly functional linear polymer precursors $\equiv(\text{OH})\text{-PSTY}_n\text{-Br}$ were synthesised by ATRP using alkyne-functional initiator, **1**, with number-average molecular weights (M_n) of 2890 (**7a**), 6470 (**7b**), 9130 (**7c**) and 17300 (**7d**), and PDI values 1.11, 1.08, 1.08 and 1.06, respectively (see Table **D1**, Appendix D). The Br chain-end functionality of **7a-d** were determined, by using the ^1H NMR integration, to be 97, 95, 96 and 95%, respectively. The LND simulation³³ based on weight distribution ($w(M)$) gave ~12 % of double molecular weight products. The formation of double molecular weight products can occur by radical termination or alkyne-alkyne coupling reaction during or after polymerization. The Br chain-ends of polymers **7a-d** were converted to azide groups quantitatively, and the linear polymers then cyclised using CuAAC³⁴ reaction. The general synthetic route to produce different functional linear and cyclic polymers and their complex architectures is shown in scheme 5.1.

An effective and rapid cyclization procedure was followed to prepare monocyclic polymer with high yield and purity. The linear polymer solution in toluene, was fed into a toluene solution of an excess (50 equiv. to polymer conc.) of Cu(I)Br and PMDETA at a feed rate of 1.24 mL min⁻¹ for **7a** 0.5 mL min⁻¹ for **7b-c** and 0.2 mL min⁻¹ for **7d** at 25 °C respectively and then stirred for further 3 h, following a procedure shown to be highly effective in producing monocyclic polymer. The reason for using the [Cu(PMDETA)Br] complex to activate the CuAAC reaction in toluene is that the complex forms a neutral, distorted square planar structure and is more soluble and thus more reactive in toluene than other ionised and partially soluble copper complexes.³⁵ The monocyclic polymers **8a-d** under these feed conditions gave conversions of 84.0, 84.8, 81.1 and 79.8% respectively, as determined from SEC distributions. SEC traces for cyclization of **8a-d** to produce **9a-d** are shown in Figure 5.1.

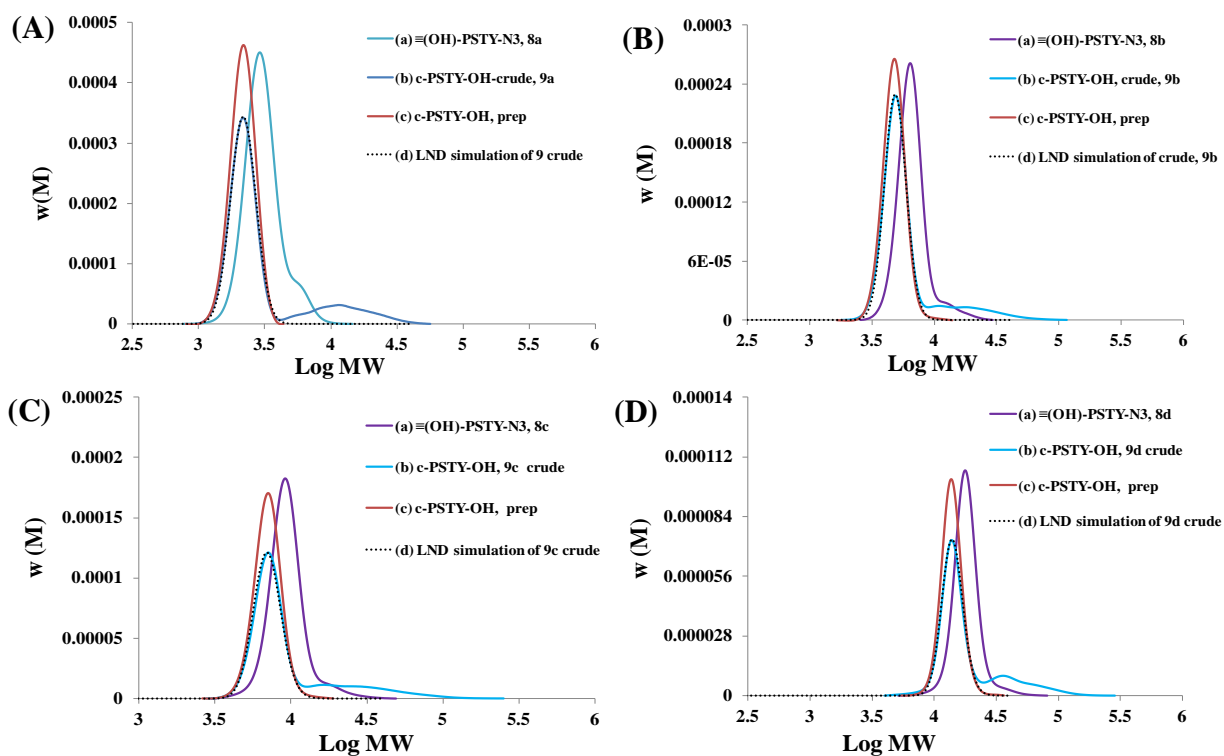


Figure 5.1. SEC chromatograms for cyclization of (A) (a) $\equiv(\text{OH})\text{-PSTY}_{25}\text{-N}_3$ **8a** (b) $\text{c-PSTY}_{25}\text{-OH}$ crude, **9a** (c) $\text{c-PSTY}_{25}\text{-OH}$ purified by prep and (d) LND simulation of **9a** crude with hydrodynamic volume change of 0.75; (B) (a) $\equiv(\text{OH})\text{-PSTY}_{58}\text{-N}_3$ **8b** (b) $\text{c-PSTY}_{58}\text{-OH}$ crude, **9b** (c) $\text{c-PSTY}_{58}\text{-OH}$ purified by prep and (d) LND simulation of **9b** crude with hydrodynamic volume change of 0.75; (C) (a) $\equiv(\text{OH})\text{-PSTY}_{84}\text{-N}_3$ **8c** (b) $\text{c-PSTY}_{84}\text{-OH}$ crude, **9c** (c) $\text{c-PSTY}_{84}\text{-OH}$ purified by prep and (d) LND simulation of **9c** crude with hydrodynamic volume change of 0.76; (D) (a) $\equiv(\text{OH})\text{-PSTY}_{163}\text{-N}_3$ **8d** (b) $\text{c-PSTY}_{163}\text{-OH}$ crude, **9d** (c) $\text{c-PSTY}_{163}\text{-OH}$ purified by prep and (d) LND simulation of **9d** crude with hydrodynamic volume change of 0.765; SEC analysis based on polystyrene calibration curve.

The resultant crude cyclic polymers were purified by prep SEC to remove any unreacted starting polymers and high-molecular-weight by-products formed through either alkyne-alkyne coupling or multi-block formation from CuAAC reactions. The M_n s of **9a-d** after prep were 2140 (PDI = 1.04), 4690 (PDI=1.04), 6890 (PDI=1.04) and 13430 (PDI=1.04) as determined by RI detection alone and was in accord with a reduced hydrodynamic volume of more compact cyclic topology 0.75, 0.75, 0.76 and 0.765 respectively. Analysis of the purified cyclic polymers by triple-detection SEC (to obtain an absolute MWD independent of topology) gave $M_n = 2780$ (PDI = 1.016) for **9a**, $M_n = 6220$ (PDI=1.005) for **9b**, $M_n = 9190$ (PDI=1.005) for **9c** and $M_n = 18330$ (PDI=1.004) for **9d** were almost identical to the starting linear polymers. For detailed characterization of **9a-d** using ^1H NMR and MALDI-ToF, see appendix D.

Functionalization of 9a-d

The free OH group on the cyclic polymers, were then further functionalised using 2-bromopropionyl bromide to obtain c-PSTY-Br, **10a-c** and subsequent azidation using NaN_3 gave c-PSTY- N_3 **11a-c** in near quantitative yields, as confirmed by ^1H NMR and MALDI analysis shown in appendix D. These polymers were further functionalised to mono-alkyne moieties (**14a-c**) using excess methyl 3,5-bis(propargyloxy) benzoate, **12** and di-alkyne moieties (**15b**) using excess 1, 3, 5-tris(prop-2-ynyloxy)benzene, **13** as small linkers. The mono and di-alkyne functionalised polymers were characterised by SEC, NMR and MALDI, see appendix D. The detailed synthesis and characterization of multi-functional cyclic polymers **23**, **24** and **30** were explained in the chapter 2.

Coupling reaction for complex topologies

The alkyne and azide functional polymers were utilised to form a variety of complex architectures using CuAAC click coupling reaction (see Scheme 5.1). c-PSTY₈₄-≡, **14c** was coupled with 1.0 equivalent of c-PSTY₈₄-N₃, **11c** and c-PSTY₅₈-≡₂, **15b** was coupled with 2.0 equivalents of c-PSTY₅₈-N₃, **11b** to produce spiro di-cyclic, **31** and star tricyclic, **32** by CuAAC reaction in 1.5 h at 25 °C gave 92.2% and 91.4 % product purity respectively as determined from the LND simulation based on weight distribution (Figure 5.2 (A)). The click efficiency of formation the coupled products were also calculated as 92.2 and 91.4% from the ratio of purity determined by LND to that of the maximum theoretical purity expected from the stoichiometric ratios of the reactants. The MW data and click efficiency are summarised in the Table D1 in appendix D. Preparative SEC gave essentially pure **31** and **32** in which most of the higher molecular weight polymers were removed. When the purified polymers were subsequently injected through the triple detection SEC (to obtain an absolute MWD independent of topology), it gave an essentially identical MWD to that of the sum of M_p of starting reactants and with narrow polydispersity index. These results demonstrate the isolation of a well-defined and essentially pure structure. The ^1H NMR of purified **31** and **32** (Figure D37 and D38 in appendix D) showed a nearly quantitative loss of CH_2 protons adjacent to alkyne moiety (denoted as k, $\delta=4.6-4.7$ ppm) from **14c** and **15b** and appearance of CH proton near triazole moieties (denoted as i, $\delta=5.0-5.2$ ppm) as determined by integration suggested quantitative click reaction without any unreacted reactants left. The purified product was further characterised by MALDI ToF mass spectroscopy gave MWD that could only result from the coupling of their starting polymers together (see Figure D42 and D43 in appendix D). The calculated $[\text{M}+\text{Ag}^+]$ values (18061.16 for **31** and 18215.25 for **32**) in expanded spectra were nearly identical with the experimental values (18061.86 for **31** and 18217.79 for **32**), suggesting that after purification there was little or no reactants species left.

Similarly, the CuAAC of **3a** with **4a** produced **15** with 92.9 % of product purity and coupling efficiency and coupling of **11a** with **10a** produced **17** with 89.5 % of product purity and coupling efficiency. **15** and **17** were also further characterised by NMR and MALDI as shown in appendix D.

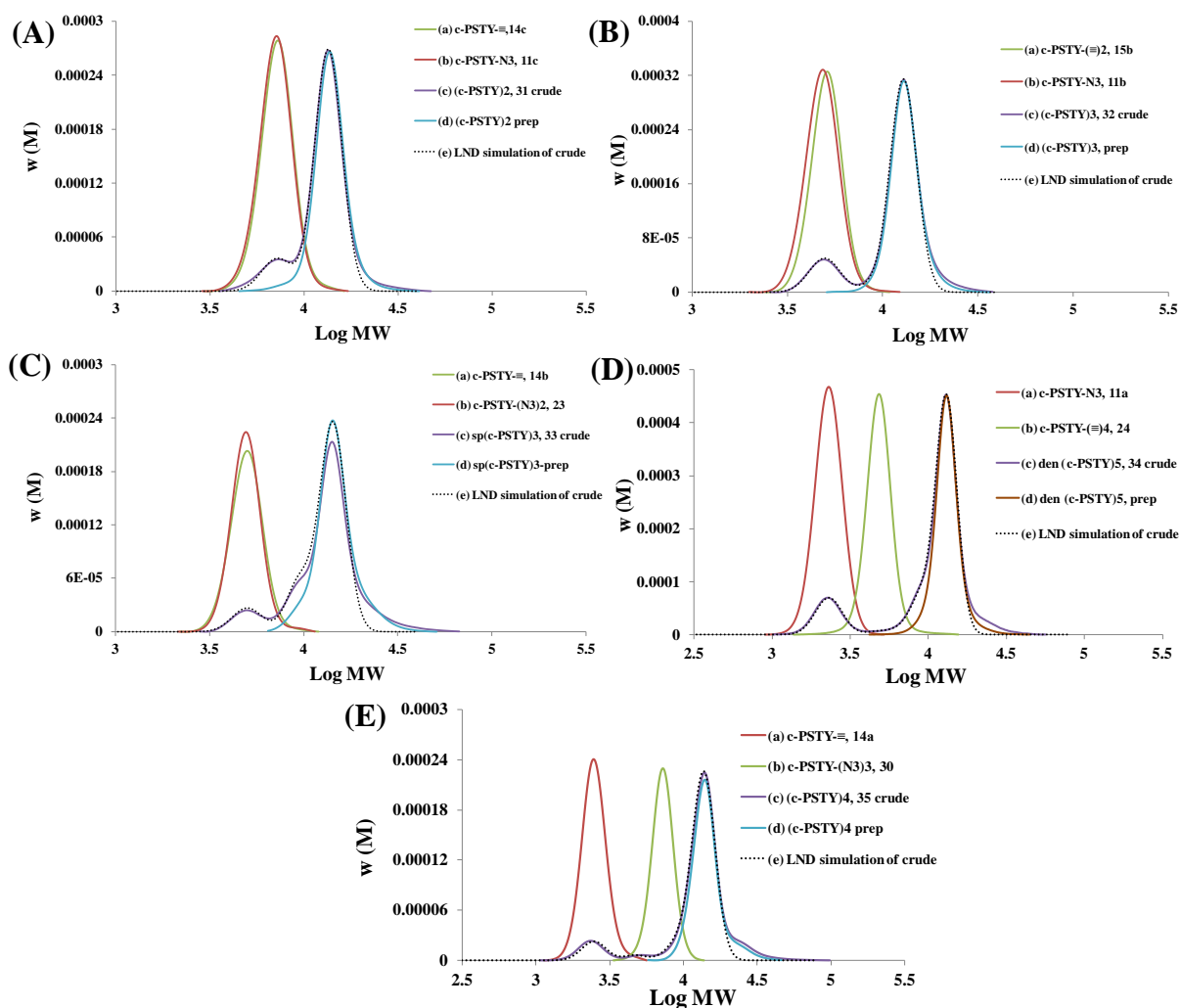


Figure 5.2: SEC of molecular weight distributions (MWDs) for the synthesis of (A) (c-PSTY)₂ **31** by CuAAC of (a) c-PSTY₈₄-≡, **14c**, and (b) c-PSTY₈₄-N₃, **11c**; (c) (c-PSTY)₂ **31**, crude, (d) (c-PSTY)₂ prepped and (e) LND simulation of crude, (B) (c-PSTY)₃, **32** by CuAAC of (a) c-PSTY₅₈-(≡)₂, **15b** and (b) c-PSTY₅₈-N₃, **11b**; (c) star (c-PSTY)₃, **32**, crude, (d) (c-PSTY)₃, prep and (e) LND simulation of crude, (C) spiro (c-PSTY)₃, **33** by CuAAC of (a) c-PSTY₅₈-≡, **14b** and (b) c-PSTY₅₀-(N₃)₂, **23**; (c) spiro (c-PSTY)₃, **33** crude, (d) spiro (c-PSTY)₃, prep and (e) LND simulation of crude, (D) den (c-PSTY)₅, **34** by CuAAC of (a) c-PSTY₅₀-(≡)₄, **24** and (b) c-PSTY₂₅-N₃, **11a**; (c) den (c-PSTY)₅, **34** crude, (d) den (c-PSTY)₅, prep and (e) LND simulation of crude and (D) G1 star (c-PSTY)₄, **35** by CuAAC of (a) c-PSTY₇₅-(N₃)₃, **30** and (b) c-PSTY₂₅-≡, **14a**; (c) G1 star (c-PSTY)₄, **35** crude, (d) G1-star (c-PSTY)₄, prep and (e) LND simulation of crude. SEC analysis based on polystyrene calibration curve. Simulation was achieved by adding M_ps of reactants (RI SEC) to fit with the crude products (RI SEC).

The topologies **33** and **35** were produced by coupling of c-PSTY₅₀-(N₃)₂, **23** and c-PSTY₇₅-(N₃)₃, **30** with 2.1 equivalents of c-PSTY₅₈-≡, **14b** and 3.15 equivalents of c-PSTY₂₅-≡, **14a** respectively. Two and three cyclic polymers attached in two and three distinct positions of same cyclic formed spiro tricyclic, **33** and G1-star like tetracyclic, **35** topologies. The product purity of **33** and **35** were calculated by LND as 83.8 and 70.5 % for crude and 91.2 and 84.1% after prep purification respectively. The changes in hydrodynamic volume by RI to triple detection SEC were observed as 0.74 and 0.71 for **33** and **35** respectively. The purified polymers were further characterised by ¹H NMR and MALDI as shown in appendix D.

G1 dendrimer pentacyclic topologies **34** was synthesised by coupling of c-PSTY₅₀-(≡)₄, **24** with 4.2 equivalents of c-PSTY₂₅-N₃, **11a** by CuAAC in 1.5 h gave 77.8% product purity. Preparative SEC allowed isolation of remarkably high purity (97%) product. The change in hydrodynamic volume by RI to triple detection SEC was 0.677. The peak MW (M_p) value of **34** from triple detection SEC was nearly identical (19400) to the sum of the M_ps (18860) of starting reactants **11a** and **24**. The purified **32** also showed low PDI values in both RI (1.04) and triple detection (1.005), strongly suggested the formation of the desired structure with high purity. The NMR analysis showed a quantitative loss of alkyne proton (denoted as l, δ=2.47 ppm), methylene protons (denoted as k, δ=4.6 ppm) near alkyne of **24** and methene proton (denoted as i, δ=3.9 ppm) near azides of **11a** (see appendix D). The methylene proton (denoted as j, δ=5.1 ppm) were suppressed for steric compactness of three triazole rings around a benzene ring. The product was further characterised by MALDI-ToF as shown in appendix D.

Effect of knots on glass transition temperature








The differential scanning calorimetry (DSC) was used to investigate the effect of knots on the glass transition temperature for polymers **8d**, **9d** and **31-35** as shown in Table 5.1. The MWs for all the topologies were close to 18 K to avoid any effects of molecular weight on T_g. It was previously shown that above a certain MW the T_g plateaus and becomes independent of the molecular weight.³⁶ In our system, we use covalent linkages to form a knot, making such knots into an irreversible. Therefore, it may be expected that the T_g for this series of polymers was not only affected by the number of knots but also the type and location of the knots.

Compared to the linear PSTY, **8d**, the cyclic PSTY, **9d**, has a higher T_g of 3.4 °C due to the absence of chain-ends. The introduction of one knot (i.e. structure **31** with two sub-cyclics) produced only a slight increase in T_g from 103.2 to 103.4 °C. One knot with three sub-cyclics (structure **32**) led to an increase in the T_g to 106.0 °C. Structure **32** has the most compact structure (i.e. ΔHDV = 0.65) in dilute solute for all the topologies made, suggesting that the higher T_g is a function of the decrease in free volume. The inclusion of two knots equally spaced and with three sub-cyclics (structure **33**)

gave a T_g of 104.4 °C, which was slightly greater than the T_g of **31** but lower than that for **32**. Increasing the number of sub-cyclics to five with just two knots (structure **34**) gave the highest T_g of 108.2 °C with a moderate decrease in Δ HDV of 0.71 compared to all other compounds. Structure **35**, with three knots and four sub-cyclics had a T_g of 104.5 °C, which was lower than **34** and similar to **33**. In addition, there seems to be no correlation between the values of T_g and the change in hydrodynamic volume.

Taken together, the data suggests that configurationally entropy instead of free volume effects play the dominant role in influencing the T_g . The core (or middle sub-cyclic) in dendrimer **34** has quite a restricted mobility, this together with the steric restriction of the outer sub-cyclics results in a lower entropy and thus higher T_g . In the case of **35**, the steric restriction is removed for the outer sub-cyclics even though the central sub-cyclic is considerably restricted.

Table 5.1: Molecular weight data and T_g results for the products (**8d**, **9d** and **31-35**).

No	Polymer code	Graphical Structures	RI detection			Triple detection			Δ HDV ^a	T_g (°C)
			M_n	M_p	PDI	M_n	M_p	PDI		
8d	\equiv (OH)-PSTY-N ₃		17300	17970	1.06	18300	18660	1.004	1	99.8
9d	c-PSTY-OH		13430	13760	1.04	18330	18580	1.003	0.78	103.2
31	(c-PSTY) ₂		13320	13590	1.04	19140	19440	1.003	0.72	103.4
32	st-(c-PSTY) ₃		12850	12940	1.04	19700	20400	1.017	0.65	106.0
33	sp-(cPSTY) ₃		14050	14280	1.06	19080	19330	1.001	0.74	104.4
34	G1-den-(c-PSTY) ₅		12890	13130	1.04	18900	18400	1.005	0.71	108.2
35	G1-st-(c-PSTY) ₄		13920	13980	1.05	19680	19800	1.002	0.74	104.5

^aThe change in hydrodynamic volume Δ HDV was calculated from $M_{n,RI}/M_{n,Theory}$.

5.4 Conclusion

A range of cyclic knot topologies with precisely controlled linkage among cyclic units were synthesised by combining 'living' radical polymerization and the highly efficient CuAAC 'click' reaction. The topologies that were synthesised included spiro-type di and tri-cyclic, star tricyclic, G1 dendrimer pentacyclic and star tetracyclic. Preparative SEC was used to purify the final products from unreacted reactants and high molecular weight impurities. The DSC was used to measure the glass transition temperatures to investigate the effect of linkage, i.e knots on their glass transition. Generally, we found that the more subcycles on one knot, the higher T_g of the structures. In this library of polymer knots, the knots number (i.e. 1, 2 and 3 in these cases) did not affect the

T_g dramatically if there were only two subcycles tethered on one knot (i.e. structure **31**, **33** and **35**). As such, structure **32** gave T_g as 106.0 °C and **35** as 108.2 °C which is a remarkable change (i.e. ~6-9 °C increase) comparing to their linear precursor **8d** or even monocyclic **9d**. These results suggested that with the same chemical composition and molecular weight, the T_g of the polymers is significantly affected by their topologies.

5.5 References

- (1) McLeish, T. *Nat Mater* **2008**, *7*, 933-935.
- (2) Whittaker, M. R.; Goh, Y.-K.; Gemici, H.; Legge, T. M.; Perrier, S.; Monteiro, M. J. *Macromolecules* **2006**, *39*, 9028-9034.
- (3) Peng, Y.; Liu, H.; Zhang, X.; Liu, S.; Li, Y. *Macromolecules* **2009**, *42*, 6457-6462.
- (4) Misaka, H.; Kakuchi, R.; Zhang, C.; Sakai, R.; Satoh, T.; Kakuchi, T. *Macromolecules* **2009**, *42*, 5091-5096.
- (5) Laurent, B. A.; Grayson, S. M. *Journal of the American Chemical Society* **2006**, *128*, 4238-4239.
- (6) Ge, Z.; Zhou, Y.; Xu, J.; Liu, H.; Chen, D.; Liu, S. *Journal of the American Chemical Society* **2009**, *131*, 1628-1629.
- (7) O'Bryan, G.; Ningnuek, N.; Braslau, R. *Polymer* **2008**, *49*, 5241-5248.
- (8) Hoskins, J. N.; Grayson, S. M. *Macromolecules* **2009**, *42*, 6406-6413.
- (9) Qiu, X.-P.; Tanaka, F.; Winnik, F. M. *Macromolecules* **2007**, *40*, 7069-7071.
- (10) Eugene, D. M.; Grayson, S. M. *Macromolecules* **2008**, *41*, 5082-5084.
- (11) Bielawski, C. W.; Benitez, D.; Grubbs, R. H. *Science* **2002**, *297*, 2041-2044.
- (12) Boydston, A. J.; Xia, Y.; Kornfield, J. A.; Gorodetskaya, I. A.; Grubbs, R. H. *Journal of the American Chemical Society* **2008**, *130*, 12775-12782.
- (13) Kudo, H.; Sato, M.; Wakai, R.; Iwamoto, T.; Nishikubo, T. *Macromolecules* **2008**, *41*, 521-523.
- (14) Culkin, D. A.; Jeong, W.; Csihony, S.; Gomez, E. D.; Balsara, N. P.; Hedrick, J. L.; Waymouth, R. M. *Angewandte Chemie International Edition* **2007**, *46*, 2627-2630.
- (15) Jeong, W.; Hedrick, J. L.; Waymouth, R. M. *Journal of the American Chemical Society* **2007**, *129*, 8414-8415.
- (16) Herbert, D. E.; Gilroy, J. B.; Chan, W. Y.; Chabanne, L.; Staubitz, A.; Lough, A. J.; Manners, I. *Journal of the American Chemical Society* **2009**, *131*, 14958-14968.
- (17) Zhang, F.; Götz, G.; Winkler, H. D. F.; Schalley, C. A.; Bäuerle, P. *Angewandte Chemie International Edition* **2009**, *48*, 6632-6635.

-
- (18) Oike, H.; Imaizumi, H.; Mouri, T.; Yoshioka, Y.; Uchibori, A.; Tezuka, Y. *Journal of the American Chemical Society* **2000**, *122*, 9592-9599.
- (19) Oike, H.; Hamada, M.; Eguchi, S.; Danda, Y.; Tezuka, Y. *Macromolecules* **2001**, *34*, 2776-2782.
- (20) Tezuka, Y.; Mori, K.; Oike, H. *Macromolecules* **2002**, *35*, 5707-5711.
- (21) Tezuka, Y.; Fujiyama, K. *Journal of the American Chemical Society* **2005**, *127*, 6266-6270.
- (22) Tezuka, Y.; Takahashi, N.; Satoh, T.; Adachi, K. *Macromolecules* **2007**, *40*, 7910-7918.
- (23) Sugai, N.; Heguri, H.; Ohta, K.; Meng, Q.; Yamamoto, T.; Tezuka, Y. *Journal of the American Chemical Society* **2010**, *132*, 14790-14802.
- (24) Igari, M.; Heguri, H.; Yamamoto, T.; Tezuka, Y. *Macromolecules* **2013**, *46*, 7303-7315.
- (25) Frisch, H. L.; Wasserman, E. *Journal of the American Chemical Society* **1961**, *83*, 3789-3795.
- (26) Alberts, B. *Molecular biology of the cell*, 4th ed. ed.; Garland Science: New York, 2002.
- (27) Shaw, S.; Wang, J. *Science* **1993**, *260*, 533-536.
- (28) Kamitori, S. *Journal of the American Chemical Society* **1996**, *118*, 8945-8946.
- (29) Sumners, D. W.; Whittington, S. G. *Journal of Physics A: Mathematical and General* **1988**, *21*, 1689.
- (30) Cai, H.; Jiang, G.; Shen, Z.; Fan, X. *Macromolecules* **2012**, *45*, 6176-6184.
- (31) Li, Y.; Mullen, K. M.; Claridge, T. D. W.; Costa, P. J.; Felix, V.; Beer, P. D. *Chemical Communications* **2009**, 7134-7136.
- (32) Jia, Z.; Lonsdale, D. E.; Kulis, J.; Monteiro, M. J. *ACS Macro Letters* **2012**, *1*, 780-783.
- (33) Cabaniss, S. E.; Zhou, Q.; Maurice, P. A.; Chin, Y.-P.; Aiken, G. R. *Environmental Science & Technology* **2000**, *34*, 1103-1109.
- (34) Kolb, H. C.; Finn, M. G.; Sharpless, K. B. *Angewandte Chemie International Edition* **2001**, *40*, 2004-2021.
- (35) Bell, C. A.; Jia, Z.; Kulis, J.; Monteiro, M. J. *Macromolecules* **2011**, *44*, 4814-4827.
- (36) Gan, Y.; Dong, D.; Hogen-Esch, T. E. *Macromolecules* **1995**, *28*, 383-385.

Chapter 6

Summary

The objective of this thesis was to synthesise complex polymer topologies by combining LRP and the CuAAC reaction. Although monocyclic polymer was efficiently synthesised by RAFT and CuAAC, an unforeseen degradation profile was observed. To overcome the unexpected degradation, we combined ATRP and CuAAC cyclization to synthesise a range of different architectures of cyclic polymers. Furthermore, a new methodology was developed to synthesise multifunctional cyclic polymers by combining ATRP and modular 'click' approach followed by CuAAC cyclization reaction. Linear polymer precursors were synthesised by the CuAAC coupling of azide from one polymer and alkyne from another. The reaction occurred in the presence of a bromine end-group, which was not affected by the Cu(I) catalyst due to the modulation of Cu(I) activity primarily towards the 'click' reaction over radical formation. Mono, di and tri-functional cyclic polymers were successfully synthesised, which upon post modification gave different and equally spaced functionalities in the precise location. These functional polymers allowed the synthesis of a variety of highly complex polymer topologies.

6.1 Cyclic polystyrene topologies via RAFT and CuAAC

The initial thesis aim was to develop a novel method to synthesise complex polymer topologies from cyclic made by combining RAFT and CuAAC reaction. The linear precursor to the cyclic was prepared using a functional RAFT agent, in which the R-group on the RAFT consisted of an alkyne moiety. This produced a telechelic polymer with an alkyne group on one end and a RAFT group on the other. The RAFT group was converted, via a two-step reaction, to an azide and OH group. High yielding OH-functional cyclics were prepared by coupling the azide and alkyne groups using the CuAAC coupling reaction. This method for forming a monocyclic was successful, and has the potential to be used for a wide range of polymer (which can be made by RAFT). However, the ester linkages were susceptible to cleavage by PMDETA (the ligand for Cu(I)) when attempting to use the OH-group as a handle to produce more complex structures. Changing the ligand to a triazole, degradation was not observed. In the next chapter we changed from the RAFT/CuAAC to the atom transfer radical polymerization (ATRP)/CuAAC to make complex topologies that were stable in a wide range of environments, thus allowing us to study the effect of topology on the glass transition temperature.

6.2 Multifunctional Cyclic Polymers and Their Complex Topologies

Atom transfer radical polymerization (ATRP) was used for the synthesis of linear precursors polymers with near uniform chain length (i.e, low polydispersity index values) and high chain-end functionality with bromine groups. We then used a modular synthetic strategy to fabricate multifunctional linear polymer precursors by modulating copper (Cu(I)) activity to favour the CuAAC 'click' reaction over bromine abstraction. In addition to this new synthetic procedure, we modified the feed process to produce cyclic polymer on a large scale, and further carry out the reaction under an inert atmosphere to avoid oxidation of the Cu(I) catalyst. This method provided a high percent of cyclic polymer with high efficiency in the synthesis of mono, di and trihydroxy functional cyclics. Bromination of the OH-groups and then azidation generated cyclic azides and alkyne building blocks. These building blocks could be coupled in desired ways to produce a range of different architectures, including spiro type tricyclic, G1 dendrimeric pentacyclic, G1 star tetra and hepta-cyclic. The purity of the products were determined by fitting the experimental SEC traces with log-normal distribution (LND) model based on fitting multiple Gaussian functions for each polymer species. The structures were produced in high yields with good click efficiency, and further purified by preparatory SEC to remove any unreacted building blocks or by-products formed during 'click' reaction. The purified products were further characterised by ^1H NMR and MALDI ToF.

6.3 Complex Polymer Topologies and Their Glass Transition Studies

In the next step, a range of different topologies of cyclic homopolystyrene, polystyrene (PSTY)/polyacrylic acid (PAA) copolymers and their linear counterparts were successfully synthesised by combining ATRP, SET-LRP and CuAAC coupling reaction. The architectures of different topologies included cyclic, linear di-block, tadpole, spiro di-cyclic, linear tri-block star, twin-tailed tadpole, twin-headed tadpole and cyclic tri-block star homopolymers and amphiphillic linear di-block, spiro di-block, mikto-arm star copolymers ($\text{AB}_2/\text{A}_2\text{B}$) of both linear and cyclic analogues. All the topologies were synthesised in high yields and were purified by preparatory SEC. The homopolystyrene topologies were characterised by ^1H NMR, SEC and MALDI ToF mass spectroscopy. We investigated the topology effect of all the complex polymers on the glass transition temperature determined by differential scanning calorimetry (DSC). The DSC results revealed that the topologies which possessed higher number of cyclic units (i.e., lower number of chain ends) showed higher T_g values. The chain ends play a significant role to increase the free

volume and lower the T_g . The self-assembled thin films of both linear and cyclic block copolymers were also characterised by AFM to investigate their morphology. The thin film of cyclic block copolymer was observed a dramatic decreased (~50%) in domain spacing compared with linear analogue due to the structural compactness arise by cyclic polymers.

In the final step of the thesis, we used different architectures of homopolystyrene - linear, cyclic, spiro di and tricyclic, star tricyclic, G1 star tetracyclic and dendrimer pentacyclic - to investigate the knot effect on glass transition temperature. Through our novel synthetic methods, we could place the knot and the number of knots within a cyclic structure. The knots through this process are considered irreversible. The experimental data revealed that the T_g depends not only the number of knots but also the types and location of the knots. Furthermore, the configurational entropy plays a dominant role in controlling the thermal response of the polymer instead of free volume.

6.4 Future Perspective of the Thesis

The synthetic approach outlined in the thesis will allow in building well-defined polymeric architectures with varying functionality and copolymer compositions. The future perspective of the thesis is to demonstrate the synthesis of well-defined functional complex topologies having cyclic polymer as building block that will help in the fabrication of slippery surface and polymeric nanostructures with tailored size, shape, conformation, and functionality.

Appendix A

Table A1: Summary of kinetic analysis data for the synthesis of 2-arm c-PSTY under three different conditions at 25 °C. Reactants; c-PSTY-N₃ (**7**) + propagyl ether.

CuBr/PMDETA		CuBr/DMF		CuBr/triazole	
Time (hours)	% of dicyclic	Time (hours)	% of dicyclic	Time (hours)	% of dicyclic
0.167	79	0.167	87	0.167	27
0.5	75	0.75	87	2.5	85
1	67	3	87	5	87
3	42	7	86	12	89
7	28	14	85	24	88
24	5	24	81		

Table A2: Summary of kinetic analysis data for the synthesis of 3-arm c-PSTY under three different conditions at 25 °C. Reactants; c-PSTY-N₃ (**7**) + tripropagylamine.

CuBr/PMDETA			CuBr/DMF			CuBr/triazole		
Time	dicyclic	tricyclic	Time	dicyclic	tricyclic	Time	dicyclic	tricyclic
10 m	7	71	10m	5	47	10 m	12	19
30m	12	60	45m	6	55	2.5 h	7	78
1h	17	50	3h	6	54	5h	6	82
2h	16	43	7h	5	56	12h	4	89
5h	8	29	14h	6	58	24h	5	88
24h	2	3	24h	6	58	--	--	--

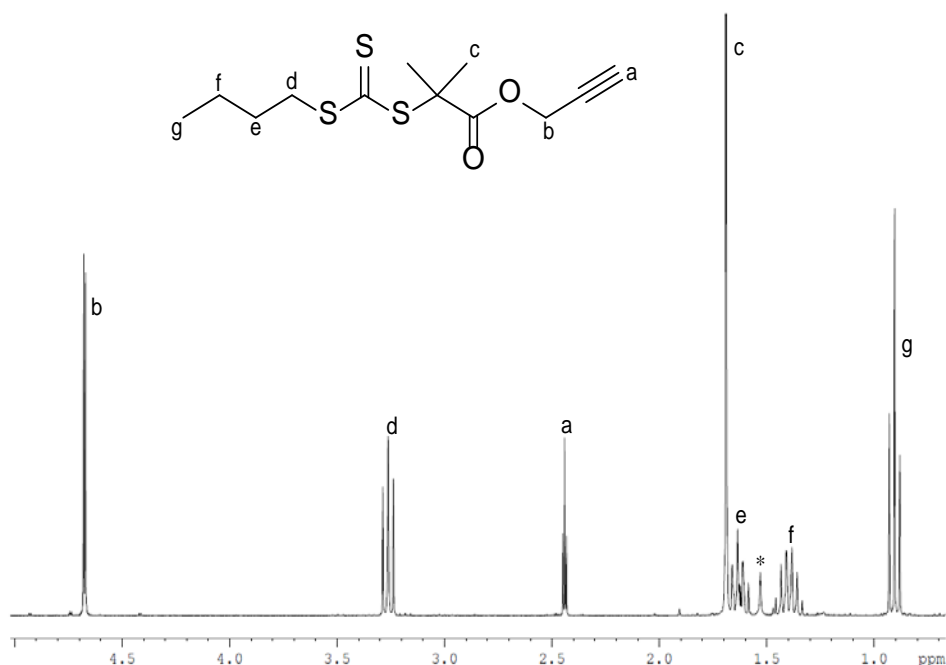


Figure A1. Prop-2-ynyl-2-(butylthiocarbonothioylthio)-2-methylpropanoate alkyne RAFT, chain transfer agent **1** in CDCl₃ (* H₂O).

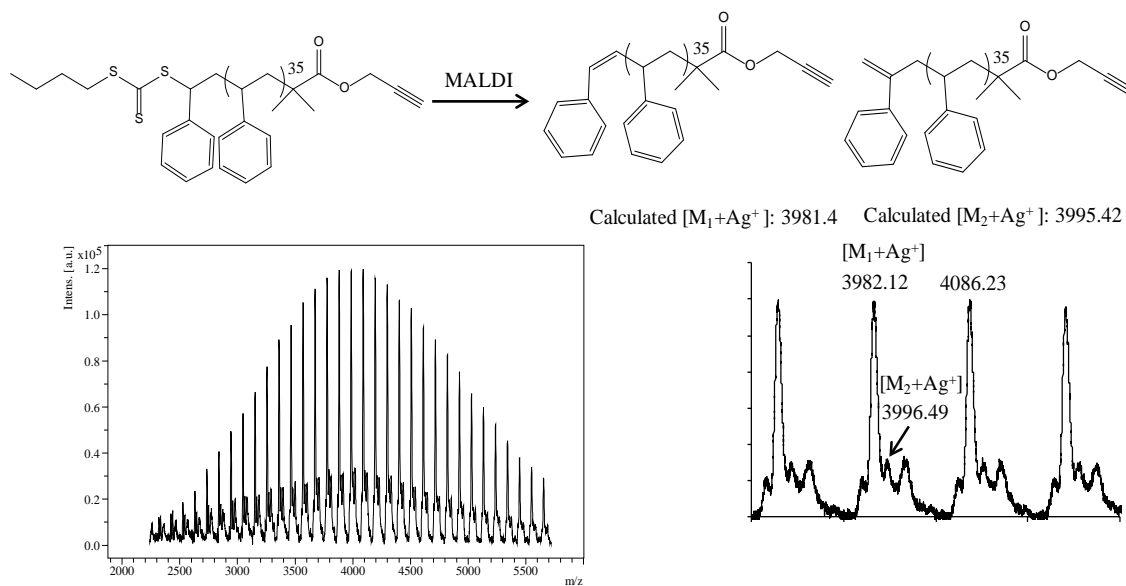


Figure A2: MALDI-ToF mass spectrum acquired in reflectron mode with Ag salt as cationizing agent and DCTB matrix. The full and expanded spectra correspond to RAFT-PSTY-≡ 2; calculated $[M+Ag^+] = 3981.4$ for the fragmentation of RAFT polymer, $DP_n = 36$.

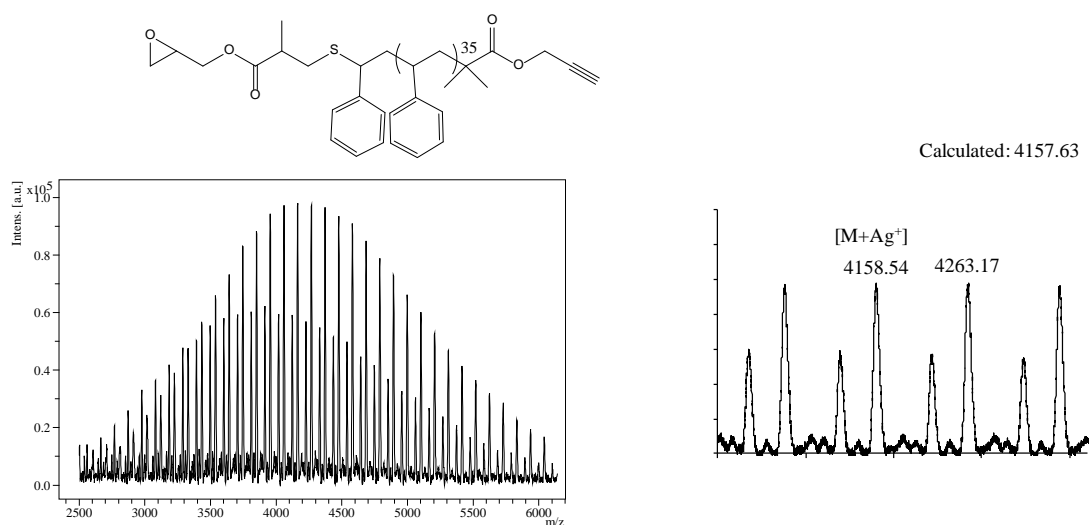


Figure A3: MALDI-ToF mass spectrum acquired in reflectron mode with Ag salt as cationizing agent and DCTB matrix. The full and expanded spectra correspond to Epo-PSTY-≡ 3; calculated $[M+Ag^+] = 4157.63$, $DP_n = 36$. The other fragmentation peak was unknown.

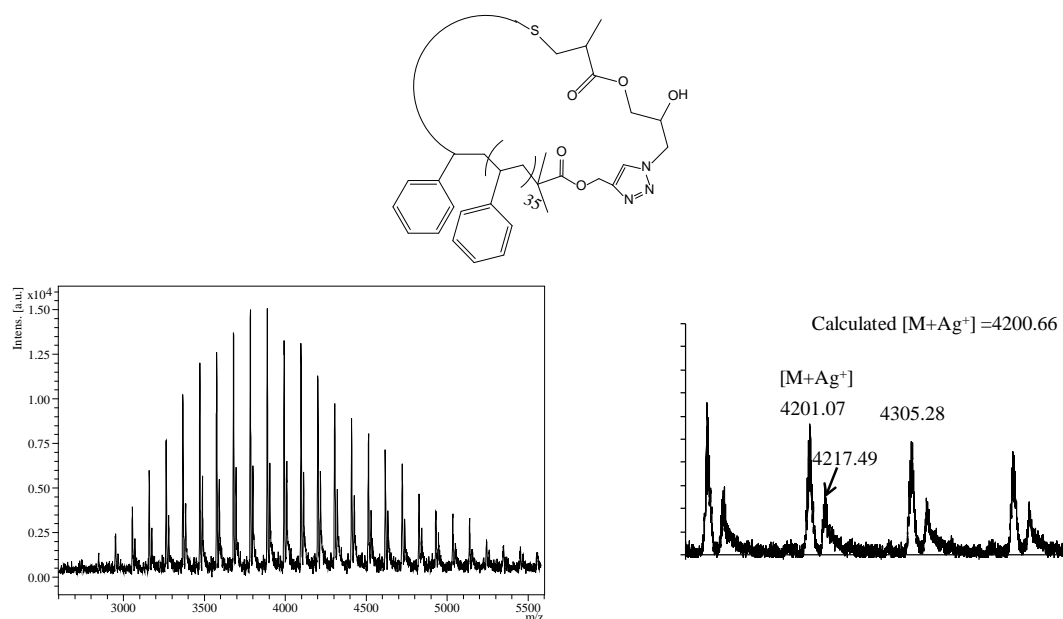


Figure A4: MALDI-ToF mass spectrum acquired in reflectron mode with Ag salt as cationizing agent and DCTB matrix. The full and expanded spectra correspond to c-PSTY-OH **5**; calculated $[M+Ag^+] = 4200.66$, $DP_n = 36$.

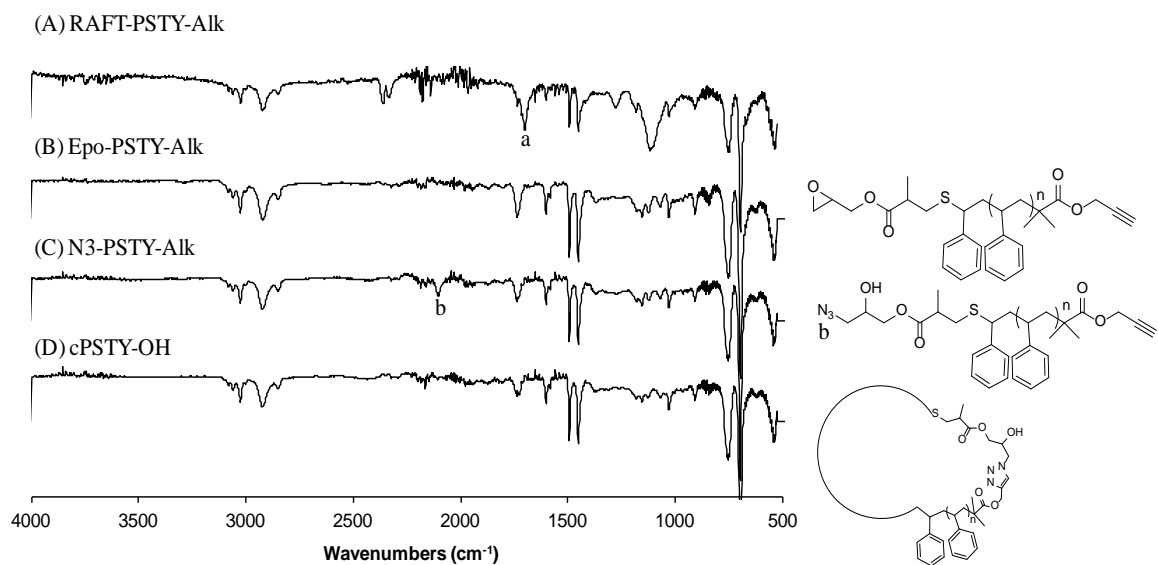


Figure A5. ATR-FTIR analysis of (A) RAFT-PSTY-≡ **2** (B) Epo-PSTY-≡ **3** (C) N₃-PSTY-≡ **4** and (D) c-PSTY-OH **5**.

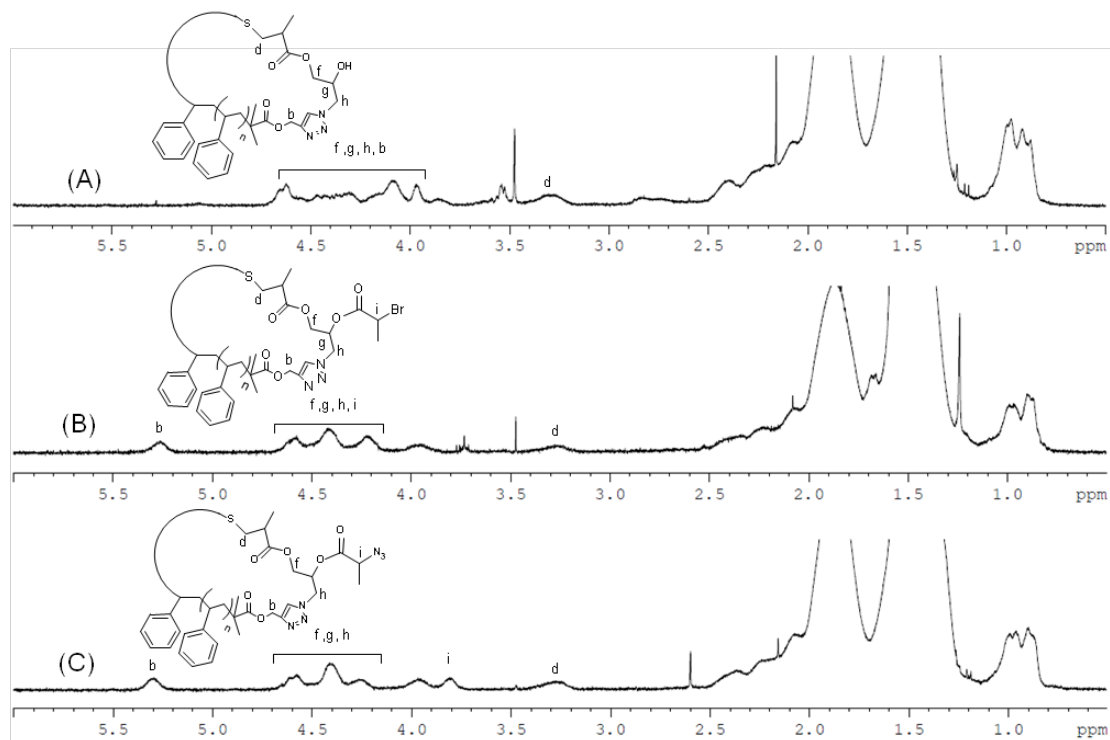


Figure A6: 500 MHz ¹H 1D DOSY NMR spectra of (A) c-PSTY-OH **5** (B) c-PSTY-Br **6** and (C) c-PSTY-N₃ **7** (*methanol).

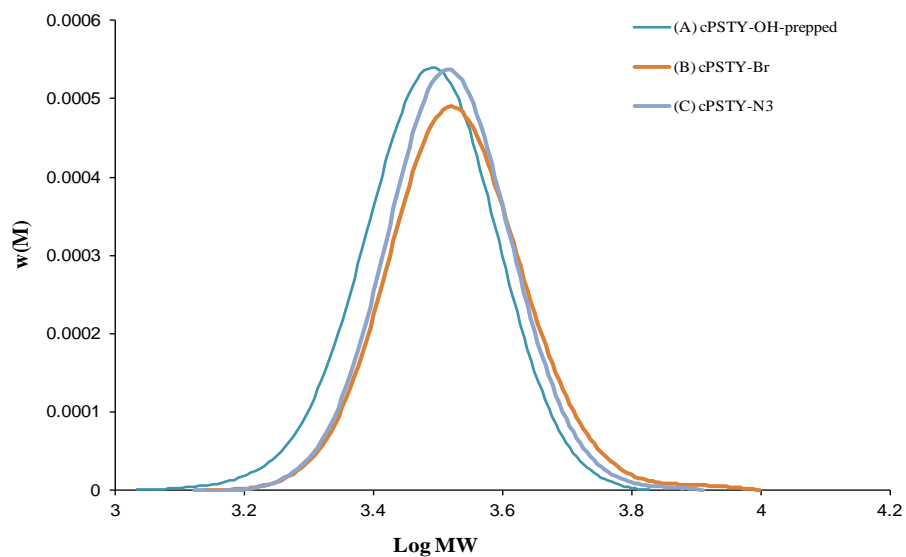


Figure A7: SEC chromatograms for cyclization of (A) c-PSTY-OH –prepped purified **5** (B) c-PSTY-Br **6** and (C) c-PSTY-N₃ **7**. SEC analysis based on polystyrene calibration curve.

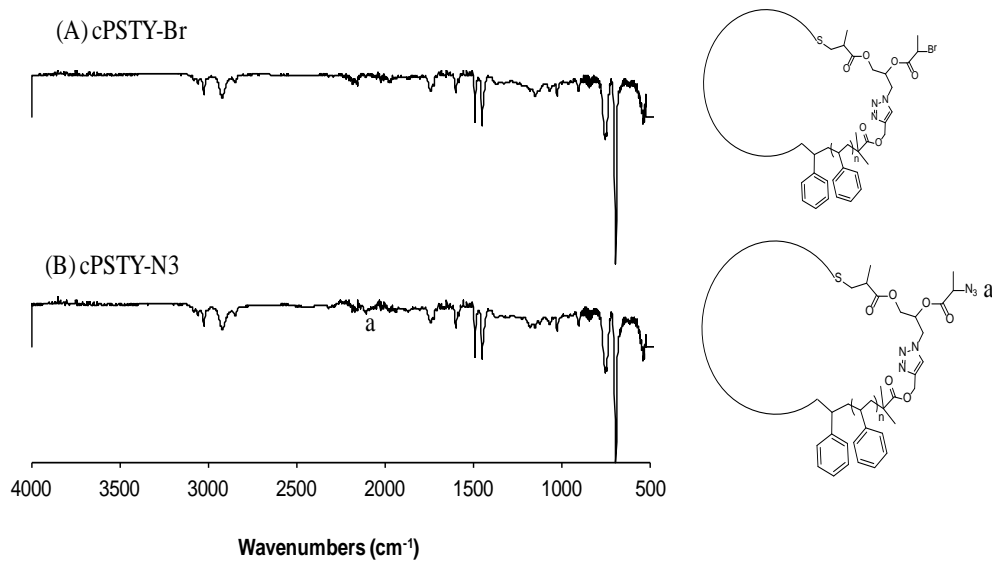


Figure A8. ATR-FTIR analysis of (A) c-PSTY-Br **6** (B) c-PSTY-N₃ **7**.

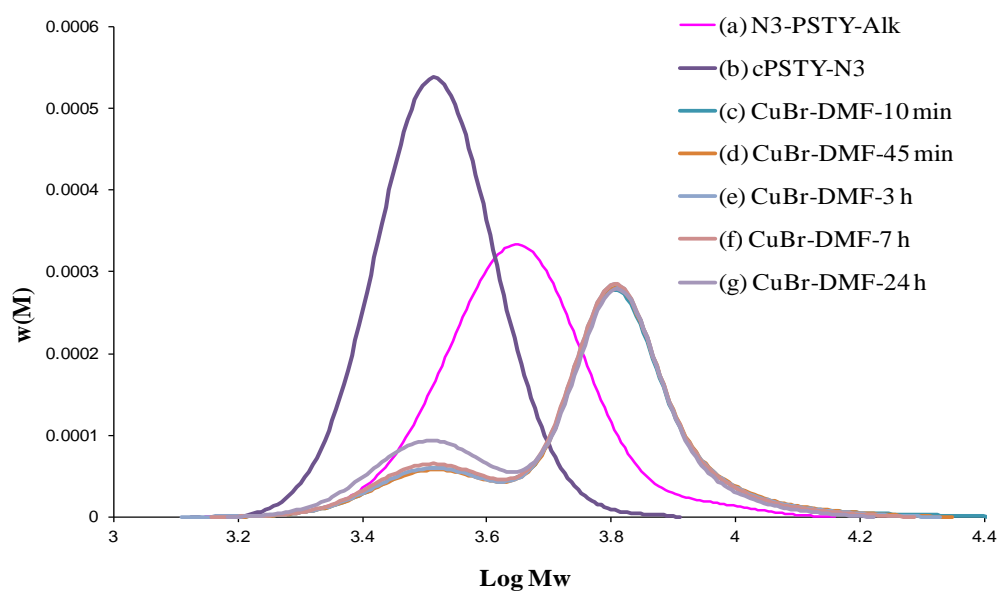


Figure A9: SEC chromatograms for the degradation studies in the synthesis of di-cyclic PSTY by one pot using CuBr/DMF; (a) N₃-PSTY-≡ **4** (b) c-PSTY-N₃ **7**; degradation after (c) 10 min (d) 45 min (e) 3 h (f) 7 h and (h) 24 h.

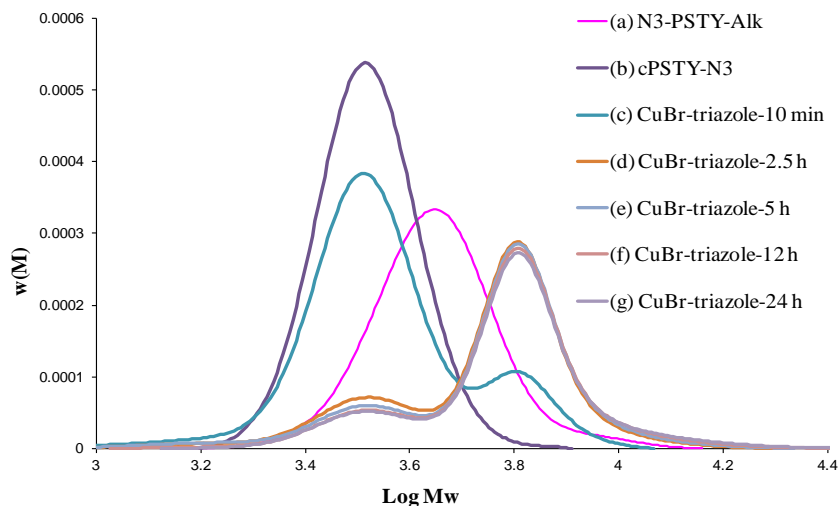


Figure A10: SEC chromatograms for the degradation studies in the synthesis of di-cyclic PSTY by one pot using CuBr/triazole in toluene; (a) N_3 -PSTY-≡ **4** (b) c -PSTY- N_3 **7**; degradation after (c) 10 min (d) 2.5 h (e) 5h (f) 12 h and (g) 24 h.

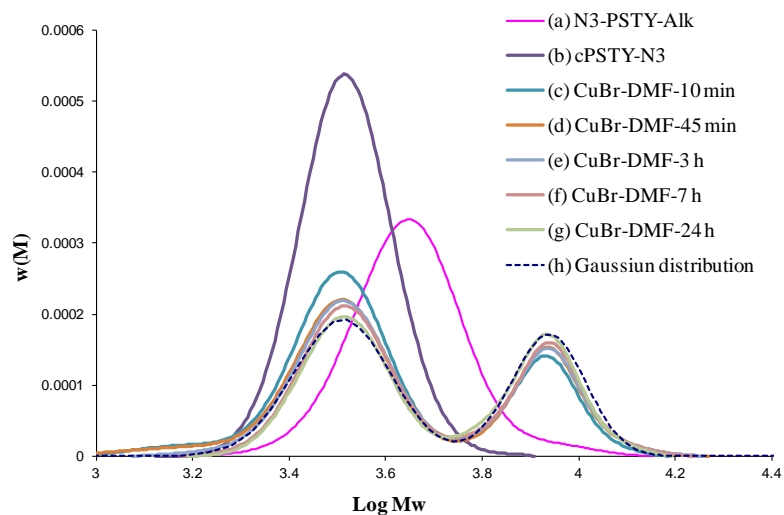


Figure A11: SEC chromatograms for the degradation studies in the synthesis of tri-cyclic PSTY by one pot using CuBr/DMF; (a) N_3 -PSTY-≡ **4** (b) c -PSTY- N_3 **7**; degradation after (c) 10 min (d) 45 min (e) 3h (f) 7 h and (g) 24 h.

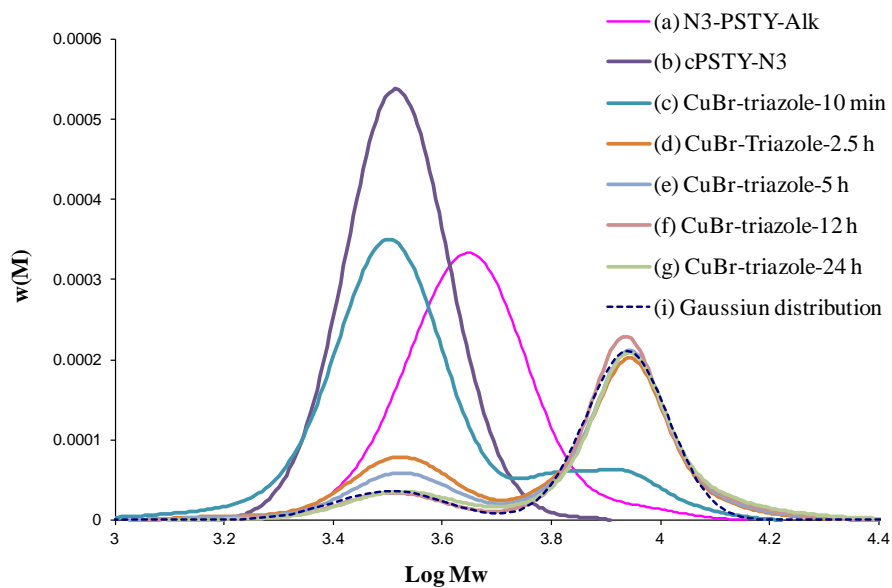


Figure A12: SEC chromatograms for the degradation studies in the synthesis of tri-cyclic PSTY by one pot using CuBr/triazole in toluene; (a) N₃-PSTY-≡ **4**, (b) c-PSTY-N₃ **7**; degradation after (c) 10 min (d) 2.5 h (e) 5 h (f) 12 h and (g) 24 h.

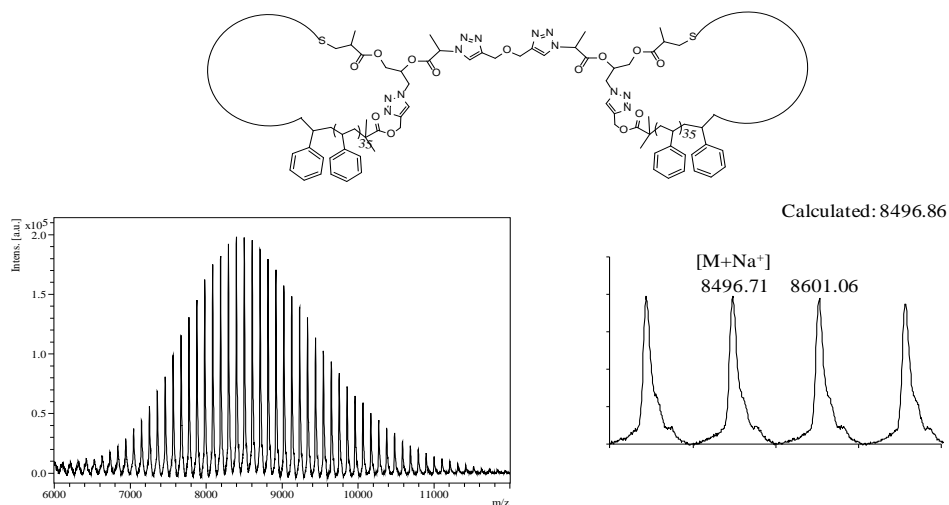


Figure A13: MALDI-ToF mass spectrum acquired in linear mode with Ag salt as cationizing agent and DCTB matrix. The full and expanded spectra correspond to (c-PSTY)₂ **8**; calculated $[M+Na^+] = 8496.86$, $DP_n = 72$.

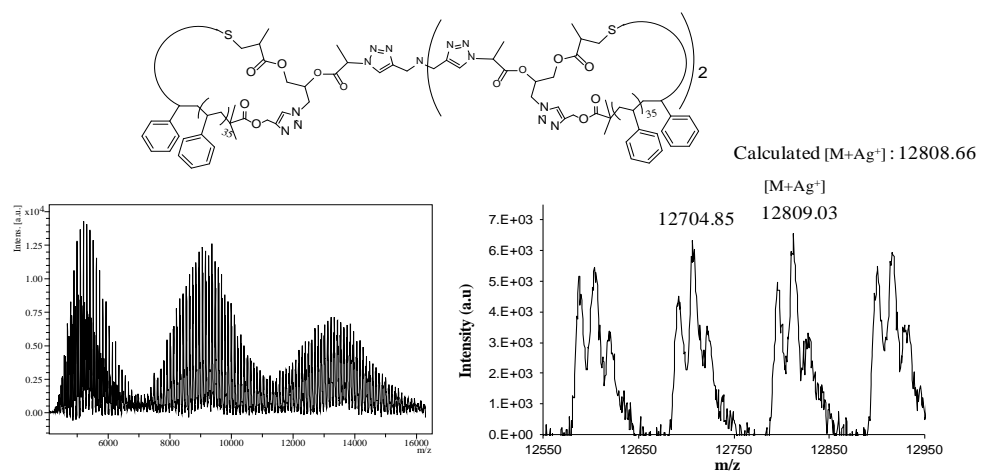
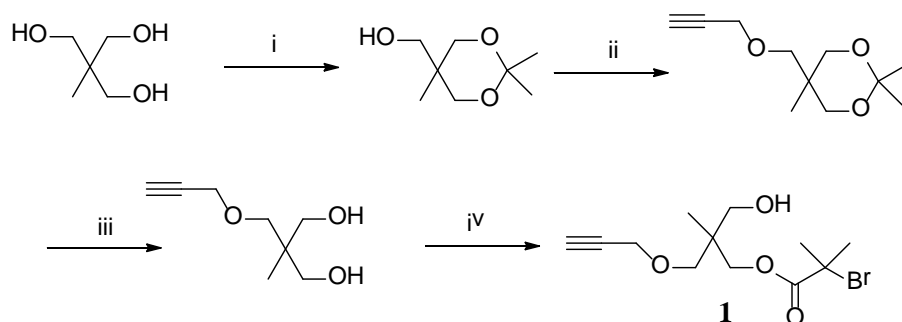


Figure A14: MALDI-ToF mass spectrum acquired in linear mode with Ag salt as cationizing agent and DCTB matrix. The full and expanded spectra correspond to $(c\text{-PSTY})_3$ **9**; calculated $[M+Ag^+] = 12808.66$, $DP_n = 108$.

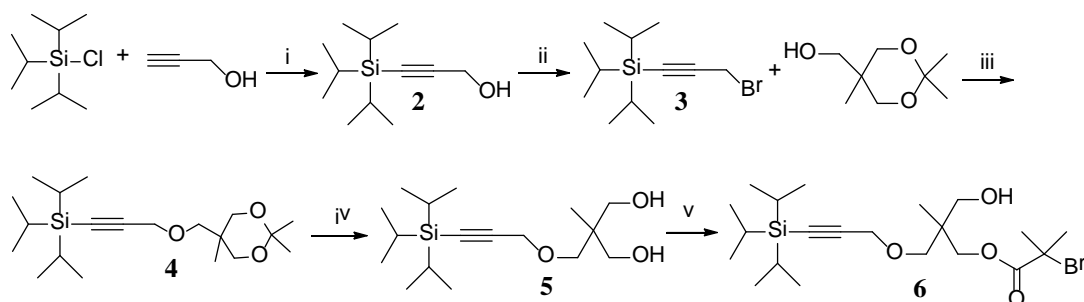
Appendix B

Scheme B1: Synthesis of alkyne (hydroxyl) functional Initiator (1)



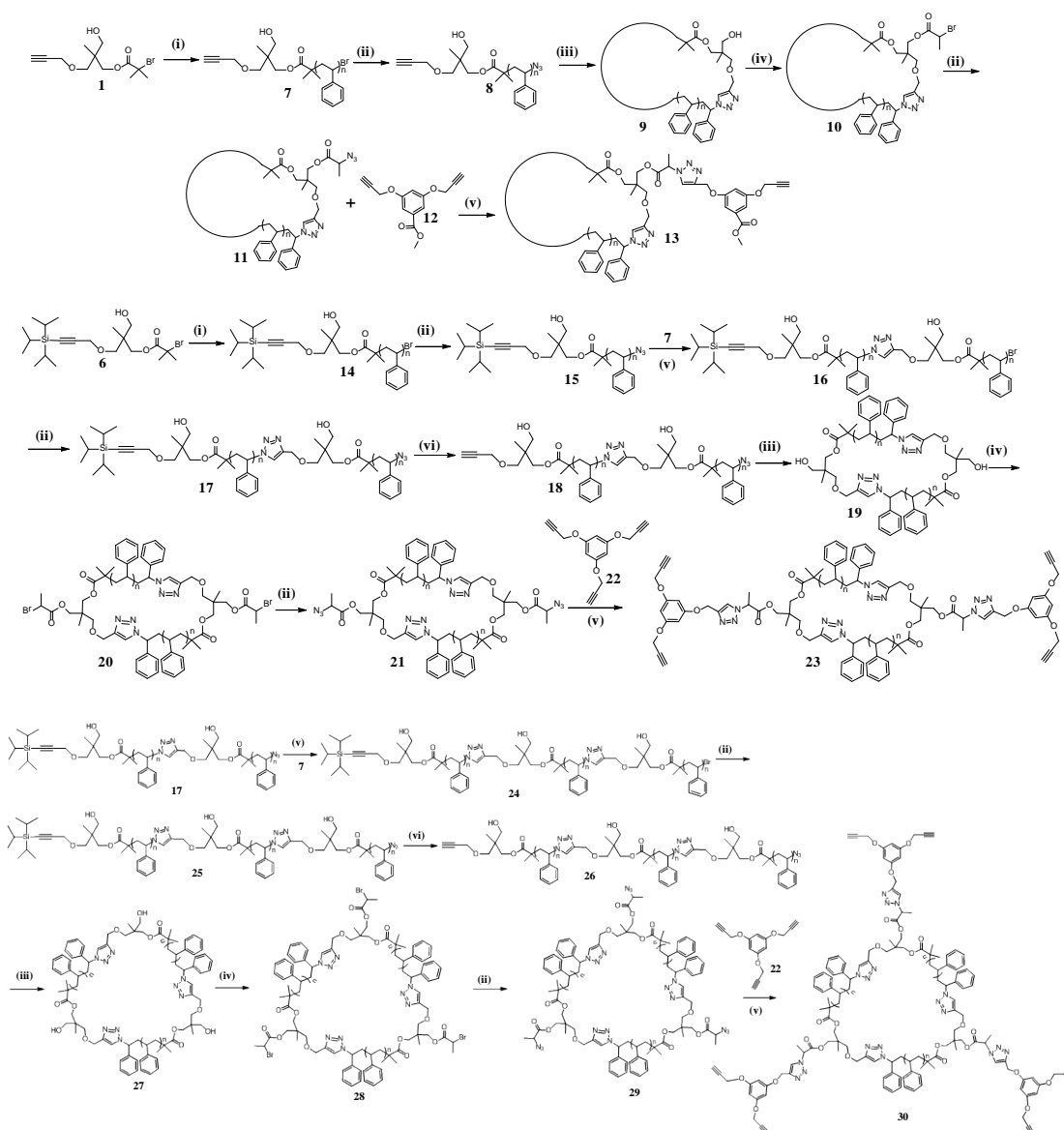
Reactants and conditions: i) Acetone, p-TsOH, RT, 16h; ii) THF, NaH, propargyl bromide, -78 °C, 16 h; iii) DOWEX, Methanol, R.T. 16 h; iv) THF, 2-bromoisobutyryl bromide, 0 °C - RT, 16 h.

Scheme B2: Synthesis of protected alkyne (hydroxyl) functional Initiator (6)

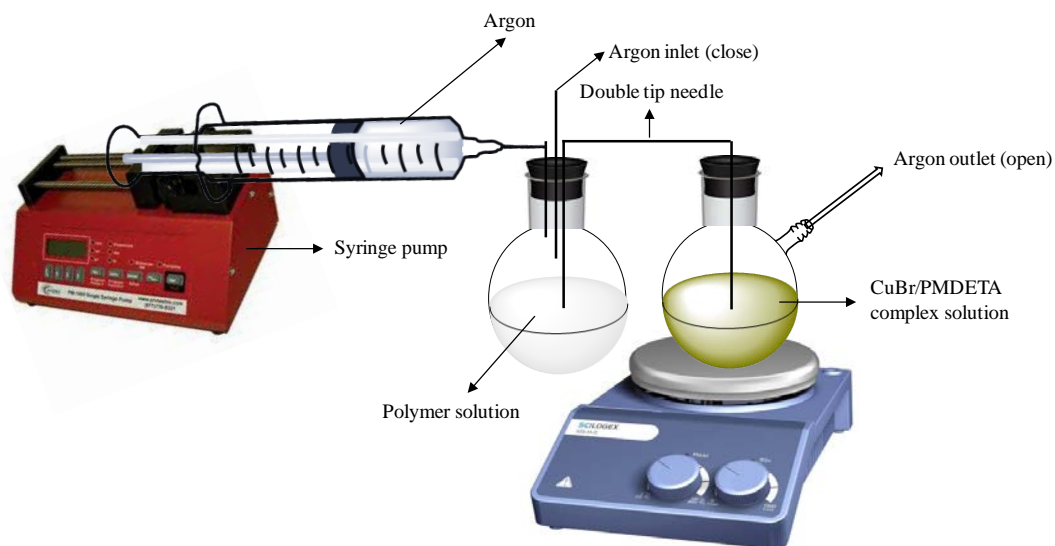


Reactants and conditions: (i) EtMgBr, THF, reflux at 76 °C, (ii) PBr₃, pyridine, ether 0 ~ 25 °C (iii) NaH/ THF, -78 °C ~ 25 °C (iv) DOWEX resin in MeOH at 40 °C (v) TEA in THF at 0 °C ~ RT for 24 h.

Scheme B3: General scheme for the synthesis of multifunctional cyclic.



Conditions: (i) **Polymerization:** Styrene, CuBr, PMDETA, CuBr₂/PMDETA in bulk at 80 °C. (ii) **Azidation:** NaN₃ in DMF at 25 °C, (iii) **Cyclization:** CuBr, PMDETA in toluene by feed at 25 °C, (iv) **Bromination:** 2-BPB, TEA in THF; 0 °C- RT, (v) **Click:** CuBr, PMDETA in toluene at 25 °C. (vi) **Deprotection:** TBAF in THF at 25 °C.



Scheme B4. Schematic illustration for the cyclization by argon feeding technique.

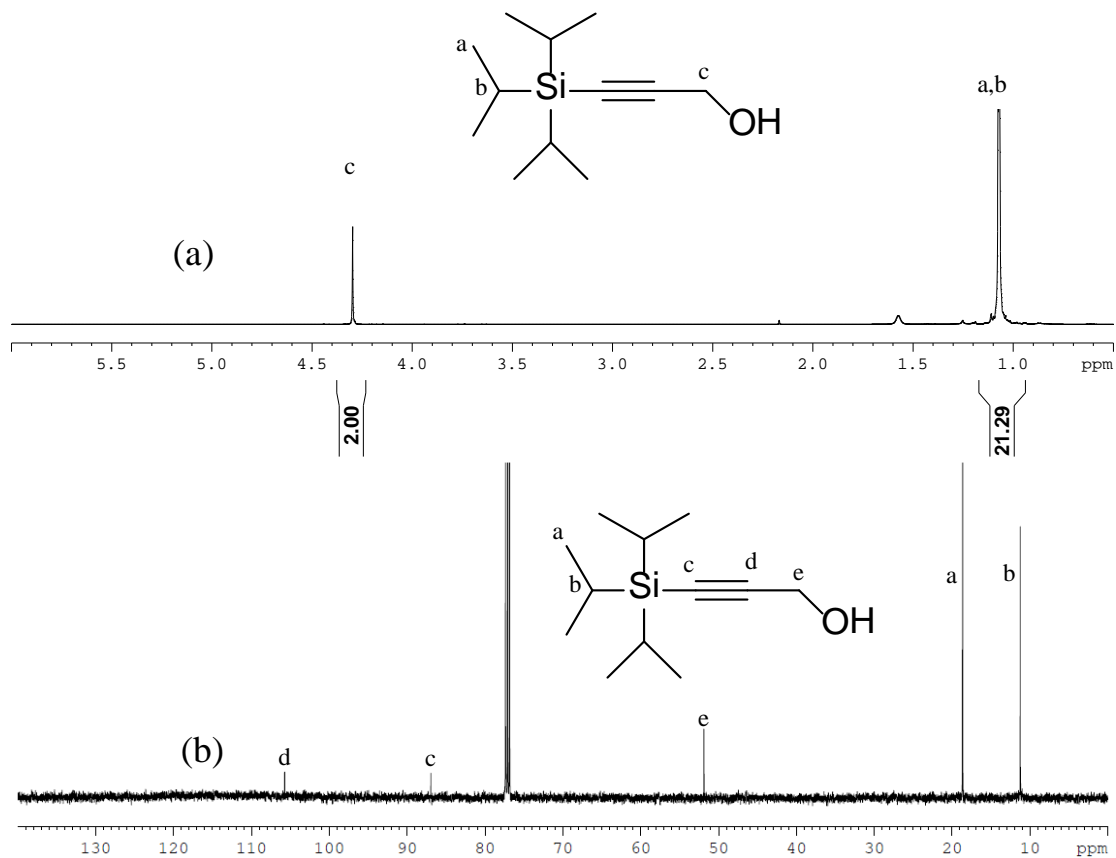


Figure B1: (a) ^1H NMR and (b) ^{13}C NMR of **2**, recorded in CDCl_3 at 298K (500 MHz).

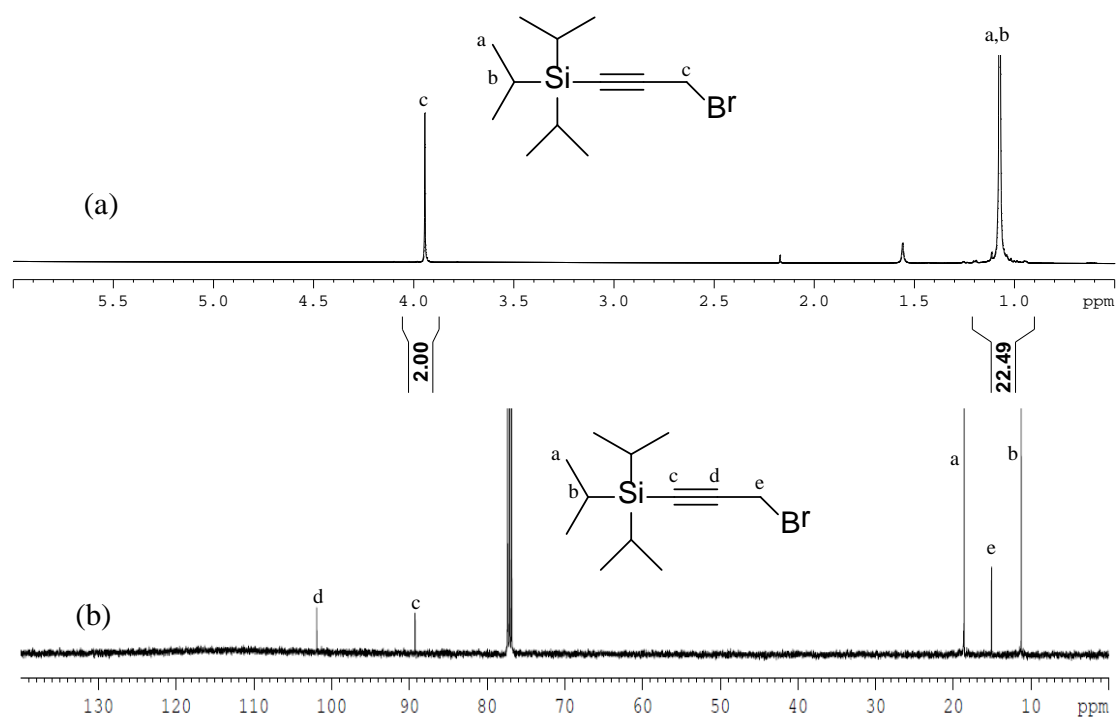


Figure B2: (a) ^1H NMR and (b) ^{13}C NMR of **3**, recorded in CDCl_3 at 298K (500 MHz).

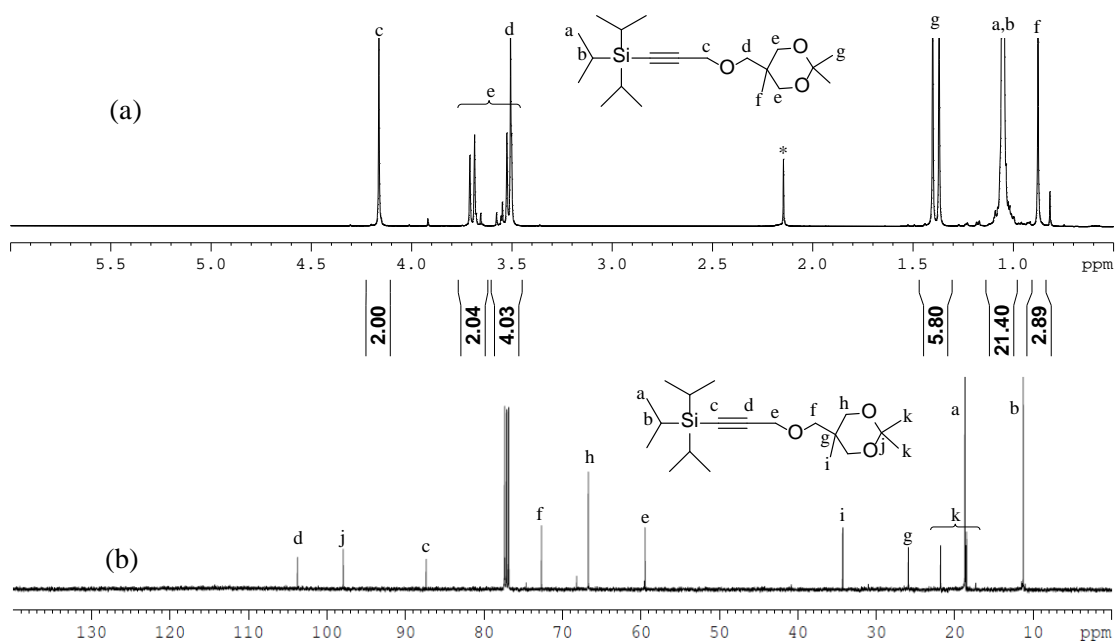


Figure B3: (a) ^1H NMR and (b) ^{13}C NMR of **4**, recorded in CDCl_3 at 298K (500 MHz). *

Acetone peak.

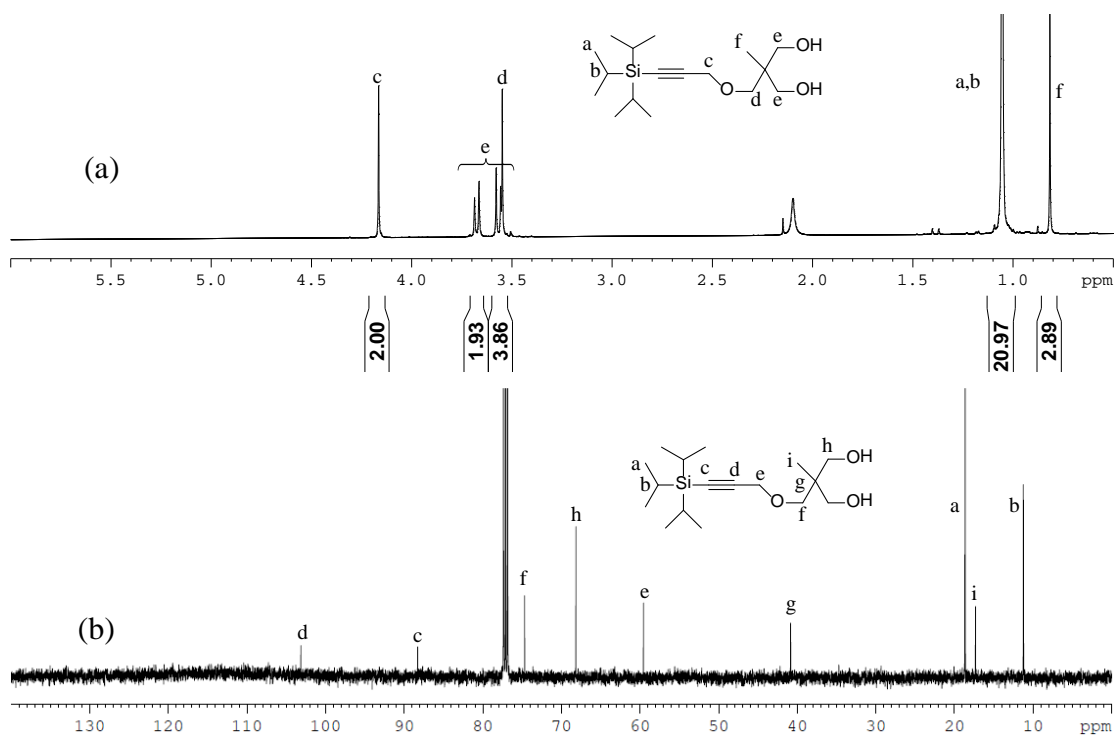


Figure B4: (a) ^1H NMR and (b) ^{13}C NMR of **5**, recorded in CDCl_3 at 298K (500 MHz).

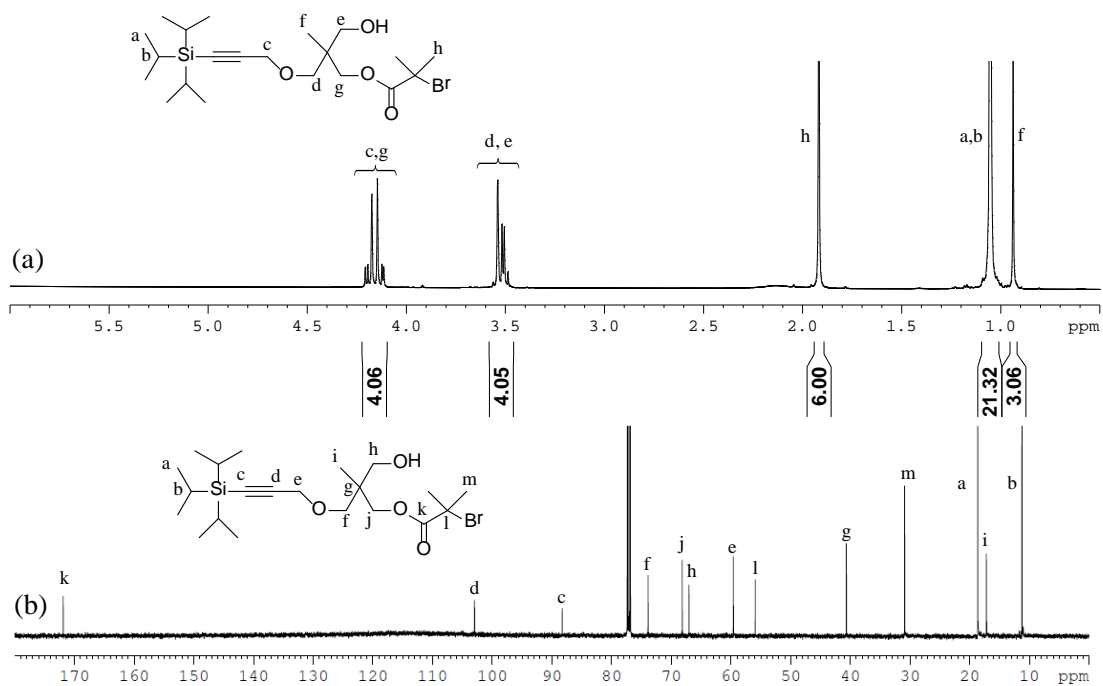


Figure B5: (a) ^1H NMR and (b) ^{13}C NMR of **6**, recorded in CDCl_3 at 298K (500 MHz).

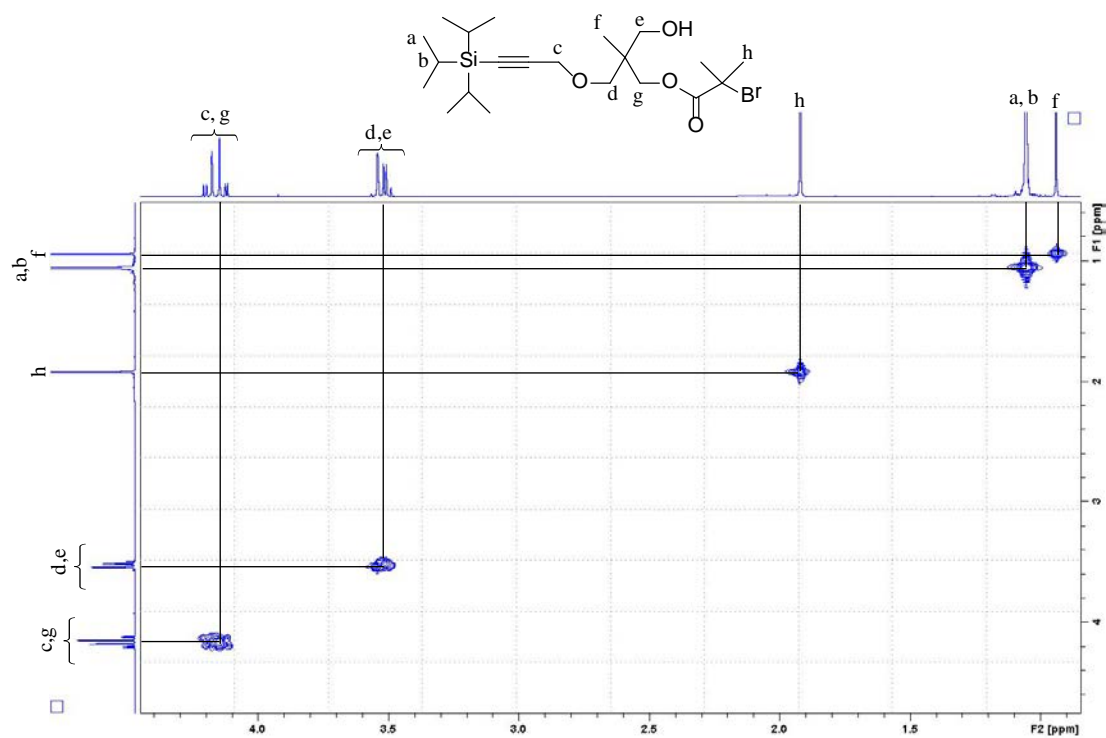


Figure B6: 2D COSY NMR spectra of **6** in CDCl_3 .

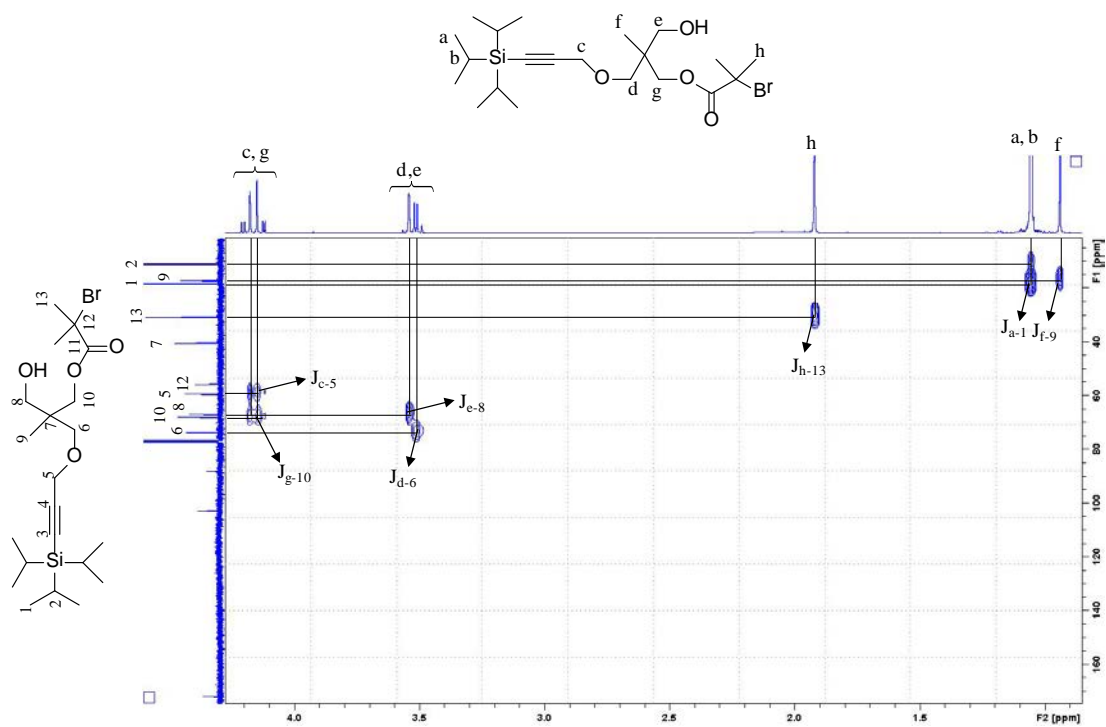


Figure B7: 2D HSQC NMR spectra of **6** in CDCl_3 .

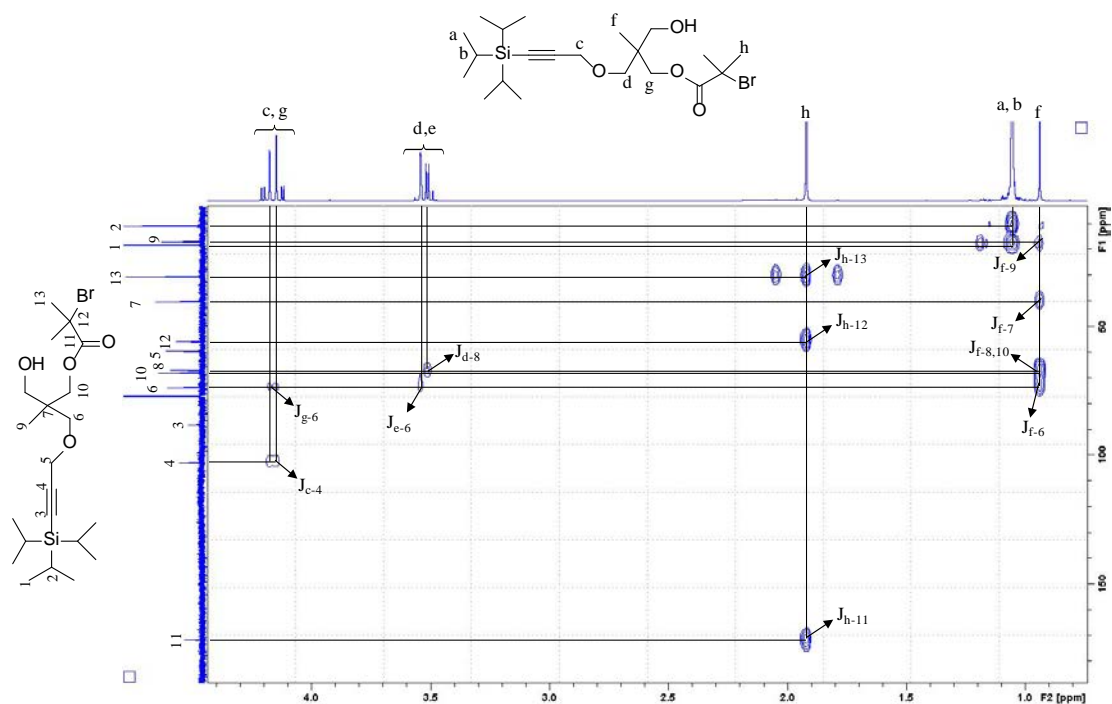


Figure B8: 2D HMBC NMR spectra of **6** in CDCl_3 .

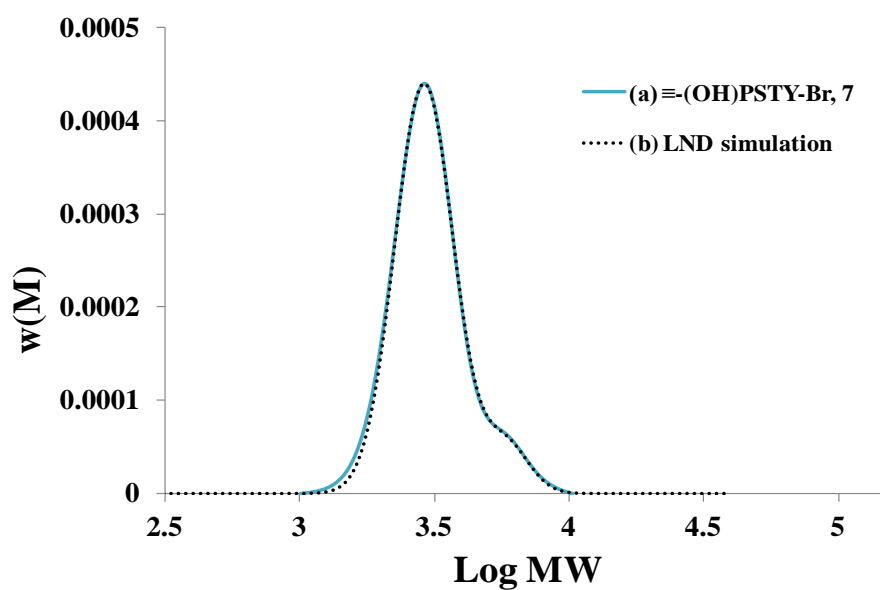


Figure B9: SEC trace of $\equiv(\text{OH})\text{-PSTY}_{25}\text{-Br}$, **7**. SEC analysis based on polystyrene calibration curve.

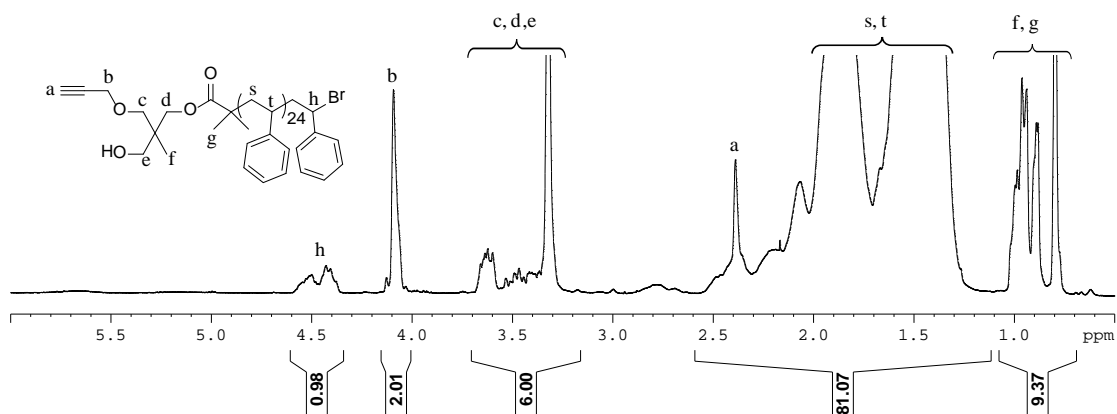


Figure B10. 500 MHz ^1H 1D DOSY NMR spectra in CDCl_3 of $\equiv(\text{OH})\text{-PSTY}_{25}\text{-Br}$ **7**.

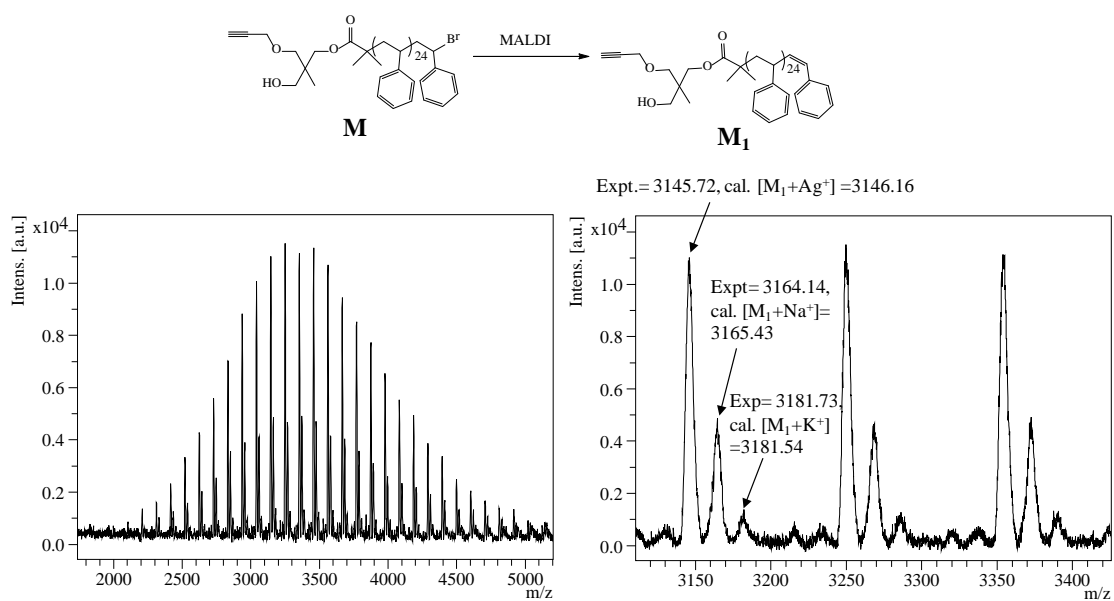


Figure B11: MALDI-ToF mass spectrum acquired in reflectron mode with Ag salt as cationizing agent and DCTB matrix. The full and expanded spectra correspond to $\equiv(\text{HO})\text{-PSTY}_{25}\text{-Br}$, **7**.

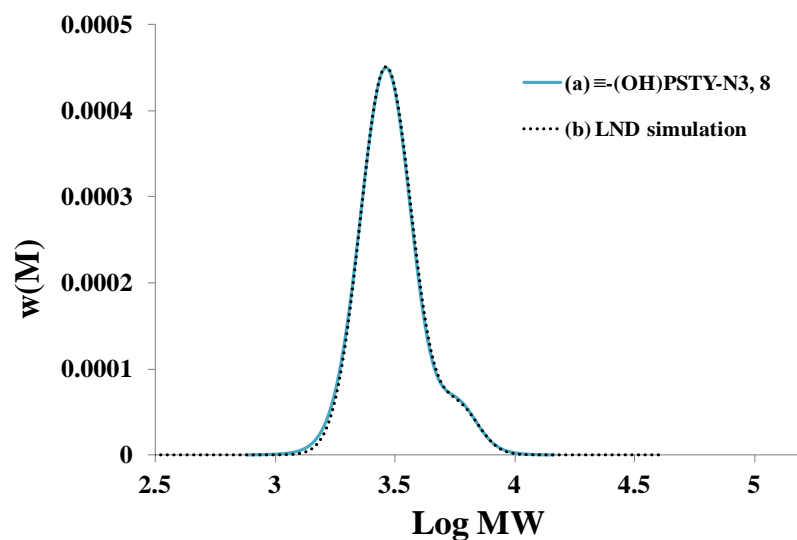


Figure B12: SEC trace of $\equiv(\text{OH})\text{-PSTY}_{25}\text{-N}_3$ **8**. SEC analysis based on polystyrene calibration curve.

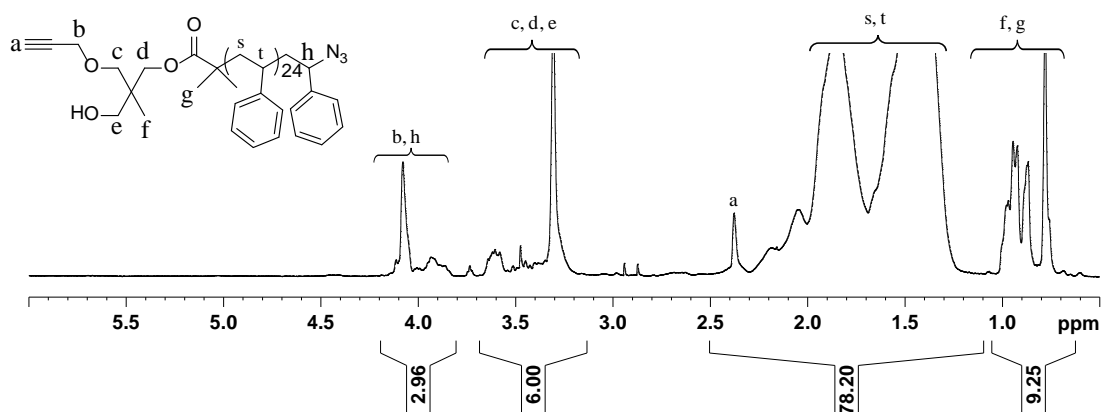


Figure B13: 500 MHz ^1H 1D DOSY NMR spectra in CDCl_3 of $\equiv(\text{OH})\text{-PSTY}_{25}\text{-N}_3$ **8**.

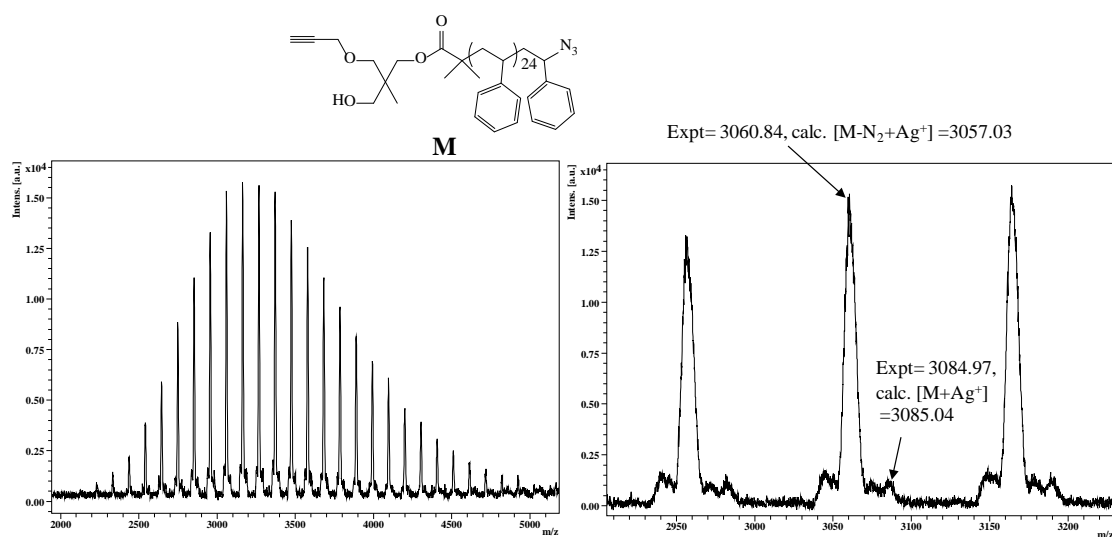


Figure B14: MALDI-ToF mass spectrum acquired in reflectron mode with Ag salt as cationizing agent and DCTB matrix. The full and expanded spectra correspond to $\equiv(\text{HO})\text{-PSTY}_{25}\text{-N}_3$, **8**.

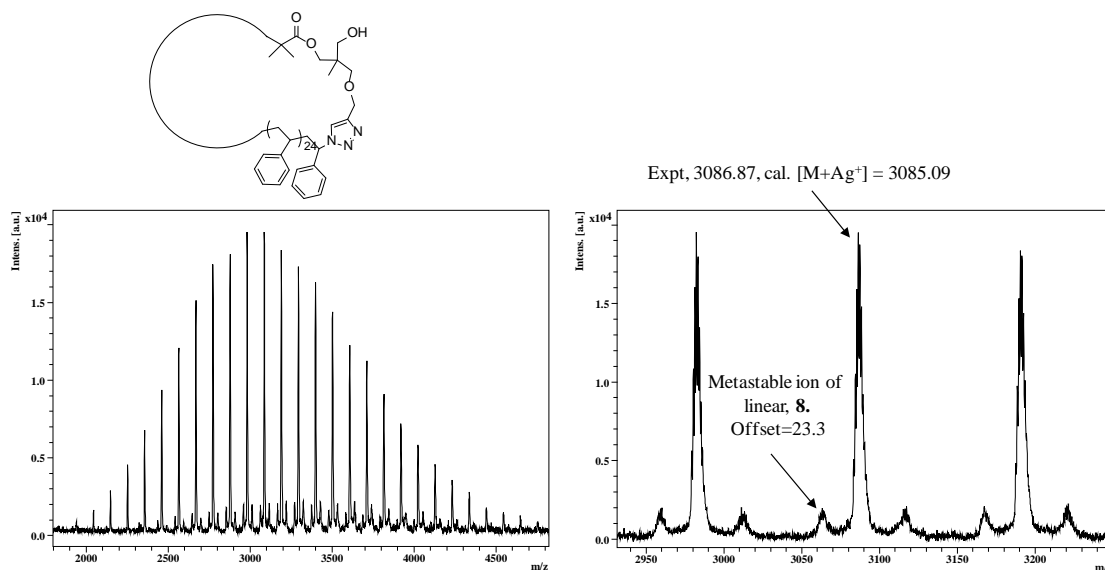


Figure B15: MALDI-ToF mass spectrum acquired in reflectron mode with Ag salt as cationizing agent and DCTB matrix. The full and expanded spectra correspond to c-PSTY₂₅-OH, **9**.

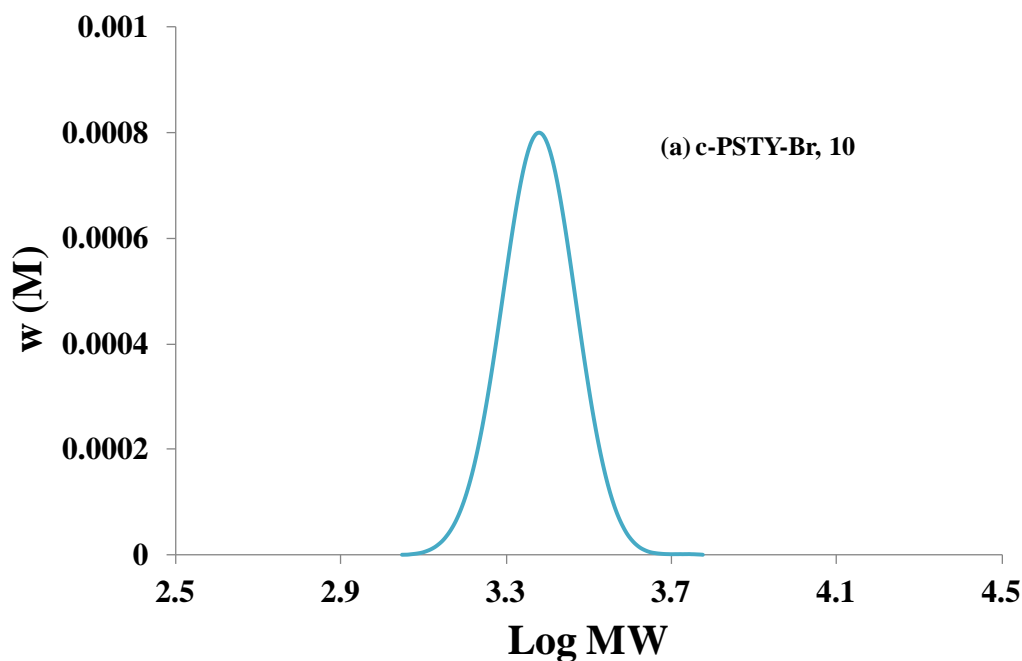


Figure B16: SEC trace of c-PSTY₂₅-Br, **10**. SEC analysis based on polystyrene calibration curve.

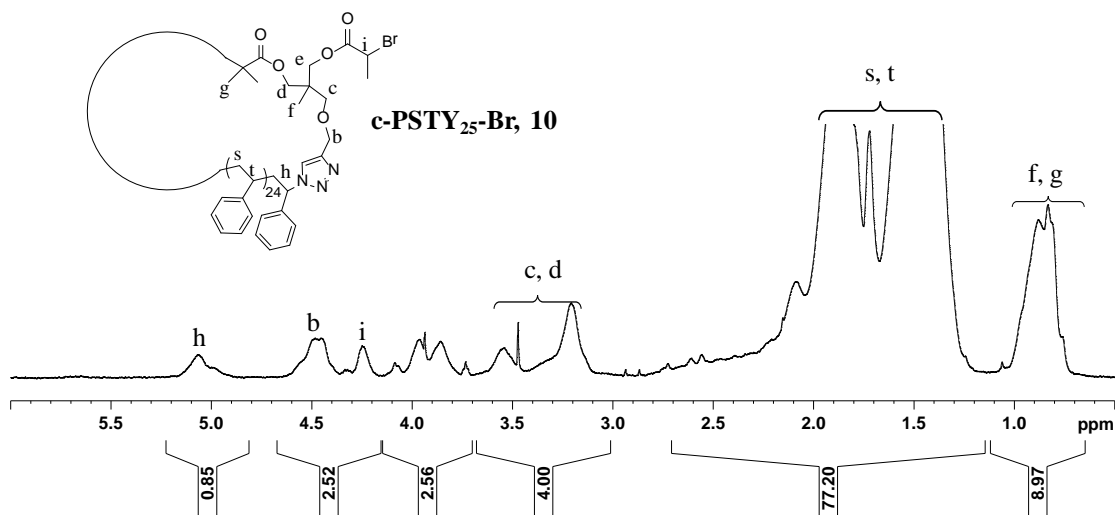


Figure B17: 500 MHz ¹H 1D DOSY NMR spectra in CDCl₃ of c-PSTY₂₅-OH 9.

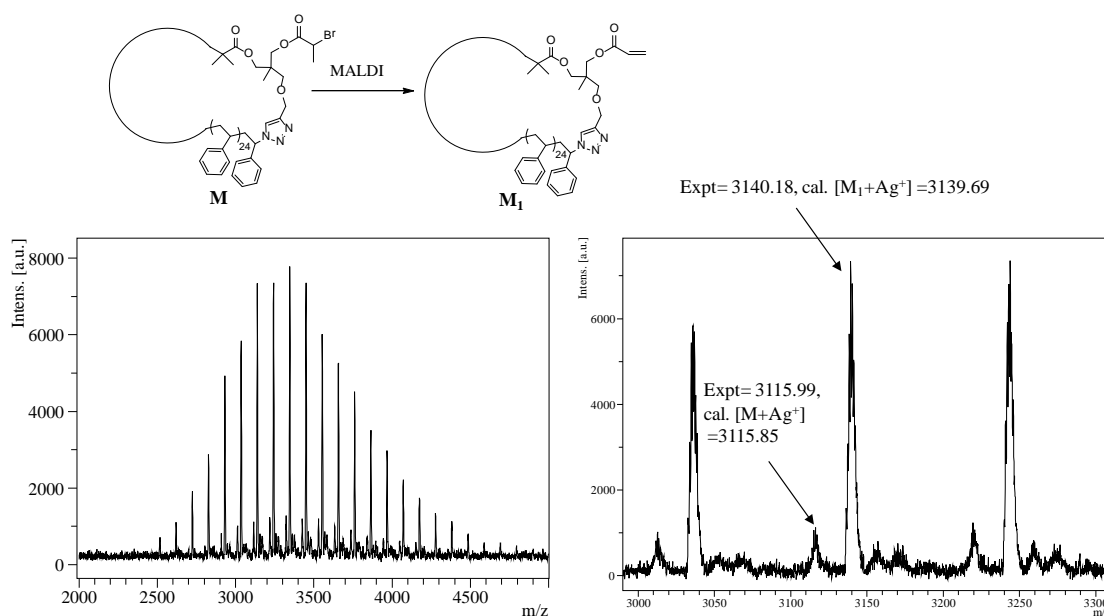


Figure B18: MALDI-ToF mass spectrum acquired in reflectron mode with Ag salt as cationizing agent and DCTB matrix. The full and expanded spectra correspond to c-PSTY₂₆-Br, 10.

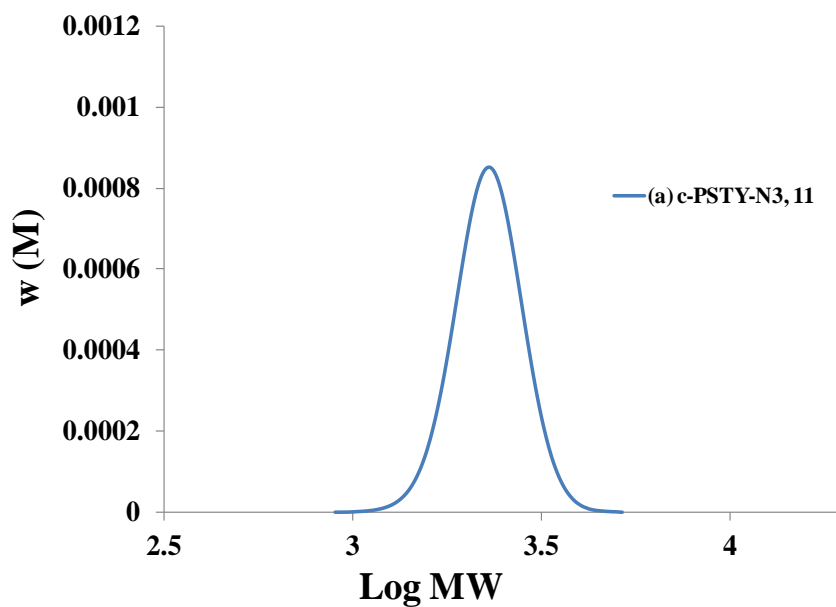


Figure B19: SEC trace of c-PSTY₂₅-N₃, 11. SEC analysis based on polystyrene calibration curve.

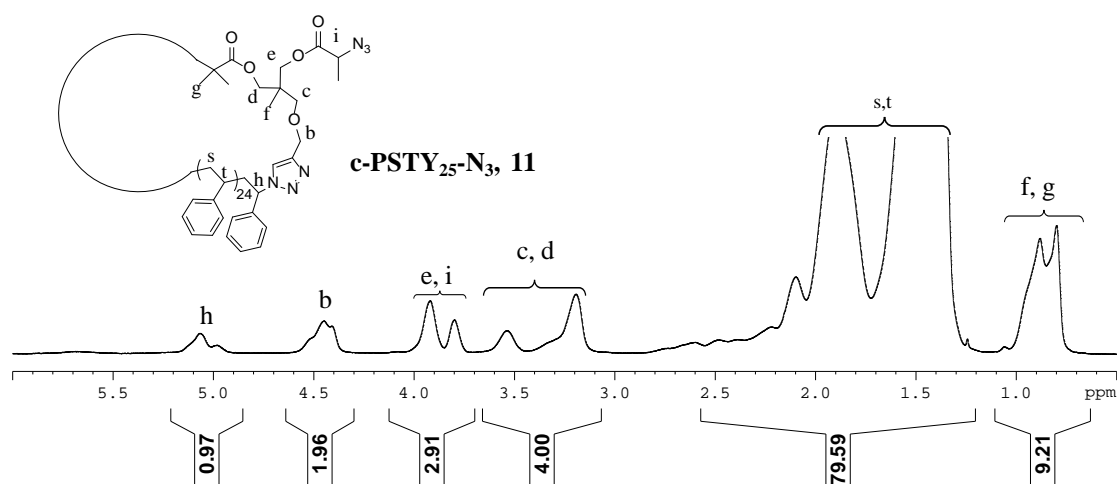


Figure B20: 500 MHz ¹H 1D DOSY NMR spectra in CDCl₃ of c-PSTY₂₅-N₃ 11.

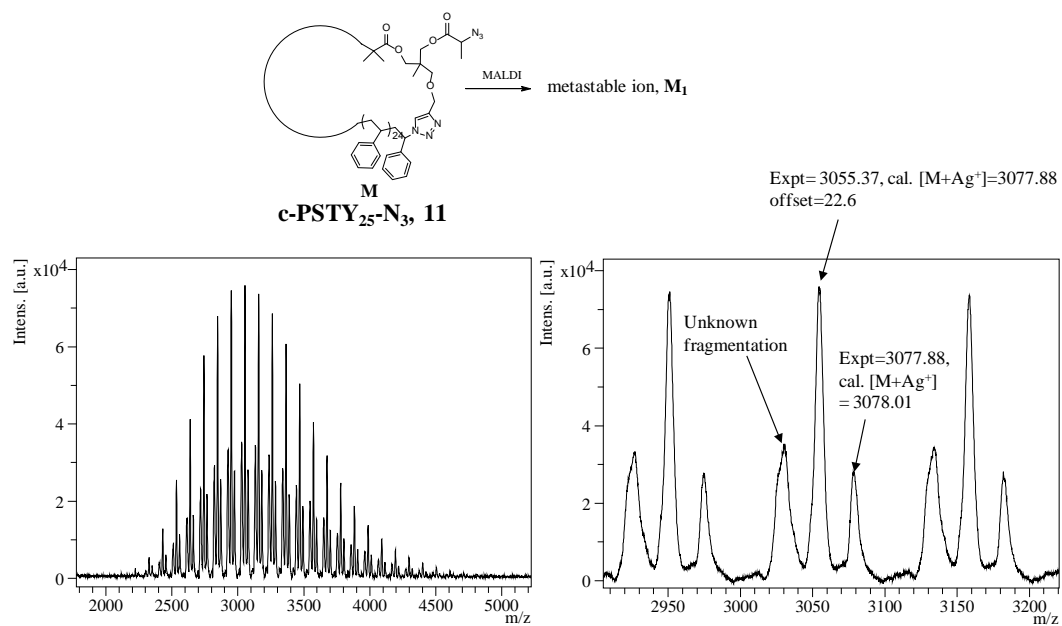


Figure B21: MALDI-ToF mass spectrum acquired in reflectron mode with Ag salt as cationizing agent and DCTB matrix. The full and expanded spectra correspond to c-PSTY-N₃, **11**.

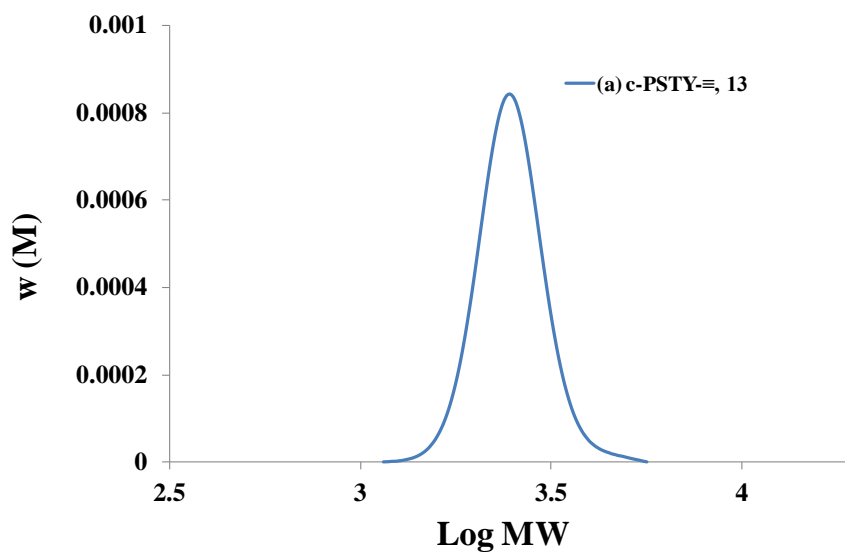


Figure B22: SEC trace of c-PSTY₂₅-N₃, **13**. SEC analysis based on polystyrene calibration curve.

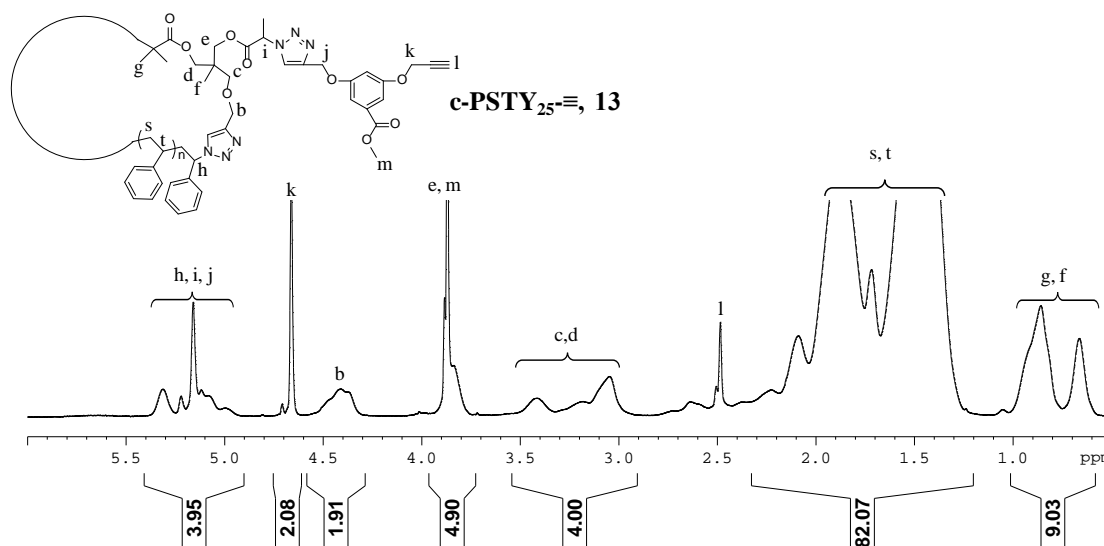


Figure B23. 500 MHz ^1H 1D DOSY NMR spectra in CDCl_3 of $\text{c-PSTY}_{25}\text{-}\equiv$ **13**.

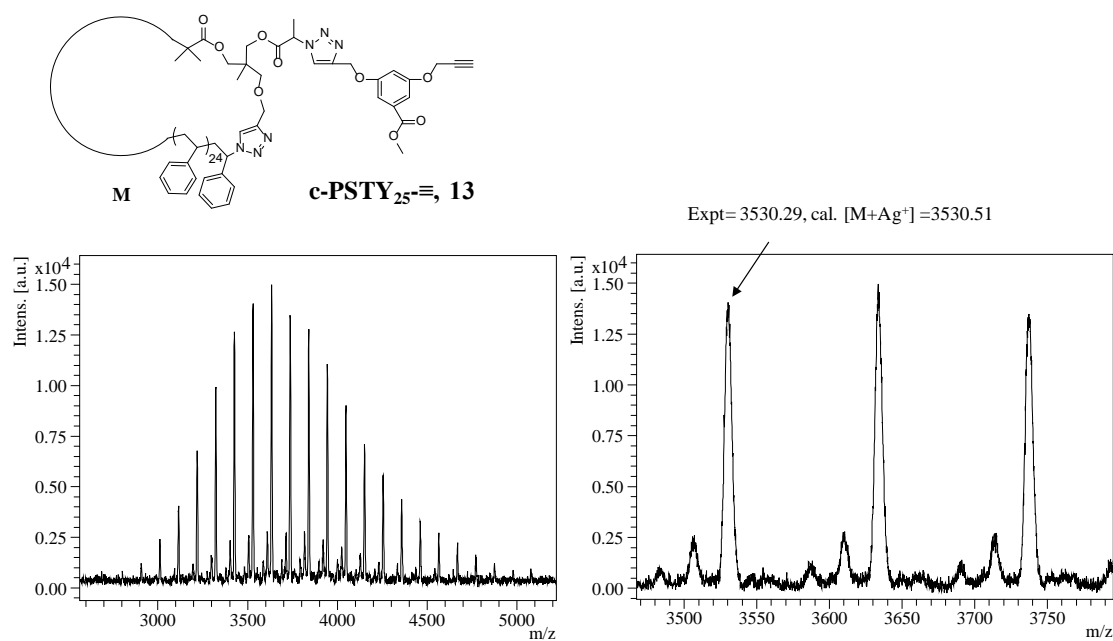


Figure B24: MALDI-ToF mass spectrum acquired in reflectron mode with Ag salt as cationizing agent and DCTB matrix. The full and expanded spectra correspond to $\text{c-PSTY}_{25}\text{-}\equiv$ **13**.

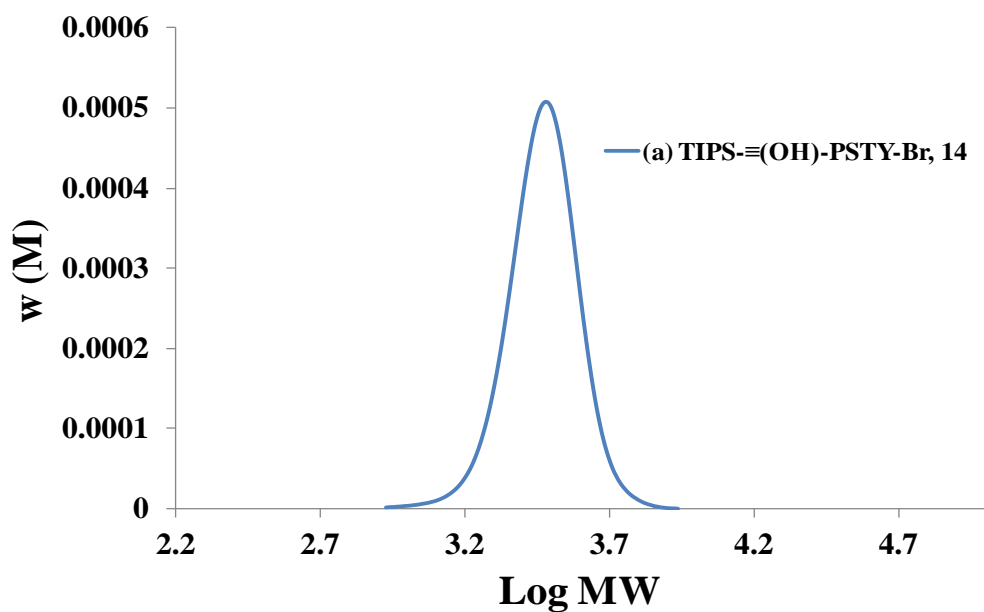


Figure B25: SEC trace of TIPS-≡(HO)-PSTY₂₅-Br, 14. SEC analysis based on polystyrene calibration curve.

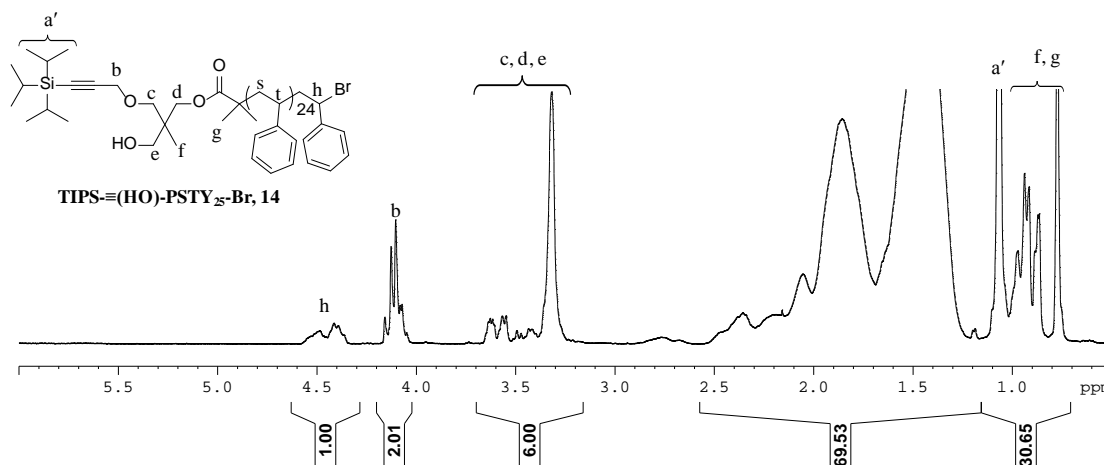


Figure B26: 500 MHz ¹H 1D DOSY NMR spectra in CDCl₃ of TIPS-≡(HO)-PSTY₂₅-Br, 14.

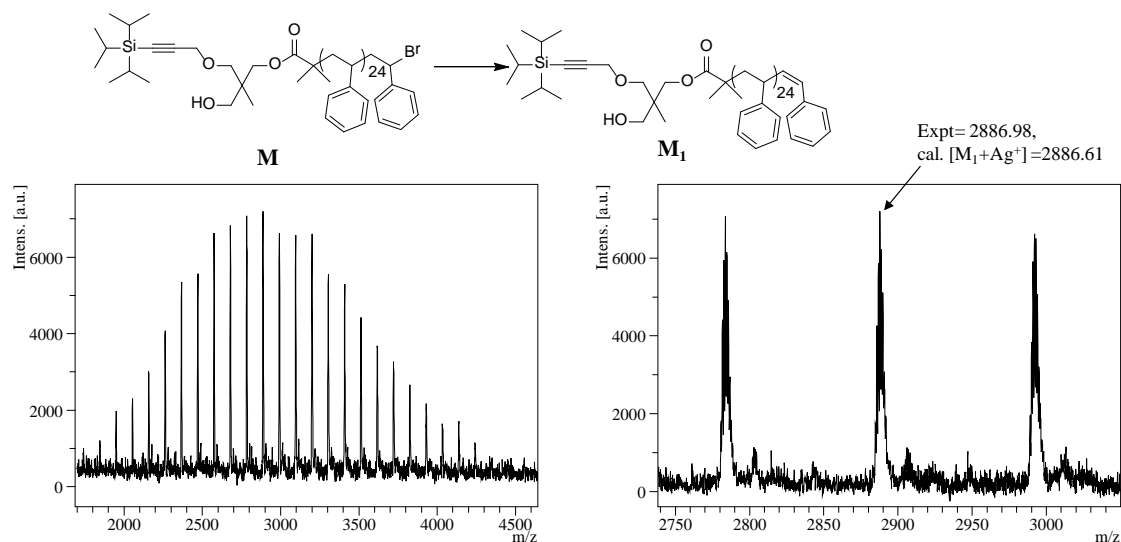


Figure B27: MALDI-ToF mass spectrum acquired in reflectron mode with Ag salt as cationizing agent and DCTB matrix. The full and expanded spectra correspond to **TIPS-≡(HO)-PSTY₂₅-Br, 14**.

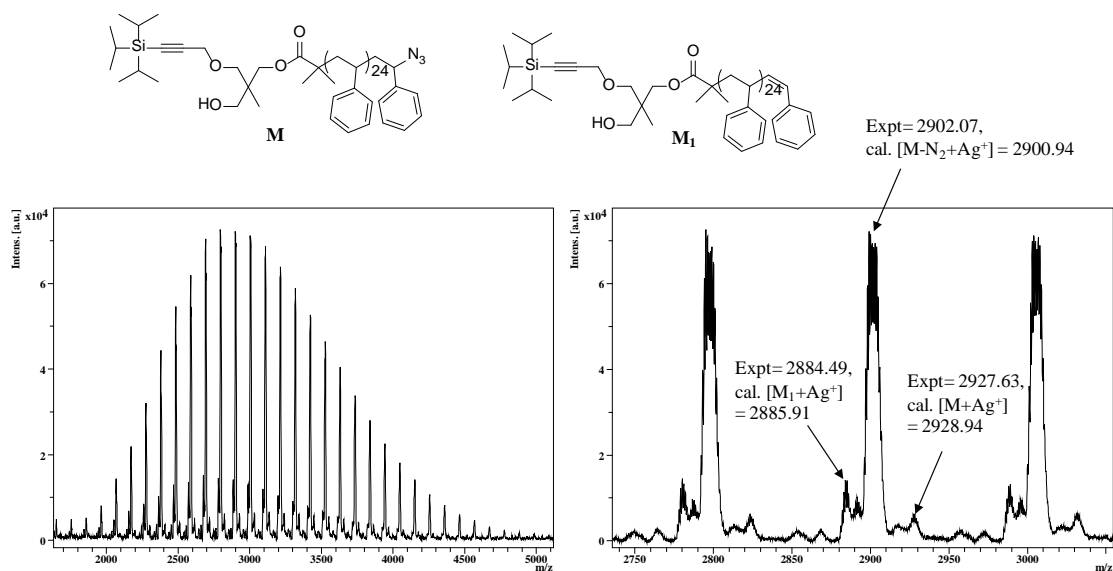


Figure B28: MALDI-ToF mass spectrum acquired in reflectron mode with Ag salt as cationizing agent and DCTB matrix. The full and expanded spectra correspond to **TIPS-≡(HO)-PSTY₂₅-N₃, 15**.

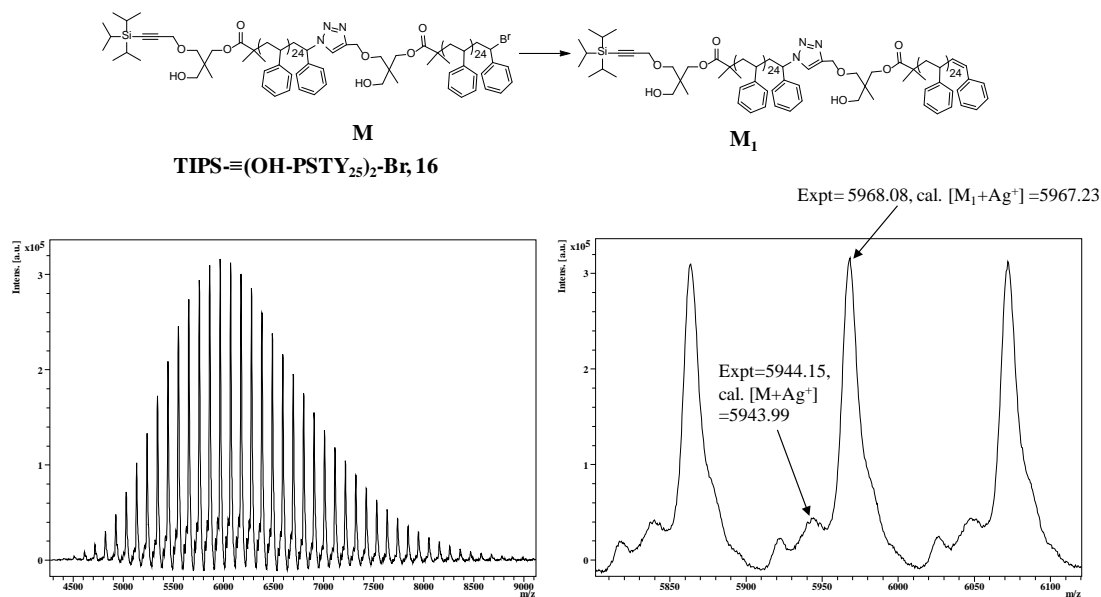


Figure B29: MALDI-ToF mass spectrum acquired in linear mode with Ag salt as cationizing agent and DCTB matrix. The full and expanded spectra correspond to **TIPS-≡(HO-PSTY₂₅)₂-Br, 16**.

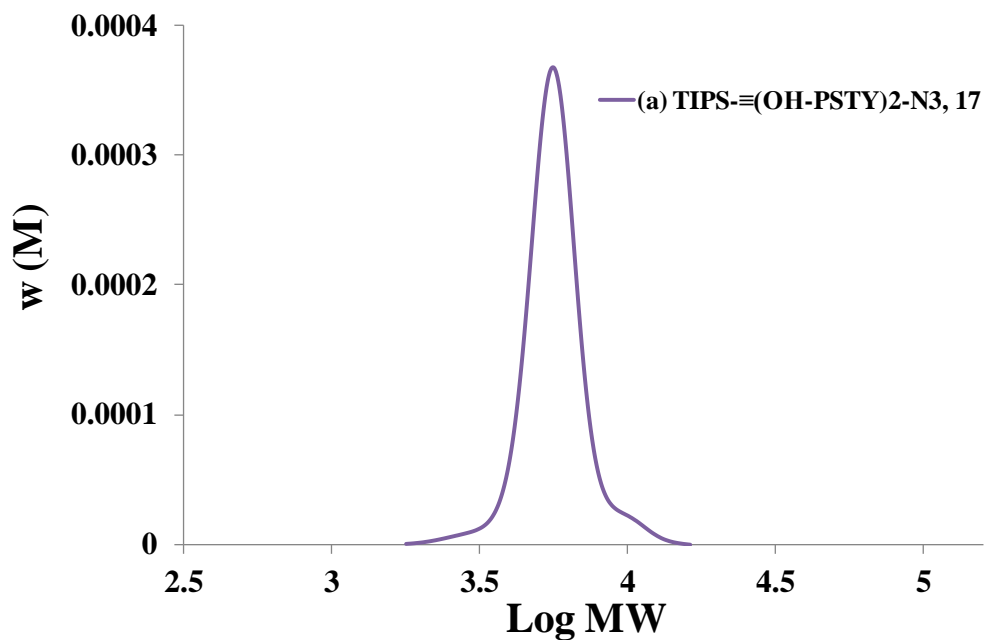


Figure B30: SEC trace of TIPS-≡(OH-PSTY₂₅)₂-N₃, 17. SEC analysis based on polystyrene calibration curve.

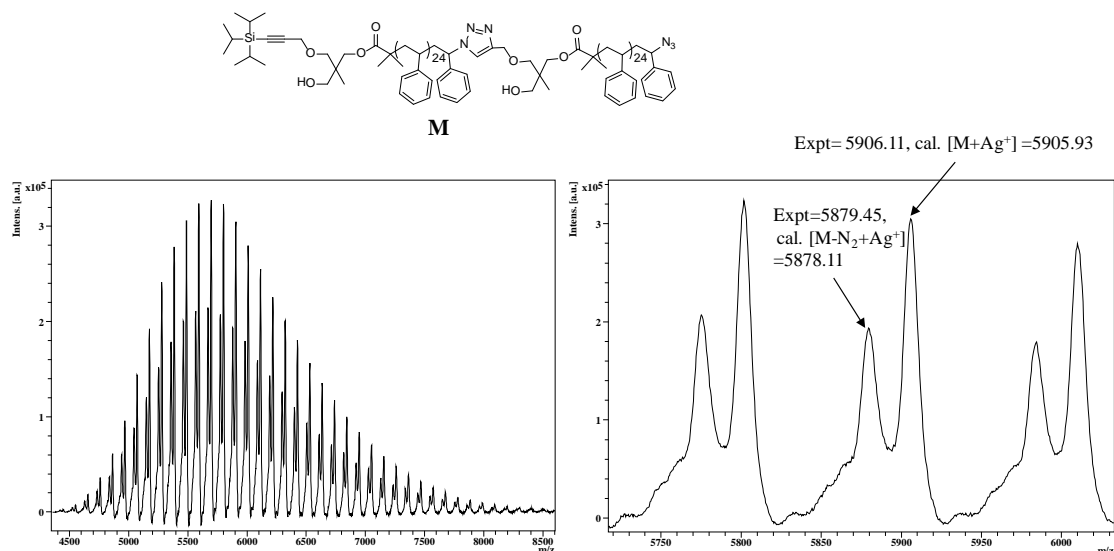


Figure B31: MALDI-ToF mass spectrum acquired in linear mode with Ag salt as cationizing agent and DCTB matrix. The full and expanded spectra correspond to TIPS-≡(HO-PSTY₂₅)₂-N₃, **17**.

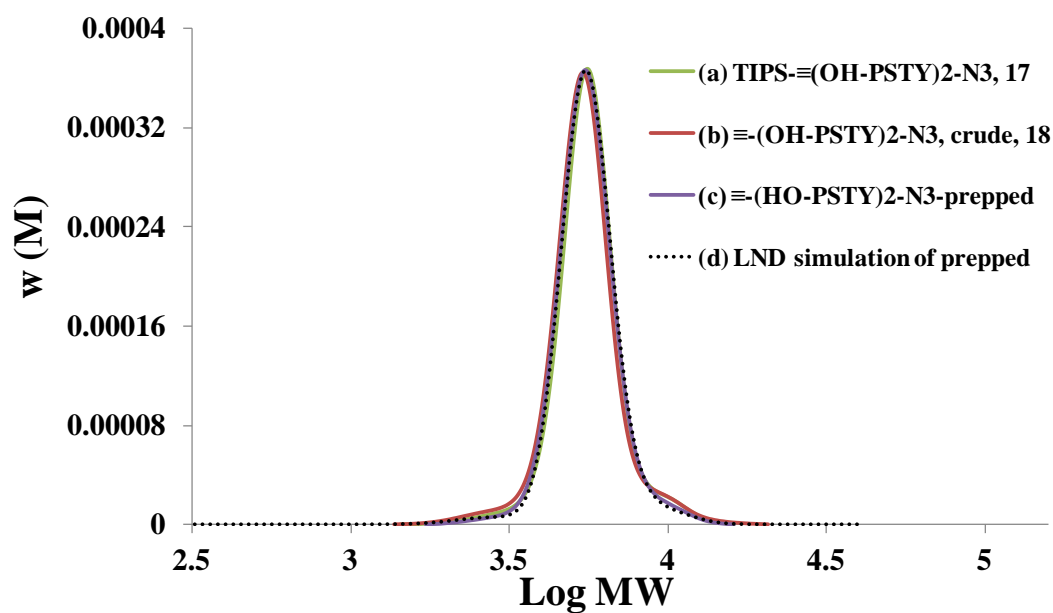


Figure B32: SEC trace of ≡(OH-PSTY₂₅)₂-N₃, **18** before and after prep. SEC analysis based on polystyrene calibration curve.

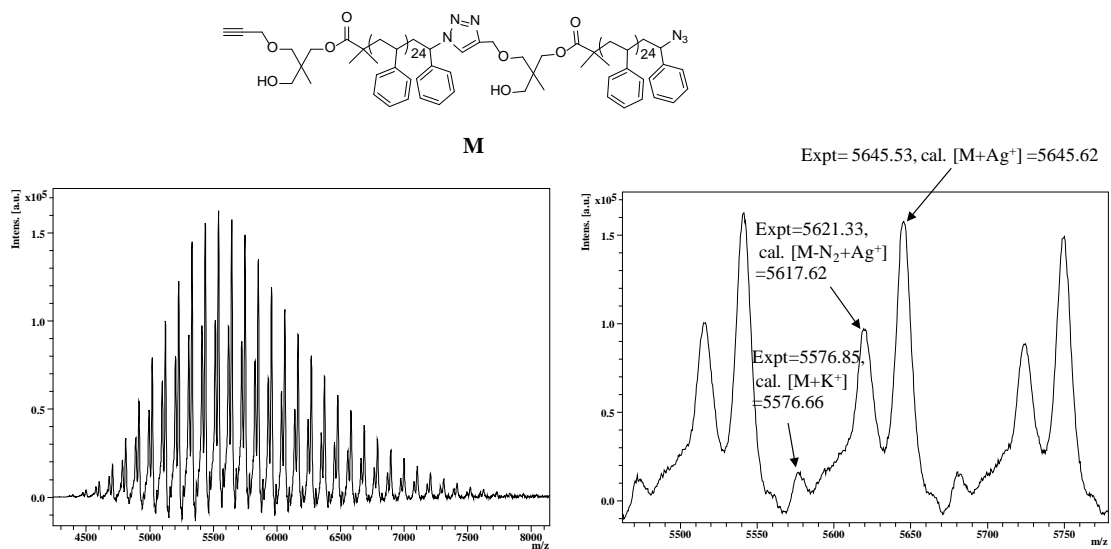


Figure B33: MALDI-ToF mass spectrum acquired in linear mode with Ag salt as cationizing agent and DCTB matrix. The full and expanded spectra correspond to $\equiv(HO-PSTY_{25})_2-N_3$, **18**.

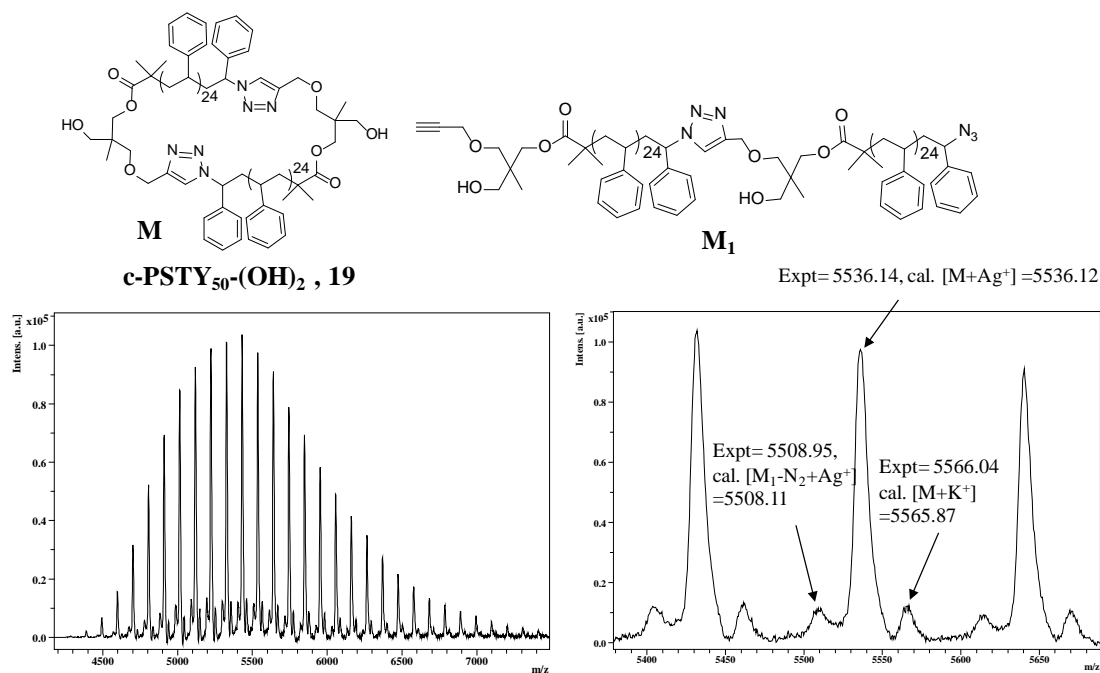


Figure B34: MALDI-ToF mass spectrum acquired in linear mode with Ag salt as cationizing agent and DCTB matrix. The full and expanded spectra correspond to $c-PSTY-(OH)_2$ **19**.

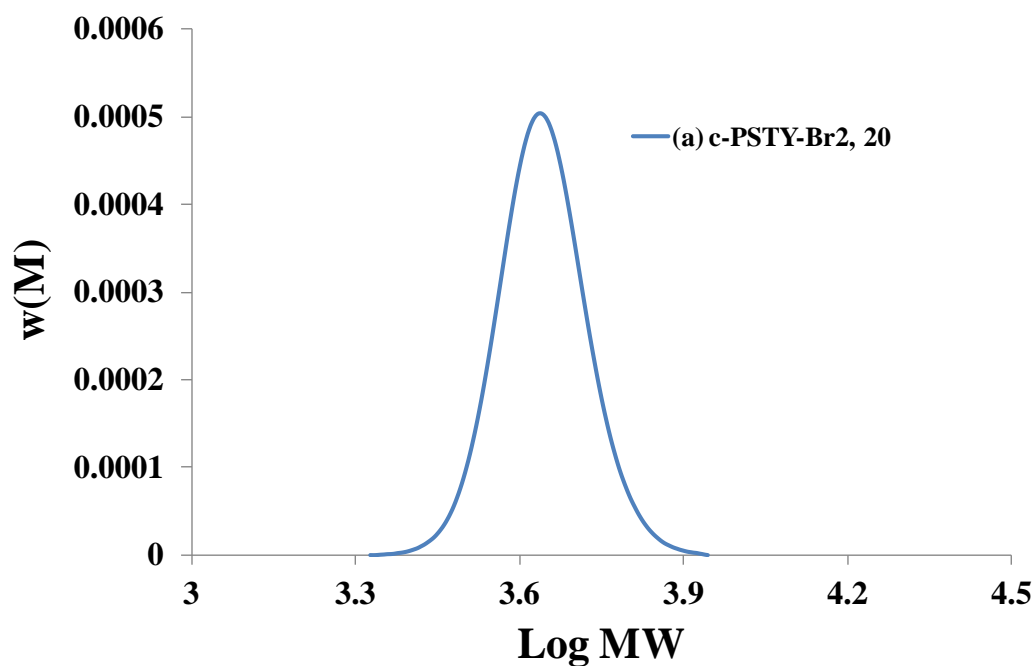


Figure B35: SEC trace of c-PSTY₅₀-Br₂, **20**. SEC analysis based on polystyrene calibration curve.

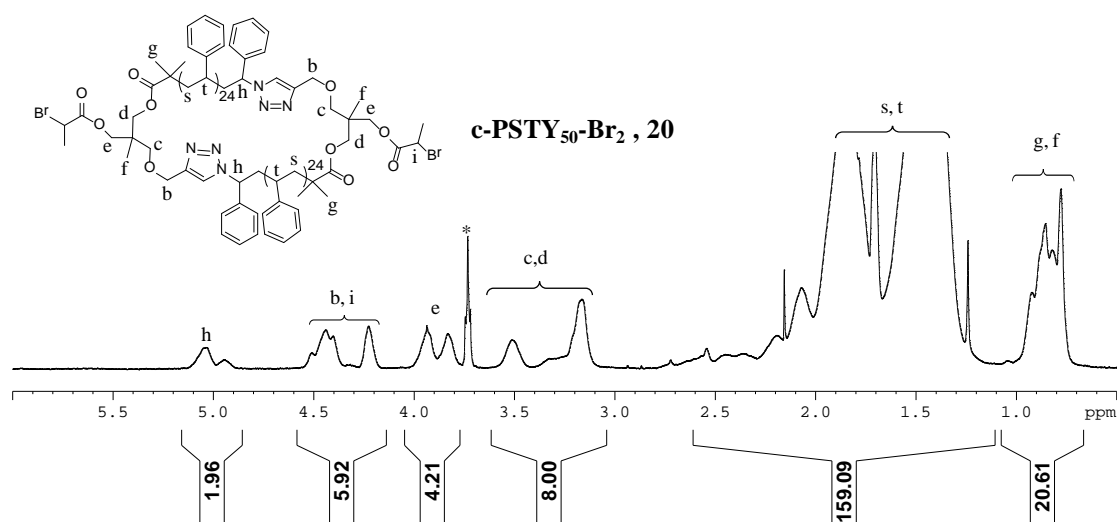


Figure B36: 500 MHz ¹H 1D DOSY NMR spectra in CDCl₃ of c-PSTY₅₀-Br₂, **20**.

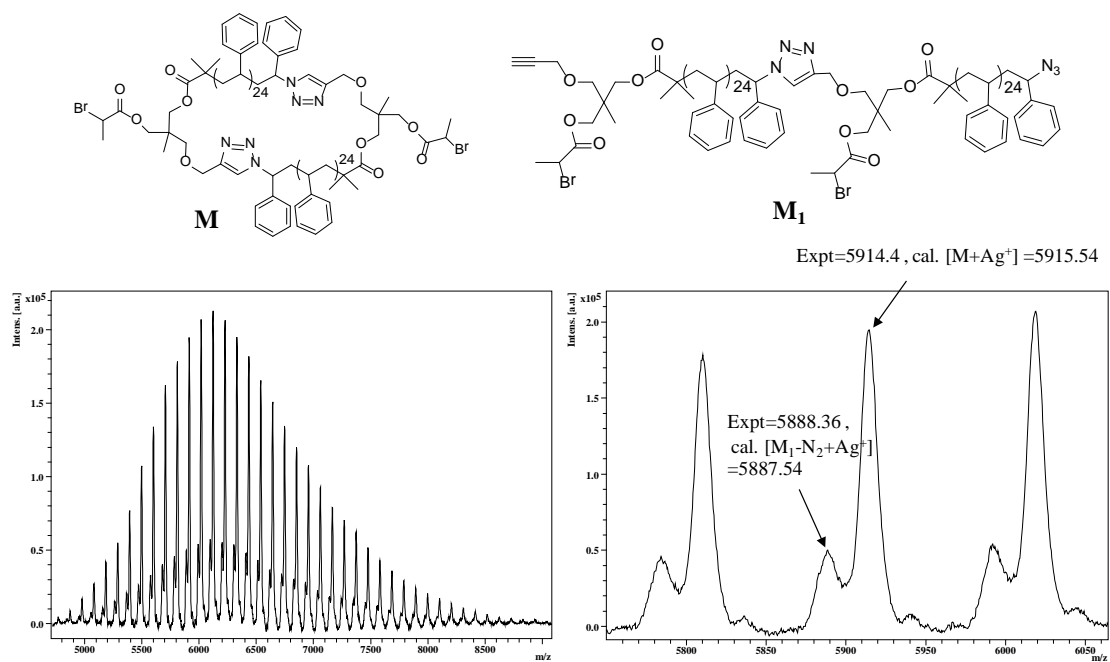


Figure B37: MALDI-ToF mass spectrum acquired in linear mode with Ag salt as cationizing agent and DCTB matrix. The full and expanded spectra correspond to c-PSTY₅₀-Br₂, **20**.

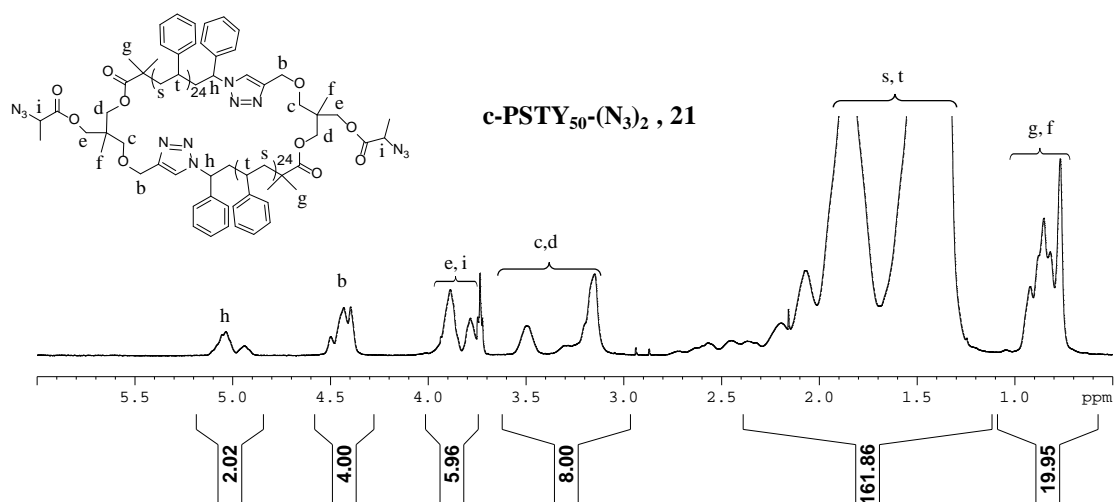


Figure B38: 500 MHz ¹H 1D DOSY NMR spectra in CDCl₃ of c-PSTY-(N₃)₂, **21**.

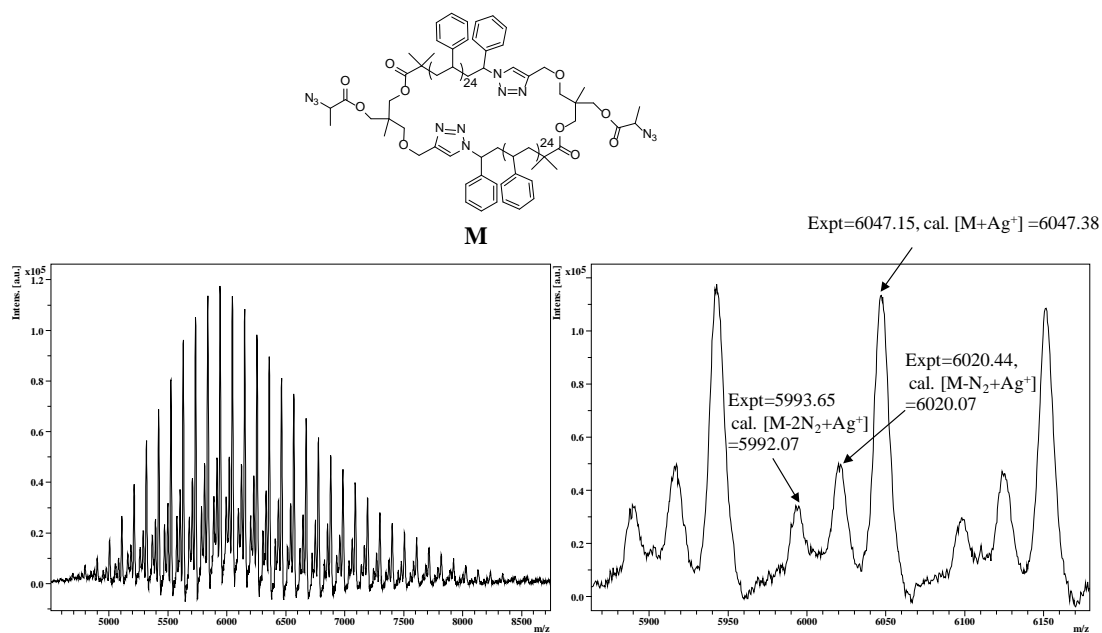


Figure B39: MALDI-ToF mass spectrum acquired in linear mode with Ag salt as cationizing agent and DCTB matrix. The full and expanded spectra correspond to c-PSTY₅₀-(N₃)₂, **21**.

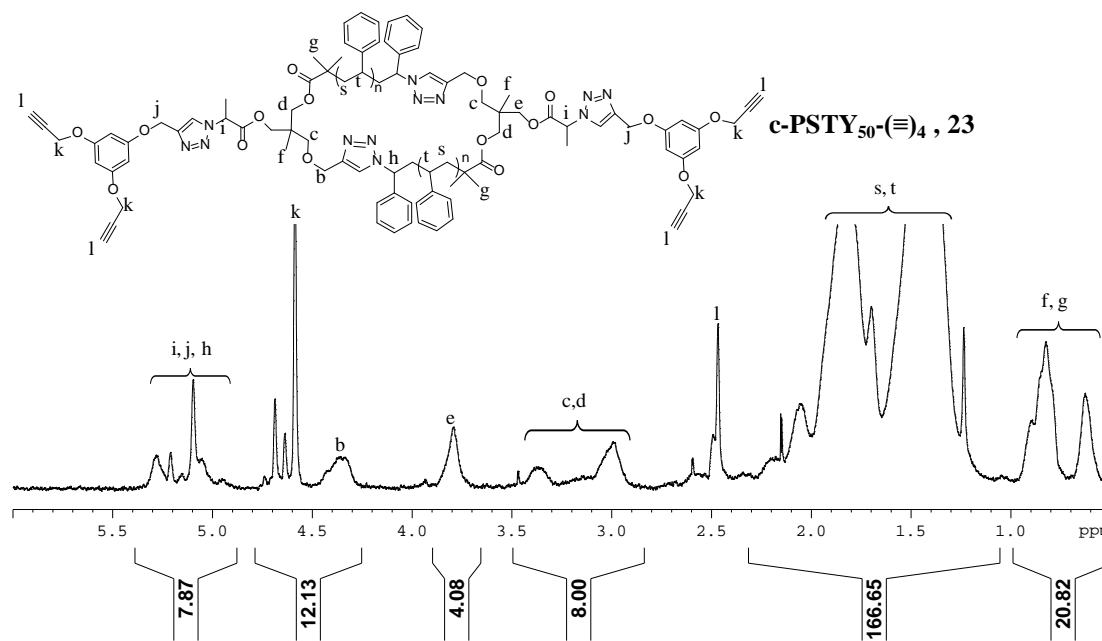


Figure B40: 500 MHz ¹H 1D DOSY NMR spectra in CDCl₃ of c-PSTY-(≡)₄, **23**.

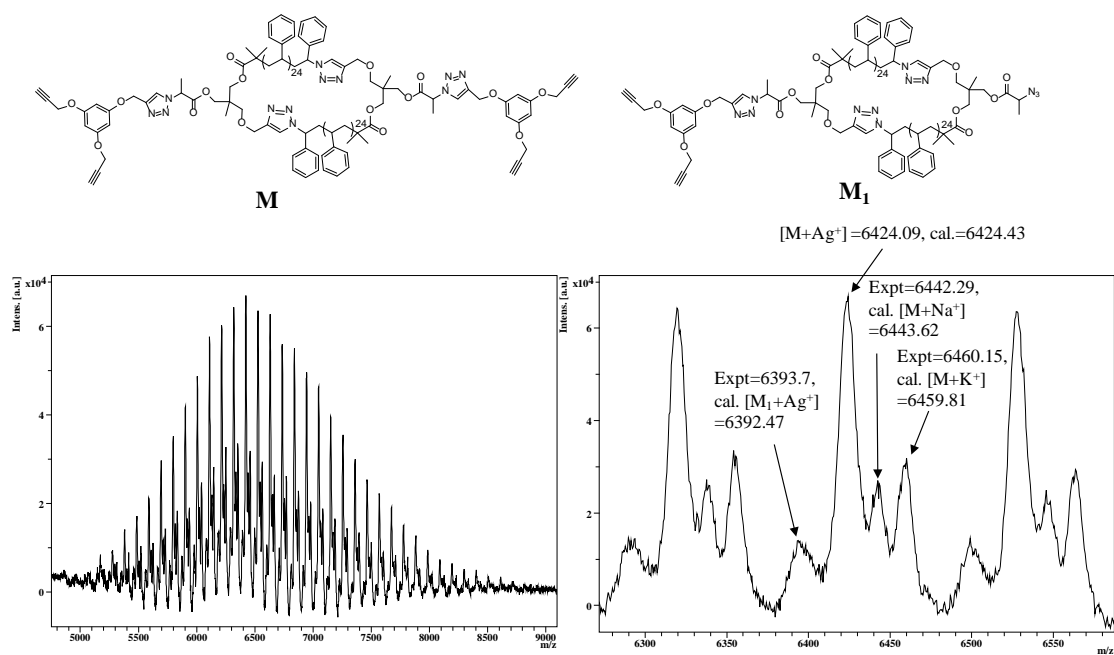


Figure B41: MALDI-ToF mass spectrum acquired in linear mode with Ag salt as cationizing agent and DCTB matrix. The full and expanded spectra correspond to c-PSTY₅₀-(≡)₄, **23**.

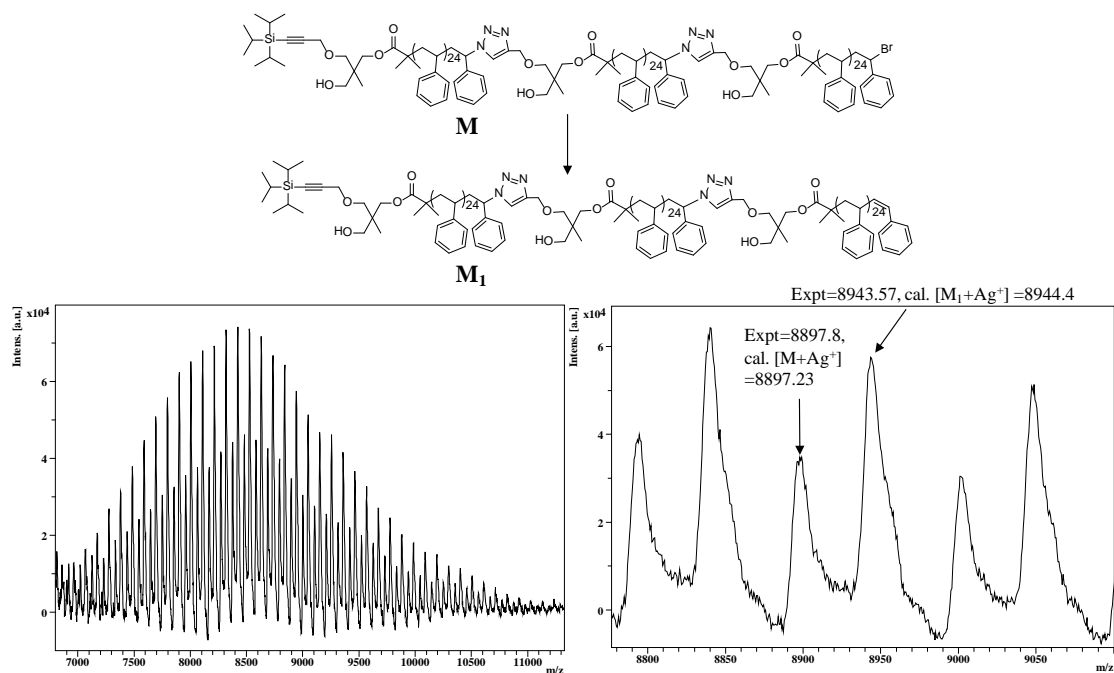


Figure B42: MALDI-ToF mass spectrum acquired in linear mode with Ag salt as cationizing agent and DCTB matrix. The full and expanded spectra correspond to TIPS-≡(OH-PSTY₂₅)₃-Br, **24**.

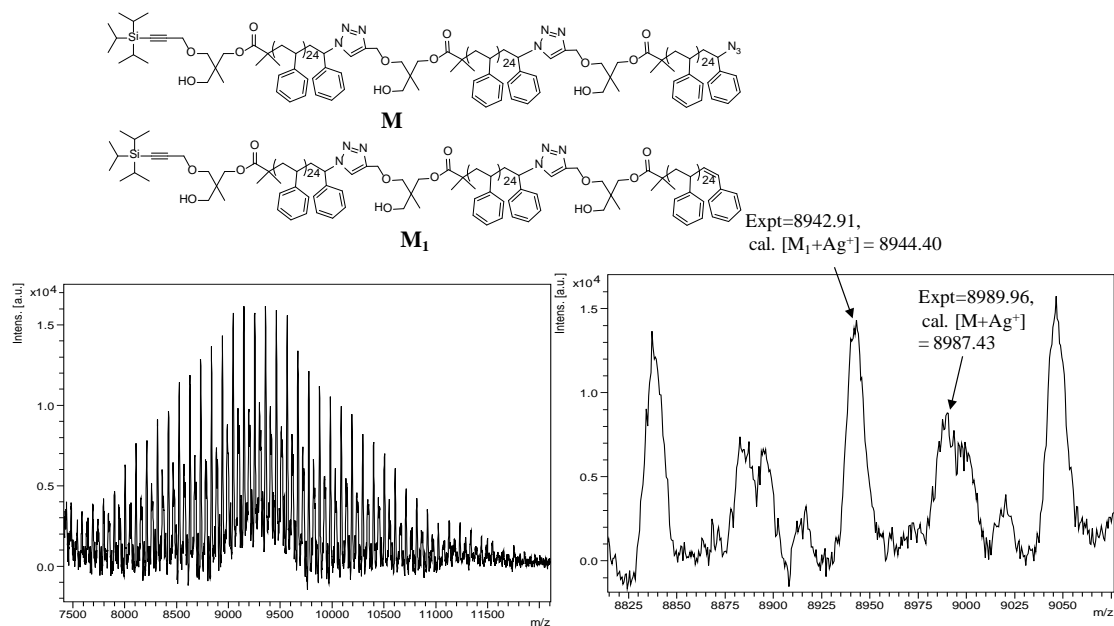


Figure B43: MALDI-ToF mass spectrum acquired in linear mode with Ag salt as cationizing agent and DCTB matrix. The full and expanded spectra correspond to TIPS-≡(OH-PSTY)₂₅-N₃, **25**.

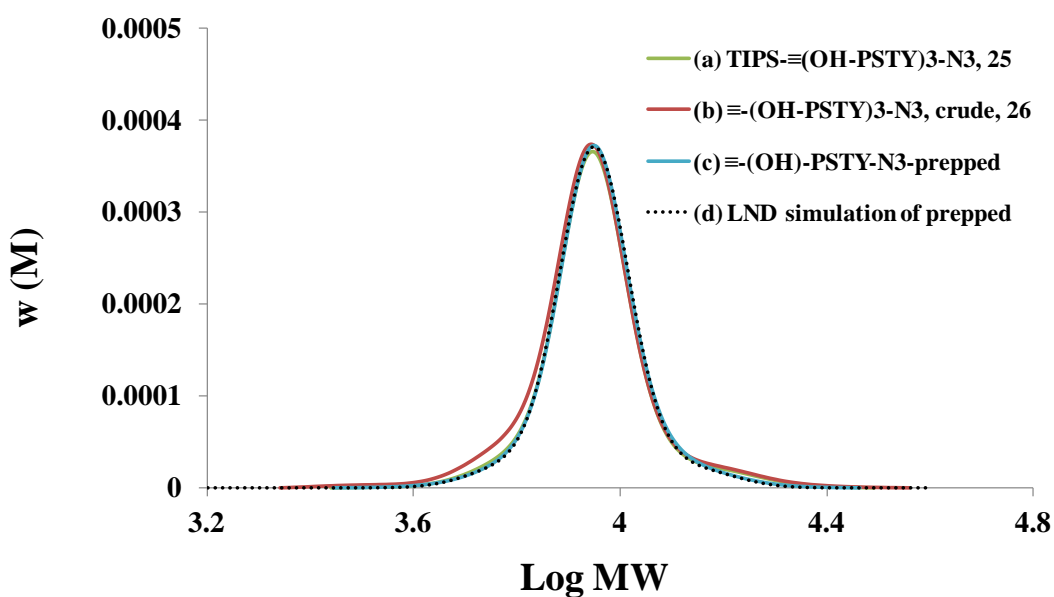


Figure B44: SEC of molecular weight distributions (MWDs) for TIPS-≡(OH-PSTY)₂₅-N₃ crude, **25**. SEC analysis based on polystyrene calibration curve.

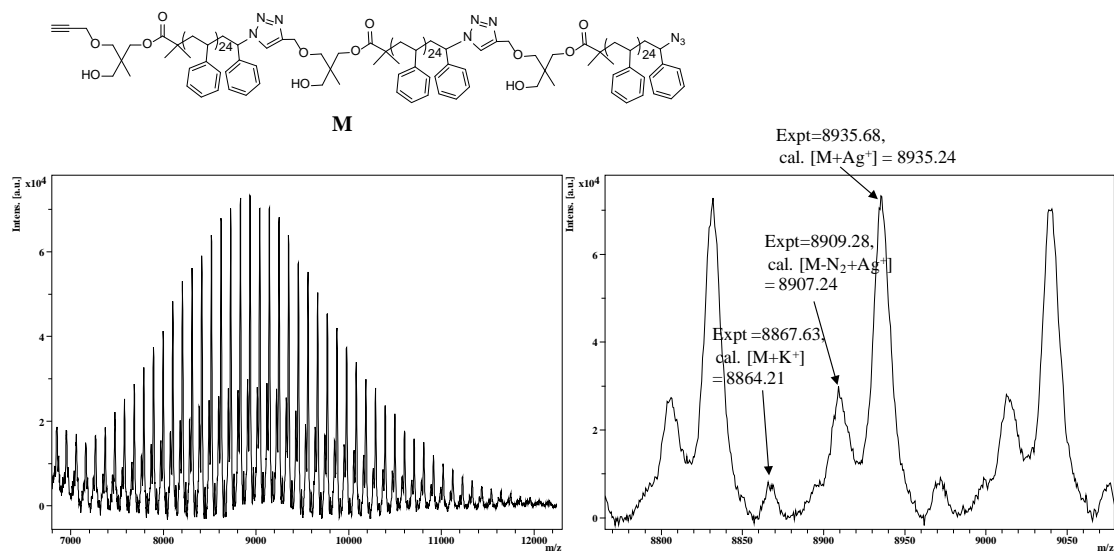


Figure B45: MALDI-ToF mass spectrum acquired in linear mode with Ag salt as cationizing agent and DCTB matrix. The full and expanded spectra correspond to $\equiv(\text{OH-PSTY}_{25})_3\text{-N}_3$, **26**.

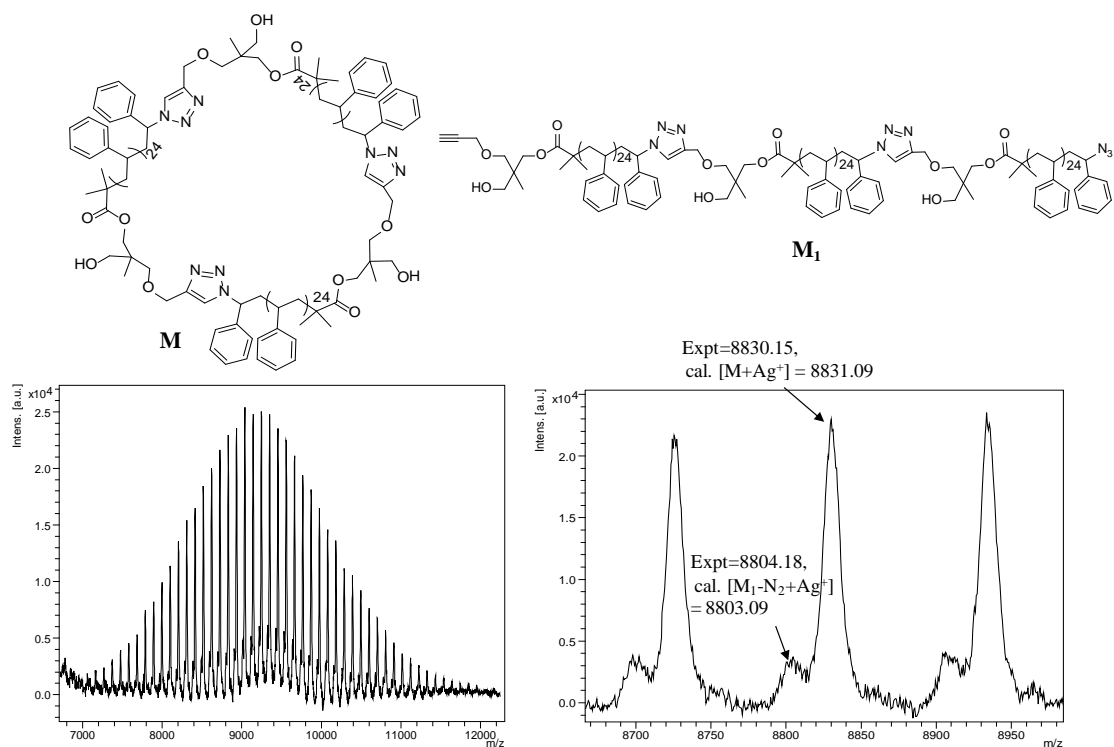


Figure B46: MALDI-ToF mass spectrum acquired in linear mode with Ag salt as cationizing agent and DCTB matrix. The full and expanded spectra correspond to $c\text{-PSTY}_{75}\text{-(OH)}_3$, **27**.

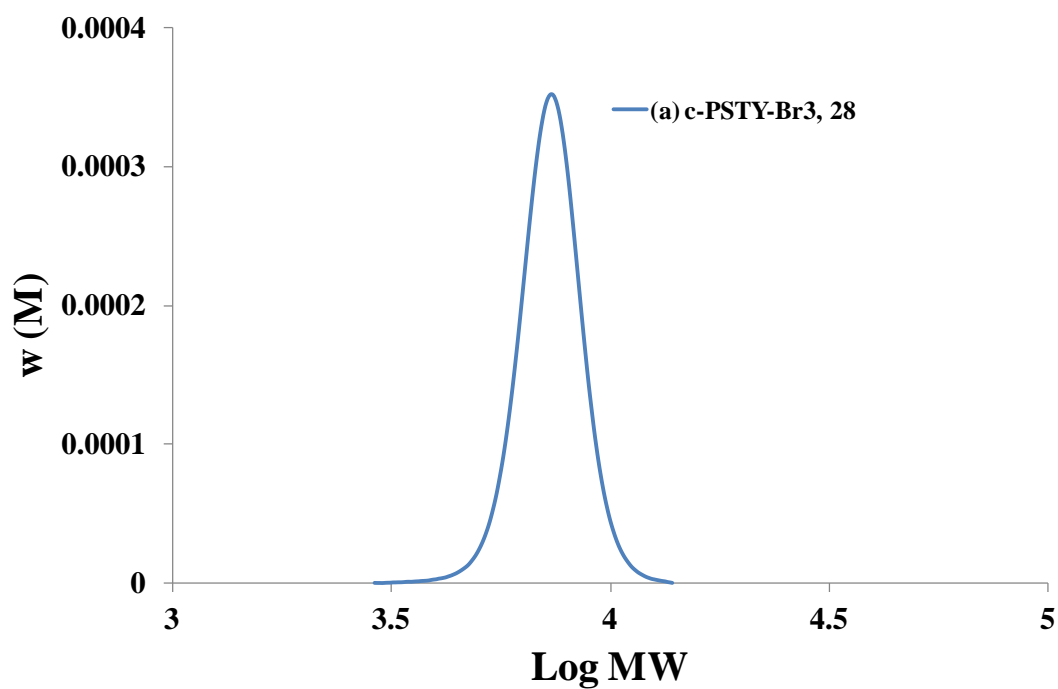


Figure B47: SEC of molecular weight distributions (MWDs) for c-PSTY₇₅-Br₃, **28**. SEC analysis based on polystyrene calibration curve.

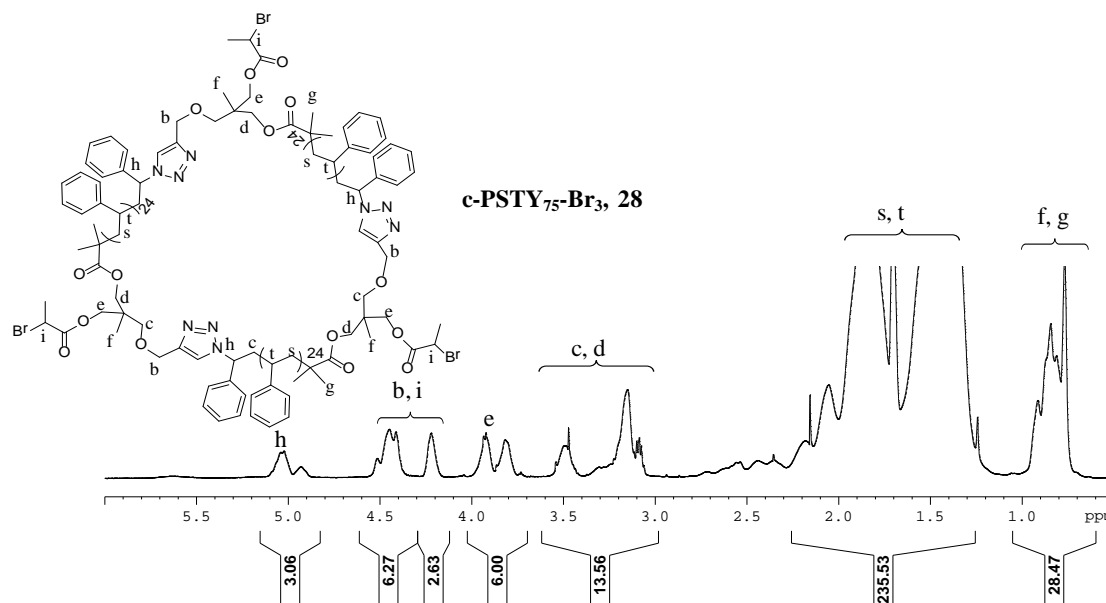


Figure B48: 500 MHz ¹H 1D DOSY NMR spectra in CDCl₃ of c-PSTY₇₅-Br₃, **28**.

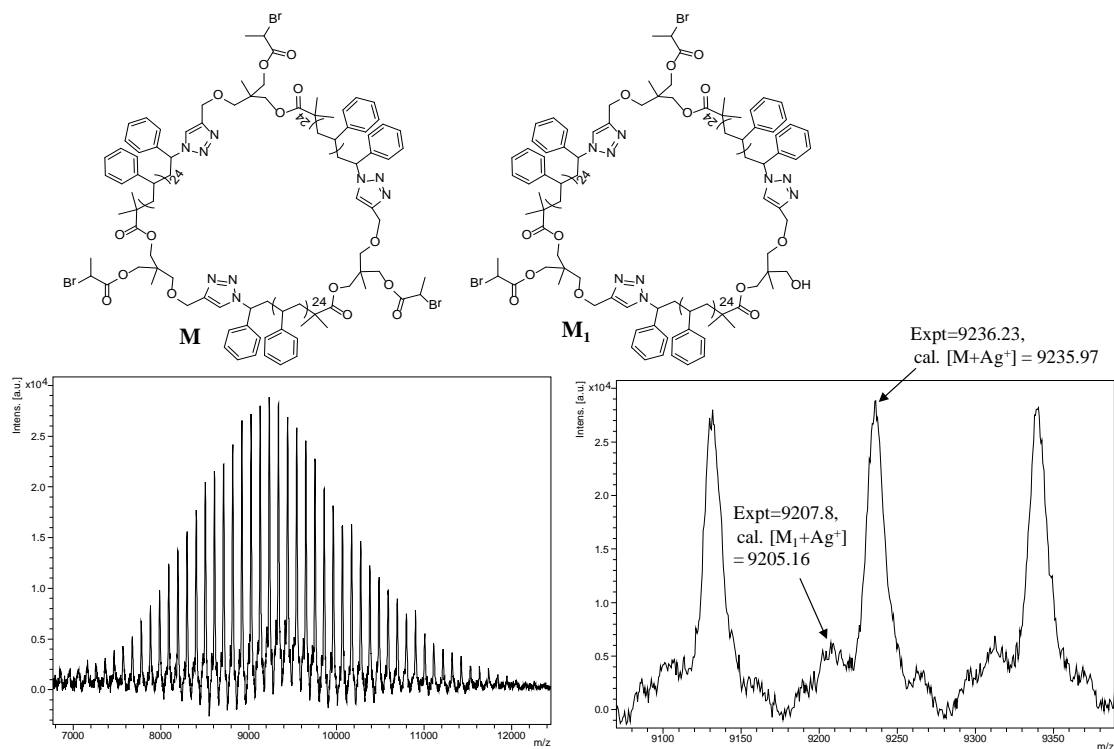


Figure B49: MALDI-ToF mass spectrum acquired in linear mode with Ag salt as cationizing agent and DCTB matrix. The full and expanded spectra correspond to c-PSTY₇₅-Br₃, **28**.

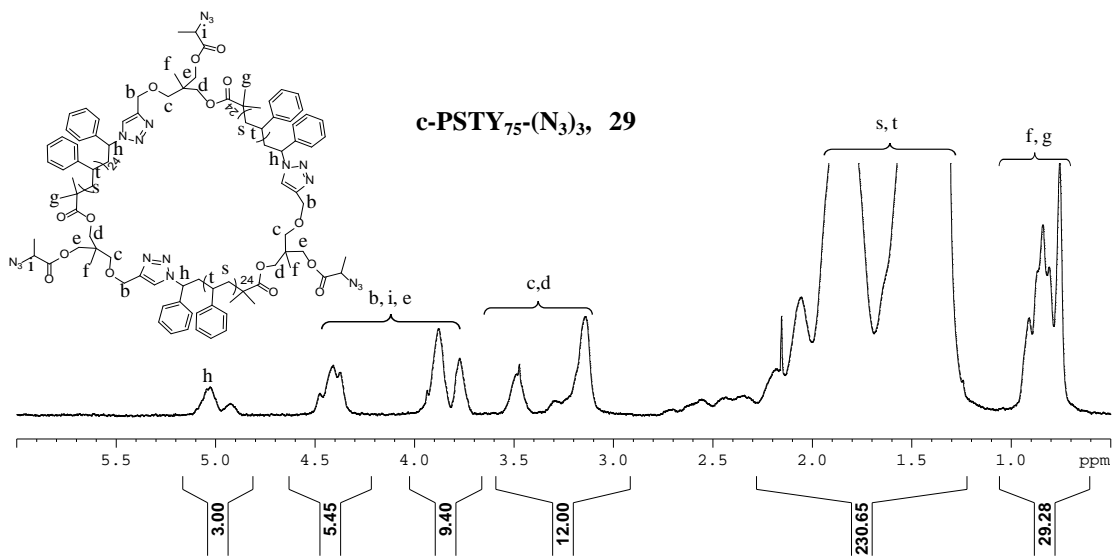


Figure B50: 500 MHz ¹H 1D DOSY NMR spectra in CDCl₃ of c-PSTY₇₅-(N₃)₃, **29**.

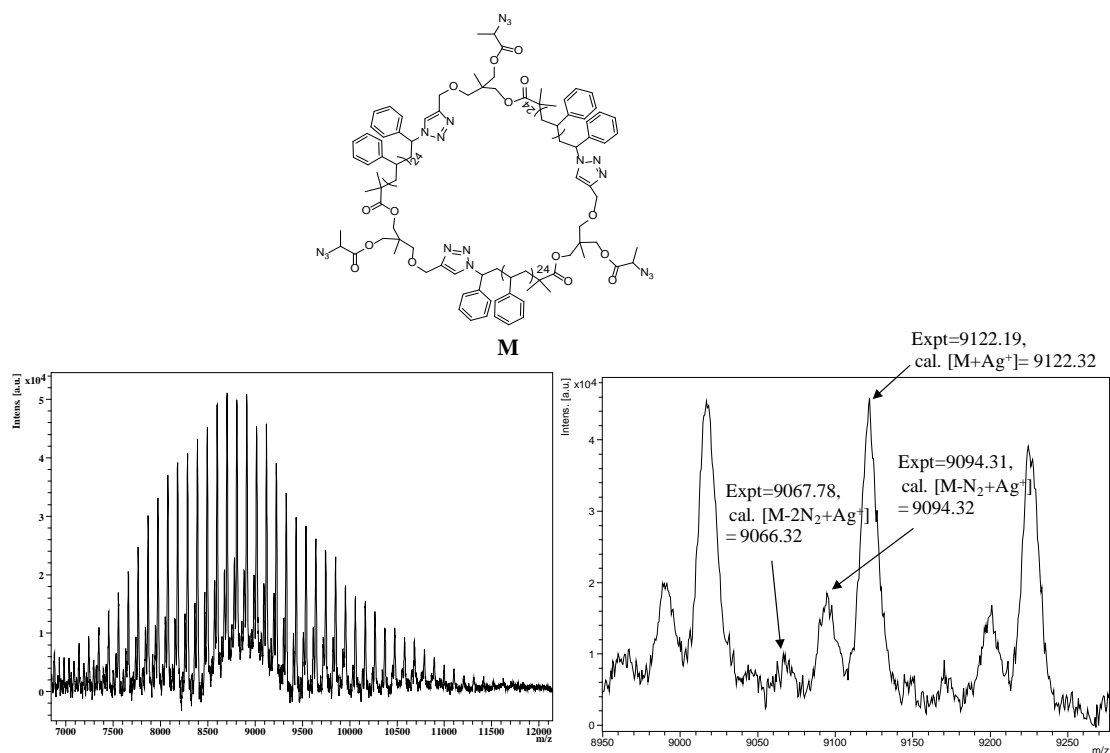


Figure B51: MALDI-ToF mass spectrum acquired in linear mode with Ag salt as cationizing agent and DCTB matrix. The full and expanded spectra correspond to $c\text{-PSTY}_{75}\text{-(N}_3)_3$, **29**.

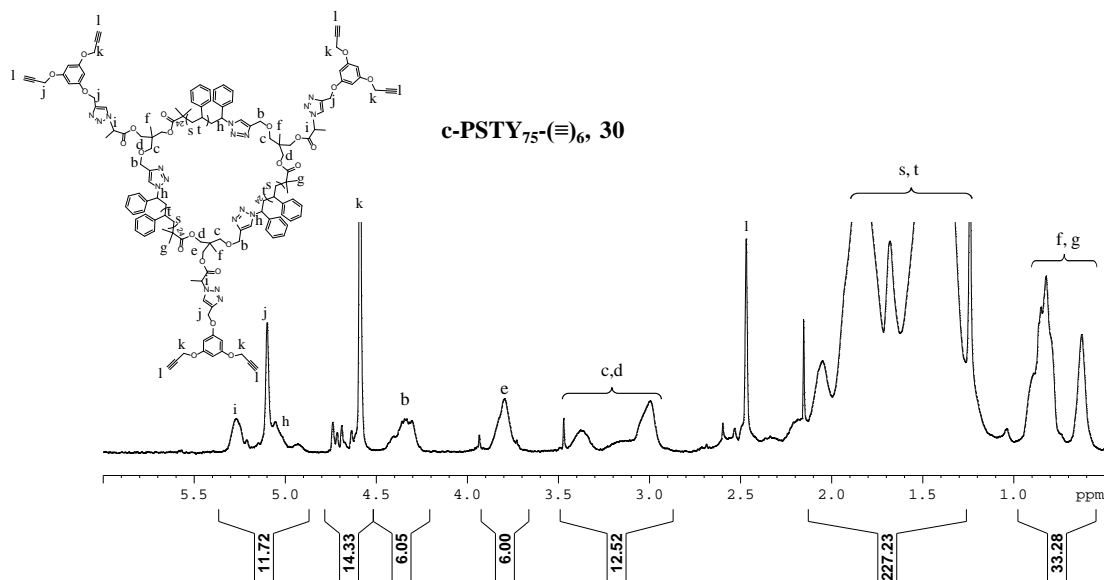


Figure B52: 500 MHz ^1H 1D DOSY NMR spectra in CDCl_3 of $c\text{-PSTY}_{75}\text{-(}\equiv\text{)}_6$, **30**.

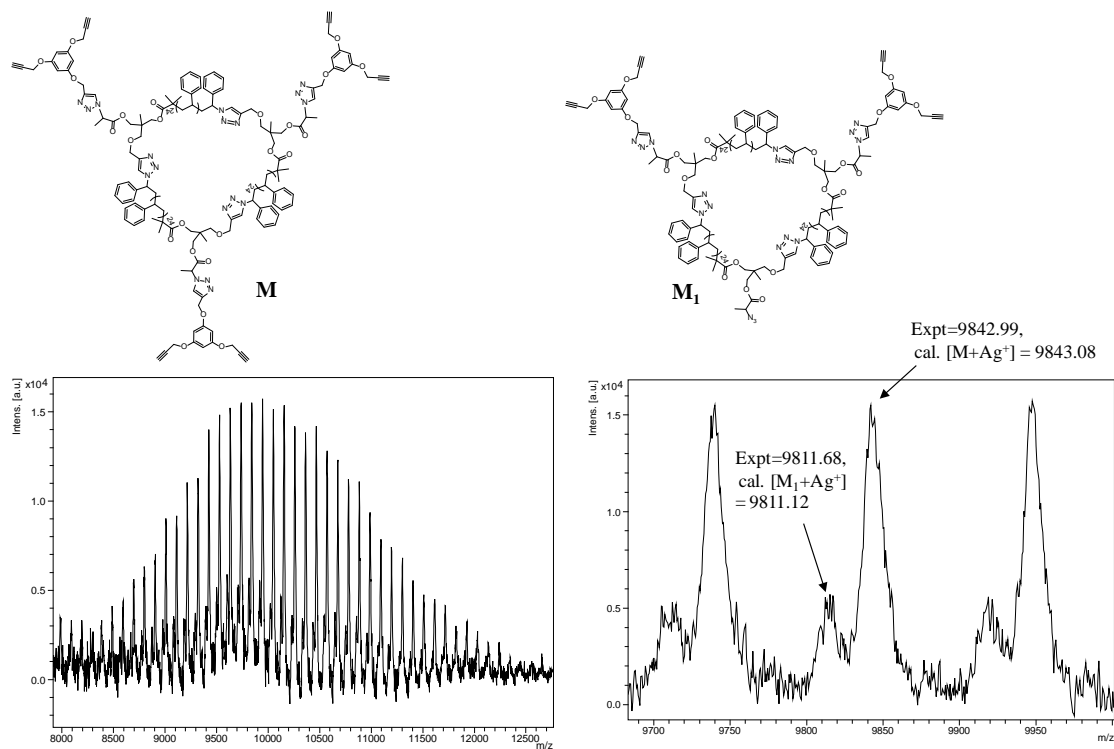


Figure B53: MALDI-ToF mass spectrum acquired in linear mode with Ag salt as cationizing agent and DCTB matrix. The full and expanded spectra correspond to *c*-PSTY₇₅-(≡)₆, **30**.

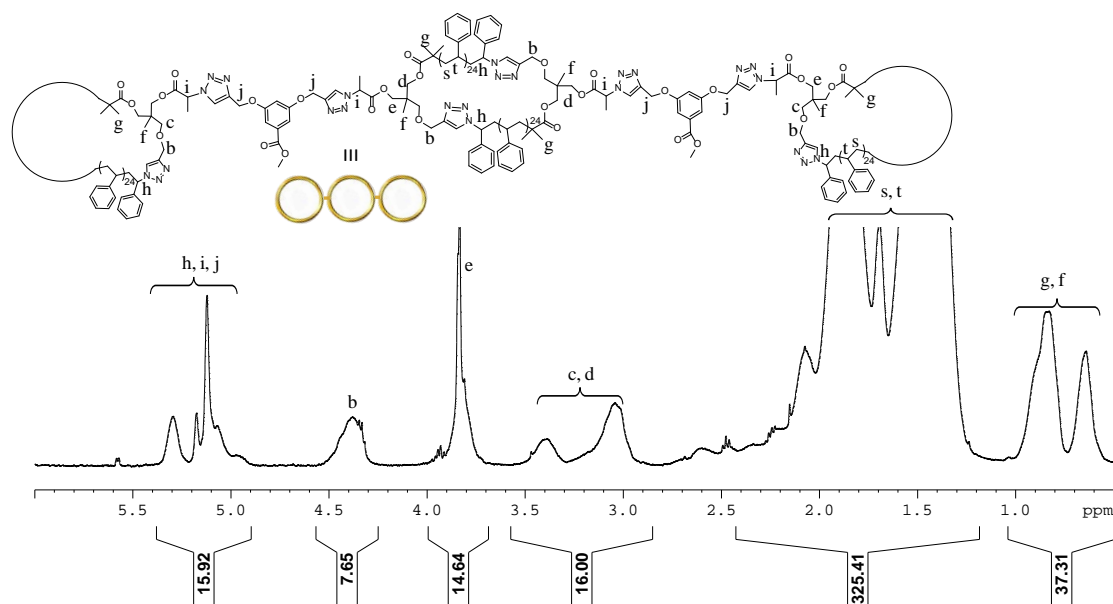


Figure B54: 500 MHz ¹H 1D DOSY NMR spectra in CDCl₃ of *c*-PSTY₇₅-(≡)₆, **31**.

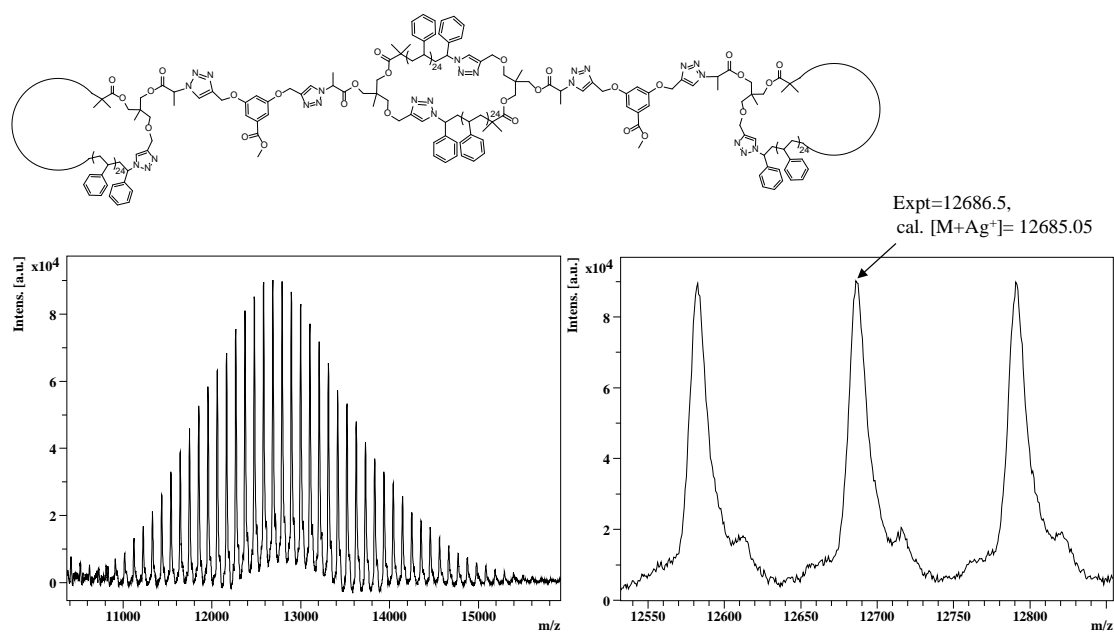


Figure B55: MALDI-ToF mass spectrum acquired in linear mode with Ag salt as cationizing agent and DCTB matrix. The full and expanded spectra correspond to Spiro (c-PSTY)₃, **31**.

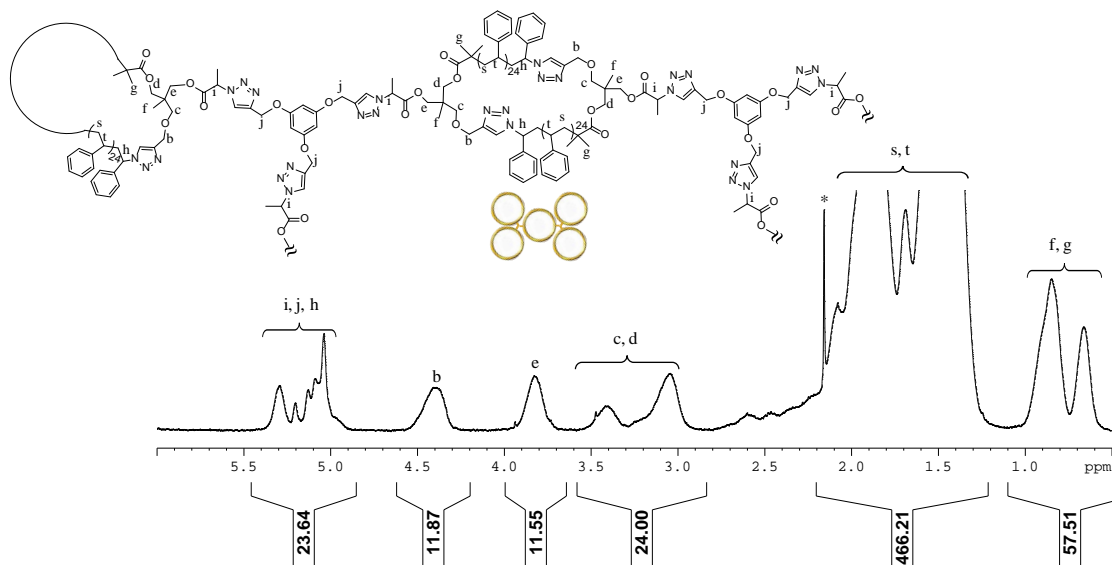


Figure B56: 500 MHz ¹H 1D DOSY NMR spectra in CDCl₃ of dendrimer (c-PSTY)₅, **32**. * Acetone peak.

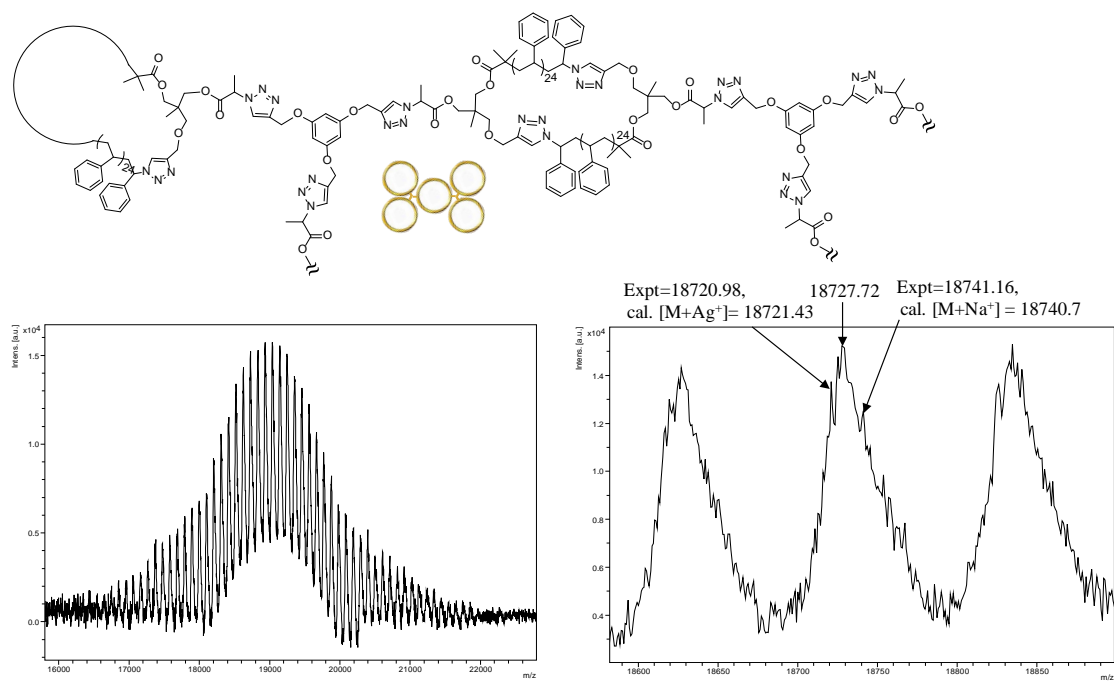


Figure B57: MALDI-ToF mass spectrum acquired in linear mode with Ag salt as cationizing agent and DCTB matrix. The full and expanded spectra correspond to Spiro (c-PSTY)₅, **32**.

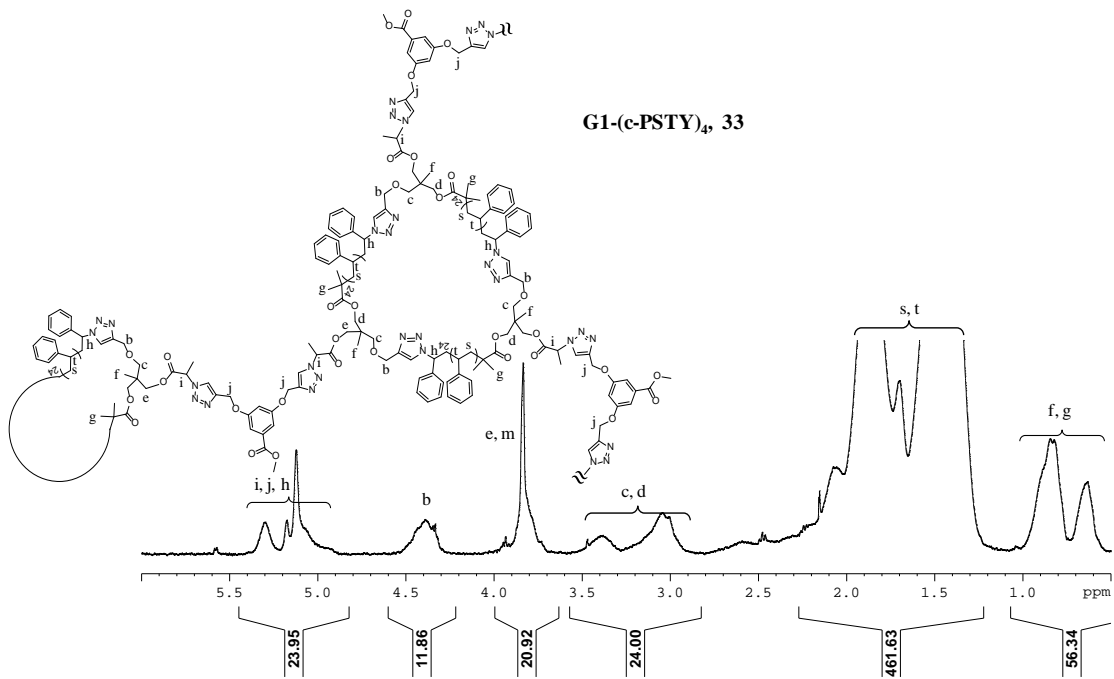


Figure B58: 500 MHz ¹H 1D DOSY NMR spectra in CDCl₃ of G1 (c-PSTY)₄, **33**.

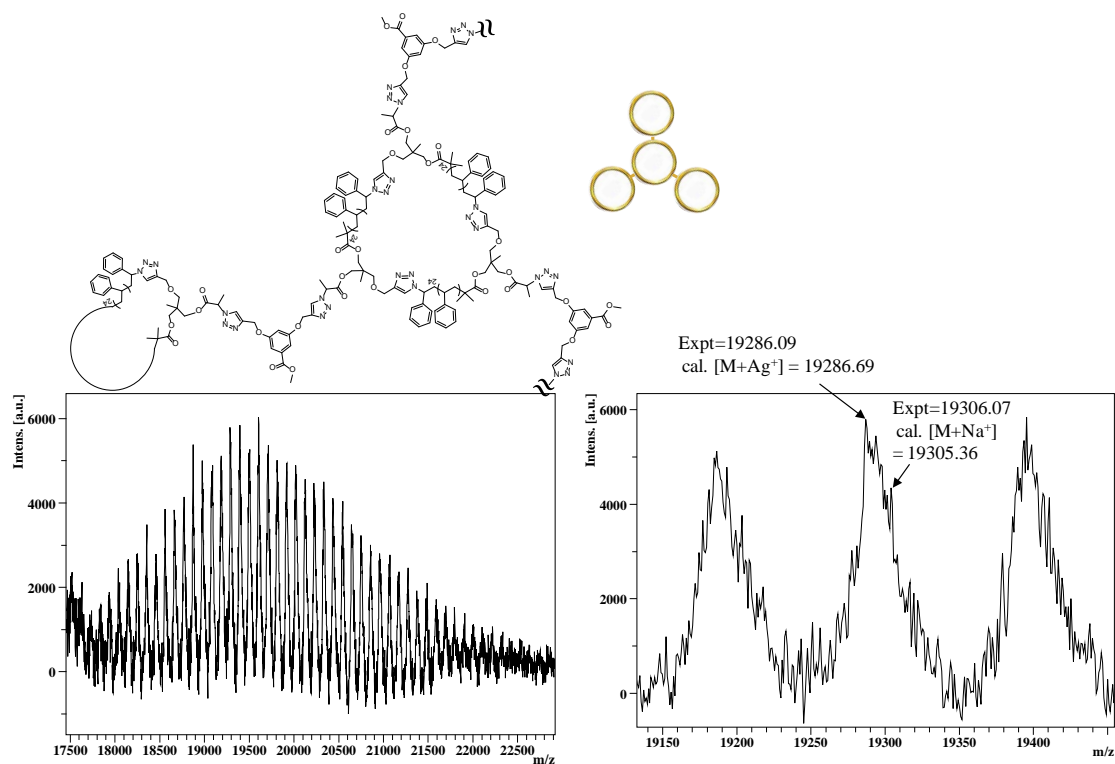


Figure B59: MALDI-ToF mass spectrum acquired in linear mode with Ag salt as cationizing agent and DCTB matrix. The full and expanded spectra correspond to Spiro (c-PSTY)₄, **33**.

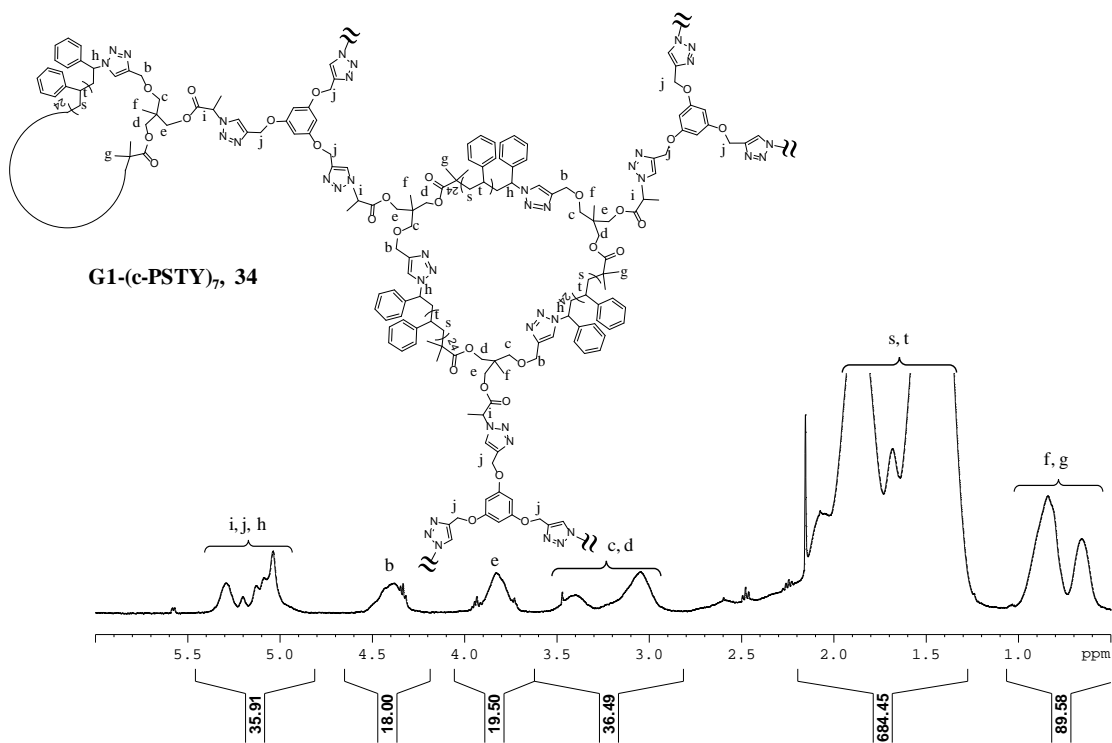


Figure B60: 500 MHz ¹H 1D DOSY NMR spectra in CDCl₃ of G1 (c-PSTY)₇, **34**.

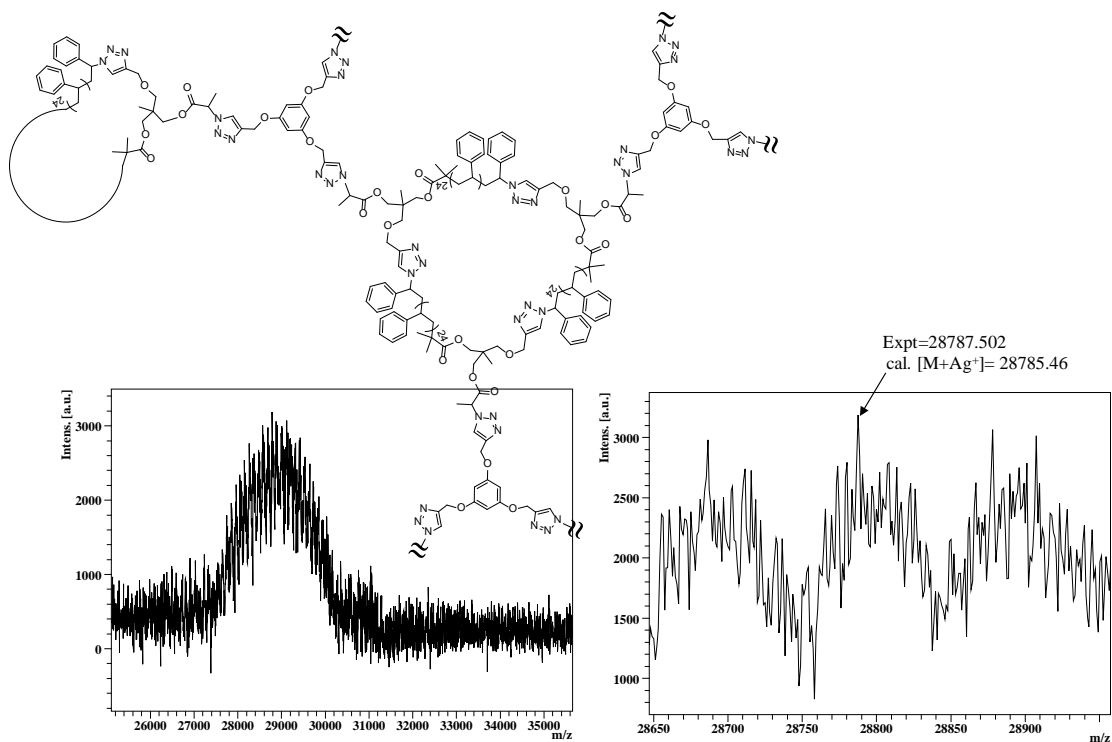
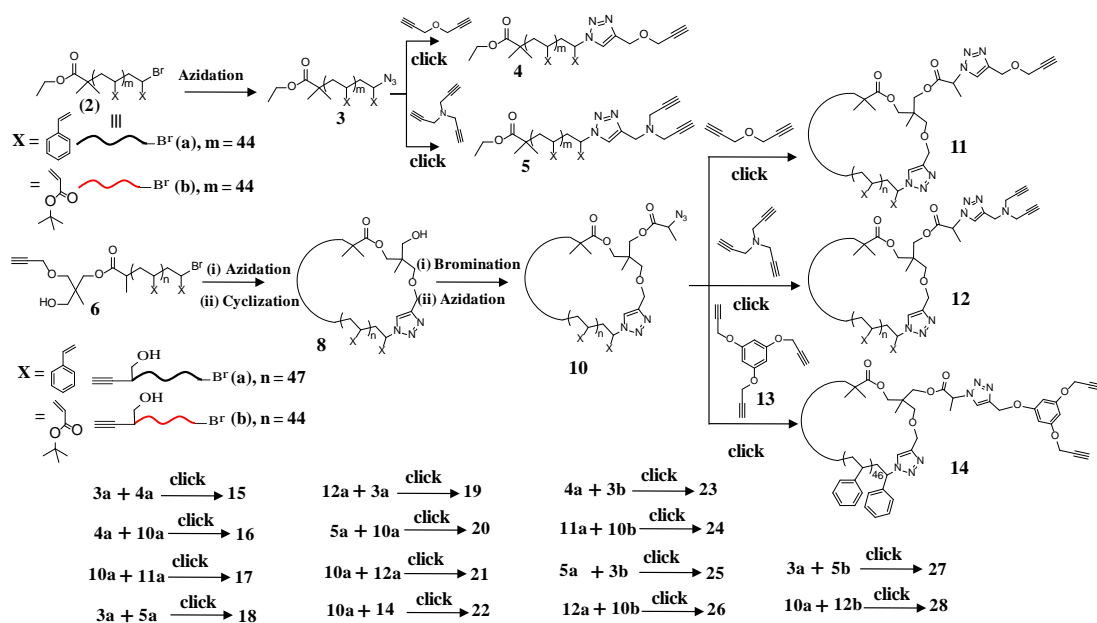


Figure B61: MALDI-ToF mass spectrum acquired in linear mode with Ag salt as cationizing agent and DCTB matrix. The full and expanded spectra correspond to Spiro (c-PSTY)₇, 34.

Appendix C



Scheme C1: Synthetic route for the preparation of functional linear and cyclic polymers and their complex architectures.

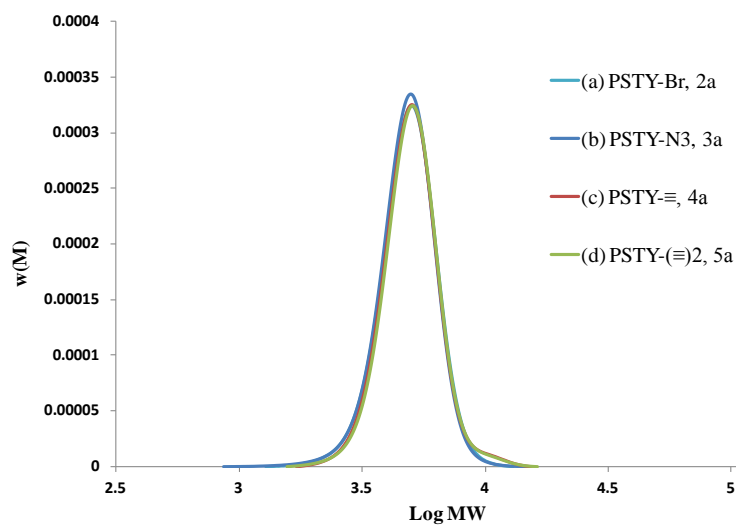


Figure C1: SEC chromatograms of functional linear PSTY (a) PSTY₄₄-Br, **2a**; (b) PSTY₄₄-N₃, **3a**, (c) PSTY₄₄-≡, **4a** and (d) PSTY₄₄-(≡)₂, **5a**. All chromatograms are based on PSTY calibration curve.

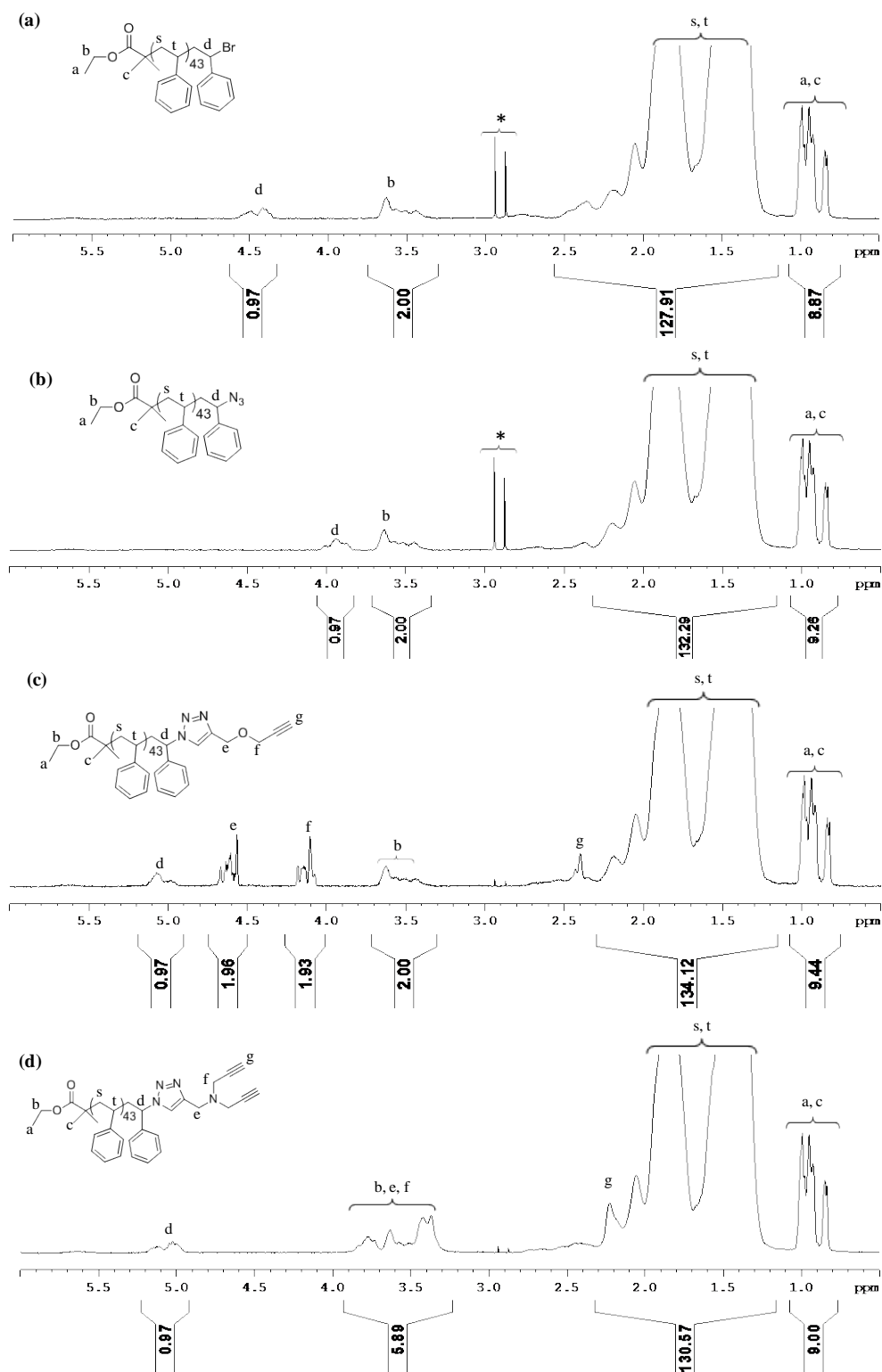


Figure C2. 500 MHz ^1H 1D DOSY NMR spectra in CDCl_3 of (a) PSTY₄₄-Br, **2a**. (b) PSTY₄₄-N₃, **3a**, (c) PSTY₄₄-≡, **4a** and (d) PSTY₄₄-(≡)₂, **5a**. *small molecule impurities.

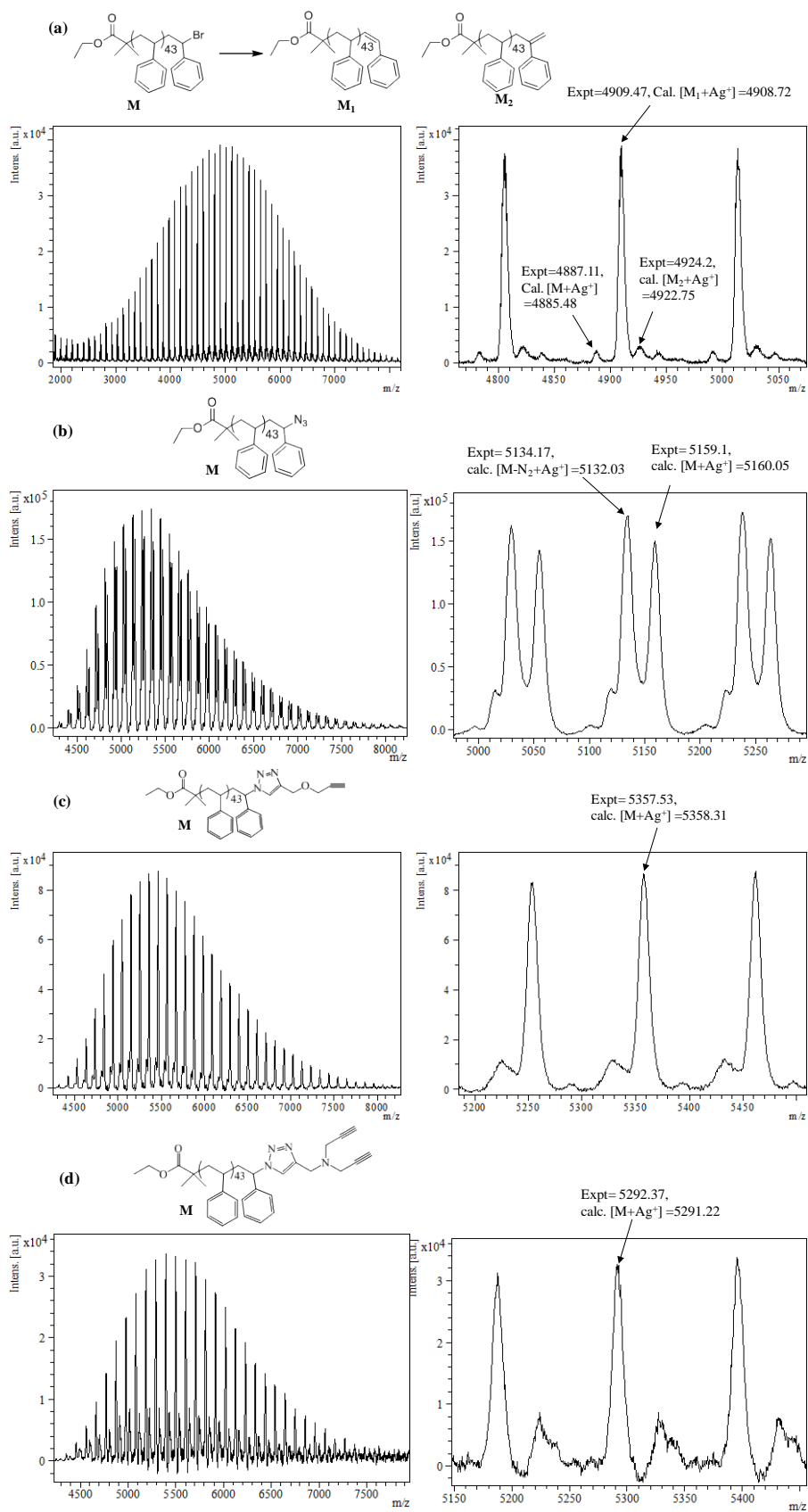


Figure C3: MALDI-ToF mass spectrum acquired in reflectron and linear mode with Ag salt as cationizing agent and DCTB matrix. The full and expanded spectra correspond to (a) $\text{PSTY}_{44}\text{-Br}$, **2a**, (b) $\text{PSTY}_{44}\text{-N}_3$, **3a**, (c) $\text{PSTY}_{44}\text{-}\equiv$, **4a** and (d) $\text{PSTY}_{44}\text{-}(\equiv)_2$, **5a**.

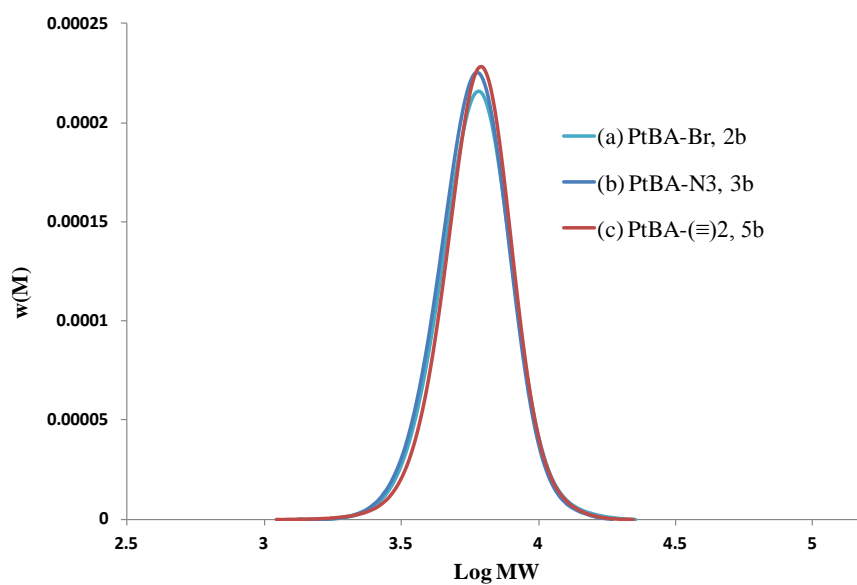


Figure C4: SEC chromatograms of functional linear P^tBA (a) $\text{P}^t\text{BA}_{44}\text{-Br}$, **2b**; (b) $\text{P}^t\text{BA}_{44}\text{-N}_3$, **3b**, (c) $\text{P}^t\text{BA}_{44}\text{-}(\equiv)_2$, **5b**. All chromatograms are based on PSTY calibration curve.

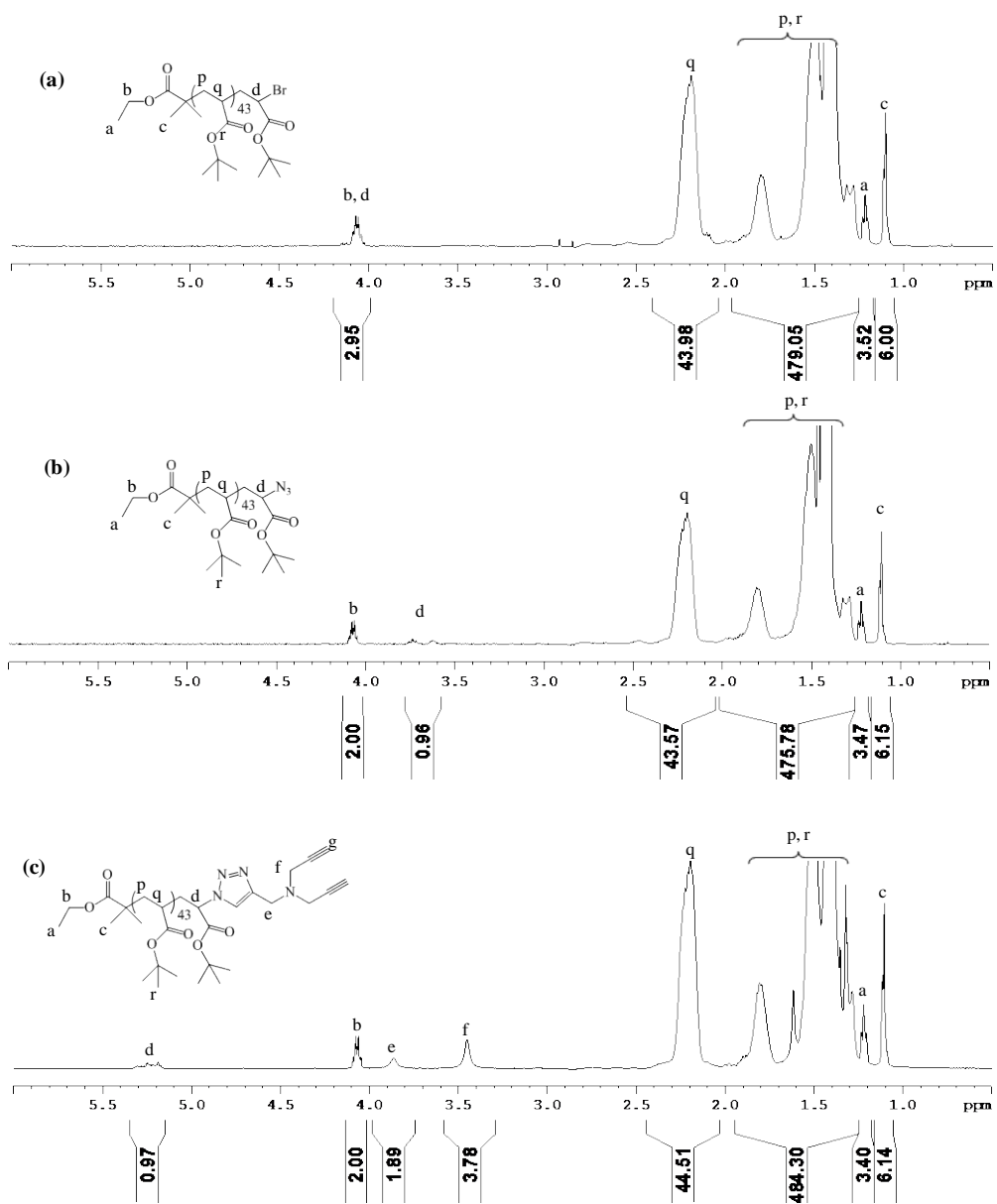


Figure C5. 500 MHz ^1H 1D DOSY NMR spectra in CDCl_3 of (a) P^tBA₄₄-Br, **2b**. (b) P^tBA₄₄-N₃, **3b**, (c) PtBA₄₄-(≡)₂, **5b**.

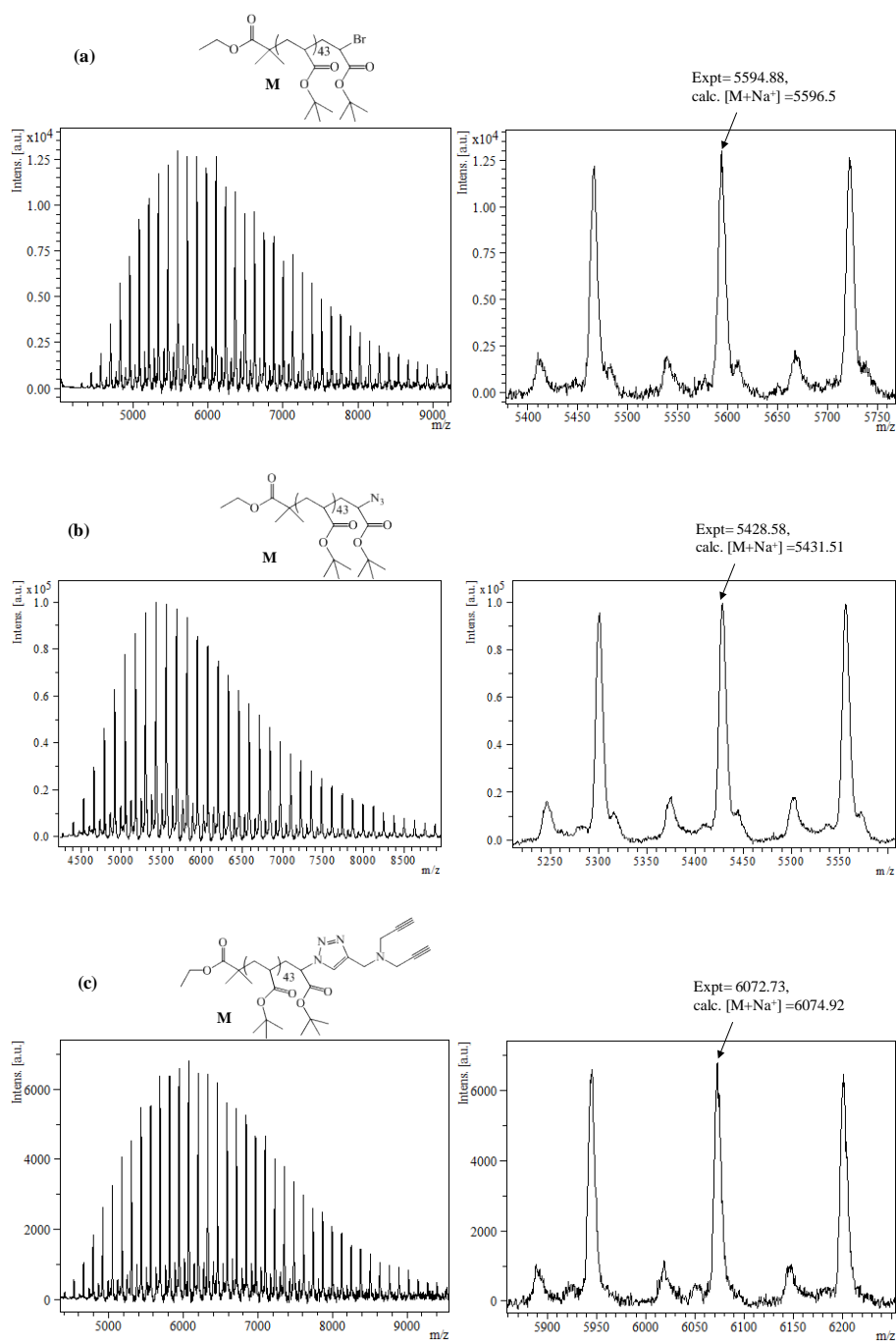


Figure C6: MALDI-ToF mass spectrum acquired in linear mode with Na salt as cationizing agent and DCTB matrix. The full and expanded spectra correspond to (a) P^tBA₄₄-Br, **2b**. (b) P^tBA₄₄-N₃, **3b**, (c) PtBA₄₄-(≡)₂, **5b**.

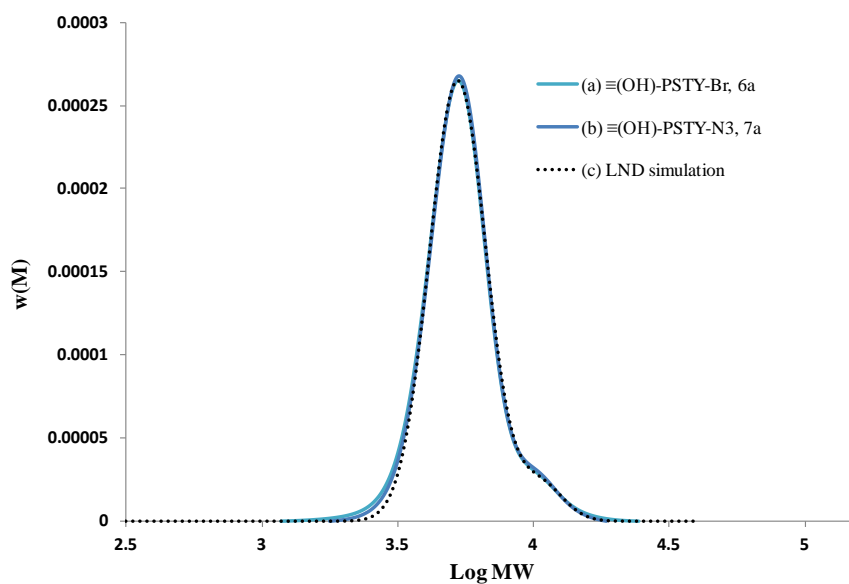


Figure C7: SEC chromatograms of (a) $\equiv(\text{OH})\text{-PSTY}_{47}\text{-Br}$, **6a**; (b) $\equiv(\text{OH})\text{-PSTY}_{47}\text{-N}_3$, **7a** (c) LND simulation of **6a**. All chromatograms are based on PSTY calibration curve.

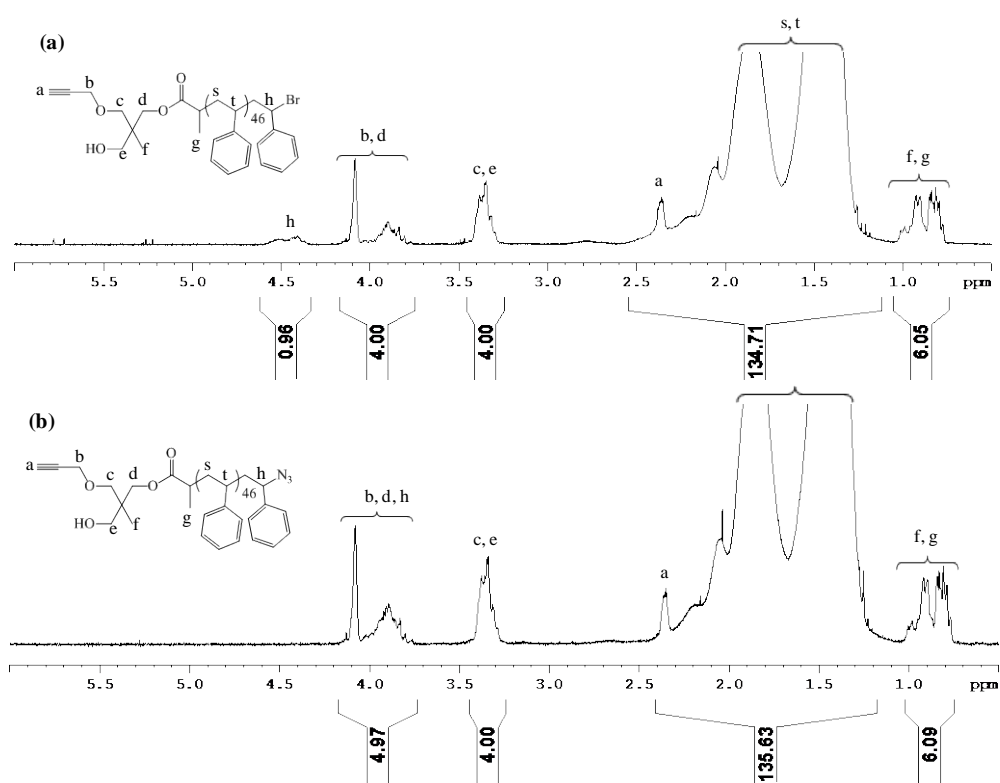


Figure C8. 500 MHz ^1H 1D DOSY NMR spectra in CDCl_3 of (a) $\equiv(\text{OH})\text{-PSTY}_{47}\text{-Br}$, **6a** and (b) $\equiv(\text{OH})\text{-PSTY}_{47}\text{-N}_3$, **7a**.

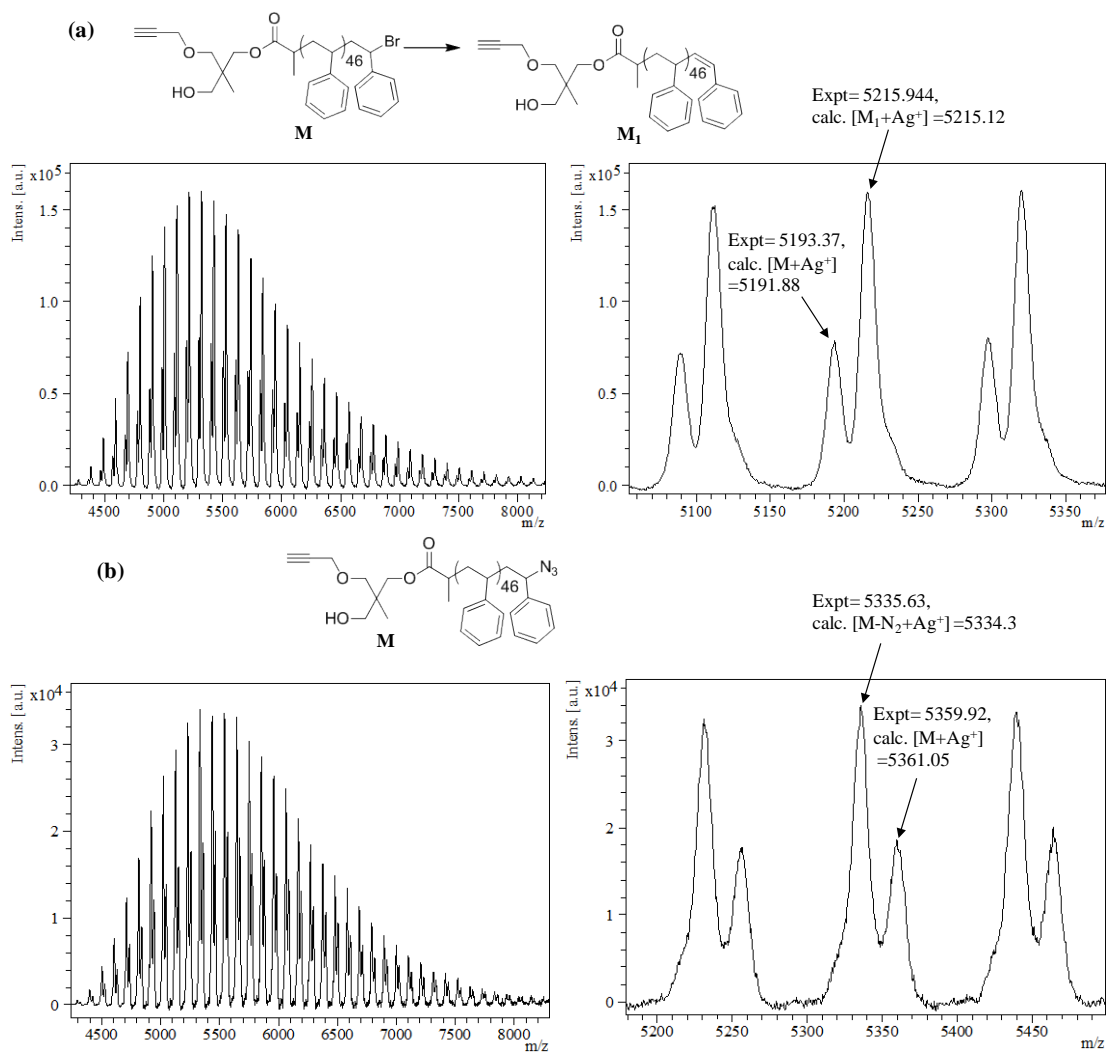


Figure C9: MALDI-ToF mass spectrum acquired in reflectron (5a) and linear (6a) mode with Ag salt as cationizing agent and DCTB matrix. The full and expanded spectra correspond to (a) $\equiv(\text{OH})\text{-PSTY}_{47}\text{-Br}$, **6a** and (b) $\equiv(\text{OH})\text{-PSTY}_{47}\text{-N}_3$, **7a**.

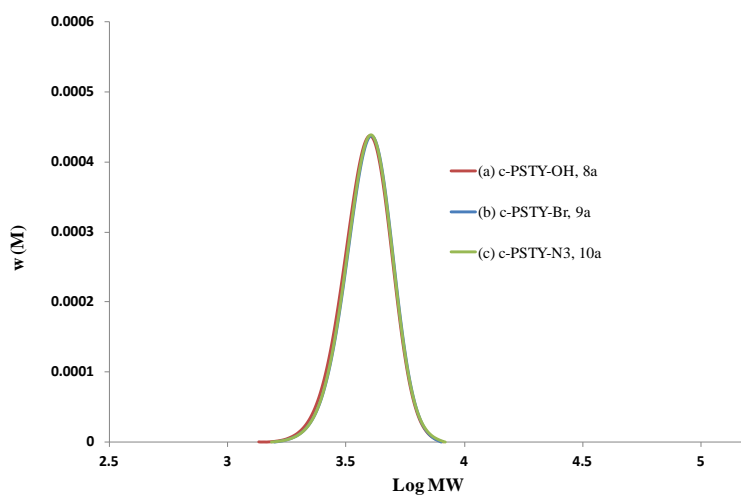


Figure C10: SEC chromatograms of (a) c-PSTY₄₇-OH, **8a**, (b) c-PSTY₄₇-Br, **9a**, (c) c-PSTY₄₇-N₃, **10a**. All chromatograms are based on PSTY calibration curve.

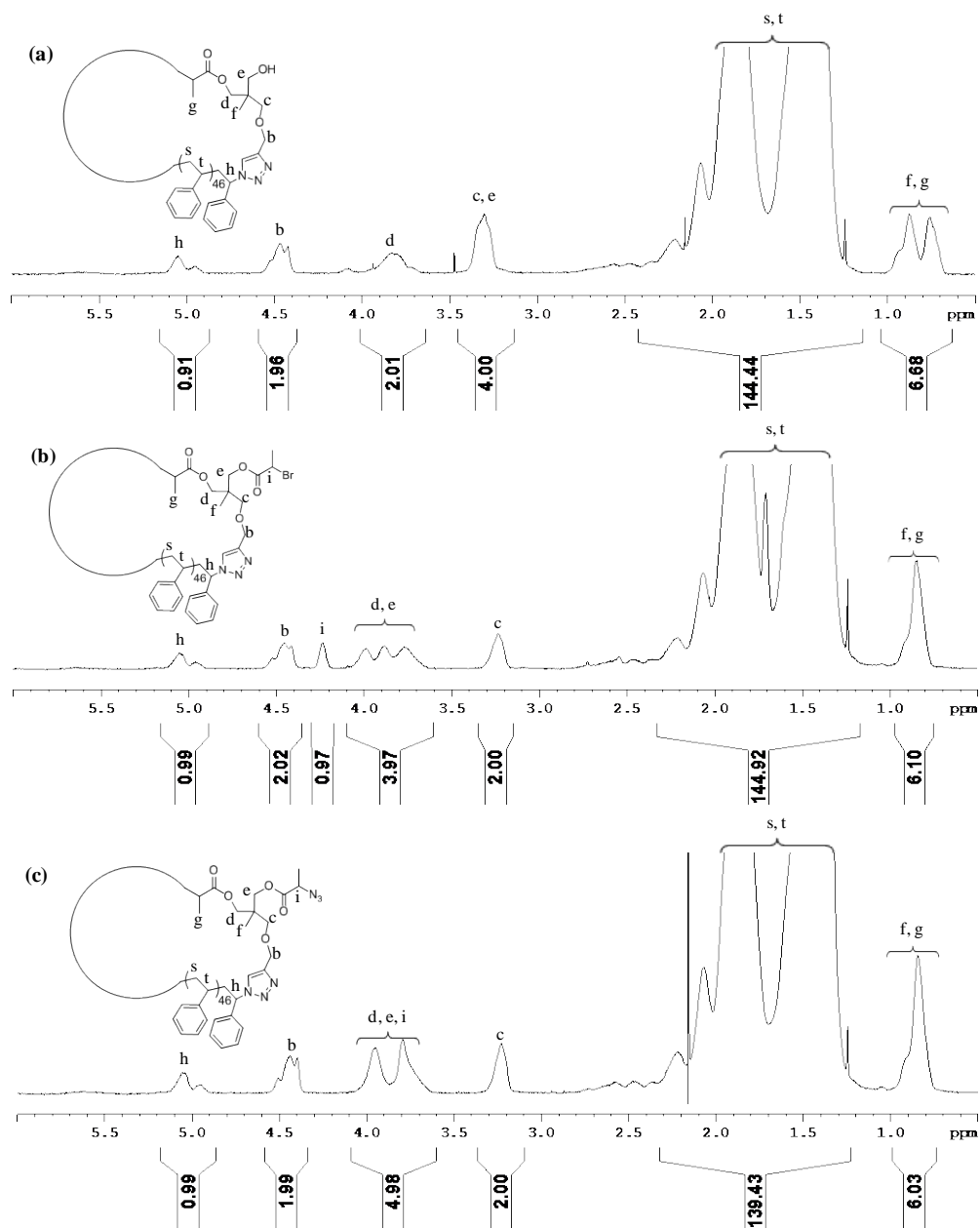


Figure C11. 500 MHz ¹H 1D DOSY NMR spectra in CDCl₃ of (a) c-PSTY₄₇-OH, **8a**, (b) c-PSTY₄₇-Br, **9a** and (c) c-PSTY₄₇-N₃, **10a**.

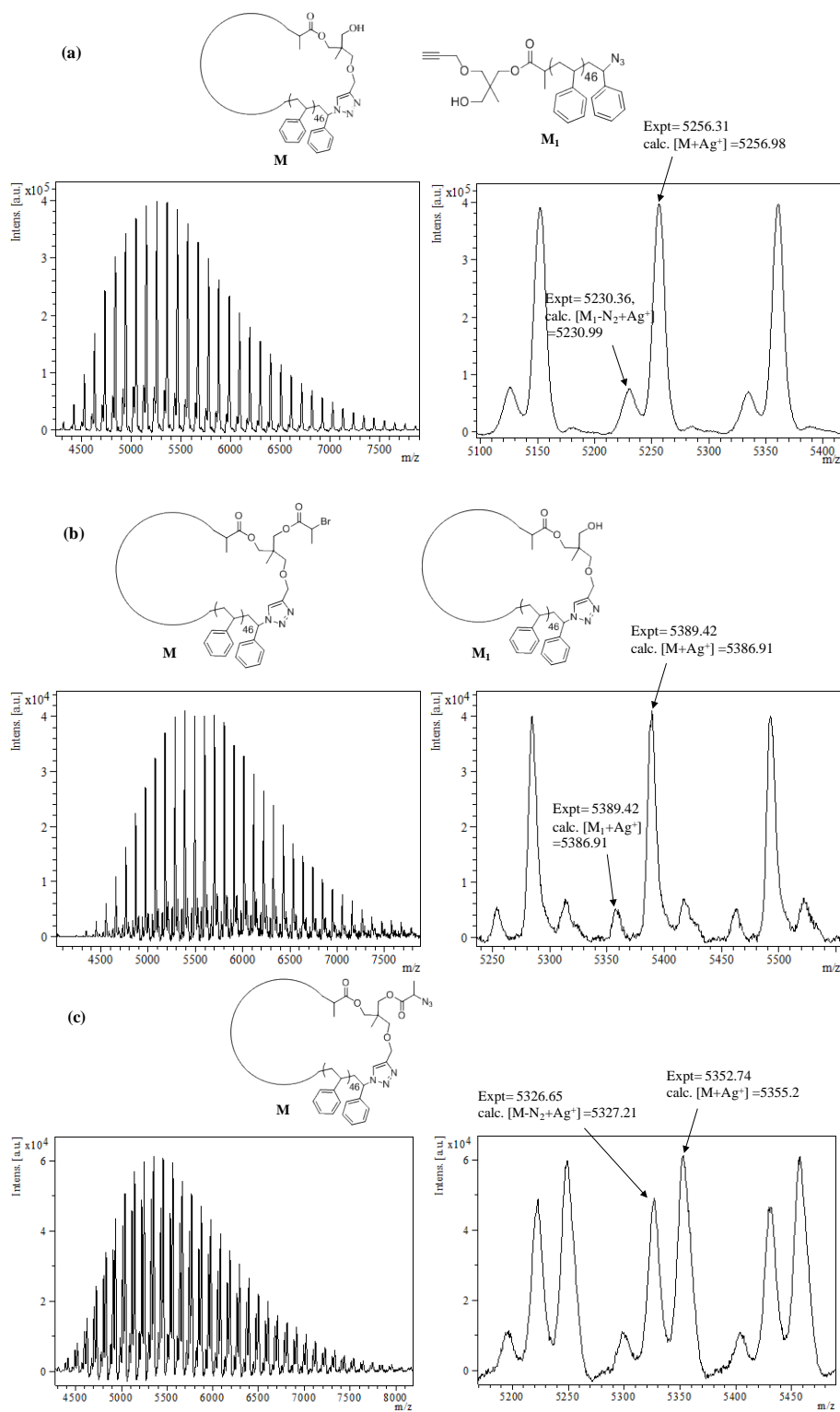


Figure C12: MALDI-ToF mass spectrum acquired in linear mode with Ag salt as cationizing agent and DCTB matrix. The full and expanded spectra correspond to (a) c-PSTY₄₇-OH, **8a**, (b) c-PSTY₄₇-Br, **9a** and (c) c-PSTY₄₇-N₃, **10a**.

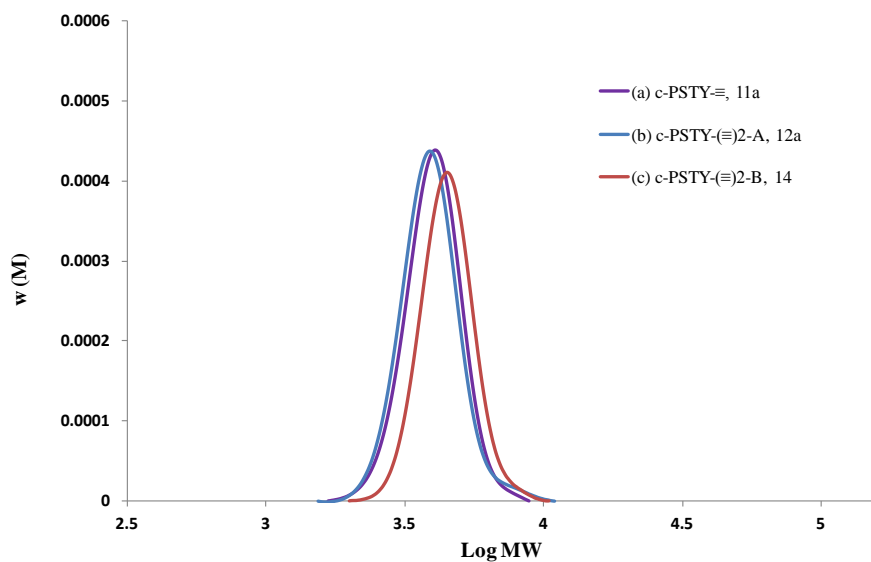


Figure C13: SEC chromatograms of (a) c-PSTY₄₇-≡, **11a**, (b) c-PSTY₄₇-(≡)₂-A (amine functional core), **12a** and (c) c-PSTY₄₇-(≡)₂-B (benzene functional core), **14**. All chromatograms are based on PSTY calibration curve.

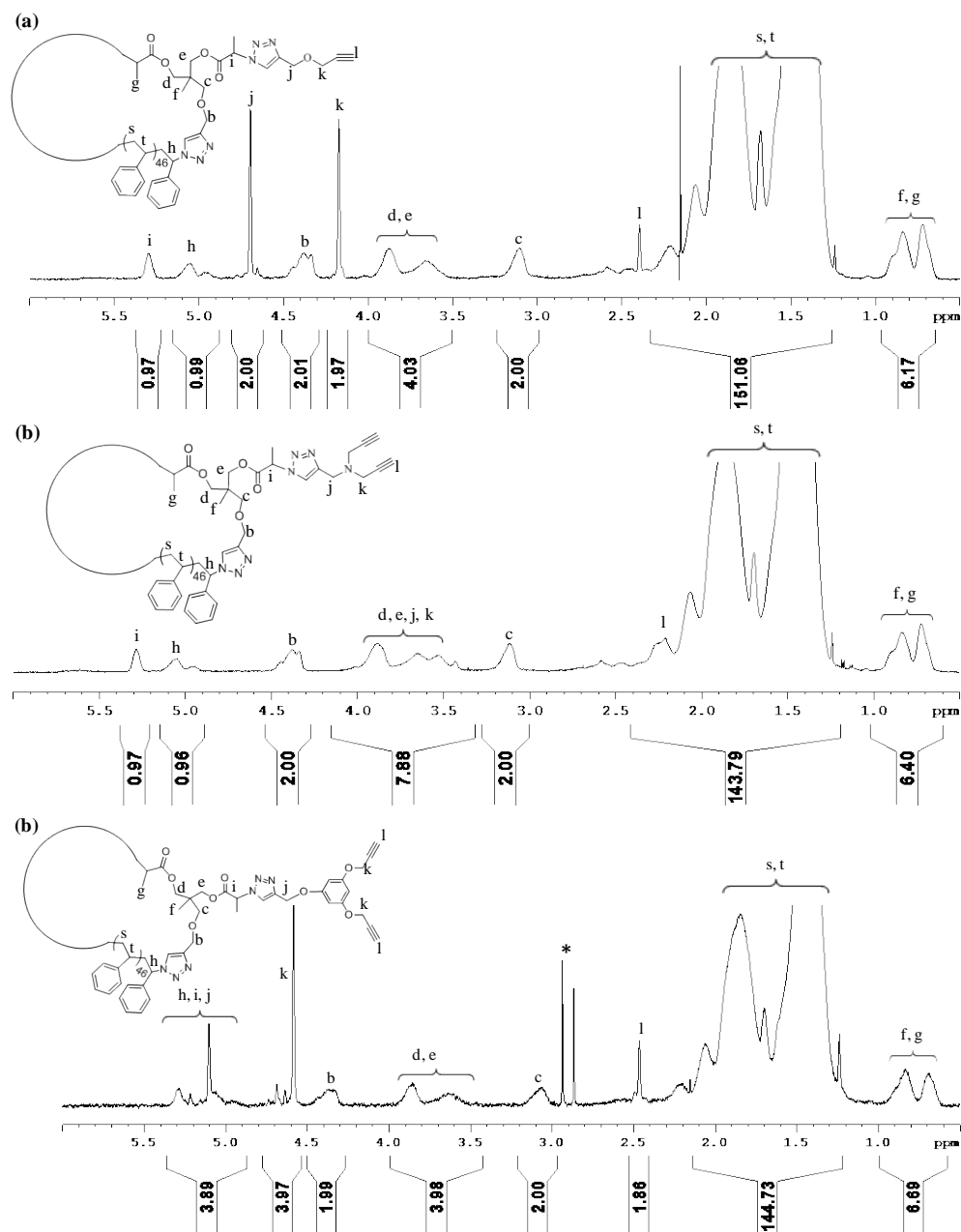


Figure C14. 500 MHz ^1H 1D DOSY NMR spectra in CDCl_3 of (a) c-PSTY₄₇-≡, **11a**, (b) c-PSTY₄₇-(≡)₂-A, **12a** and (c) c-PSTY₄₇-(≡)₂-B, **14**. * Small molecules impurities.

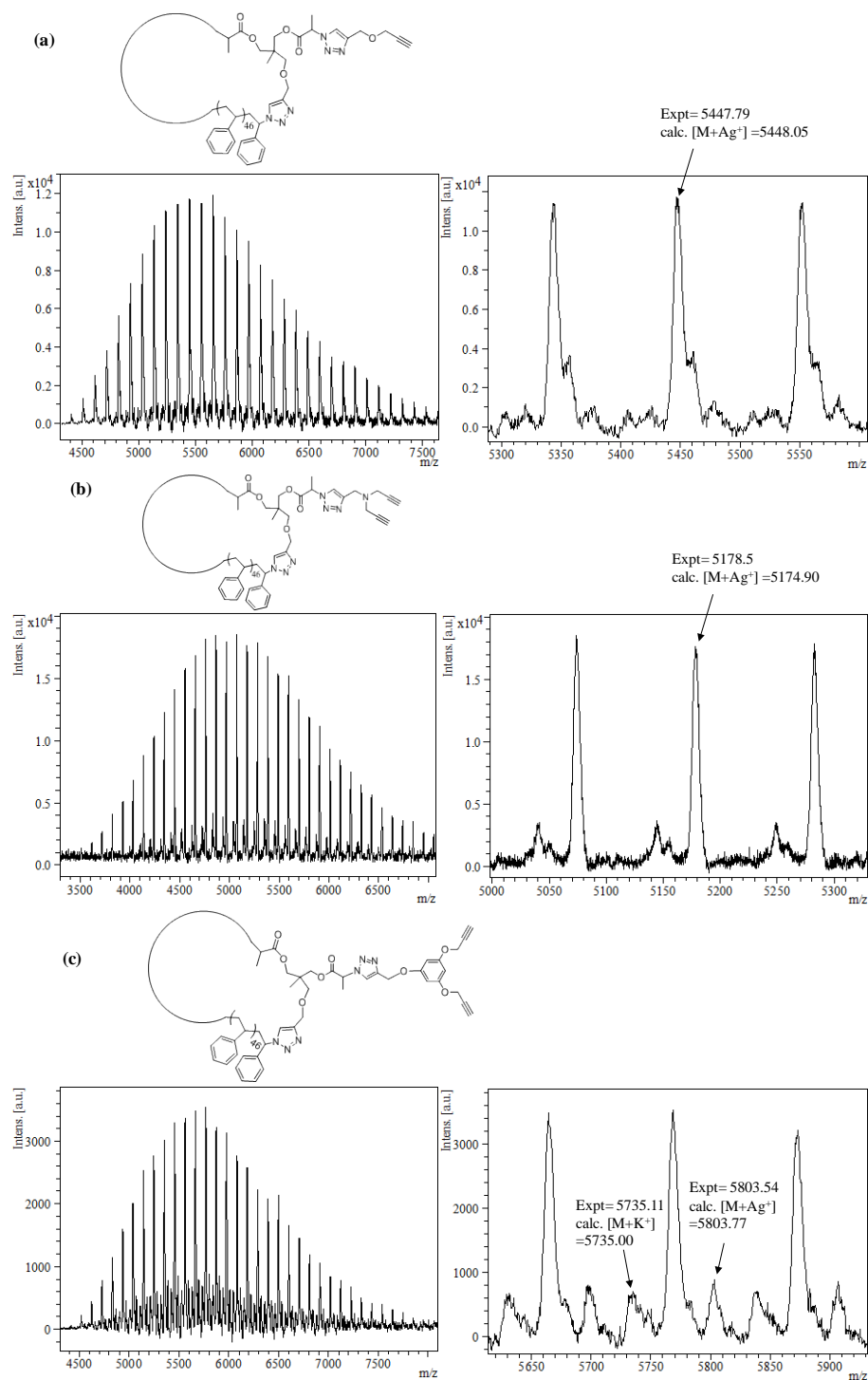


Figure C15: MALDI-ToF mass spectrum acquired in reflectron mode with Ag salt as cationizing agent and DCTB matrix. The full and expanded spectra correspond to (a) c-PSTY₄₇-≡, **11a**, (b) c-PSTY₄₇-(≡)₂-A, **12a** and (c) c-PSTY₄₇-(≡)₂-B, **14**.

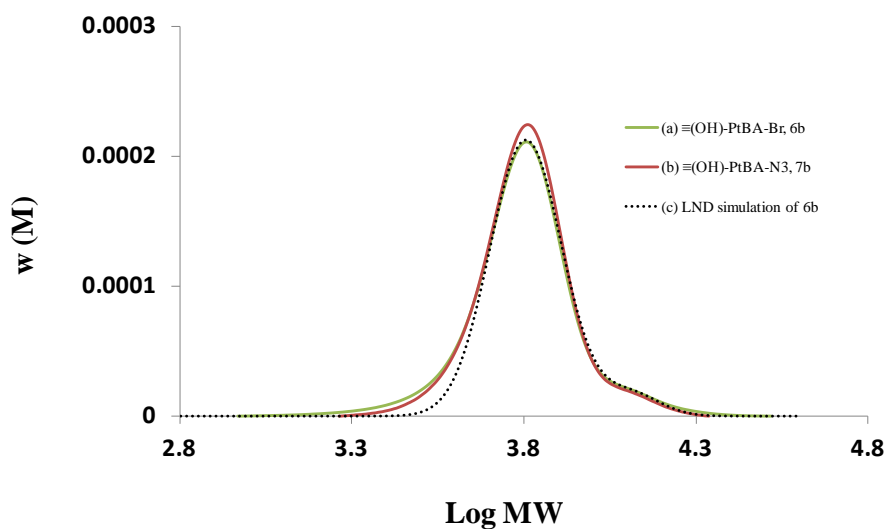


Figure C16: SEC chromatograms of (a) $\equiv(\text{OH})\text{P}^t\text{BA}_{44}\text{-Br}$, **6b**, (b) $\equiv(\text{OH})\text{P}^t\text{BA}_{44}\text{-N}_3$, **7b** and (c) LND simulation of **6b**. All chromatograms are based on PSTY calibration curve.

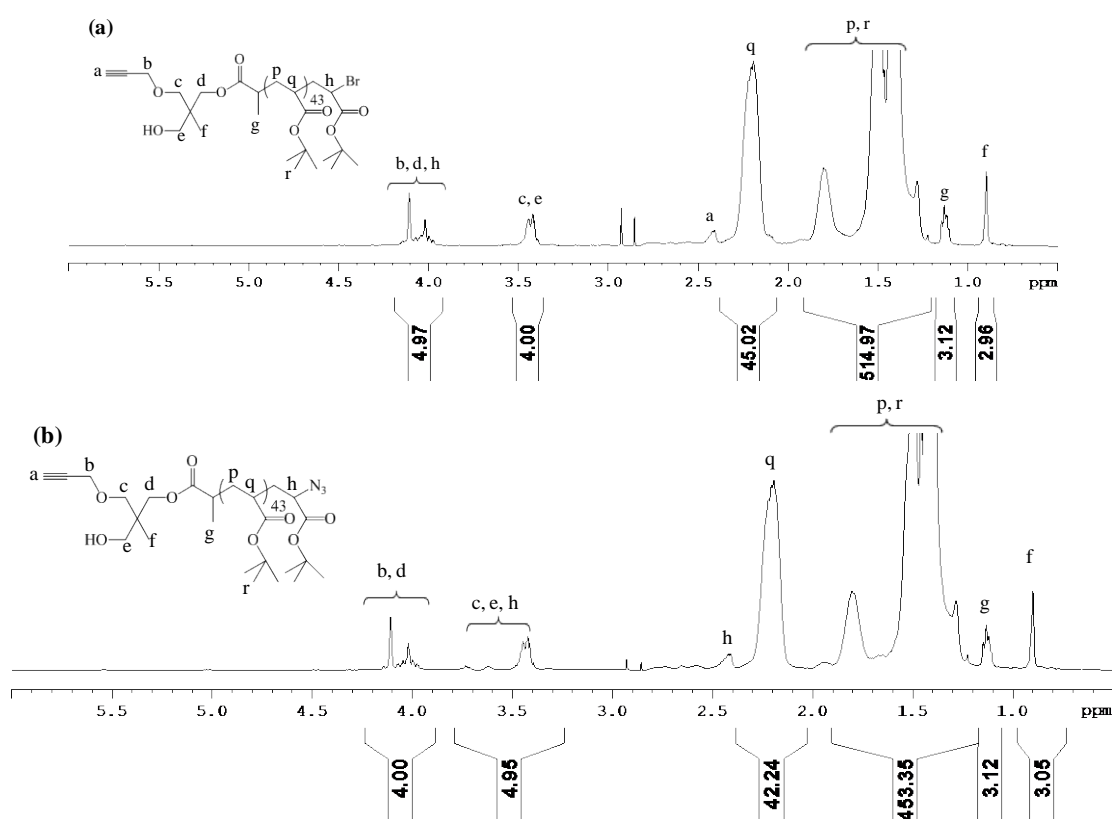


Figure C17. 500 MHz ^1H 1D DOSY NMR spectra in CDCl_3 of (a) $\equiv(\text{OH})\text{-P}^t\text{BA}_{44}\text{-Br}$, **6b** and (b) $\equiv(\text{OH})\text{-P}^t\text{BA}_{44}\text{-N}_3$, **7b**.

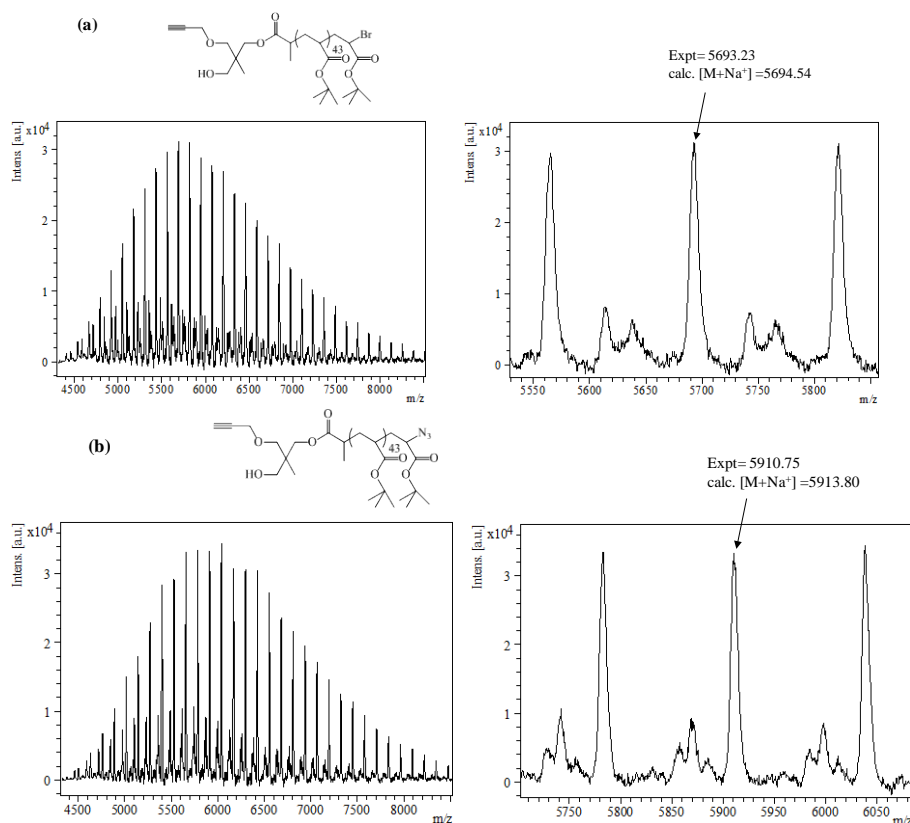


Figure C18: MALDI-ToF mass spectrum acquired in linear mode with Na salt as cationizing agent and DCTB matrix. The full and expanded spectra correspond to (a) $\equiv(\text{OH})\text{-P}^t\text{BA}_{44}\text{-Br}$, **6b** and (b) $\equiv(\text{OH})\text{-P}^t\text{BA}_{44}\text{-N}_3$, **7b**.

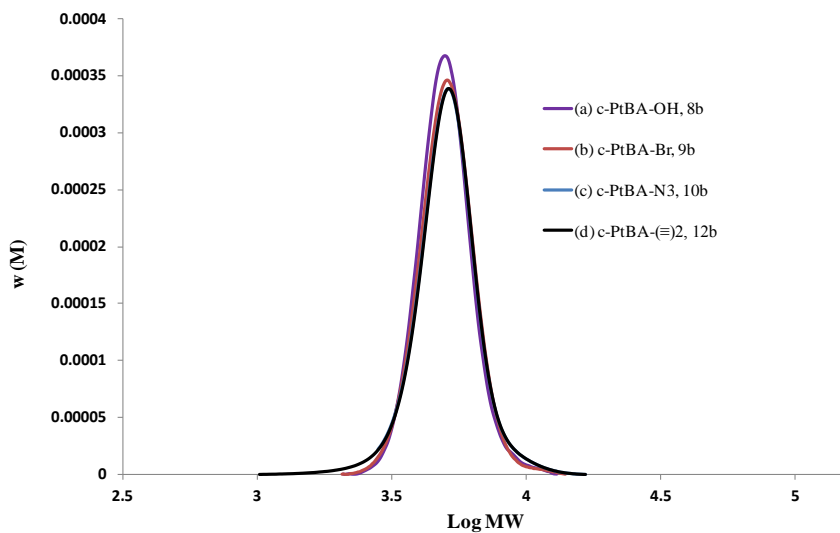


Figure C19: SEC chromatograms of (a) c-P^tBA₄₄-OH, **8b**, (b) c-P^tBA₄₄-Br, **9b**, (c) c-P^tBA₄₄-N₃, **10b** and (d) c-P^tBA₄₄-(\equiv)₂, **12b**. All chromatograms are based on PSTY calibration curve.

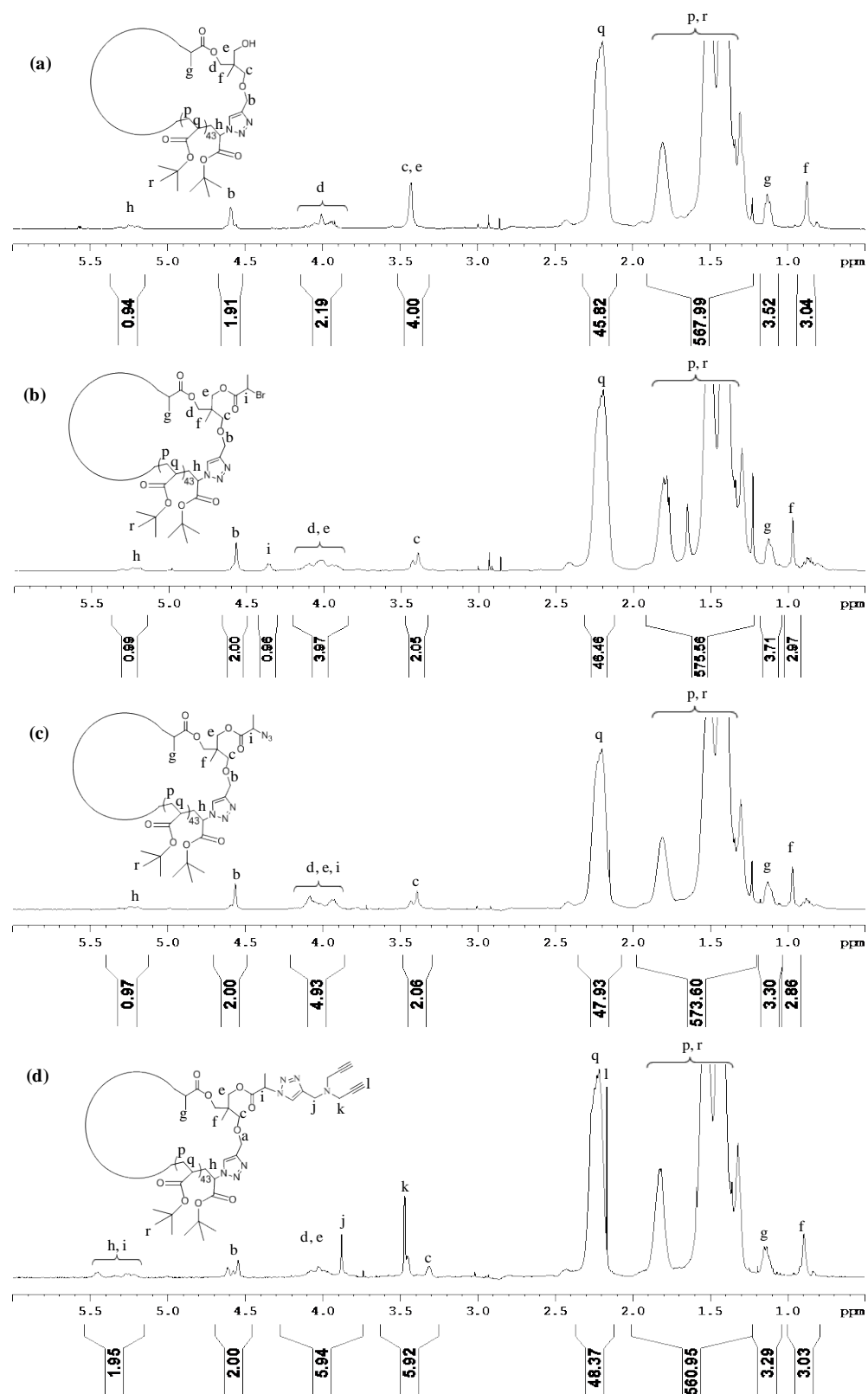


Figure C20. 500 MHz ^1H 1D DOSY NMR spectra in CDCl_3 of (a) c-PBA₄₄-OH, **8b**, (b) c-PBA₄₄-Br, **9b**, (c) c-PBA₄₄-N₃, **10b** and (d) c-PBA₄₄-≡, **12b**.

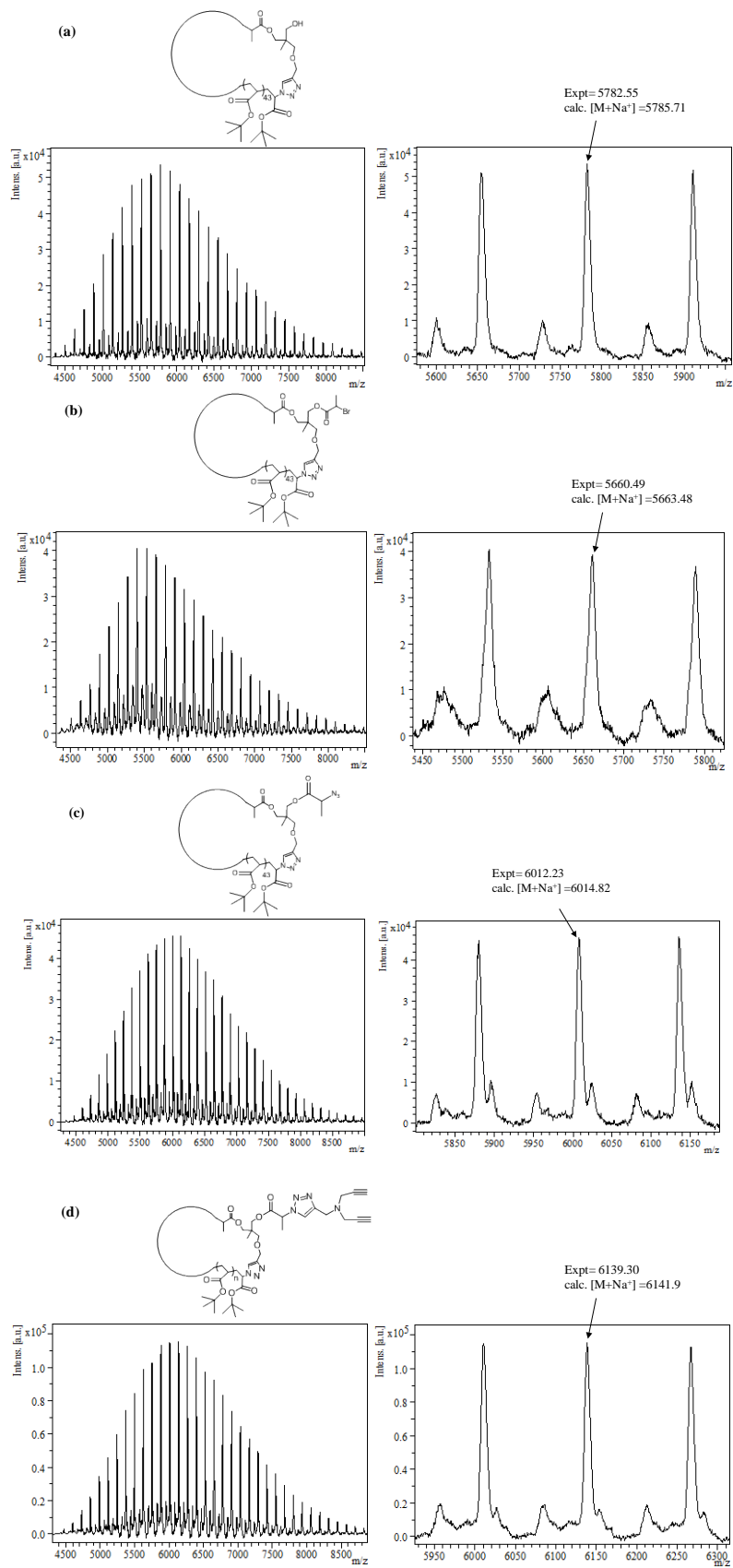


Figure C21: MALDI-ToF mass spectrum acquired in linear mode with Na salt as cationizing agent and DCTB matrix. The full and expanded spectra correspond to (a) c-P^tBA₄₄-OH, **8b**, (b) c-P^tBA₄₄-Br, **9b**, (c) c-P^tBA₄₄-N₃, **10b** and (d) c-P^tBA₄₄-(≡)₂, **12b**.

Table C1. Molecular weight data for linear and cyclic polymers to build up complex architectures.

Polymer	Purity by LND (%)		RI detection ^a			Triple detection ^b			M _n by NMR	Δ HDV ^c
	Crude	Prep	M _n	M _p	PDI	M _n	M _p	PDI		
2a			4670	5010	1.07				4670	
3a			4650	4990	1.07				4740	
4a			4800	5050	1.07				4940	
5a			4850	5060	1.07				4870	
2b			5660	6080	1.10				5830	
3b			5540	5960	1.10				5800	
5b			5770	6190	1.09				5800	
6a	87.7		5220	5245	1.10	4890	4860	1.05	4980	
7a	87.0		5070	5130	1.10	4920	4900	1.05	4940	
8a^d	81.46	81.46	3780	3970	1.06	5450	5550	1.04	5250	0.71
9a			3870	4080	1.05				5390	
10a			3850	4030	1.05				5140	
11a			3920	4080	1.05				5650	
12a			3820	3900	1.06				5380	
14			4420	4470	1.05				5690	
6b	88.1		5890	6400	1.13				6060	
7b	89.3		6040	6480	1.13	6040	6210	1.09	5640	
8b^d	71.63	71.63	4890	5130	1.05	6260	6570	1.04	6150	0.78
9b			4930	5080	1.05				6290	
10b			4940	5080	1.05				6500	
12b			4940	5120	1.07				6380	

^aThe data was acquired using SEC (RI detector) and is based on PSTY calibration curve.

^bThe data was acquired using Triple Detection SEC.

^cΔHDV was calculated by dividing M_p of RI with M_p of triple detection.

^dPurity was calculated by using LND simulation based on number distribution (f(N)).

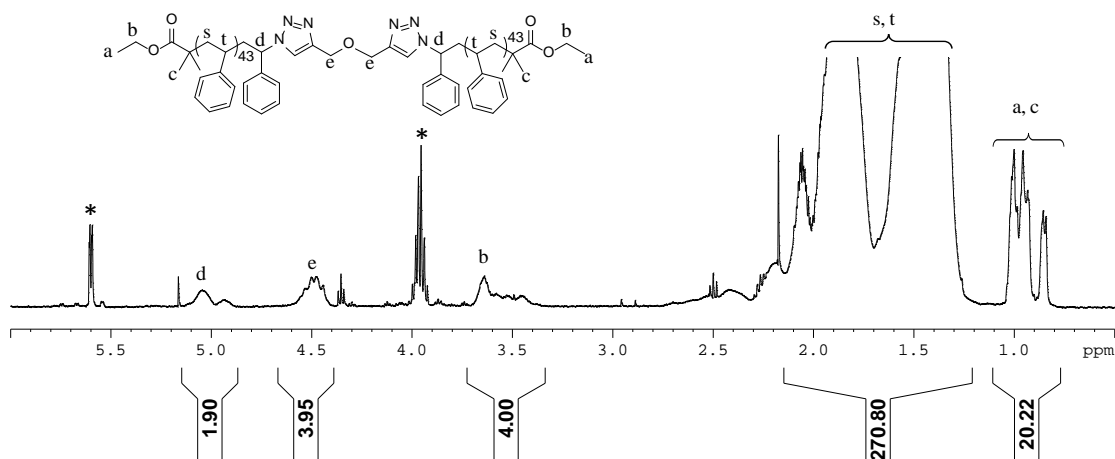


Figure C22. 500 MHz ^1H 1D DOSY NMR spectra in CDCl_3 of $(\text{PSTY})_2$ **15**.

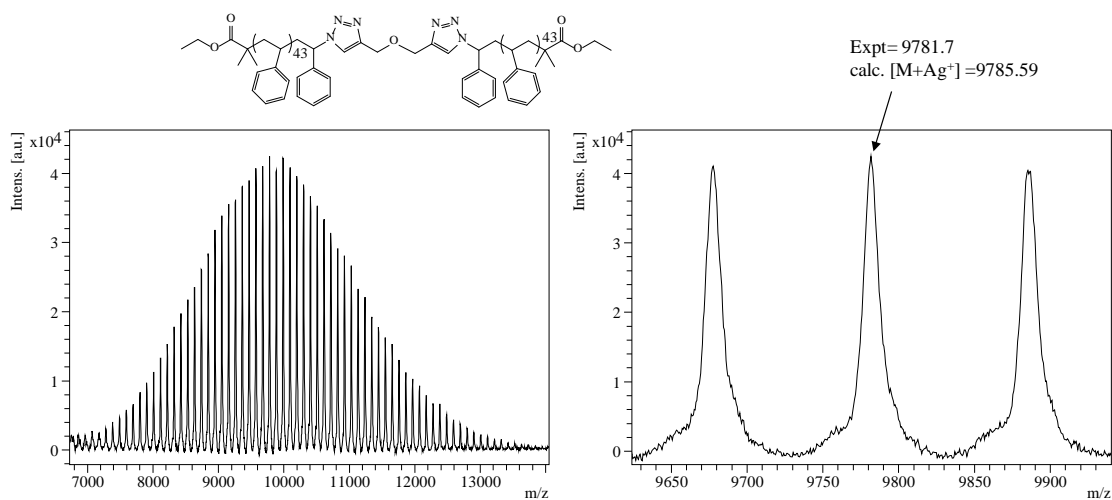


Figure C23: MALDI-ToF mass spectrum acquired in linear mode with Ag salt as cationizing agent and DCTB matrix. The full and expanded spectra correspond to $(\text{PSTY})_2$, **15**.

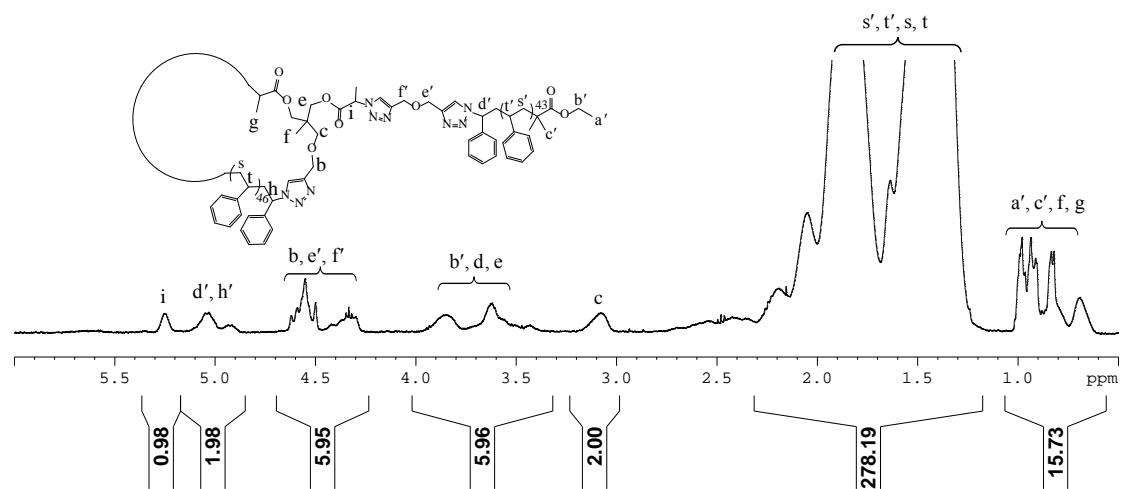


Figure C24. 500 MHz ^1H 1D DOSY NMR spectra in CDCl_3 of c-PSTY₄₇-b-PSTY₄₄, **16**.

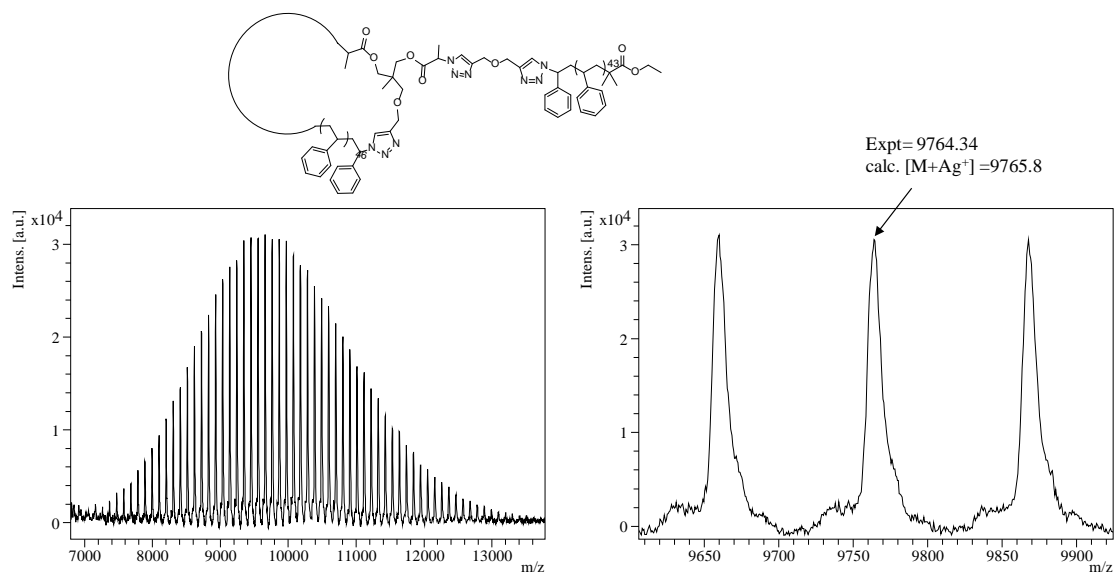


Figure C25: MALDI-ToF mass spectrum acquired in linear mode with Ag salt as cationizing agent and DCTB matrix. The full and expanded spectra correspond to $c\text{-PSTY}_{47}\text{-}b\text{-PSTY}_{44}$, **16**.

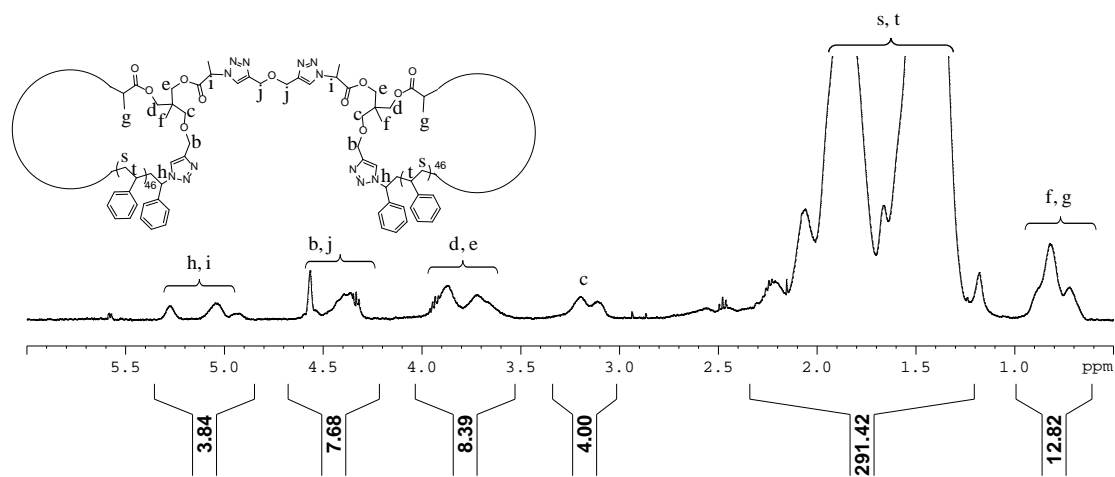


Figure C26. 500 MHz ^1H 1D DOSY NMR spectra in CDCl_3 of $(c\text{-PSTY}_{47})_2$, **17**.

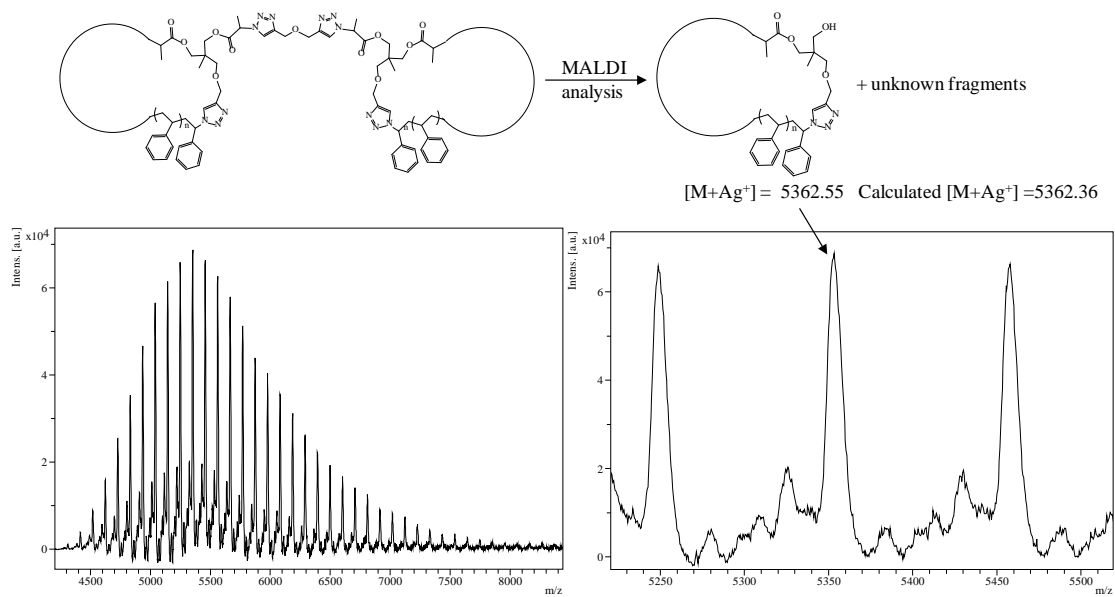


Figure C27: MALDI-ToF mass spectrum acquired in linear mode with Ag salt as cationizing agent and DCTB matrix. The full and expanded spectra correspond to $(c\text{-PSTY}_{47})_2$, **17**.

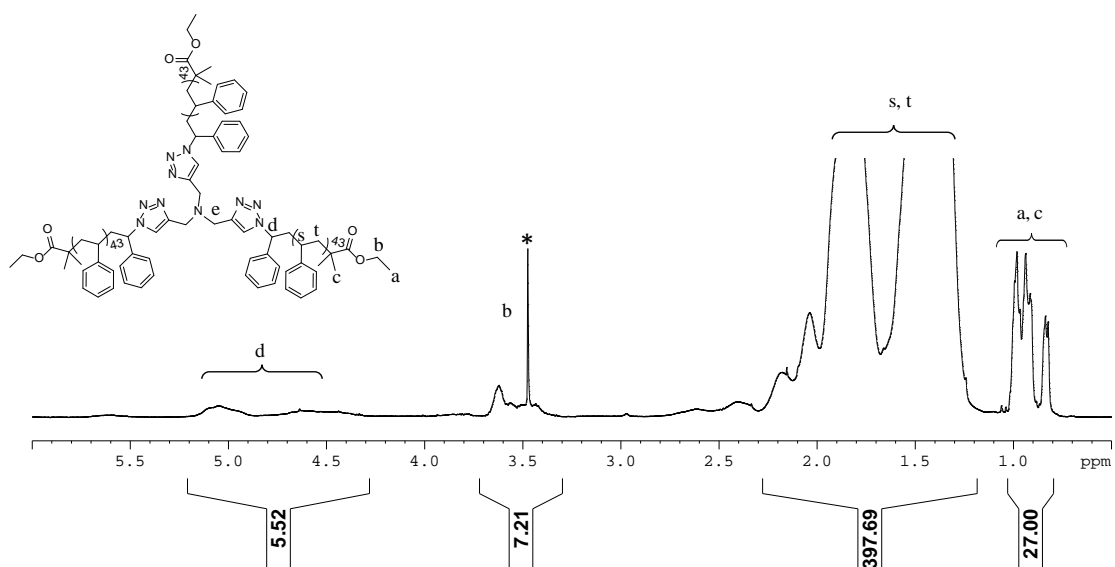


Figure C28. 500 MHz ^1H 1D DOSY NMR spectra in CDCl_3 of $(\text{PSTY}_{44})_3$ **18**. * small molecules impurities.

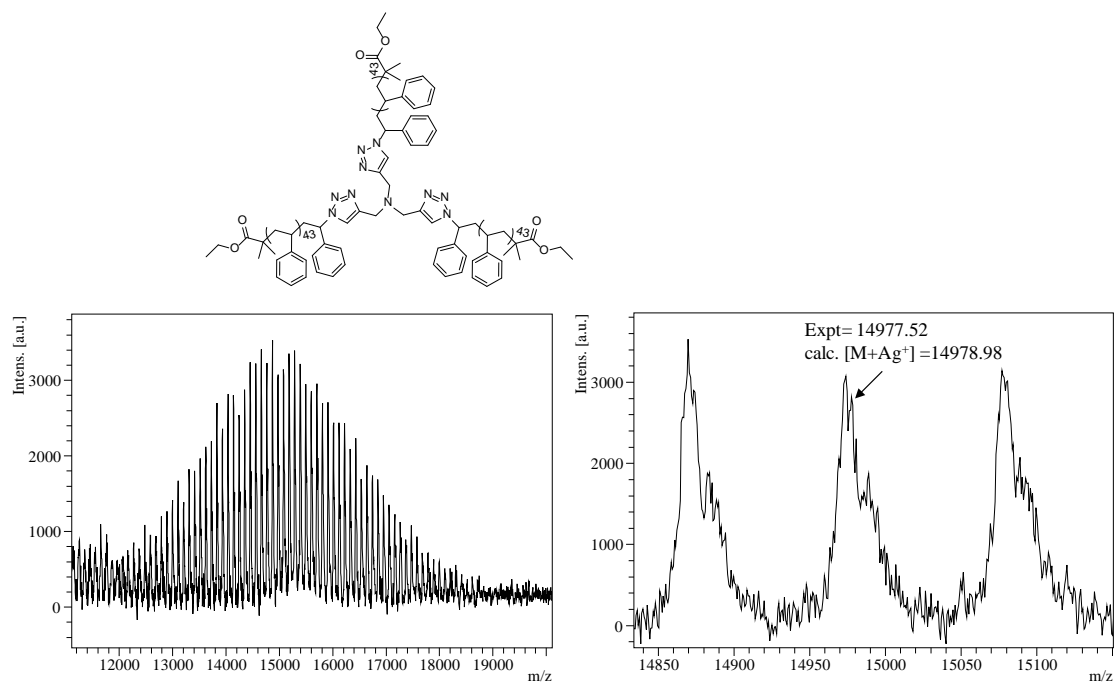


Figure C29: MALDI-ToF mass spectrum acquired in linear mode with Ag salt as cationizing agent and DCTB matrix. The full and expanded spectra correspond to (PSTY₄₄)₃ **18**.

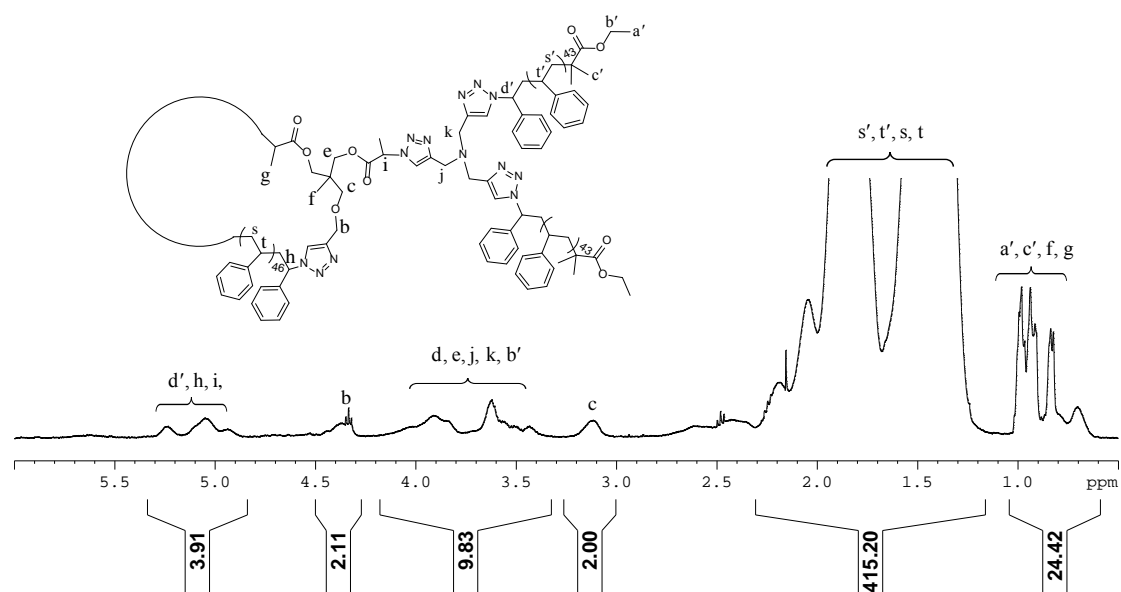


Figure C30. 500 MHz ¹H 1D DOSY NMR spectra in CDCl₃ of c-PSTY₄₇-b-(PSTY)₂ **19**.

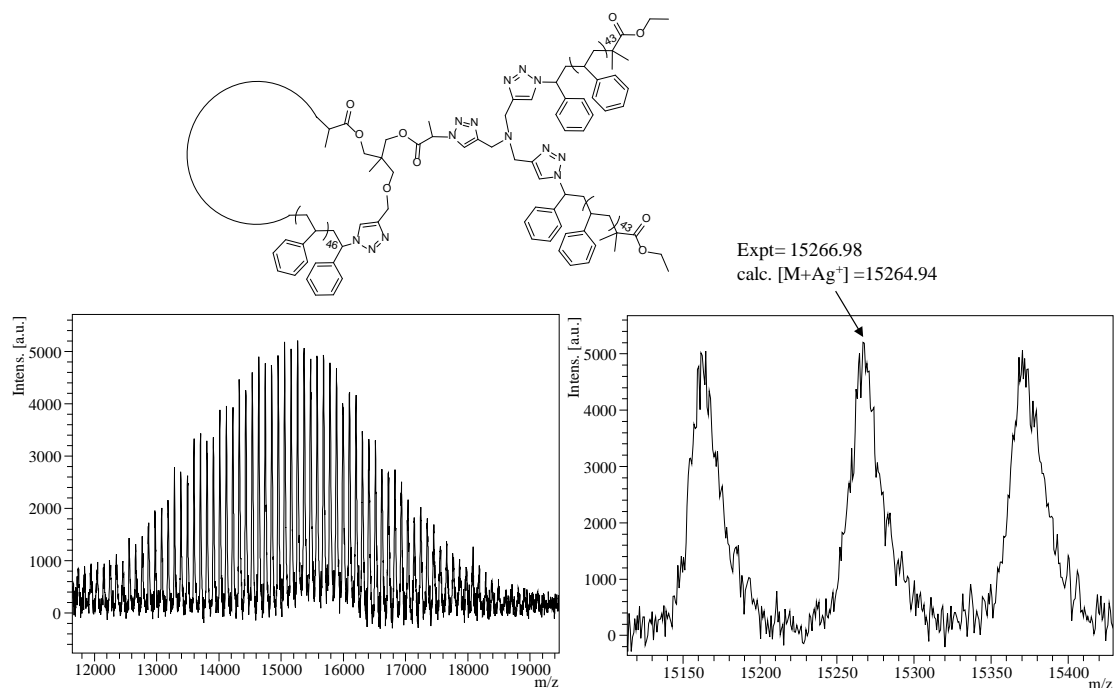


Figure C31: MALDI-ToF mass spectrum acquired in linear mode with Ag salt as cationizing agent and DCTB matrix. The full and expanded spectra correspond to $c\text{-PSTY}_{47}\text{-(PSTY}_{44})_2$ **19**.

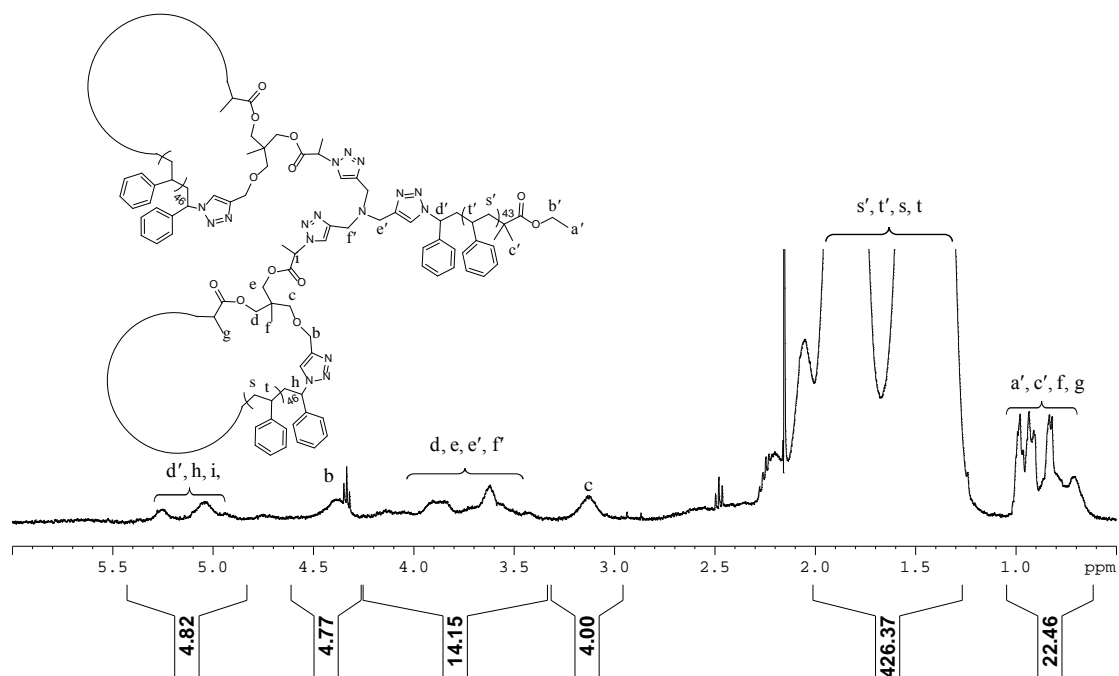


Figure C32. 500 MHz ^1H 1D DOSY NMR spectra in CDCl_3 of $(c\text{-PSTY}_{47})_2\text{-PSTY}_{44}$, **20**.

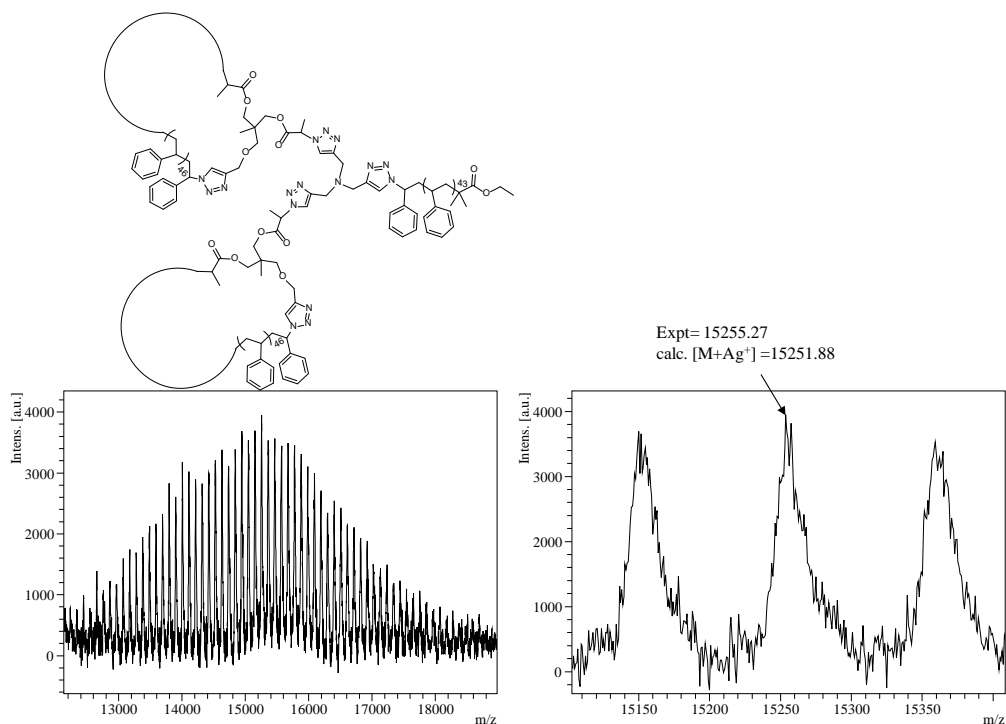


Figure C33: MALDI-ToF mass spectrum acquired in linear mode with Ag salt as cationizing agent and DCTB matrix. The full and expanded spectra correspond to $(c\text{-PSTY}_{47})_2\text{-PSTY}_{44}$, **20**.

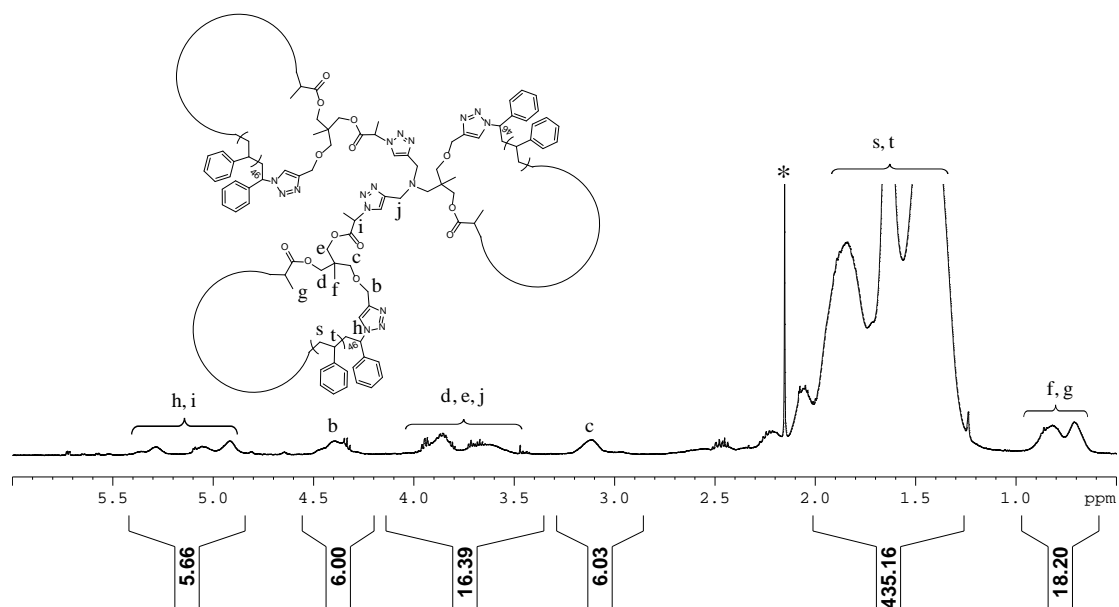


Figure C34. 500 MHz ^1H 1D DOSY NMR spectra in CDCl_3 of $(c\text{-PSTY}_{47})_3\text{-A}$, **21**, * acetone.

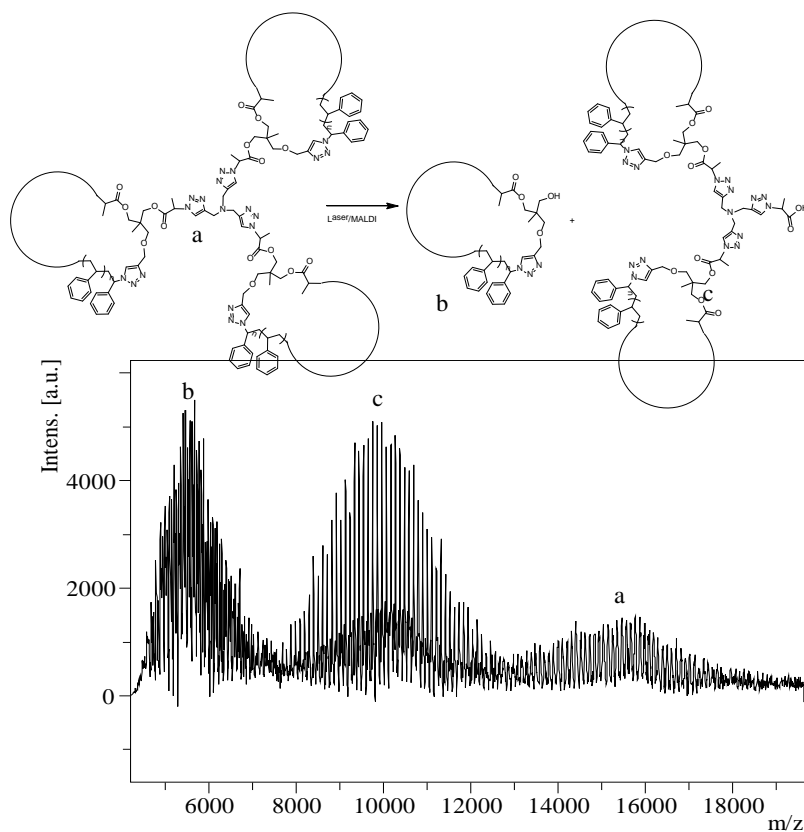


Figure C35: MALDI-ToF mass spectrum acquired in linear mode with Ag salt as cationizing agent and DCTB matrix. The full and expanded spectra correspond (c-PSTY₄₇)₃-A, **21**.

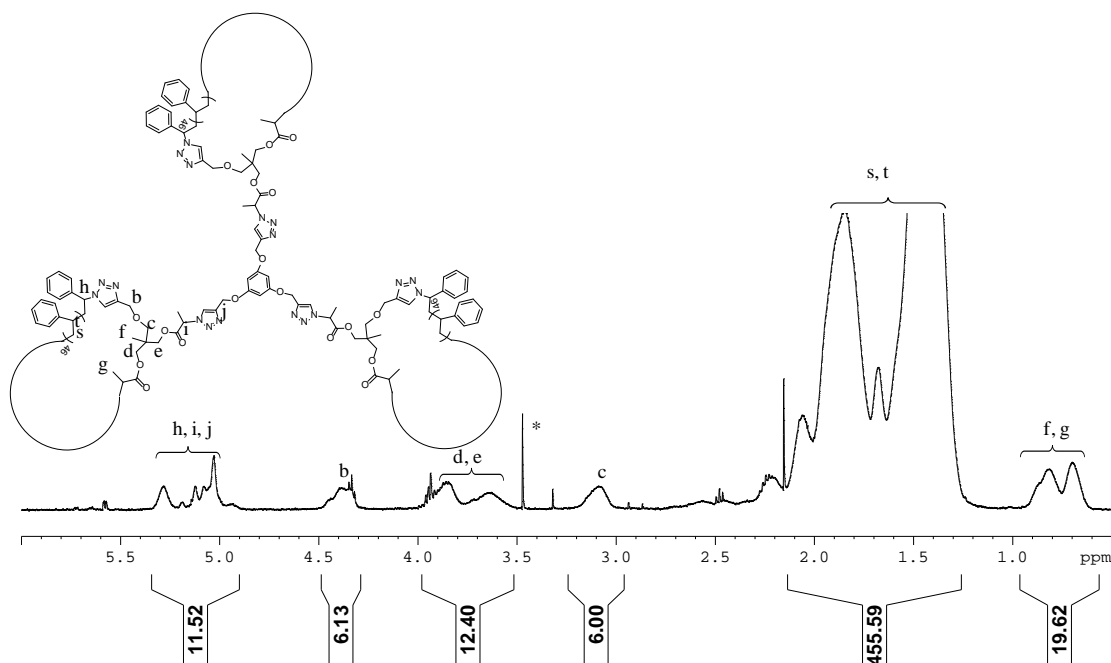


Figure C36. 500 MHz ¹H 1D DOSY NMR spectra in CDCl₃ of (c-PSTY₄₇)₃-B, **22**, * Small molecules impurities.

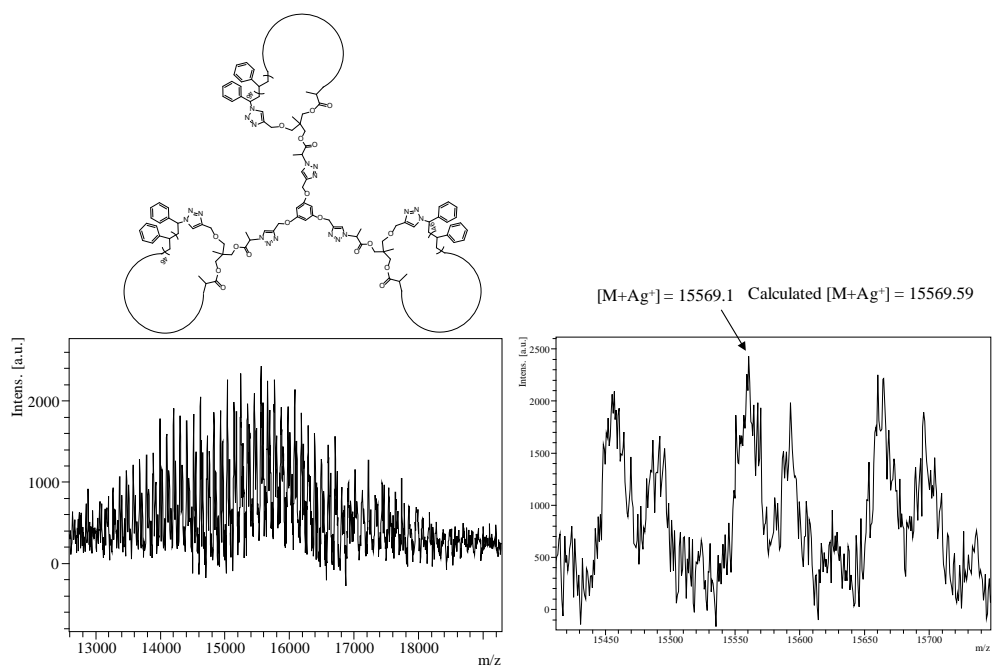


Figure C37: MALDI-ToF mass spectrum acquired in linear mode with Ag salt as cationizing agent and DCTB matrix. The full and expanded spectra correspond to $(c\text{-PSTY}_{47})_3\text{-B}$, **22**.

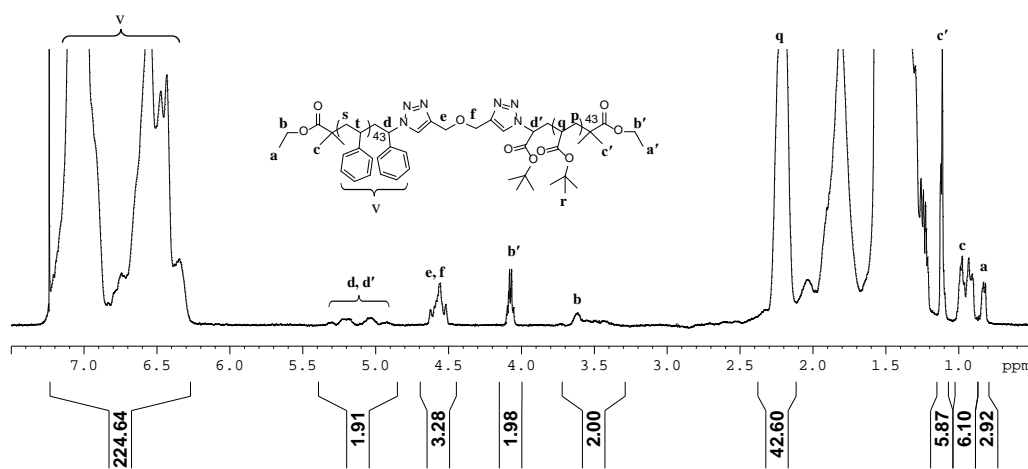


Figure C38. 500 MHz ^1H 1D DOSY NMR spectra in CDCl_3 of $\text{PSTY}_{44}\text{-b-PtBA}_{44}$, **23**.

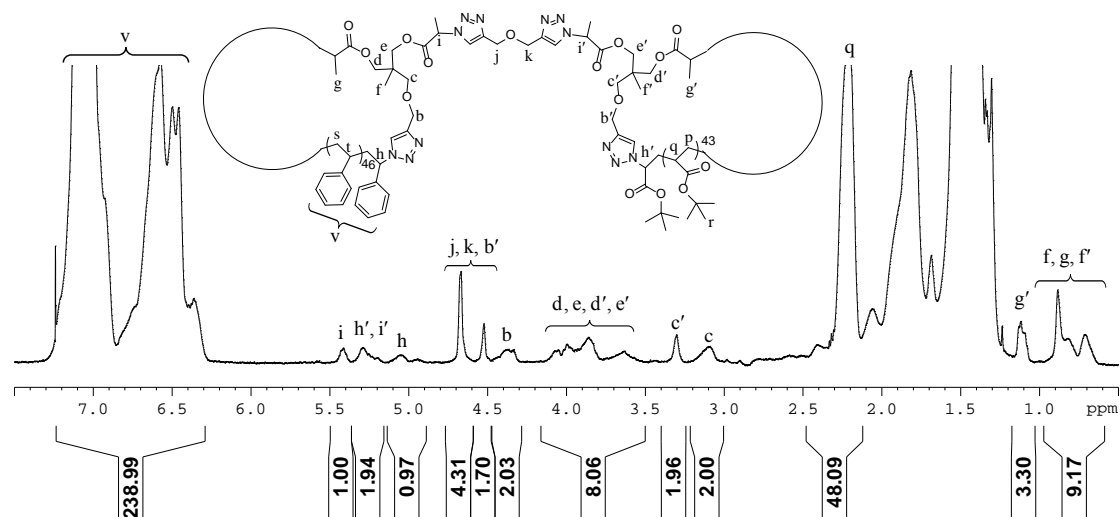


Figure C39. 500 MHz ^1H 1D DOSY NMR spectra in CDCl_3 of **c-PSTY₄₇-b-c-PtBA₄₄**, **24**.

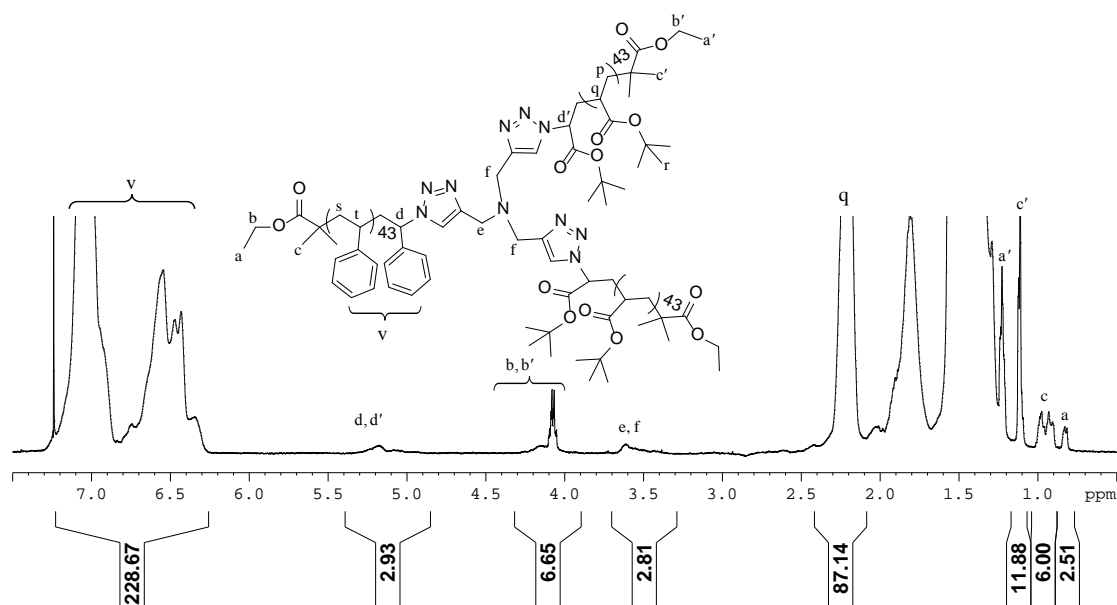


Figure C40. 500 MHz ^1H 1D DOSY NMR spectra in CDCl_3 of **PSTY₄₄-b-(PtBA₄₄)₂**, **25**.

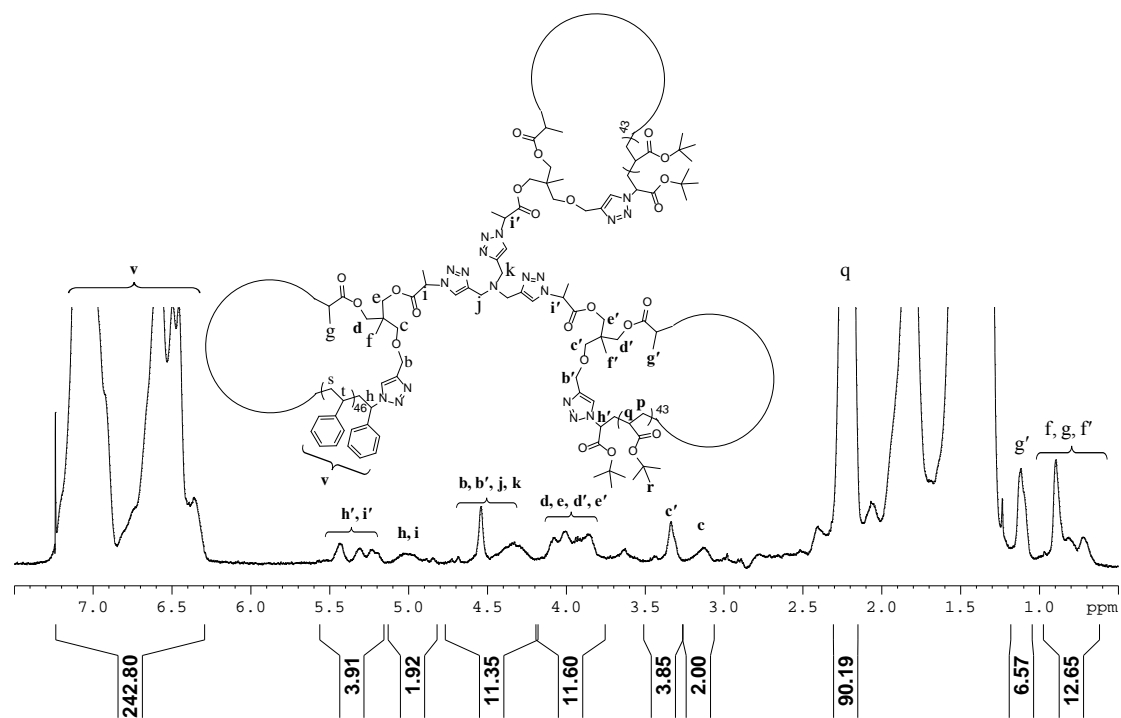


Figure C41. 500 MHz ^1H 1D DOSY NMR spectra in CDCl_3 of $c\text{-PSTY}_{44}\text{-}b\text{-(cPtBA}_{44})_2$, **26**.

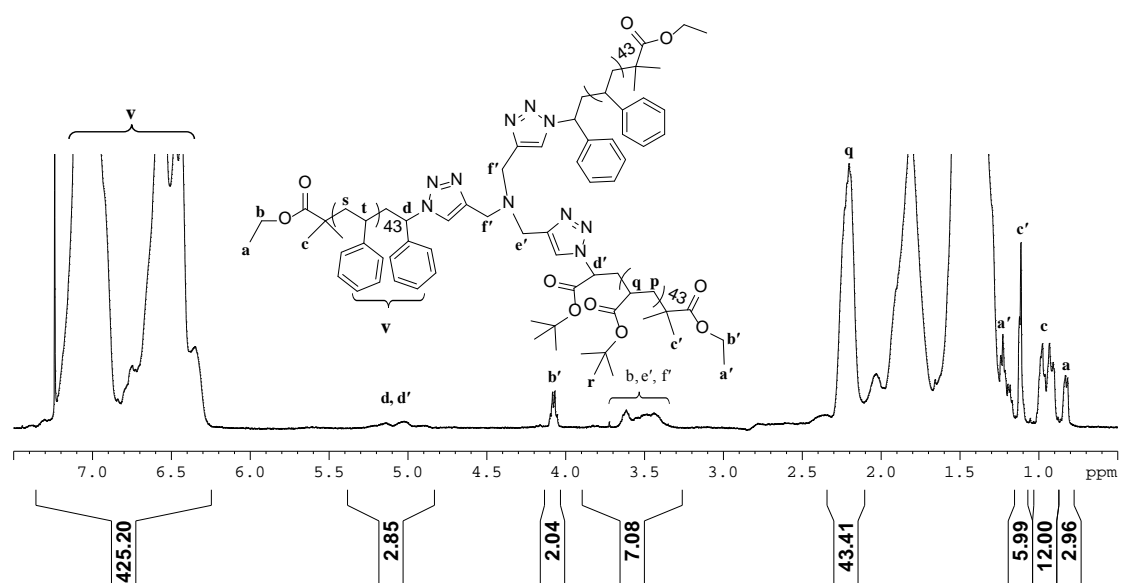


Figure C42. 500 MHz ^1H 1D DOSY NMR spectra in CDCl_3 of $(\text{PSTY}_{44})_2\text{-PtBA}_{44}$, **27**.

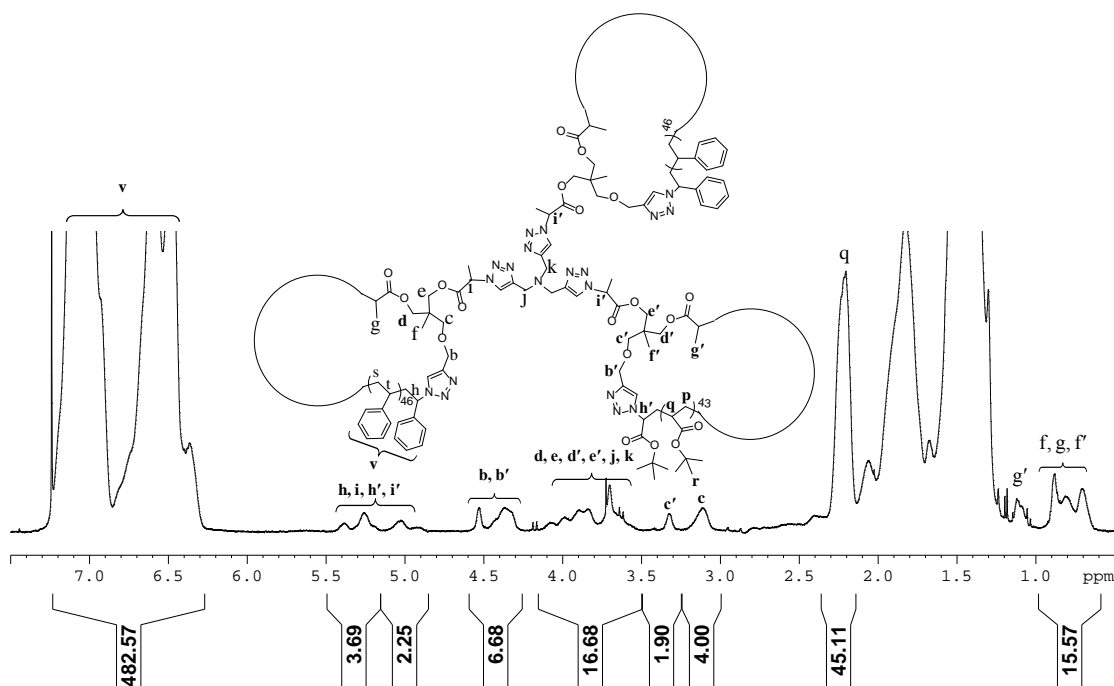


Figure C43. 500 MHz ^1H 1D DOSY NMR spectra in CDCl_3 of $(\text{c-PSTY}_{47})_2\text{-b-c-PtBA}_{44}$, **28**.

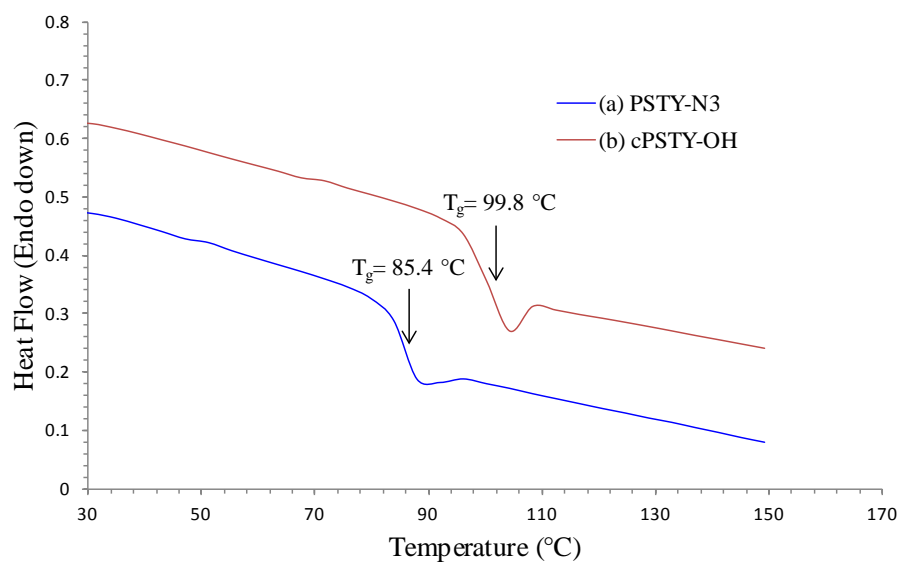


Figure C44. Differential scanning calorimetry (DSC) thermograms recorded for (a) $\text{PSTY}_{44}\text{-N}_3$, **3a** and (b) $\text{c-PSTY}_{47}\text{-OH}$, **8a**. Samples were first heated from 20 to 150 $^\circ\text{C}$ at a heating rate of 5 $^\circ\text{C}/\text{min}$ under nitrogen atmosphere, followed by cooling to 20 $^\circ\text{C}$ at a rate of 5

°C/min after stopping at 150 °C for 3 min, and finally heating to 150 °C at the rate of 5 °C/min.

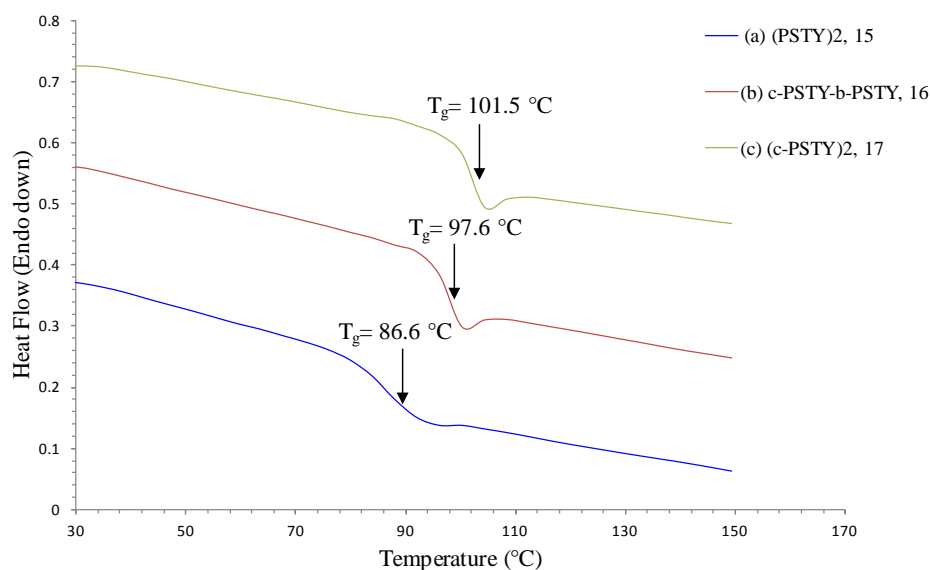


Figure C45. Differential scanning calorimetry (DSC) thermo-grams recorded for (a) (PSTY₄₄)₂, **15** and (b) c-PSTY₄₇-b-PSTY₄₄, **16** and (c) (c-PSTY₄₇)₂, **17**. Samples were first heated from 20 to 150 °C at a heating rate of 5 °C/min under nitrogen atmosphere, followed by cooling to 20 °C at a rate of 5 °C/min after stopping at 150 °C for 3 min, and finally heating to 150 °C at the rate of 5 °C/min.

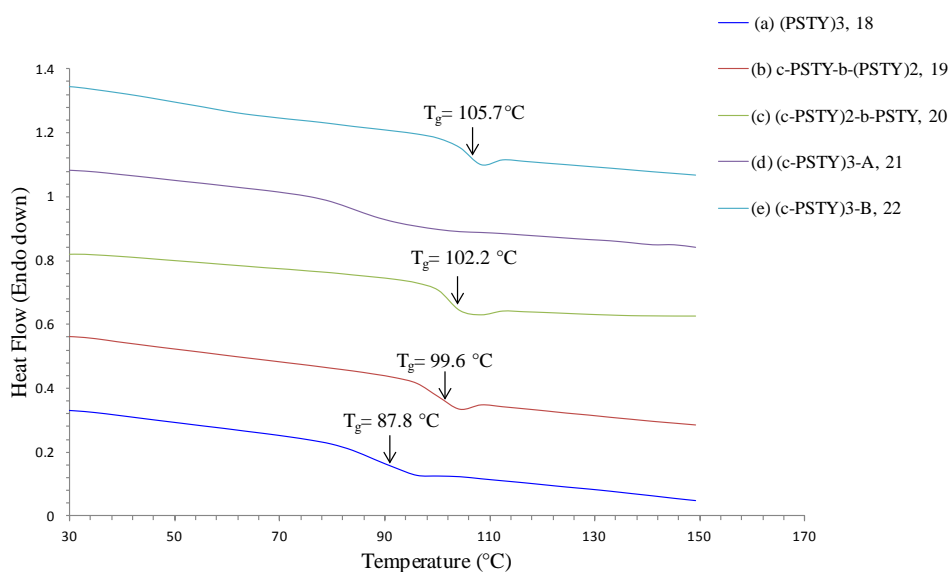


Figure C46. Differential scanning calorimetry (DSC) thermograms recorded for (a) (PSTY₄₄)₃, **18** and (b) c-PSTY₄₇-b-(PSTY₄₄)₂, **19**, (c) (c-PSTY₄₇)₂-PSTY₄₄, **20**, (d) (c-

PSTY₄₇)₃-A, **21** and (e) (c-PSTY₄₇)₃-B, **22**. Samples were first heated from 20 to 150 °C at a heating rate of 5 °C/min under nitrogen atmosphere, followed by cooling to 20 °C at a rate of 5 °C/min after stopping at 150 °C for 3 min, and finally heating to 150 °C at the rate of 5 °C/min.

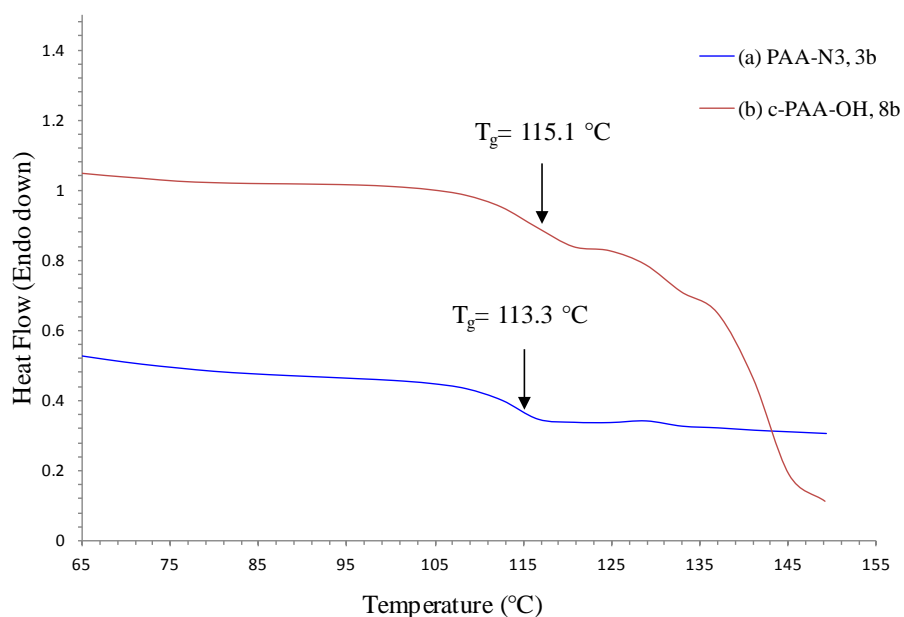


Figure C47. Differential scanning calorimetry (DSC) thermograms recorded for (a) PAA₄₄-N₃, **3b** and (b) c-PAA₄₄-OH, **8b**. Samples were first heated from 20 to 150 °C at a heating rate of 5 °C/min under nitrogen atmosphere, followed by cooling to 20 °C at a rate of 5 °C/min after stopping at 150 °C for 3 min, and finally heating to 150 °C at the rate of 5 °C/min.

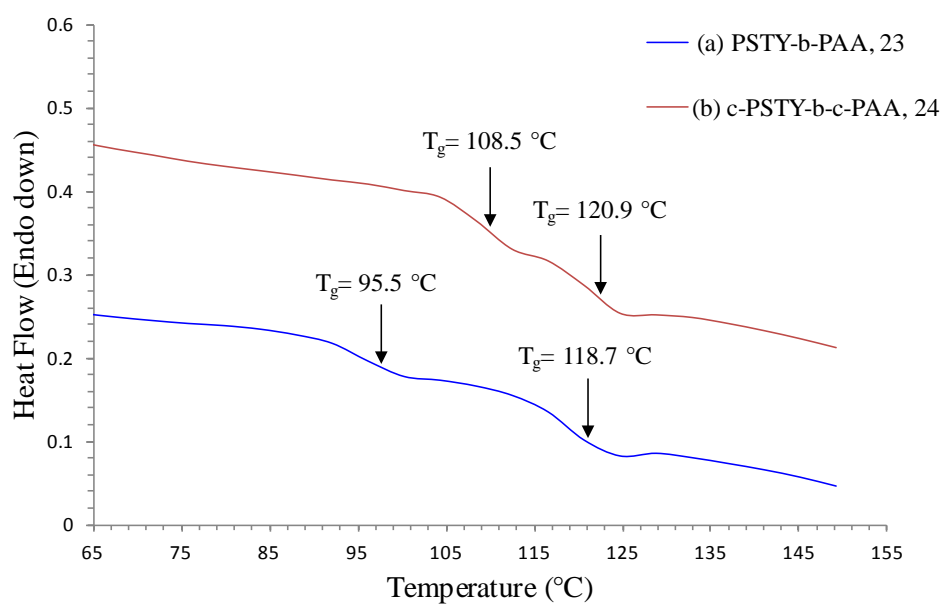


Figure C48. Differential scanning calorimetry (DSC) thermograms recorded for (a) PSTY₄₄-b-PAA₄₄, **23** and (b) c-PSTY₄₇-b-c-PAA₄₄, **24**. Samples were first heated from 20 to 150 °C at a heating rate of 5 °C/min under nitrogen atmosphere, followed by cooling to 20 °C at a rate of 5 °C/min after stopping at 150 °C for 3 min, and finally heating to 150 °C at the rate of 5 °C/min.

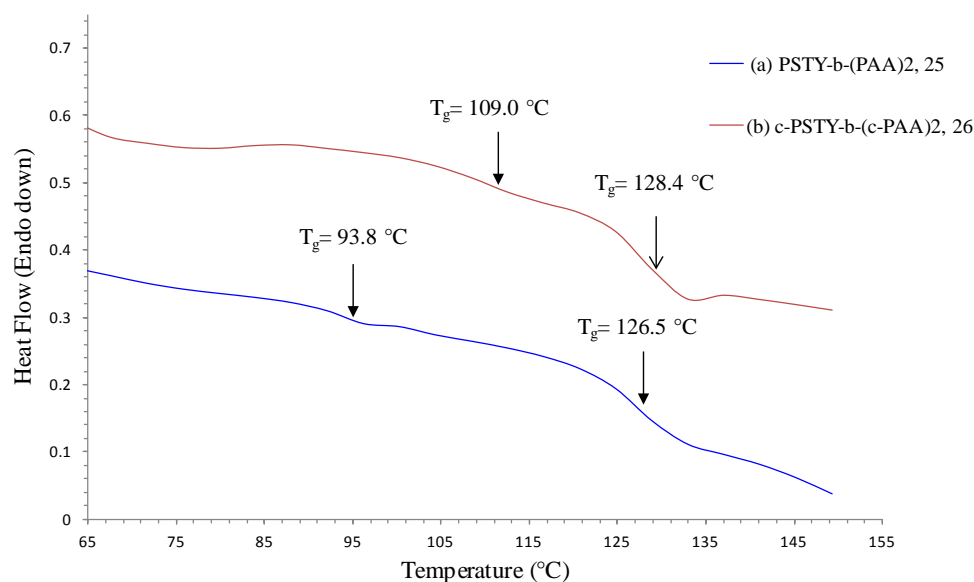


Figure c49. Differential scanning calorimetry (DSC) thermograms recorded for (a) PSTY₄₄-b-(PAA₄₄)₂, **25** and (b) c-PSTY₄₇-b-(c-PAA₄₄)₂, **26**. Samples were first heated from 20 to 150

°C at a heating rate of 5 °C/min under nitrogen atmosphere, followed by cooling to 20 °C at a rate of 5 °C/min after stopping at 150 °C for 3 min, and finally heating to 150 °C at the rate of 5 °C/min.

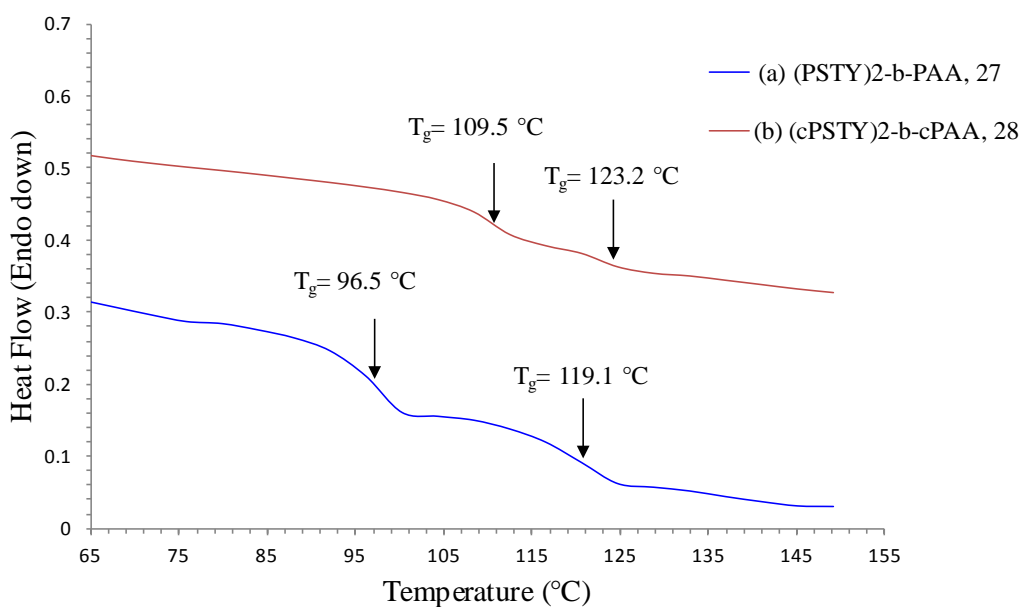


Figure C50. Differential scanning calorimetry (DSC) thermograms recorded for (a) (PSTY₄₄)₂-b-PAA₄₄, **27** and (b) (c-PSTY₄₇)₂-b-c-PAA₄₄, **28**. Samples were first heated from 20 to 150 °C at a heating rate of 5 °C/min under nitrogen atmosphere, followed by cooling to 20 °C at a rate of 5 °C/min after stopping at 150 °C for 3 min, and finally heating to 150 °C at the rate of 5 °C/min.

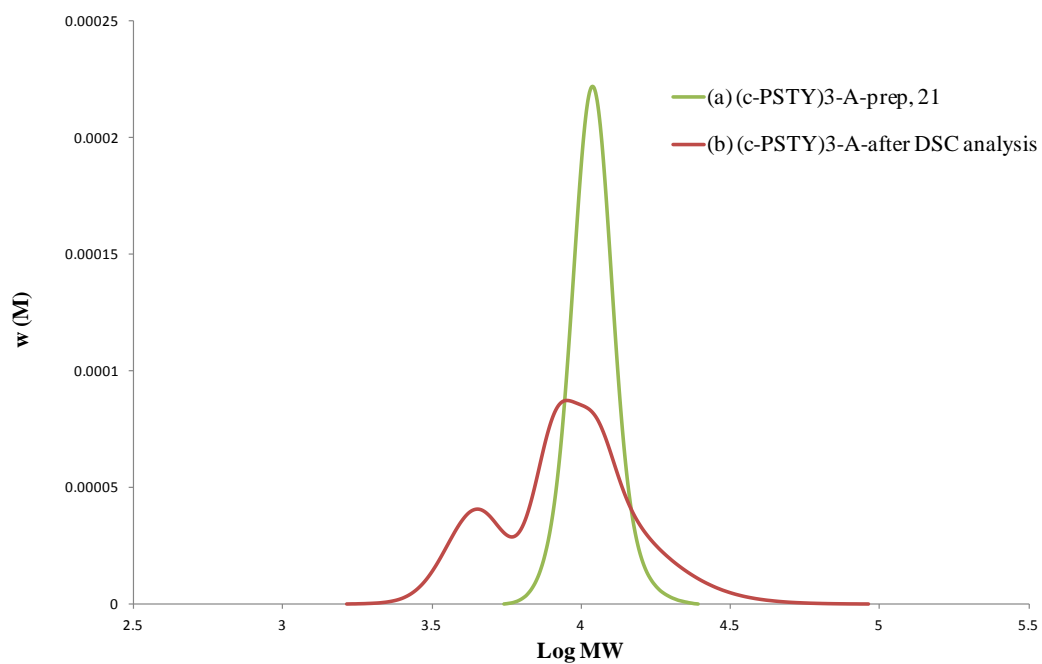
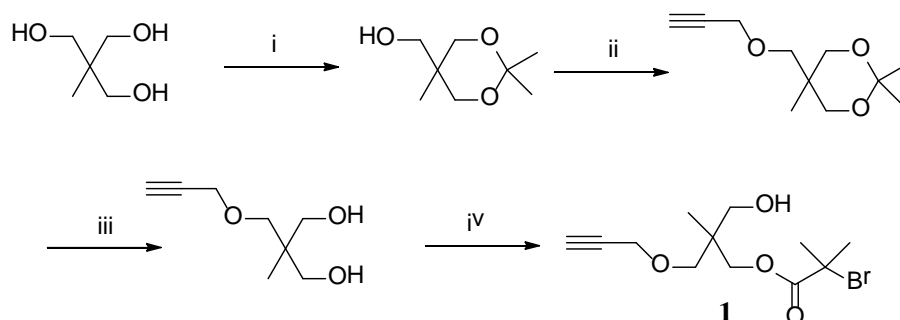


Figure C51: SEC traces of (c-PSTY)₃-A-21 for polymer cleavage (a) before and (b) after DSC analysis.

Appendix D

Synthesis of Alkyne (hydroxyl) functional Initiator (1)



Scheme D1: Synthetic scheme for Alkyne (hydroxyl) functional initiator.

Reactants and conditions: i) Acetone, p-TsOH, RT, 16h; ii) THF, NaH, propargyl bromide, -78 °C, 16 h; iii) DOWEX, Methanol, R.T. 16 h; iv) THF, 2-bromoisobutyryl bromide, 0 °C - RT, 16 h.

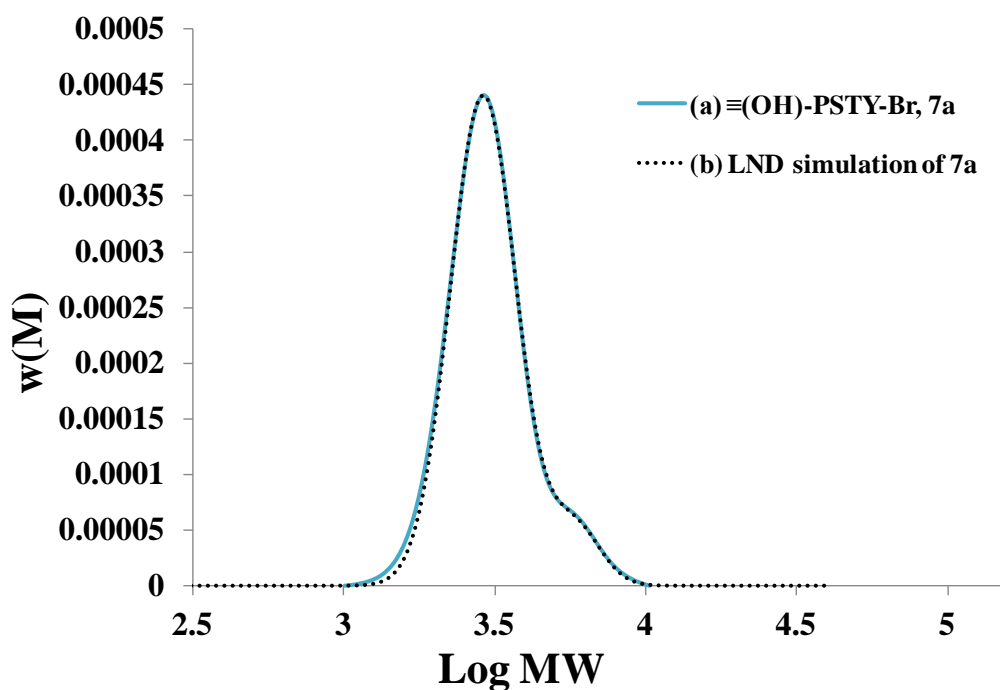


Figure D1: SEC trace of (a) $\equiv(\text{OH})\text{-PSTY}_{25}\text{-Br}$ 7a and (b) LND simulation. SEC analysis based on polystyrene calibration curve.

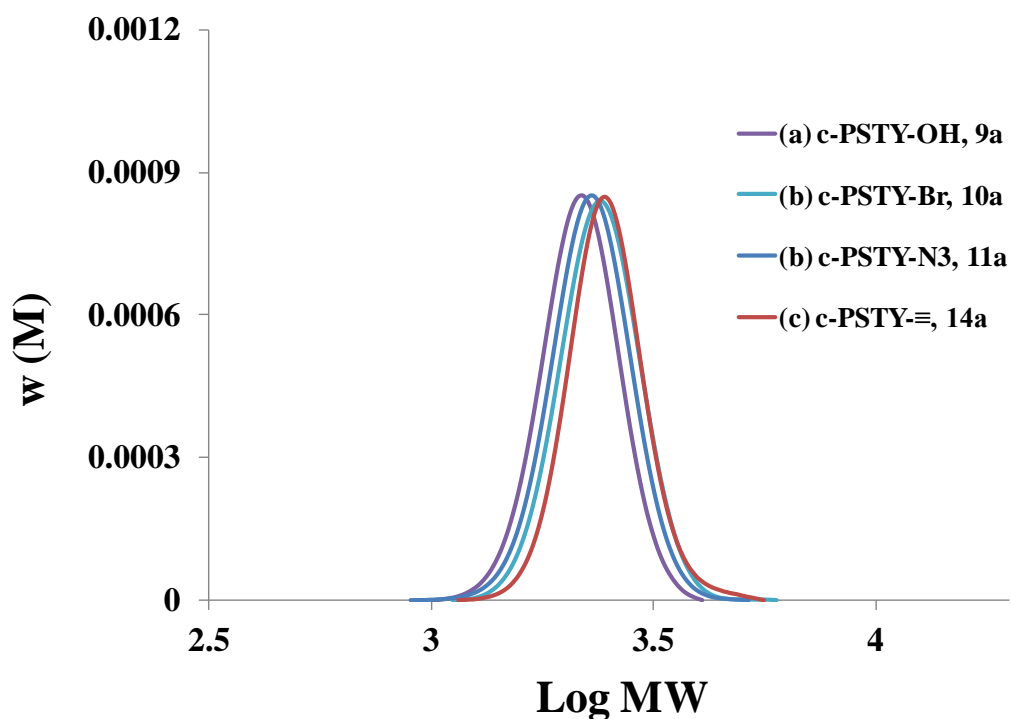


Figure D2: SEC trace of (a) c-PSTY₂₅-OH, **9a**, (b) c-PSTY₂₅-Br, **10a**, (c) c-PSTY₂₅-N₃, **11a** and (d) c-PSTY₂₅-≡, **14a**. SEC analysis based on polystyrene calibration curve.

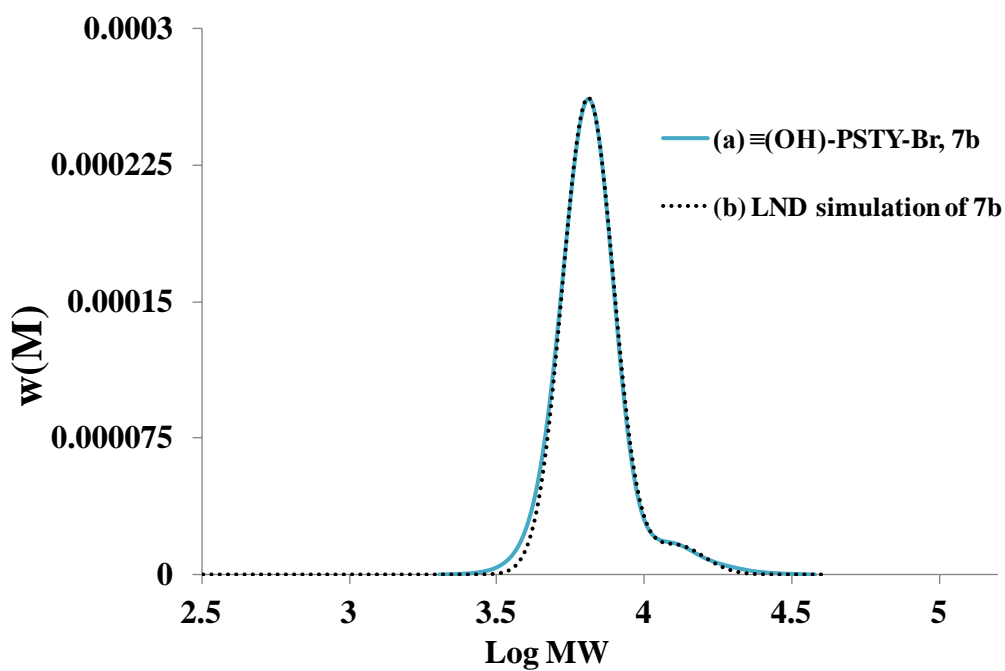


Figure D3: SEC trace of (a) ≡(OH)-PSTY₅₈-Br **7b** and (b) LND simulation. SEC analysis based on polystyrene calibration curve.

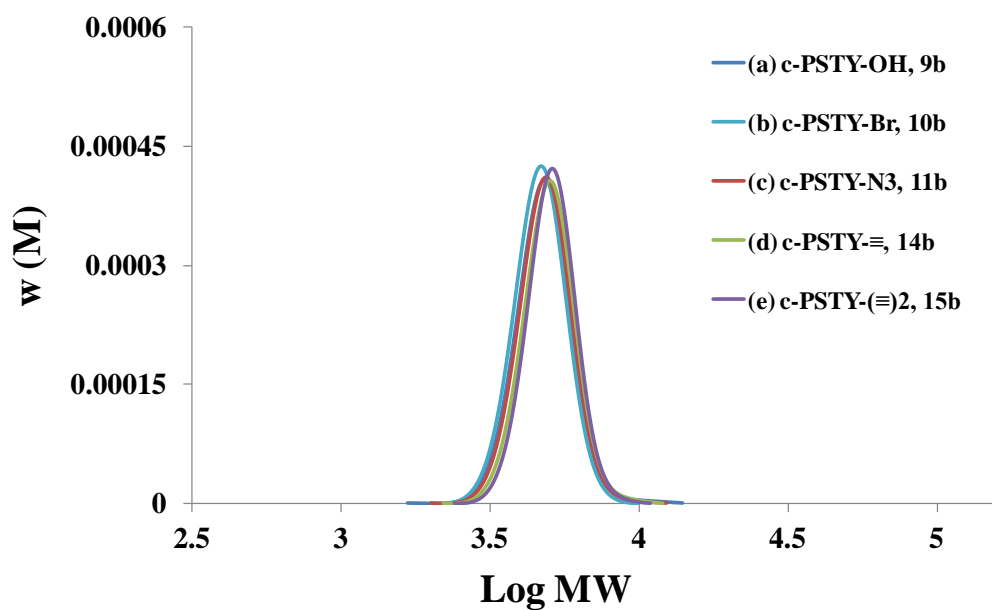


Figure D4: SEC trace of (a) c-PSTY₅₈-OH, **9b**, (b) c-PSTY₅₈-Br, **10b**, (c) c-PSTY₅₈-N₃, **11b**, (d) c-PSTY₅₈-≡, **14b** and (e) c-PSTY₅₈-(≡)₂, **15b**. SEC analysis based on polystyrene calibration curve.

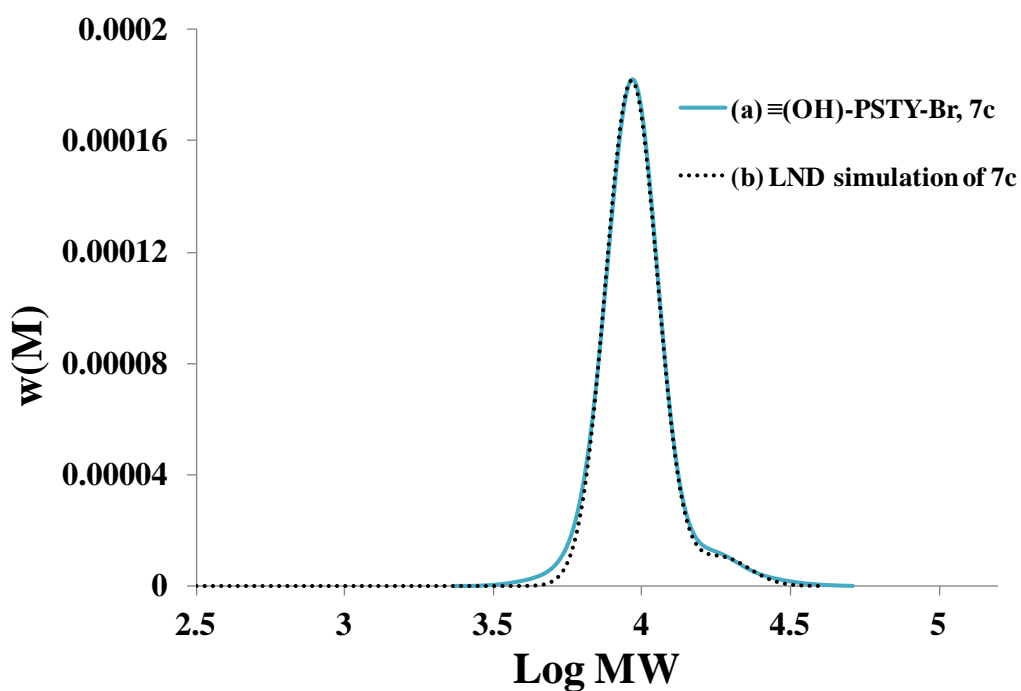


Figure D5: SEC trace of (a) ≡(OH)-PSTY₈₄-Br **7c** and (b) LND simulation. SEC analysis based on polystyrene calibration curve.

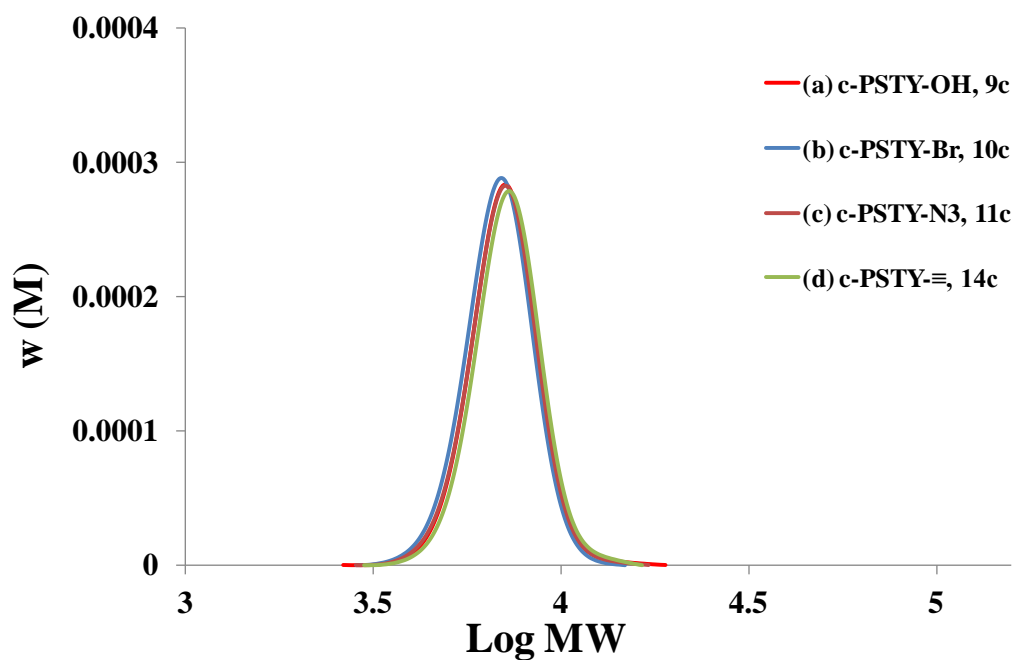


Figure D6: SEC trace of (a) c-PSTY₈₄-OH, **9c**, (b) c-PSTY₈₄-Br, **10c**, (c) c-PSTY₈₄-N₃, **11c** and (d) c-PSTY₈₄-≡, **14c**. SEC analysis based on polystyrene calibration curve.

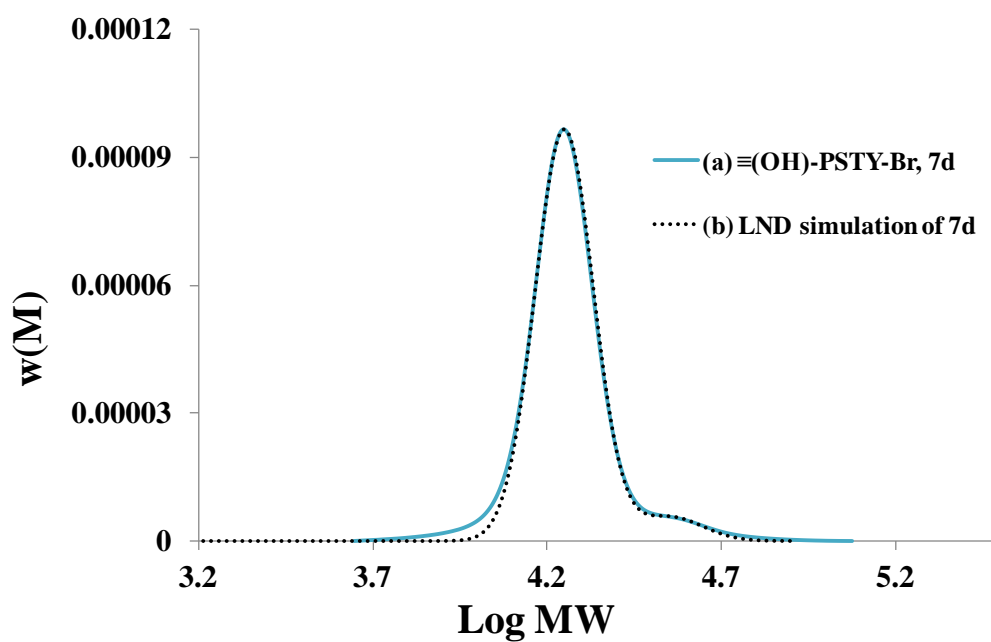


Figure D7: SEC trace of (a) ≡(OH)-PSTY₁₆₄-Br **7d** and (b) LND simulation. SEC analysis based on polystyrene calibration curve.

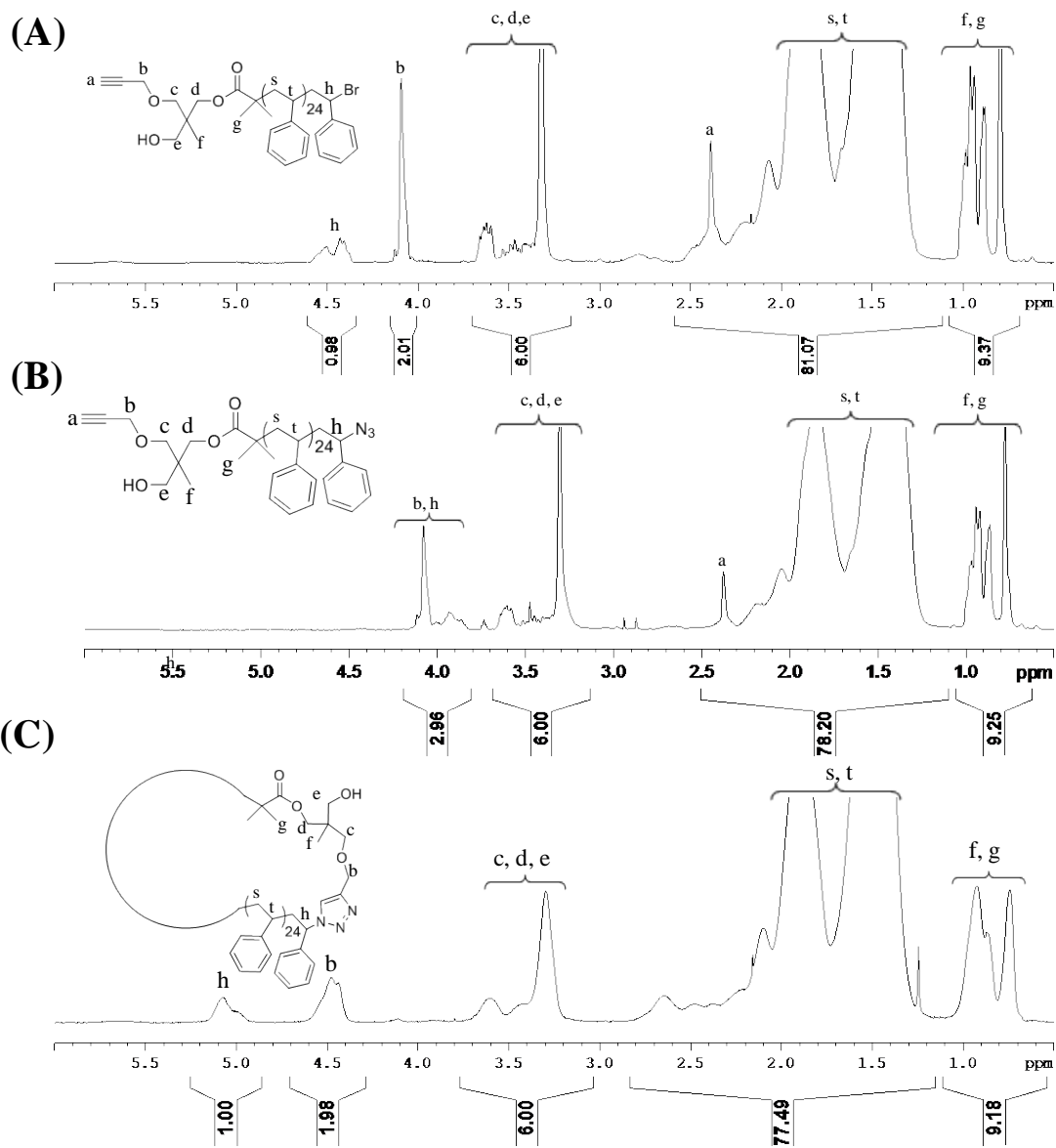


Figure D8. 500 MHz ^1H 1D DOSY NMR spectra in CDCl_3 of (a) $\equiv(\text{OH})\text{-PSTY}_{25}\text{-Br}$ **7a**, (b) $\equiv(\text{OH})\text{-PSTY}_{25}\text{-N}_3$ **8a**, (c) c-PSTY₂₅-OH **9a**.

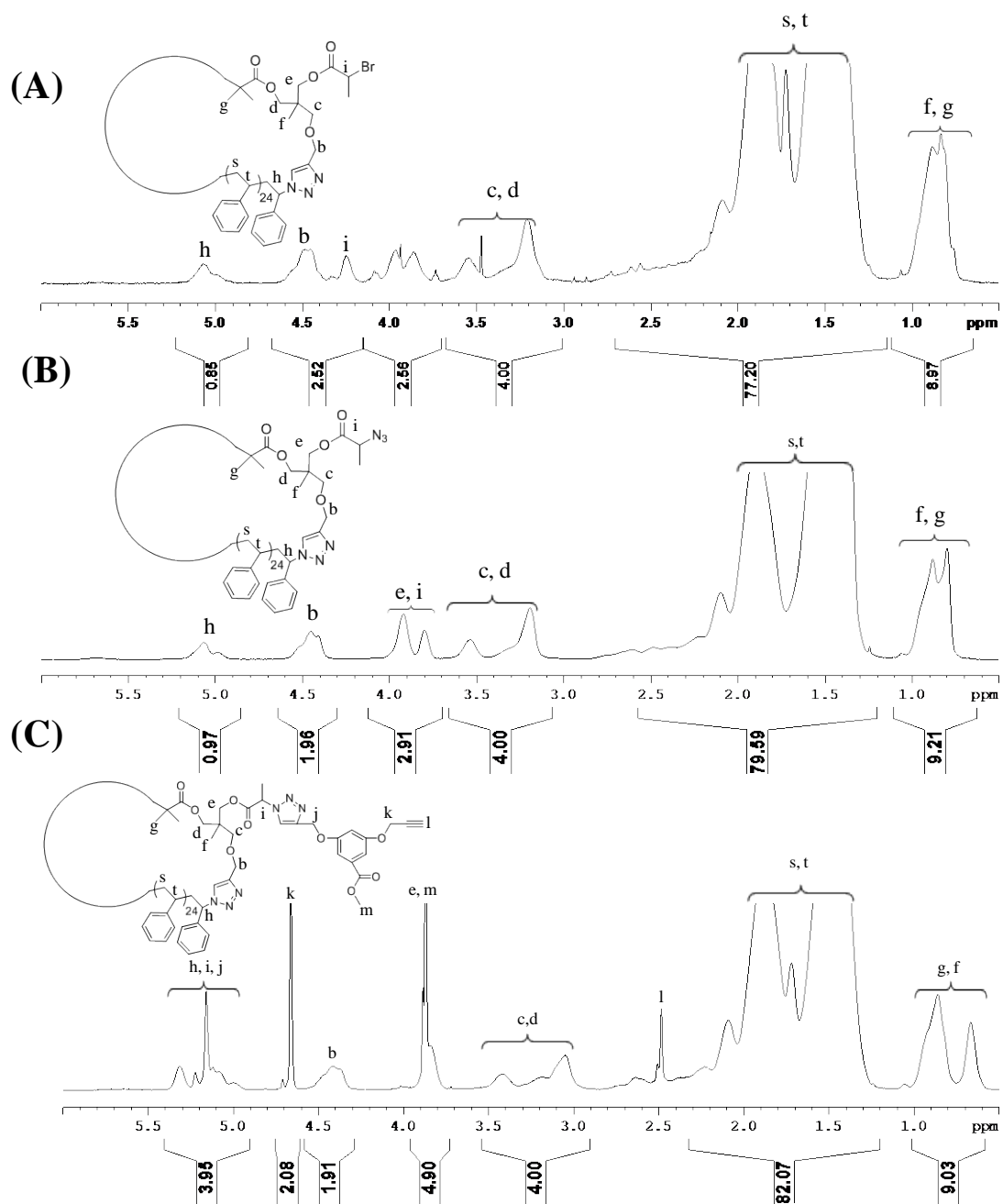


Figure D9. 500 MHz ^1H 1D DOSY NMR spectra in CDCl_3 of (a) c-PSTY₂₅-Br **10a**, (B) c-PSTY₂₅-N₃ **11a**, (C) c-PSTY₂₅≡ **14a**.

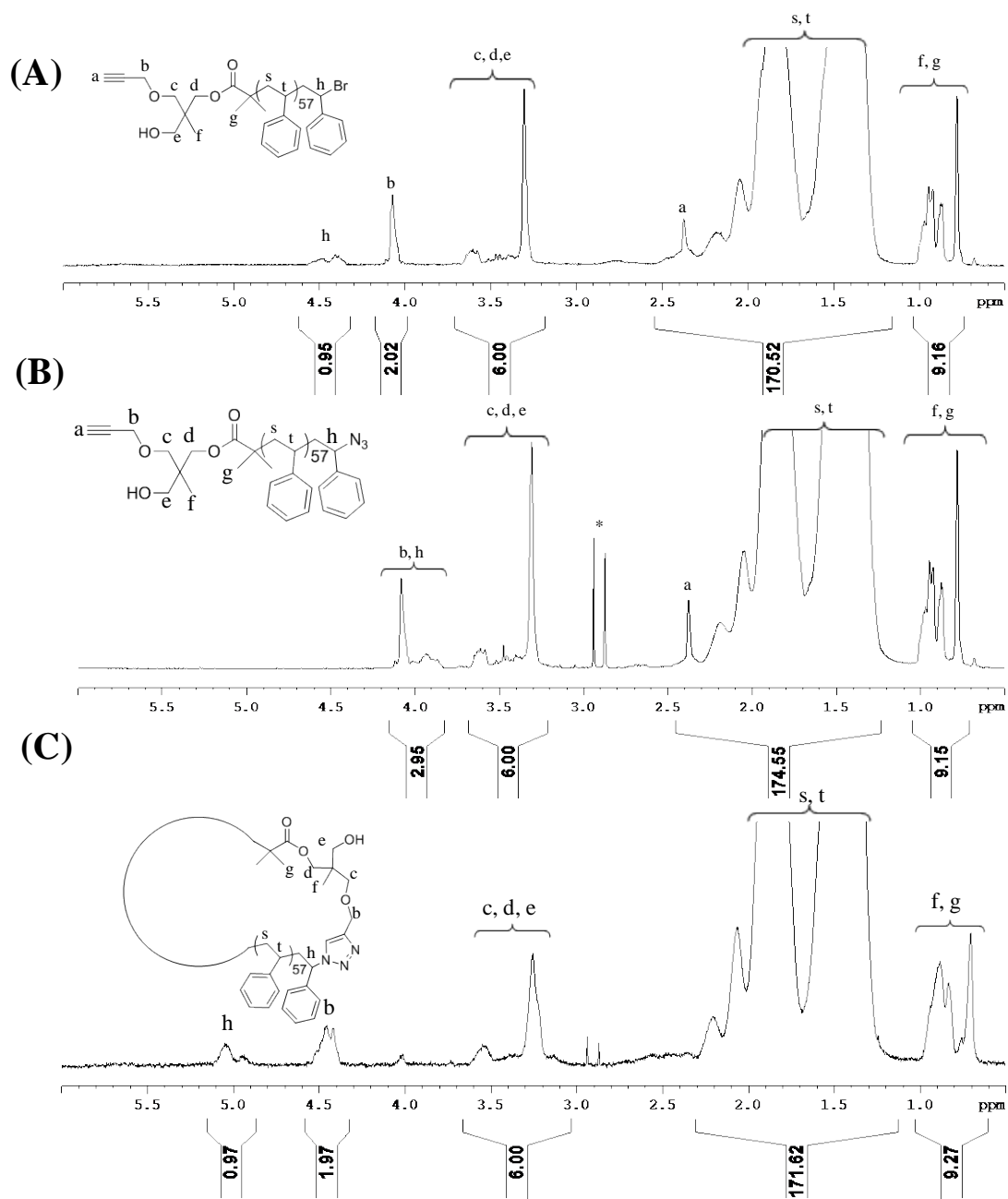


Figure D10. 500 MHz ^1H 1D DOSY NMR spectra in CDCl_3 of (a) $\equiv(\text{OH})\text{-PSTY}_{58}\text{-Br}$ **7b**, (b) $\equiv(\text{OH})\text{-PSTY}_{58}\text{-N}_3$ **8b**, (c) c-PSTY₅₈-OH **9b**.

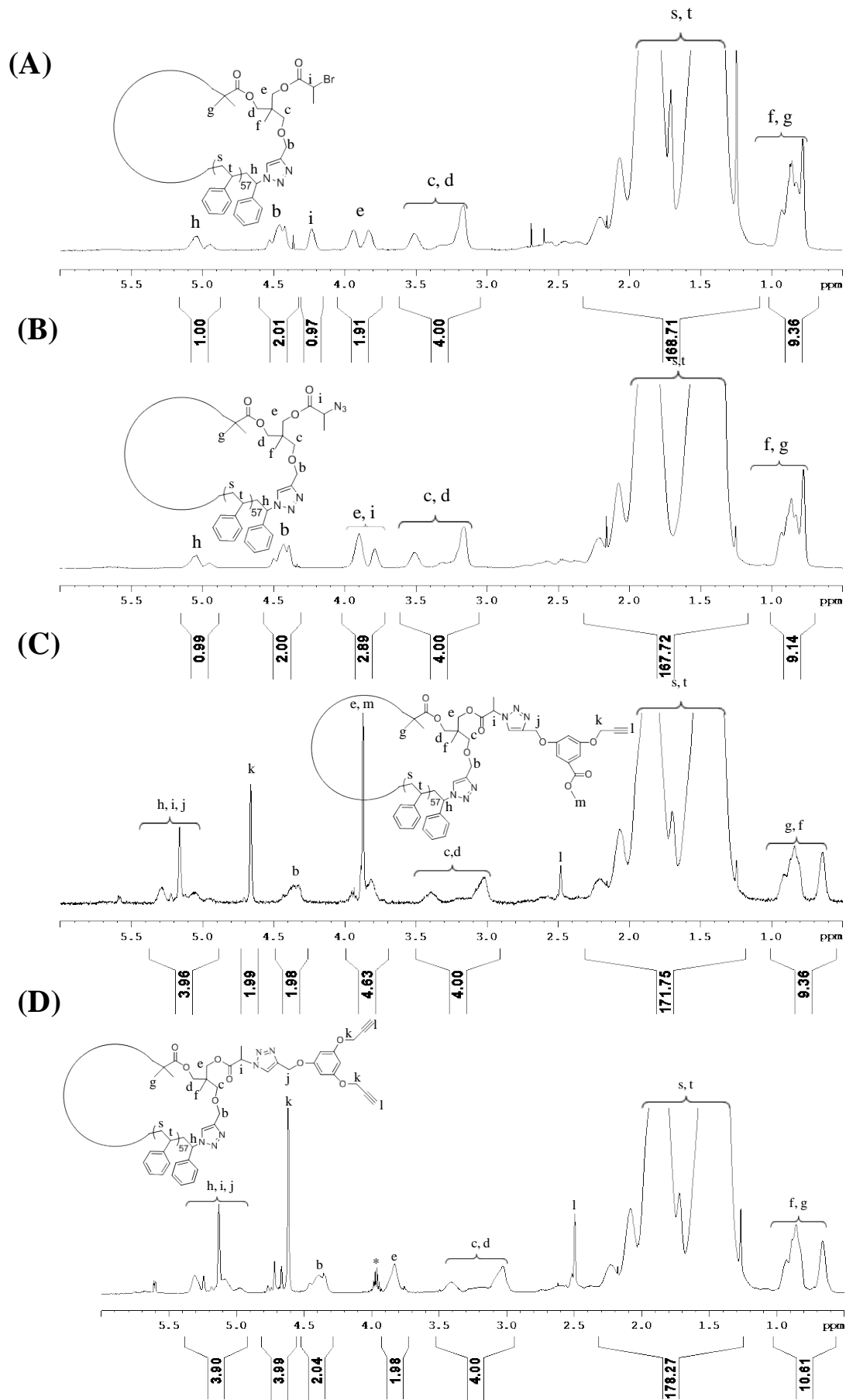


Figure D11. 500 MHz ^1H 1D DOSY NMR spectra in CDCl_3 of (A) c-PSTY₅₈-Br **10b**, (B) c-PSTY₅₈-N₃ **11b**, (C) c-PSTY₅₈-≡ **14b** and (D) c-PSTY₅₈-(≡)₂ **15b**.

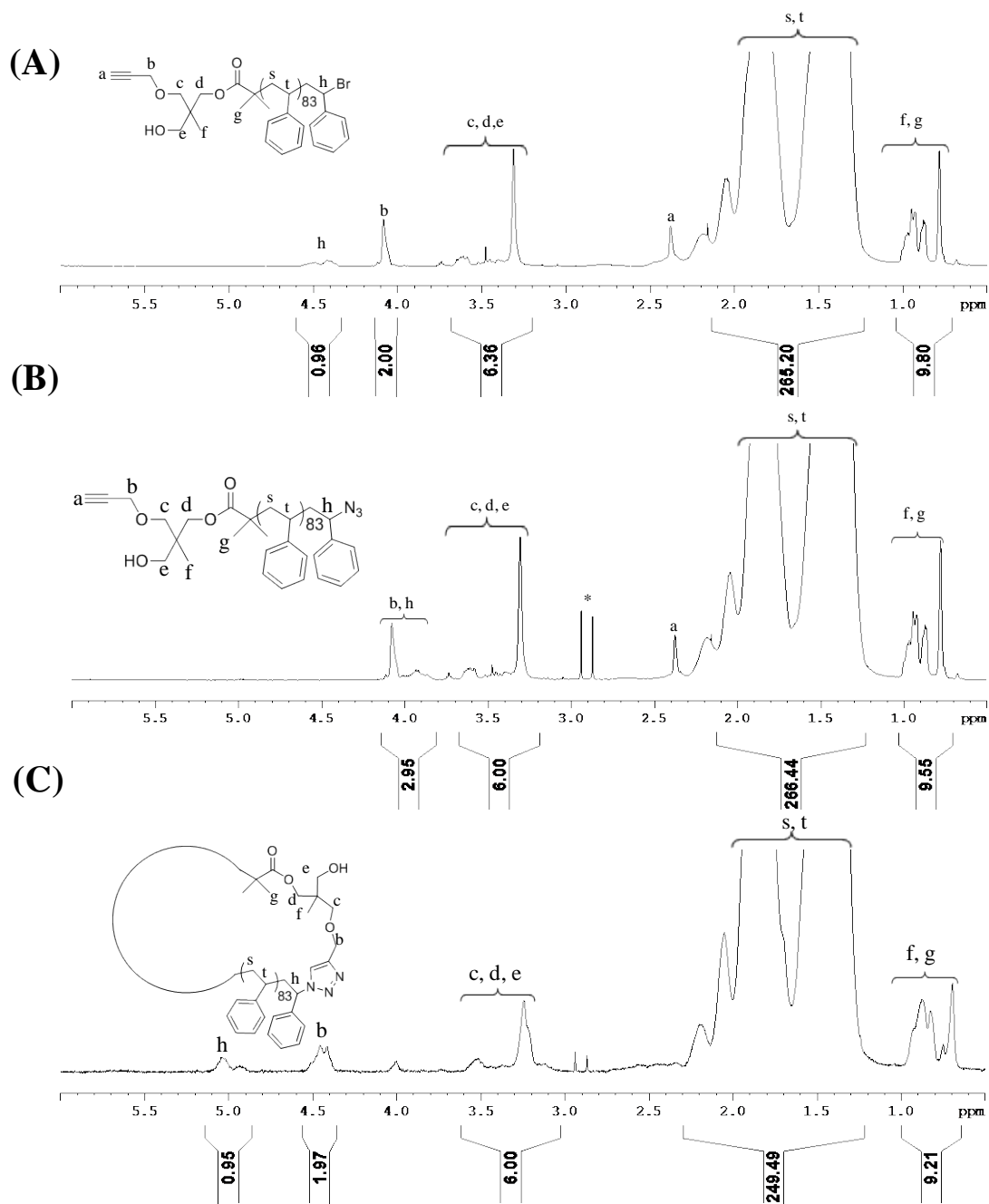


Figure D12. 500 MHz ^1H 1D DOSY NMR spectra in CDCl_3 of (a) ≡(OH)-PSTY₈₄-Br **7c**, (b) ≡(OH)-PSTY₈₄-N₃ **8c**, (c) c-PSTY₈₄-OH **9c**.

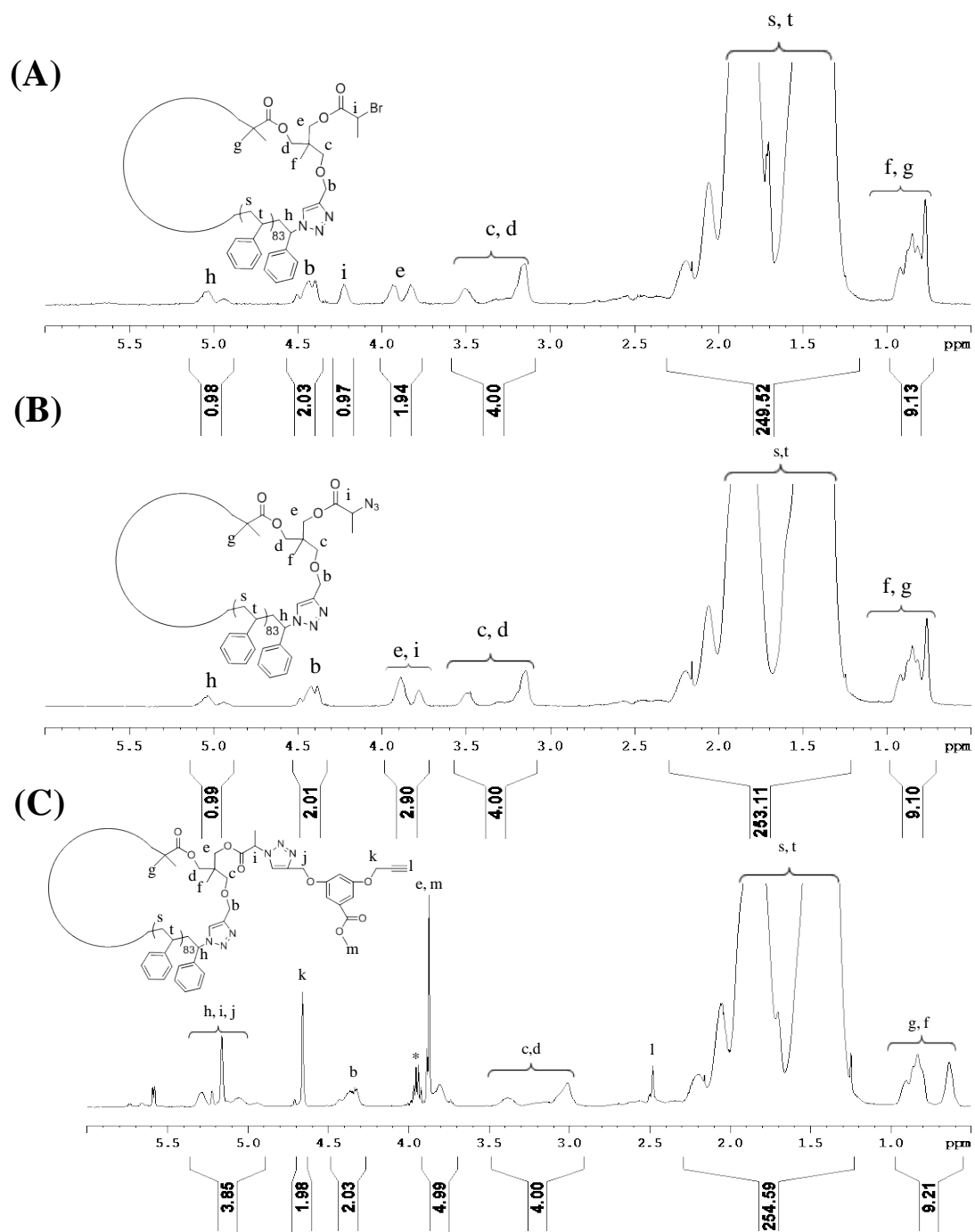


Figure D13. 500 MHz ^1H 1D DOSY NMR spectra in CDCl_3 of (a) c-PSTY₈₄-Br **10c**, (B) c-PSTY₈₄-N₃ **11c** and (C) c-PSTY₈₄-≡ **14c**.

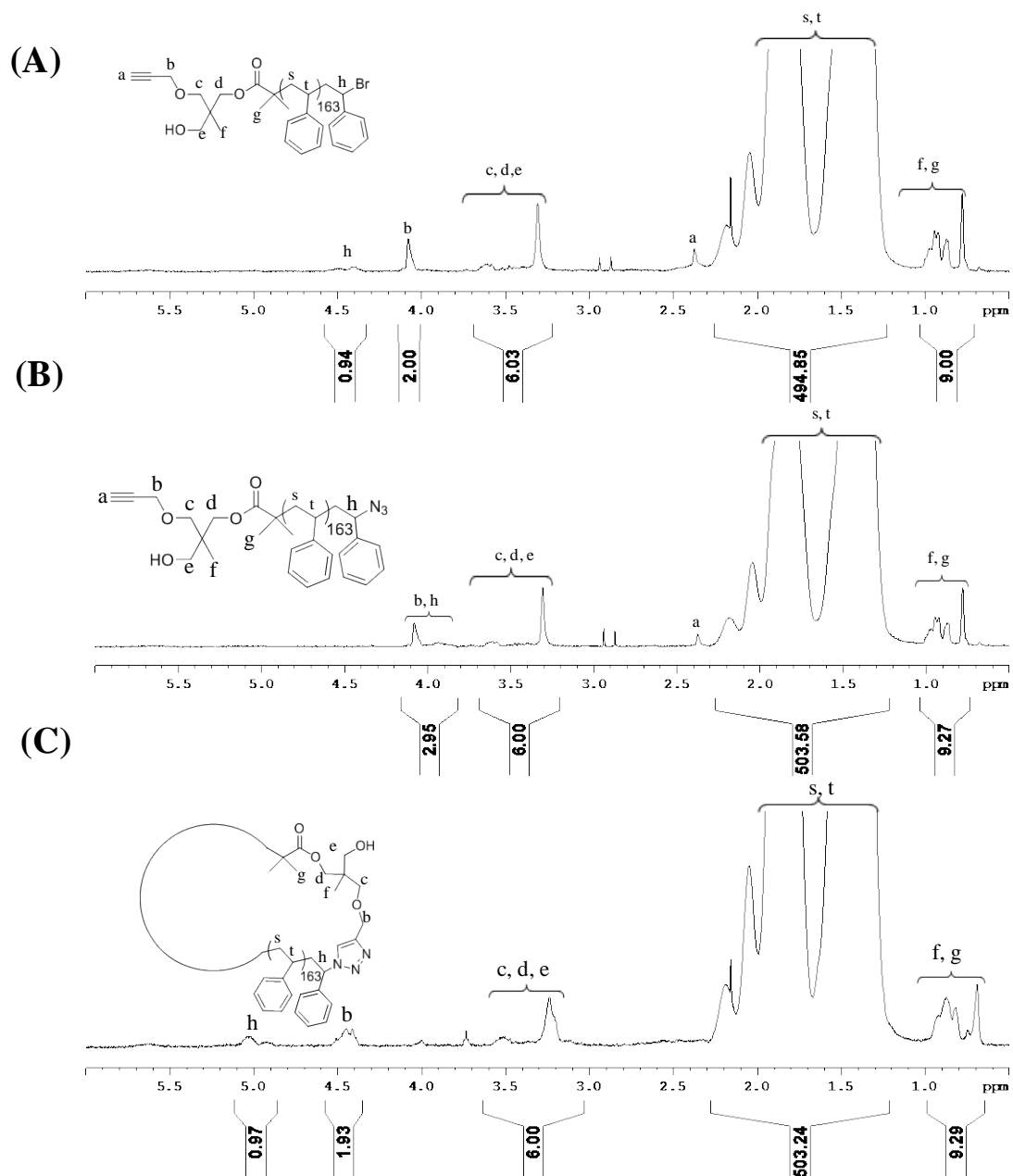


Figure D14. 500 MHz ^1H 1D DOSY NMR spectra in CDCl_3 of (a) $\equiv(\text{OH})\text{-PSTY}_{164}\text{-Br}$ **7d**, (b) $\equiv(\text{OH})\text{-PSTY}_{163}\text{-N}_3$ **8d**, (c) $\text{c-PSTY}_{164}\text{-OH}$ **9d**.

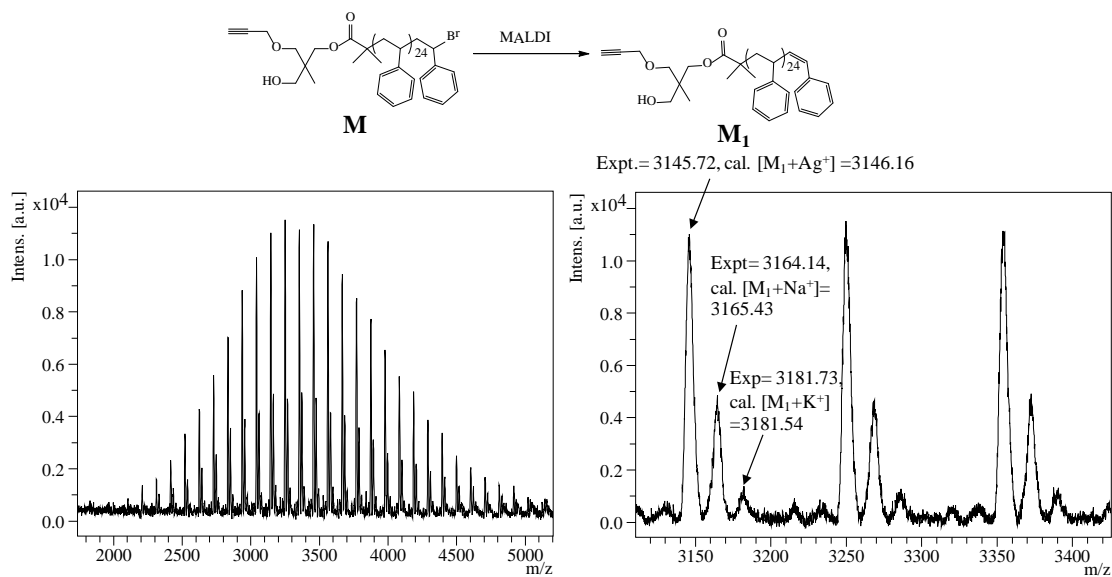


Figure D15: MALDI-ToF mass spectrum acquired in reflectron mode with Ag salt as cationizing agent and DCTB matrix. The full and expanded spectra correspond to $\equiv(\text{HO})\text{-PSTY}_{25}\text{-Br}$, **7a**.

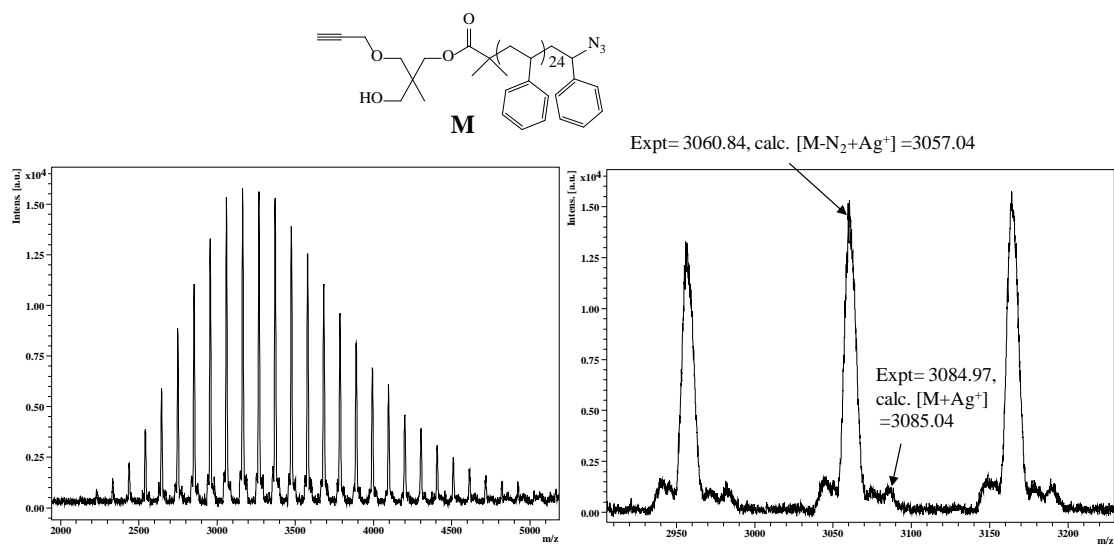


Figure D16 : MALDI-ToF mass spectrum acquired in reflectron mode with Ag salt as cationizing agent and DCTB matrix. The full and expanded spectra correspond to $\equiv(\text{HO})\text{-PSTY}_{25}\text{-N}_3$, **8a**.

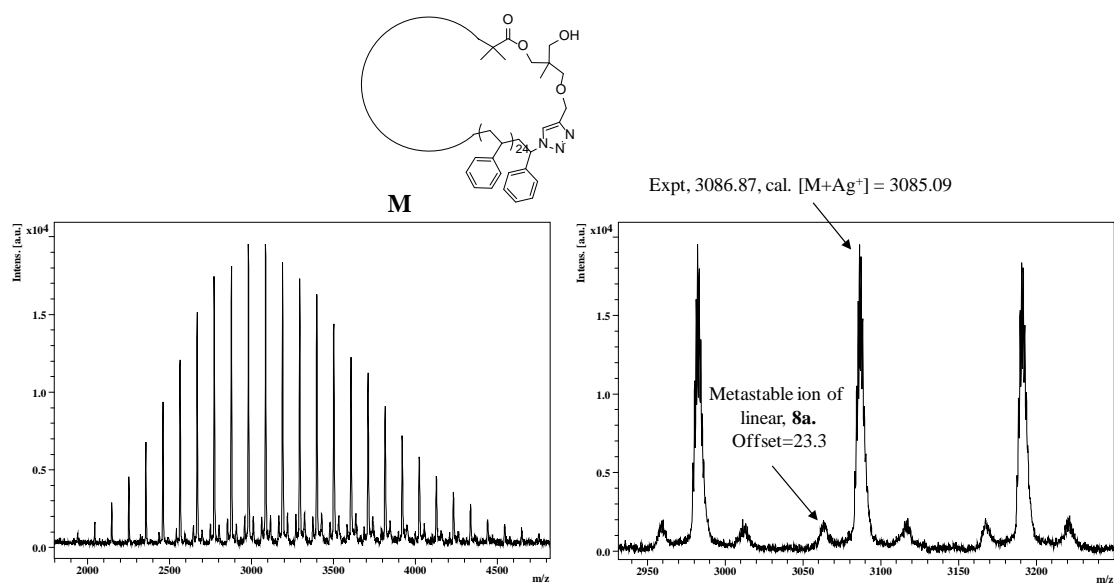


Figure D17: MALDI-ToF mass spectrum acquired in reflectron mode with Ag salt as cationizing agent and DCTB matrix. The full and expanded spectra correspond to c-PSTY₂₅-OH, **9a**.

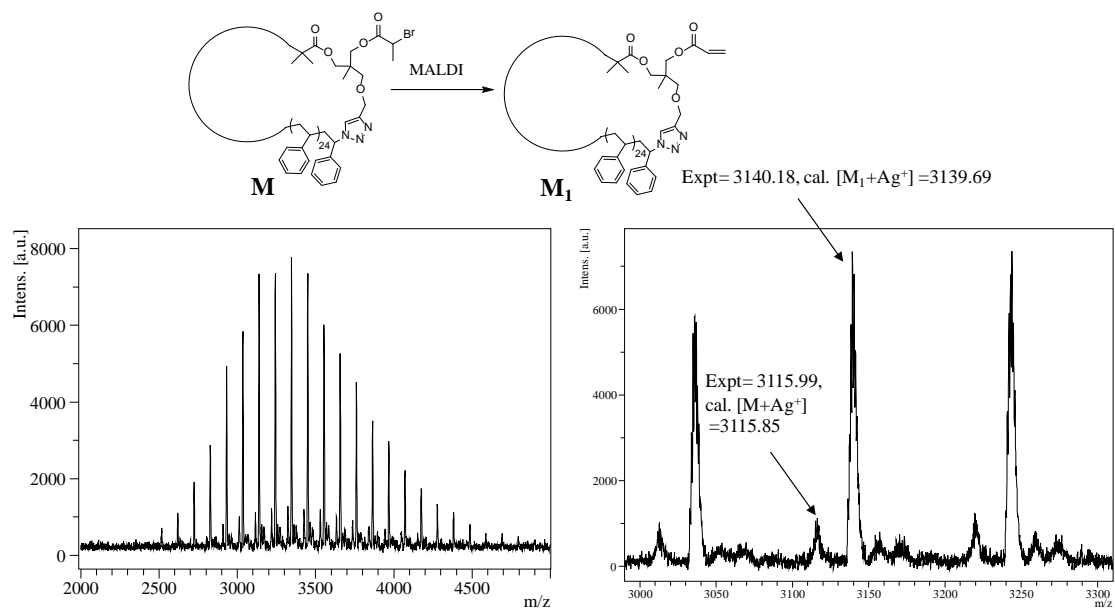


Figure D18: MALDI-ToF mass spectrum acquired in reflectron mode with Ag salt as cationizing agent and DCTB matrix. The full and expanded spectra correspond to c-PSTY₂₅-Br, **10a**.

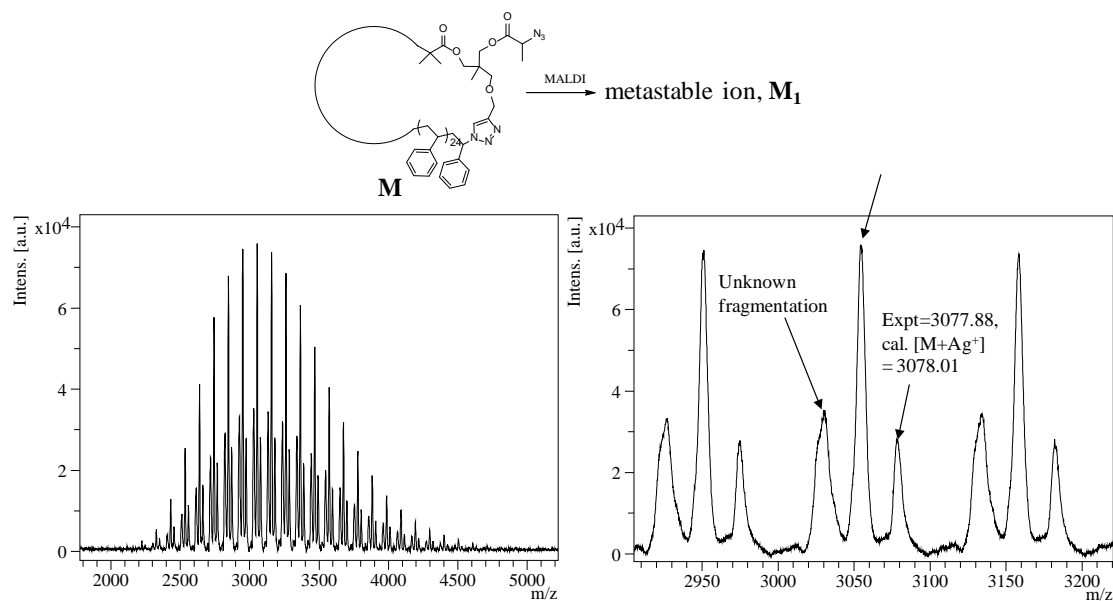


Figure D19: MALDI-ToF mass spectrum acquired in reflectron mode with Ag salt as cationizing agent and DCTB matrix. The full and expanded spectra correspond to c-PSTY₂₅-N₃, **11a**.

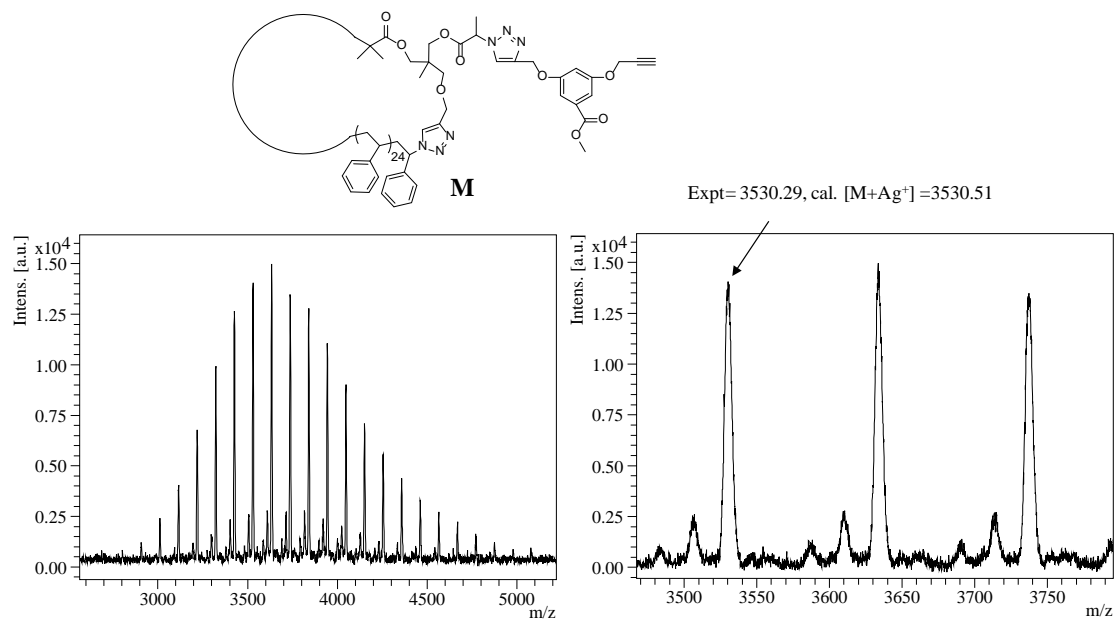


Figure D20: MALDI-ToF mass spectrum acquired in reflectron mode with Ag salt as cationizing agent and DCTB matrix. The full and expanded spectra correspond to c-PSTY₂₅-≡, **14a**.

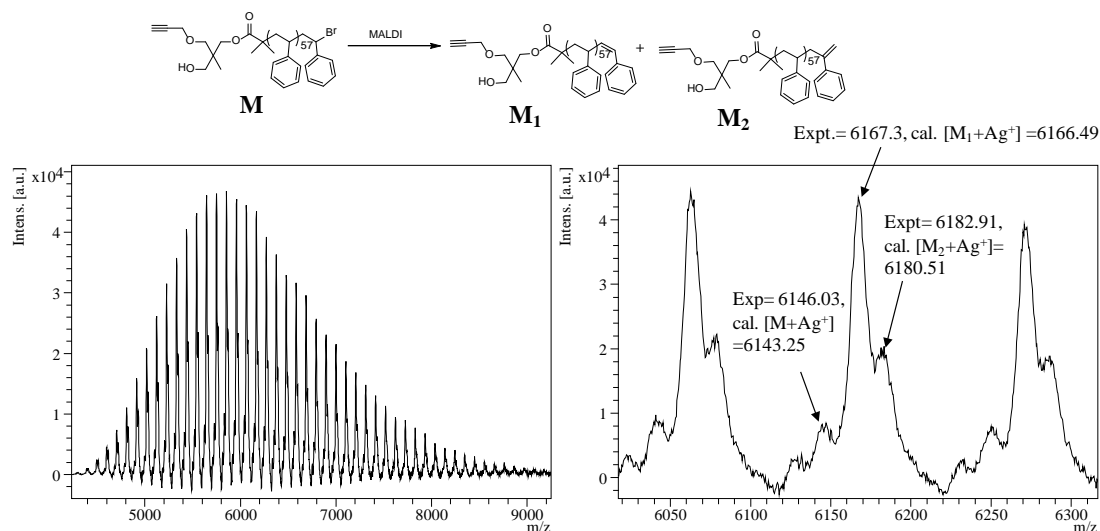


Figure D21: MALDI-ToF mass spectrum acquired in linear mode with Ag salt as cationizing agent and DCTB matrix. The full and expanded spectra correspond to $\equiv(\text{HO})\text{-PSTY}_{58}\text{-Br}$, **7b**.

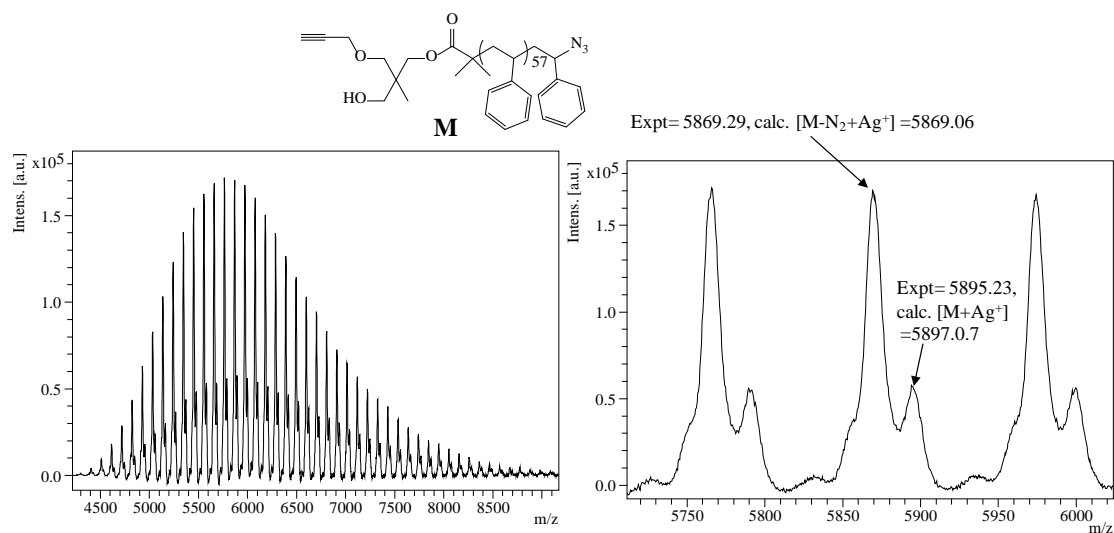


Figure D22: MALDI-ToF mass spectrum acquired in linear mode with Ag salt as cationizing agent and DCTB matrix. The full and expanded spectra correspond to $\equiv(\text{HO})\text{-PSTY}_{58}\text{-N}_3$, **8b**.

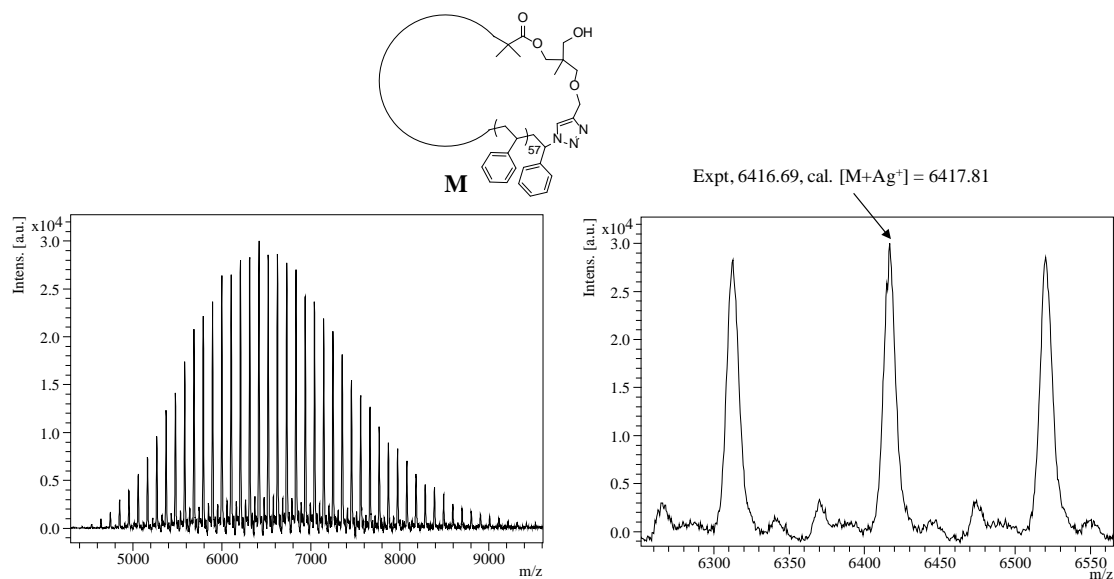


Figure D23: MALDI-ToF mass spectrum acquired in linear mode with Ag salt as cationizing agent and DCTB matrix. The full and expanded spectra correspond to c-PSTY₅₈-OH, **9b**.

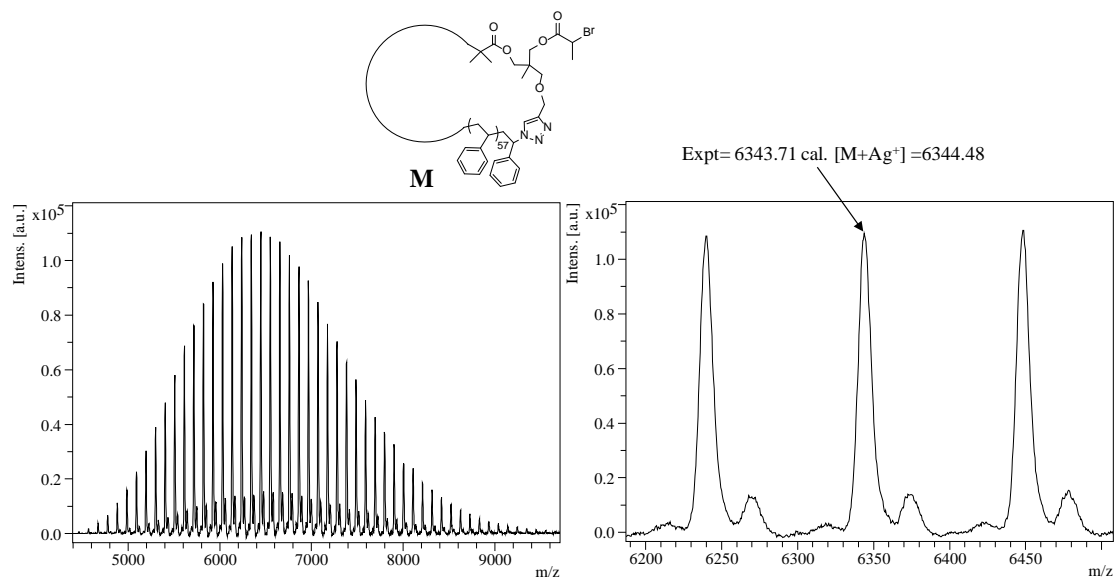


Figure D24: MALDI-ToF mass spectrum acquired in linear mode with Ag salt as cationizing agent and DCTB matrix. The full and expanded spectra correspond to c-PSTY₅₈-Br, **10b**.

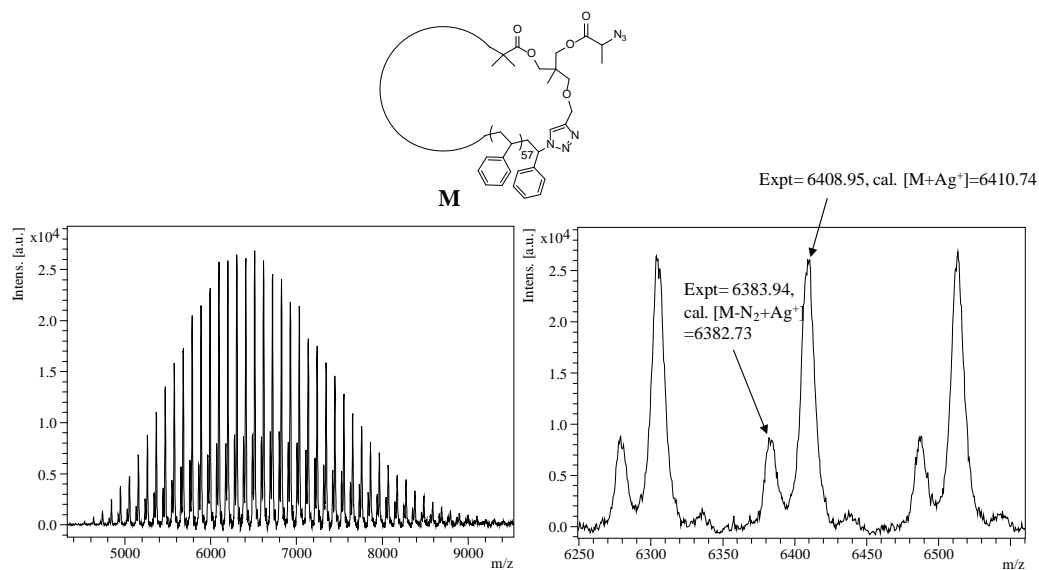


Figure D25: MALDI-ToF mass spectrum acquired in linear mode with Ag salt as cationizing agent and DCTB matrix. The full and expanded spectra correspond to c-PSTY₅₈-N₃, **11b**.

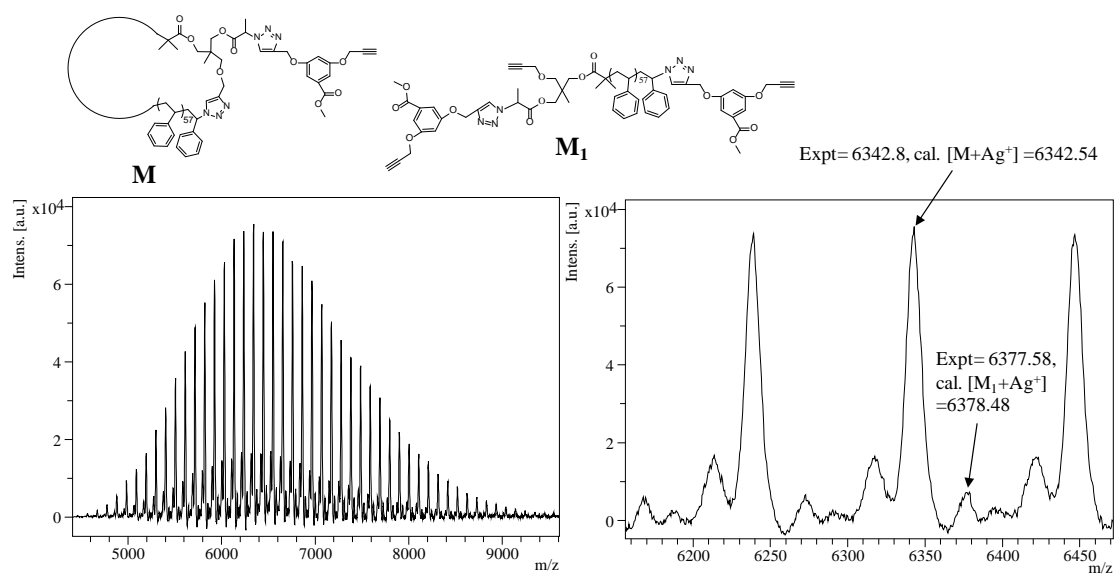


Figure D26: MALDI-ToF mass spectrum acquired in linear mode with Ag salt as cationizing agent and DCTB matrix. The full and expanded spectra correspond to c-PSTY₅₈-≡, **14b**.

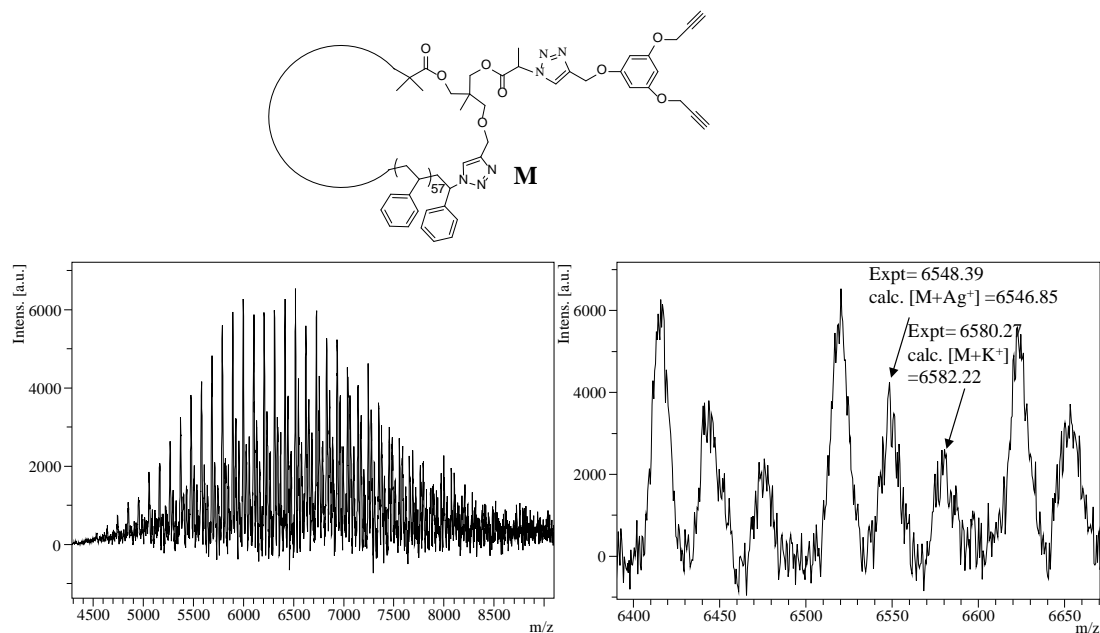


Figure D27: MALDI-ToF mass spectrum acquired in linear mode with Ag salt as cationizing agent and DCTB matrix. The full and expanded spectra correspond to c-PSTY₅₈-(≡)₂, **15b**.

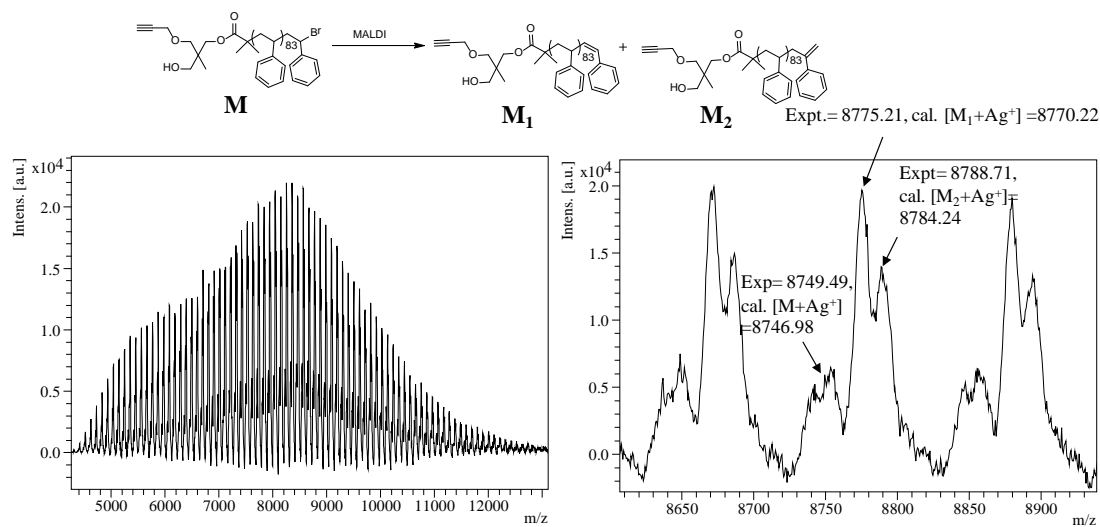


Figure D28: MALDI-ToF mass spectrum acquired in linear mode with Ag salt as cationizing agent and DCTB matrix. The full and expanded spectra correspond to ≡(HO)-PSTY₈₄-Br, **7c**.

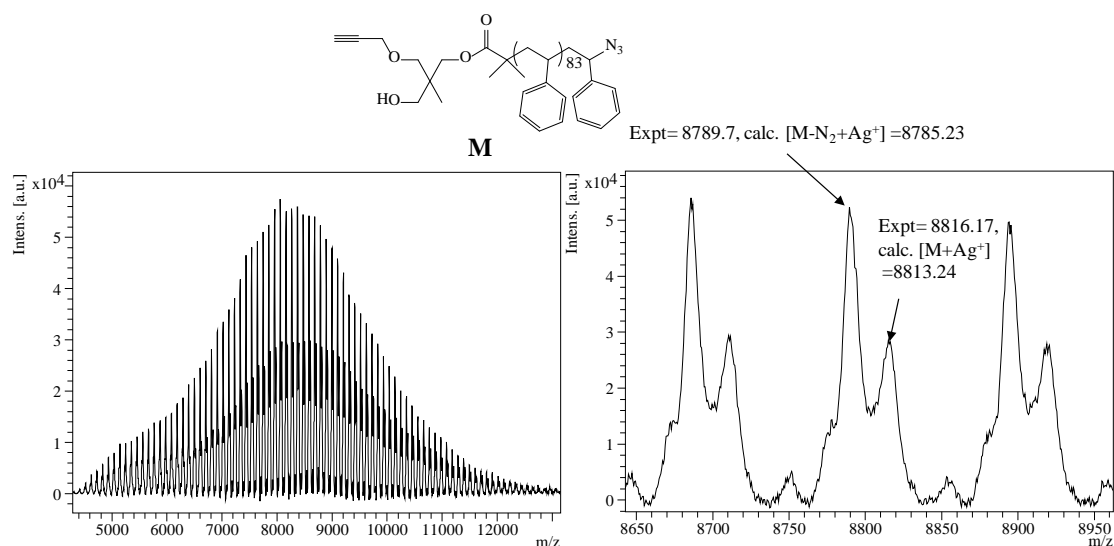


Figure D29: MALDI-ToF mass spectrum acquired in linear mode with Ag salt as cationizing agent and DCTB matrix. The full and expanded spectra correspond to $\equiv(\text{HO})\text{-PSTY}_{84}\text{-N}_3$, **8c**.

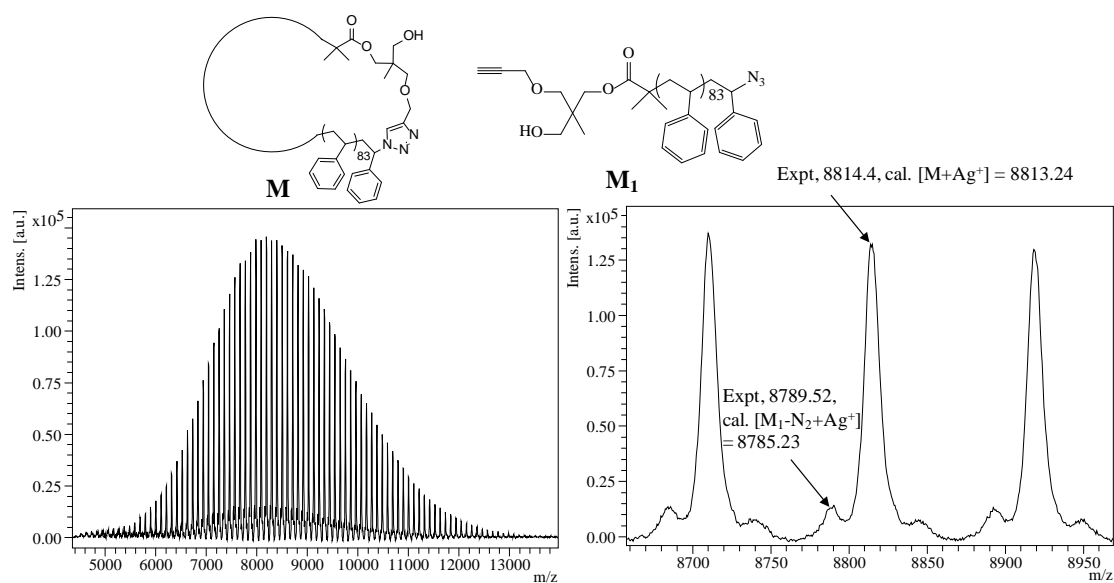


Figure D30: MALDI-ToF mass spectrum acquired in linear mode with Ag salt as cationizing agent and DCTB matrix. The full and expanded spectra correspond to $c\text{-PSTY}_{84}\text{-OH}$, **9c**.

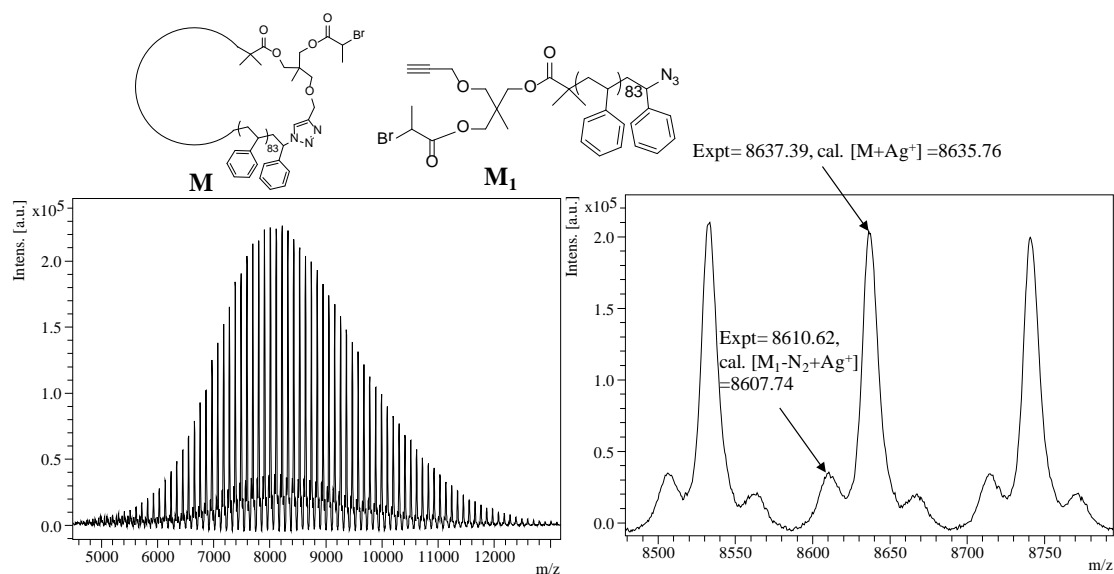


Figure D31: MALDI-ToF mass spectrum acquired in linear mode with Ag salt as cationizing agent and DCTB matrix. The full and expanded spectra correspond to c-PSTY₈₄-Br, **10c**.

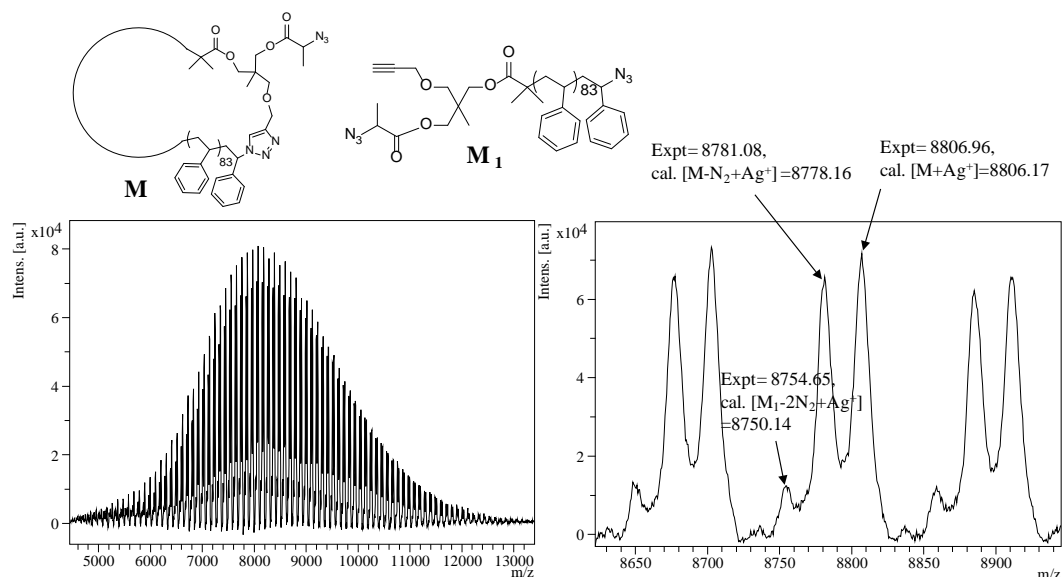


Figure D32: MALDI-ToF mass spectrum acquired in linear mode with Ag salt as cationizing agent and DCTB matrix. The full and expanded spectra correspond to c-PSTY₅₈-N₃, **11c**.

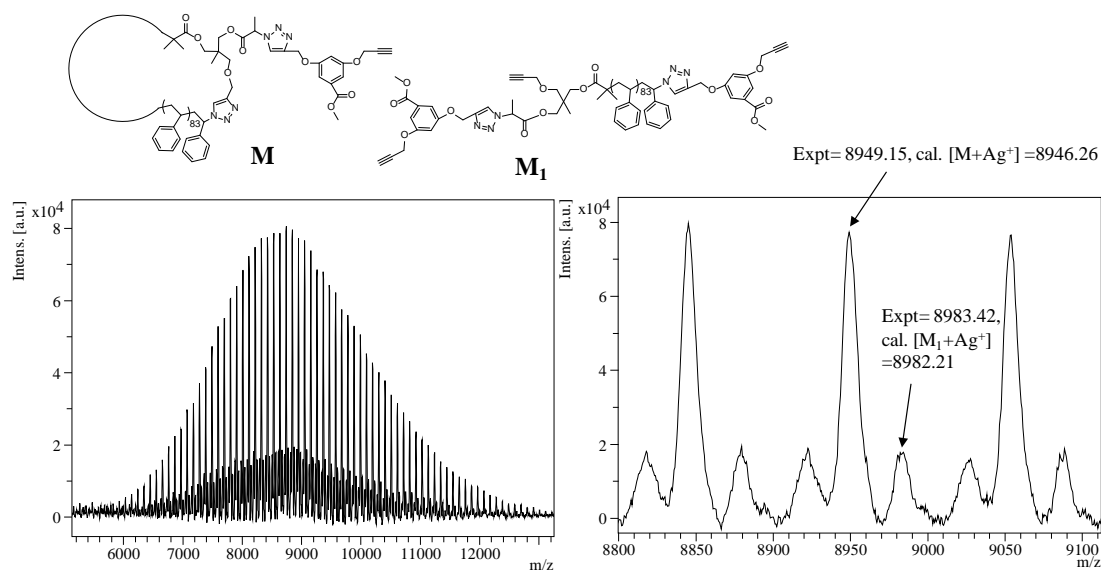


Figure D33: MALDI-ToF mass spectrum acquired in linear mode with Ag salt as cationizing agent and DCTB matrix. The full and expanded spectra correspond to c-PSTY₈₄-≡, **14c**.

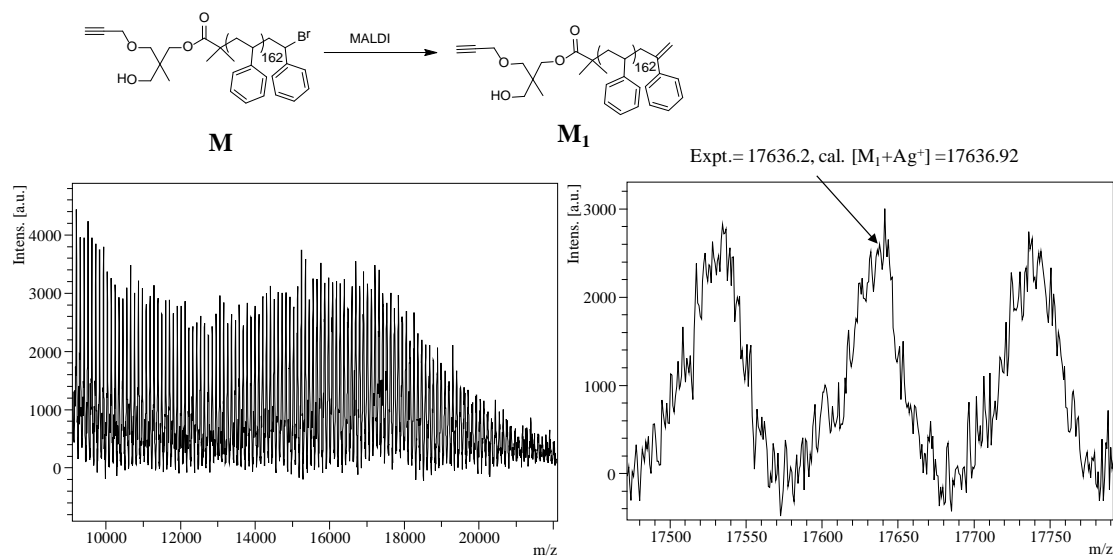


Figure D34: MALDI-ToF mass spectrum acquired in linear mode with Ag salt as cationizing agent and DCTB matrix. The full and expanded spectra correspond to ≡(HO)-PSTY₁₆₃-Br, **7d**.

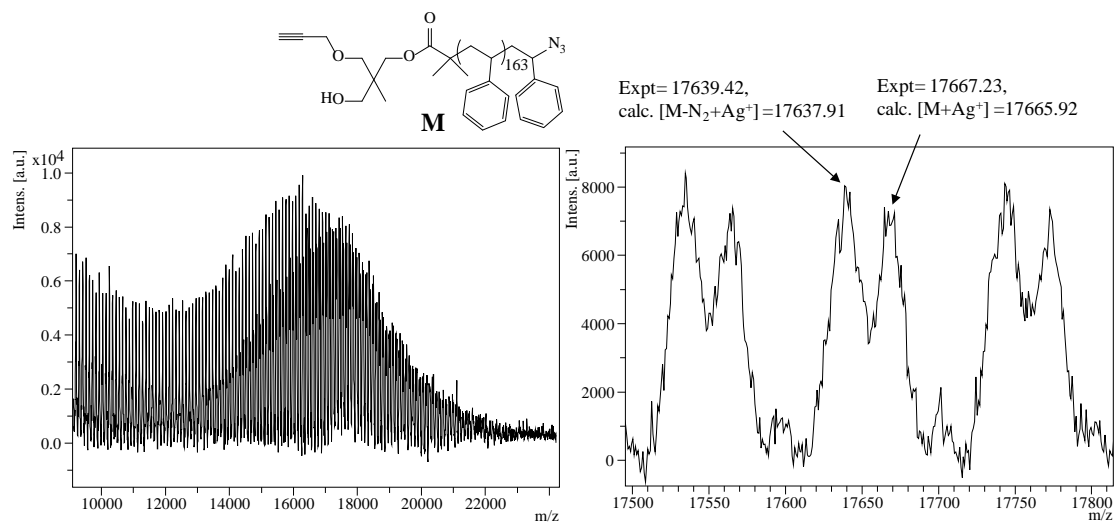


Figure D35: MALDI-ToF mass spectrum acquired in linear mode with Ag salt as cationizing agent and DCTB matrix. The full and expanded spectra correspond to $\equiv(\text{HO})\text{-PSTY}_{163}\text{-N}_3$, **8d**.

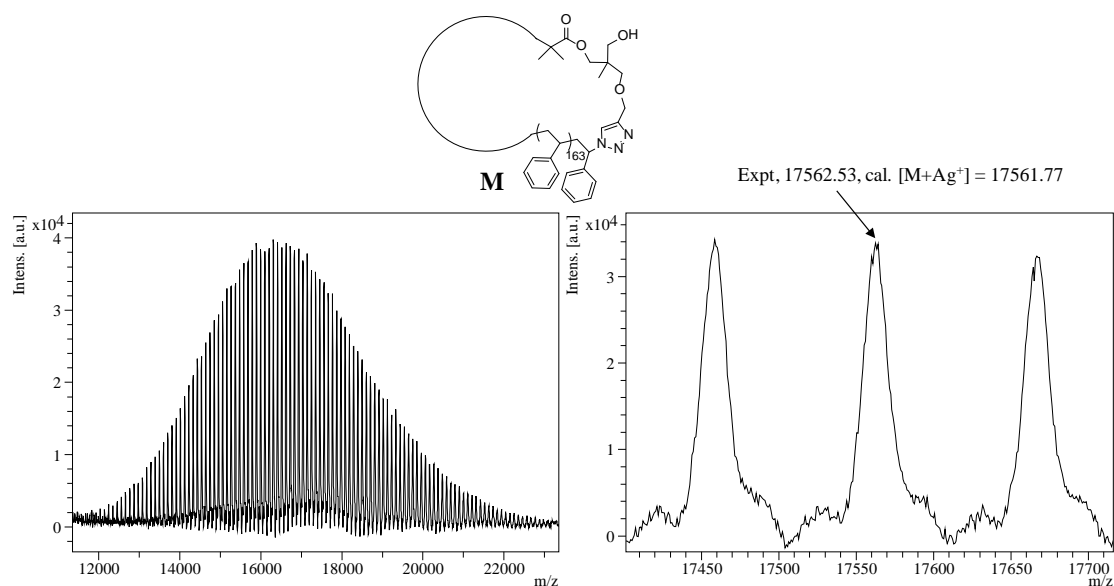


Figure D36: MALDI-ToF mass spectrum acquired in linear mode with Ag salt as cationizing agent and DCTB matrix. The full and expanded spectra correspond to $c\text{-PSTY}_{163}\text{-OH}$, **9d**.

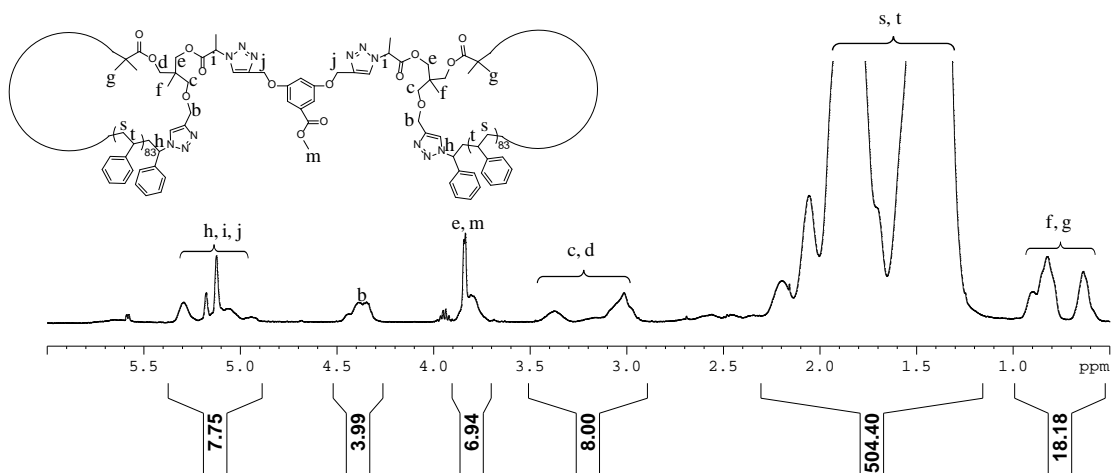


Figure D37. 500 MHz ¹H 1D DOSY NMR spectra in CDCl₃ of (c-PSTY₈₄)₂, **31**.

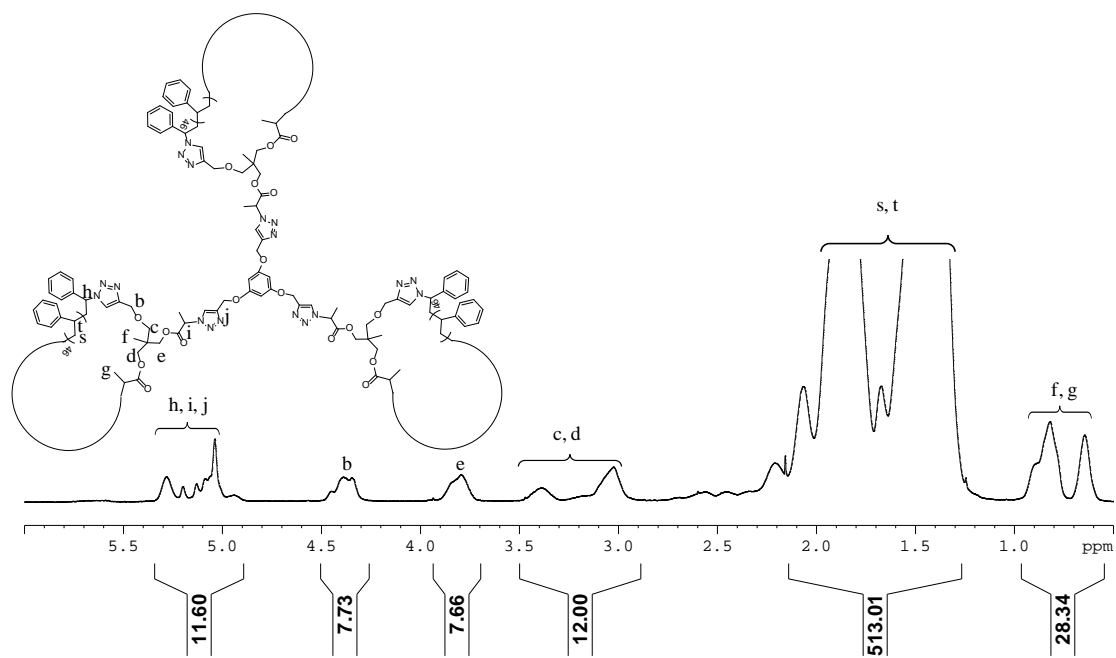


Figure D38. 500 MHz ¹H 1D DOSY NMR spectra in CDCl₃ of st-(c-PSTY₅₈)₃, **32**.

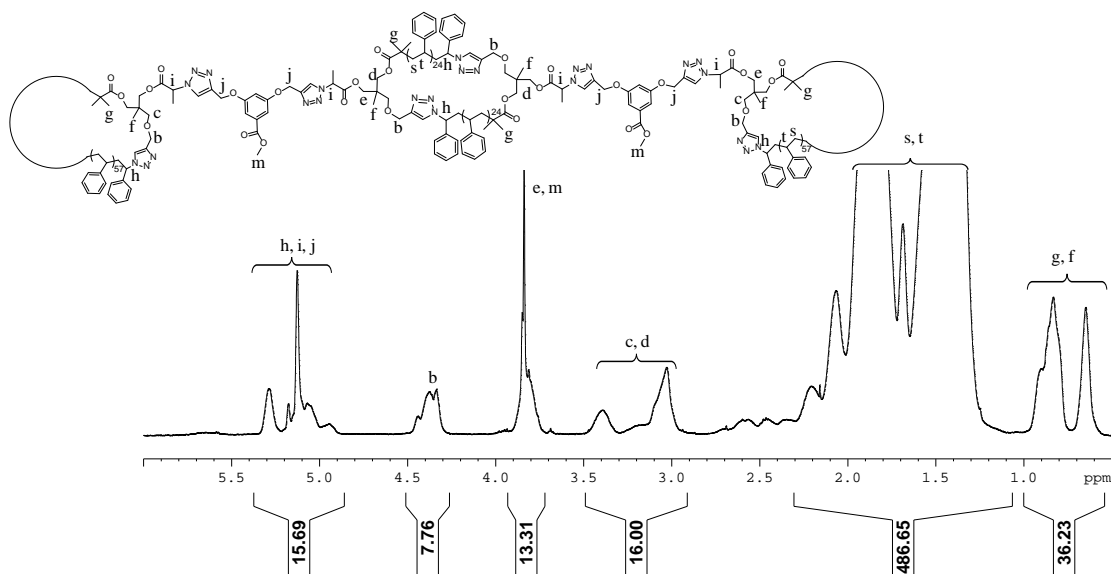


Figure D39: 500 MHz ¹H 1D DOSY NMR spectra in CDCl₃ of sp-(c-PSTY)₃, **33**.

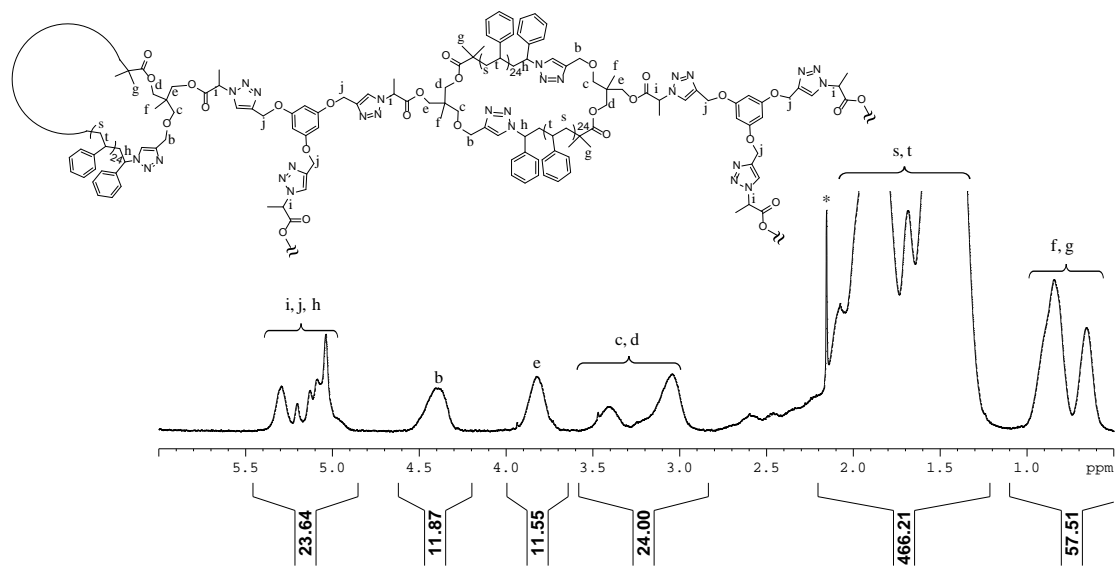


Figure D40: 500 MHz ¹H 1D DOSY NMR spectra in CDCl₃ of dendrimer (c-PSTY)₅, **34**.

*Acetone peak.

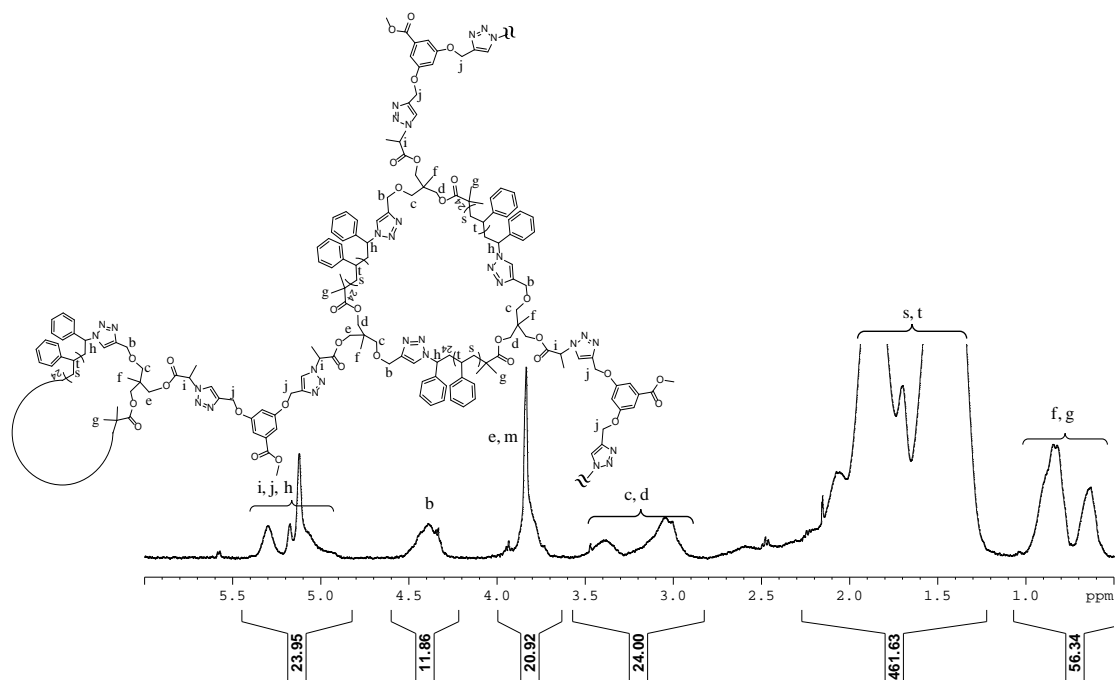


Figure D41: 500 MHz ^1H 1D DOSY NMR spectra in CDCl_3 of G1 (c-PSTY) $_4$, **35**.

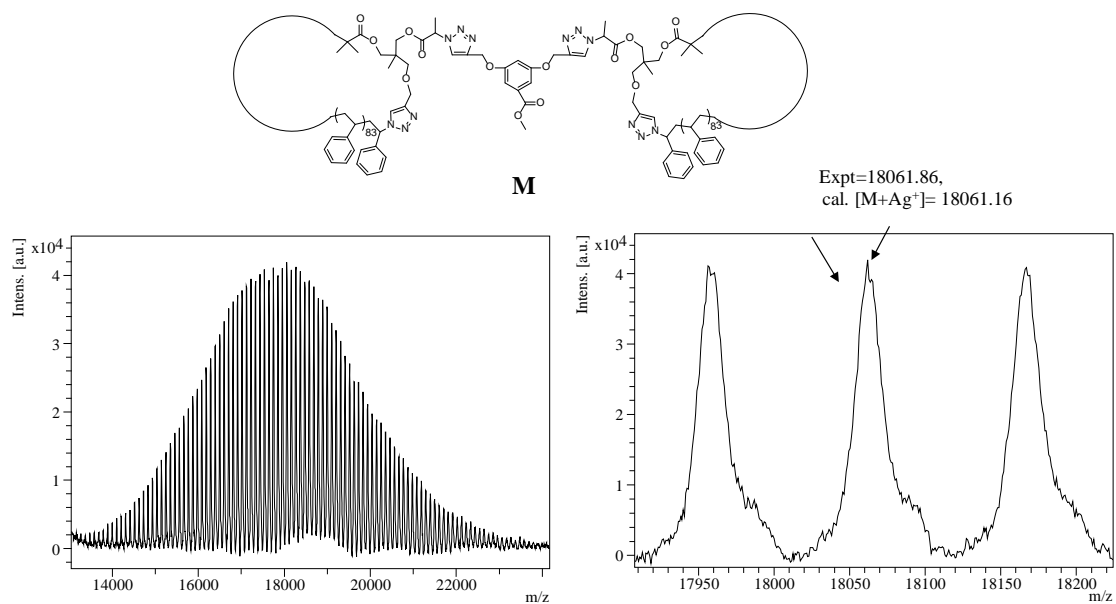


Figure D42: MALDI-ToF mass spectrum acquired in linear mode with Ag salt as cationizing agent and DCTB matrix. The full and expanded spectra correspond to (c-PSTY) $_{84}$) $_2$, **31**.

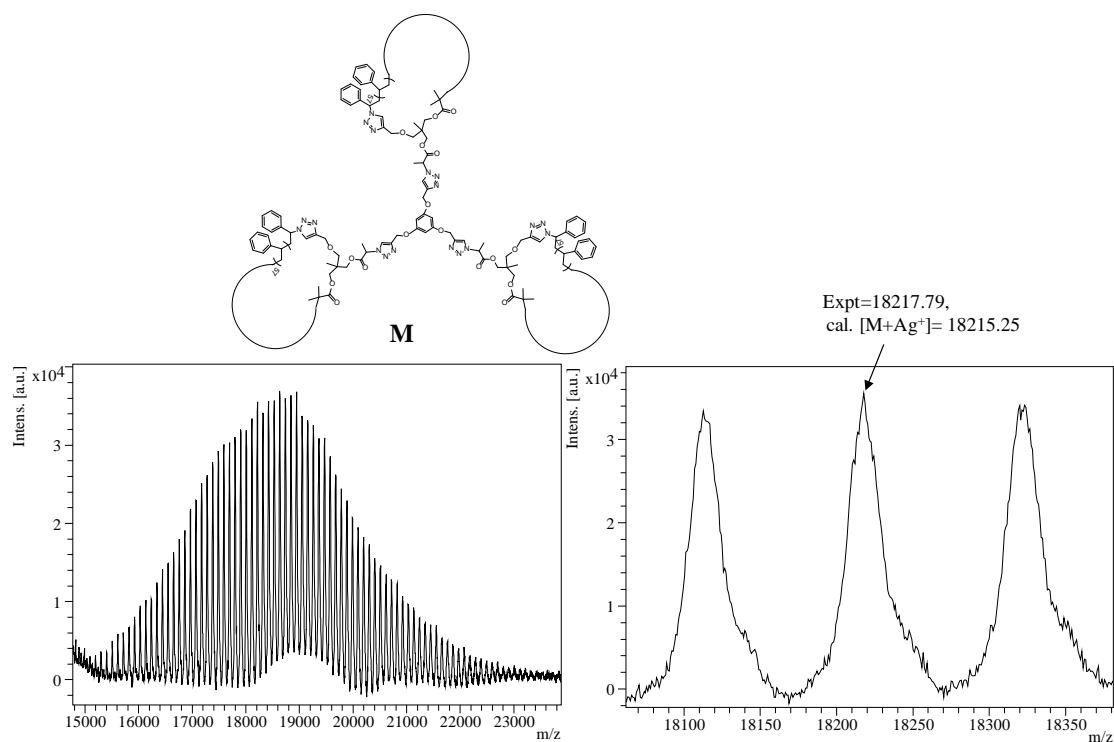


Figure D43: MALDI-ToF mass spectrum acquired in linear mode with Ag salt as cationizing agent and DCTB matrix. The full and expanded spectra correspond (c-PSTY₅₈)₃, **32**.

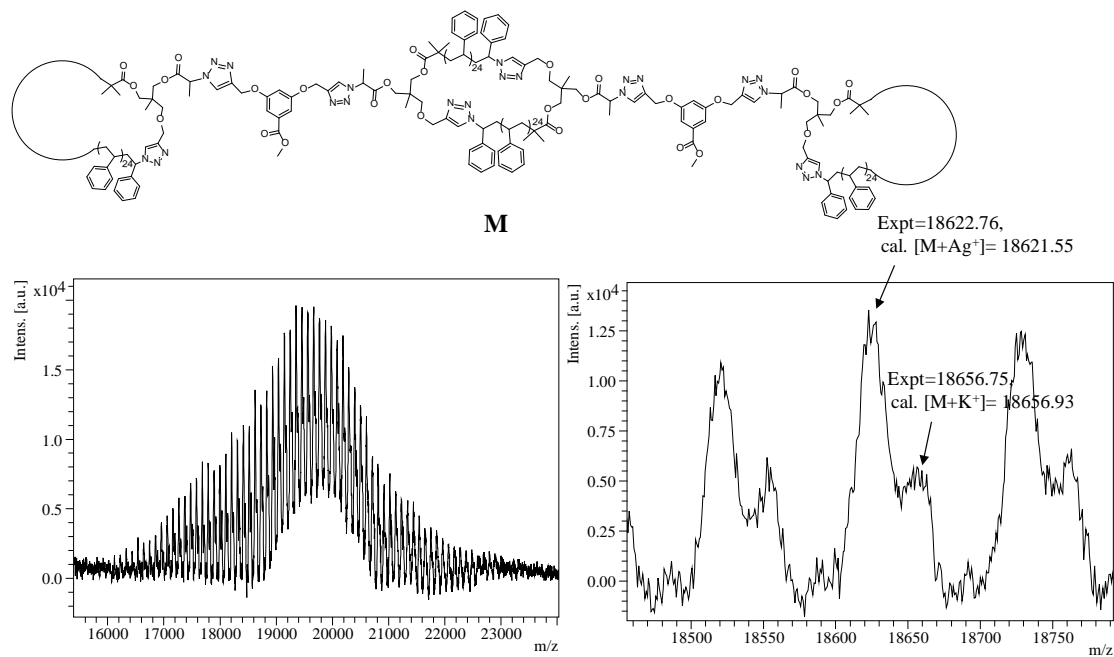


Figure D44: MALDI-ToF mass spectrum acquired in linear mode with Ag salt as cationizing agent and DCTB matrix. The full and expanded spectra correspond to Spiro (c-PSTY)₃, **33**.

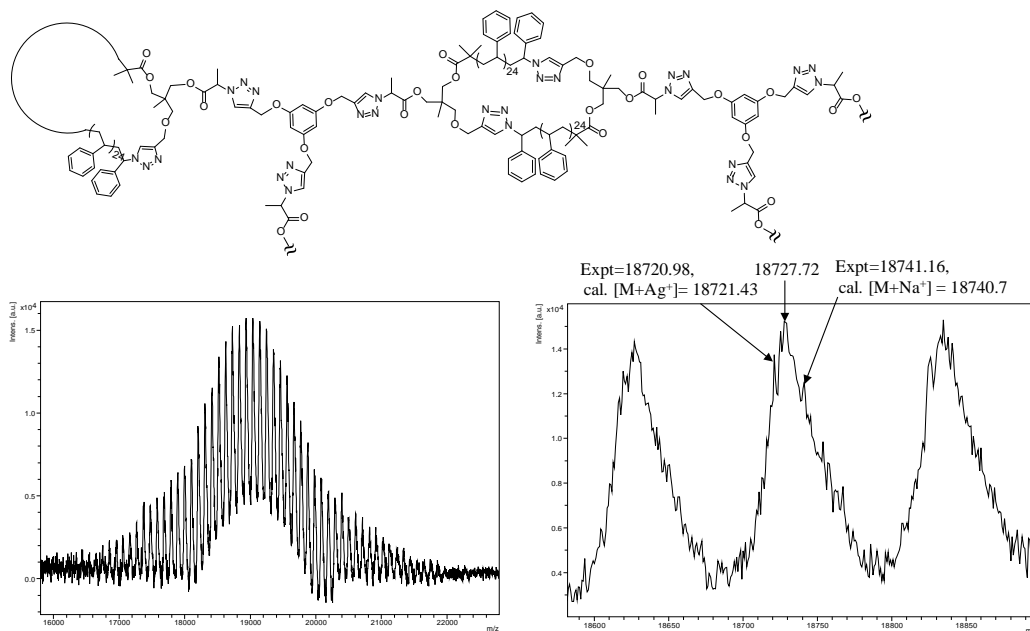


Figure D45: MALDI-ToF mass spectrum acquired in linear mode with Ag salt as cationizing agent and DCTB matrix. The full and expanded spectra correspond to G1-den-(c-PSTY)₅, **34**.

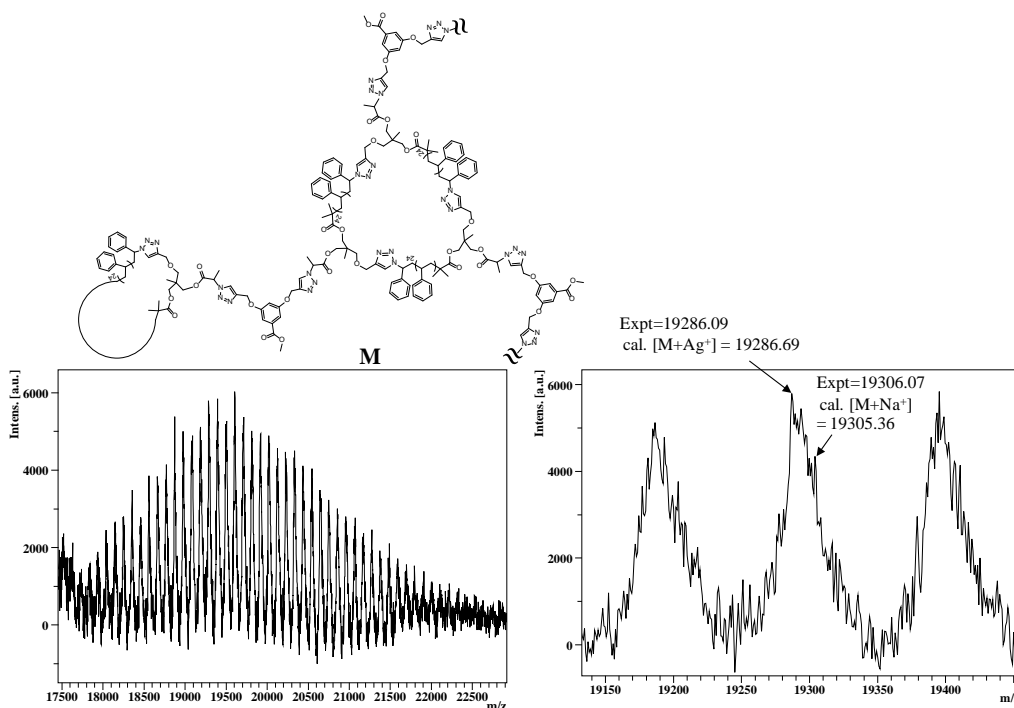


Figure D46: MALDI-ToF mass spectrum acquired in linear mode with Ag salt as cationizing agent and DCTB matrix. The full and expanded spectra correspond to G1-st-(c-PSTY)₄, **35**.

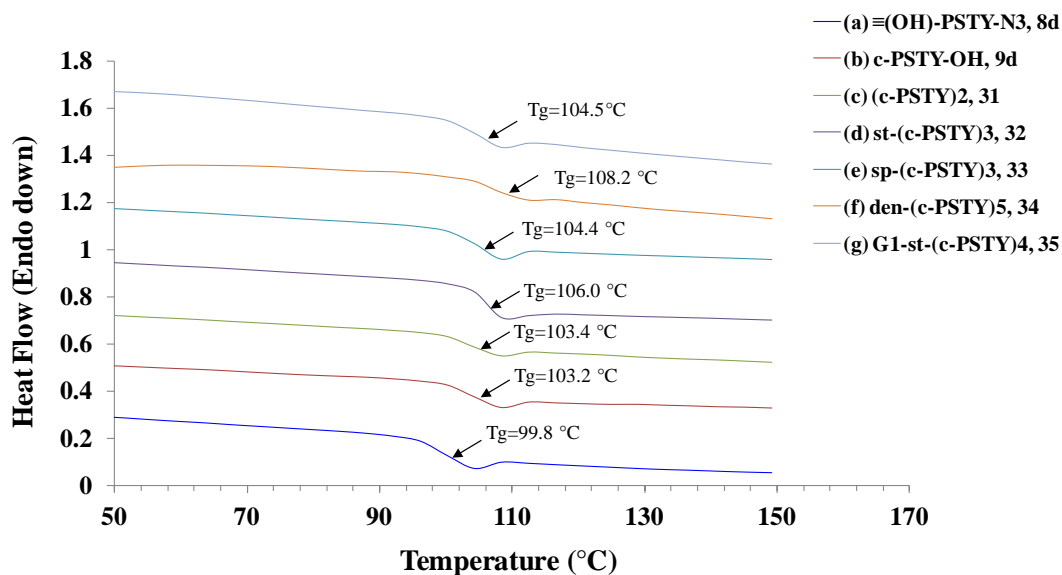


Figure D47. Differential scanning calorimetry (DSC) thermograms recorded for (a) ≡(OH)-PSTY₁₆₃-N₃, **8d**, (b) c-PSTY₁₆₃-OH, **9d**, (c) (c-PSTY)₂, **31**, (d) st-(c-PSTY)₃, **32**, (e) sp-(c-PSTY)₃, **33**, (f) G1-den-(c-PSTY)₅, **34** and (g) G1-st-(c-PSTY)₄, **35**. Samples were first heated from 20 to 150 °C at a heating rate of 5 °C/min under nitrogen atmosphere, followed by cooling to 20 °C at a rate of 5 °C/min after stopping at 150 °C for 3 min, and finally heating to 150 °C at the rate of 5 °C/min.

Table D1: Molecular weight and simulation data for the starting building blocks and their products.

Polymer	Purity by LND (%)		Coupling efficiency (%) ^a	RI detection ^b			Triple detection ^c			M _n by NMR	Δ HDV ^d			
	Crude	Prep		M _n	M _p	PDI	M _n	M _p	PDI					
7a	84.0	> 99.0		2890	2900	1.11	2780	2860	1.01	3120	0.76			
8a				2880	2900	1.11				2980				
9a				2140	2180	1.04				2980				
10a				2350	2400	1.04				3110				
11a				2250	2300	1.04				3178				
14a	84.8	> 99.0		2440	2470	1.04	6220	6390	1.00	3520	0.77			
7b				6470	6450	1.08				6240				
8b				6390	6440	1.08				6310				
9b				4690	4900	1.04				6310				
10b				4580	4670	1.04				6340				
11b	81.1	> 99.0		4750	4850	1.04	9190	9400	1.00	6200	0.73			
14b				4930	5030	1.04				6670		1.01	6200	
15b				5020	5100	1.03				6520		6660	1.00	6650
7c				9130	9240	1.08				6500		6650	1.00	6860
8c				9020	9130	1.08				9580				
9c	79.8	> 99.0		6890	7100	1.04	18300	18660	1.00	8910	0.76			
10c				6670	6950	1.04				9150				
11c				6880	7100	1.04				9220				
14c				7050	7280	1.04				9460				
7d				17110	17730	1.09				17490				
8d	90.8		90.8	17300	17970	1.06	18330	18580	1.00	17770	0.96			
9d				13430	13760	1.04				17770				
16				2870	3040	1.08				2960				
17				2890	2910	1.06				3030				
18				5510	5600	1.05				6350				
19	82.1	> 99.0		5510	5550	1.06	5350	5500	1.02	6210	0.76			
20				5350	5400	1.06				6420				
21				4110	4170	1.03				6475				
22				4350	4370	1.03				6220				
23				4470	4590	1.03				6250				
24	82.0		82.0	4720	4830	1.04	8830	8980	1.00	6830	0.74			
25				8830	8990	1.06				9230				
26				8750	8860	1.06				9400				
27				8720	8880	1.05				9660				
28				76.5	> 99.0					6600		6780	1.03	8830
29				7210	7320	1.03				9230				
30				7070	7220	1.03	9250	9390	1.00	8910				
31	92.2	98.5	92.2	13320	13590	1.04	19140	19440	1.00	18580				
32	91.4	99.0	91.4	12850	12940	1.04	19700	20400	1.01	19250				
33	83.8	91.23	86.6	14050	14280	1.06	19080	19330	1.00	19030				
34	77.75	97.02	80.9	12890	13130	1.04	18900	19400	1.00	18400				
35	70.53	84.15	74.25	13920	13980	1.05	19680	19800	1.00	18450				

^aCuAAC coupling efficiency was determined from the RI traces of SEC. Coupling efficiency calculated as follows: $\text{purity (LND)}/\text{max. purity by theory} \times 100$. ^bThe data was acquired using SEC (RI detector) and is based on PSTY calibration curve. ^cThe data was acquired using DMAc Triple Detection SEC with 0.03 wt% of LiCl as eluent. ^d ΔHDV was calculated by dividing M_p of RI with M_p of triple detection.